UNITED STATES DEPARTMENT OF THE INTERIOR

GEOLOGICAL SURVEY

NATIONAL EARTHQUAKE HAZARDS REDUCTION PROGRAM,
SUMMARIES OF TECHNICAL REPORTS VOLUME XX

Prepared by Participants in

NATIONAL EARTHQUAKE HAZARDS REDUCTION PROGRAM

July 1985

OPEN-FILE REPORT 85-464

This report (map) is preliminary and has not been reviewed for
conformity with U.S.Geological Survey editorial standards
(and stratigraphic nomenclature). Any use of trade names
is for descriptive purposes only and does not imply
endorsement by the USGS.

Menlo Park, California

1985

UNITED STATES
DEPARTMENT OF THE INTERIOR
GEOLOGICAL SURVEY

———————

NATIONAL EARTHQUAKE HAZARDS REDUCTION PROGRAM,
SUMMARIES OF TECHNICAL REPORTS VOLUME XX

Prepared by Participants in

NATIONAL EARTHQUAKE HAZARDS REDUCTION PROGRAM

———————

Compiled by

Muriel L. Jacobson

Thelma R. Rodriguez

The research results described in the following summaries were submitted by the investigators on May 10, 1985 and cover the 6-months period from October 1, 1984 through May 1, 1985. These reports include both work performed under contracts administered by the Geological Survey and work by members of the Geological Survey. The report summaries are grouped into the three major elements of the National Earthquake Hazards Reduction Program.

Open File Report No. 85-464

The data and interpretations in these progress reports may be reevaluated by the investigators upon completion of the research. Readers who wish to cite findings described herein should confirm their accuracy with the author.

CONTENTS

Earthquake Hazards Reduction Program

Objective (P-1):   Prediction Methodology and Evaluation

Develop methods to provide a rational basis for estimates of increased earthquake potential. Evaluate the relevance of various geophysical, geochemical, and hydrological data for earthquake prediction.

Objective (P-2):   Earthquake Prediction Experiments

Conduct data collection and analysis experiments in areas of California capable of great earthquakes, where large populations are at risk. The experiments will emphasize improved coordination of data collection, data reporting, review and analysis according to set schedules and standards.

Objective (P-3):   Theoretical, Laboratory and Fault Zone Studies

Improve our understanding of the physics of earthquake processes through theoretical and laboratory studies to guide and test earthquake prediction observations and data analysis. Measure physical properties of those zones selected for earthquake experiments, including stress, temperature, elastic and anelastic characteristics, pore pressure, and material properties.

Objective (P-4):   Induced Seismicity Studies

Determine the physical mechanism responsible for reservoir-induced seismicity and develop techniques for predicting and mitigating this phenomena.

ELEMENT III   Evaluation of Regional and Urban Earthquake Hazards

Delineate, evaluate, and document earthquake hazards and risk in urban regions at seismic risk.   Regions of interest, in order of priority, are:

1)   The Wasatch Front

2)   Southern California

3)   Northern California

4)   Anchorage Region

5)   Puget Sound

6)   Mississippi Valley

7)   Charleston Region

ELEMENT IV   Earthquake Data and Information Services

ELEMENT V: Engineering Seismology

Most of the technical summaries contained in this volume are for research contracts solicited by RFP-1284. The description in the previous table of contents corresponds to respective Elements and Objectives of that RFP. Additionally some of the summaries are for research objectives that were initiated in earlier years. These objectives are covered in the descriptions found in the following table of contents.

Southern California Seismic Arrays

Contract No. 14-08-0001-21854

Clarence R. Allen
Seismological Laboratory, California Institute of Technology
Pasadena, California 91125 (818-356-6904)

Investigations

This semi-annual Technical Report Summary covers the six-month period from 1 October 1984 to 31 March 1985. The contract's purpose is the partial support of the joint USGS-Caltech Southern California Seismographic Network, which is also supported by other groups, as well as by direct USGS funding of its own employees at Caltech. According to the contract, the primary visible product will be a joint Caltech-USGS catalog of earthquakes in the southern California region; quarterly epicenter maps and preliminary catalogs are also required and have been submitted as due during the contract period. About 250 preliminary catalogs are routinely distributed to interested parties.

Results

Figure 1 shows the epicenters of all cataloged shocks that were located during the six-month reporting period. Some of the seismic highlights during this period are as follows:

Number of earthquakes processed: 9184
Number of earthquakes of M = 3.0 and greater: 253
Number of earthquakes of M = 4.0 and greater: 26
Largest shock within network area: M = 4.7 (8 February, near Bakersfield)
Largest nearby shock: M = 6.2 (23 November, near Bishop)
Smallest felt earthquake: M = 2.3 (3 December, Buena Park)
Number of earthquakes for which systematic telephone notification to
    emergency-response agencies was made: 13

The most significant seismicity during the period occurred northwest of Bishop (Inyo County); this activity was slightly outside of the Network area but is shown in Figure 1. Other interesting activity included the following:

(1) Activity in the Desert Hot Springs area (Riverside County) was somewhat higher than usual, especially during January and February of 1985 (Fig. 2). The largest event (M = 4.1, 1/2/85) was not associated with reported damage. Nevertheless, these sequences included 940 cataloged events, 7 of which were reported to the Seismological Laboratory as having been felt. The activity was the cause of a large number of inquiries from members of the public. The epicentral area was very similar to that of the M = 6-1/2 event of 1948.

(2) The entire Santa Barbara-Ventura-Malibu area has shown activity during this period somewhat higher than normal. In fact, this activity was noticed as early as April 1984, and Figure 3 shows the epicentral distribution since that

1

time. Of these events, 22 were reported as felt, and 1 (of M = 4.5) caused minor damage in Solvang (Santa Barbara County).

During the reporting period, the Network remained relatively stable, with no new stations installed, and with no significant hardware or software modifications to the data-analysis operation. The USGS did, however, begin the conversion of a number of the outlying stations from telephone to microwave telemetry. With the publication of the 1975-1983 catalog in April 1985 (see below), final listings for southern California earthquakes of M = 3.0 and greater have now been published for 1932 through 1983.

Publication

Hutton, L. K., Allen, C. R., and Johnson, C. E., 1985, Seismicity of southern California: Earthquakes of ML 3.0 and greater, 1975 through 1983: Pasadena, Calif. Inst. Technology, 142 p. (Copies available through the Caltech Bookstore; $5.00 plus shipping)
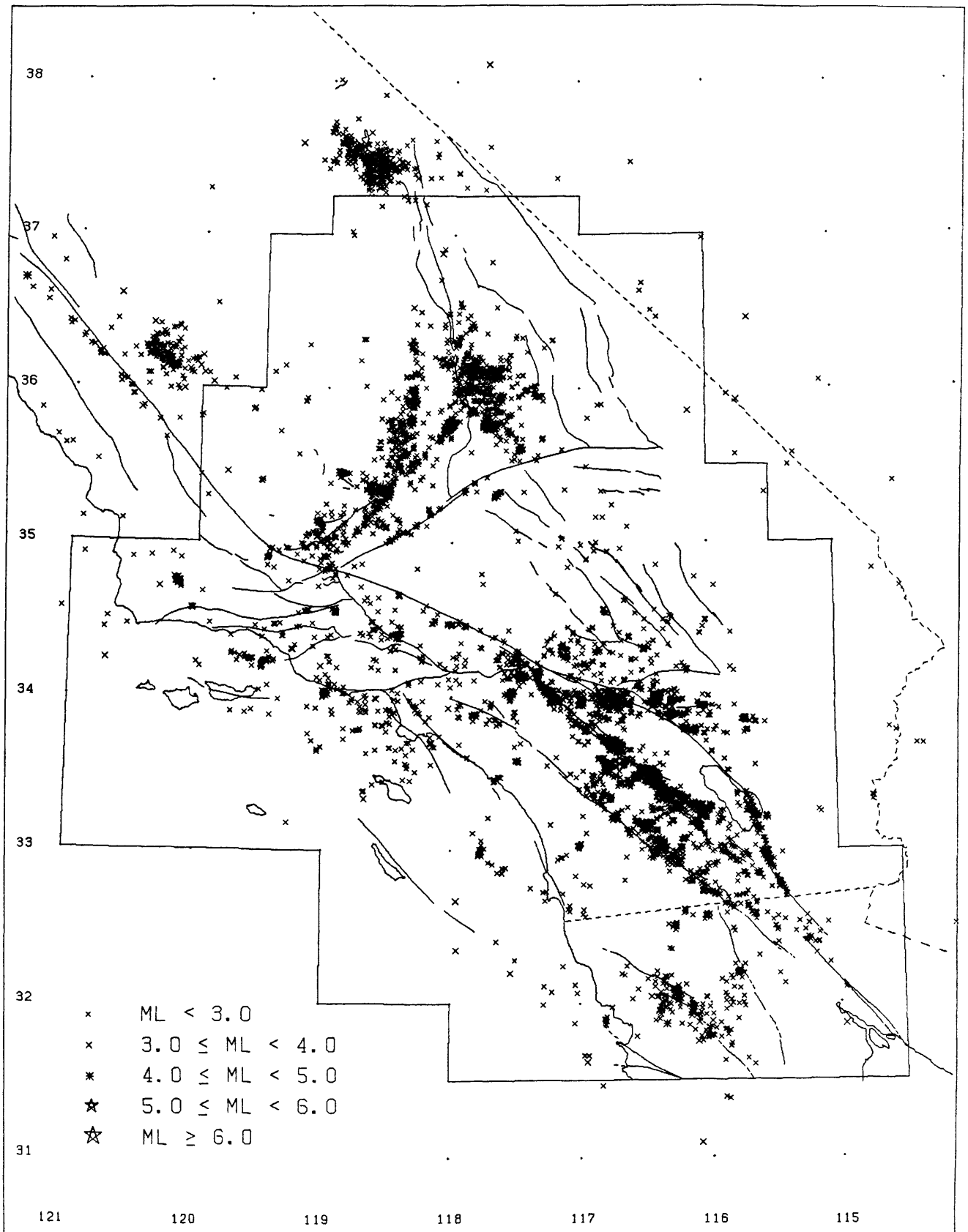
Figure 1.--Epicenters of larger earthquakes in the southern California region, 1 October 1984 to 31 March 1985.
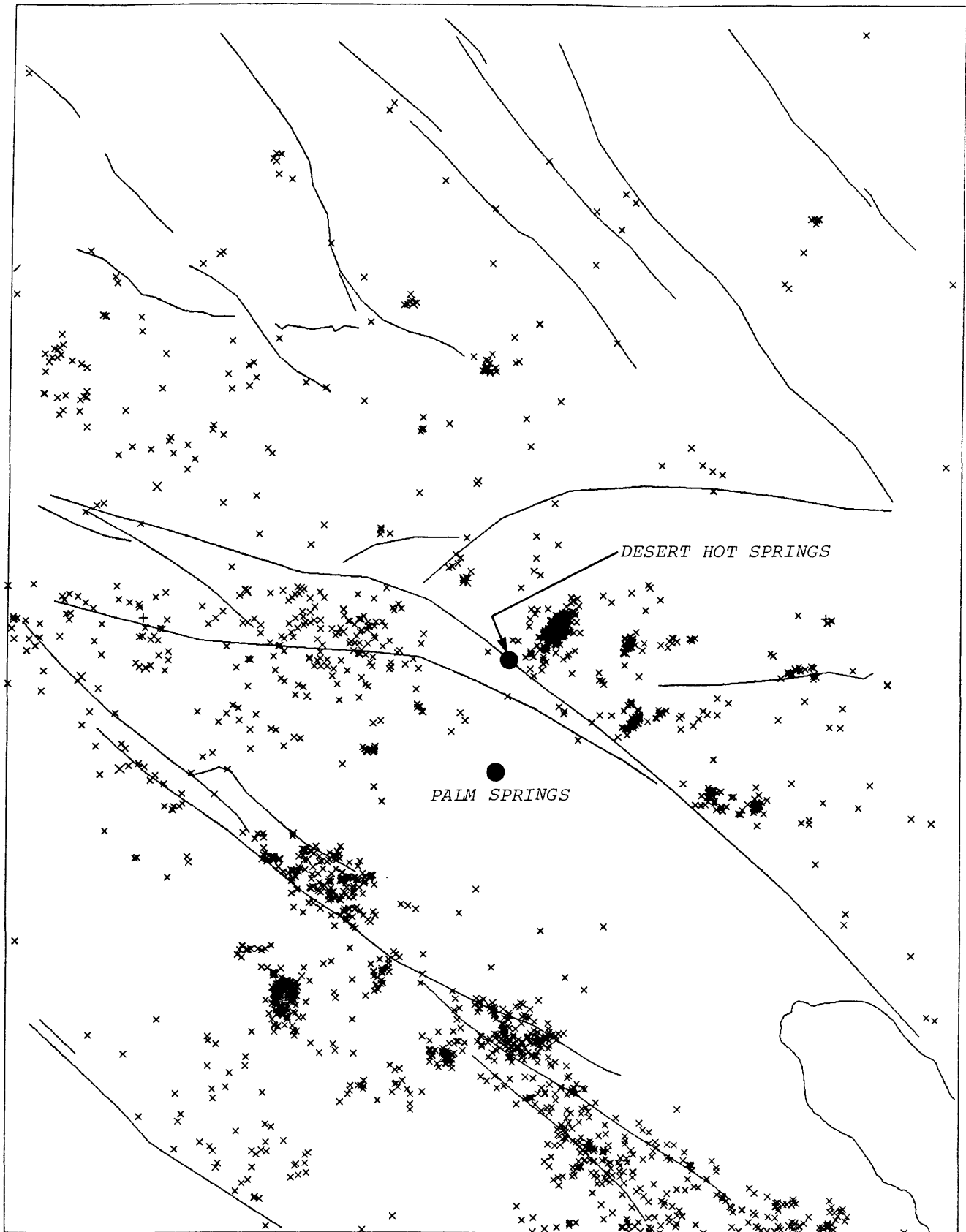
Figure 2.--Clusters of events in the Desert Hot Springs-Palm Springs area, most of which occurred in January and February 1985. "Anza gap" is near bottom. For location of map area, compare with Figure 1.
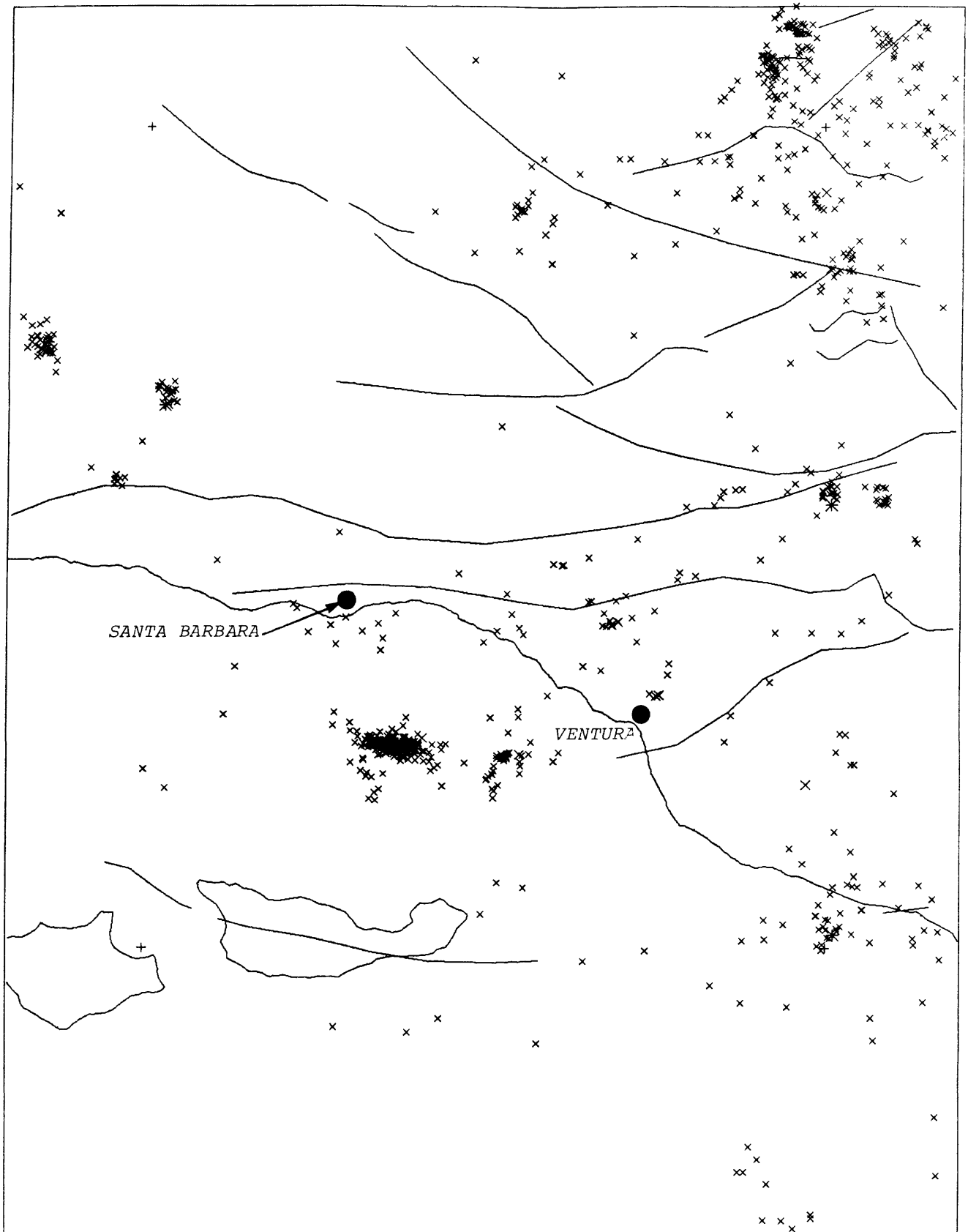
Figure 3.--Activity in the Santa Barbara-Ventura-Malibu area, from April 1984 through March 1985. For location of map area, compare with Figure 1.

REGIONAL SEISMIC MONITORING ALONG THE WASATCH FRONT URBAN
CORRIDOR AND ADJACENT INTERMOUNTAIN SEISMIC BELT

14-08-0001-21857

W. J. ARABASZ, R.B. SMITH, J.C. PECHMANN, and W.D. RICHINS
Department of Geology and Geophysics
University of Utah
Salt Lake City, Utah 84112
(801)581-6274

Investigations

This contract supports "network operations" (including a computerized central recording laboratory) associated with the University of Utah 80-station regional seismic telemetry network. USGS support focuses on the seismically hazardous Wasatch Front urban corridor of north-central Utah but also encompasses neighboring areas of the Intermountain seismic belt (ISB). The University of Utah maintains de facto responsibility for earthquake surveillance, including emergency response and direct public interface, for an 800-km-long segment of the ISB between Yellowstone Park and southernmost Utah. The State of Utah, the U.S. Bureau of Reclamation, the National Park Service and the U.S. Geological Survey (Geothermal Research Program) also contributed support to operation of the University of Utah network during the report period.

Primary products of this USGS contract are quarterly earthquake catalogs and a semi-annual data submission, in magnetic-tape form, to the USGS Data Archive.

Results

Figure 1 shows the epicenters of 282 earthquakes located in the Utah region (lat. 36.75°-42.5°N, long. 108.75°-114.25°W) during the six-month period October 1, 1984, to March 31, 1985. The seismicity sample includes 5 events of local magnitude (M_L) greater than or equal to 3.0, and 5 felt events. The largest event, of M_L 3.6, occurred on January 26, 1985 in the Utah-Idaho border area north of the Great Salt Lake. It was followed one day later by an M_L 3.3 event with nearly the same epicenter. Both events were felt locally. A third felt event of M_L=3.4 occurred 15 km southeast of this pair of events three months previous to them on October 15, 1984. Two other earthquakes reported felt in the Utah region during this time period were shocks of magnitude 2.5 and 2.4 on November 25, 1984, located near, and felt at, St. George, Utah.

The two most outstanding features of the seismicity map in Figure 1 are: (1) the intense activity along the Utah-Idaho border north of the Great Salt Lake and (2) clustered small-magnitude earthquake activity in the vicinity of active underground coal mining southwest, west, and north of Price in central Utah. Both of these features are characteristic of recent seismicity in Utah. The two events in southwestern Wyoming shown on the map may be local blasts.

Reports and Publications

Richins, W. D., 1984, Utah earthquake activity, October through December 1984, Wasatch Forum, v. 1, no. 3, 7.

Utah Earthquakes: Oct 1, 1984 – Mar 31, 1985

Figure 1

Seismological Data Processing

Barbara Bekins, Thomas Jackson, and Richard Jensen

Branch of Seismology
U.S. Geological Survey
345 Middlefield Rd. MS 977
Menlo Park, California, 94025
(415) 323-8111 ext. 2965

Investigations

Computer data processing is absolutely necessary in modern seismological research; digital seismic data can be analyzed in no other way, and problems of earthquakes and seismic wave propagation usually require numerical solution. The purpose of this project is to develop and operate a simple, powerful, well human-engineered computer data processing system and to write general application programs to meet the needs of scientists in the earthquake prediction program and monitor earthquakes in northern California. This goal includes maintaining the ability to transfer data and programs over a network and the ability to share data and programs with external contractors.

Results

The PDP11-70 UNIX system has continued to operate smoothly, and performs a large amount of computing for program projects. Some current statistics:

158	registered users
460654	1024-byte disk storage blocks used
58	login sessions per weekday

Considerable effort has been spent on the software which processes the data from the real time Ppicker. (See Earthquakes and the statistics of Crustal Heterogeneity by Bruce Julian). The role of this software has grown in importance to the point where it had to be redesigned to run more efficiently and tolerate faults more robustly. Ultimately, this software will run on the new Ppicker system which will come with System V UNIX.

This project has concluded an investigation into super micro-computers which run the UNIX system. The object of this investigation was to find a computer system which would replace the PDP 11/70 for under $50,000. To replace the 11/70, the system must have at least 24 terminal ports, a fast graphics subsystem, an SMD disk controller, a nine track tape drive, an ethernet controller, a floating point processor, at least two million bytes of memory and a 16 bit parallel input device. It must run the 4.2BSD UNIX system and demand paged virtual memory is also a requirement. A requisition has been issued recommending the purchase of an Integrated Solutions Optimum System.

The Seismology Branch Vax 11/750 is now running under VMS version 4.1+. Development is proceeding on combining data from the real time Ppicker, the CUSP system, Calnet group processing into one unified database. These data will be accessed through the CUSP database system which runs under VMS version 4.1+. In addition there are plans to bring up the SAC system written at Lawrence Livermore Labs. This system provides interactive analysis of seismic waveforms.

A plan has been created to replace the current system for digitizing of selected earthquakes off analog FM tapes. This work is presently performed on Data General

Eclipse systems. The plan is to use an IBM PC/XT for positioning the tape and a Tustin digitizer to digitize the data. These data will then be sent to the Vax 750 for storage and analysis with the CUSP system.

This project also handles one third of the support for the office Vax 780 operation. This support consisted of weekly and monthly disk backups to tape, authorizing new users, redistributing Seismology branch disk quotas, assisting users, and occasional miscellaneous activities related to computer operations and system management.

Other project activities include the following major efforts. A survey of existing and projected terminal to computer connections by branch computer users was conducted in order to specify the data requirements for the new ROLM PABX system. These requirements have been forwarded to ROLM. A floor plan for moving the Vax 780, and the two Vax 750 systems into the Information Systems Division computer room was created and approved.

Central Aleutian Islands Seismic Network

Contract No. 14-08-0001-21896

Selena Billington and Carl Kisslinger
Cooperative Institute for Research in Environmental Sciences
Campus Box 449, University of Colorado
Boulder, Colorado   80309

(303) 492-8028

Brief Description of Instrumentation and Data Reduction Methods

The Adak seismic network consists of 13 high-gain, high-frequency, two-component seismic systems and one six-component system (ADK) located at the Adak Naval Base. Station ADK has been in operation since the mid-1960s; nine of the additional stations were installed in 1974, three in 1975, and one each in 1976 and 1977.

Data from the stations are FM-telemetered to recording sites near the Naval Base, and are then transferred by cable to the Observatory on the Base. Data were originally recorded by Develocorder on 16 mm film; since 1980 the film recordings are back-up and the primary form of data recording has been on analog magnetic tape. The tapes are mailed to CIRES once a week.

At CIRES the analog tapes are played back at four-times the speed at which they were recorded into a computer which digitizes the data, automatically detects events, and writes an initial digital event tape. This tape is edited to eliminate spurious triggers, and a demultiplexed tape containing only seismic events is created. All subsequent processing is done on this tape. Times of arrival and wave amplitudes are read from an interactive graphics display terminal. The earthquakes are located using a program developed for this project by E. R. Engdahl, which uses corrections to the arrival times which are a function of the station and the source region of the earthquake.

Data Annotations

Earthquake locations are complete through February, 1985. Our normal lag time for hypocenter locations is three-to-six weeks, dependent on the postal service from Adak. The network was last serviced in July and August, 1984. Because of logistic problems, the westernmost station could not be reached at that time, and we were also unable to make necessary return trips to two other far-west stations. Of the 28 short-period vertical and horizontal components, 20 were operating for the period of August 1984 through February 1985.

Current Observations

334 earthquakes were located with data from the network during the seven-month time period from August 1, 1983, through February 28, 1985. Epicenters of these events are shown in Figure 1, a vertical cross-section is

given in Figure 2 and a plot of the cumulative number of events for the time period from May, 1976, through February, 1985, is given in Figure 3. Six of the events located within the past seven months were large enough to be located teleseismically (USGS PDEs). Three events had m_b greater than or equal to 5.0. The largest of these was a m_b 5.5 event in November; its aftershocks show up as a site of activity at about 175.3 ° W longitude. Another feature of the seismicity during this time period is a swarm of seven earthquakes during a 1-1/2 hour period on December 8, at about 176.1 ° W.

More detailed information about the network status and a catalog of the hypocenters determined for the time period reported here are included in our semi-annual data report to the U.S.G.S. Recent research using these data is reported in the Technical Summary for U.S.G.S. Grant No. 14-08-001-G881 in this volume.

LEGEND

• = 2.2 and below
○ = 2.3 to 3.0
○ = 3.1 to 3.9
○ = 4.0 to 4.9
□= PDE magnitude

ADAK SEISMICITY: AUGUST 1984–FEBRUARY 1985

UNIVERSAL TRANSVERSE MERCATOR PROJECTION

|====|
15 km

334 EVENTS
ALL DEPTHS
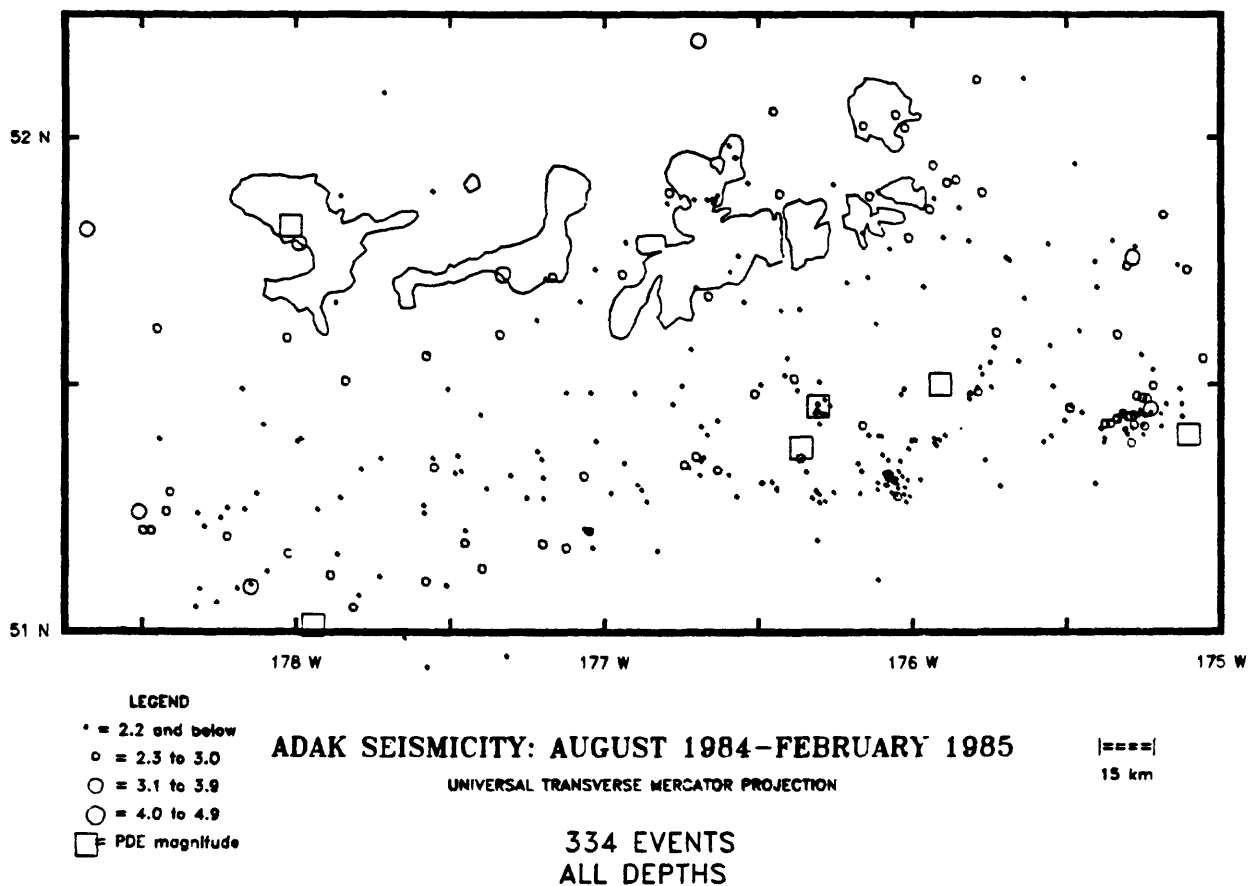
Figure 1: Map of seismicity which occurred from August 1, 1984, through February 28, 1985. All epicenters were determined from Adak network data. Events marked with squares are those for which a teleseismic body-wave magnitude has been determined by the USGS; all other events are shown by symbols which indicate the duration magnitude determined from Adak network data. The islands mapped (from Tanaga on the west to Great Sitkin on the east) indicate the geographic extent of the Adak seismic network.
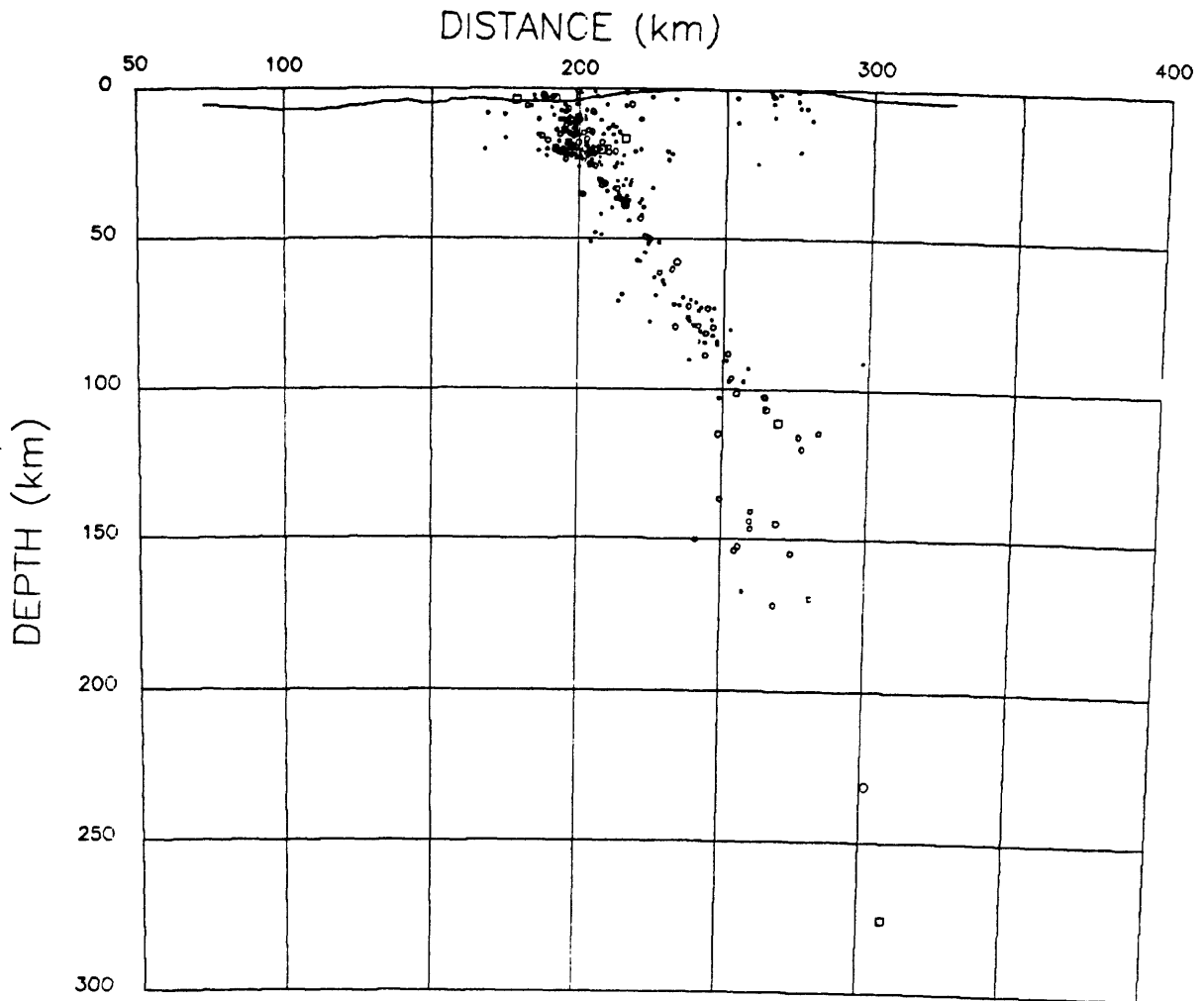
ADAK SEISMICITY: AUGUST 1984—FEBRUARY 1985

Figure 2: Vertical cross section of seismicity which occurred from August 1, 1984, through February 28, 1985. Events are projected according to their depth (corresponding roughly to vertical on the plot) and distance from the pole of the Aleutian volcanic line. The zero-point for the distance scale marked on the roughly-horizontal axis of the plot is arbitrary. Events marked with squares are those for which a teleseismic body-wave magnitude has been determined by the USGS; all other events are shown by symbols which indicate the duration magnitude determined from Adak network data. The irregular curve near the top of the section is bathymetry. Earthquakes deeper than about 100 km depth are mislocated too far south (left) as an effect of the slab on their ray paths to the local stations.

CUMULATIVE NUMBER OF EVENTS
MAY 1976 – FEBRUARY 1985

Legend:
- —— all events
- — — 1.5<m<=2.2
- - - - - 2.2<m<=3.0
- —- — m>3.0
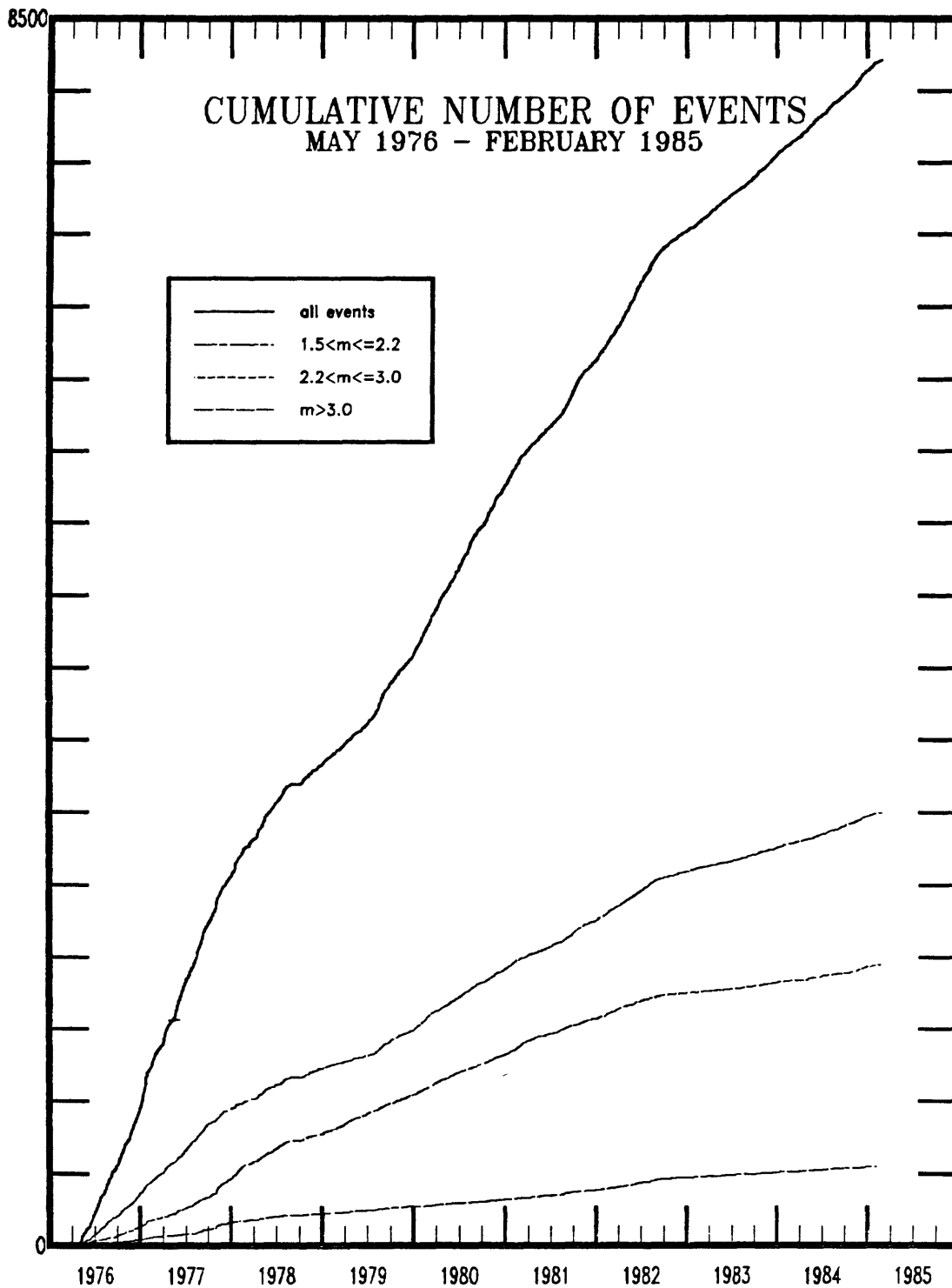
Figure 3: Plot of the cumulative occurrence of earthquakes as a function of time in the Adak region for the time period from May, 1976, through February, 1985. Vertical axis is number of events in intervals of 500. Horizontal axis is date in intervals of years. The four curves show the cumulative number of events within the specified magnitude ranges.

Regional Seismic Monitoring in Western Washington

14-08-0001-21861

R.S. Crosson and S.D. Malone
Geophysics Program
University of Washington
Seattle, WA 98195
(202) 543-8020

Investigations

Operation of the western Washington regional seismograph network and routine preliminary analysis of earthquakes in western Washington are carried out under this contract. Quarterly catalogs of seismic activity in Washington and Northern Oregon are funded jointly with other contracts. The time period for this summary is the six months from October 1, 1984 through March 31, 1985. Data are provided for USGS contract 14-08-0001-21862 as well as for other research programs. Network calibration and data assembly efforts are closely related to and overlap objectives under contract 21862, also summarized in this volume. Publications are listed in the 21862 summary.

Results

Network operation for stations in western Washington continued normally. No unusual regional earthquake activity was recorded and the Mt. St. Helens region remained generally quiet. A new station (MEW) sited on McNeil Island in the south part of Puget Sound began operation in early 1985, improving coverage of the central Puget Sound region. A nearby station on the Kitsap Peninsula near Port Gamble is presently being installed, and should further enhance the network. Network coverage in the northeast part of the Puget Sound basin will improve with the installation and reinstallation of stations in the Skagit Valley. The telemetry link for these stations is now available, and one station in the Skagit Valley, BLS, is operational but noisy. Signal quality should be improved by a planned telemetry re-routing. Station RMW was restored in November, 1984 after an outage of several months. Stations APW (vandalized in late 1984) and STW (destroyed by machinery in July, 1984) were repaired in March, 1985. Stations RVW, NLO, and HDW ceased operation during the winter and are scheduled for repair. Loss of several stations is typical in winter months, and stations are restored as good weather permits. A skeletal network of calibrated stations is being installed, to improve our ability to study earthquake spectra, source parameters and transmission characteristics.

To improve the consistency of magnitude estimation, we are using our new automatic picking program to determine coda lengths by fitting an exponential curve to a derived amplitude envelope of trace data. These coda lengths are being calibrated to Wood-Anderson amplitudes for a suite of events.

We are working to establish a uniform base of arrival time data. This effort includes reformatting 'pickfiles' of arrival times and relocating events using an updated velocity model and a revised location routine. Western Washington data from 1970 through 1983 have been processed and checked and eastern Washington data are partially processed.

Central California Network Operations

9930-01891

Wes Hall
Branch of Seismology
U.S. Geological Survey
345 Middlefield Road, Mail Stop 977
Menlo Park, California 94025
(415) 323-8111, Ext. 2509

Investigations

1. Maintenance and recording of 399 seismograph stations, located in Northern Calif., Central Calif. Recording 70 stations from other agencies. The area covered is from the Oregon border south to Santa Maria.

Results

1. Replaced 20 VCO's in Parkfield area with new J502's. The improved version has improved dynamic range (60db) and was designed to exhibit a temperature coefficient of less than ±50 PPM/oC (this is equivalent to ±2HZ per 1000 HZ/40oC).

2. Reduced the number of Develocorders from 10 to 5.

3. Questa Peak - Co-located a microwave site within a television facility at Questa Peak and Williams Hill. Install 6 ft. parabolic microwave antennas on each facility tower. Fabricated mounts and installed 10 Yaggi antennas on the facility towers to receive telemetry signals.

4. Mt. Tamalpais - Mission Peak - Installed a second 6 ft. parabolic antenna and modified the receiver for space diversity at Mission Peak. A 10 ft. addition to the Mt. Tamalpais antenna tower was completed to allow proper mounting of the Corp of Engineer parabolic antennas and to disperse Yaggi antennas for optimum reception of telemetry signals.

5. Cal Tech - Tuned all micro receivers and transmitters to their authorized frequencies. Installed the microwave receiver site within the seismic telemetry room. Installed a 28 ft. tower and mounted a 8 ft. parabolic antenna on the roof of Mudd Building.

6. Currently, the Northern and Central Calif. seismic network microwave system is carrying 23 phone lines (this equates to 171 signal channels).

Seismological Field Investigations

9950-01539
LANGER
Branch of Engineering Geology and Tectonics
U.S. Geological Survey
Box 25046, MS 966, Denver Federal Center
Denver, CO 80225
(303) 236-1593

Investigations

1. Guinea, West Africa, earthquake aftershock study—local investigation of aftershocks resulting from M_s = 6.2 earthquake of December 22, 1983.

2. Laramie Mountains, Wyoming, earthquake aftershock study — local investigation of aftershocks resulting from M_L = 5.5 earthquake of October 18, 1984.

3. Borah Peak, Idaho, earthquake aftershock study — local investigation of aftershocks resulting from M_s = 7.3 earthquake of October 18, 1983.

4. Western Argentina (Cancete) earthquake aftershock study — local investigation of aftershocks resulting from M_s = 7.4 earthquake of November 23, 1977.

Results

1. The investigation and interpretation of geologic and seismic field data obtained following the Guinea, West Africa, earthquake of December 22, 1983, has been completed. A somewhat "better" velocity model than that used in Langer and others (1985) reduced the hypocentral error statistics generated by HYPOELLIPSE (Lahr, 1979) but resulted in no significant changes in the aftershock locations or composite focal mechanism solutions. A final report is being prepared for publication in the BSSA.

2. The magnitude 5.5 (M_L) Laramie Mountains, Wyoming, earthquake of October 18, 1984, is possibly the largest documented earthquake to occur in the eastern Wyoming area during historical time. The felt region covered some 287,000 km^2 that extended into the neighboring states of Utah, Montana, South Dakota, Nebraska, and Colorado and also a part of Kansas (Stover, 1985). Although the shock was felt over a wide area, there were only minor structural damage effects to homes and businesses close to the epicenter. A focal mechanism solution for the main shock (D. W. Gordon and R. E. Needham, written commun., 1985) indicates that the predominant mode of faulting is strike-slip along near-vertical fault planes, i.e., dextral motion on a plane striking N. 69° E., or sinistral motion on a plane striking N. 26° W. The "T" axis strike is N. 23° E., plunge = 9°; the "P" axis strike is N. 71° W., plunge = 25°.

A 23-station portable seismic network (16 smoked-paper plus 7 digital systems) was installed around the epicentral area and recorded aftershocks for a period of 10 1/2 days (October 19-29). The field work was conducted with the assistance of personnel and equipment from the Geologic Services Branch, U.S. Bureau of Reclamation. Approximately 250 aftershocks were recorded, of which we have now located 49 events from data obtained by our best network configuration. Duration magnitudes range from 1.8 to 3.7 and for 35 of these events, the epicentral standard errors are

less than ±0.50 km; both the horizontal and vertical standard errors did not exceed ±1.0 km for all located aftershocks.

The epicentral locale for most of the aftershocks is within a 13 km^2 area. Depths extend from about 21.0 to 25.5 km with the deepest events occurring in the southern part of the aftershock zone. Focal mechanism solutions were determined for 45 of the 49 located aftershocks which indicate normal and strike-slip modes of faulting. In all cases, the location of the "T"-axes is near horizontal and they trend to the northeast at about the same angle as for the main shock (N. 23° E.).

Art Tarr has calculated moments and stress drops for most of the digitally recorded aftershocks. Although it is somewhat premature to report on his results, some stress drops appear to be very high (350 bars ±100). Systems calibrations are being verified before the final calculations can be made.

3. Following the October 28, 1983, Borah Peak earthquake, hypocenters for 402 aftershocks recorded from October 29 through November 19, 1983, were located with HYPOELLIPSE (Lahr, 1979). Locations were determined using P- and S-wave arrival times from our portable MEQ-800 network, as well as times provided through a cooperative effort with the University of Utah, Boise State University, Idaho National Engineering Laboratory, University of Washington, and Montana Bureau of Mines and Geology. Of the selected events, 374 are well-located (HYPOELLIPSE "A" or "B" quality), and have been studied in greater detail.

Locations of the events have been plotted and the relationship between surface rupture and faulting at depth has been examined. The epicenters are concentrated in two northwesterly-trending elongated clusters, separated by a gap of a few kilometers in which there appear to be no aftershocks. This gap is associated with the junction point in the surface rupture where the faulting has been diverted westward, away from its primary northwest trend.

Depth sections have been constructed separately for the northern and southern clusters. The southern events clearly define a plane dipping 45 to 55 degrees SW. The northern events are more diffused and cannot be explained by a single plane. It now appears that these aftershocks lie on two intersecting planes, one dipping about 45 degrees SW (an extension of the fault plane in the south) and another dipping about 45 degrees NE. These depth sections also indicate that the deeper events occur in the south in part of the aftershock zone.

Focal mechanisms have been determined for about 60 aftershocks. With the exception of five events, the focal mechanisms show a great deal of consistency: normal faulting with a strike of about 155 degrees, dip of 45 degrees, and a strike-slip component (left-lateral) 5-10 degrees away from pure dip-slip displacement. Of the five inconsistent events, four indicate primarily strike-slip faulting, and one event shows reverse faulting.

We plan to continue our investigation of the aftershocks, concentrating our efforts in the northern splay section. Very soon we expect to have 3-dimensional plots of our hypocenters (provided by NOAA), which should help to interpret the complexities in this area.

4. Aftershocks of the Western Argentina (Cancete) earthquake of November 23, 1977, are being reexamined. We think there is good evidence for conjugate faulting that can be verified by a more rigerous analysis of existing data.

References Cited

Lahr, J. C., 1979, HYPOELLIPSE -- a computer program for determining local earthquake hypocentral parameters, magnitude, and first-motion pattern: U.S. Geological Survey Open-File Report 79-431, 53 p.

Langer, C. J., Bonilla, M. G., and Bollinger, G. A., 1985, The Guinea, West Africa, earthquake of December 22, 1983 -- Reconnaissance geologic and seismologic field studies: U.S. Geological Survey Open-File Report 85-282, 33 p.

Stover, C. W., 1985, Preliminary isoseismal map and intensity distribution for the Laramie Mountains, Wyoming, earthquake of October 18, 1984: U.S. Geological Survey Open-File Report 85-137, 9 p.

Reports

Langer, C. J., Bonilla, M. G., and Bollinger, G. A., 1985, The Guinea, West Africa, earthquake of December 22, 1983 -- Reconnaissance geologic and seismologic field studies: U.S. Geological Survey Open-File Report 85-282, 33 p.

Langer, C. J., Bonilla, M. G., and Bollinger, G. A., 1985, Geologic and seismologic field studies following Guinea, West Africa, earthquake of December 22, 1983 abs. : Earthquake Notes, v. 55, p. 22.

Langer, C. J., Martin, R. A., and Wood, C. K., 1985, Preliminary results of the aftershock investigation of the October 18, 1984, Laramie Mountains, Wyoming, earthquake abs. : Earthquake Notes, v. 55, p. 24.

ALASKA SEISMIC STUDIES

9930-01162

John C. Lahr
Branch of Seismology
U. S. Geological Survey
345 Middlefield Road, MS 977
Menlo Park, California 94025
(415)323-8111, Ext. 2510

Investigations

1) Continued collection and analysis of data from the high-gain, short-period seismic network extending across southern Alaska from Juneau to Cook Inlet and inland across the Chugach Mountains.

2) With funding from the Division of Geological and Geophysical Surveys of the State of Alaska, continued operation of four seismic stations in the northern Prince William Sound region which experienced two magnitude 6 earthquakes during 1983.

3) Continued monitoring of the region around the proposed Bradley Lake hydroelectric project on the Kenai Peninsula, a cooperative effort with the Alaska Power Authority.

4) Cooperated with the Engineering Seismology and Geology Branch in operating 19 strong-motion accelerographs in southern Alaska, including 13 between Icy Bay and Cordova in the area of the Yakataga seismic gap. Fourteen accelerographs are connected to the high-gain station telemetry network so that absolute trigger times can be obtained.

Results

1) During the past six months preliminary hypocenters were determined for 1805 earthquakes that occurred between August 1984 and January 1985 (Figure 1). Fifteen of these events had magnitudes of 4 m_b and larger, and four were larger than 5 m_b. The two largest shocks both had magnitudes of 5.7 m_b and had significant aftershock sequences. One shock occurred on August 14 along the Castle Mountain fault about 80 km NE of Anchorage (see below), and the second occurred on January 9 at a depth of about 15 km near the U.S.-Canada border north of Icy Bay within the aftershock zone of the 1979 St. Elias earthquake (7.1 M_s). The largest aftershock of the January 9 earthquake was a magnitude 3.9 M_L shock that occurred about 2-1/2 minutes after the mainshock. Eleven aftershocks with coda-duration magnitudes of 2 or larger occurred by the end of January, nine within the first day following the mainshock. On September 20, two shocks with magnitudes of 5.4 and 5.1 m_b and nearly identical epicenters occurred about 11 minutes apart at shallow depth southeast of Hinchinbrook Island. The pair of events did not have a detectable aftershock sequence, but in the surrounding offshore region it is not unusual for double or single events shocks of comparable magnitude to occur without significant aftershock activity. In and around the Yakataga seismic gap the pattern of microearthquake activity was similar to that

observed over the past several years.

2) Detailed investigation of the location of the August 14, 1984 Sutton mainshock (5.7 m_b, 5.2 M_s) and its aftershocks has continued. Aftershocks recorded by two stations installed in September have been used to refine the crustal velocity model and develop station corrections. The mainshock and 49 well-recorded aftershocks were located using arrivals from only the nearest seven stations. The resulting locations are more tightly clustered and have considerably less scatter in depth than solutions using all available data. The aftershocks range in depth from 12 to 20 km and define a steep, NW-dipping plane; the mainshock is located at 20 km depth.

Shallow seismicity that occurred in the vicinity of the Castle Mountain fault from the installation of the USGS network in 1971 to the time of the Sutton earthquake has been reviewed in the context of the Sutton aftershock pattern. A few events located less than about 5 km north of the mapped fault trace are now interpreted as having occurred on the fault. This fault-related activity includes a swarm of events in 1980 near the southwest end of the Sutton aftershock zone. The most prominent feature in the seismicity, however, is a number of earthquake concentrations 5 to 20 km north of the mapped fault trace that are attributed to faulting within the Talkeetna Mountains.

The new seismic evidence for activity of the Talkeetna segment of the Castle Mountain fault, together with unequivocal geologic evidence of Holocene activity on the Susitna segment, suggest that at least 130 km of the Castle Mountain fault should be considered as active for the purposes of hazard evaluation.

3) During the period July-December 1984, the level of shallow (depth less than 20 km) seismicity near Bradley Lake on the southern Kenai Peninsula was comparable to that observed during the previous six-month period. Seven events with S-P time intervals in the range 1.5 to 3.0 seconds were detected at the station BRLK, about 2 km northwest of the lake. These events all had magnitudes less than 1 and were too small to be located by the regional network because all but one of the seismographs in the local array were removed in June 1984.

4) Development work on the ELOG (remote earthquake detection and logging instrument) has continued. Based on the results of a deployment in 1984, a new algorithm which reduces false triggers and increases pick accuracy has been developed and incorporated into the software. Four new units were built and tested for deployment in Alaska in 1985. A solid-state mass storage device (RAM cassette, 128k) prototype was designed and built; it will be tested this summer in Alaska.

A prototype for an analog telemetry interface (ATI) was built and tested in the laboratory and will be deployed in Alaska for testing this summer. These units will be installed at telephone exchanges where signals are multiplexed. The ATI will incorporate many new features, such as periodically sending test tones to verify correct phone operation, sending information on the squelch status of radio receivers, a built-in digital meter giving signal level in db's, and translation from one center frequency to another.

5) Liu (1984) has suggested that the decay in the rate of earthquake occurrence with time after a large shock is a useful diagnostic, in the context of earthquake prediction, for identifying an earthquake sequence as either a foreshock or an aftershock sequence. A critical analysis of this paper has found Liu's contention not to be adequately supported by the data presented in the paper. An error in his graphical method of quantifying the decay rate of seismicity in an earthquake sequence introduces an unknown systematic bias in the reported decay rates. Furthermore, ambient background seismicity, if not recognized, can cause the decay rate of aftershocks to be underestimated. A rigorous statistical re-analysis of Liu's data is required to determine whether the apparent difference in decay rates for foreshock and aftershock sequences is real or an artifact of Liu's method.

References cited

Liu, Z. R., 1984, Earthquake frequency and predition, Seismological Society of America Bulletin, v. 74, p. 255-265.

Reports

Lahr, J. C., Page, R. A., Fogleman, K. A., and Miller, T. P., 1985, The 1984 Sutton earthquake: new evidence for activity of the Castle Mountain fault [abs.], Earthquake Notes, Eastern Section, Seismological Society of America, v. 55, p. 23.

Page, R. A., 1985, Earthquake frequency and prediction - a critical examination, Earthquake Notes, Eastern Section, Seismological Society of America, v. 55, p. 16.
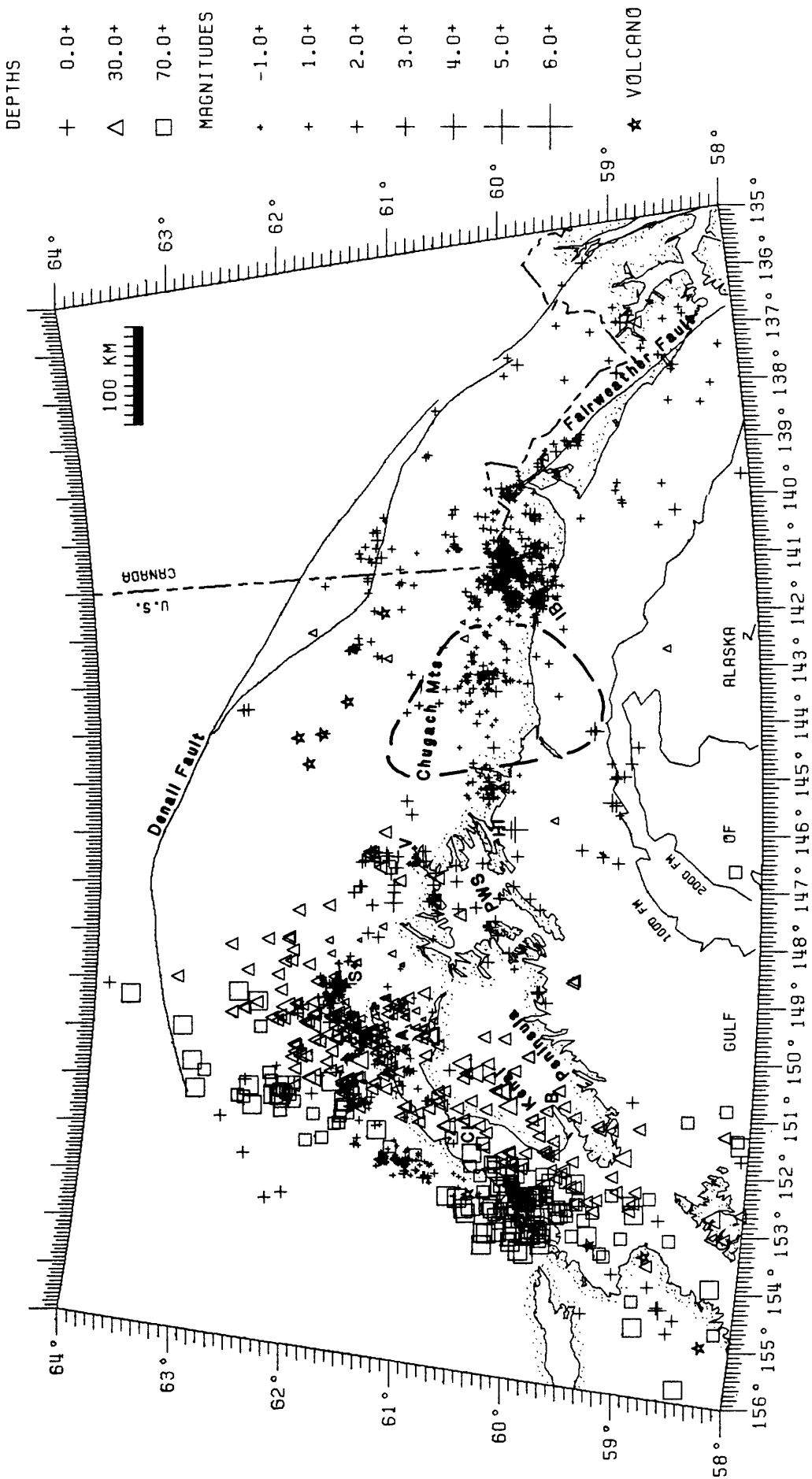
Figure 1. Earthquakes located by the USGS southern Alaska seismograph network during August 1984 – January 1985. Epicenters of 1805 events are plotted. Magnitudes are determined from coda-duration or maximum amplitude, and for events of magnitude 3 and larger can be as much as one unit smaller than the teleseismic m_b magnitude. The lowest magnitude level to which data is processed varies across the mapped area due to uneven station distribution and to criteria used to select earthquakes for processing. Heavy dashed contour indicates inferred extent of Yakataga seismic gap. Abbreviations are: A – Anchorage, B – Bradley Lake, CI – Cook Inlet, HI – Hinchinbrook Island, IB – Icy Bay, PWS – Prince William Sound, S – Sutton, V – Valdez. A few earthquakes near Anchorage have been masked for clarity.

23

Northern and Central California Seismic Network Processing

9930-01160

Fredrick W. Lester
Branch of Seismology
U.S. Geological Survey
345 Middlefeld Road M/S 977
Menlo Park, California 94025
(415) 323-8111, ext. 2149

Investigations

1. Signals from 429 stations of the multipurpose Northern and Central California Seismic Network (Calnet) are telemetered continuously to the central laboratory facility in Menlo Park. They are supplemented with signals from up to 50 stations from other institutions. The data are recorded, reduced, and analyzed to determine the origin times, magnitudes, and hypocenters of the earthquakes that occur in or near the network. Data on these events are presented in the forms of lists, computer tape and mass data files, and maps to summarize the seismic history of the region and to provide basic data for further research in seismicity, earthquake hazards, and earthquake mechanics and prediction. A magnetic tape library of "dubbed" unprocessed analog tape records of the network for significant local earthquakes and teleseisms is maintained to facilitate futher detailed studies of crust and upper mantle structure and physical properties, and of the mechanics of earthquak sources.

2. Quarterly reports were prepared on seismic activity around Lake Shasta, Warm Springs Dam, the Auburn Dam site and Melones Dam for the appropriate funding agencies. Quarterly reports on seismic activity in the Mount Shasta area and in Lassen Volcanic National Park were also prepared and distributed to interested agencies and individuals.

Results

1. Figure 1 shows the seismic activity of Northern and Central California for the period October 1, through March 31, 1985. The 10854 earthquakes plotted are all reliable locations using 4 or more phase readings in the solution. The phase readings were obtained either by hand timing, or by the automatic Real Time Picker (RTP), or by the Caltech-USGS Seismic Processing System (CUSP), or they are a combination of all sources. The data have been screened for blasts and those found have been eliminated. Identification of quarries in the Sierra Nevada Foothills is a constant problem so that all quarry data have not yet been eliminated from the catalog. We feel that the catalog of location data maintained by Calnet is complete for earthquakes magnitude 1.5 and larger.

Currently all data are processed through the CUSP system and are available from the CUSP data base, including the digitial seismograms. Events that are detected on Develocorder films or by the RTP that are not detected by CUSP are added to the data base as quickly as time permits. This is being accomplished by digitizing the earthquakes from the analog

magnetic tapes on another computer. These digital data are then input into the CUSP system and processed to completion using standard CUSP timing and analysis techniques. Any events missed by CUSP and not available for digitizing from the magnetic tapes are processed by hand from Develocorder films and the final location and phase data are added to the data base. These hand processed events are the only ones for which there are no digital seismograms in the data base. At the present time less than 10 percent of the earthquakes located go undetected by CUSP, and in the past six months only one event was timed by hand.

2. Final processing of data for the first half of calendar year 1978 is complete and those data will be published this month. Work is currently underway on the final processing of the 1984 data. It is expected that those data will be published by June or July 1985.

Reports

Berg, P. A., and Walter, Stephen, R., 1984, Upper crustal structure of the Lassen Peak area, northern California, from seismicity and refraction data (abs.) submitted to the AGU fall meeting.

NORTHERN AND CENTRAL CALIFORNIA SEISMICITY
OCTOBER 1984 - MARCH 1985

MAGNITUDE   SYMBOL

5.0 TO 6.0-   ⬡

4.0 TO 5.0-   ⬡

3.0 TO 4.0-   ○

2.0 TO 3.0-   ○
LESS THAN 2.0   ·

100 KILOMETERS
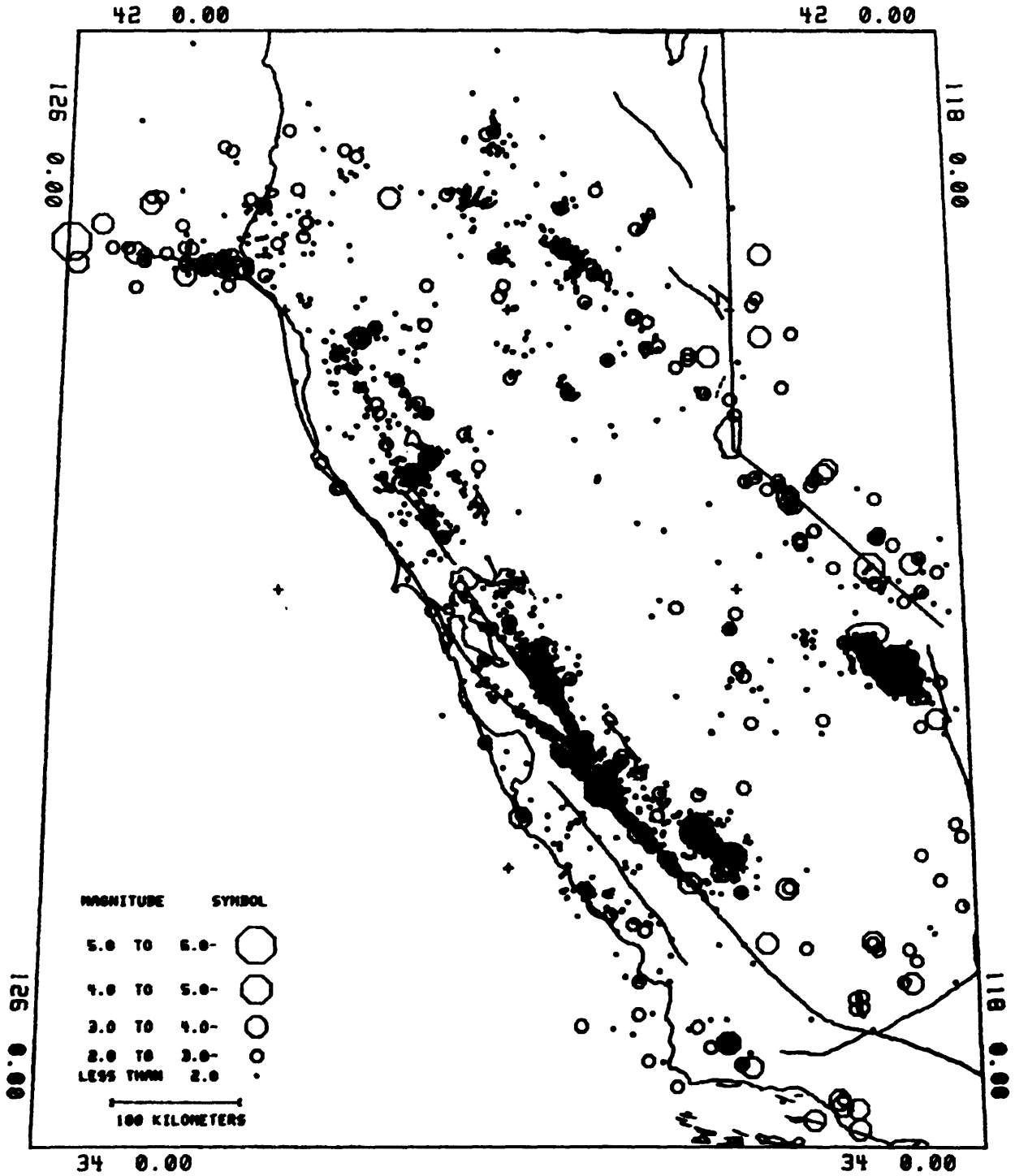
FIGURE 1

WESTERN GREAT BASIN-EASTERN SIERRA NEVADA SEISMIC NETWORK

Contract 14-08-0001-21867

A.S. Ryall, W.F. Nicks, and E.J. Corbett
Seismological Laboratory
University of Nevada
Reno, NV 89557
(702) 784-4975

Investigations

This program supports continued operation of a seismographic network in the western Great Basin of Nevada and eastern California, with the purpose of recording and location of earthquakes occurring in the western Great Basin; and acquiring a data base of phase times and analog and digital seismograms from these earthquakes. These data are used for research on: (1) ongoing seismicity in the western Great Basin with emphasis on the Long Valley caldera; (2) source mechanisms studies of these earthquakes; (3) possible precursory seismicity patterns in the White Mountains gap; (4) seismicity near reservoirs in the Lake Tahoe region; and (5) evaluation of the contribution that high-quality digital broad-band seismic stations can make to regional network-seismic studies.

Results

A. *Seismic Network Operation*

As is typical during the winter months, relatively few changes have been made to our telemetered network. During the contract period, two new stations have been installed: DLH and DSX. DLH is a 3-component short-period (8 Hz) station located at the bottom of a 1,000-foot deep drill hole situated in the northern Long Valley Caldera. The station was originally installed by Sandia National Laboratory for research they did last summer and recording has been taken over by University of Nevada at their request. DSX was installed in Dixie Valley, Nevada, primarily to monitor sonic booms generated at the U.S. Navy's supersonic training facility. Two stations have been removed: ANT and ADH; both located about 25 km NE of the Long Valley Caldera. Of of the 3 "temporary" stations installed in the Sierra Nevada wilderness south of Mammoth Lakes, 2 have unexpectedly managed to survive the winter. HOP succumbed to the snows in January, but PRB and STR are still operating as of April 30. This is most fortunate because these stations have been instrumental in recording aftershocks of the November 23 Round Valley earthquake. In summary, the University of Nevada is now operating 55 short-period analog seismographic stations, four of which are multi-component. In addition we are recording signals from 11 USGS stations, 2 U.C. Berkeley stations, and 1 from the California Division of Water Resources. All 69 of these stations are being recorded on analog magnetic tape at Reno as well as digitally by our on-line system.

In addition to the analog stations, the University of Nevada operates 3 remote digital seismographic stations. The digital stations provide broad-band (0.05-30 Hz), wide dynamic-range (96 dB) digitization of signals from a 3-component set of seismometers, and telemeter the data to the Reno facility where it is continuously recorded. The data is currently being recorded at 25 samples per second, but we are in the process of upgrading the system to 50 sps. In addition, the vertical components of these stations are also being recorded on our on-line recording system. The three stations are now operating

in mine tunnels at Mina, Bodie, and Washoe Lake (MNA, BDE, and WCN). A fourth station is planned for the Las Vegas area in the near future, but its installation has been delayed due the fact that the most desirable sites are in Bighorn sheep wilderness areas, which require an involved permitting process.

We are in the process of acquiring a microwave system to replace some of our major VHF radio links. Although the initial investment is substantial, the savings in telephone line costs will offset the expense in about 2 years. The principal advantages of the microwave system are increased reliability, especially during the winter months, less susceptibility to nearby lightning ground strikes, reduced radio interference, and a substantial increase in the number of signals we can transmit.

B. *On-line System*

A computer-based earthquake recording system has been operating successfully since May 1984. It provides on-line event detection and digitization of the analog seismic signals transmitted to the Reno data facility. This system facilitates analysis of large numbers of earthquakes and will allow waveform analysis of the network data. The triggering algorithm has been tuned sufficiently so that false triggers are now reduced to about 10%. We are still plagued by noise triggers during lightning storms, due to our dependence on VHF radio telemetry, but we expect this problem to be alleviated by the installation of the microwave system. We are currently recording 80 seismic signals and 4 time signals on the 96-channel on-line system. For the period May 11, 1984 to April 30, 1985, we have recorded and archived digital seismograms for 6129 seismic events. Of this number 3544 (58%) are local earthquakes that we have located and cataloged. The remainder of the data are teleseisms, regional events, nuclear tests, and local events of less than 10 seconds duration, (roughly magnitude < 1.5 M_L), for which we save the traces but do not time the arrivals.

C. *Data Analysis*

Our earthquake data have been timed and located through April 30, 1985. This is with the exception of some data gaps that exist between November 23 and December 31, 1984. These gaps resulted from our analysis staff being swamped by the large number of aftershocks following the magnitude 6 earthquake at Round Valley, and are being filled as time permits. Since the beginning of the contract period on November 1, 1984, the University of Nevada Seismological Laboratory registered 1,468 earthquakes. Of these events:

552 were magnitude 2 or greater;
70 were magnitude 3 or greater;
14 were magnitude 4 or greater;
3 were magnitude 5 or greater;
1 was magnitude 6 or greater.

As the figure shows, most of the activity since the first of the year is continuing aftershocks of the November 23, 1984 Round Valley earthquake. In addition, a high level of seismic activity continues in the mountain block south of the Long Valley Caldera.

△MGN

△LMC
△DHL

△DMP

△BEN

△BCK

△MLK

△CHS

△DOE

△ORC

△MMP

△HL

△CC

△CAS

△MLN

△LLK

△K

△MC

△C

△RSM

△CWC

△PRB

△RCC

△HOP

△STR

△BHP

△POC

△SCH

0   10   20   km
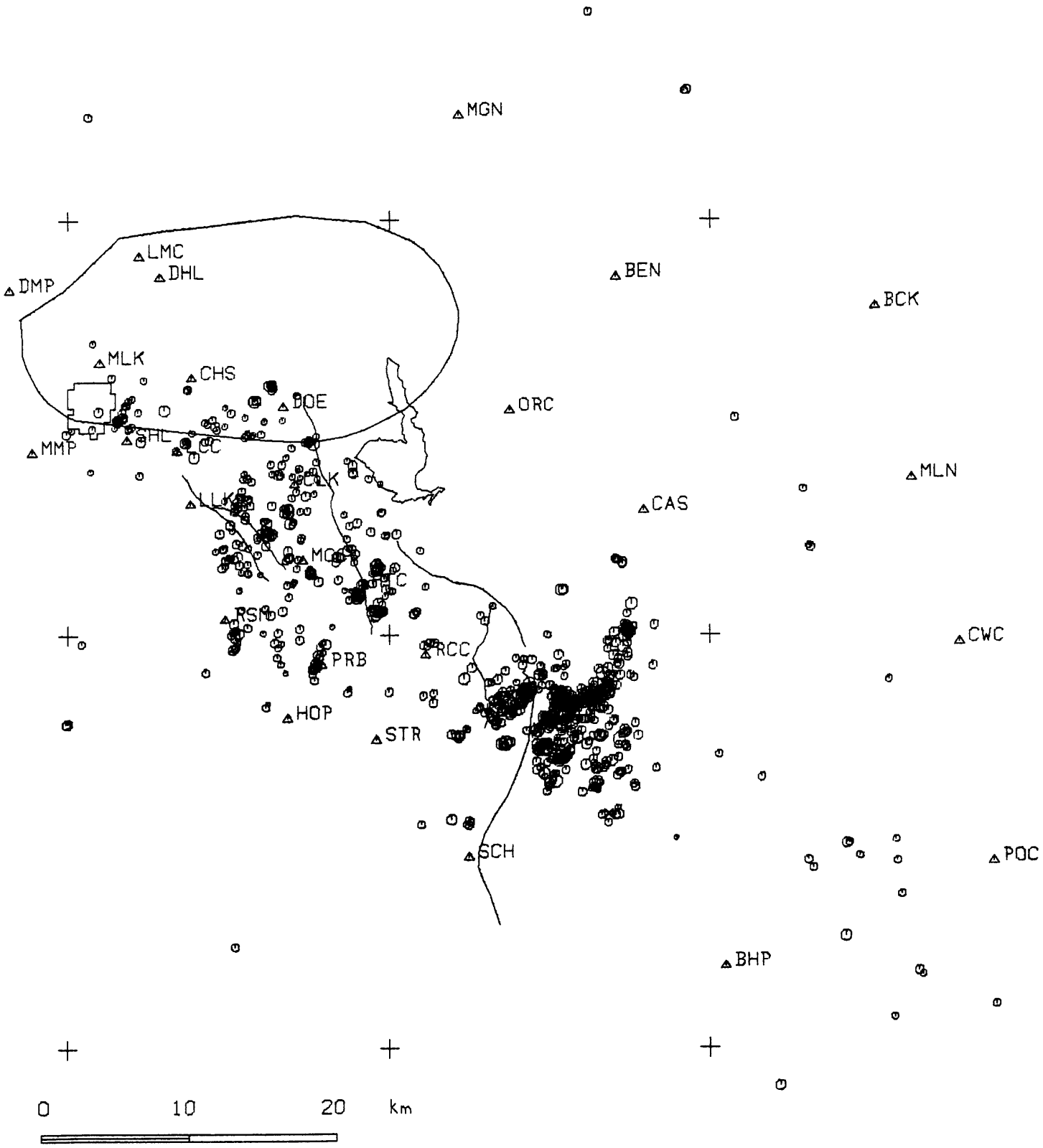
magnitude

○   ⊙   ⊙   ⊙   ×

2   3   4   5   nm

Mammoth Seismicity -- Jan-April 1985

Consolidated Digital Recording and Analysis

9930-03412

Sam W. Stewart
Branch of Seismology
U.S. Geological Survey
345 Middlefield Road, Mail Stop 977
Menlo Park, California 94025
(415) 323-8111, Ext 2577

Investigations

The goal is to operate, on a routine and reliable basis, a computer-automated system that will detect and process earthquakes occurring within the USGS Central California Earthquake Network (also known as CALNET). Presently, the output from more than 450 short-period seismic stations is telemetered to a central recording point in Menlo Park, California. Two DEC PDP 11/44 computers, and a VAX/750, are used on this project. The 11/44A is dedicated to the task of online, realtime detection of earthquakes and storing the waveforms for later analysis. The 11/44B is used for offline processing and archiving of earthquakes. Both computers have a 512 channel analog-to-digital converter, so the 11/44B can serve as backup to the online system whenever necessary. The two computers can communicate with each other via a simple digital-bit I/O "semaphore" system, and can transfer large amounts of data via a dual-ported disk subsystem or a dual-ported magnetic tape subsystem. The VAX/750 is a general purpose computer used by the Branch of Seismology. We use it as the primary "research" computer for the CUSP system. It holds the primary data base of the earthquake summary data and phase card data, which is available for research purposes. We update and maintain the CALNET data on this computer.

Both 11/44 computers use the RSX11M-PLUS (v2.1) operating system. The VAX/750 uses the DEC VMS operating system. Software has been developed largely by Carl Johnson in Pasadena, but with considerable modification by Peter Johnson, Bob Dollar and Sam Stewart, to meet Menlo Park's specific needs. Our applications are all written in Fortran-77, but with heavy use of system functions unique to the RSX or VMS operating systems.

Results

1. During the period October 1984 through March 1985 approximately 11,429 events were processed through the CUSP system. This includes 9419 events that were classified as 'LOCAL' events, i.e., they occurred within or near enough to the network that hypocenters were calculated and the data entered into the catalogs. The remaining 2010 events were either regional or teleseismic events, or unprocessed copies of local events that were too small (M1 < 1.0) to be timed, or copies of very large events that had to be 'split' in order to be accommodated by the 11/44 hardware limitations. In addition, a few

thousand non-seismic, noise events detected by the online 11/44A computer had to be examined and deleted. Considering only the seismic events, this projects to an annual rate of processing about 23,000 events per year.

2. A second interactive processing station (Tektronix 4014 graphics terminal) was added to the offline 11/44B. (It can also be switched to the Seismology VAX/750.) This greatly increases our flexibility in scheduling analyst's time, as well as increasing thruput and providing backup capability.

3. The final processing steps, and online CUSP database itself, were moved from the 11/44B to the VAX/750. The necessary program conversion was done mainly by Carl Johnson in Pasadena, while Peter Johnson made the necessary mods for Menlo Park. This gives the research staff more convenient access to the CUSP data, and to the necessary programs to analyze the data.

4. Several types of MERGE operations have to be done with data on the VAX/750. The RTP data need to be merged with the equivalent CUSP events, into one CUSP event file. Data digitized by the Eclipse system, and processed on the 11/44B, need to be merged with the equivalent CUSP event, both the phase data and the digitized seismograms. By the end of this report period these operations were just getting started.

5. Conversion of the seismic telemetry systems from leased telephone lines to our own microwave transmission system was started (by other projects, not this one). As conversion proceeded, dropouts, or fading, in the microwave signals produced many, very long and extensive noise triggers in the online detection system. The problem was quite serious, but is being attacked vigorously and seems better now. In order to control the problem, we have had to increase our detection thresholds throughout most of the network. This will result in some, small events being missed. If these missed events are seen on the Develocorder scan films, or the Helicorder records, then they can be digitized from the telemetry tapes on the Eclipse system, and entered into the CUSP system via Eclipse 800 bpi digital tapes.

Reports

None.

Seismic Monitoring of the Shumagin Seismic Gap, Alaska

USGS 14-08-0001-21919

John Taber and Klaus H. Jacob
Lamont-Doherty Geological Observatory of Columbia University
Palisades, New York 10964
(914) 359-2900

Investigations

Seismic data from the Shumagin seismic network were processed to obtain origin times, hypocenters, and magnitudes for local and regional events. The processing resulted in files of hypocenter solutions and phase data, and archive tapes of digital data. These files are used for the analysis of possible earthquake precursors, seismic hazard evaluation, and studies of regional tectonics and volcanicity (see Analysis Report, this volume). A published bulletin for 1984 will be available in spring 1985.

Results

The seismicity of the Shumagin Islands region from January 1 to December 30, 1984 is shown in map view in Figure 1 and in cross section in Figure 2. The overall pattern over this time period is similar to the long term seismicity, though the double-planed seismic zone is only weakly determined. The highest concentration of events occurs at the base of the shallow thrust zone with the thrust zone itself poorly defined. West of the network the seismicity is more diffuse and extends closer to the trench.

A shallow (less than 10 km) earthquake swarm began in August, 1984 under Mt. Dutton, an extinct volcano of uncertain age near 55.25, 162.25. This was the largest swarm we have recorded on the peninsula since the network was installed in 1973. There were 35 events located between 8-20-84 and 12-30-84 with at least 20 additional smaller events near the beginning of the swarm. Occasional events have continued into March, 1985. The biggest event in the swarm was $Ml=2.9$ with most magnitudes measuring below 1.5. Though the number and size of events is still very small, renewal of volcanic activity can't be ruled out.

The network is capable of digitally recording and locating events as small as $Ml=0.4$ with uniform coverage at the 2.0 level. Onscale recording is possible to at least $Ml=5.0$ on a telemetered 3 component force-balance accelerometer. Larger events are recorded by one digitally recording acelerometer and on photographic film by 12 strong-motion accelerometers.
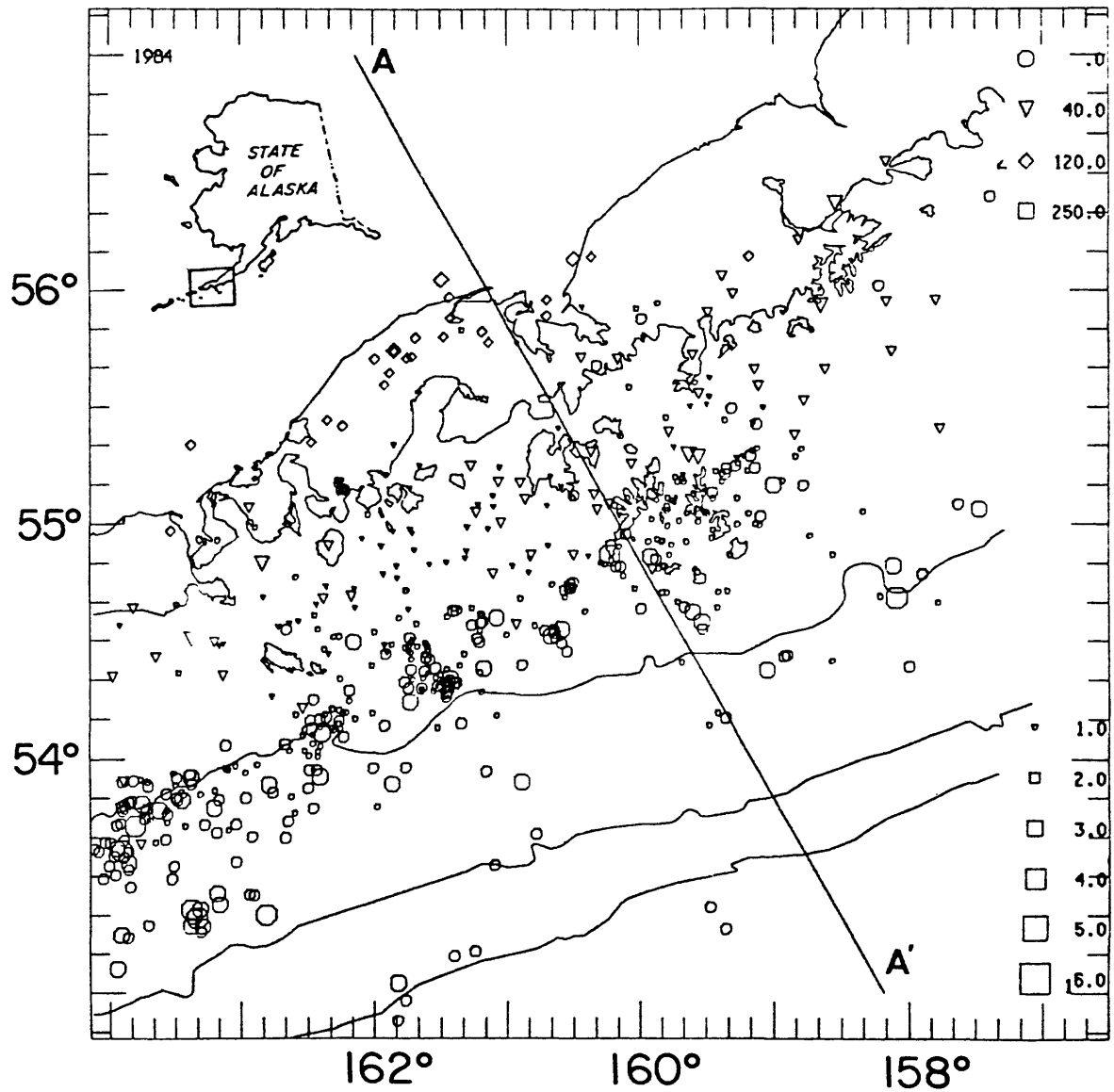
Figure 1. Seismicity recorded by the Shumagin Island seismic network from January 1 to December 30, 1984. Depth is shown by symbol type and magnitude by symbol size.
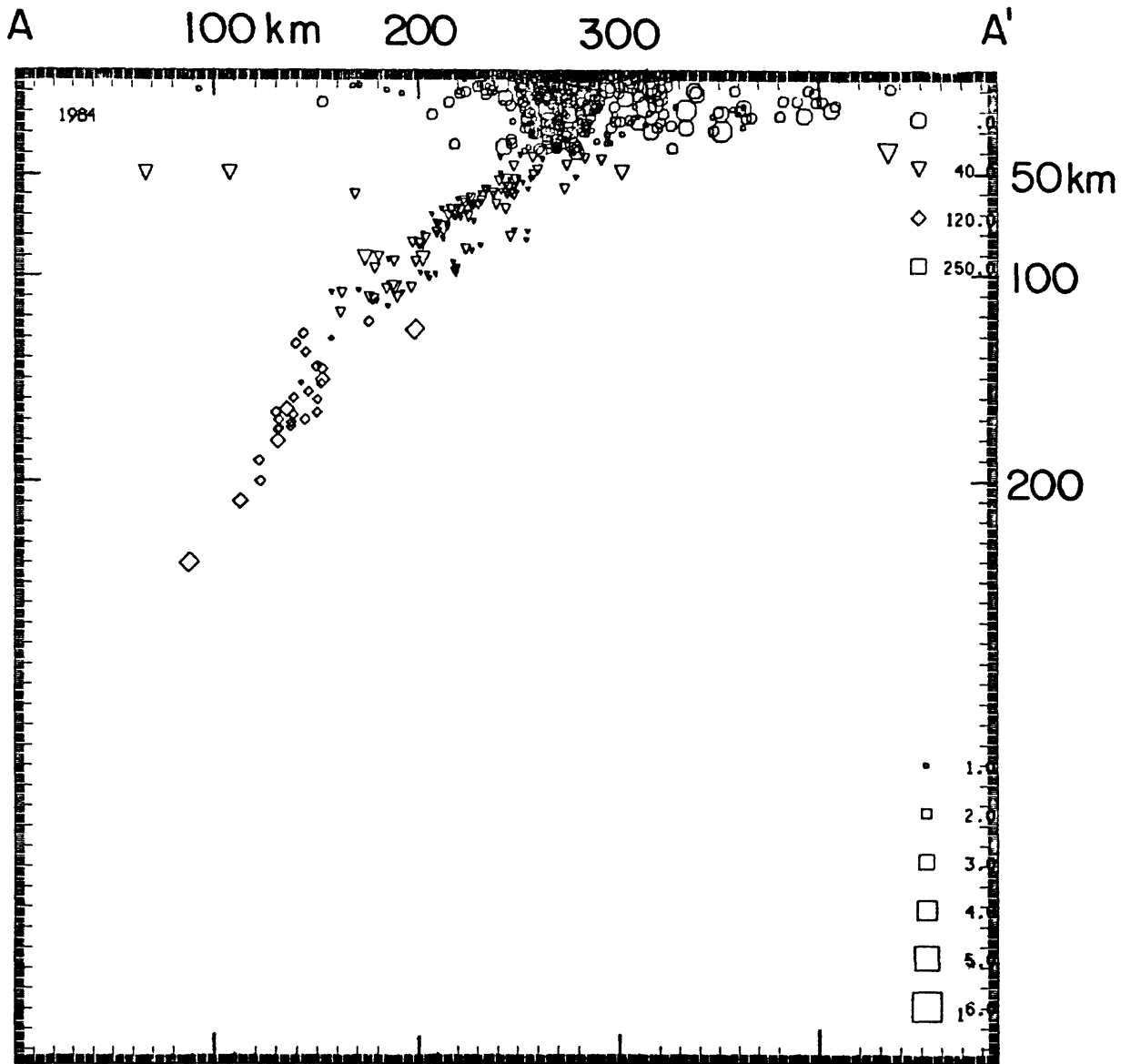
Figure 2. Cross section of seismicity projected along the line A-A' in
Figure 1. Symbols are the same as in Figure 1.

Earthquake Hazard Research in the Greater Los Angeles Basin
and Its Offshore Area

#14-08-0001-21858

Ta-liang Teng
Thomas L. Henyey
Egill Hauksson

Center for Earth Sciences
University of Southern California
Los Angeles, CA 90089-0741
(213) 743-6124

INVESTIGATIONS

(1) Monitor earthquake activity in the Los Angeles Basin and the adjacent offshore area.

(2) Analyze data from a swarm of small earthquakes that occurred in the Santa Barbara Channel during 20-25 April 1984. The swarm that consisted of at least 400 earthquakes in the magnitude range from 0.5 to 4.0 was located approximately 20 km southeast of the City of Santa Barbara.

RESULTS

(1) The earthquake activity that occurred in the Los Angeles Basin and the adjacent offshore area during 1984 is shown in Figure 1. The seismicity rate during 1984 is similar to the rate that was recorded during the previous three years. The earthquake activity is characterized by single shocks that are scattered throughout the Los Angeles Basin. A significant trend of seismicity is observed offshore, extending from Malibu in the north to the San Pedro channel in the south. This trend is subparallel to the Newport-Inglewood fault as well as the Palos Verdes fault. A cluster of earthquakes is observed to the south of the Wilmington oil field in Long Beach. Many of the small events that occurred along the northern section of the Newport-Inglewood were felt locally.

(2) The Santa Barbara Channel Easter swarm was strongly clustered in both space and time. The epicentral distribution of this earthquake activity that consists of more than 300 located earthquakes is shown in Figure 2. Most of the earthquake activity is located within a 4 km by 10 km area, a few kilometers to the south of our Ocean Bottom Seismometer, DCG. The Union Platform C is situated 5 km to the north of the station DCG, approximately in the middle of the Ocean Bottom Seismometer Network. The stations, DCG and DCF made it possible to determine the hypocentral depths for these events. Nearly all of the earthquakes occurred in the depth range between 10-17 km.

One of the characteristics of this swarm is very strong temporal clustering. During the previous week only two earthquakes were reported in the vicinity of the epicentral area of the swarm. The activity peaked on April 22, but the four largest events of magnitude (3.8, 3.8, 4.0 and 3.9) in this sequence occurred on April 21 22h and 23h; April 22 05h and 23h, respectively.

Over 300 earthquakes in the swarm were recorded digitally by the PDP 11/34 computer that is now dedicated to record the U.S.C.-southern California Coastal Zone Network. These data that are currently being analyzed will not only permit us to determine accurate hypocentral parameters but also source parameters such as seismic moment, stress drops and source radius. In addition, crosscorrelation of the digital waveforms from the Ocean Bottom Seismometers may provide more accurate relative hypocentral locations than available previously.

REPORTS

Hauksson, E. and G. Saldivar, Recent seismicity (1970-1984) along the Newport-Inglewood fault, Los Angeles Basin, southern California, EOS, vol. 65, no. 45, p. 996, 1984.

Hauksson, E., T. L. Teng, T. L. Henyey, J. K. McRaney, L. Hsu and G. Saldivar, Earthquake Hazard Research in the Los Angeles Basin and its Offshore Area, U.S.C. Geophysics Laboratory Technical Report #85-1, 1985.

Hauksson, E., T. L. Teng and J. McRaney, The Santa Barbara Channel Easter Swarm of April 1984, USGS Semi-Annual Data Review Meeting in Santa Barbara, California, September, 1984.

LOS ANGELES BASIN EARTHQUAKES
1984 PRELIMINARY EARTHQUAKE LOCATIONS
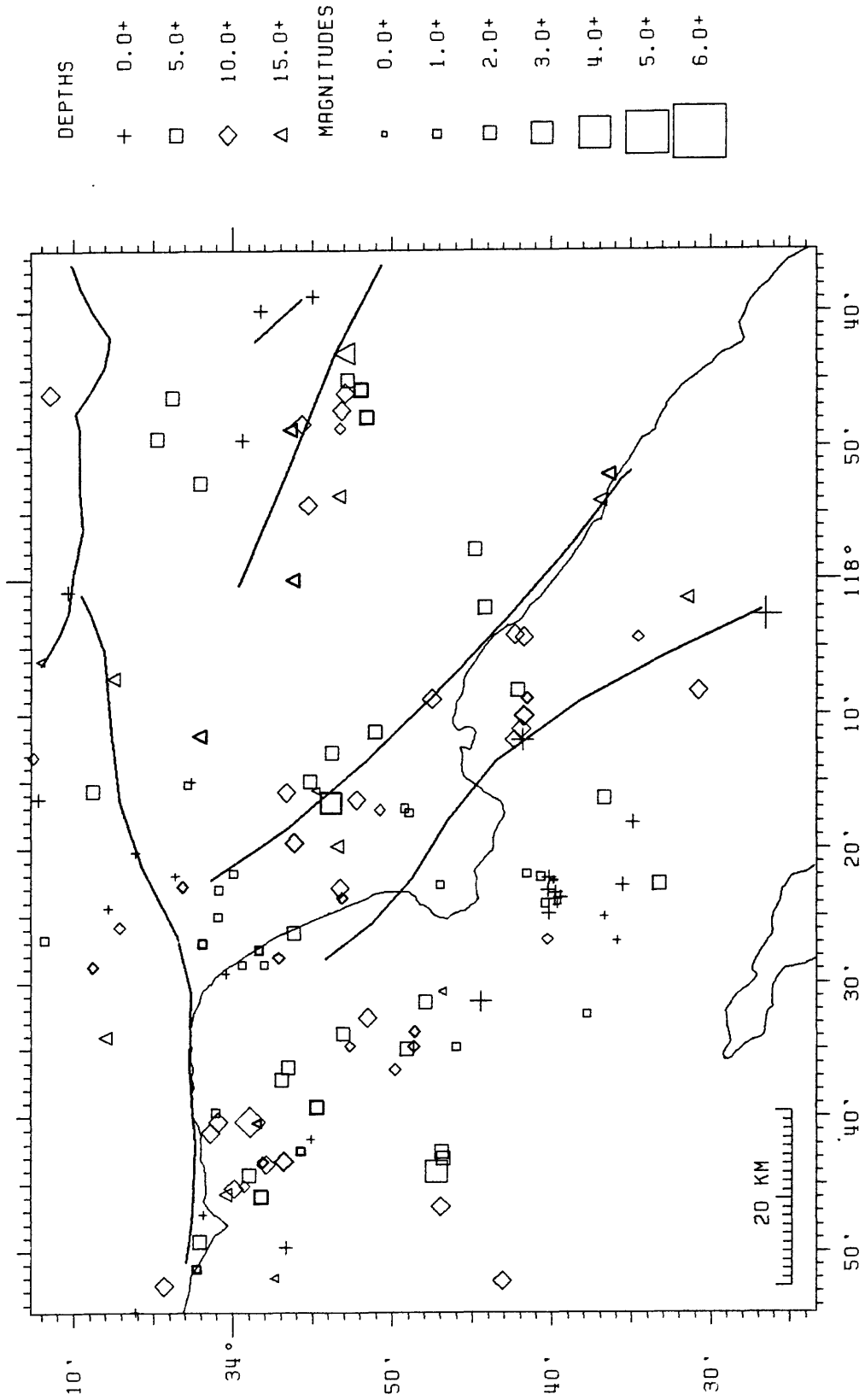
Figure 1. Los Angeles Basin seismicity 1984 recorded by the U.S.C. Seismic Network.

SANTA BARBARA CHANNEL EARTHQUAKES

1984 PRELIMINARY EARTHQUAKE LOCATIONS
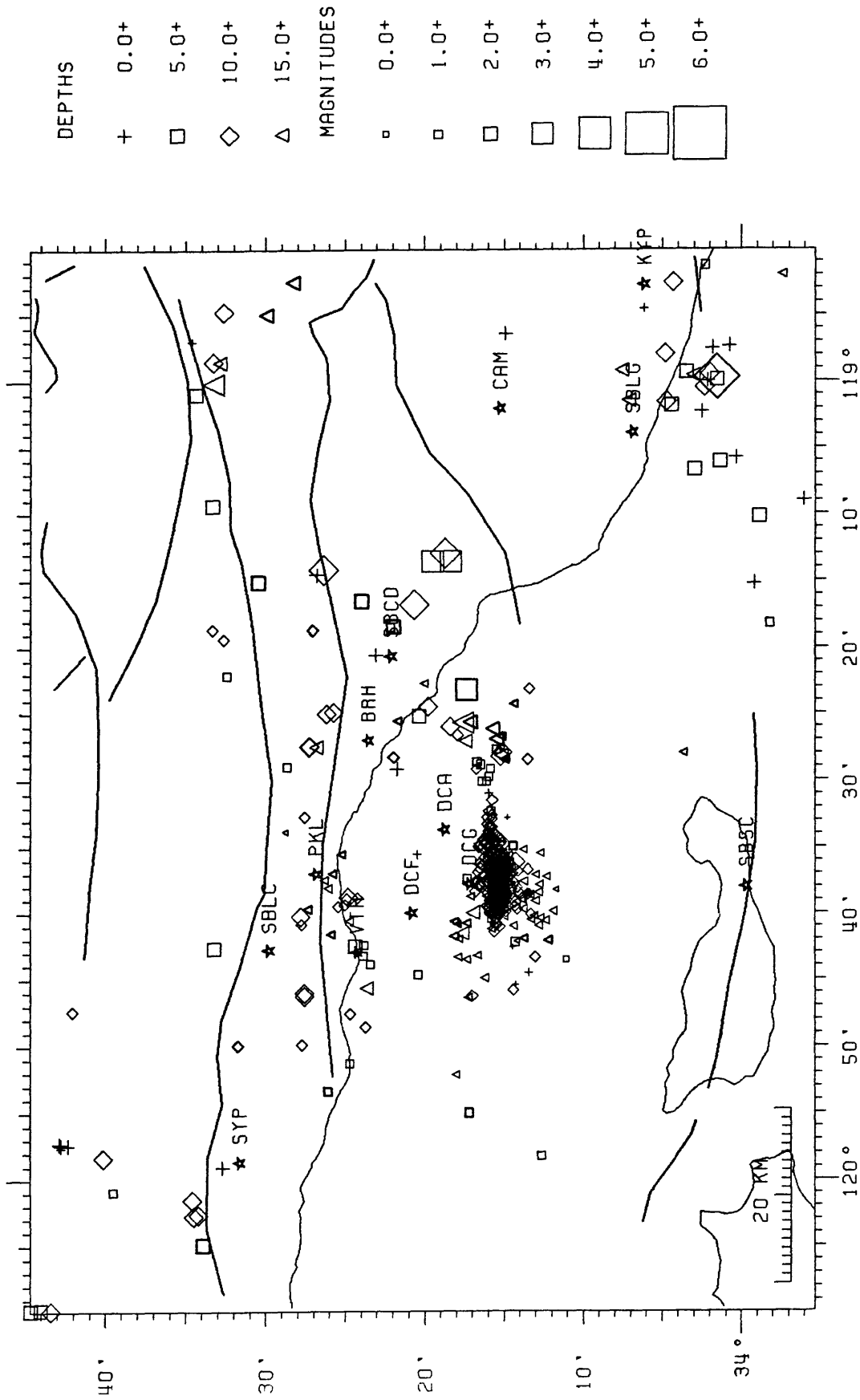
Figure 2. Santa Barbara Channel seismicity 1984 recorded by the U.S.C. Ocean Bottom and Land Seismic Network. The cluster of earthquakes near DCG is the April 1984 swarm of over 300 earthquakes.

Field Experiment Operations

9930-01170

John Van Schaack
Branch of Seismology
U. S. Geological Survey
345 Middlefield Road MS-977
Menlo Park, California 94025
(415) 323-8111, ext. 2584

Investigations

This project performs a broad range of management, maintenance, field operation, and record keeping tasks in support of seismology and tectonophysics networks and field experiments. Seismic field systems that it maintains in a state of readiness and deploiys and operates in the field (in cooperation with user projects) include:

a. 5-day recorder portable seismic systems.
b. "Cassette" seismic refraction systems.
c. Portable digital event recorders.
d. Smoked paper recorder portable seismic systems

This project is responsible for obtaining the required permits from private landowners and public agencies for installation and operation of network sensors and for the conduct of a variety of field experiments including seismic refraction profiling, aftershock recording, teleseism P-delay studies, volcano monitoring, etc.

This project also has the responssibility for managing all radio telemetry frequency authorizations for the Office of Earthquakes, Volcanoes, and Engineering and its contractors.

Results

Seismic Refraction
One hundred twenty seismic cassette recorders were used in 2 separate experiments to gather deep crustal velocity and structural data. Record sections were produced and preliminary analysis was done in the field for the first experiment. These 2 experiments were:
1. Maine; Eight deployments were completed consisting of approximately 1,000 Km. of profiles with about 45 shots being fired
2. Nevada; Three deployments were completed consisting of 360 total recording sites along 120 Km. of profile. More than 30 shots were fired.

Telemetry Networks
A number of modifications have been made to the Central California Seismic Network telemetry system to reduce telemetry costs. Approximately 100 stations are being carried on the microwave network.

This network has been installed between Mount Tamalpias and San Luis Obispo with Menlo Park being the receiving point.

<u>Portable Networks</u>

Ten 5-day recorders were installed and operated in a cooperative network with the University of California at Los Angeles. This network ran between Vernal Utah and Lubbock Texas and was operated from December 1984 through February 1985.

Data Processing Center Operations

9930-01499

John Van Schaack
Branch of Seismology
U. S. Geological Survey
345 Middlefield Road- Mail Stop 977
Menlo Park, California 94025
(415) 323-8111, Ext. 2584

Investigations

This project has the general housekeeping, maintenance and management authority over the Earthquake Prediction Data Processing Center. Its specific responsibilities include:

1. Day to day operation and performance quality assurance of 5 network magnetic tape recorders.
2. Day to day management, operation, maintenance, and performance quality assurance of 2 analog tape playback stations.
3. Day to day management, operation, maintenance and performance quality assurance of the U.S.G.S. telemetered seismic network event library tape dubbing facility (for California, Alaska, and Hawaii).
4. Projection of usage of critical supplies, replacement parts, etc., maintenance of accurate inventories of supplies and parts on hand, uninterrupted operation of the Data Processing Center.

Results

Procedures and staff for fulfilling assigned responsibilities have been developed and the Data Processing Center is operating smoothly and serving a large variety of scientific user projects.

Northern San Andreas Fault System

9910-03831

Robert D. Brown
Branch of Engineering Seismology and Geology
U.S. Geological Survey
345 Middlefield Road, MS 977
Menlo Park, California 94025
(415) 323-8111, ext. 2461

Investigations

Project objectives, previously focused on northern California faults of the San Andreas system (north of Monterey Bay), have been broadened to include the region west of the San Andreas fault and north of the Transverse Ranges. This was done to facilitate review of the Long Term Seismic Program (LTSP) for the Diablo Canyon Power Plant. The LTSP is being conducted by Pacific Gas and Electric (PG&E) Company as part of a license condition required of the utility by the Nuclear Regulatory Commission (NRC).

Field and office review of geophysical and geological data and interpretations continued during the period October 1 through March 31, with effort divided between the original project area and that related to Diablo Canyon issues. Research activities were diluted somewhat by meetings with NRC and PG&E staff and with the Policy Advisory Board of the Bay Area Regional Earthquake Preparedness Project.

Results

Provided NRC staff with review comments on program plan for geological investigations related to Diablo Canyon LTSP and recommended related USGS activities to be supported in FY 1985.

Completed, with Bill Kockelman, an invited paper for the University of California Public Affairs Report: *Geology for Decisionmaking*.

Reports

Brown, Robert D., and Kockelman, William J., in preparation, Geology for Decisionmaking--Reducing Hazards and Protecting Resources: *Public Affairs Report, Bulletin of the Institute of Governmental Studies*, University of California, Berkeley, 31 ms. p. (Director's approval, March 29, 1985).

Characteristics of Active Faults

9950-03870

Robert C. Bucknam
Branch of Engineering Geology and Tectonics
U.S. Geological Survey
Box 25046, MS 966, Denver Federal Center
Denver, CO 80225
(303) 236-1604

Investigations

1. Geologic studies of paleoseismicity make a critical contribution to the understanding of fault behavior by providing a long-term base of data on the distribution and timing of large earthquakes. Because dating of faulting events plays a key role in evaluating the earthquake potential of a fault zone, there is an important need to improve our ability to assign ages to paleoearthquakes. Geomorphic methods of dating fault scarps have proven to be widely useful in studies of paleoseismicity, but the influence of lithologic properties of the faulted alluvium on the rate of degradation is virtually unknown. Lithologic properties of alluvium almost certainly exert a very strong influence on the erosion of fault scarps, particularly on the rate at which the free face degrades. Variations in this rate may be significant when estimating the ages of fault scarps of Holocene age from geomorphic data.

   Studies undertaken this fiscal year under this new project focus on location of sites along late-Holocene and historic fault scarps in the Great Basin showing variability in the degree of erosion of the scarp. Reconnaissance measurements of the morphology of the scarps will be made and samples for determination of physical properties and mineralogy of cementing materials will be collected at the sites.

2. Produce, in collaboration with other scientists, an atlas of maps and illustrations characterizing the geological/geophysical setting and relationships, the geomorphic character, and the seismicity of selected major active faults of the world. This work is part of International Geological Program Project No. 206, "Worldwide Comparison of the Characteristics of Major Active Faults," R. C. Bucknam, U.S. Geological Survey and Ding Guoyu, State Seismological Bureau, Peoples Republic of China, co-organizers. Currently, a dozen countries are participating in this project which held its organizational meeting in Kobe, Japan in June 1984.

Comparative Earthquake and Tsunami Potential for Zones
in the Circum-Pacific Region

9600-98700

George L. Choy
Stuart P. Nishenko
William Spence
Branch of Global Seismology and Geomagnetism
Denver Federal Center, MS 967
Denver, Colorado 80225
(303) 236-1506

Investigations

1. Prepare detailed maps and text of comparative earthquake potential for the west coasts of Mexico, Central America, and South America.

2. Conduct investigations of the rupture processes of large earthquakes that have produced tsunamis. Compare the faulting parameters of these earthquakes to parameters determined for other tsunami-producing earthquakes.

3. Develop a working model for the interaction between forces that drive plate motions and the occurrence of great subduction zone earthquakes.

Results

1. A study of comparative earthquake potential is complete for the west coasts of Chile and southern Peru. A paper describing the results is in press with the Journal of Geophysical Research. A major success of our program is that the great Chilean earthquake of March 3, 1985 had been correctly forecast. However, this earthquake ruptured only 1/3 the total length of the Valparaiso seismic gap defined by the length of the 1906 earthquake. The southern third of the Valparaiso gap now has the highest hazard in central Chile for the next one or two decades. Work on the earthquake potential for the west coast of Mexico is nearly done. The Mexican subduction zone has been divided into 11 zones based on patterns of prior earthquake occurrence. Four of the segments have low probabilities (<30 percent) for earthquake recurrence. Five segments have conditional probabilities of greater than 30 percent for large earthquakes during the next 20 years.

2. We have detailed the rupture processes of three large earthquakes which have produced tsunamis. The Samoa Islands earthquake of 1 September 1981, which occurred at the extreme northern end of the Tonga trench ruptured two separate but offset faults. The Peru earthquake of 1974 was a shallow focus thrust event consisting of several small breaks. It is concluded that the maximum likely earthquake to occur in central Peru would be M_S 8.4. A primary conclusion of the study of the great Sumba earthquake of 1977 was that a great thrust earthquake will not occur at the central Sunba arc, but that a great normal-faulting earthquake is possible at the central Sunda arc.

3. An evaluation of the ridge push and slab pull forces in the context of the stress that leads to great subduction zone earthquakes has been completed and a paper submitted to Nature.

Reports

Choy, G. L., 1984, Broadband body-wave analysis of the complex rupture process of the Samoa earthquake of September 1, 1981: Submitted to the Journal of Geophysical Research.

Nishenko, Stuart P., 1984, Seismic potential for large and great interplate earthquakes along the Chilean and southern Peruvian margins of South America: A quantitative reappraisal: Scheduled for publication on April 10, 1985, in the Journal of Geophysical Researach.

Nishenko, S. P., and Singh, S. K., 1984, Conditional probabilities for the occurrence of large plate boundary earthquakes along the Mexican subduction zone: 1985-2005: In preparation.

Singh, S. K., Ponce, L., and Nishenko, S. P., The great Jalisco, Mexico earthquakes of 1932 and the Rivera subduction zone: Submitted to the Bulletin of the Seismological Society of America.

Spence, William, The 1977 Sumba earthquake series: Direct evidence for slab pull: Submitted to the Journal of Geophysical Research.

Spence, William, Slab pull: Submitted to Nature.

Investigation of Seismic-Wave Propagation for Determination of Crustal Structure

9950-01896

Samuel T. Harding
Branch of Engineering Geology and Tectonics
U.S. Geological Survey
Box 25046, MS 966, Denver Federal Center
Denver, CO   80225
(303) 236-1572

Investigations

1. Conducted high-resolution seismic-reflection surveys at the following locations in South Carolina:

   (a) In and around Hollywood, S.C., to determine if the recently discovered sandblows were related to possible subsurface faulting.

   (b) Along Dorchester Road in Charleston, S.C.

   (c) West of Summerville, S.C., to determine if deeper faulting seen by Vibroseis work done by V.P.I. and industry could be seen higher in the section.

2. A short survey was conducted across the Meers fault in Oklahoma.

3. Reprocessed Vibroseis reflection lines in the Mississippi embayment near Caruthersville, Mo., and Marked Tree, Ark., in an area that coincides with the earthquake zone.

Results

The high-resolution seismic-reflection line across the Meers fault shows reflection offset of about 30 m at a depth fo 171 m. This subsurface fault has the same sense of movement as the surface exposure of the Meers fault and can be projected updip to the surface exposures.

The work conducted in South Carolina is still being analyzed and no definitive results can be reported at this time.

New information on mid-crustal structure in part of the New Madrid seismic zone between Caruthersville, Mo., and Marked Tree, Ark., has been interpreted from reprocessed industry seismic-reflection profiles. One line has been processed to 7 s and several others are being processed to 11 s. (All times are two-way traveltime.) The lines were originally processed to 5 s, and interpretations of them by other investigators delimited a disrupted structural zone coincident with the seismicity. A migrated record section of the 7-s line shows that generally incoherent reflectors in the disrupted zone extend beneath the maximum depth of the hypocenters of about 15 km. In addition to an approximately 10-km-wide shallow fault zone, coincident with the seismicity, the reprocessed lines show mid-crustal structure. Adjacent to the disrupted zone, several prominent zones of reflectors occur at depths

correlative with depths of velocity discontinuities interpreted from seismic-refraction surveys reported in the literature. A zone of strong reflectors overlying magnetic basement correlates with a 4.9-km/s zone which is known from drill-hole exploration to be composed of clastic sediments. Another group of reflectors at 5-6 s (15-18 km) appears to correlate with a 6.2-km/s layer which overlies a 6.6-km/s layer. Preliminary interpretation of a line being reprocessed to 11 s shows reflections at about 30 km which are interpreted to be the top of a 7.3-km/s layer. The zones of mid-crustal reflectors are strong but discontinuous and commonly appear to be lenticular.

Reports

Dwyer, R. A., and Harding, S. T., 1985, Mid-crustal seismic reflectors from part of the New Madrid seismic zone [abs.]: Earthquake Notes, v. 55, no. 1, p. 26.

Harding, S. T., 1984, High-resolution seismic-reflection line conducted east of Jackson Dam, Jackson Lake, Wyoming: Administrative report to Bureau of Reclamation.

Harding, S. T., 1985, Preliminary results of a high-resolution reflection survey across the Meers fault, Comanche County, Oklahoma [abs.]: Earthquake Notes, v. 55, no. 1, p. 2.

Harding, S. T., The use of seismic-reflection data to unravel the earthquake history associated with intracraton earthquakes [abs.]: SEG, Annual Meeting, Washington, D.C. (in press)

Seismic Source Characteristics of Western States Earthquakes

Contract No. 14-08-0001-21912

Donald V. Helmberger

Seismological Laboratory,
California Institute of Technology
Pasadena, California 91125
(818)-356-6998

Investigation

There are strong suggestions that earthquakes occurring at particular locations tend to reproduce nearly identical signals, for example see Richter (1958). The phenomenon of certain regions having higher stress drop than others has been discussed for many years, Thatcher (1971) and more recently Nava and Brune (1983). Thus, we suggest that a good appreciation of the characteristics of faulting in the various regions should be included along with the seismicity patterns in hazard appraisal. We address the problem of determining the source parameters with magnitudes greater than about 4.5 by applying a semi-automated inversion technique. Many of the earthquakes in this magnitude class are not well suited to the waveform analysis of the teleseismic body waves or surface waves because they are not large enough to produce usable records at large distances. On the other hand, the earthquakes are small enough to produce on-scale recordings at regional distances (2° to 12°). Recently, we have shown that it is possible to retrieve the source parameters of moderate size earthquakes from long-period seismograms at these distances, for example see Figure 1.

We plan to analyze the waveforms of 30 to 40 WUS and Northern Mexico earthquakes (Baja) which were recorded on the LRSM and WWSS networks during the post-1962 years. We hope that these results will provide the ground work (reference events and paths) for extending the waveform analysis to pre-1962 data.

Results

This project has just begun and most of the efforts have gone into data collection and digitization. A six-month no-cost extension has been requested because of the slow rate of obtaining the LRSM data. Complete data sets for about 10 events have been assembled and will be reported on shortly.

References

Helmberger, D. V. and G. R. Engen, 1980, Modeling the long-period body waves from shallow earthquakes at regional distances, Seismol. Soc. Amer., Bull., 70, pp. 16 1714.

Nava, F. A. and J. N. Brune, 1983, Source mechanism and surface wave excitation for two earthquakes in Northern Baja, California, Mexico, Seismol. Soc. Amer., Bull., in press.

Richter, C. R., 1958, Elementary Seismology, W. H. Freeman and Company, San Francisco, California.

Thatcher, W., 1971, Surface wave propagation and source studies in the Gulf of

California region, Ph.D. thesis, Caltech, Pasadena, California.

Wallace, T. C., D. V. Helmberger and G. R. Mellman, 1981, A technique for the inversion of regional data in source parameter studies, J. Geophys. Res., 86, pp. 1679-1685.
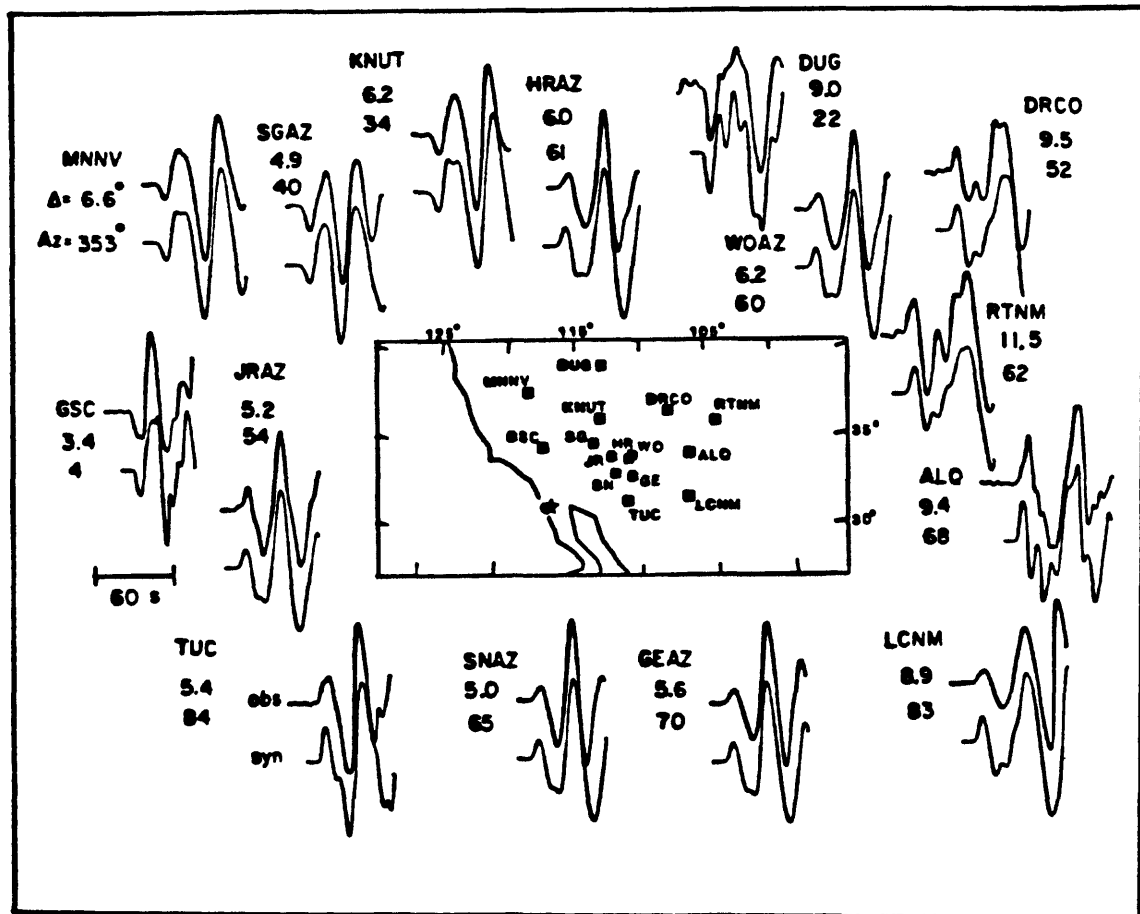
Figure 1. Location of the 12-22-64 San Miguel earthquake (star) and the recording stations. The stations with two and four letter designations are LRSM while those with three letters are WWSSN. Also shown are the vertical component (top trace) and synthetics (bottom trace) computed with the inversion fault orientation. The fault parameters are strike = 312°, dip = 85° and rake of 177°. The moment is 8 x 10^{24} dyne-cm.

Pleistocene Faulting in Coastal San Diego County
Contract Number: 14-08-21898
Principal Investigator: Philip Kern
Contractor: San Diego State University Foundation
San Diego, CA 92182-1900
Telephone of P.I.: (619) 265-6443

Investigations

This study is part of a project to map the Pleistocene geology of coastal
San Diego County. During the past half year mapping of marine and non-marine
shorelines, associated sediments, and geologic structures has been carried
out in the Oceanside and San Luis Rey Quadrangles. This work brings to
completion mapping of the terraced coastal zone from San Diego to Oceanside.

Results

At least 17 and perhaps as many as 19 or more marine terraces with shoreline
elevations from just below sea level to 400 m are present along the San Diego
County coast between San Diego and Camp Pendleton, north of Oceanside.
(On-going mapping on Camp Pendleton will resolve the number of terraces
during the next few months.) The shorelines of at least the nine youngest
terraces, and perhaps the older ones as well, are horizontal from Del Mar to
Oceanside, showing that the coastal strip has been subjected to regionally
uniform uplift. No new fossil occurrences have been found, so still only
five terraces have been dated, four of them uncertainly by amino-acid
racemization.

Postglacial uplift in northeastern United States
9510-03207

Carl Koteff
U.S. Geological Survey
National Center, MS928
703/860-6503   FTS 928-6503

INVESTIGATIONS

The postglacial uplift profile for the Connecticut River Valley from central Connecticut to northeastern Vermont and northwestern New Hampshire has been extended for a total distance of over 245 km from south to north. Altitudes of the contact between topset and foreset beds in 28 ice-marginal deltas that were constructed in glacial Lake Hitchcock were analyzed by an ordinary least squares regression. The topset/foreset contacts are believed to represent the former water level with an accuracy of 1 m. Ice-marginal deltas were especially singled out because they provide a relative physical chronology of the northward growth of a glacial lake during ice retreat. The ice retreat is known to have been very systematic in the region for the time represented by glacial Lake Hitchcock, from about 17,000 B.P. to about 14,000 B.P., although ice retreat over the northern half of the region was about twice as fast as over the southern half. Thus, the profile derived from the delta altitudes is a variable-rate time-transgressive depiction of about 3000 years.

RESULTS

The regression analysis of the altitudes of topset/foreset contacts for the 28 ice-marginal deltas that were constructed in glacial Lake Hitchcock show a refined profile of postglacial uplift that bears N20 $\frac{1}{2}$ W. The profile is a very straight line; only two of the plotted altitudes depart more than 2 sigma (less than 2 m) from the projection. 22 of the altitudes plot within 1 m of the profile. A projected altitude of the water level of Lake Hitchcock at the threshold in the spillway at New Britain in central Connecticut is 25.07 m, and the altitude of the topset/forest contact in the northernmost ice-marginal delta at South Ryegate in northeastern Vermont is 244 m. The differential uplift is 219 m over a distance of 245.8 km along the N20 $\frac{1}{2}$ W projection and shows a gradient of 0.9 m/km up to the northwest.

Because the profile is so straight and because it represents a time transgression of 3000 years, the concept of a considerable delay to uplift response during early stages of deglaciation is confirmed. It is reasonable to extend this delay to include the beginning of deglaciation at about 19,000 B.P. Thus there appears to have been a 5000-year period of ice unloading before initiation of upward crustal movement. Significantly, perhaps as much as 50% of the ice load had disappeared in this time.

Uplift began in this region after 14,000 B.P., and uplift rates are calculated to have been between 7-12 cm/year for at least a thousand years. Isobases of uplift show a regular and consistent pattern, which suggests that there has been no noticeable effect by this event on any known crustal structure in this area.

52

REPORTS

Koteff, Carl, and Larsen, F. D. 1985 Postglacial uplift in the Connecticut
    Valley, western New England [abs.]: Geological Society of America
    Abstracts with Programs, v. 17, no. 1, p. 29.

Fault Mapping to Determine Source Zone Structure and
Influence on Variable Rupture Mode of Earthquakes in California

14-08-0001-21991

Dr. Karen McNally
Charles F. Richter
Seismological Laboratory
Earth Sciences Board
University of California,
Santa Cruz
Santa Cruz, California   95064
(408) 429-4137

Objectives:

To obtain detailed information and physical descriptions of structural heterogeneities, commonly referred to as fault 'asperities' or 'barriers', in seismogenic zones. Such heterogeneities may influence variable fault rupture and recurrence periods of major earthquakes. A technique using P-waves refracted laterally at the fault plane will be used to provide a detailed mapping of velocity contrast variations along the San Andreas fault in central California. P-waves of approximately 400 earthquakes occurring from 1975 to 1984 will be analyzed; the results will integrated with previous data (1969-1975) (McNally and McEvilly, 1977) for final interpretation. The size of the mapping region is 35 km long (along the fault) and 12 km deep. A mobile seismograph array will be operated to determine velocity contrast variations along the fault zone to within about 2%. Three-dimensional ray tracing will be used to improve the precision of the results. The results will be used in conjunction with detailed studies of the San Andreas fault in southern California.

Progress Summary:

All earthquakes $M_L > 2.5$, 1975-1982, have been relocated and fault mechanism solutions determined. Teleseismic events have been used to check USGS stations polarities as necessary. Refraction angle measurements are being finalized. We identify high refraction angles near 36 40'N - 36 43'N, where none were observed previously. (Distinctive clustering of seismicity is also observed at this location.) This could indicate stress changes locally, a change in rupture medium, or fault gauge zone. The mobile array is now operating in the San Benito area.

Northeastern Seismicity and Tectonics
9510-02388

Nicholas M. Ratcliffe
U.S. Geological Survey, MS 925
Reston, Virginia 22092
(703) 860-6406
and
John K. Costain
Virginia Polytechnic Institute and State University
Blacksburg, Virginia 24061

INVESTIGATIONS

1. Interpretation of VIBROSEIS reflection profiles of the Ramapo seismic zone in New Jersey and Eastern Pennsylania.

2. Geologic mapping along VIBROSEIS routes.

3. Analysis of proprietary industry reflection data across the Newark basin.

RESULTS

1. A preliminary interpretation of Ramapo 1, shot in August and October of 1983, is shown in Figures 1 and 2. These data were collected in a cooperative effort with Virginia Polytechnic Institute with funds provided by the Nuclear Regulatory Commission. The line extends 32 km from the gneiss of the Reading Prong, southeastward across the Triassic border fault into the Newark basin south of the Watchung Syncline in central New Jersey. A line drawing and geologic section are shown in Figure 2. The prominent southeast dipping grain in basement rocks west of the Newark basin is associated with Paleozoic thrust faults. This grain extends beneath the Triassic basin to about 4 seconds, with dips of about 30 degrees. The border fault (Flemington fault) is interpreted to consist of a series of downward converging faults that merge at depth with the reflectors in the footwall.

2. The field, reflection data and coring of the border fault along this line support shallow 36° dips for the Triassic border fault and similar shallow dips for Paleozoic thrust faults. Reactivation of Paleozoic thrust faults during Mesozoic extension is the preferred explanation for the formation of the Newark basin here.

3. Earthquake hypocenters recorded by Lamont Doherty (Regional Seismicity Bulletin of the Lamont-Doherty Network) for the area adjacent to the line are plotted in Figure 3. Despite the large uncertainties in depths, many events plot within crystalline rocks in a prism of rock between the Schooley Mountain thrust and Flemington faults. Similar relationships are seen in our other profiles that extend northward into New York State.

55

REPORTS

Ratcliffe, N. M., and Burton, W. C., 1985, Fault reactivation models for the origin of eastern North American Mesozoic basins and relationship to current seismicity, in Proceedings of the Second U.S. Geological Survey Workshop on the Early Mesozoic Basins of the Eastern United States: U.S. Geological Survey Circular no. _____, in press.
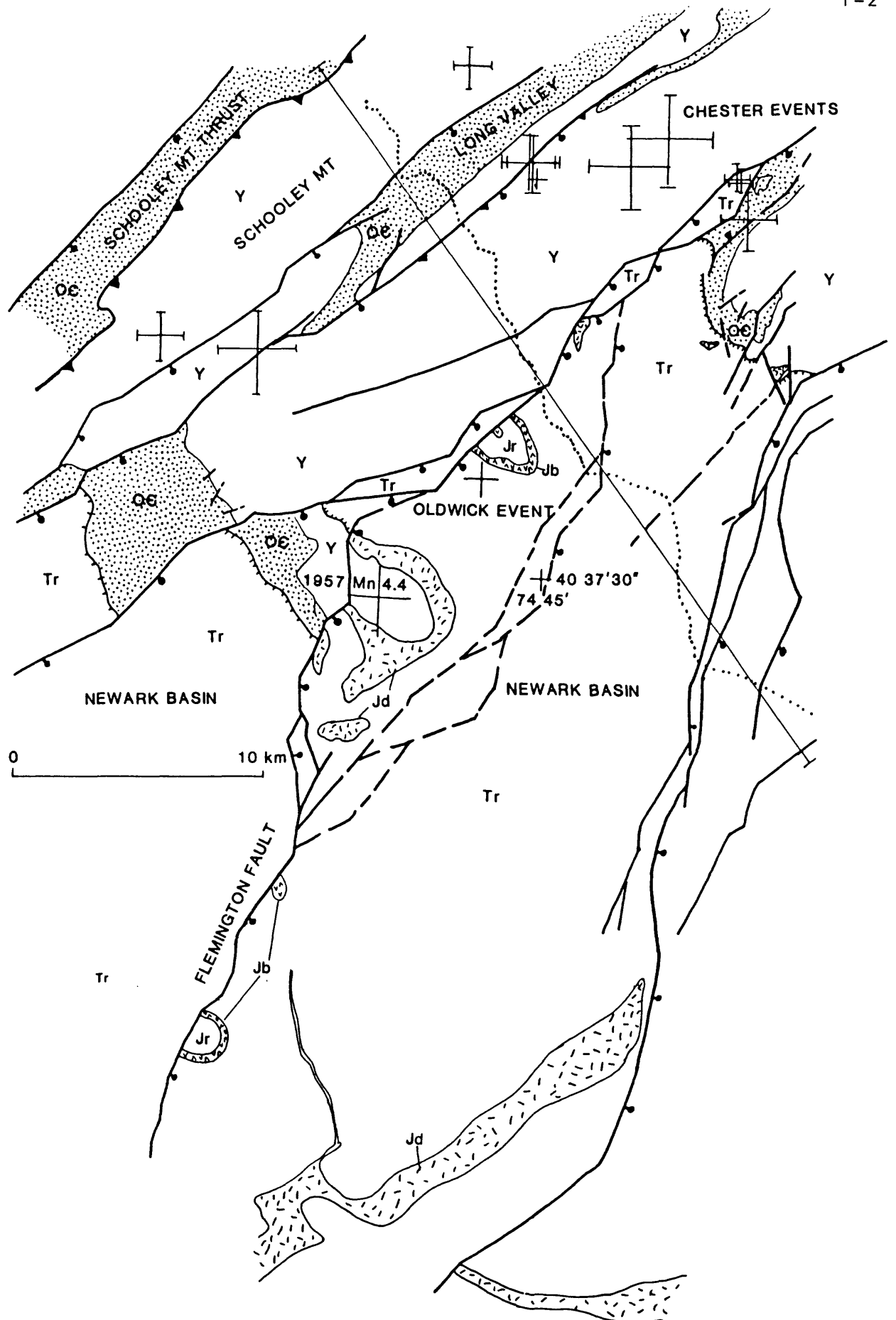
MESOZOIC FAULTS AND EPICENTERS LINE 1

Figure 1.--Location of Ramapo seismic line 1 and epicenters.
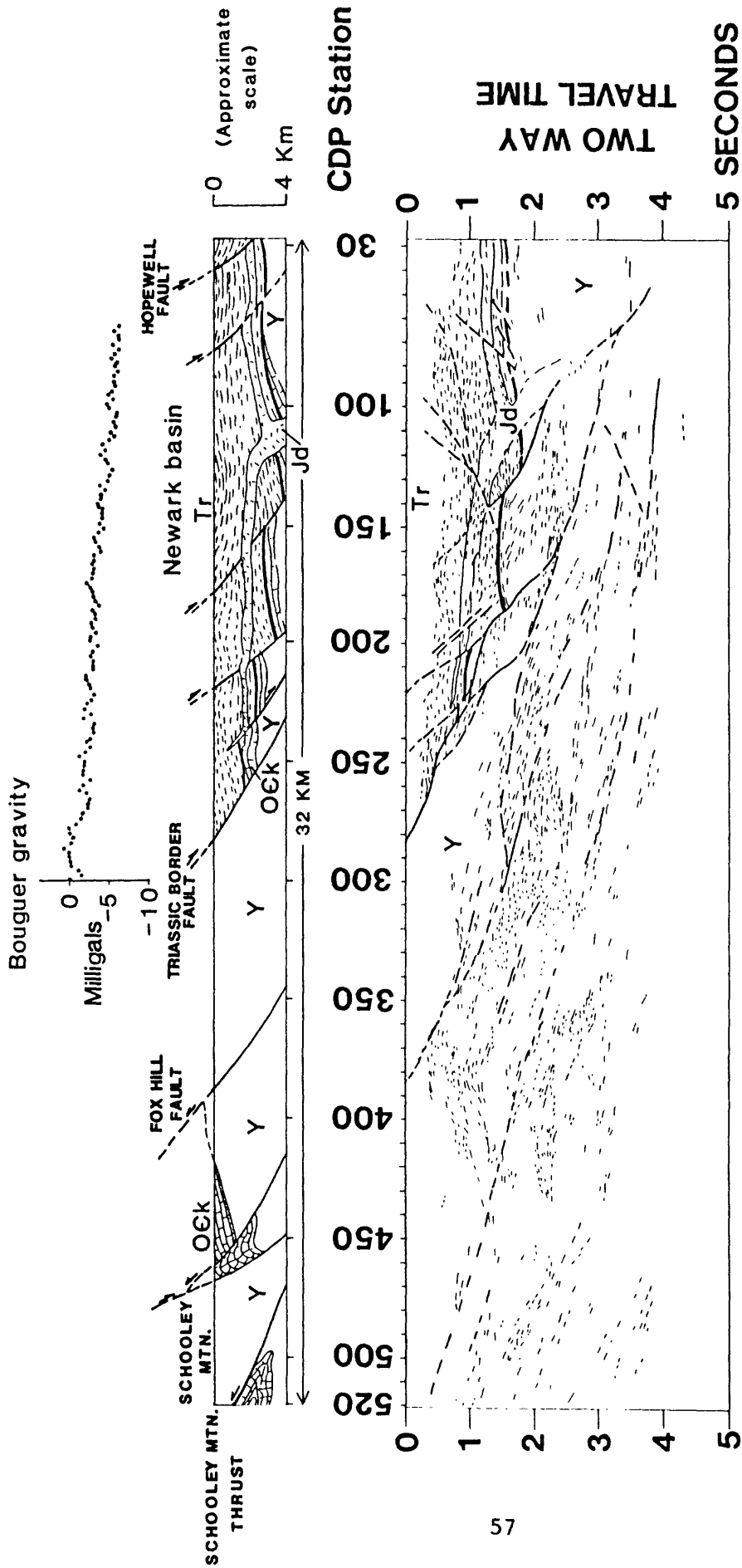
RAMAPO LINE 1: LINE DRAWING AND GEOLOGIC REFERENCE SECTION
AND BOUGUER GRAVITY DATA OF KODAMA

Figure 2.--Interpretive line drawing of Ramapo line 1.

57

CROSS SECTION RAMAPO LINE 1 and HYPOCENTERS

NEWARK BASIN

LONG VALLEY EVENTS

Tr

BERNARDSVILLE EVENT

Y

FLEMINGTON FAULT

Y

OLDWICK EVENT

Y gneiss

SCHOOLEY MT THRUST

OЄ

OЄ

Y

0

12 km

0

10 km
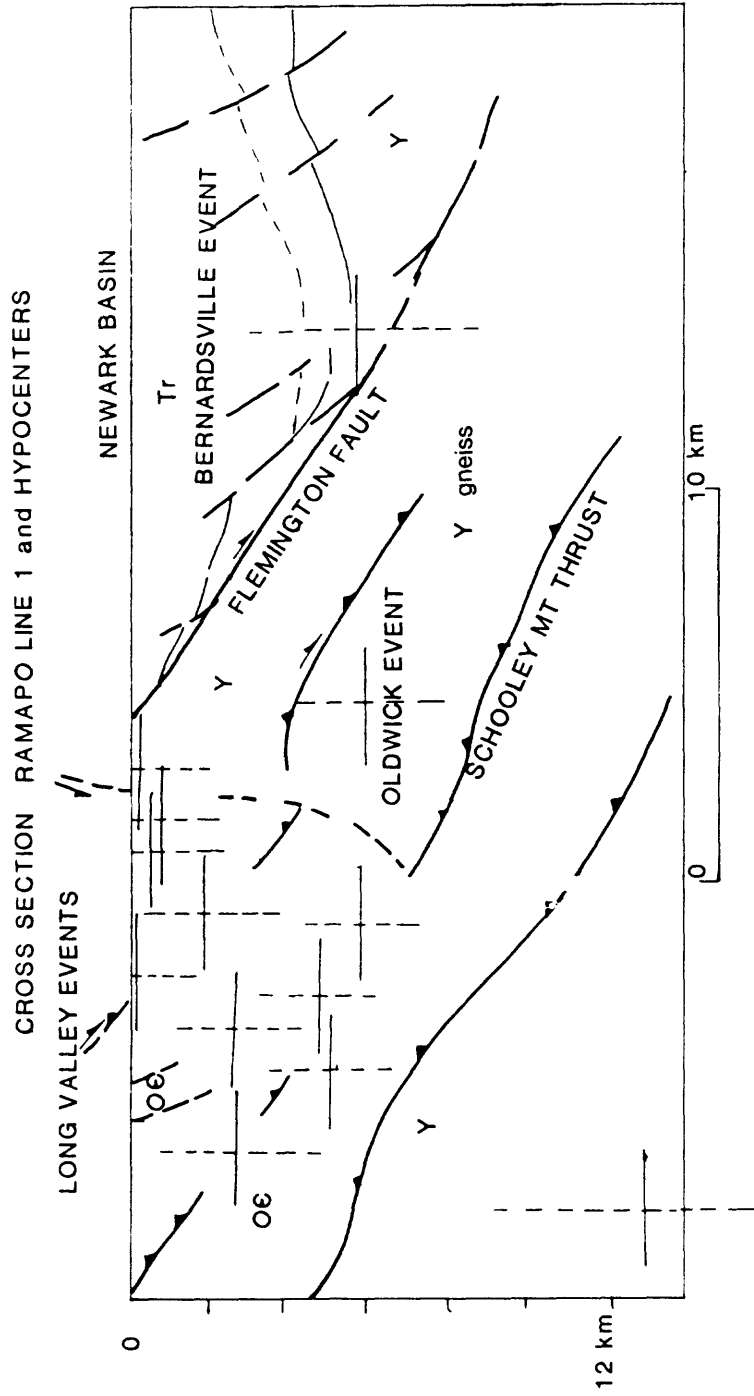
Figure 3.--Depth section and location of hypocenters along Ramapo line 1.

58

Basement Tectonic Framework Studies
Southern Sierra Nevada, California

9910-02191

Donald C. Ross
Branch of Engineering Seismology and Geology
U.S. Geological Survey
345 Middlefield Road, MS 977
Menlo Park, CA 94025
(415) 323-8111, ext. 2341

Investigations

1. Field studies of plutonic and metamorphic rocks east of the White Wolf-Breckenridge-Kern Canyon to the eastern Sierra Nevada frontal fault.

2. Compilation of all granitic modal data for the southern Sierra Nevada and preparation of index maps for each granitic unit.

3. Revision of the Bulletin manuscript and illustrations on basement rock correlations across the White Wolf-Breckenridge-southern Kern Canyon fault, southern Sierra Nevada.

Results

1. Field studies in October and November, 1984, disclosed and, in part, delineated a large foliated granitic body in the area of Walker Pass that contains abundant mafic minerals and some mafic dikes. These features suggest that the body is Jurassic. If so, this is the southernmost Jurassic pluton in the Sierra Nevada, and the only one so far identified south of lat 36°00' N.

2. Preliminary evaluation of Rb-Sr isotopic data determined and interpreted by R.W. Kistler (Isotope Geology Branch) indicate that some of the mafic rocks east of the large body of amphibolitic- to granulitic-grade "oceanic" rocks in the Sierra Nevada tail are more related to "continental" basement than to the "oceanic" basement of the Sierran tail.

Reports

Clark, J.C., Brabb, E.E., Greene, H.G., and Ross, D.C., 1984, Geology of Point Reyes peninsula and implications for San Gregorio fault history, in Crouch, J.K., and Bachman, S.B., eds., Tectonics and sedimentation along the California margin: Pacific section, Society of Economic Paleontologists and Mineralogists, v. 38, p. 67-86.

Ross, D.C., 1984, Possible correlations of basement rocks across the San Andreas, San Gregorio-Hosgri, and Rinconada-Reliz-King City faults, California: U.S. Geological Survey Professional Paper 1317, 37 p.

---1985, Mafic gneissic complex (batholithic root?) in the southernmost Sierra Nevada, California: Geology, v. 13, no. 4, p. 288-291.

---In press, Basement-rock correlations across the White Wolf-Breckenridge-southern Kern Canyon fault zone, southern Sierra Nevada, California: U.S. Geological Survey Bulletin 1651 (Director's approval, December 12, 1984.

---In press, Metamorphic and plutonic rocks of the southernmost Sierra Nevada, California, and their tectonic framework: U.S. Geological Survey Professional Paper 1381 (Director's approval, March 5, 1985).

INTEGRATED STUDIES OF EARTHQUAKE SOURCE ZONE CHARACTERISTICS, HAZARDS, AND
PREDICTION IN THE WASATCH FRONT URBAN CORRIDOR AND ADJACENT
INTERMOUNTAIN SEISMIC BELT

14-08-0001-21983

R.B. SMITH, W. J. ARABASZ, J.C. PECHMANN, and W.D. RICHINS*
Department of Geology and Geophysics
University of Utah
Salt Lake City, Utah 84112
(801)581-6274

Investigations

1. Calibration of a seismic network for earthquake source studies using teleseisms and local earthquakes.
2. Tests using local blast data of a technique for determining relative earthquake locations by cross-correlation of waveforms.
3. Further studies of the M_L 4.0 Richfield earthquake of May 24, 1982, and associated seismicity.

Results

1. We have developed and successfully tested an indirect approach to calibrating amplitude response for individual stations of our network by using amplitude displacement spectra of initial P-waves from deep focus teleseisms (M5.5 or greater). For a given teleseism the displacement spectra for a large set of stations, corrected for instrument frequency response, are combined in the 1.2 to 2.4 Hz frequency band to form an average, which is then compared with individual spectra to yield relative gain values. Knowledge of the absolute gain of one or more key stations allows calibration of the entire set.

An absolute gain value for the University of Utah network was calibrated using seismic moment measurements made by J. Boatwright of the U.S. Geological Survey for aftershocks of the October 28, 1983 Boran Peak, Idaho, earthquake. Boatwright's measurements were made using data from 12 GEOS digital event recorders deployed in the epicentral area following the mainshock. Fourteen of the aftershocks studied by Boatwright were examined, ranging in magnitude from M_L 2.0 to 4.0 (a range constrained by limitations of instrumental dynamic range for the U of U stations). Low-frequency P-wave spectral amplitudes for these events were determined using a suite of fourteen stations of the U of U network in southeastern Idaho and northern Utah. After establishing an absolute gain value for the U of U network using these data, the seismic moments calculated from the U of U data agree very well (within about a factor of 3) over the entire range of moment values with those determined independently by Boatwright. It therefore appears that spectral data from regional seismic stations at distances greater than 100 km can provide accurate information on relative seismic moments, even though the assumptions on which the moment calculations are based are not valid at such large distances.

2. Geller and Mueller (1980) hypothesized that earthquakes producing nearly identical waveforms must have similar focal mechanisms and hypocenter

---

*J. F. Peinado and B. S. Thorbjarnardottir also contributed significantly to this project during the report period.

within 1/4 of the shortest wavelength to which the similarity extends. Various investigators have subsequently applied this argument to studies of small-scale earthquake clustering before and after moderate to large earthquakes. We have recently tested the 1/4-wavelength argument of Geller and Mueller (1980) using seismograms of blasts in the Getty-Mercur Mine in the Oquirrh Mountains southwest of Salt Lake City. Seismograms from four different stations were filtered in four one-octave passbands with third-order recursive Butterworth filters. Cross correlations were then calculated for all possible event pairs from the filtered records for each station. The mean peak cross correlation values are plotted versus blast separation distance in Figure 1. This figure clearly demonstrates that the highest cross correlation values are found for nearby events. The vertical bars indicate the 1/4 wavelength values at the high frequency cutoffs of the filters assuming a velocity of 3.4 km/sec, which is the P-wave velocity for the uppermost crust measured on a nearby refraction line (Keller et al., 1975). The horizontal bars are drawn at 0.6, which is the arbitrary cutoff value used by Pechmann and Kanamori (1982) to separate "well correlated" events from "poorly correlated" events. With very few exceptions, correlation values of 0.6 or greater correspond to event separation distances ot less than the 1/4 wavelength values shown. Thus, these data support the hypothesis of Geller and Mueller (1980) that events with similar waveforms occur within one-quarter of the shortest wavelength for which the similarity is observed.

3. The waveform cross correlation technique was used to investigate preshocks and aftershocks of the M_L 4.0 Richfield earthquake that occurred on May 24, 1982 at 12:13. Four preshocks occurred in a location 5 km NW of the mainshock epicenter during a four-hour period on July 16, 1981. Clear dilatational first motions observed at some stations demonstrate that these events are not blasts. Seismograms of these four preshocks are extremely similar at frequencies up to at least 16 Hz. (Figure 2), implying that the hypocenters cluster within about one-quarter of the 16 Hz wavelength or 80 m. In contrast, none of the aftershocks show high cross correlations in the 8-16 Hz passband and only two pairs have cross correlations of 0.6 or greater in the 4-8 Hz passband. Likewise, no events highly correlated at 8-16 Hz and only one pair highly correlated at 4-8 Hz were found among a group of 11 preshocks centered 15 km SW of the mainshock epicenter. Thus, the four very similar preshocks near the mainshock epicenter appear to be fairly unusual. We suggest that these 4 events may have represented the breaking of a critical fault asperity, the failure of which resulted in a transfer of stress to the location of the mainshock.

Using the method of Frankel and Kanamori (1983), we estimate a fault radius for the mainshock of about 1.1 -1.6 km. Combining this with a moment measurement of 1.3×10^{23} dyne-cm determined from P-wave spectra yields a stress drop of 15-41 bars for this earthquake.

Reports and Publications

Bruhn, R. L., R. B. Smith, W. T. Parry, D. S. Chapman, and M. D. Zoback, 1984, Proposed deep drilling of the Wasatch normal fault zone, Utah, Eos Trans. AGU, 65, 1097.

Doser, D. I., and R. B. Smith, 1985, Source parameters of the October 28, 1983 Borah Peak, Idaho, earthquake from body wave analysis, submitted to Bull. Seismol. Soc. Am.

Pechmann, J. C., W. D. Richins, and R. B. Smith, 1984, Evidence for a "double moho" beneath the Wasatch front, Utah, Eos Trans. AGU, 65, 988.

Peinado, J. F., and W. J. Arabasz, 1985, "Size" estimates and source properties of selected earthquakes in southeastern Idaho, Geol. Soc. Am. Abstracts with Programs, 17, 260.

Richins, W. D., and W. J. Arabasz, 1985, Seismicity of southeastern Idaho based on seismic monitoring using regional and temporary local networks, Geol. Soc. Am. Abstracts with Programs, 17, 261.

Smith, R. B., W. D. Richins, D. I. Doser, J. C. Pechmann, L. L. Leu, and G. J. Chen, 1984, The 1983, M_s 7.3 Borah Peak, Idaho earthquake: a model for active crustal extension, Eos Trans. AGU, 65, 989.

Thorbjarnardottir, B. S., and J. C. Pechmann, 1985, Waveform analysis of local Utah earthquakes using digital data, Geol. Soc. Am. Abstracts with Programs, 17, 267.

Figure 1. (a) Location map for Mercur Mine blasts. (b) Mean of the maximum cross correlations calculated for filtered seismograms of Mercur Mines blasts from four different stations. Values are plotted versus separation distances between blasts, measured between the approximate centers of the blasts areas. Typical blast dimensions are 60 x 160 m. The vertical lines represent 1/4 wavelength at the upper limit of each passband, assuming a velocity of 3.4 km/sec. The horizontal lines are drawn at 0.6 and indicate a possible dividing line between "well correlated" and "poorly correlated" events. 19.5 sec of record, beginning with the P-wave, were used for the cross correlation calculations.
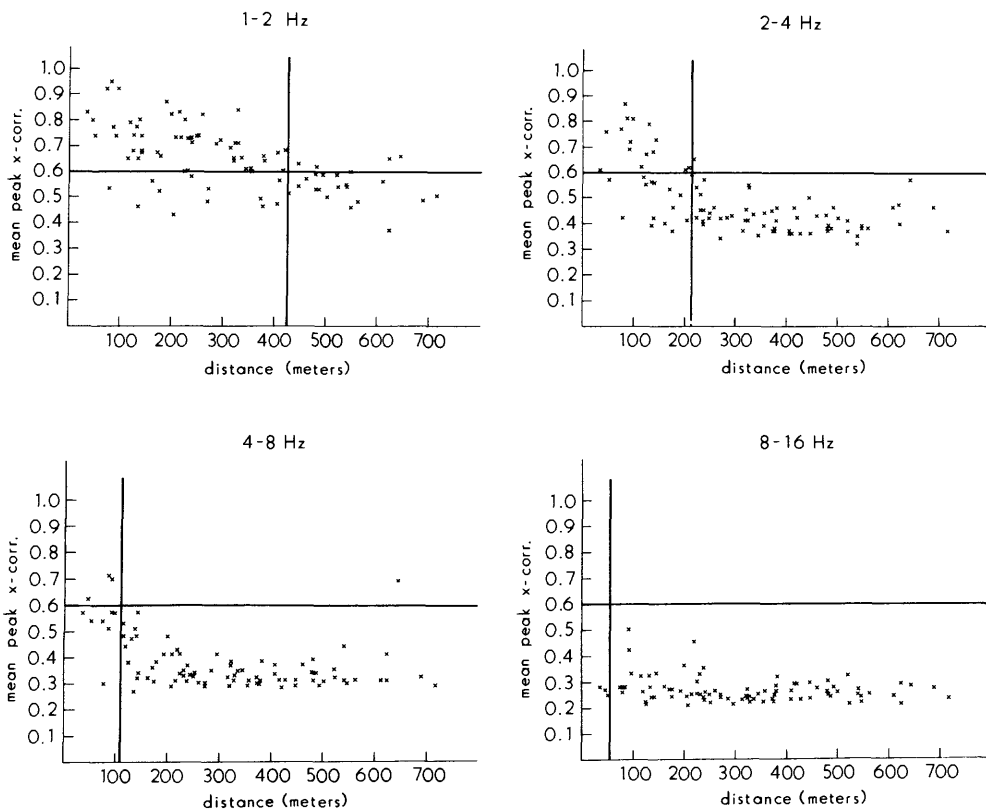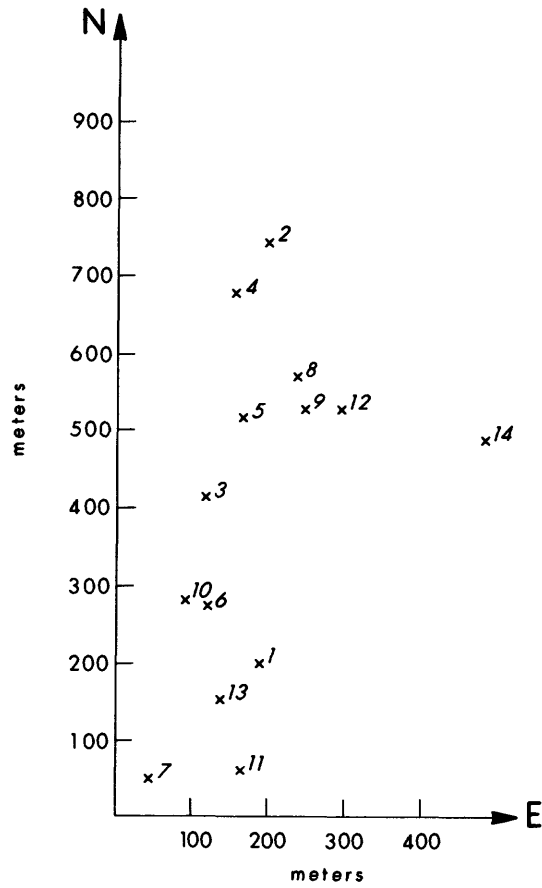
RICHFIELD CROSS-CORRELATION MATRICES

Unfiltered

2-4 Hz

4-8 Hz

8-16 Hz
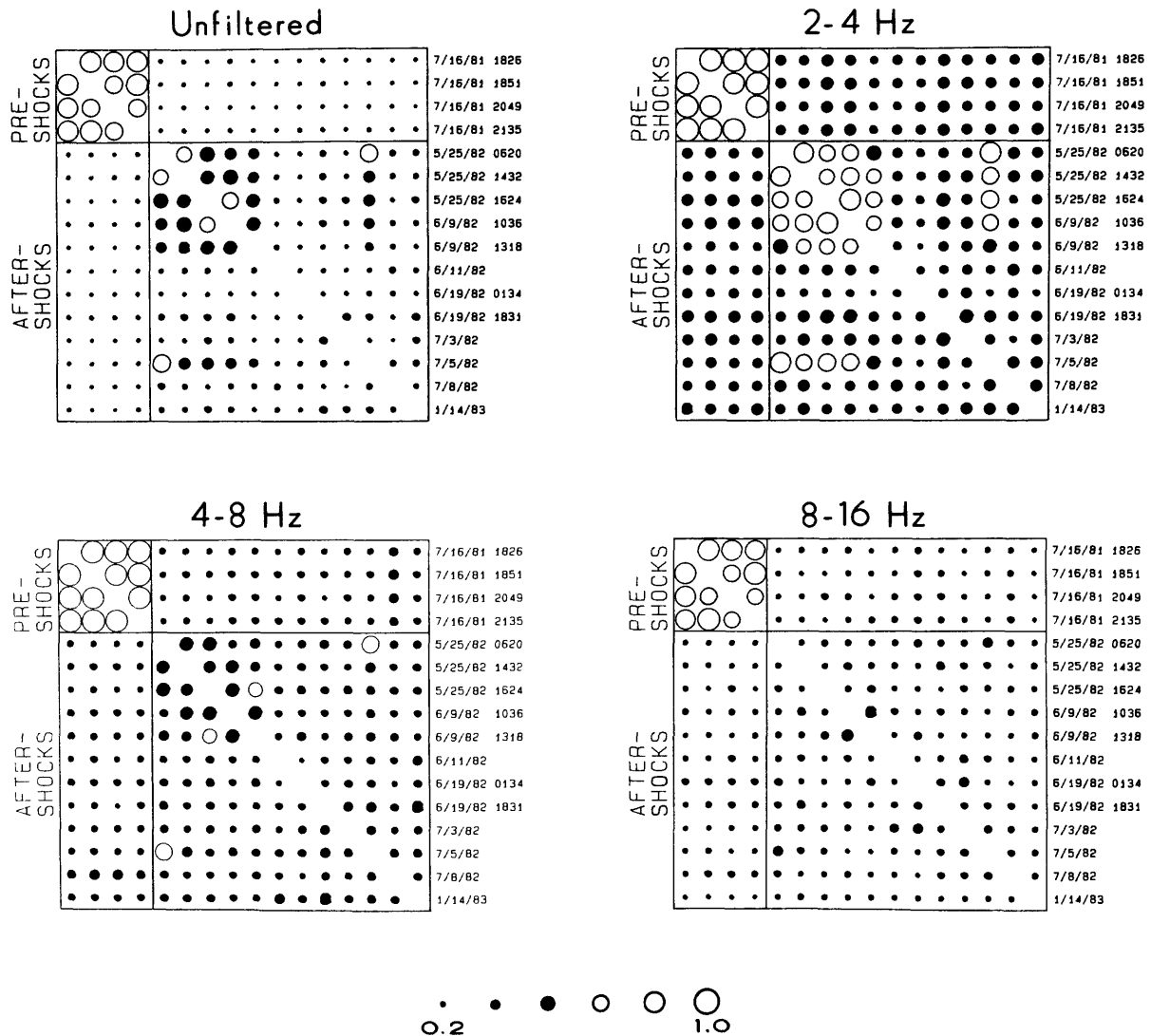
Figure 2. Correlation coefficients calculated from filtered and unfiltered seismograms recorded at station MSU ($\Delta \sim 25$ km) for all possible pairs of events within 7 km of the M_L 4.0 Richfield mainshock (May 24, 1982) during 1981-83. Each circle represents the maximum value of the normalized cross correlation function for the event pair corresponding to its position in the matrix. The radius of the circle is proportional to the correlation value, and circles representing values less than 0.6 are solid. 19.5 sec of record were used for the cross correlations.

Geothermal Seismotectonic Studies

9930-02097

Craig S. Weaver
Branch of Seismology
U. S. Geological Survey
at Geophysics Program AK-50
University of Washington
Seattle, Washington 98195
(206) 442-0627

Investigations

1. Continued analysis of the seismicity and volcanism patterns of the Pacific Northwest in an effort to develop an improved tectonic model that will be useful in updating earthquake hazards in the region. (Weaver, Michaelson, Yelin)

2. Continued acquisition of seismicity data along the Washington coast, directly above the interface between the North American plate and the subducting Juan de Fuca plate. (Weaver, UW contract)

3. Continued seismic monitoring of the Mount St. Helens area, including Spirit Lake (where the stability of the debris dam formed on May 18, 1980 is an issue) and Elk Lake. (Weaver, Grant, UW contract)

4. Study of an earthquake sequence between 1958-1962 that occurred near Swift Reservoir (the largest event has an M_L=5.1). The events near Swift Reservoir were probably on the southern segment of the SHZ. (Grant, Weaver)

5. Detailed analysis of the seismicity sequence accompanying the May 18, 1980 eruption of Mount St. Helens. Earthquakes are being located in the ten hours immediately following the onset of the eruption, and the seismic sequence is being compared with the detailed geologic observations made on May 18. (Weaver, Shemeta, UW contract)

Results

1. The earthquakes that followed the May 18 eruption of Mount St. Helens show a pronounced deepening immediately following the onset of the eruption at 1532 (GMT). Prior to the eruption onset, nearly all of the earthquakes beneath Mount St. Helens were low-frequency type in the very shallow crust, approximately 0-2 km beneath the surface of the crater floor formed on May 18. As the initial eruption event decreased in amplitude, small magnitude (< 2.5), high-frequency, tectonic-like earthquakes began. These events were located at depths between about 4 km and 10 km, The rate of seismic activity slowly decreased for the first three hours following the eruption onset, then began to build to a higher rate. For the next 3 hours (3-6 hours after the eruption onset), earthquakes occurred primarily between 4 and 10 km depth, but most events were clustered near 4 km (Figure 1). Finally, about 6 1/2 hours after the eruption onset, seismic records were nearly saturated with continuous activity.

The period of saturated activity has been studied using the Wood-Anderson seismograph records from Seattle (165 km distant) and low-gain recordings from USGS 5-day tape recorders located at close-in epicentral distances (12-40

km) that ran throughout the sequence. These data clearly show that the period of most intense seismic activity on May 18, is a series of moderate magnitude earthquakes (up to 4.5), and that the majority of these events are located at depths of 3 km to about 7 km (Figure 1). The maximum of the seismic energy release is co-incident with the period of maximum number of earthquakes, and correlates with the probable emplacement of a shallow magma body beneath the crater floor at Mount St. Helens. We interpret the earthquakes between 3-7 km as fracturing of the upper part of the magmatic system. Once this volume had been sufficiently fractured, the magma body was able to move quickly through the system, resulting in the "boiling over" of the crater described by observers in the field on May 18.

After this emplacement phase, seismicity and volcanic activity changed very quickly. Mount St. Helens ceased erupting within a few hours of the probable time of emplacement, and earthquakes began to occur as deep as 20 km beneath the system (Figure 1). We interpret these later events as adjustment on regional faults that bound the magmatic system. On May 19 earthquakes continued at depths between 5 and 14 km, although most of these events were of small magnitude (<1.5). This swarm-like sequence of small events continued until May 21.

2. Earthquake hypocenters that are interpreted to be within the Juan de Fuca plate beneath western Washington indicate that the plate has a non-planar geometry south of Puget Sound. Available hypocenters indicate that beneath southwestern Washington, the Juan de Fuca plate dips both to the northeast (parallel to the relative direction between the Juan de Fuca plate and the North American plate) and to the southeast.

Reports

Weaver, C. S. and C. A. Michaelson, Seismicity and volcanism in the Pacific Northwest: evidence for the segmentation of the Juan de Fuca plate, *Geophysical Research Letters, v. 12,* (in press), 1985.

Michaelson, C. A., and C. S. Weaver, Upper mantle structure from teleseismic P-wave arrivals in Washington and northern Oregon, submitted to *Journal Geophysical Research,* (Director's approval, 2/85).

Shemeta, J. E., Weaver, C. S., and Grant, W. C., Details of the May 18, 1980 post-eruption seismicity at Mount St. Helens, Washington, (abs), *EOS, Transactions, American Geophysical Union, v. 65,* 1001, 1984.

Baker, G. E., A long period focal mechanism for the magnitude 7.1 south Puget Sound, Washington, event of April 13, 1949, (abs), *EOS, Transactions, American Geophysical Union, v. 65,* 986, 1984.

Shemeta, J. E. and Weaver, C. S., Seismicity accompanying the emplacement of a shallow magma body, (abs), submitted to *Mount St. Helens: Five years later,* symposium at Cheney, Washington, (in press), 1985.
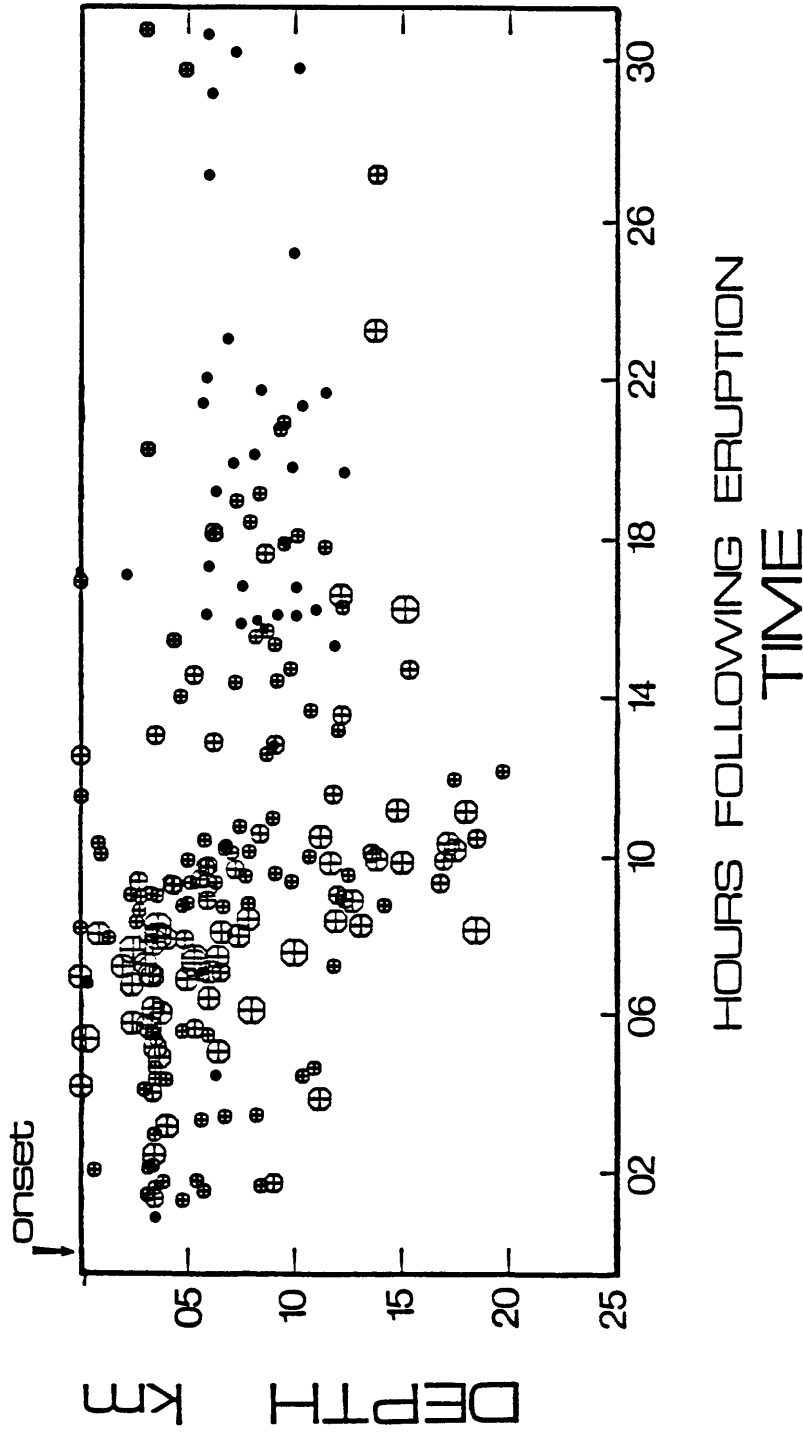
Figure 1. Depth vs. time plot for earthquakes located beneath Mount
St. Helens on May 18 and 19, 1980. Eruption onset was at
1532 (GMT) on May 18. The earthquakes are scaled by
magnitude, with the largest symbols representing events
greater than 4.0, whereas the smallest symbols represent
events with magnitudes less than 1.0.

Holocene deformation near Coalinga, California

9540-02190

Brian F. Atwater, Project Chief
Branch of Western Regional Geology
U. S. Geological Survey
345 Middlefield Road, MS 975
Menlo Park, CA 94025
(415) 323-8111   x2031   FTS 467-2031

Investigations

(1) Completion of radiocarbon dating of Holocene alluvium capable of expressing uplift on the Coalinga anticline, hence also providing constraints on the repeat time of major fold-building earthquakes akin to that of 3 May 1985.

(2) Preparation of final report, intended as a chapter in the Coalinga Professional Paper.

Results

Geomorphic and stratigraphic evidence together favor long (250 years or greater) average repeat times for major fold-building earthquakes of late Holocene age near Coalinga. An estimate in the range 200-600 years, allowed by R.S. Stein and G.C.P. King on the basis of their structural interpretation of a hump in the present alluvial plain of an anticline-crossing creek, should be shortened to reflect the hump's nearly synclinal location but lengthened greatly to acknowledge that the hump probably formed hydraulically. Comparison of late Holocene and modern alluvial-plain profiles suggests no uplift faster than one meter per thousand years. This in turn signifies a repeat time of at least 250 years if all the uplift has accompanied major earthquakes and if the amount of coseismic uplift has averaged 0.25 m along the anticline-cross creek. These and other results are now (6 May 1985) undergong coauthor review, and should be ready for formal peer review within three weeks.

Reports

Atwater, B.F., Tinsley, J.C., Stein, R.S., Trumm, D.A., and Wert, S.L., 1985, Late Holocene alluvial plains as structural datums across the Coalinga Nose - Guijarral Hills anticline, Fresno County, California in Rymer, M.J. and Ellsworth, W.L., eds., Proceeding of Workshop XXVII, Mechanics of the May 2, 1983 Coalinga earthquake: U.S. Geological Survey Open-File Report 85-44, p. 437-438 (published).

Tucker, A.B., Tinsley, J.C., Atwater, B.F., Trumm, D.A., Robinson, S.W., Stein, R.S., Donahue, D.J., and Jull, A.J.T., 1985, Accelerator dating of detrital and burned-in-place charcoal from the alluvium of Los Gatos Creek, Fresno County, California, U.S.A.: submitted to Radiocarbon Congress, Trondjheim, Norway (approved by Director).

SURFACE FAULTING STUDIES

9910-02677

M. G. Bonilla
Branch of Engineering Seismology and Geology
U. S. Geological Survey
345 Middlefield Road, MS 977
Menlo Park, CA 94025
(415) 323-8111, Ext. 2245

Investigations

1. Appearance of active faults in exploratory trenches.
2. Field investigations of surface faulting.

Results

1. Data from 119 trench exposures that contain more than 1000 fault strands were analyzed. More than 10% of the strands have one or more obscure segments (i.e., segments in which the fault is not visible or is obscure). Of the strands for which the position of the ground surface at time of faulting is known, about 80% of them die out upward. Thus a fault strand that seems to be overlain by an apparently undisturbed deposit is not necessarily older than the deposit. No consistent relation was found between the amount of fault displacement and the occurrence of obscure segments or strands that die out upward. Most obscure segments occur on faults with small displacement, but many occur on faults with displacements >1.5 m. A large fraction of obscure segments occur in coarse-grained materials and soil horizons. Most obscure segments are of substantial length, with nearly 60% of them longer than 0.3 m and about 20% of them longer than 1 m. A manuscript on these and other characteristics of active faults exposed in exploratory trenches is in preparation.

2. An Open-File report on the Guinea, west Africa earthquake of December 22, 1983 was prepared. The Open-File report was modified for publication in a journal.

Reports:

Bonilla, M.G., Mark, R.K., and Lienkaemper, J.J., 1984, Statistical relations among earthquake magnitude, surface rupture length, and surface fault displacement: Seismological Society of America Bull., v. 74, no. 6, p. 2379-2411.

Harms, K.K., Clark, M.M., Rymer, M.J., Bonilla, M.G., Harp, E.L., Herd, D.G., Lajoie, K.R., Lienkaemper, J.J., Mathiesen, S.A., Perkins, J.A., Wallace, R.E., and Ziony, J.I., 1984, The search for surface faulting, in Bennett, J.H., and Sherburne, R.W., eds., The 1984 Morgan Hill, California earthquake: California Division of Mines and Geology Special Publication 68, p. 149-160.

Langer, C.J., Bonilla, M.G., and Bollinger, G.A., 1985, Geologic and seismologic field studies following the Guinea, west Africa, earthquake of December 22, 1983 [abs.]: Earthquake Notes, v. 55, no. 1, p. 22.

Langer, C.J., Bonilla, M.G., and Bollinger, G.A., 1985, The Guinea, west Africa, earthquake of December 22, 1983--Reconnaissance geologic and seismologic field studies: U.S. Geologic Survey Open-File Report 85-282.

Lienkaemper, J.J., 1984, Comparison of two surface-wave magnitude scales: M in Gutenberg and Richter (1954) and M_s of Preliminary Determination of Epicenters: Seismological Society of America Bull., v. 74, no. 6, p. 2357-2378.

SOIL DEVELOPMENT AND DISPLACEMENT ALONG THE HAYWARD FAULT

14-08-0001-21929

Glenn Borchardt
California Department of Conservation
Division of Mines and Geology
380 Civic Drive
Pleasant Hill, CA 94523-1997

(415) 671-4926

Investigations

Its high rate of activity (>5 mm/yr) and urban location make the Hayward fault potentially the most destructive in the San Francisco Bay Area (Steinbrugge and others, 1985). The fault may be due for a major earthquake--the most recent occurred on the southern segment 117 years ago, while the most recent on the northern segment occurred at least 149 years ago. The objective of this work is **to use soils and sediments to determine the recurrence interval and the amount of displacement to be expected for major earthquakes on the Hayward fault.**

This phase of the investigation concentrated on developing background information and doing the reconnaissance for site selection. Consultants' reports on sites within the Alquist-Priolo Special Studies Zone were evaluated for precise fault locations and for information on soil sites that might yield information on displacement history and recurrence interval. In addition to the Point Pinole site, the Niles alluvial cone was selected for detailed study. A late Holocene soil was described and sampled in Fremont and the late Holocene deposits in the Alameda Creek area in Niles were examined for evidence of faulting.

Work is continuing at the Point Pinole study site. A precise map of fault location is being prepared through evaluation of cultural features and geomorphic evidence. Two transects were bored at 1-m intervals across the fault in Reyes silty clay loam in the tidal marsh. A late Quaternary section containing a well drained Holocene soil and a paleosol offset by a subsidiary fault were described in the sea cliff northeast of the fault. Samples for carbon dating have been obtained from a landslide at the northwest end of the fault, and from a buried A horizon and a peat deposit from the tidal marsh.

Results

1. Of 339 seismic investigations performed within the Alquist-Priolo Special Studies Zone along the Hayward fault, 46 report evidence for offset soils. Fully half of these offset soils occur in the late Holocene alluvium in the Niles quadrangle. The upper 2 m of the alluvium near Alameda Creek appears to be less than 2,000 years old. For these reasons the Niles cone has been chosen as the second site for detailed study. Exposures at Alameda Creek Quarries were examined for evidence of soil development and fault displacement. Although there is clear evidence for fault creep in the streets to the northwest, the artificial fill overlying the offset sand and gravel deposits in the quarry does not appear to be disturbed. The interbedded silt and sand units reported in consultants' reports from the Niles cone probably are indicative of young alluvial soils useful for determining recurrence interval and displacement per event.

2. Curb offsets at 608 Banks, 613 Banks, and 704 Phanor in Parchester Village south of Point Pinole averaged 15 cm on 3/21/85. Offset from 1950 to 1971 was 11 cm. By this measure, the aseismic creep rate on this part of the fault appears to have decreased from about 5 mm/yr to about 3 mm/yr during the last decade.

3. Borings across the fault in the tidal marsh at the Point Pinole study site reveal an Ab/Bgb/Bkcgb/Cb sequence overlain by 60 cm of young alluvium on the east side of the fault and a Bgb/Bkcgb/Cb sequence overlain by 100 cm of bay mud and salt pan deposits on the west side. The youngest deposits overlying the fault may correlate with bay mud deposits overlying a distinctive peat layer that occurs at a depth of 30 cm throughout the marsh. Bay mud deposits in the northwest portion of the marsh appear to dip gently toward the fault. During the next phase of the tidal marsh study we will explore the possibility that the dense collection of modern driftwood in this area has accumulated in response to subsidence that occurred during the 1836 earthquake. Samples of the peat and of the buried A horizon will be submitted for carbon dating.

Publications in Preparation

Borchardt, Glenn, 1986 (forthcoming), Smectites, in J. B. Dixon and S. B. Weed, eds., Minerals in soil environments (2nd edition): Soil Science Society of America, Madison, WI.

Borchardt, Glenn, and Hill, R. L., 1985 (in press) Smectitic pedogenesis and late Holocene tectonism along the Raymond fault, San Marino, California, in D. L. Weide and M. L. Faber, eds., Soils and Quaternary geology of the southwestern United States: Geological Society of America Special Paper 203.

Steinbrugge, K. V., Davis, J. F., Lagorio, Henry, Bennett, John, Borchardt, Glenn, and Toppozada, Tousson, 1985 (forthcoming), Earthquake planning scenario for a magnitude 7.5 earthquake on the Hayward fault: California Division of Mines and Geology Special Publication.

Applied Global Tectonics

9950-03899

C. G. Bufe
Branch of Engineering Geology and Tectonics
U.S. Geological Survey
Box 25046, MS 966 Denver Federal Center
Denver, CO 80225
(303) 236-1585

The objective of this project is an improved understanding of occurrence patterns of earthquakes and volcanic eruptions in time and space through the development and testing of deterministic recurrence and triggering models.

Investigations

1. Annual and longer period occurrence patterns of earthquakes and volcanic eruptions are being examined and implications for recurrence models assessed.

2. Space and time variations in magnitude-frequency relations and their implications for earthquake recurrence and prediction are being assessed in collaboration with J. H. Pfluke in Menlo Park and A. M. Rogers in Golden.

Results

Examination of annual variations in earthquake and volcano activity has shown the presence in several regions of significant minima in activity near mid-year. This is a time of annual acceleration in earth rotation resulting from angular momentum transfer between the atmosphere and the solid Earth. Longer-term patterns of earthquake recurrence and volcano repose time show evidence of site-specific triggering at periods near 11 years and 22 years. These periods correspond to the sunspot and the Hale heliomagnetic cycles respectively, suggesting trigger mechanisms based on solar-terrestrial interactions. Evidence of paleoclimatic variations near these periods has been derived by several investigators from tree ring, ice core, and varve data. Other investigators have detected the 11-year period in earth rotation variations and global seismic energy release. A global model relating local phase of event triggering to latitude and principal stress orientation is currently being tested.

Report

Bufe, C. G., 1984, Possible solar influence on repeat times of Parkfield, California earthquakes: Earthquake Notes, v. 55, no. 1, p. 16.

DETAILED GEOMORPHIC STUDIES TO DEFINE LATE QUATERNARY FAULT BEHAVIOR AND SEISMIC HAZARD, CENTRAL NEVADA SEISMIC BELT

Contract #21970

William B. Bull, Julia Fonseca, and Suzanne Hecker
Department of Geosciences
University of Arizona
Tucson, AZ 85721
(602)621-6024

Investigations

1. Hecker completed detailed age analysis of Holocene fault scarps along the eastern base of the Stillwater Range, at the northern end of the 1954 Dixie Valley surface rupture and the southern portion of the Stillwater seismic gap (see Fig. 1). Dating methods involved a) diffusion-equation modeling of scarp-profile data, using the diffusivity constant determined for Lake Bonneville and Lahontan shoreline scarps (Hanks and others, 1984; Hanks and Wallace, in press); b) estimation of faulted and unfaulted surface ages through quantified soil-profile field descriptions (after Harden, 1982) and comparisons to dated soils in the area; and c) use of a buried ash unit to calibrate rates of sedimentation in a small graben formed during Holocene faulting. The magnitude of the prehistoric earthquake was estimated using the moment-magnitude relationship of Hanks and Kanamori (1979). Measurements of fault plane dip and focal depth for the 1954 earthquake allowed approximation of the seismic moment.

2. Fonseca studied patterns of Quaternary faulting around the Sou Hills, a transverse bedrock structure at the southern end of the 1915 Pleasant Valley earthquake rupture.

Results

1. The three independent dating techniques (see #1 above) yielded mutually consistent results, suggesting that large magnitude faulting occurred 2.7-3.2 ka along the eastern Stillwater Range front. Given dating resolution, the timing of prehistoric Holocene faulting was synchronous in the historically ruptured and unruptured positions of the Stillwater Range, suggesting that the historical pattern of incremental filling of the Central Nevada seismic belt (CNSB) with successive, large events may continue and eventually close the Stillwater seismic gap.

The size of the prehistoric earthquake is estimated to be M_w 7.2-7.5. The former estimate uses a total rupture length of $\sim$40 km, the length of the set of nearly continuous prehistoric Holocene scarps. The latter estimate assumes that the entire 80 km Stillwater Range front ruptured simultaneously.

Earliest Holocene soils are displaced no more than younger soils, indicating an absence of faulting during at least the first 8000 years of the Holocene. Average long-term recurrence intervals of 7-13 ka and 6-8 ka are estimated for the late Quaternary and late Cenozoic, respectively, based on cumulative offset of late Pleistocene alluvium and late Miocene basalts. In view of the observed variability of recurrence during the Holocene, individual return periods may vary considerably

from long-term average recurrence intervals. Conversely, average recurrence intervals should be used with caution when predicting actual return periods between faulting events.

2. Ongoing study of late Quaternary ruptures in the Sou Hills portion of the central Nevada seismic belt (CNSB) reveals a complex normal faulting style. The Sou Hills block is an area of uplifted Tertiary bedrock transverse to the north-south trend of the CNSB. In contrast to the pattern seen in adjacent segments of the CNSB, where ruptures are concentrated along well-defined mountain fronts, ruptures in the Sou Hills are distributed along faults both bounding and internal to the block, as well as along faults scattered across the piedmont. Individual rupture segments are characterized by shorter lengths (generally 1-2 km) and smaller displacements (less than or equal to 1 m) as compared to the more continuous ruptures of several meters offset found along the adjacent Tobin and Stillwater Ranges.

Studies of historic normal faulting events such as the 1915 Pleasant Valley earthquake (Wallace, 1984) and the 1983 Borah Peak earthquake (Crone and Machette, 1984) seem to indicate that this style of discontinuous, spatially distributed faulting typifies ruptures which die out in transverse bedrock structures. If these historic events may serve as analogues, then the pattern of prehistoric faulting suggests that ruptures have repeatedly died out in the Sou Hills structure.

Other evidence that ruptures propagating along the Tobin and Stillwater Ranges often die out in the Sou Hills comes from analysis of landform parameters that reflect rates of relative uplift. Using measurements of mountain front sinuosity, the ratio of valley floor widths to heights, and triangular facet stages, mountain front segments have been classified on the basis of relative tectonic activity. Both the Stillwater and Tobin Range show a decline in activity where they join the Sou Hills.

Furthermore, late Cenozoic geologic displacements of pre-extension basalts and a decline in basin fill thickness towards the Sou Hills suggest that the total amount of tectonic offset is considerably less in the Sou Hills segment as compared to adjacent segments of the CNSB.

A change in the sense of Quaternary fault displacement from down-to-the-east to down-to-the-west occurs within the Sou Hills, but no through-going fault appears to link the two zones. This, together with the fact that the 1915 rupture ends just north of this transition (Wallace, 1984), may indicate that the Tobin and Stillwater Range fronts do not rupture simultaneously. Transverse structures like the Sou Hills may be an important factor in limiting the size of earthquakes, as suggested by Zoback (1983).

References

Crone, A.J., and Machette, M.N., 1984, Surface faulting accompanying the Borah Peak earthquake, central Idaho: Geology, v. 12, p. 664-667.

Hanks, T.C., and Kanamori, H., 1979, A moment magnitude scale: Journal of Geophysical Research, v. 84, n. B5, p. 2348-2360.

Hanks, T.C., Bucknam, R.C., Lajoie, K.R., and Wallace, R.E., 1984, Modification of wave-cut and faulting-controlled landforms: Journal of Geophysical Research, v. 89, p. 5771-5790.

Hanks, T.C., and Wallace, R.E., 1984, Morphological analysis of the Lake Lahontan shoreline and Beachfront fault scarps, Pershing County, Nevada: Seismological Society of America Bulletin, in press.

Harden, J.W., 1982, A quantitative index of soil development from field descriptions: examples from a chronosequence in central California: Geoderma, v. 28, p. 1-28.

Wallace, R.E., 1984, Fault scarps formed during the earthquake of October 15, 1915, Pleasant Valley, Nevada and some tectonic implications: U.S. Geological Survey Professional Paper 1274-A.

Zoback, M.L., 1983, Structure and Cenozoic tectonism along the Wasatch fault zone, Utah, in Tectonic and Stratigraphic Studies in the Eastern Great Basins, Geological Society of America Memoir 157, p. 3-27.

MAP LOCATION

PLEASANT VALLEY

1915

TOBIN RANGE

SOU HILLS

SEISMIC GAP

STILLWATER RANGE

DIXIE VALLEY

1954

HISTORIC SURFACE RUPTURE

SCALE
0   5   10
MILES

N

LOCATION MAP
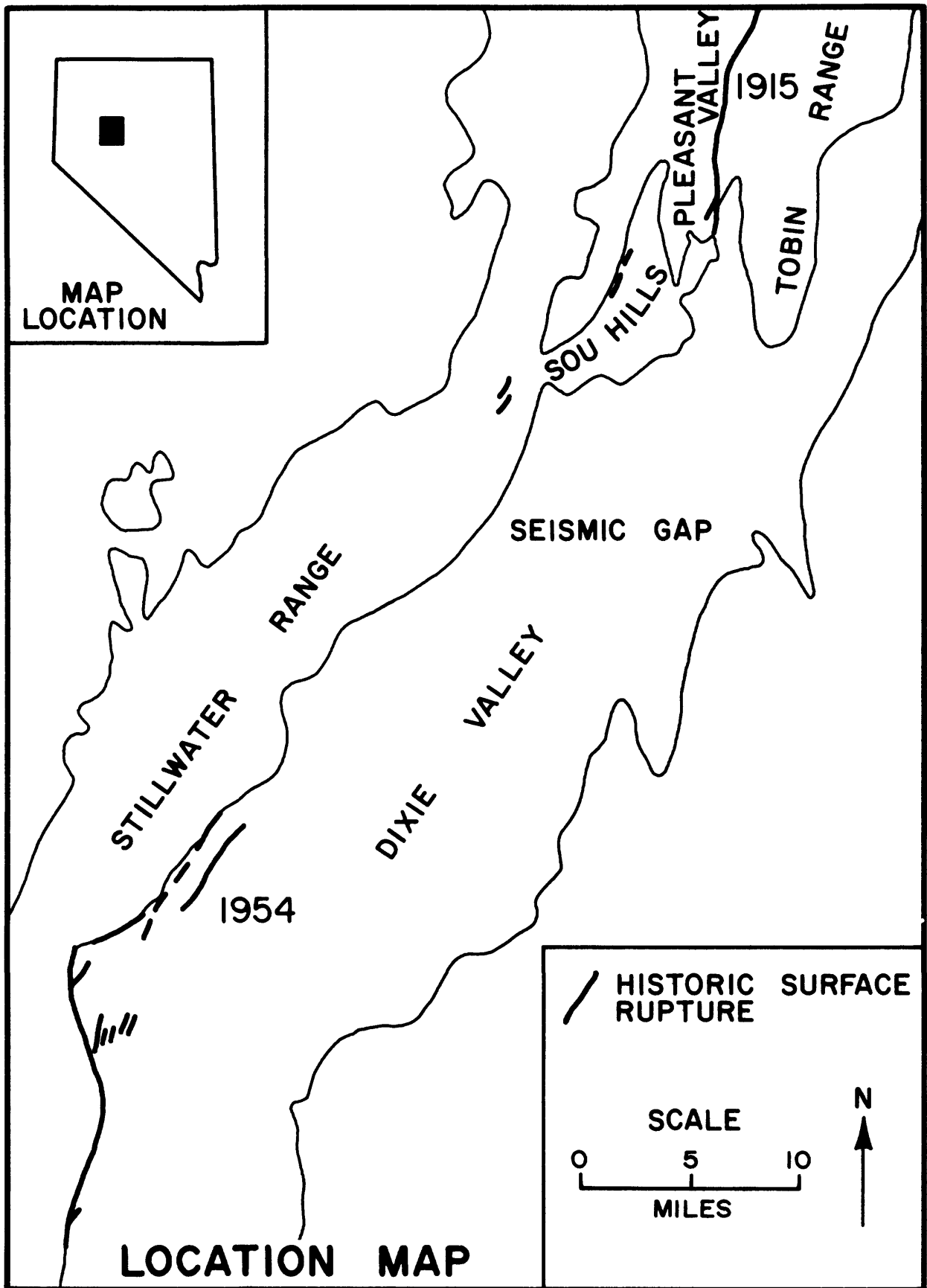
Figure 1

Holocene and Quaternary Geologic Studies

9540-03787

Robert O. Castle
Branch of Western Regional Geology
345 Middlefield Road MS 975
Menlo Park, CA 94025
(415) 323-8111, ext. 2353

Investigations

1. Continued investigations, data analyses, and preparation of report on historic surface deformation in the Salton Trough and adjacent parts of southeastern California--a report which emphasizes the contrast in contemporary tectonic activity between southeastern California and southwestern Arizona.

2. Continued preparation and editing of two reports on the magnitude and predictability of the so-called unequal-refraction error in geodetic leveling.

Results

Comparisons among the results of repeated geodetic levelings in the Salton Trough, with respect to a tectonically invariant San Diego reference mark, reveal both considerable variability and complexity in the nature and range of vertical displacements throughout southeastern California, even during the relatively short, approximately 80-year span of the historic record. Regional patterns of vertical crustal deformation in the Salton Trough have changed markedly through both space and time and variously involve periods of relative tectonic quiescence, abrupt episodes of accelerated aseismic movement and tilting and periodic reversals in tilt direction. The detailed vertical displacement histories of many individual bench marks are commonly characterized by a long-term trend or tilt that reflects an apparent continuation of trends recognized in the latest Quaternary geologic record. Cumulative regional geodetic trends define a net structural deepening in the Salton Sea area, but most other areas, including both the Coachella Valley and the Imperial Valley, have sustained significant net uplift during the period of historic record. Moreover, contemporary crustal movement in southeastern California has actually ranged broadly beyond the Salton Trough and involves considerable historic uplift and tilting within a relatively aseismic portion of the southern Peninsular Ranges extending nearly as far west as the metropolitan San Diego area. The magnitude of cumulative uplift declines rapidly east of the Colorado River but persists as several relatively irregular steps as far east as The Gila Mountains, about 70 km east of Yuma. With the possible exception of the effects of compaction-induced subsidence attributable to localized ground-water withdrawls, no significant vertical displacements have otherwise occurred along the reach from the Gila Mountains to the Hassayampa area. These geodetic comparisons are thus consistent with the general absence of any historic seismicity and the geologically inferred stability within this part of southwestern Arizona.

In many places, particularly in the Imperial Valley, the long-term
geodetic trend has been periodically or cyclically interrupted by abrupt and
rapidly developed, short-term pulses of uplift and subsequent partial
collapse, specifically during the 1930s and in the 1970s. The overall gross
similarities in both the timing and character of these pulses, which are
regionally widespread and range in magnitude up to about 0.4 m, suggest that
these patterns may somehow be associated with subsequent large-magnitude
earthquakes along the Imperial fault in 1940 and again in 1979. A more
localized episode of accelerated surface tilting may have preceded the 1968
Borrego Mountain earthquake along the San Jacinto fault in the epicentral
region west of the Salton Sea. Localized vertical crustal deformation and/or
pronounced tilting has continued along or adjacent to other active fault zones
throughout southeastern California inlcuding the Imperial, Brawley, San
Jacinto, San Andreas, and La Nacion faults. There is additional evidence from
the geodetic record obtained from both the Salton Trough and the Peninsular
Ranges of contemporary aseismic activity or vertical offset along several
mapped faults not otherwise known to have sustained historic displacement, and
for progressively increasing, but narrowly restricted, active fault-like
movement in areas where no known faults have been mapped. Regionally
widespread uplift during the mid-1970s in southeastern California was
temporally coincident with widespread uplift during this same period in other
parts of Southern California. At its probable culmination around 1974,
broadly developed crustal swelling straddled the entire plate margin from the
southernmost Coast Ranges, across the Transverse Ranges and the Big Bend
region of the San Andreas fault, through the Salton Trough and was apparently
increasing in magnitude when last seen heading south across the International
boundary.

Reports

Castle, R. O., Elliott, M. R., Church, J. P., and Wood, S. H., 1984, The
evolution of the southern California uplift, 1955 through 1976; U.S.
Geological Survey Professional Paper 1342, 136 p.

Castle, R. O., Elliott, M. R., and Gilmore, T. D., 1985, An early 20th-century
uplift in southern California: U.S. Geological Survey Professional Paper
1362 (in press).

Castle, R. O., Gilmore, T. D., Mark, R. K., and Shaw, R. H., 1985, Empirical
estimates of cumulative refraction errors associated with procedurally
contrained levelings based on the Gaithersburg-Tucson refraction tests of
the National Geodetic Survey: (approved by Director)

LATE QUATERNARY SLIP RATES ON ACTIVE FAULTS OF CALIFORNIA

9910-03554

Malcolm M. Clark
Branch of Engineering Seismology and Geology
U.S. Geological Survey
345 Middlefield Road, MS 977
Menlo Park, CA 94025
(415) 323-8111, ext. 2591

Investigations

1. Late Quaternary traces of the Calaveras fault in the epicentral area of the 1984 Morgan Hill earthquake (K.K. Harms, M.M. Clark).

2. The Nunez fault near Coalinga (M.J. Rymer, J.J. Lienkaemper).

3. Holocene history of Lone Pine fault, Owens Valley (L.K.C. Lubetkin, USFS; M.M. Clark).

4. Continuing investigation of late-Quaternary slip rates along California faults for update of slip rate table and map (M.M. Clark, J.J. Lienkaemper, K.K. Harms).

Results

1. In April we checked lineations and mapped traces east of the active trace of the Calaveras fault in search of any recent movement. The 1984 Morgan Hill earthquake seismicity is systematically offset to the east of the mapped active trace and prompted this search. We checked Dibblee's (1972) East Branch Calaveras fault and its splay to the west at all road crossings from northeast of San Felipe Valley to the notch east of hill 2477, south of Henderson Ridge. We checked Dibblee's Madrone Springs fault in Packwood Valley and on the road to the north and above the valley, as well as unmapped lineations east of San Felipe Valley. We did not find any preserved ground rupture associated with the 1984 Morgan Hill earthquake, nor any unequivocal evidence for recent movement.

2. Clastic dikes are exposed parallel to and only in the hanging wall of the Nunez fault. Some dikes are truncated at the base of a Quaternary terrace deposit and other dikes intrude the deposit. All clastic dikes checked in the area have similar mineralogies to that of the local Great Valley sequence sandstones, the inferred source beds. The clastic dikes were apparently to be caused by the strong shaking of earthquakes and, if so, indicate that large earthquakes on the Nunez fault both predate and postdate deposition of the Quaternary terrace. The age of the terrace deposit is inferred to be tens to hundreds of thousands of years old, from its position 20 m above the bed of Los Gatos Creek and a ^{14}C age of 1800 yr in deposits only 1 m above the creek.

Analysis of trench walls in the modern flood plain of Los Gatos Creek gives an approximation of recency of pre-1983 movement on the Nunez fault. A 10 cm high monoclinal flexure developed at the trench site in the 1983 earthquake sequence. Fine-grained strata exposed in the trench walls show this 10 cm flexure, but no additional offset. ^{14}C ages of sediments exposed in the trench are 140+230 and 255+220 yr at depths of 0.5 to 0.9 m and 1800+124 yr at 2.1 m depth. The ^{14}C ages and lack of any offset greater than the 10 cm developed in 1983 indicate no large earthquakes on the Nunez fault in the last 1,700 to 1,900 yrs.

3. The Lone Pine fault is a north-trending secondary break in the Owens Valley fault zone, 1.4 km west of Lone Pine, Calif. This fault forms a proiminent east-facing scarp across an abandoned fan of the Tioga (latest Pleistocene) glaciation, and was the site of significant displacement during the 1872 Owens Valley earthquake. Knowledge of the character and amount of slip at this site in 1872 may be of value in assessing earthquake potential in this region and in other parts of the Great Basin.

   Dip slip along this scarp from the 1872 earthquake was 1 to 2 m. A young debris flow that crosses the scarp has been offset 6 to 7 m right laterally and 1 to 1.5 m vertically, apparently in 1872. Average total dip slip of this fan surface is about 5.5 m. About three 1872-size earthquakes could have produced the scarp. This number of events is also indicated by desert varnish patterns on boulders in the fault scarp and by scarp morphology. An average recurrence interval for three such events is 3,300 to 10,500 yrs. This estimate is based on the age of the fan surface, which is bracketed by a 21,000 year-old shoreline of Lake Owens, and by the time of abandonment of the fan, about 10,000 years ago. This average recurrence interval, combined with the total 1872 offset of the debris flow, gives an average late Quaternary slip rate of 0.6-2 mm/yr for the Lone Pine fault. The average recurrence interval applies to the Lone Pine fault only, rather than to the Owens Valley fault zone as a whole. Other fault scarps near Lone Pine suggest that earthquakes occur in this region more frequently than every 3,300 to 10,500 years.

4a. Increased use of late Quaternary slip rates has produced better tectonic analyses and earthquake hazard estimates, yet we are concerned that users may lose sight of the significant limitations in most slip rates. Slip rates (slip/time) are deceptively simple, but estimates of both slip and time generally include crucial assumptions and significant measurement errors.

   The principal sources of uncertainties in measurements of slip are (1) imprecise boundaries to the features that have been offset, (2) measurements that fail to span the entire zone of faulting or deformation, (3) no measurement for one of the components of slip, and (4) incorrect identification of apparently offset features.

Most estimates of elapsed time have large uncertainties. Dates commonly must be obtained indirectly from associated deposits or features, and involve assumptions about that association. Such dates generally bracket the elapsed time, often by wide margins. Dating techniques themselves may contain major assumptions and analytical uncertainties. In addition, if recurrence interval is large relative to the time period, a major uncertainty in slip rate arises if the measured time period does not begin and end at the same place on an assumed earthquake recurrence cycle.

Estimates of both slip and elapsed time should include minimum and maximum allowed by the data. These extremes should be combined to produce the extreme ranges of resulting slip rate. Those who report slip rates should fully disclose and discuss all aspects of methods, assumptions, and uncertainties that produced those rates. They should also evaluate the quality of the slip and age estimates, and, where possible, give a qualified opinion, based on experience and judgment, of preferred value if the range of slip rates is large.

Slip rates will improve as more and better data become available. For now, we urge those who use slip rates to use caution and common sense and to clearly identify how uncertainties affect their results.

4b. Quaternary faults of California as compiled by Jennings (1975) were scanned by an automatic laser digitizer by U.S. Geological Survey National Mapping Division in a cooperative cartographic experiment with the Branch of Engineering Seismology and Geology. Using computer programs for raster to vector conversion and for inverting the original fault map projection grid, the Quaternary fault traces were made generally available for computer driven plotting (Lienkaemper, 1985).

c. J.J. Lienkaemper's compilation of all historic slip rates in California at a minimal data standard is nearing completion for northern and central California. Two goals have been set for this study: (1) to estimate the macroseismic slip fraction for late-Quaternary faults in California, (2) to identify important segments of late-Quaternary faults in California for which no reliable historic slip indicators yet exist. Historic slip-rate data standards cannot be improved using only published sources; the oldest slip indicators need to be carefully reevaluated and freshly measured and documented in several cases. Several important segments of late-Quaternary faults do require installation of slip indicators such as quadrilaterals.

d. Investigation by literature review of afterslip on reverse faults other than the Nunez uncovered a mistaken report of afterslip in the 1971 San Fernando earthquake, California. A 42 cm difference in Little Tujunga Canyon reported by Savage, Burford and Kinoshita (1975) was actually attributable to mistaking a backsight (Lienkaemper and Burford, 1985). The afterslip at line N2 (>6 cm) at Nunez fault is therefore the largest reported for a reverse fault within 50 m of a surface rupture.

Reports

Lienkamper, J.J., 1985, Quaternary fault map of California in digital format: U.S. Geological Survey Open-File Report 85-211, 14 p.

Lienkamper, J.J., and Burford, R.O., 1985, No large afterslip in Little Tujunga Canyon following the 1971 San Fernando earthquake: Bulletin Seismological Society America, v. 75, no. 2, p. 627.

Lubetkin, L.K.C., and Clark, M.M., 1985, Late Quaternary activity along the Lone Pine fault, eastern California: U.S. Geological Survey Open-File Report 85-290, p. 118-140.

Rymer, M.J., in press, Estimation of late Quaternary activity on the Big Valley fault, Lake County, California, in Sims, J.D., ed., Geological Society of America Special Paper.

Rymer, M.J., W.L. Ellsworth, eds., 1985, Mechanics of the May 2, 1983 Coalinga, California earthquake: U.S. Geogical Survey Open-File Report 85-44, 438 p.

Rymer, M.J., Roth, Barry, Bradbury, J.P., and Forester, R.M., in press, Depositional environments of the Cache, Lower Lake, and Kelseyville Formations, Lake County, California, in Sims, J.D., ed., Late Quaternary climate, tectonism, and sedimentation in Clear Lake, northern California Coast Ranges, Geological Society of America Special Paper.

Sims, J.D., Rymer, M.J., and Perkins, J.A., in press, Late Quaternary deposits beneath Clear Lake, California--physical stratigraphy, age, and paleogeographic implications, in Sims, J.D., ed., Geological Society of America Special Paper.

Dating Holocene Fault Movements in East-central
Idaho using Primary Tephra

14-08-0001-21992

B. Cochran, K. Sprenke and P. Sablock
Department of Geology
University of Idaho
Moscow, ID 83843
(208)885-7977

Investigations:

The goals of the investigation are to locate offset tephra
along the Lost River Range fault system in south central Idaho.
These offset tephra will be used to measure and date late
Quaternary faulting in the area. A second goal of this project is
to establish a late Quaternary tephrochronology of the study area.

Results:

1. The initial phase of this project involved the construction of
   a hand operated, 10.0 cm diameter, modified Livingston soft
   sediment coring sampler capable of extracting up to thirty
   meters of lake sediment, in two meter sections.

2. Several high altitude lakes, in south-central Idaho, were
   cored during the winter months of 1985. The purpose of this
   coring was to provide a complete late Quaternary
   tephrochronological and sedimentological record of the area.
   The lakes were selected on the basis of low estimated
   sedimentation and high organic production. We estimate that
   niether lake is older than the last major glacial advance,
   probably about 15,000 years B.P. Ten meters of continuous,
   overlapping, core were extracted from Little Redfish Lake in
   the Stanley Basin. A single, non-overlapping, twenty meter
   core section was extracted from Jimmy Smith Lake near Challis,
   Idaho, before weather conditions forced a shutdown of
   operations. Additionally, exposures of late Quaternary alluvium
   and colluvium in the Challis area, which contained tephra,
   were sampled and documented.

3. The core sections from Little Redfish Lake have been
   examined, described and documented. Initial petrographic
   analysis of the sediments reveals the presence of four tephra,
   one of which is possibly reworked. About sixteen organic
   samples, bounding the tephra, have been collected for
   radiocarbon dating. Electron microprobe analyses of the glass

shards in the various tephra has begun. Neither the radiocarbon dates nor the results of the microprobe analysis are available at this time.

4. Preliminary petrographic analysis of the four tephra found in the Little Redfish Lake core indicate the presence of a tephra layer petrographically identical to Mt. Mazama layer O (ca. 6700 BP). There is one primary tephra below the Mazama layer which appears to resemble various Glacier Peak tephra deposited between ca. 14,000 and 11,000 BP. Another tephra, stratigaphically superior to the Mazama layer, is petrographically similar to the younger Mt. St. Helens ejecta. The fourth tephra, lies above the Glacier Peak layer and is, as yet, unidentified. This tephra is contained in a turbidite sequence and has been reworked. Preliminary analysis of this tephra indicates that it is unlike any of the other tephra and may be derived from pre-Holocene ash deposits.

Continuing Research:

Field investigations along the Lost River fault system will begin early in the summer of 1985. These investigations will focus on locating primary and secondary tephra deposits along the Willow Creek scarp.

Presentations:

Cochran, B. and Sprenke, K., 1984, Dating of Holocene Fault Movements in east-central Idaho using Primary Tephra: USGS Workshop XXVII on the Borah Peak Earthquake, Sun Valley, Idaho, October 1984.

Earthquake Hazard Investigations in the Pacific Northwest

14-08-0001-21862

R.S. Crosson
Geophysics Program
University of Washington
Seattle, WA 98195
(202) 543-8020

Investigations

The objectives of this research are to provide fundamental data and interpretations for earthquake hazard investigations. Currently, we are focusing on seismicity, structure, and tectonic questions related to the occurrence of a hypothetical major subduction earthquake on the Juan de Fuca - North American plate boundary. Specific tasks which we have worked on in this contract period are:

1. Analysis and interpretation of Pn observations for both eastern and western Washington

2. Development and implementation of automated processing of seismic events using digital network data

3. Development of a revised crustal structure model for the greater Puget Sound Region

4. Locations, focal mechanisms and occurrence characteristics of crustal and subcrustal earthquakes beneath western Washington and their relationship to subduction processes

Results

1. Previously reported results from Pn analysis are being prepared for publication by C. Zervas and R. S. Crosson.

2. Our algorithm for automated phase and coda length picking is operating in a testing and verification mode. The routine performs well for events above a specific size. We anticipate that the autopicking will improve our network magnitude calibration by providing quantitative and consistent estimates of coda lengths. We are calibrating auto-processed coda duration measurements to Wood-Anderson amplitude measurements for the purpose of improving the consistency and accuracy of local magnitude determinations. Use of automatic processing in routine network data analysis appears feasible and we will begin trial implementation soon.

3. Using auto-picked digital data for 58 seismic events (48 earthquakes, 10 explosions), we inverted for a coupled P and S velocity model for the greater Puget Sound region. The final model, although similar to our previous model in the depth range from about 12 km to 30 km, has a thinner surface layer of velocity 5.4 km/sec and a slight velocity reversal in the interval 30-40 km. km. The constraint on the velocity in the 30-40 km depth range, an earthquake free zone, with our new model appears to be better than that previously obtained. This structure inversion effort is preliminary to undertaking a reexamination of deep earthquake seismicity.

4. Various studies of PNW focal mechanisms have been undertaken previously, but no system has been established to comprehensively compile and classify all available mechanisms. Therefore, we are creating a data base of events for which focal mechanisms have been determined and trace data checked. A search is also being made to identify other events for which focal mechanisms

can be determined and to compile a comparatively complete data base of focal mechanisms. To date, evidence from focal mechanisms is difficult to reconcile with regional stress; focal mechanism data seem to favor NS compression rather than the N70E direction predicted on the basis of geodetic strain measurements, or the N50E direction of plate convergence determined from ocean-floor magnetic anomalies. Focal mechanisms are observed that reflect stress orientations which contradict the expectation from locked subduction. If earthquakes occur on preexisting fractures which are planes of weakness, then the apparent stress direction from focal mechanisms does not necessarily define the true stress direction (McKenzie, 1969). McKenzie made the single assumption that the slip vector is always parallel to the direction of resolved shear stress in the fault plane. Using this assumption, for a particular ratio of principal stresses and a particular fault surface, all allowable orientations of true principal stress can be defined. In the extreme case, the actual axis of greatest principal stress may be as much as 90 degrees away from the apparent axis determined by the P axis of a focal mechanism. Recently, Gephart and Forsyth (1984) have devised a method of determining tectonic stress orientation, which also gives information about the ratio of principal stresses. This method depends on a statistical distribution of focal mechanisms and uses physical principles stated by McKenzie (1969) in addition to a 'minimum rotation' criteria. We have begun implementation of their analysis programs. This method, or a modification of it, promises to provide a powerful tool for extracting stress information from focal mechanism data; and may help resolve the question of tectonic stress in the Pacific Northwest margin area.

Articles:

Crosson, R.S., 1985 (in preparation), A New Algorithm for Automated Determination of Phase Arrival Times and its Application to Regional Network Data, to be submitted to B.S.S.A..

Noson, Linda Lawrance, Ruth S. Ludwin, Robert S. Crosson, 1985, Compilation of Earthquake Hypocenters in Western Washington - 1979, State of Washington Department of Natural Resources, Information Circular 79.

Ludwin, R. S., S.D. Malone, R.S. Crosson, 1985 (in press), Washington Earthquakes 1983, National Earthquake Information Service.

Zervas, C.E., and R.S. Crosson, 1985 (in preparation), Pn Observations and Interpretations in Washington.

Abstracts:

Zervas, C., and R.S. Crosson, Pn velocities and station delays in Washington, EOS, 65, no. 17, p. 330, 1984.

Ludwin, R. S. and R.S. Crosson, The Azimuth of Regional Tectonic Compression in the Pacific Northwest from Shallow Thrust Earthquakes, EOS, 65, no. 45, p. 986, 1984.

Reports:

Univ. of Wash. Geophysics Program, 1985, Regional Seismic Monitoring in western Washington and Earthquake Hazard Investigations in the Pacific Northwest, 1983-1984 Final Technical Report U.S.G.S. Contracts 14-08-0001-21861 14-0001-21861.

Univ. of Wash. Geophysics Program, 1984, Quarterly Network Report 84-C on Seismicity of Washington and Northern Oregon July 1 through September 30, 1984, 25p.

Univ. of Wash. Geophysics Program, 1984, Quarterly Network Report 84-D on Seismicity of Washington and Northern Oregon October 1 through December 31, 1984, 23p.

Soil Development as a Time-Stratigraphic Tool

9540-03852

Jennifer W. Harden
Branch of Western Regional Geology
U.S. Geological Survey
345 Middlefield Road, MS 975
Menlo Park, California 94025
(415) 323-8111 ext. 2039

Investigations

1. The first objective of this project is to use soil development as age control for studies on the recency and timing of tectonic events. Geomorphic surfaces that have been offset by faults are correlated across the fault and approximately dated by the degree of soil development. In some studies, the surfaces include both Pleistocene and Holocene deposits, thereby providing information on the evolution of fault activity.

2. The second objective is to develop methods for sampling and data analysis to (a) establish rates of soil development in areas where soils have been studied and dated radiometrically; (b) test comparability of development rates between different geographical and geologic settings; and (c) establish statistical methods for estimating the ages of deposits based on soil development and calibration curves.

3. These methods are to be applied in areas along faults such as the San Andreas and Calaveras (in conjunction with J. C. Matti and M. M. Clark, U.S. Geological Survey; FY-85, 86).

Results

1. Soils sampled near Tres Pinos, Palo Alto and Yucaipa in 1984 were prepared and analysed for particle size, bulk density, dithionite iron and percent magnetite. Approximately 150 samples were analyzed for a total of about 600 samples runs (M. J. Singer, P. Janitzky, J. Aniku contract number (4-9540-0074).

2. A statistical method has been devised for the computer for estimating rates of soil development and for comparing rates in different areas. Soil parameters are plotted against deposit age in calibration areas, and statistical methods are used to estimate long-term rates of soil development. Ordinary least squares is not appropriate for soil studies, because this method assumes that there is no error in calibration dates.

A maximum likelihood estimate (MLE) procedure was designed to estimate long-term rates of soil development. The MLE method, designed by Paul Switzer (Stanford University) and programmed by Robert Mark (U.S.G.S.), assumes that soil variability may be different on different-aged surfaces and can be estimated by examining multiple soil profiles on a given-aged surface. The method also allows calibration dates to have uncertainties associated with them; ages with error are assigned to each surface according to radiometric dates with uncertainties from laboratory error and from geologic

considerations such as stratigraphic position of the dated material relative to the geomorphic surface. The slope of the curve, or rate of soil development, is similar to that obtained from a two-error regression.

Errors or uncertainties of the slope are estimated by a Monte Carlo resampling technique. This method involves resampling soil data, assuming that the data can be described by a Gaussian distribution. Each time a new data set is generated, the MLE method is used to estimated the slope or soil-development rate. The error associated with the slope are then estimated as the standard deviation of the 100 simulated slopes calculated from resampling.

To estimate the age of a surficial deposit from the degree of soil development, the same MLE method is used. Errors or uncertainties in the ages are calculated by resampling the soil data from the deposit of unknown age, as well as the calibration data. One hundred recalculations of the age are used to represent error bars of the age estimate.

Publications

Harden, J. W., 1984, Techniques and uncertainties in using soil development for stratigraphic, geomorphic, and age analyses (abs): Earthquake Notes, Vol. 55, no. 1, p. 7.

Harms, K. K., Harden, J. W., Hoose, S. N., and Clark, M. M., 1984, Estimating slip rates along Calaveras Fault, California, using soil chronology and geometry of stream terraces: Earthquake Notes, Vol. 55, no. 1, p. 9.

Singer, M. J. and Peter Janitzky, 198_ , A field and laboratory manual for a study on soil chronosequences: U.S. Geological Survey Bulletin No. 1648, p. 180, text figures 17.

Tectonics of Central and Northern California

9910-01290

William P. Irwin
Branch of Engineering Seismology and Geology
U.S. Geological Survey
345 Middlefield Road, MS 977
Menlo Park, CA   94025
(415) 323-8111, ext. 2065

Investigations

1. Preparation of a geologic map of the Klamath Mountains and adjacent areas, California and Oregon, at a scale of 1:500,000, for purposes of tectonic analysis of the region.

2. Revisions and final drafts of geologic maps of the Dubakella Mountain and Hyampom 15-minute quadrangles, California, following reviews by the Branch of Western Technical Reports.

3. Compilation of the geology of the Garberville 100,000-scale quadrangle, California, in cooperation with M.C. Blake and others.

4. Preparation of a geologic map of the Redding 2-degree sheet, California, in cooperation with J.P. Albers.

5. Preparation for outside publication of manuscripts entitled "Cryptic tectonic domains of the Klamath Mountains, California and Oregon" and, with C.D. Blome, "Significance of equivalent radiolarian ages from Cyprus and Oman."

Results

Project work has shed light on the tectonic problem of determining the time of accretion of the Klamath Mountains province to the North American continent. The numerous fragments of oceanic crust and island arcs that make up the Klamath Mountains province were joined together (amalgamated) in an oceanic setting during Paleozoic and Mesozoic tectonic events. They must have accreted to North America as a composite unit during latest Jurassic or earliest Cretaceous time before deposition of the Cretaceous Great Valley overlap sequence. Their time of accretion to North America would be ascertained most readily by direct observation of the boundary relations between the Klamath terranes and the continental bedrock, such as the development of a datable zone of metamorphism along the boundary or by the presence of datable plutons that crosscut the boundary. However, the boundary is concealed by a broad area of overlap sequences of Cretaceous and younger sedimentary and volcanic strata.

Paleomagnetic study of the problem, done in collaboration with E.A. Mankinen and C.S. Gromme, has so far yielded the best evidence for the time of accretion of the Klamath terranes to North America. The rocks drilled in the Eastern Klamath terrane generally show substantial clockwise rotation relative to stable North America; the Permian and Triassic strata have rotated about 100 degrees and the Jurassic about 50 degrees. During the last report period we drilled Shasta Bally batholith which is Early Cretaceous (135 Ma) in age and which cannot be more than a few million years older than the Lower Cretaceous (Hauterivian) strata of the overlap sequence that rest on the batholith's eroded surface. Previous study had shown that the Lower Cretaceous overlap sequence has rotated little--probably no more than 12 degrees. This led us to predict that Shasta Bally batholith, unlike other plutons that had been drilled in the Klamath Mountains, also would show little rotation.

The preliminary laboratory results obtained during the present report period indicate little rotation for Shasta Bally batholith. This lack of substantial rotation relative to stable North America and the similarity in this regard to the Lower Cretaceous overlap sequence suggests that the Early Cretaceous emplacement of Shasta Bally batholith approximates the time of accretion of the Klamath Mountains province to North America. These and other data also indicate that the time-honored concept of the Nevadan orogeny needs major revision.

Reports

Irwin, W.P., 1985, Cryptic tectonic domains of the Klamath Mountains, California and Oregon, in R. H. Jahns Memorial Volume: Elsevier Scientific Publishing Co., in press.

Blome, C.D., and Irwin, W.P., 1985, Significance of equivalent radiolarian ages from ophiolitic terranes of Cyprus and Oman: Geology, in press.

Mankinen, E.A., Irwin, W.P., and Gromme, C.S., 1984, Implications of paleomagnetism for the tectonic history of the Eastern Klamath and related terranes in California and Oregon, in Nilsen, T.H., ed., Geology of the Upper Cretaceous Hornbrook Formation: Society of Economic Paleontologists and Mineralogists, Pacific Section, v. 42, p. 221-229.

Coastal Tectonics, Western U.S.

9910-01623

Kenneth R. Lajoie
Branch of Engineering Seismology and Geology
U.S. Geological Survey
345 Middlefield Road, MS 977
Menlo Park, CA 94025
(415) 323-8111, ext. 2642

Investigations

1. Uplift and deformation of Pleistocene marine strandlines and deposits along the Palos Verdes fault, Los Angeles County, California.

2. Set up and computerize amino-acid geochronology laboratory. Inter- and intraspecies and outcrop variability of amino-acid analysis in fossil molluscan shells.

Results

1. Geomorphic and amino-acid data indicate that the "first terrace" mapped by Woodring in the San Pedro area (1946) consists of at least two and possibly as many as four separate marine terraces that may range in age from 85 ka-300 ka B.P. Woodring used the warm-water aspect of fossil molluscan faunas as a basis for correlating isolated or widely separated terrace remnants in the San Pedro area. However, the temperature aspect of the faunas may be controlled by local marine conditions (shallow embayment) rather than paleosea level. Consequently, the temperature aspect may not be a useful correlating tool for emergent terraces and subsurface strata in this area.

2. Amino acid data on fossil shells from about 30 m of deformed strata exposed in a road cut along Gibson Boulevard on the basin margin west of the fault may range from 300 ka-700 ka(?) B.P. This age range is probably represented by much thicker sections of strata in deeper parts of the basin east of the fault. Fossil shells from deep boreholes west of the fault are being analyzed to affect correlations across the fault and to determine relative fault displacement throughout late Holocene time. Preliminary analysis of well logs and sample cuttings from deep boreholes east of the Palos Verdes fault indicate that there may be unconformities in the late Pleistocene strata. Preliminary paleontological analysis of fossil molluscan fauna from these boreholes indicate that most of the strata were deposited under shallow-water conditions. Therefore, the depth of each assemblage may be a rough approximation of tectonic subsidence and sediment compaction.

Reports

None.

Neogene Paleomagnetic Stratigraphy, Transverse Ranges, California:
Timing and Deformation Rates of Potentially Active Faults

14-08-0001-21901

Shaul Levi
Geophysics, College of Oceanography
Oregon State University
Corvallis, Oregon 97331
(503) 754-2912

Neogene formations are widely exposed in parts of the Transverse Ranges, in areas undergoing rapid urbanization north and west of Los Angeles. These formations from oldest to youngest include the Modelo, Towsley, Pico and Saugus. Our paleomagnetic (PM) investigations of the continental Saugus Formation, in the East Ventura Basin along the Santa Clara River and transmission line sections at Castaic Junction, indicate that the Saugus was deposited mostly in the Matuyama reversed polarity epoch and is younger than 2.48 Ma (million years). The youngest Saugus exposed in both sections was deposited during the normal polarity Brunhes epoch and is younger than 0.7 Ma. Furthermore, our results indicate an average sedimentation rate of 0.9 km/Ma for both the transmission line and Santa Clara River sections. The marine Pico Formation in this area is less well suited for PM, and even most of its fine-grain horizons are severely overprinted. However, reversed sites from the upper Pico suggest that they, too, were deposited during the Matuyama. The sections of Pico Formation in Lyons Canyon and Modelo and Towsley Formations of Towsley Canyon were extensively overprinted by the present field and have thus far not yielded useful PM results.

Currently we are working in the southern foothills of the San Gabriel and Santa Susana Mountains in Los Angeles County, where initial sampling has been conducted (from east to west) along Little Tujunga Canyon (Towsley/Pico and Saugus Formations), Marek Ridge (Towsley/Pico and Saugus Formations) and Lower Van Norman Lake (Sunshine Ranch and upper members of the Saugus Formation). Our results to date are as follows:

1. All usable Saugus sites along Little Tujunga Canyon, which stratigraphically overlie the Marek Ridge section, are reversely magnetized. (Three of the twenty-one sampled sites did not yield polarity information.)

2. At Marek Ridge thirty-two sites were sampled from the Towsley/Pico and Saugus Formations. The approximately 700 m section is predominantly reversed, presumably of Matuyama age, and four normal polarity events were identified in Saugus strata (Figure 2). As in the Castaic Junction area, the Saugus Formation PM results are clearly superior to those of the Towsley/Pico for reasons that are not yet known.

3. At the Lower Van Normal reservoir nine of the ten horizons sampled are reversed and presumably of Matuyama age. The lowest site of the approximately 900 m stratigraphic section has normal polarity (Figure 3).
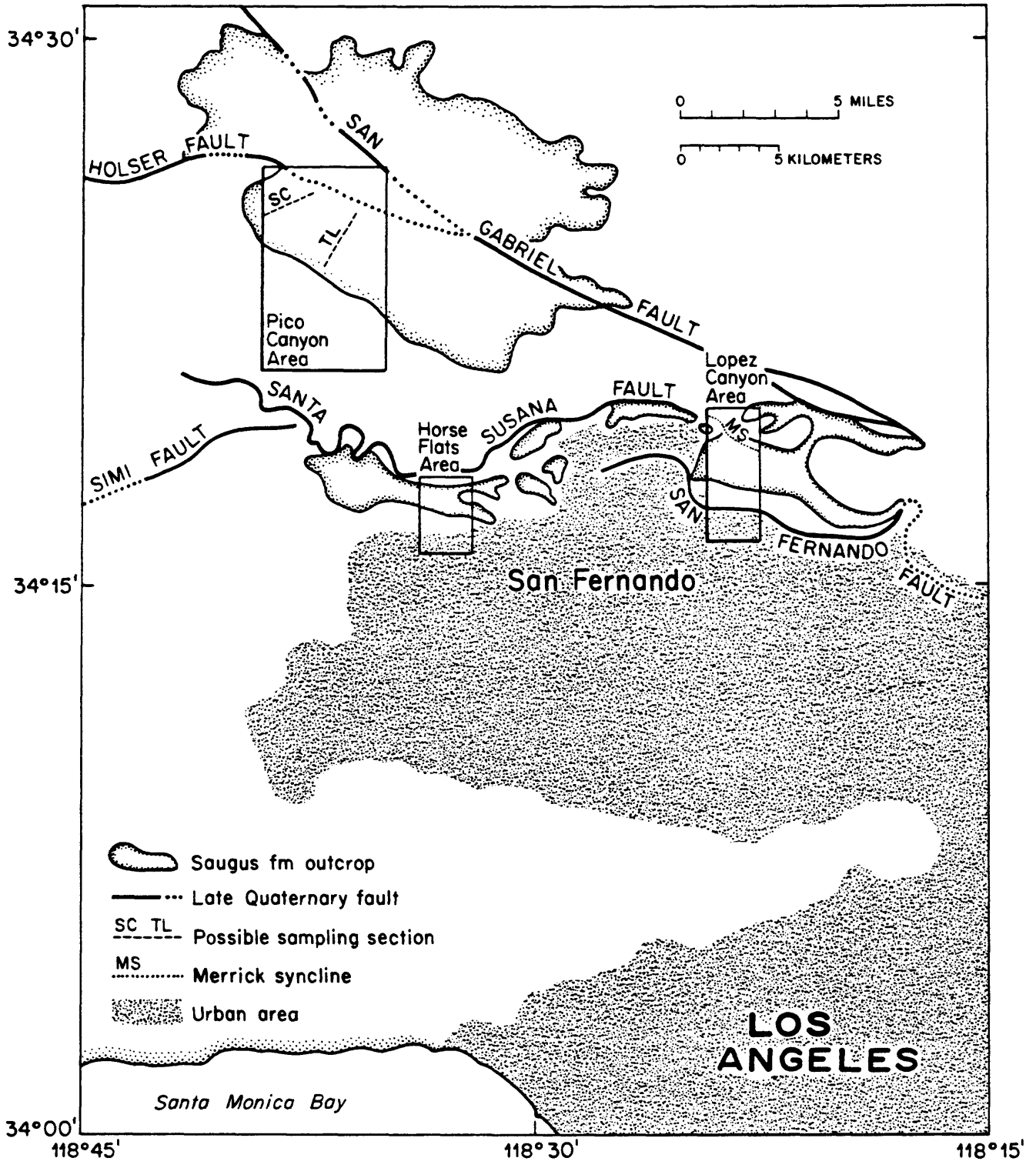
Figure 1. Location of Saugus outcrops in the East Ventura Basin.
The rectangles enclose the stratigraphic sections of this PM study.
The Pico Canyon area contains the transmission line (TL) and Santa
Clara River (SC) sections; the Horse Flats area includes the Lower
Van Norman Lake section; the Lopez Canyon area encompasses the Little
Tujunga Canyon and Marek Ridge sections. Adapted from "Geologic Map
of the San Gabriel Mountains, California," 1:250,000, by W.G. Bruer,
California Division of Mines and Geology Bull., 196, 1975.
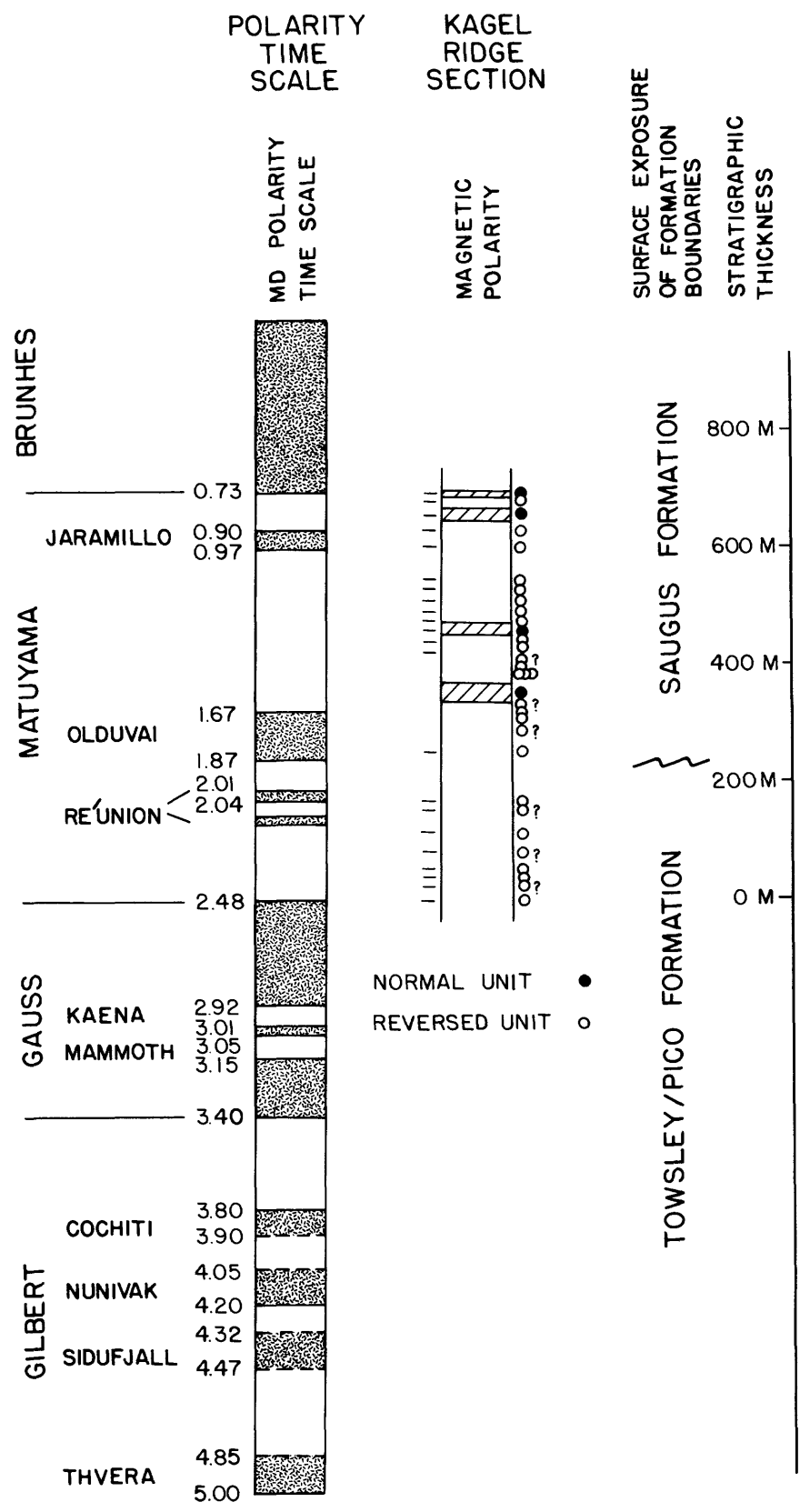
Figure 2. Magnetostratigraphy of the Marek Ridge section (labeled above as Kagel Ridge) and the magnetic polarity time scale after Mankinen and Dabrymple (1979). Circles indicate the stratigraphic position of sampling sites. 0 = reversed, 0 = normal, ? = questionable polarity.

POLARITY   VAN NORMAN
TIME   LAKE
SCALE   SECTION

MD POLARITY TIME SCALE

MAGNETIC POLARITY

STRATIGRAPHIC THICKNESS

BRUNHES

——————— 0.73

JARAMILLO 0.90
0.97

MATUYAMA

OLDUVAI   1.67

1.87
2.01
RE'UNION < 2.04

——————— 2.48

GAUSS

KAENA   2.92
3.01
MAMMOTH   3.05
3.15

——————— 3.40

COCHITI   3.80
3.90

NUNIVAK   4.05
4.20

GILBERT

SIDUFJALL 4.32
4.47

THVERA   4.85
5.00

SAUGUS FORMATION

1000 M
800 M
600 M
400 M
200 M
0 M

NORMAL UNIT   ●
REVERSED UNIT ○

Figure 3. Magnetostratigraphy of the Lower Van Norman Lake section and the magnetic polarity time scale after Mankinen and Dabrymple (1979). Other symbols as in Figure 2.

Earthquake Hazards Studies, Upper Santa Ana
Valley and Adjacent Areas, Southern California

9540-01616

Jonathan C. Matti
Branch of Western Regional Geology
U. S. Geological Survey
345 Middlefield Road, MS 975
Menlo Park, California 94025
(415) 323-8111 ext. 2358, 2353

Investigations

1. Studies of the Quaternary history of the upper Santa Ana River Valley. Emphasis currently is on: (a) generation of a liquefaction susceptibility map; and (b) the three-dimensional distribution of the valley fill and its lithologic, lithofacies, and pedogenic character.

2. Neotectonic studies of the Crafton Hills-Yucaipa Valley, Banning, and San Andreas fault zones. The study has focused on: (a) mapping fault strands that deform crystalline basement rocks, Tertiary sedimentary rocks, and Quaternary surficial units; (b) identification of Quaternary units to establish Quaternary depositional patterns and the relative ages of displacements along various fault strands; and (c) interpreting relationships between the Banning fault system and the south branch of the San Andreas fault.

Results

1. S. E. Carson and J. C. Matti have reached the report-writing stage of a liquefaction evaluation for the San Bernardino Valley. No new results to report.

2. A report by Matti, Morton, and Cox (1985) outlines the tectonic framework of the central Transverse Ranges and vicinity, and identifies paleotectonic and neotectonic faults that evolved in the region during late Miocene through Holocene time. These faults can be grouped into four systems: (1) The San Andreas fault system (2) the San Gorgonio Pass fault system, (3) the Crafton Hill horst-and-graben system, and (4) the Cucamonga fault zone.

San Andreas fault system

Banning fault zone. The Banning fault zone is an old strand of the San Andreas fault system that formerly was a throughgoing fault that extended from the Coachella Valley region, through San Gorgonio Pass, and west to the vicinity of the San Gabriel Mountains; there, the Banning fault probably once was continuous with the San Gabriel fault. The Banning-San Gabriel fault generated about 60 km of right-lateral displacement during the period between 10-12 m.y. B.P. and about 5 m.y. B.P. The Banning-San Gabriel fault was abandoned by the San Andreas system about 5 m.y. ago.

San Andreas fault zone.--In the vicinity of the central Transverse Ranges the San Andreas fault zone consists of these segments that have different degrees of structural complexity (fig. 1). The Mojave Desert segment forms a relatively simple fault zone that extends from the Tejon Pass region to the Cajon Pass region. The segment has been the site of Pliocene through Holocene displacements. The Coachella Valley segment forms a relatively simple fault zone that extends from the Brawley seismic zone northwestward through the Coachella Valley. This segment also has been the site of Pliocene through Holocene displacements. The Transverse Ranges segment forms a complex zone of multiple fault strands that had sequential movement histories; to the northwest and southeast these strands merge to form the Mojave Desert and Coachella Valley segments.

From oldest to youngest, fault strands within the Transverse Ranges segment includes the Wilson Creek, Mission Creek, Mill Creek, and San Bernardino strands (fig. 1). Together, these strands represent the total amount of Pliocene through Recent right-lateral displacement on the San Andreas fault zone (sensu stricto) in southern California (4 or 5 m.y. B.P. to Recent). The Wilson Creek strand represents the first generation strand of the San Andreas. Following a prolonged period of right-lateral displacements on a throughgoing fault that generated more than 100 km of offset, the Wilson Creek strand in the vicinity of the San Bernardino Mountains was deformed and compressed into a sinuous trace before being truncated on its outboard side by the Mission Creek strand. The Mission Creek strand in turn generated about 45 km of right-lateral displacement (the same displacement as that of the Punchbowl fault in the San Gabriel Mountains, which I infer to be a continuation of the Mission Creek strand), before it too was deformed in the vicinity of the San Bernardino Mountains and succeeded by the Mill Creek strand. Both the Wilson Creek and Mission Creek strands may have been deformed as a result of left-lateral displacements on the adjacent Pinto Mountain fault. The Mill Creek strand developed inboard (east) of a westward projection of San Bernardino Mountains basement created as the Mission Creek strand and adjacent rocks were deflected and rotated to the west and southwest. Subsequent right-lateral movements on the Mill Creek strand nipped off this projection and displaced it 8 to 10 km to the northwest; subsequently, the Mill Creek strand also was deformed by left-lateral displacements on the Pinto Mountain fault and was terminated as a throughgoing right-lateral strand. The San Bernardino strand marks the trace of the modern neotectonic strand of the San Andreas fault within the Transverse Ranges segment. The strand is continuous with the Mojave Desert segment, and extends for 60 km along the western base of the San Bernardino Mountains to the vicinity of the Crafton Hills fault system, beyond which the San Bernardino strand loses its clear surface expression. Continuity of the San Bernardino strand with neotectonic right-lateral faults in the Coachella Valley is doubtful. In my view the San Bernardino strand has reactivated the Mission Creek strand which formerly was an active trace of the San Andreas along the base of the San Bernardino Mountains.

The Wilson Creek, Mission Creek, and Mill Creek strands all merge into the Coachella Valley segment of the San Andreas fault to the southeast; similarly, the Mill Creek, Wilson Creek, and Mission Creek-Punchbowl strands all merge into the Mojave Desert segment to the northwest. This relation requires that while multiple strands were evolving sequentially within the

Transverse Ranges segment, the adjacent Mojave Desert and Coachella Valley segments were routinely generating right-lateral displacements within their relatively uncomplicated, narrow fault zones. This contrast in structural style between the Transverse Ranges segment and the two adjacent segments persisted for much of the history of the San Andreas fault (sensu stricto), which may require fundamental differences in crustal structure between the complex and simple fault segments.

Complications that developed in the Transverse Ranges segment during Pliocene and early Quaternary time also have characterized the late Pleistocene and Holocene neotectonic regime. Specifically, late Quaternary right-lateral displacements as the Coachella Valley segment of the San Andreas fault apparently are not carried through the southeastern San Bernardino Mountains on any of the throughgoing right-lateral faults: not only are the Mill Creek, Mission Creek, and Wilson Creek strands buried by unfaulted Quaternary alluvium of progressively older age, but the Coachella Valley segment (Mission Creek fault of some workers) appears to lose its fresh appearance and demonstrable Holocene displacements in the vicinity of Desert Hot Springs. The Coachella Valley segment of the Banning fault appears to have fresher tectonic geomorphology in the northwestern Coachella Valley, and I suggest that right-slip on the Coachella Valley segment of the San Andreas fault may have stepped left onto the Banning fault during late Quaternary time (fig. 1). Assuming that right-slip on the Coachella Valley segment is comparable to that on the Mojave Desert in Cajon Pass (25 mm/year), then 25 mm/year may have been transferred from the San Andreas fault to the Banning fault and thence into San Gorgonio Pass. In this capacity the Coachella Valley segment of the fault probably is not a new southern strand of the San Andreas fault zone, but instead represents late Quaternary reactivation of the old Pliocene Banning fault as right-slip is transferred southwestward.

San Gorgonio Pass and Crafton Hills fault system

Late Quaternary tectonism in the San Gorgonio Pass and Crafton Hills fault system represent compressional convergence and extensional pull-apart, respectively. The San Gorgonio Pass fault system is a late Pleistocene and Holocene complex of east-trending reverse and thrust faults separated by northwest-trending faults that I infer to be right-lateral tear or wrench faults developed in the upper plates of the thrusts. The San Gorgonio Pass fault zone thus is a compressional system that is overprinted on the older Banning fault in the San Gorgonio Pass region. The reactivated neotectonic Coachella Valley segment of the Banning fault feeds into the San Gorgonio Pass compressional system, and may or may not work its way through this structural maze and continue on to the northwest. The Crafton Hills fault zone is a northeast-trending series of normal faults that represent late Quaternary crustal extension normal to faults of the San Andreas system.

Neotectonic synthesis

Late Quaternary tectonism in the vicinity of the south-central Transverse Ranges may reflect a regional tectonic regime where right slip is passed from the Coachella Valley segment of the San Andreas fault onto the Banning fault, through San Gorgonio Pass and onto the San Jacinto fault, and then back onto the modern trace of the San Andreas fault in the San Bernardino valley region

(fig. 1). The San Gorgonio Pass fault system may have taken up all of the slip on the neotectonic Banning fault through convergence within the thrust-fault belt. Alternatively, an unknown but possibly large amount of slip may have stepped left onto the San Jacinto fault, locally accelerating that fault above the 8 to 12 mm/year rate determined by Sharp (1981). If this extra slip steps back onto the San Andreas fault in the San Bernardino valley, then two relations could be achieved: (1) The modern San Andreas fault would extend as a youthful neotectonic feature southeastward from Cajon Pass to the Crafton Hills region, but would not necessarily continue through the San Gorgonio Pass region and on into the Coachella Valley. This would explain the difficulty most workers have in mapping the modern San Andreas fault through San Gorgonio Pass. The San Bernardino strand shows this distribution pattern. (2) Right-slip on the San Bernardino strand would not continue very far to the southeast beyond the Crafton Hills fault system. As a result, extensional pull-apart would be expected in this zone of normal faults.

Neotectonic relations in the vicinity of the south-central Transverse Ranges thus reflect a complex knot in the modern San Andreas fault zone. However, this setting is not new. Instead, the modern neotectonic framework merely is the latest phase of a complex history that has characterized the Transverse Ranges segment of the San Andreas fault for the last 2 to 2.5 million years. This history can be viewed as a consequence of the repetitive development of a left step in the San Andreas fault zone in the vicinity of the Transverse Range segment. Northwest and southeast of this left step the Mojave Desert and Coachella Valley segments of the San Andreas have relatively uneventful histories; however, where the left step developed, the San Andreas fault has responded by evolving multiple strands that succeeded each other through time as the parent fault attempted to retain its continuity through the region. These successive attempts are represented by the Wilson Creek, Mission Creek, and Mill Creek strands. The modern San Andreas fault is responding to the most recent left step by transferring slip from the Coachella Valley segment to the Banning fault. Virtually all of the modern neotectonic faults in the vicinity of the south-central Transverse Ranges are a manifestation of this left step in the San Andreas fault zone--which poses challenging problems for siting instrument packages designed to monitor regional strain in anticipation of recognizing premonitory signals for a large earthquake on the San Andreas or San Jacinto fault zone.

References Cited

Matti, J.C., Morton, D.M., and Cox, B.F., 1985, Distribution and geologic relations of fault systems in the vicinity of the central Transverse Ranges, southern California: U.S. Geological Survey Open-File Report 85-365, scale 1:250,000.

Sharp, R.V., 1981, Variable rates of late Quaternary strike slip on the San Jacinto fault zone, southern California: Journal of Geophysical Research, v. 86, no. B3, p. 1754-1762.
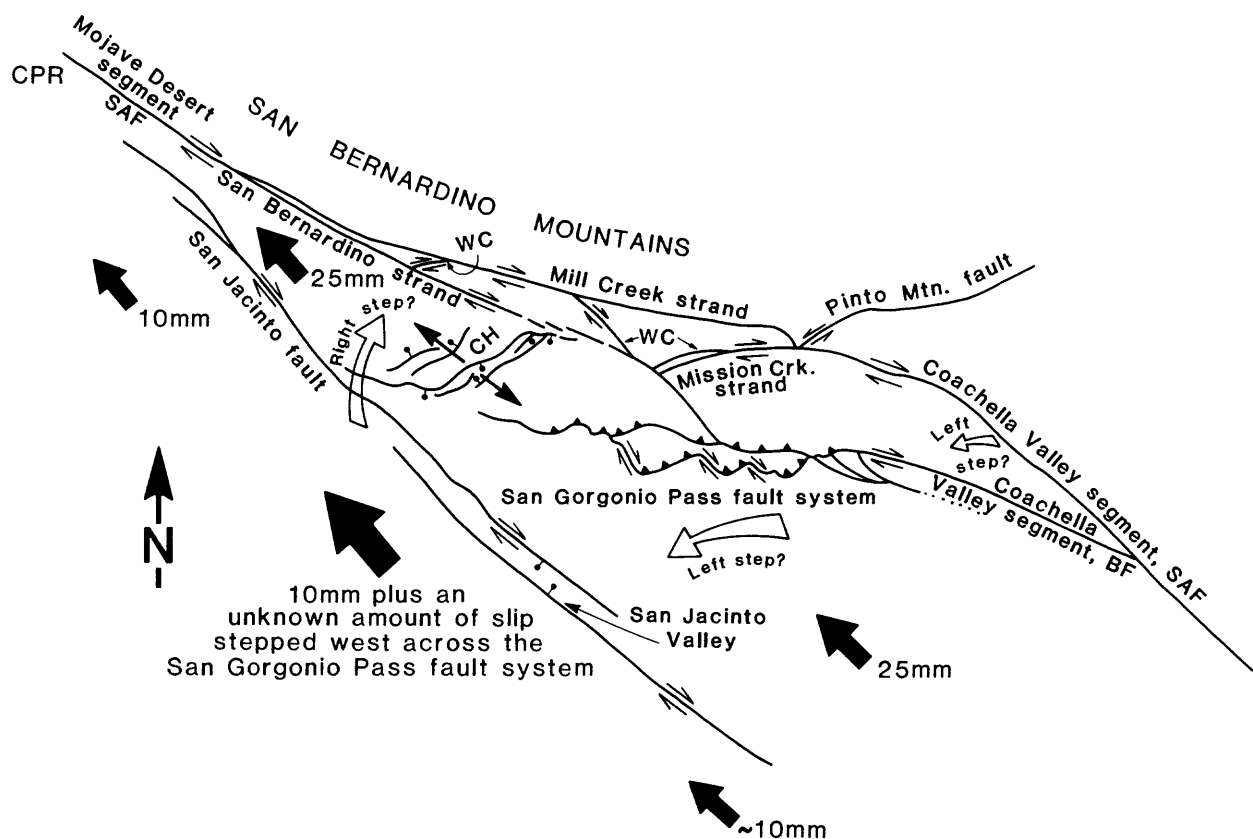
Figure 1. -- Schematic diagram illustrating relations between faults and crustal blocks in the vicinity of the south-central Transverse Ranges, southern California. Large solid arrows indicate the relative motion of crustal blocks; large hollow arrows indicate lateral transfer slip. Small solid arrows in the Crafton Hills area indicate crustal extension in the Crafton Hills fault system. BF, Banning fault; CH, Crafton Hills, CPR, Cajon Pass region; SAF, San Andreas fault; WC, Wilson Creek strand, San Andreas fault. Geology taken from Matti and others, 1985. Ten mm slip-rate on the San Jacinto fault is an average of the 8 to 12 mm rate determined by Sharp (1981).

QUATERNARY FAULT HISTORY AND EARTHQUAKE POTENTIAL
OF THE HANSEL VALLEY AREA, NORTH-CENTRAL UTAH

14-08-001-21899

James McCalpin
Department of Geology
Utah State University
Logan, UT 84322
(801) 750-1220

Investigations

1. Surficial geologic mapping of Hansel Valley at 1:50,000, including detailed subdivisions of Lake Bonneville lacustrine deposits.
2. Mapping and profiling of fault scarps on the west and east margins of the valley.
3. Detailed logging of the walls of an arroyo which intersects a Quaternary fault zone on the west side of Hansel Valley.
4. Relative and absolute dating of sediments deformed by Quaternary faulting.

Results

1. Surficial geologic mapping of Hansel Valley is now complete. Although considerable littoral deposition occurred on the valley margins in Lake Bonneville time, much of the floor of the valley is composed of pre-Bonneville, semi-indurated fanglomerates and sandstones (Tertiary?) overlain by less than 2m of Bonneville-cycle silts and clays.

2. Two small, discontinuous fault scarps which occur on the east valley margin at the base of the Northern Promontory Mountains have been described previously (McCalpin, 1985). Major effort was devoted to profiling and examining the 10 km-long extension of the 1934 fault scarp on the west side of the valley. Vertical displacement values calculated from scarp profiles vary widely, with no correlation to age of shorelines displaced (Fig. 1). The fault scarp has been increased in height by slumping in its central portion, as it ascends a larger escarpment (throw values 3.9 m, 6.2 m, 9.0 m, 5.1 m). Throw values from unslumped portions of the scarp range from 1.2 to 2.5 m, which probably represents displacement at depth.

The timing of faulting can be constrained by using conceptual models of geomorphic relations between shorelines and fault scarps. Faulting could conceivably occur 1) before the lake was present, 2) during the transgression, 3) during the highstand, 4) during the regression, or 5) after the lake had dessicated. Small fault scarps (1-2 m high) formed before a transgression would be reworked and destroyed, gauging from the size and coarseness of Bonneville transgressive bars on exposed prominences. A scarp which offset shorelines during a trangression would be destroyed above the elevation of the shoreline when faulting occurred, but transgressive shorelines formed prior to faulting would be offset and preserved if below effective wave base. If faulting occurred during the highstand, all transgressive shorelines would preserve evidence of faulting. If faulting occurred during a regression, regressive shorelines already formed as the lake receded would be faulted. Future regressive shorelines would be controlled by the position of the fault scarp, since regressive shorelines in the Bonneville Basin were generally ineffective at erosion and deposition compared to transgressive shorelines. Faulting

after the lake had dried up would displace all transgressive and regressive shorelines. Field evidence from western Hansel Valley shows that the 10 km-long scarp was formed sometime after the transgression had risen to the highest shoreline (4600 ft) offset by the scarp, but before the regression had reached the elevation of 4350 ft, where small regressive shoreline features do not extend across the scarp. Lake elevation dates (Scott et al, 1983) bracket this interval as roughly 26-12 ka.

Independent evidence for scarp age from scarp height-slope angle plots suggests that the scarp was formed between 15 ka and 10 ka (Fig. 2). The overlap between the two estimates (15-12 ka) is probably close to the true scarp age. Notably, a surface displacement of 1.2 m to 2.5 m correlates with historic ruptures which were 25 to 55 km long (Bonilla, 1982, p.60) much longer than the 10 km scarp length found here. It is possible that the displacement values actually represent two fault events within the specified time interval; subsurface evidence also suggests two Bonneville-age events.

3. Exposures in a 10 m-deep arroyo (West Gully of Fig. 1) expose a complex of normal faults where the scarp would project across the gully. Twelve faults in an 80-m wide zone define a broad graben structure (Fig. 3), with net displacement across the zone 1.3 m down to the east, a similar value to that on the scarp north of the gully. Tectonic fractures in the basal Little-Valley silts are clearly truncated by the Bonneville transgression, indicating at least one event in the period 140 ka - 26 ka. Other faults offset the Bonneville transgressive gravels as much as 2.5 m; these faults cannot be traced to the surface in the gully vicinity, but instead die out into one of two convoluted silt units which overlie the Bonneville gravels. The intense deformation in these two units, (which are separated by undeformed laminar silts) is restricted to the vicinity of fault traces. We infer that each convolution episode was initiated by seismic shaking, resulting from two earthquake events within the period roughly 26-12 ka. Since 12 ka, there has been only one surface rupturing event on the fault trace (1934 AD). The overall temporal pattern seems to be one or more event from 150-26 ka, two events from 26-12 ka, and one event since 12ka. The apparent short recurrence times during the Lake Bonneville epoch may have resulted partly from crustal loading, or could be an artifact of examining faults which offset mainly Bonneville-age deposits.

4. Relative dating and correlation of ostracod faunas by Rick Forrester, USGS, suggests that Little Valley, interpluvial, and Bonneville-age deposits are all offset in the west Gully. Absolute dates will be obtained both ^{14}C on gastropods and TL dating of inorganic silts.

Reports
McCalpin, James, 1985, Quaternary fault history and earthquake potential of Hansel Valley, north-central Utah: Summaries of Technical Reports, Vol. XIX, U.S. Geological Survey Open-File Report 85-22, p. 126-129.

Robison, R. M. and McCalpin, James, 1985, Evidence for recurrent Quaternary normal faulting along the trace of the 1934 Hansel Valley fault scarp, north-central Utah: Geological Society of America, Abstracts with Programs, vol. 17, no. 4, p. 262.
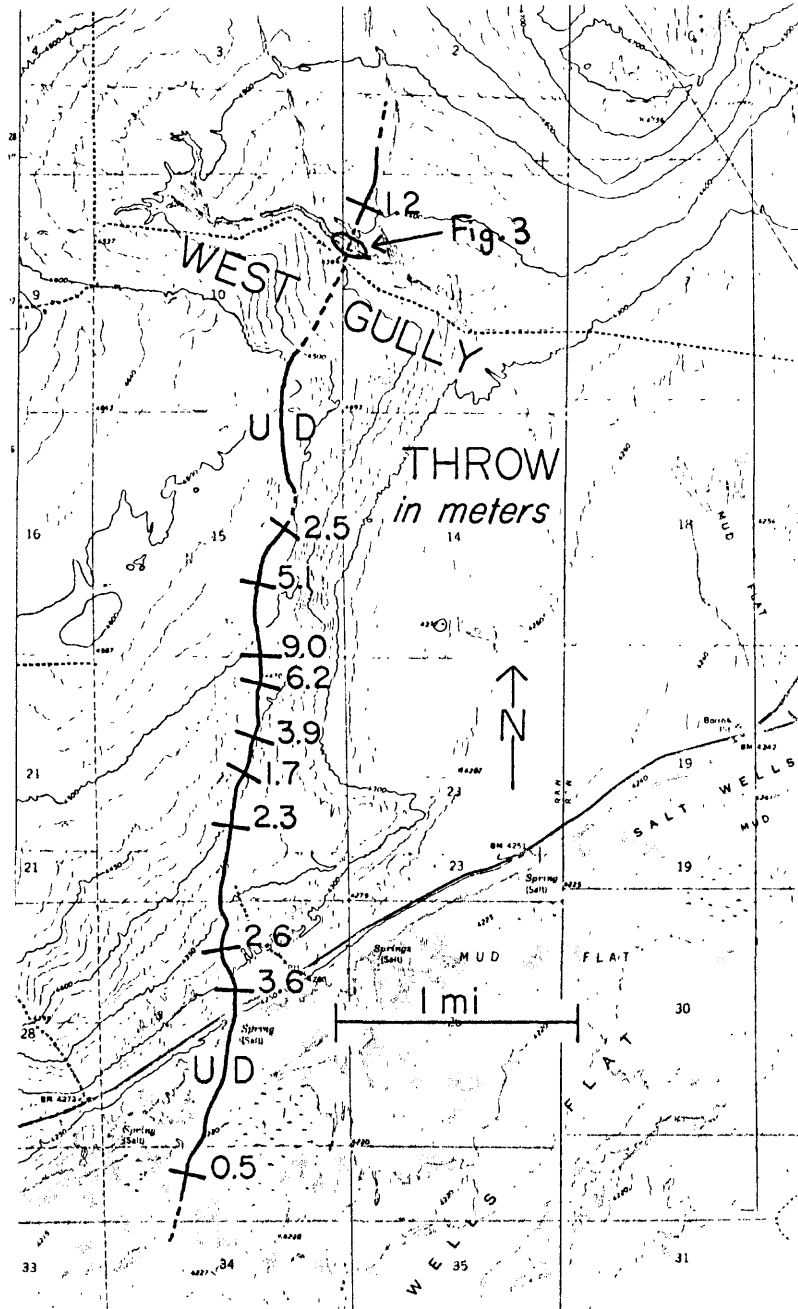
Figure 1. Map of the trace of the main 1934 Hansel Valley fault
scarp (south end of heavy line to the 3.6m throw), and the
pre-historic scarp further north. High throw values in the
center result from syntectonic slumping. This scarp is the
result of at least one, and possibly two, faulting events in
the period 26ka to about 12 ka.
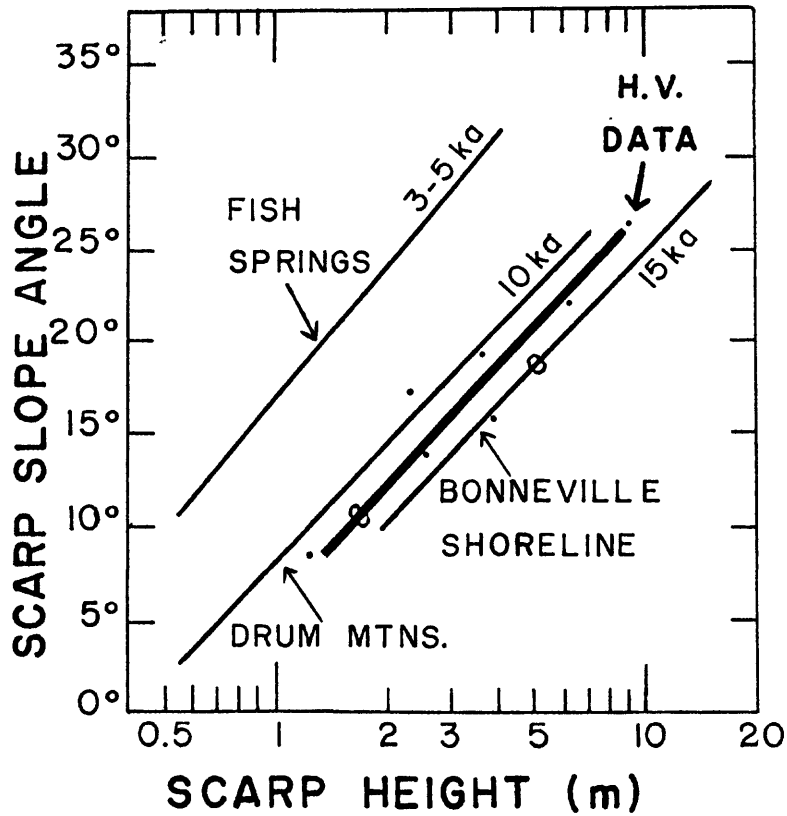
Figure 2. Scarp height-slope angle relations for the pre-historic
Hansel Valley scarp, with reference data from other dated scarps.
Accurate dating is not possible because scarps formed underwater
do not weather exactly like subaerially-formed scarps.
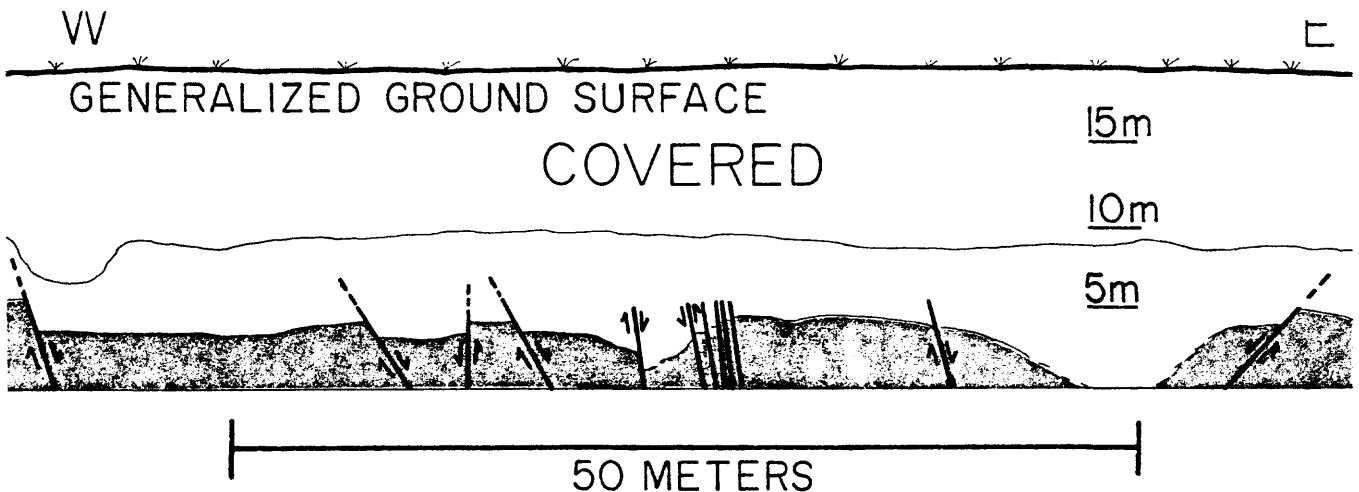
Figure 3. Schematic diagram of the overall fault pattern observed
in the bottom of the West Gully (see Fig.1).Net displacement was
about 1.3m down to the east.

Regional extent of pre-1886 sand blows near Charleston

9950-03868

Stephen F. Obermeier
Branch of Engineering Geology and Tectonics
MS 926, National Center
Reston, VA 22029
(703) 860-6406; 928-6406 (FTS)

Investigations

A detailed examination has been made of many pre-1886 sand blows near Hollywood, South Carolina, for the purpose of discussing and describing the characteristics of sand blows, and for the purpose of collecting ^{14}C samples for age dating. A search has been made for 1886 and pre-1886 sand blows in a three county area surrounding Charleston, with the idea that the areal extent of sand blows indicates the strength of the pre-1886 sand blows discovered at Hollywood.

Results

^{14}C data indicate there are at least three Holocene liquefaction events at Hollywood. Many sites with earthquake-induced liquefaction have been located at widely scattered sites (see attached sheets for locations and field-interpreted ages). Many of the pre-1886 sand blows appear to be the same age, based on soil development on the vented material. At a few sites, ^{14}C testing can bracket the date of the event, but at most there is not enough carbon preserved for dating.

Reports

Obermeier, S. F., Gohn, G. S., Weems, R. E., Gelinas, R. L., and Rubin, Meyer, 1985, Geologic evidence for recurrent moderate to large earthquakes near Charleston, South Carolina: Science, v. 227, p. 408-411.

Obermeier, S. F., Weems, R. E., Gohn, G. S., and Rubin, Meyer, 1985, Distribution and recurrence of prehistoric earthquakes near Charleston, South Carolina; Annual meeting, SSA, Austin, Texas, April 1985

Obermeier, S. F., Gohn, G. S., and Weems, R. E., 1984, Geologic evidence for prehistoric earthquake-induced liquefaction and ground deformation near Charleston, South Carolina: 56th Annual Meeting, Eastern Section, SSA, St. Louis University, Oct. 1984.

List of Holocene liquefaction sites

1. FM I, II, III; pre-1886 and probable 1886 liquefaction;
    Cainhoy quad; sand pit; long 79°49.1', lat 32°59.8'

2. CH I, II; pre-1886 and 1886 liquefaction; Cainhoy quad; road
    cuts; CH I at long 79°45.5', lat 32°53.45'; CH II at long
    79°45.35', lat 32°53.9'

3. WV I, II; two liquefaction events widely spaced in time,
    pre-1886 and probable 1886; Sewee Bay quad; road cut; long
    79°43.75', lat 32°55.65'

4. BB I, II, III; pre-1886, and possible 1886 liquefaction;
    Sewee Bay quad; road cut' long 79°38.2', lat 32°59.8'

5. AR I, II; two liquefaction events widely spaced in time,
    pre-1886 and probable 1886; Adams Run quad; ditch; long
    89°19.3', lat 32°43.9'

6. AR III; pre-1886 liquefaction; Adams Run quad; ditch; long
    80°20.7', lat 32°44.0'

7. FC I, II, III; pre-1886 and probable 1886 liquefaction;
    Clubhouse Crossroads quad; ditch; long 80°18.7', lat
    32°55.2'

8. CR I; very probable 1886 liquefaction; Wadmalaw Island quad;
    ditch; long 80°08.6', lat 32°44.3'

9. BR I; two pre-1886 liquefaction events, long separated in
    time; Jacksonboro quad; road cut; long 80°27.9', lat
    32°48.0'

10. BR IV; pre-1886 liquefaction; Jacksonboro quad; ditch; long
    80°25.9', lat 32°48.0'

11. DD I; very probable 1886 liquefaction; Johns Island quad;
    sand pit; long 80°04.5', lat 32°45.1'

12. MP I; 1886 liquefaction; Charleston quad; ditch; long
    79°53.5', lat 32°48.1'

13. HW; probably at least three pre-1886 and 1886 liquefaction
    events; Wadmalaw Island quad; drainage ditch; long
    80°13.7', lat 32°43.1'

14. McL; pre-1886 liquefaction; Awendaw quad; ditch; long 79°
    31.4', lat 33°04.3'

15. SAN; probable pre-1886 liquefaction; Santee quadrangle; sand
    pit; long 79°24.25'; lat 33°14.95'
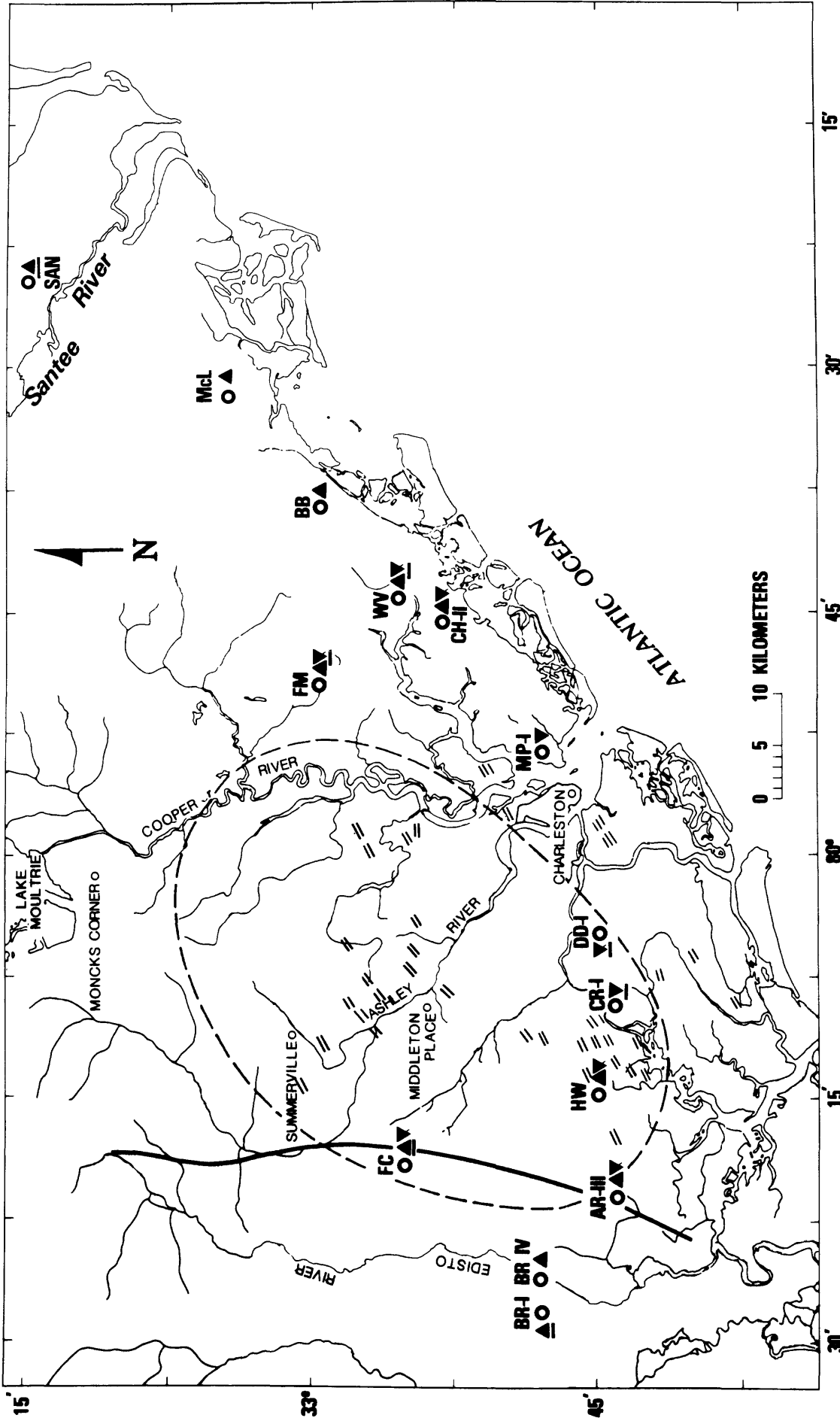
Approximate boundary of 1886 meizoseismal zone (MMI-X)

Western limit of 1886 craters   ≡ 1886 craters (Dutton)

▲   Pre-1886 sand blow

▼   1886 sand blow

—   Underline indicates probable sand blow date

111

EARTHQUAKE RESEARCH IN THE WESTERN GREAT BASIN

Contract 14-08-0001-21986

A.S. Ryall, W.A. Peppin, U.R. Vetter, and E.J. Corbett
Seismological Laboratory
University of Nevada
Reno, NV 89557
(702) 784-4975

Investigations

This program supports continued studies with research focused on: (1) seismicity in the White Mountains Gap; (2) magmatic processes in Long Valley Caldera; (3) the UNR experimental digital network; (4) systematic variations in focal mechanisms with depth; (5) attenuation changes in earthquake regions connected with volcanism; (6) relocations of Mammoth Lakes earthquakes; (7) improved depth control on Mammoth Lakes earthquakes; (8) analysis of digital waveforms; and (9) digitization of field tapes for a more detailed analysis of the 1978 Wheeler Crest earthquakes. Progress in selected areas of this program is described below.

Results

A. *Systematic variations in focal mechanisms.*

The frequency-depth distribution of earthquakes in the western Great Basin shows a maximum at 8-12 km depth, which corresponds to a temperature of 200°-300° C. (Lachenbruch and Sass, 1978). There are strong indications that the focal mechanisms change with depth from strike slip in the upper 6-9 km to mainly oblique and normal slip at greater depths (Vetter, 1985). The depth range of this change coincides roughly with the depth of maximum earthquake occurrence. The seismicity in the western Great Basin is mainly restricted to the uppermost 17 km, where the temperature gradients for the Great Basin would predict temperatures below 400°-500° C. If we divide the crust according to its seismic behavior into three regions, the frictional, the transitional, and the plastic: then the frictional regime consists of the uppermost crust to the depth of maximum seismicity; the transitional regime extends from there to the maximum depth of earthquakes; and the plastic regime is the aseismic lower crust (Meissner and Strehlau, 1982). We find most strike-slip and some oblique-slip earthquakes in the frictional regime, while most oblique and all normal-slip events occur in the transitional regime. Frequency-depth distributions of the seismicity in different sub-regions of the western Great Basin indicates that the crustal temperature gradient increases from western Nevada to the Mono Lake and Mammoth Lakes regions and is highest in the Long Valley caldera. Thus the temperature gradient for these sub-regions may be roughly estimated from the seismicity (Vetter, 1984).

B. *Analysis of Wideband Digital Data.*

Some 4,500 wideband (0.1-50 Hz) digital displacement seismograms have been recorded for half a dozen earthquake sequences in the western Great Bassin, including the 1980 Mammoth Lakes events (Peppin, 1984a). These data have formed the basis for two abstracts presented at recent meetings of the AGU and SSA (Peppin, 1984b, 1985). Because of the discrepancy in results obtained from these excellent records as compared with work done by personnel from the

USGS (Archuleta *et al.*, 1982), we found it necessary to present the results of this analysis in December 1984 and April 1985, the latter after completely redoing the analysis of spectral parameters. Based on consultation with attendees at these meetings, we have now satisfied ourselves that our analysis methods are valid, and are writing up the results for publication. Two results of importance have emerged. *First,* spectral corner frequencies published by Archuleta *et al.* are likely to be estimates of processes other than the source because of strong local (factor of 2.5) site effects. *Second,* again because of site effects and because the data used by Archuleta *et al.* sampled "non-hardrock" sites, the seismic moments inferred may be substantially overestimated by use of Brune's (1970) theory (factor of 4 or 5 when compared with a "hardrock" site.) Similar strong site effects have recently been observed at Mammoth (Archuleta *et al.*, 1985) and predicted theoretically (Barker, 1985.)

C. *1978 Wheeler Crest Aftershocks.*

The first significant earthquake generally associated with the Mammoth Lakes sequence occurred on October 4, 1978 under the Wheeler Crest segment of the Sierra Nevada. The University of Nevada recorded aftershocks of this event for 10 days following the event on seven radio-telemetered and 2 three-component wideband digital seismographs. We have completed hardware and software needed to convert the data to digital format so that the University of Washington interactive timing software can be used to analyze the events. Several tens of aftershocks had been dumped to disc before the November 1984 earthquake forced us to set this project aside. We will soon be resuming work on this task, aimed at master-event location of a suite of these aftershocks, and will have completed the first phase of this work prior to termination of this contract. As this earthquake is arguably associated with magma injection (Julian, 1983; Ryall and Ryall, 1984), careful delineation of the aftershock locations has taken on new importance.

D. *The Round Valley earthquake and its aftershocks.*

On November 23, 1984, a magnitude 6 earthquake was felt widely throughout eastern California and western Nevada. The epicenter was located 22 km northwest of Bishop, California, just east of the Wheeler Crest, at the eastern escarpment of the Sierra Nevada. Preliminary results presented by Ryall and Hill (1984) indicated that the mainshock and the first few hours of aftershocks delineate a linear zone trending N 30° E. First motion studies on a few large events during these first few hours indicated strike-slip focal mechanisms with NE-trending nodal planes corresponding to left-lateral motion. Subsequent analyses by Corbett (1985) indicate that the aftershock pattern became much more complex with time. To date, 727 events have been timed and located, which is estimated to be only one third of the available data. Over the first two weeks the primary NE-trending zone increased in length from 6 to 12 km. Commencing on November 24, the aftershocks began to spread westward under the high mountains of the Wheeler Crest. By December 9, the aftershock zone was roughly triangular in shape, with 12 km on a side. Much of the activity, along the N 30° E trending zone was deeper than 6 km and outlined a vertically dipping zone suggestive of a fault. Nearly all of the aftershocks west of this zone were shallower than 6 km and appeared to shoal to the west. The mainshock was preceded by 4.8 seconds by a foreshock which obscured the exact arrival times and the first motions of the mainshock at all of the nearby stations. Consequently, it is not possible to locate the mainshock as accurately as the foreshock and the aftershocks. Relocations of the mainshock relative to the foreshock indicate
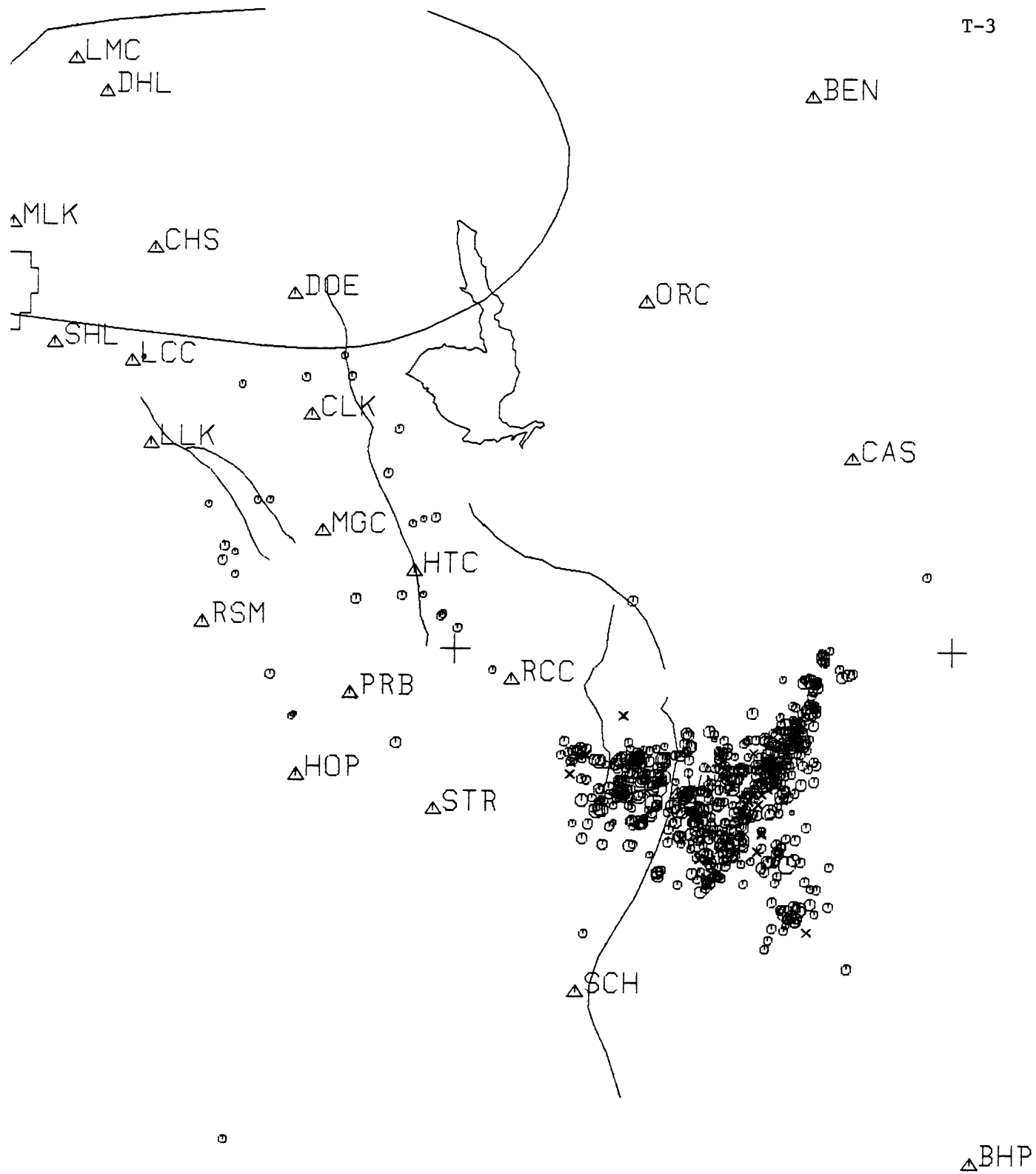
Round Valley Nov. 23 - Dec. 9 727 eq's

that its epicenter is probably within half a kilometer of the foreshock epicenter and it may be as much as one and a half kilometers deeper.

Due to the foreshock, it has not yet been possible to derive a good focal mechanism for the mainshock, but we are in the process of assimilating data from other sources. To date, focal mechanisms have been derived for 80 aftershocks, and they indicate quite a bit more variability than the preliminary study suggested. Left-lateral strike slip on a NE-trending plane is shown for 40% of the solutions, 25% would show dip-slip down-to-the-west movement on vertical NE-trending planes, 30% show oblique-normal movement, and 5% of the mechanisms can be classified as compressional. The oblique-normal mechanisms would infer down-to-the-west movement on NNE-trending planes or down-to-the-northeast movement on NW-trending planes.

The aftershock zone is directly astraddle the Round Valley fault zone which has recognized down-to-the-east normal-fault movement as young as Holocene. Despite the proximity of this major Quaternary range-front fault, none of the aftershock trends and none of the focal mechanisms show evidence for motion on this fault. The temporal development of the aftershock zone is similar to the pattern of simple NNE trends developing into pervasive seismicity that was observed for the 1980 Mammoth Lakes sequence (Lide and Ryall, 1985).

References

Archuleta, R.J., E. Cranswick, C. Mueller, and P. Spudich (1982). Source parameters of the 1980 Mammoth Lakes, California earthquake sequence, *J. Geophys. Res.* **87**, 4595-4608.

Archuleta, R.J., J. Gibbs, E. Etheridge, J. Sena, R. Warrick, and R. Borcherdt (1985). Downhole measurements of strong ground motion, *Earthquake Notes*, **56 no. 1**, 5.

Barker, J.S. (1985). Modeling local structure using aftershocks of the May 1980 Mammoth Lakes earthquakes, *Earthquake Notes*, **56, no.** 1, 31.

Brune, J.N. (1970). Tectonic stress and the spectra of seismic shear waves from earthquakes, *J. Geophys. Res.* **75**, 4997-5009. (Correction (1971), *J. Geophys. Res.* **76**, 5002.)

Corbett, E.J. (1985). The Round Valley, California earthquake of November 23, 1984. *Earthquake Notes*, **56, no.1**, 30.

Julian, B.R. (1983). Evidence for dyke intrusion earthquake mechanisms near Long Valley caldera, California, *Nature*, **303**, 323-325.

Lachenbruch, A.H., and J.H. Sass (1978). Models of an extending lithosphere and heat flow in the Basin and Range province, *Geol. Soc. Am. Memoir 152*, 209-250.

Lide, C.S. and A.S. Ryall (1985). Relationship between aftershock locations and mechanisms of the May, 1980 Mammoth Lakes earthquakes, *J. Geophys. Res.*, submitted.

Meissner, R. and J. Strehlau (1982). Limits of stresses in continental crusts and their relation to the depth-frequency distribution of shallow earthquakes, *Tectonics*, 1, 73-89.

Peppin, W.A. (1984a). The University of Nevada, Reno, portable digital event recording seismograph system, *Seismological Laboratory rpt.*, Univ. Nevada, 115p.

Peppin, W.A. (1984b). Seismic moment of Mammoth Lakes earthquakes from close-in displacement seismograms, *EOS, Trans. Am. Geophys. Union*, **65**, 1117.

Peppin, W.A. (1985). What do spectral corner frequencies mean anyway? *Earthquake Notes*, **56, no.1**, 14.

Ryall, A.S. and F.D. Ryall (1984). Shallow magma bodies related to lithospheric extension in the western Great Basin, western Nevada and eastern California, *Earthquake Notes*, **55, no.1**, 11.

Ryall, A.S. and D.P. Hill (1984). The Round Valley earthquake sequence, unscheduled presentation at the Fall American Geophysical Union meeting, December 7, 1984, San Francisco, Ca.

Vetter, U.R. (1984). Earthquake frequency, focal mechanisms, and temperature in the western Great Basin-Mammoth Lakes Region, Nevada and eastern California. *EOS, Trans. Am. Geophys. Union*, **65**, 1118.

Vetter, U.R. (1985). Focal mechanisms and frequency-depth distribution of earthquakes in the Mammoth Lakes area, *J. Geophys. Res.*, in preparation.

Very Precise Dating of Earthquakes
at Pallett Creek
and Their Interpretation

14-08-0001-22026

Kerry Sieh
(Co-Investigators: Minze Stuiver, David Brillinger)
Division of Geological and Planetary Sciences
California Institute of Technology
Pasadena, California 91125
(818) 356-6115

In early February of this year we collected our first samples for
very precise dating of the peats at Pallett Creek. These peats are
now being analyzed in Minze Stuiver's laboratory at the University of
Washington, but no results are yet available. Additional samples will
be collected during the remainder of 1985.

Active Tectonics of the San Andreas Fault
System in Southern California

14-08-0001-22011

Kerry Sieh
Division of Geological and Planetary Sciences
California Institute of Technology
Pasadena, California 91125
(818) 356-6115

During the past six months I and my students have made several new investigations along the southern half of the San Andreas fault. In addition, Ray Weldon has continued to complete writing of various chapters of his Ph.D. thesis, most of the data for which was collected with support under this contract.

In early April, Carol Prentice and I selected a site southeast of Cholame, in the Bitterwater Valley, for excavation. This site is in the middle of the segment which in 1857 experienced only 3.5 meters of slip. This is the segment along which Sieh and Jahns (1984) have forecast a magnitude 7.5 earthquake within the next several decades. Our initial excavations were conducted in mid-April and proved that our site does not have a stratigraphic record that will enable detailed investigation of the amount of offset in 1857 and previous earthquakes and will not allow dating of previous earthquakes. Extensive bioturbation by rodents appears to have destroyed virtually the entire 3 meters of alluvial sands and gravels that we exposed.

In December and January, Pat Williams conducted investigations along the dormant southern part of the San Andreas fault near the Salton Sea. His investigations revealed one locality at which the flooding of the Salton Sea in 1907 covered the San Andreas fault. This site, at Salt Creek, on the east side of the Salton Sea, may well prove to contain a record of 20th-century slip on the San Andreas fault. Triggered slip was documented by us in 1979 (Sieh, 1982) and by Allen and others (1972) at Salt Creek. Williams discovered milled lumber underlying lake sediments which are cut by the fault. Later in the year Williams will return to determine the amount of offset on these sediments. This offset will provide a slip rate for the past 75 to 80 years, and will enable us to determine whether the slip rate has accelerated, decelerated or remained constant at this site during this period. Williams also discovered well-bedded lacustrine clays, silts and sands within the channel of Salt Creek. These may well help constrain the age of offset of Salt Creek and may enable paleoseismic investigations there.

Field work at the Indio site resumed in mid-February and continues at the present time (May). We have nearly completed excavation and analysis of one of the four major fault traces at the site and have made progress in understanding the amount of slip during prehistoric earthquakes along one of the other traces. We now are quite confident that several large slip events have happened since

1200 A.D. The two best-constrained events appear to be separated by only about 150 ± 50 years.

About 1 km southeast of the Indio site and 1 km northwest of Clarence Allen's Dillon Road alinement array, we have discovered an 11 cm offset of both sides of a concrete canal. The canal was built in about 1940 and thus yields an average slip rate of about 2.4 mm per year. This is very similar to Louie and others' (1985) estimate of the slip rate at the Dillon Road site for the period 1972 to 1977.

Quaternary Framework for Earthquake Studies
Los Angeles, California

9540-01611

John C. Tinsley
Branch of Western Regional Geology
U.S. Geological Survey
345 Middlefield Road, MS 975
Menlo Park, California 94025
(415) 323-8111, x 2037

Investigations

1. Completed editing of first galley proofs, and continued editing proof copy
   of maps and illustrations for inclusion in chapters 5 and 11, U.S.
   Geological Survey Professional Paper 1360 "Evaluating earthquake hazards
   in the Los Angeles region -- an earth science perspective (J.I. Ziony,
   editor). (J.C. Tinsley)

2. Conducted shallow seismic refraction studies to determine the thicknesses
   of late Pleistocene and Holocene alluvium overlying the Tulare Formation
   where the channel of Los Gatos Creek crosses the Coalinga Nose-Guijarrel
   Hills anticlinal structures. (J.C. Tinsley, J.C. Yount, and E.A.
   Rodriguez)

3. Completed site selections in the Los Angeles basin and Wasatch Front areas
   for a series of experiments to determine the capability of high-resolu-
   tion seismic reflection profiling to serve as a predictor of relative
   ground motion. (K.W. King, D. Steeples (Kansas Geological Survey),
   J.C. Tinsley, A.M. Rogers, and D. Carver)

4. Initiated collection of geologic and geotechnical data to characterize
   relative ground motion in terms of site geology at about 50 instrument
   stations scattered along the Wasatch Front, from Logan, Utah to Cedar
   City, but concentrated in the Salt Lake City, Provo, and Ogden areas.
   (J. Tinsley, D. Carver, K. Parish, R. Van Horn)

Results

1. Initial page proofs for USGS Professional Paper 1360, Chapters 4, 5, 9,
   11, and 15, have been received, corrections have been made, and the
   galleys returned to the editor for preparation of second-galleys. The
   maps and illustrations have been received in draft form from the
   illustrators in Menlo Park; the maps have been colored to check the
   linework, and changes, deletions, and additions to the artwork are being
   made.

2. Seismic refraction profiles along Los Gatos Creek indicate that sediments
   having an average P-wave velocity (Vp) of about 450 m/sec directly
   overlie cemented sandstone of the Tulare Formation (Vp = 1800-2200
   m/sec), where Los Gatos Creek crosses the anticline. Comparison of

velocities obtained by working in areas where the age of the deposits is known enables us to describe the following seismic stratigraphy for the deposits we have studied (Table 1). This information may be useful to others who are studying relative ground response in the Coalinga area, or who are obtaining high-resolution seismic reflection profiles. A Bison Model 1580 signal enhancement seismograph and a sledgehammer were used to record the data; this is neither a paid political announcement nor a commercial endorsement of any product by the U.S. Government. A draft manuscript is in co-author review, prior to inclusion in the forthcoming USGS professional paper devoted to the Coalinga earthquake.

3. Seismic reflection profiles have been recorded from sites in the Los Angeles area (near the site of Upper Van Norman Reservoir, near Lower Van Norman Reservoir, near Sylmar High School, and near Chino Airport) and in the Wasatch Front area near Hobble Creek Canyon, Provo Airport, Youd Farm, and Spanish Fork airport. The reflection data are being processed; initial indications are that the quality of the records is excellent.

4. Initial contacts have been made in the Salt Lake City area, and procurement of geotechnical and geologic information concerning near-surface deposits and depth-to-bedrock is underway. The stations at which relative ground response has been determined are localities where past USGS researchers have recorded ground motion emanating from the Nevada Test Site and generated by underground nuclear explosions. The sites selected have exhibited a wide range of spectral amplification relative to bedrock; the alluvium:bedrock spectral amplification ratios range from 2 to 11. Using multivariate statistical analyses, we will investigate comparisons among geotechnical parameters such as thickness, shear-wave velocity or void ratio of various layers of sediment obtaining the data from conventional borehole studies. The results should enable us to recognize statistically significant sets or clusters of geotechnical parameters that contribute to relatively high or relatively low amplification or site-resonance effects at a site, owing to the wave-propagation characteristics of the basin fill. Relative ground response maps can then be drawn up, by using the grouped data to characterize seismically distinct units, as has been done in the Los Angeles area by A.M. Rogers, J.C. Tinsley, and R.D. Borcherdt.

Reports

The following is published:

Atwater, B.F., Tinsley, J.C., Stein, R.S., Trumm, D.A., and Wert, S.L., 1984, Late Holocene alluvial plains as structural datums across the Coalinga Nose - Guijarral Hills anticline, Fresno County, California in Rymer, M.J. and Ellsworth, W.L., (eds.), Proceedings of Conference XXVII - Mechanics of the May 2, 1983, Coalinga earthquake: U.S. Geological Survey Open-File Report 85 - 44, p. 437-438.

Table 1: Seismic stratigraphy along Los Gatos Creek, near Coalinga, CA

Geologic Unit	Vp m/sec
1. Modern channel Alluvium and late Holocene overbank alluvium	340-420
2. Early Holocene(?) or Late Pleistocene alluvium	470-850
3. Tulare Formation	1625-2050

The following have Director's approval:

Tinsley, J.C. and Fumal, T.E., 1985, Mapping Quaternary sediments for areal variations in shaking response--Chapter 5 in U.S. Geological Survey Professional Paper 1360.

Fumal, T.E. and Tinsley, J.C., 1985, Mapping shear-wave velocities of near-surface geologic materials: Chapter 6 in U.S. Geological Survey Professional Paper 1360.

Rogers, A.M., Tinsley, J.C., and Borcherdt, R.D., 1985, Predicting relative shaking response: Chapter 9 in U.S. Geological Survey Professional Paper 1360.

Tinsley, J.C., Youd, T.L., Perkins, D.M., and Chen, A.T.F., 1985, Evaluating liquefaction potential: Chapter 11 in U.S. Geological Survey Professional Paper 1360.

Ziony, J.I., Evernden, J.F., Fumal, T.E., Harp, E.L., Hartzell, S.H., Joyner, W.B., Keefer, D.K., Spudich, P.A., Tinsley, J.C., Yerkes, R.F., and Youd, T.L., 1985, Predicted geologic and seismologic effects of a postulated magnitude 6.5 earthquake along the northern part of the Newport-Inglewood zone: Chapter 15 in U.S. Geological Survey Professional Paper 1360.

Central California Deep Crustal Study
(Neotectonic Synthesis of U.S.)

9540-02191

Carl M. Wentworth
Branch of Western Regional Geology
U.S. Geological Survey
345 Middlefield Road, MS 975
Menlo Park, California 94025
(415) 323-8111 ext. 2474

Investigations

The objective of the project is to examine crustal structure between the California Coast Ranges and the Sierran foothills using deep seismic reflection profiling in concert with surface geology, aeromagnetic and gravity analysis, and seismic refraction profiling. The experiment was framed to trace the Coast Range thrust eastward to depth in the mantle and in so doing, explore the source of the Great Valley magnetic anomaly.

1. Reflection line CC-2 (see map, p.149, USGS Open-File Report 85-22) was extended another 35 km eastward from the east margin of the Northern San Joaquin Valley into the Sierran foothills. The extension crosses well into the exposed granitic batholith. Excellent data were obtained to a depth of 15 s.

2. Analysis has continued of data at Coalinga (SJ-19, see map, as above) and the northern San Joaquin valley and Diablo Range (CC-1, see map, as above).

3. A tentative scientific drilling experiment was designed to test the tectonic wedge hypothesis of Wentworth and others (1984).

Results

1. Extension of reflection line CC-1 into the Sierran foothills has yielded extraordinary results. A suite of strong, west dipping events rises eastward from beneath the San Joaquin valley, crosses beneath the valley margin at about 4 s (unmigrated), and in crude fashion connects eastward with similar events as shallow as 1 s (3 km at 6 km/s) beneath the Sierran batholith. Gently east-dipping events as shallow as 1.3 s underlie the steep batholith boundary. A multitude of deeper events occur thoroughout the 15-s record. The moderately dipping events at such shallow depth beneath the exposed batholith raise the possibility of post batholith thrusting or detachment sliding, neither of which is incorporated in present views of Sierran structure. No similarity with the COCORP reflection line across the northern sierras is evident.

2. Generation of the 1983 Coalinga earthquake by northeastward directed thrusting associated with a northeastwardly emplaced tectonic wedge of Franciscan rock raises the possibility of similar behavior elsewhere along the Coast Range - Great Valley margin. Similar wedge tectonics seem to

characterize the whole 600-km-long margin (Wentworth and others, 1984), as may Pliocene and Quaternary uplift.

3. Inference of wedge-like obduction of Franciscan rock onto the continental margin and beneath marine strata of the Great Valley sequence defines an attractive target for scientific continental drilling. Structural relations between the Mesozoic Franciscan assemblage and Great Valley sequence in the California Coast Ranges have long been considered a type example of subductive accretion of trench and oceanic sediments against a continent. The Coast Range thrust emplaces Franciscan rocks of blueschist grade beneath unmetamorphosed Great Valley sequence and has been assumed to extend eastward to depth into the mantle. To the contrary, extensive geophysical control (seismic reflection and refraction profiles and preliminary gravity and magnetic modeling) all suggests that the Franciscan overlies west-dipping Great Valley basement and that the Coast Range thrust butts downdip against that basement (see figure 1). The structural geometry requires wedge-like obduction of the Franciscan mass and associated thrusting and this style of deformation may be widespread in the Coast Ranges and elsewhere. Deep drilling would not only test the wedge relations but would provide subsurface information for a host of ongoing Coast Range investigations, including in situ and heat flow studies.

Reports

Zoback, M.D., and Wentworth, C.M., 1985, Crustal studies in central California using an 800-channel seismic reflection recording system: American Geophysical Union Geodynamics series: International Symposium on Deep structure of the Continental Crust: Results from Reflection Seismology, Ithica, N.Y., June 1984, in press.
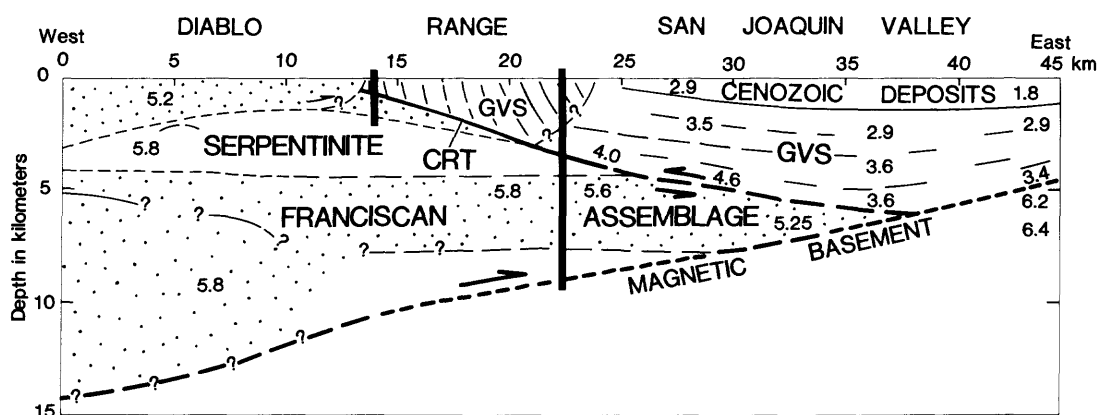
Figure 1. Tentative drill holes (vertical bars) on a cross section along seismic reflection line CC-1 (Garzas Creek-Hwy 140 at lat. 37.25 N). Subhorizontal boundaries are mainly from the reflection record section; the solid line representing the CRT beneath steeply dipping GVS is from gravity modeling by R. Jachens and the short dashed boundaries are from magnetic modeling by A. Griscom. The serpentinite lens is the preferred, shallowest of a series of possible lenses that all satisfy the magnetic data. Queried lines are inferred. Velocities are from seismic reflection and refraction data.

Recognition of Individual Earthquakes on Thrust Faults
(New Zealand)

USGS Contract No. 14-08-0001-21984

Robert S. Yeats, Ian Madin
Department of Geology
Oregon State University
Corvallis, Oregon 97331-5506
(503) 754-2484

Kelvin R. Berryman, Sarah Beanland
Earth Deformation Section
New Zealand Geological Survey, D.S.I.R.
P.O. Box 30 368
Lower Hutt, New Zealand
(644) 699-059

Investigations

Field work by Ian Madin and Sarah Beanland on the Dunstan fault in central Otago resumed in January, 1985 to continue through April. Robert Yeats and Kelvin Berryman visited the area in February and March.

Results

For a discussion of the geologic setting of this project, see Volume XIX of the Summaries of Technical Reports (USGS OFR 85-22), p. 276-282.

The Manuherikia basin contains fine-grained Tertiary strata overlain by weathered gravels (Maori Bottom) which have clasts composed predominantly of gray-wacke derived from northwest-trending ranges northeast of the basin and not from the immediately-adjacent Dunstan Range, composed of schist. This suggests that the northwest-trending ranges (Hawkdun, St. Bathans) were uplifted and presumably faulted prior to uplift and faulting of the northeast-trending Dunstan Range and Raggedy Ridge. The Maori Bottom gravels are overlain with angular unconformity by late Quaternary gravels responding to the present topography and drainage. These gravels contain schist detritus and are faulted; however, most of the uplift of the Dunstan Range had already occurred by the time they were deposited.

New mapping in the northern part of the Manuherikia basin has identified a formation younger than the Maori Bottom and older than the Waikerikeri and Devonshire fan gravels. This formation, informally named the St. Bathans formation, consists of very coarse-grained angular schist detritus derived from the immediately-adjacent Dunstan Range, alternating with finer grained deposits which appears to be loessic sediments reworked by water. We suggest that the St. Bathans formation was deposited during the main period of movement on the Dunstan fault.

Late Quaternary fault traces continue northeast toward the village of St. Bathans (Drybread and Cambrians traces). However, no late Quaternary traces have yet been found associated with northwest-trending faults at the north end of the Manuherikia basin (St. Bathans, Hawkdun, or Stranraer faults).

FIGURE 1. KNOWN ACTIVE AND POTENTIALLY ACTIVE FAULTS OF CENTRAL OTAGO
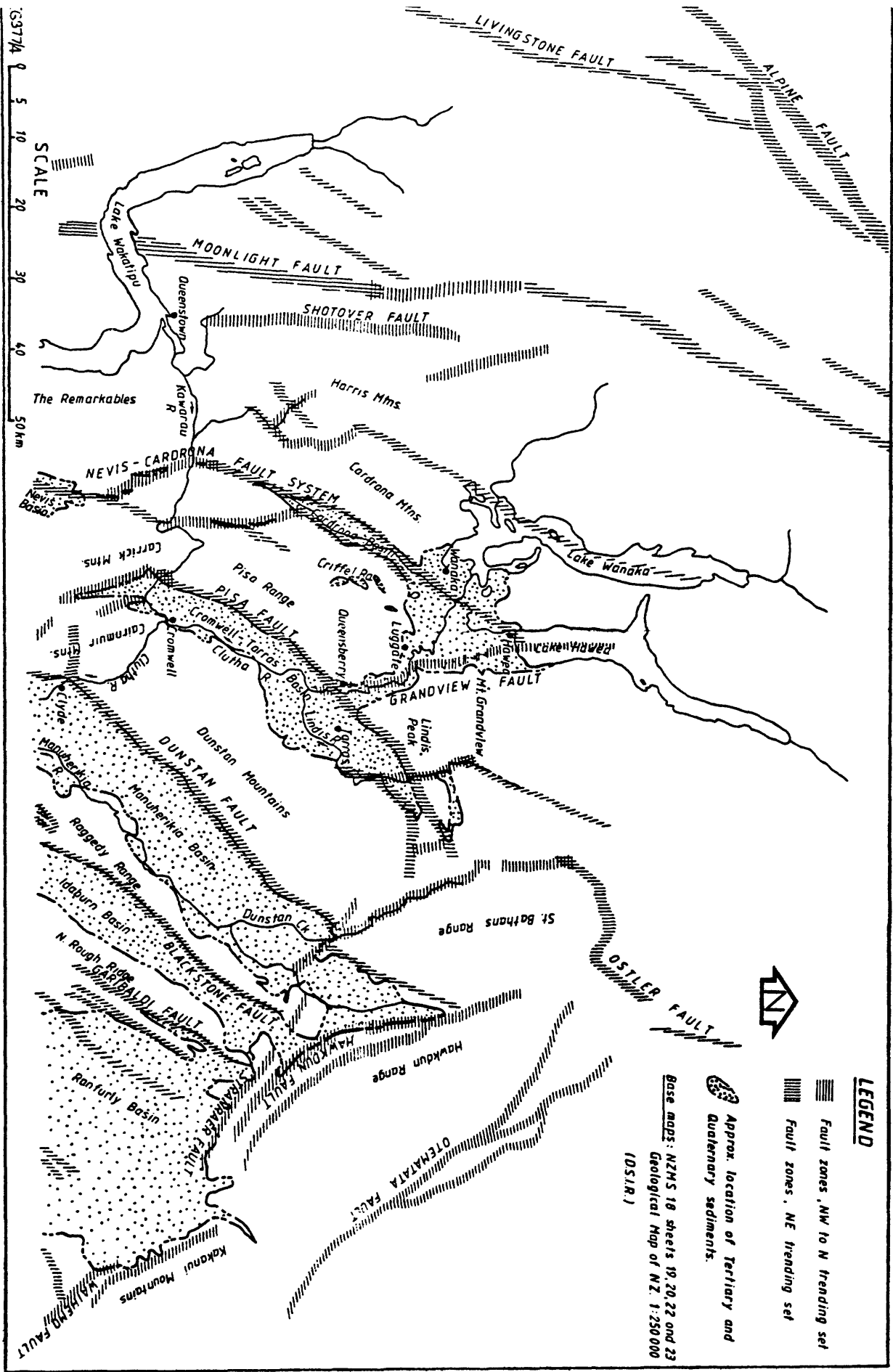
Earthquake Hazards Studies, Metropolitan Los Angeles-
Western Transverse Ranges Region

9540-02907

R. F. Yerkes
Branch of Western Regional Geology
345 Middlefield Road   MS 975
Menlo Park, California   94025
(415) 323-8111 x2350

Investigations and results

1. Historic earthquake data (W. H. K. Lee). No change.

2. Earthquake hazards studies (Yerkes). (A) Completed two chapters for Professional Paper report on the 1983 Coalinga earthquake (before the second anniversary!). Abnormally high fluid pressures (pressure/depth ratio > 13.6 kPa/m) are identified from records of more than 300 deep wells; they extend to the depth limit of drilling (~7 km) throughout southwest San Joaquin Valley and the adjoining Lost Hills-Kettleman Hills-Coalinga anticline chain of folds. Below about 4.5 km the average P/D ratio increases with depth at a rate greater than the lithostatic gradient, suggesting an inverse relation between crustal strength and depth. Sonic logs for a number of wells show abrupt reversals in the velocity/depth gradient at the top of the abnormally high-pressure field, and where seismic profile data are available, this reversal coincides with the top of a seismic low-velocity zone. Several likely sources of abnormally high pressures are identified, but their relative contributions cannot be determined. Chief of these are diagenetic-metamorphic generation of fluids in the Franciscan and Great Valley sequence, compaction disequilibrium and aquathermal pressuring in thick Tertiary mudstone sequences, and regional tectonic compression. We infer the presence of near-lithostatic fluid pressures in Franciscan and Great Valley sequence rocks at seismogenic depths below Coalinga anticline on the basis of mapped seismic low-velocity zones, active generation of metamorphic fluids, and southward and downward propagation of the 1983 mainshock rupture (implying an inverse relation between depth and crustal strength), indicating rupture on the gently southwest-dipping surface of the fault-plane solution. Identification of a near-horizontal maximum compressive stress axis compatible with more than 100 fault-plane solutions of the 1983 earthquake sequence, assuming frictional failure, also favors the gently southwest-dipping fault. (B). This investigation was extended to the western Transverse Ranges, widely known for its regional-scale, active compressional deformation. Abnormally high fluid pressures, much more extensive than previously reported, have been identified and mapped along the Pitas Point-Red Mountain-San Cayetano zone of reverse faults in the eastern Santa Barbara Channel-Ventura basin area. In both the southwest San Joaquin Valley and western Transverse Ranges we note an apparent correlation between isolated clusters of reverse/thrust earthquakes and abnormally high fluid pressures.

3. Quaternary stratigraphy, chronology, and tectonics, Ventura area (A.M. Sarna-Wojcicki)

A) Completed report documenting correlations of widespread late Cenozoic volcanic ash layers in continental sediments of the western conterminous United States and in uplifted on-land marine sediments of the Humboldt and Ventura basins of coastal California, and in sediments of DSDP sites 34, 36, 173, and 470, in the northeastern Pacific Ocean. These ash layers, erupted from vents in the Yellowstone area of Wyoming and Idaho (Y), the Cascade Range of the Pacific Northwest (C), and Long Valley, California (L), are the informally-named Huckleberry Ridge (ca. 1.8 m.y.; Y), Rio Dell (ca. 1.3 m.y.; C), Bishop (ca. 0.7 m.y.; L), Lava Creek-B (ca. 0.6 m.y.; Y), and Loleta (ca. 0.36 m.y.; C) ash beds. Because these tephra layers were erupted, transported, and deposited within a short period of time (several hours to several days), they are essentially isochronous datum planes that allow direct comparison of chronologic and climatic data between marine and terrestial sequences, without complications arising from dating errors. Ages of some marine biostratigraphic datums are shown to be time transgressive; conversely, isotopic ages of some tephra layers are corrected using reliable biostratigraphic datums.

B) Continued study of oxygen-isotope analysis of foraminifera in on-land Quaternary marine sections, Ventura Basin, in order to improve existing age control for upper Cenozoic sections by correlation with deep-ocean secular oxygen-isotope variations, and in order to derive a climatic history that can be correlated to non-marine sections in the western United States by means of tephra layers. About 75 samples collected in Balcom Canyon, Ventura Basin, have been processed; about 300 planktonic and benthic foraminifera specimens have been picked from each for biostratigraphic, bathymetric, and isotopic analysis (coop. with Kris McDougall, BP&S).

Reports

Sarna-Wojcicki, A.M., and Meyer, C.E., 1984, Tephrochronology applied to studies of Quaternary depositional basins in the western conterminous United States: Geological Society of America, Abstracts with Programs, v. 16, no. 6, p. 644.

Sarna-Wojcicki, A.M., Meyer, C.E., Bowman, H.R., Hall, N.T., Russell, P.C., Woodward, M.J., and Slate, J.L., 1985, Correlation of the Rockland ash bed, a 400,000-year-old stratigraphic marker in Northern California and Western Nevada, and implications for middle Pleistocene Paleogeography of central California: Quaternary Research, v. 23, p. 236-257.

Sarna-Wojcicki, A.M., Meyer, C.E., Roth, P.H., and Brown, F.H., 1985, Ages of tuff beds at East African early hominid sites and sediments in the Gulf of Aden: Nature, v. 313, p. 306-308.

Segall, P., and Yerkes, R.F., 1985, Stress and fluid pressure changes associated with oil field operations--a critical assessment of effects in the focal region of the 1983 Coalinga earthquake: U.S. Geological Survey Open-File Report 85-44, p.313-343.

Yerkes, R.F., McGarr, A.F., Wentworth, C.M., and Walter, A.W., 1984, Abnormally high fluid pressures near the Coast Range-Great Valley boundary California, may aid northeast-directed thrusting responsible for the 1983 Coalinga earthquakes (abs.): EOS, vol. 65, no. 45, p. 995-996.

Yerkes, R.F., Levine, Paia, and Wentworth, C.M., 1985, Abnormally high fluid pressures in the region of the Coalinga earthquakes—a preliminary report: U.S. Geological Survey Open-File Report 85-44, p. 344-375.

ANALYSIS OF CENTRAL CALIFORNIA NETWORK DATA FOR EARTHQUAKE PREDICTION

The goals of this study are to evaluate the ability of coda wave analysis to further our understanding of the earth's structure in tectonically active regions, and to clarify the cause of precursory variation in coda Q reported for various seismic regions.

For these purposes, it is essential to separate the source, site and path effects on coda waves.

The methods used here are the simple extensions of single station coda wave techniques used by many workers (e.g., Aki and Chouet, 1975). Under non-restrictive assumptions of coda stability, a method is constructed to isolate source or site effects on high frequency waves (1.5-24 Hz). These techniques allow incorporation of data from earthquakes of many sizes, and from stations lying great distances apart. Digital data is drawn from the U.S.G.S. California Network (CALNET) archives; over 1200 records are used from over 90 earthquakes in the Coast Ranges of California between San Francisco and San Luis Obispo. Application of our techniques yields a variance reduction of 75-90% depending on data processing details. The methods of Aki (1980a) and Aki and Chouet (1975) are also used in order to evaluate the path effect (Q) of both coda and direct shear waves.

The site effect on coda waves is calculated for the data set which was specially collected for this purpose. In spite of a bias toward hard rock sites in the CALNET, a tremendous variation in site reponse is found. At low frequencies the results spread over a range that is too large to be explained solely by the impedence effect. Other processes such as inefficiently damped trapped modes must exist in extreme cases. The model of coda waves as backscattered waves from randomly-situated heterogeneities in the earth must be exteneded to include this possibility. At high frequencies, attenuation controls the site effect, although strange variations, especially at granite sites, remain unexplained.

The source effect is calculated for the data set in much the same manner as for the site study. The results are compared to simple -square and -cube source models. The -square model fits the best, except for the group of Coyote Lake earthquakes that exhibit a constant corner frequency independent of size. This indicates that a source-controlled limiting corner frequency, or f_{max}, exists in the Coyote Lake data. The result is not strong and should be investigated further with a more apporiate distribution of data.

An exhaustive search is carried out to determine the factors upon which the quality factor of coda waves (Q_c) depends. The most interesting result is a dramatic change in crustal Q_c (by a factor of 2) at high frequencies between the high Q Salinian and the low Q Franciscan regions. This could be due to scattering loss at high frequencies in the highly-deformed Franciscan, or to low, thermally-activated intrinsic Q. The latter hypothesis is supported by the observation that the difference in Q_c between the granite

and Franciscan regions is similar to differences between normal and "hot" areas. The quality factor of shear waves (Q_β) is found to agree with <u>crustal</u> Q_c within error bars. Temporal variations in Q_c and M_L-M_{coda} are also investigated. M_L-M_{coda} is observed to decrease after the magnitude 5.0 Bear Valley Earthquake corresponding to an increase in Q or decrease in seismic attenuation after the earthquake.

Theory and Strategy of Earthquake Prediction
Contract No. 14-08-0001-G-990
Principal Investigator: Keiiti Aki
University of Southern California
University Park
Los Angeles, California 90089-0741
(213) 743-3510

Numerical simulations of fault motion and earthquake occurrence provide a convenient test-bed for examining models of earthquake source mechanisms and for exploring their dynamic consequences. Three equally important elements of earthquake phenomena (Aki, 1983), namely, (1) the loading of tectonic stress, (2) the friction law governing fault slip, and (3) the structural heterogeneity of the earthquake source region, can be taken into account in the simulation. Many of the observed large-scale phenomena associated with earthquakes and fault motions have been reproduced by numerical simulations (Burridge and Knopoff,1967; Mikumo and Miyatake, 1978, 1979, 1983), including the occurrence of foreshocks, mainshocks, and aftershocks, correlation among various source parameters, and the occurrence of stable, preseismic and postseismic slips. However, none of these models were able to predict the observed stationary frequency-magnitude relation (Andrews, 1978). Andrews (1975, 1978) found that this difficulty in the construction of a model for recurring earthquakes is posed because tectonic loading cannot change the fault's self-energy (Eshelby, 1957). He also indicated that this difficulty is not removed by letting friction be a function of position because the difference between fault strength and stress will tend to become spatially smoother after each event. We call this difference as the stress deficit because it is the amount of stress needed to be increased in order to initiate a rupture. The consequence of this stress deficit smoothing process on seismicity along a fault is that after a certain time only large events repeat themselves regularly but very few small events happen between these large events. This violates the observed stationary magnitude-frequency relation.

In the present study, we introduced a laboratory inferred friction law, the rate and state dependent friction law, to our numerical simulations. This friction law was proposed by Dieterich (1979, 1980, 1981) and Ruina (1980, 1983). We first examined the dynamic motion and stability of a single degree of freedom elastic system undergoing frictional slip. The system consists of a sliding block connected to an elastic spring which is driven at a constant velocity. The frictional slip is governed by the rate and state dependent friction law. Then, we extended the solution to a one-dimensional mass-spring model with the same friction law. This model predicts non-uniform slip and stress drop on the length scale of the rupture of a heterogeneous fault. This result is very different from earlier modelings of dynamic slip based on Byerlee's law in which the stress and slip functions become smoother with time on the length scale of the rupture, and cannot explain the universally observed stability of magnitude-frequency relation. Our new modeling with a rate and state dependent friction law appears to show no such smoothing effect and provides a physical mechanism for the roughening process of the difference between fault strength and stress that is necessary to explain the observed stationary magnitude-frequency relation. The non-instantaneous healing involved in the evolution of the state variable in the friction law is

responsible for the recurring non-uniform slip and stress drop, and may be explained by the reduction of the interaction between fault segments as compared to Byerlee's law in which the healing is instantaneous. The simulations also indicate that the existence of strong patches on a fault is needed for the occurrence of a large earthquake. The creeping section of a fault such as the one along the San Andreas fault, on the other hand, can be simulated by the rate and state dependent friction law using a fault model without strong patches but with patches having certain material constants which, according to the instability criterion of fault motion which was derived from the rate and state dependent friction law, insure that only creep will happen. In this case, small earthquakes and aseismic creep relieve the accumulating strain without any large events. The maximum characteristic sliding displacement, which gives adequate simulation of seismicity, was found to be remarkably consistent with the slip-weakening critical displacement inferred from seismicity simulations by Cao and Aki with a slip-weakening friction law and inferred from strong motion data using the specific barrier model by Papageorgiou and Aki.

REFERENCES

Aki, K., Theory of earthquake prediction with special reference to Monitoring of the Quality Factor of Lithosphere by the Coda Method, Submitted to Proceedings of the U.S.-Japan Symposium on Earthquake Prediction, Tokyo, Nov., 1983.

Andrews, D.J., From antimoment to moment: plane-strain models of earthquakes that stop, Bull. Seismol. Soc. Am., 65, 163-182, 1975.

Andrews, D.J., Coupling of energy between tectonic processes and earthquakes, J. Geophys. Res., 83, 2259-2264, 1978.

Burridge, R., and L. Knopoff, Model and theoretical seismicity, Bull. Seismol. Soc. Am., 57, 341-371, 1967.

Dieterich, J.H., Modeling of rock friction, 2. Simulation of preseismic slip, J. Geophys. Res., 84, 2169-2175, 1979.

Dieterich, J., Experimental and model study of fault constitutive properties, ASME Appl. Mech. Div., Solid Earth Geophysics and Geotechnology, ed. S. Nemat-Nasser, ASME, New York, 21-29, 1980.

Dieterich, J., Constitutive properties of faults with simulated gouge, Mechanical Behavior of Crustal Rocks, Monograph 24, eds. N.L. Carter, M. Friedman, J.M. Logan, and D.W. Stearns, American Geophysical Union, 103-120, 1981.

Eshelby, J.D., The determination of the elastic field of an ellipsoidal inclusion, and related problems, Proc. Roy. Soc. London, Ser. A, 241, 376-396, 1957.

Mikumo, T., and Miyatake, T., Dynamical rupture process on a three-dimensional fault with non-uniform frictions, and near-field seismic waves, Geophys. J.R. Astr. Soc., 54, 417-438, 1978.

Mikumo, T., and Miyatake, T., Earthquake sequences on a frictional fault model with non-uniform strengths and relaxation times, Geophys. J.R. Astr. Soc., 59, 497-522, 1979.

Mikumo, T., and Miyatake, T., Numerical modeling of space and time variations of seismic activity before major earthquakes, Geophys. J.R. Astr. Soc., 74, 559-583, 1983.

Ruina, A., Friction Laws and Instabilities: A Quasi-static Analysis of Some Dry Friction Behavior, Ph.D. Thesis, Brown University, 1980.

Ruina, A., Slip instability and state variable friction laws, J. Geophys. Res., 1983.

Remote Monitoring of Source Parameters for Seismic Precursors

9920-02383

George L. Choy
Branch of Global Seismology and Geomagnetism
U.S. Geological Survey
Denver Federal Center, MS 967
Denver, Colorado   80225
(303) 236-1506

Investigations

1. __Rupture process of moderate-sized earthquakes.__ We are using methods of seismogram synthesis to model features of broadband seismograms generated by the Coalinga earthquake of May 2, 1983.

2. __Teleseismic estimates of radiated energy from shallow earthquakes.__ We are developing a method for obtaining radiated energy direct measurements ofbroadband teleseismic body waves.

Results

1. The broadband content of digitally recorded body waves from the GDSN permits detailed resolution of the rupture process. Our modelling technique combines realistic source models with propagation operators computed by the reflectivity method. We have determined that the Coalinga mainshock was a complex rupture consisting of two events. The crustal structure at the source was responsible for later complexities in the broadband records.

2. We have developed a method for computing radiated energy that has several advantages: (1) it analyzes frequencies about and above the corner frequency by using digitally recorded broadband data; (2) it accounts directly for frequency dependent attentuation; and (3) its accuracy is unaffected by rupture complexity. Indirect estimates of energy (e.g., those depending on simplistic relations with seismic moment) may overestimate energy if the rupture process involves a sizeable component of aseismic slip. We are in the process of implementing a scheme to automate computation of energy using as input digitally recorded data from the GDSN.

Reports

Choy, G. L., 1984, Source parameters of the Coalinga, California earthquake of May 2, 1983, inferred from broadband body waves: U.S. Geological Survey Open-File Report, 85-44, p. 83-131.

Boatwright, J., and Choy, G. L., 1984, Teleseismic estimates of the energy radiated by shallow earthquakes: Journal of Geophysicial Research, in press.

Choy, G. L., and Boatwright, J., 1985, Estimates of teleseismic source parameters of shallow earthqukes from broadband waveforms [abs.]: To be presented at the 23rd General Assembly of IASPEI, Tokyo, Japan.

Analysis of Earthquake Data from the Greater Los Angeles Basin
and Adjacent Offshore Area, Southern California

#14-08-0001-G-983

Egill Hauksson
Ta-liang Teng

Center for Earth Sciences
University of Southern California
Los Angeles, CA 90089-0741
(213) 743-7007

INVESTIGATIONS

We are analyzing earthquake data recorded by the USC and CIT/USGS networks during the last 11 years in the Los Angeles Basin. Below we present some of the preliminary results of seismotectonic analysis of recent earthquakes along the Newport-Inglewood fault zone which cuts across the eastern half of the Los Angeles Basin.

RESULTS

The main results of this study consist of improved earthquake locations that can be used to infer the tectonic structure and the mode of strain release along the Newport-Inglewood fault. Further, the set of fault plane solutions provides new insight about the state of stress around the NIF and forms the basis for a seismotectonic interpretation.

Earthquake Locations. The recalculated hypocenters are shown in Figure 1. Earthquakes of magnitude between 3.0 and 4.0 are shown as large symbols. The epicenters are still scattered in space mainly to the east of the southern section of the Newport-Inglewood fault. Along the northern end of the fault most of the seismicity falls within the width of the fault zone. The Newport-Inglewood fault is considered to be locked and the occurrence of small earthquakes off the fault reflects accumulation of elastic strain around the fault that leads to brittle failure on favorably oriented small scale faults.

Fault Plane Solutions. The majority of the fault plane solutions determined for earthquakes along the Newport-Inglewood fault show reverse faulting on steeply dipping planes. A few solutions show right lateral strike-slip motion.

Fault plane solutions determined for the northern section of the NIF are shown in Figure 2. These are lower hemisphere equal area mechanisms. The black quadrants indicate regions of tension (the position of the tension or T-axis is indicated by an open small circle) and the white quadrants represent regions of compression (the position of the maximum compression or P-axis is similarly indicated by a filled small circle).

The strike-slip solutions are shown in the center lower section of Figure 2. The only pure strike-slip solutions are shown by events numbers 1 and 14, which are located in the Baldwin Hills and 8 km further to the south along the NIF itself. Toward the right and above in Figure 2, we show reverse mechanisms, which in most cases have steeply dipping planes. Most of these earthquakes have magnitudes in the range 2.9-3.7 and the variability in the orientation of the nodal planes may reflect real variations in the fault structure as well as somewhat quality or the accuracy with which we can determine these solutions. No obvious depth dependence on the type of faulting was found. Locally, in some cases, we appear to have similar solutions (e.g. solutions number 7, 25 and 27) and (e.g. 3 and 13).

The numerous earthquake focal mechanisms of events located on small subsidiary faults several kilometers away from the NIF itself remain mostly unexplained so far. Clusters of events in the Baldwin Hills, south of Newport Beach and the northeast of Long Beach show both strike-slip and reverse faulting occurring within a spatially limited area. These focal mechanisms could be indicative of block rotations or heterogeneous material properties that permit faulting along an ensemble of planes of weaknesses with different strike and dip.

REPORTS

Hauksson,. E. and G. Saldivar, Recent seismicity (1970-1984) along the Newport-Inglewood fault, Los Angeles Basin, southern California, EOS, vol. 65, no. 45, p. 996, 1984.

NEWPORT — INGLEWOOD FAULT ZONE
## RELOCATED EARTHQUAKES 1973 — 1984
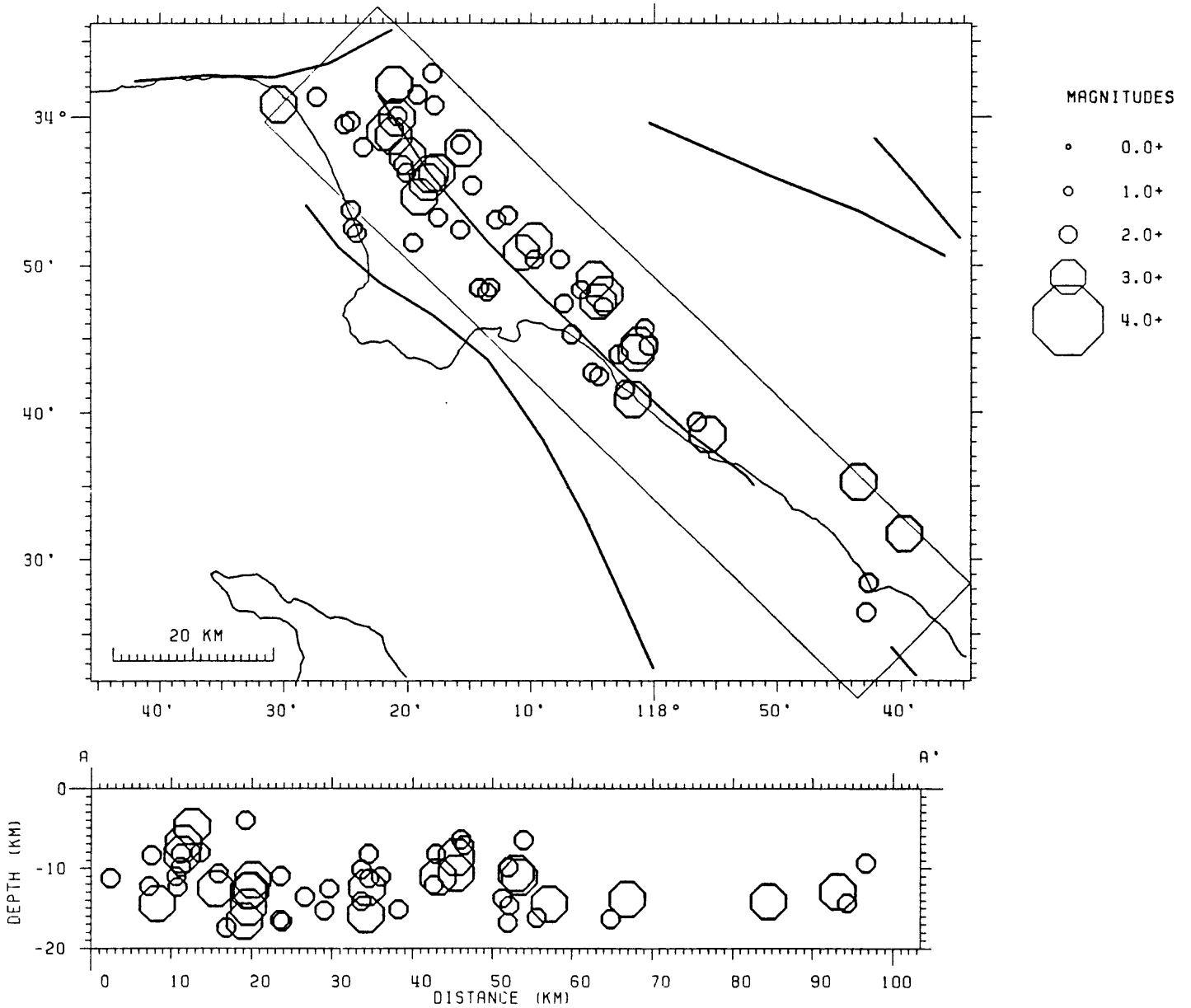
Figure 1. Newport-Inglewood fault: relocated seismicity for 1973-1984.
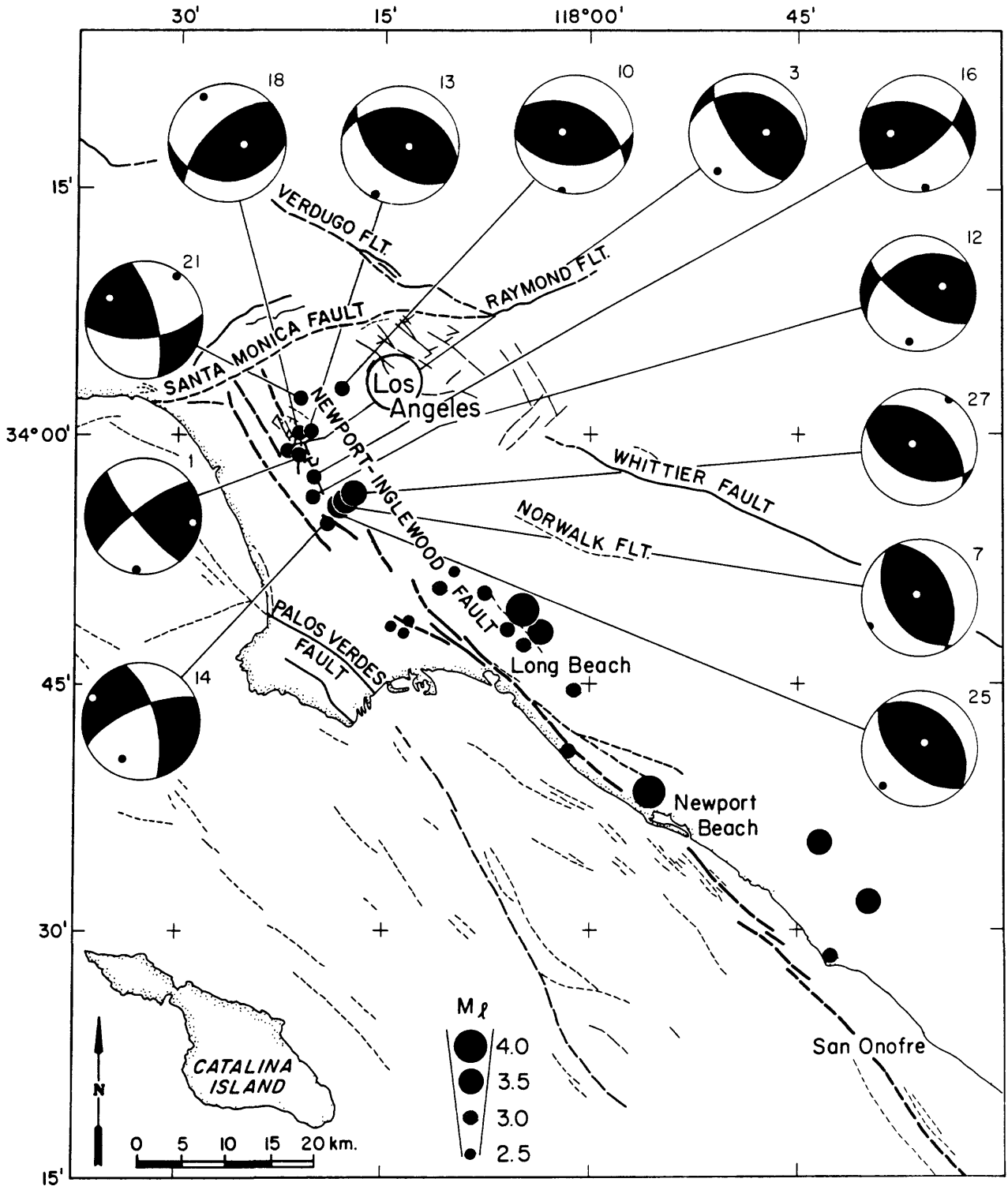
Figure 2. Single event lower hemisphere fault plane solutions for earthquakes along the northern section of the Newport-Inglewood fault.

Northwest U.S. Subduction Zone
Risk Assessment
9930-03790

Thomas H. Heaton and Stephen H. Hartzell
Branch of Seismology
U.S. Geological Survey
525 S. Wilson Avenue
Pasadena, CA 91106
(818) 405-7809

The primary purpose of this project is to assess the potential seismic hazard due to great shallow thrust earthquakes along the Juan de Fuca subduction zone of the northwestern United States. Despite good evidence of 3 to 4 cm/yr of present-day plate convergence, historic (150 yr) and instrumentally located seismicity has been remarkably low in the shallow part of the subduction zone lying beneath the continental margin of the northwestern United States. Although it may be that interplate slip along this 900 km by 100 km interface is occurring entirely aseismically, the Juan de Fuca subduction zone shares many characteristics with other zones that have experienced great shallow subduction earthquakes. In order to assess the potential hazard due to such earthquakes, we (1) estimate the size, recurrence time, and rupture characteristics of potential subduction earthquakes by identifying analogous subduction zones and studying earthquakes that have occurred there and (2) we estimate the nature of strong ground motions by studying strong ground motion records from other large subduction earthquakes.

In addition to our work on seismic hazards in the northwestern U.S., we are also constructing models of the rupture history of the 1984 Morgan Hill earthquake as inferred from waveform modeling of strong ground motions using a finite fault in a layered half-space.

Investigations

1.   Compare physical characteristics of subduction in the northwestern United States with those of other world-wide subduction zones. Investigate the characteristics of earthquakes that have occurred on analogous subduction zones.

2.   Estimate the potential strong ground motions from shallow subduction earthquake that could be postulated for the northwestern United States.

3.   The strong ground motion waveforms for the April 24, 1984 Morgan Hill earthquake are modeled to obtain the coseismic distribution of slip. The Calaveras Fault is subdivided into a gridwork of equal-sized subfaults. The ground motion due to a unit amount of slip on each one of these subfaults is computed separately for each local strong motion station. These synthetics, along with the data, for the input to a least-squares inversion scheme. The inversion program then calculates the best fitting spatial and temporal distribution of slip in the frequency band of 0.2 Hz to 5.0 Hz.

Results

1.   We have compared age of subducted plate, rate of convergence, trench bathymetry, free-air gravity, heat-flow, seismicity, trench sediments, and overall geometry of the Juan de Fuca subduction zone with other world-wide subduction zones. We conclude that the subduction zones in southwestern Japan, southern Chile, Colombia, and Mexico are most similar to subduction in the northwestern United States. The convergence rate in southwestern Japan is about 3 to 4 cm/yr and this region has experienced earthquakes of up to M_w 8.6. It appears that sometimes the entire zone ruptures during a single event and that at other times the zone breaks in several smaller (M_w 8) events. The recurrence times for these events has ranged from 100 to 250 years with an average of about 180 years. Southern Chile has a convergence rate of about 9 cm/yr and, based on the occurrence of 4 great earthquakes, has an average repeat time of about 130 years. All of these events appear to be very large, and the 1960 earthquake is the largest world-wide event of this century (M_w 9.5). Colombia has a convergence rate of about 8 cm/yr and has experienced a M_w 8.8 earthquake in 1906 and a M_w 8.2 earthquake in 1979. The area near Jalisco, Mexico is subducting at a rate of about 55 cm/yr and is also similar to the northwestern United States. This area experienced an M_w 8.2 earthquake in 1932 and the recurrence time is not established for this type of event. All of the areas that share physical characteristics with the Juan de Fuca subduction zone have experienced shallow subduction earthquakes with energy magnitudes of greater than 8. While this does not prove that great earthquakes will occur in the northwestern United States, it does suggest that we should not ignore their possibility. Based on the comparison with other zones, we postulate that earthquakes of up to M_w 9 with recurrence times of 300-500 years cannot be ruled out.

2.   An interesting report of Indian legends of a dramatic sea-level disturbance has been brought to our attention by Park Snavely Jr. (U.S.G.S., Menlo Park). James G. Swan (1868, Smithsonian Contributions to Knowledge, no. 220) reported that Indians from the Makah, Kwilleyute, and Chemakum tribes all maintained a tradition that vaguely resembles the occurrence of a great prehistoric tsunami along the Washington coast.

3.   We have collected over 50 strong ground motion recordings from more than 20 shallow subduction earthquakes having magnitudes of 7 or greater. Fourteen of these earthquakes were also considered in our teleseismic study of the 60 largest subduction earthquakes in the last 50 years. There appears to be a good agreement between the duration of energy release as inferred from the teleseismic records and the duration of the observed strong ground motions for many (but not all) of these earthquakes. We have prepared a set of figures summarizing the ground motions for the 25 large subduction earthquakes as well as the spatial geometry of the stations relative to the aftershock zones. Response spectra have been calculated for all components of acceleration. These spectra have been sorted by magnitude and horizontal distance to the rupture surface. Comparison of spectra at similar distances and earthquake magnitudes shows a very large scatter (about one order of magnitude). These records provide sufficient data to estimate the ground motions for earthquakes having magnitudes of up to 8 1/4. There are no strong motion records available for earthquakes of M_w greater than 8 1/2. In order to estimate motions from such earthquakes, we will sum

records from smaller earthquakes using a model of the rupture characteristics of giant earthquakes. The rupture characteristics will be chosen in such a way that the summation process will be compatible with observed teleseismic records of giant earthquakes.

4.   A plane-layered approximation to the velocity structure of Blumling et al. (1985, Bull. Seism. Soc. Am. 75, 193-209) is used to calculate the required Green's functions. The timing of phases at several strong motion stations shows a 15% reduction in the S-wave velocity for travel paths within the fault zone compared with travel paths perpendicular to the fault. An inspection of the strong motion records suggests that the earthquake consisted of two main sources, or alternatively a single source which produced a prominent "starting phase" and "stopping phase". Inversion of the strong motion data indicates that the two source model is the favored interpretation. However, there is also considerable associated slip of lower amplitude. One source is located near the hypocenter at a depth of about 10 km. The second and larger source broke about 4.5 sec later and is located under Anderson Lake at a depth of about 8 km. The maximum dislocations are between 1.5 m and 2.0 m. The average rupture velocity is approximately 90% of the shear wave velocity. The limited spatial extent and sharpness of the dislocation patterns for the Morgan Hill earthquake make it a good example of the asperity model of faulting.

Reports

Hartzell, S.H. and T.H. Heaton (1985). Teleseismic time functions for large, shallow subduction zone earthquakes, Bull. Seism. Soc. Am., in press.

Hartzell, S.H. and T.H. Heaton (1985). Strong ground motion for large subduction zone earthquakes, Earthquake Notes, vol. 55 No. 1, 6.

Heaton, T.H. and S.H. Hartzell (1985). Estimates of potential shallow subduction earthquakes in the northwestern U.S., Earthquake Notes, vol. 55 No. 1, 16.

Heaton, T.H. (1985). A model for a seismic computerized alert network, Science, in press.

Heaton, T.H. and H. Kanamori (1985). Reply to H. Acharya's "comments on seismic potential associted with subduction in the northwestern United States", Bull. Seism. Soc. Am., in press.

Hartzell, S.H. and T.H. Heaton (1985). Teleseismic time functions for large shallow subduction earthquakes, Ewing Symposium on Fault Rupture Dynamics, Spring 1985.
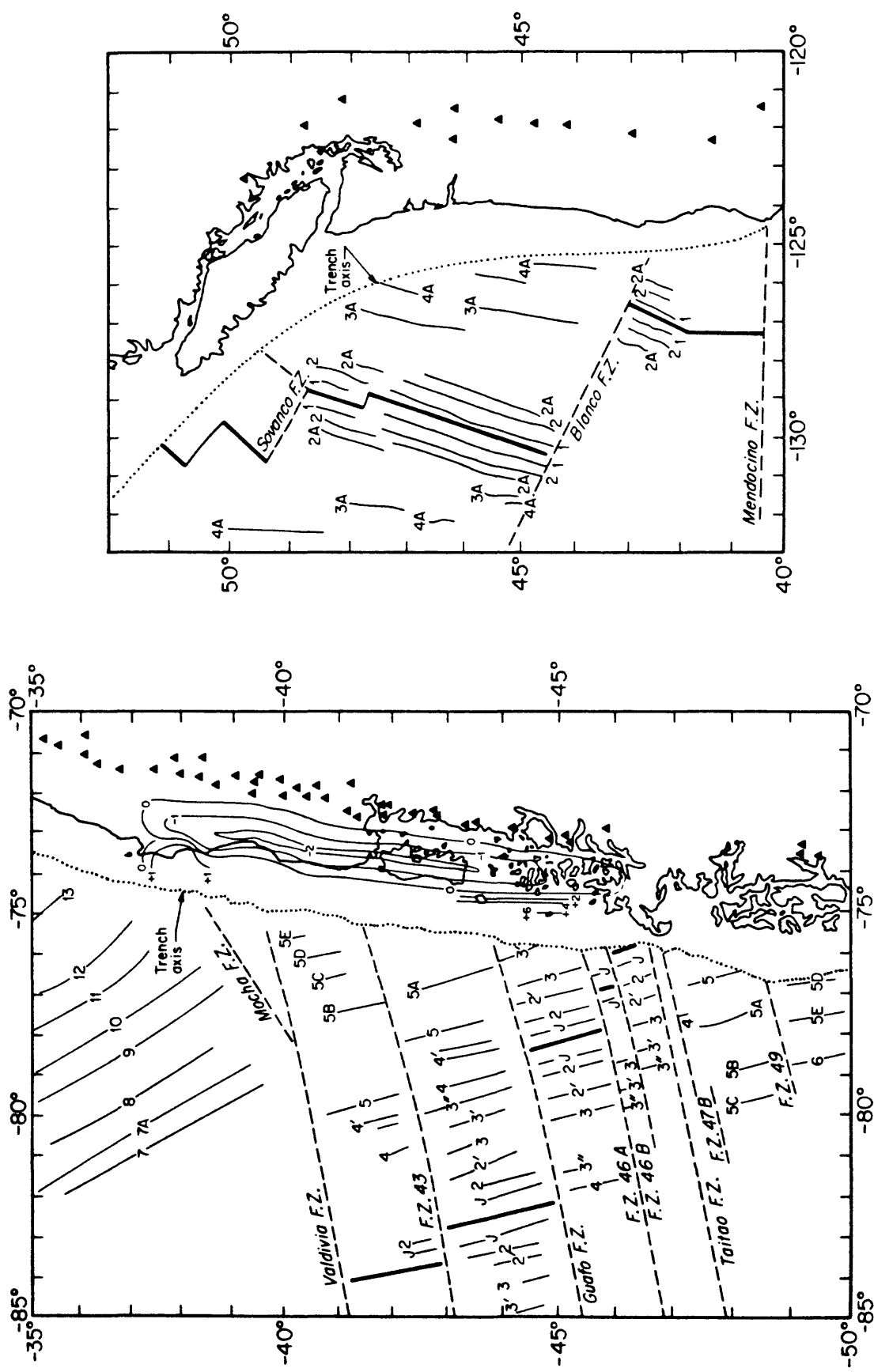
Figure 1. Comparison of the geometry of subduction in the northwestern United States with that in southern Chile. Maps are on the same scale. Sea-floor magnetic lineations and Quaternary volcanoes are shown. Coseismic vertical deformation from the 1960 M_w 9.5 earthquake is also shown.

SEARCH FOR PRECURSORS TO EARTHQUAKES IN THE VANUATU ISLAND ARC BY MONITORING TILT AND SEISMICITY

14-08-0001-18350

Bryan L. Isacks
Department of Geological Sciences
Cornell University
Ithaca, NY 14853
(607)256-2307

Investigations

This report covers the period October 1, 1984 to March 31, 1985 for the operation and analysis of data from the Vanuatu seismograph and tilt networks. The networks include twenty stations distributed along 500 km of the arc, seven bubble-level tiltmeter stations, two periodically releveled arrays of benchmarks (1 km aperature), and a 100 m two-component water tube tiltmeter. Our investigations during the period covered by this report have concentrated on analyses of data from the seismograph network and from the long-baseline tiltmeter.

Results

1.   The most important earthquakes caught since the commencement of the local networks occurred near Efate island. The events comprise a spatially coherent sequence that began in 1978 after four years of relative quiescence. This sequence can be divided into a "precursory" episode in 1978-1979 (three magnitude 6 events), the magnitude 7.1 "mainshock" in July 1981, and a "post-seismic" episode in 1983 (three events with magnitudes between 5.8 and 6.1). A paper describing the 1978-1983 Efate sequence is nearing completion. The paper describes the intricate spatial-temporal relationships among the mainshock epicenters, aftershock sequences and clusters of events that define the 1978-1983 sequence. The results strongly suggest specific structural features of the interacting plates (or "asperities") which localize and concentrate the seismicity. In some cases those features appear to form temporary "barriers" to the spatial development of seismicity, while in other cases specfic areas seem to be repeatedly activated. The epicenters of previous moderate to large sized earthquakes are also found to concentrate in the repeatedly activated areas revealed in the 1978-1983 sequence. Another result of the study is that a clear difference can be seen between the locations of

aftershocks and clusters versus the locations of the remaining "background" activity. The aftershocks and clusters tend to be located trenchward (up-dip) of the more continuously active background activity. This suggests a variation with depth in the mode of slip along the plate boundary from stick-slip at shallow depths to creep at greater depths.

Ongoing investigations are concentrated on more detailed resolution of the spatial structure of the aftershock sequences and clusters of the 1978-1983 sequence, and on related variations in source properties, particularly focal mechanism orientations. Cooperative work with S. Roecker is underway to invert the local network data for the three-dimensional velocity structure of the central New Hebrides.

2.   During the past year and a half the region of Efate-Malekula islands where the 1978-1983 sequence took place has been relatively quiet. In fact, during the past 6 months no events have been located by the PDE in the region of Malekula and Efate islands. The largest event during the past six months occurred nearly 100 km south of Efate in October, 1984. This event (Ms = 5.9) is located very close to the magnitude 6 earthquake of January, 1979 and to the magnitude 7.1 earthquake of 1961. The area is just south of the region affected by the 1978-1983 sequence. The 1984 event had a well-developed aftershock zone (its focal mechanism is not yet determined). The area of the aftershock zone is smaller - about 10-15 km across - and is more typical of a earthquake of its magnitude than the anomalously large aftershock areas developed near Efate island. No foreshocks were detected for the 1984 earthquake.

3.   Modification of the long-baseline (100 M) water-tube tiltmeter made during August, 1984 led to significant improvement in the long-term stability of the instrument, as seen in recordings to January, 1985. The previous system had end pots open to the system atmosphere (while the system as a whole was sealed from the environment). Condensation on the float appeared as instrumental drift. During August, 1984 a controlled test was initiated for one of the end pots. The exposed water surface surrounding the float was sealed by floating a film of oil the surface. The records from this pot during the following four months showed that this modification was successful in removing the condensation induced drift. The remaining three detectors will be conditioned in the same way. In addition , a very flexible diaphragm will be installed in the system air return passage tubes in each detector pot. In conjunction with the oil, this diaphragm will help isolate the float-transducer elements from any exposure to moist air.

Reports

Marthelot, J.-M., J.-L. Chatelain, B. L. Isacks, R. K.
Cardwell, E. Coudert, 1985, Seismicity and Attenuation in the
Central Vanuatu (New Hebrides) Islands: A New Interpretation
of the Effect of Subducting the D'Entrecasteaux Fracture Zone,
J. Geophys. Res., 90, in press.

Instrument Development and Quality Control

9930-01726

E. Gray Jensen
Branch of Seismology
U.S. Geological Survey
345 Middlefield Road - Mail Stop 977
Menlo Park, California 94025
(415) 323-8111, Ext. 2050

Investigations

This project supports other projects in the Office of Earthquake, Volcanoes and Engineering by designing and developing new instrumentation and by evaluating and improving existing equipment in order to maintain high quality in the data acquired by the Office. During this period some personnel from this project were assigned to the GEOS project (9940-03009) on a part-time basis.

Results

Expansion of the CALNET microwave network is continuing. The network now extends to Hog Canyon to the south and Mt. Tamalpais to the north. During this period an effort was initiated to identify the causes of and eliminate losses of signal experienced by the network. Addition of a "space diverse" antenna to the Mt. Tamalpais-Mission Peak link seems to have improved its reliability and may be the solution at other locations as well. Development and construction of improved telemetry VCO's for seismic data has continued. Twenty-five of the prototype J501 VCO-preamp packages which included an EXAR VCO for higher stability and dynamic range have been built and installed. An additional 100 units of the improved J502 version are currently under construction. Also under construction are 100 each of the V02H and V02L modification circuits for conversion of J402's for more stability and dynamic range.

A system for keeping an array of portable recorders synchronized to less than 1 microsecond was developed and installed at Anza. The inputs to the CUSP digitizer were modified to provide shielding and reduce noise in the system. An improved squelch circuit has been developed for the Motorola telemetry radios. Also development has begun on the following project: an alarm system for the microwave network, a new discriminator with higher-dynamic range, digital seismic telemetry and recording, and an integrated circuit replacement for the mercury battery calibration reference in seismic telemetry packages.

Ongoing projects include maintenance of the 16 seismic stations and monitoring equipment of the Yellowstone network. Installation of seismic telemetry equipment at 20 sites in the Parkfield area was performed. Sixteen pairs of telemetry radios were prepared for use in the USSR and maintenance of PDR-2 event recorders was provided for the PRC. Maintenance was also provided for the Seismic Cassette Recorder system during projects in Maine and Nevada. Repair or modification of 85 telemetry radios and calibration of 100 seismometers was performed.

Southern California Cooperative Seismic Network

9930-01174

Carl E. Johnson
Branch of Seismology
U.S. Geological Survey
Seismological Laboratory 252-21
Pasadena, California   91125

Investigations

1. Southern California Network Operations
   Operations and maintenance of the southern Caifornia seismic network continued through the reporting period without significant failure. At present 248 predominantly short-period, vertical instruments are telemetered to Caltech for analysis.

2. Routine Network Analysis
   Routine processing using stations of the southern California cooperative seismic network was continued for the period October 1984 through March 1985. Routine analysis in cooperation with Caltech personnel includes the interractive timing of phases, event location, magnitude calculation, and final catalog production using the CUSP analysis system. At present 2000 events detected each month are being analyzed in this manner with a regional magnitude threshold approaching 1.2.

3. Hawaiian CUSP
   The real-time component of CUSP has been developed and implemented at HVO (Hawaiian Volcano Observatory) where it is being used to digitize volcanic events associated with the Kilauea and Mauna Loa volcanoes. Running on one of a pair of VAX 11/750 microcomputers, the real-time module is used to process, display, and archive events from an array of 72 instruments with a digitization rate of 100 hz. This consumes roughtly 5% of available CPU time on the real-time machine leaving the remainder available for automatic processing as well as on-line interractive analysis. A unique asynchronous design was used at HVO that permits scientists to access the real-time data steam for such purpose as sampling tremor, or event counts. The current implementation provides a substantially lower threshold for the detection of small volcanic microquakes and tremor events with a better than 5 fold increase in capture rate over other automatic systems used at HVO during the past several years.

4. Seismotectonics of the Cajon Pass
   Three of the largest faults in southern California, the San Andreas, San Jacinto and Transverse Ranges Frontal faults, intersect at Cajon Pass. This complex region is the southern terminus of the 1857 rupture and one of the most persistently seismically active areas of southern California. Focal mechanisms of all the $M \geq 2.6$ earthquakes in the region from 1978 to 1984 are being determined from first motion data. Earthquake locations are also being re-analyzed to determine the seismogenic structures within the area. The focal mechanism data are being analyzed and inverted to determine the state of stress along the San Andreas fault.

5. Earthquake Activity in the Southern Sierra Nevada

We have been conducting a special study of a recent swarm at Durrwood Meadows in the southern Sierra Nevada. The southern Sierra Nevada has been one of the most seismically active regions of southern California during 1984. The spatial and temporal distribution of this earthquake activity has been analyzed to determine the cause of the activity and the importance of these events in estimating the seismic hazard of the region. The focal mechanisms of the M > 3.0 events within the swarm have also been determined from first motion data.

6. Seismicity Statistics Based on 2nd Order Moment

Analysis of the second order seismic moment of the southern California catalogue is being carried out in collaboration with Paul Reasenburg in Menlo Park, CA. With this technique, spatial and temporal patterns of seismicity associated with moderate earthquakes are examined. In addition, Reasenburg's clustering algorithm is being applied to the southern California catalogue. The resulting clusters will be analyzed to quantify seismic patterns and search for possible seismic precursors in southern California.

Results

1. Seismotectonics of the Cajon Pass

Re-analysis of the earthquakes in the region from 1978 to 1984 has shown that while two strands of the San Jacinto fault are very active, both the Tranverse Ranges and San Andreas faults are quiescent. Almost all of the earthquakes are confined to the western side of the San Andreas fault. Focal mechanisms were determined from P-wave first motions for all M > 2.6 earthquakes from 1978 to May 1980 and August 1912 through 1984. All of these earthquake mechanisms had one plane striking subparallel to the San Andreas fault and dipping slightly to the northeast. Two thirds of these mechanisms showed almost pure right-lateral, strike-slip motion along the northwest trending plane, while the rest had a significant component of reverse motion (rake of 120° to 150°). The reverse mechanisms are more common north of the Transverse Ranges Frontal fault and close to the San Andreas fault. Inversion of these data for stress state using the methods of Angelier shows the maximum principal stress is horizontal along a north-south direction. The minimum stress is also horizontal and strikes east-west.

2. Earthquake Activity in the Southern Sierra Nevada

The Durrwood swarm was located within a 100-km long linear belt of seismicity that trends through the southern Sierra Nevada along a north-south strike. This seismic belt was one of the most seismically active features in southern California during 1984. The Durrwood swarm itself was characterized by a complex spatial distribution and a simple pattern of focal mechanisms. At the beginning of the swarm, the earthquakes were located along a northwest trend. Later periods of high seismicity were distributed along a northeast trend forming a Y-shape structure and other north and northwest trends. In spite of this complexity, the focal mechanisms of the 35 M > 3.0 earthquakes within the swarm were all similar to each other with almost pure normal faulting along a north-south strike. The strikes of the planes in the focal mechanims and the spatial distribution of the epicenters form an en echelon pattern. The

consistency of the focal mechanism with each other and the en echelon pattern imply a homogeneous stress field and the lack of a continuous fault structure. A 100 km linear belt of seismicity in an area with no through-going fault structure is interpreted as the beginning of a Basin and Range type normal fault presently forming within the Sierra Nevada.

Reports

1. Jones, L.M., Foreshocks and time-dependent earthquake hazard assessment in southern California, Trans. Amer. Geophys. U., 65, no.45, p.988, 1984.

2. Jones, L.M., Seismotectonics of the Cajon Pass region of the southern San Andreas fault, Trans. Amer. Geophys. U., 66, p.383, 1985.

Earthquakes and the Statistics of Crustal Heterogeneity

Bruce R. Julian

Branch of Seismology
U.S. Geological Survey
345 Middlefield Road - MS77
Menlo Park, California 94025
(415) 323-8111 ext. 2931

Investigations

Both the initiation and the stopping of earthquake ruptures are controlled by spatial heterogeneity of the mechanical properties and stress within the earth. Ruptures begin at points where the stress exceeds the strength of the rocks, and propagate until an extended region ("asperity") where the strength exceeds the pre-stress is able to stop rupture growth. The rupture termination process has the greater potential for earthquake prediction, because it controls earthquake size and because it involves a larger, and thus more easily studied, volume within the earth. Knowledge of the distribution of mechanical properties and the stress orientation and magnitude may enable one to anticipate conditions favoring extended rupture propagation. For instance, changes in the slope of the earthquake frequency-magnitude curve ("b-slope"), which have been suggested to be earthquake precursors and which often occur at the time of large earthquakes, are probably caused by an interaction between the stress field and the distribution of heterogeneities within the earth.

The purpose of this project is to develop techniques for determining the small-scale distributions of stress and mechanical properties in the earth. The distributions of elastic moduli and density are the easiest things to determine, using scattered seismic waves. Earthquake mechanisms can be used to infer stress orientation, but with a larger degree of non-uniqueness. Some important questions to be answered are:

** How strong are the heterogeneities as functions of length scale?

** How do the length scales vary with direction?

** What statistical correlations exist between heterogeneities of different parameters?

** How do the heterogeneities vary with depth and from region to region?

Scattered seismic waves provide the best data bearing on these questions. They can be used to determine the three-dimensional spatial power spectra and cross-spectra of heterogeneities in elastic moduli and density in regions from which scattering can be observed. The observations must, however, be made with seismometer arrays to enable propagation direction to be determined. Three-component observations would also be helpful for identifying and separating different wave types and modes of propagation.

The stress within the crust is more difficult to study. Direct observations require deep boreholes and are much too expensive to be practical for mapping small-scale variations. Earthquake mechanisms, on the other hand, are easily studied and reflect the stress orientation and, less directly, its magnitude, but are often not uniquely determined by available data.

This investigation uses earthquake mechanisms and the scattering of seismic waves as tools for studying crustal heterogeneity.

Results

Estimating Earthquake Locations

A new earthquake hypocenter-location computer program, *qloc*, has been written. It is small, so that it can treat events with hundreds of readings, even on small machines with limited memories, and at the same time is faster than other existing programs. It uses modern algorithms, and is designed to be general and flexible, so that these algorithms can be replaced as better ones are invented. This flexibility also enables specialized methods (for example, three-dimensional ray tracing) to be used when they are needed. Three features of the program deserve special mention:

** The ability to compute confidence estimates that are much more realistic than those provided by most other programs.

** Stable optimization algorithms, which combine large domains of convergence with rapid convergence rates.

** A method for estimating the expected size of travel-time anomalies, based on a statistical model of seismic-wave-speed variations in the earth. These estimates are used to compute optimal weights to be applied to observations at different epicentral distances, as well as to identify grossly erroneous data. and ,

An open-file report describing the program and a journal article on the algorithms used are in preparation.

Monitoring Earthquakes in Real Time

In cooperation with Barbara Bekins (see report for project 9930-03354), many improvements have been made to the software that analyzes earthquakes using data generated by the Real-Time Processors (RTP). These changes, which make the software more robust, more efficient, and more flexible, have become necessary because of the growing role played by RTP data in earthquake monitoring and prediction research. Up-to-the-minute seismicity maps can now be displayed continuously on CRT computer terminals in Menlo Park, California and Reston, Virginia, and an automatic alarm system using radio-controlled beepers alerts seismologists to unusual earthquake activity.

The main changes that have been made to the software are:

** The programs have been made smaller, so they can run on small mini- or micro-computers such as the PDP-11/23.

** The software has been made much faster, so it can keep up with intense earthquake swarms and aftershock sequences.

** The alarm facilities have been made more general and flexible. Alarms can be sounded for individual large events or for earthquake swarms, and the criteria used can vary from region to region.

** The connection to the RTP devices has been made more reliable. Hardware character buffers have been installed which largely eliminate instances of data being lost. Furthermore, the software now recovers from various abnormal conditions (unplugging an RTP, for example) without the need for human intervention.

** The software can simultaneously process data from multiple RTP devices. Currently, two RTPs are used to monitor earthquakes in central and northern, California.

** Either *hypo71* or *qloc,* the program described above, can be used to estimate earthquake hypocenters and origin times. It is planned that *qloc* will become the primary hypocenter program in the near future.

** The software now incorporates algorithms developed by Dr. Allan G. Lindh for identifying spurious events caused by factors such as transmission noise.

This software system is largely hardware-independent (it has been tested on four different computers). An open-file report describing it is in preparation.

Modelling seismic-wave codas

Investigations are continuing into seismic-wave coda shapes predicted from a physical model of elastic-wave scattering. This model takes into account the earthquake source mechanism, the vector nature of elastic waves, and possible anisotropy in the statistical distribution of heterogeneities in the earth. Preliminary investigations indicate that coda shapes for different source mechanisms and types of scattering (P-to-S, S-to-S, etc.) show surprisingly large variations in coda shapes, and suggest the possibility that coda shapes might be used in determining earthquake mechanisms.

Long Valley caldera Dilatometer

In order to gather data bearing on the earthquake mechanisms at Long Valley caldera, a Sacks-Evertson dilatometer was installed in 1983 and 1984 near the Devil's Postpile, immediately southwest of the caldera. The installation is now complete, and both low- and high- frequency data are being telemetered to Menlo Park. This instrument recorded the Wheeler Crest earthquake of November 23, 1984 (magnitude 5.8), which was about 45 km from the dilatometer, producing an interesting record that showed both a static offset and complex strain changes within the first few hours following the earthquake. The static strain offset agrees with the value computed from the seismic moment of the earthquake, but the causes of the changes following the earthquake are not yet understood. No premonitory strain changes immediately before the earthquake were detectable.

Seismic Study on Rupture Mode of Seismic Gaps

Contract No. 14-08-0001-G-979

Hiroo Kanamori
Seismological Laboratory, California Institute of Technology
Pasadena, California 91125 (818-356-6914)

Investigations

1) The vertical extent of faulting of the May 26, 1983, Akita-Oki earthquake.

2) Consistency of moment tensor source mechanisms with first-motion data.

Results

1) The vertical extent of faulting of the May 26, 1983, Akita-Oki earthquake.

We have investigated the depth extent of faulting of the May 26, 1983, Akita-Oki, Japan, earthquake by using long-period surface waves. Two methods were used. In the first method, we inverted long-period Rayleigh and Love waves assuming various point source depths and searched for a depth that gives a best fit. In this inversion we used a recently obtained laterally heterogeneous earth model. The use of the laterally heterogeneous model together with a finite rupture model reduced significantly the mismatch between the observed and calculated source phases. The result of this inversion indicates that the vertical extent of the faulting of the Akita-Oki earthquake is from 5 to 25 km, which agrees well with the vertical extent of the aftershock zone.

In the second method, the amplitude ratio of overtones to the fundamental mode Rayleigh waves is used to constrain the depth. Using the overtones (2 to 5) at a period around 80 sec and the fundamental mode at a period of about 200 sec, we determined the depth that best explains the observed amplitude ratio. The result indicates that a fault model which extends from 5 to 30 km explains the data best.

2) Consistency of moment tensor source mechanisms with first-motion data (A part of this project was done during the previous contract period. Since the work was completed and published during the current contract period, we are reporting the result here.)

Moment tensor source mechanisms for the largest twenty-nine shallow earthquakes from 1981 ($M_s \geq 6.5$) have been determined using long-period Rayleigh-wave spectra and P-wave first-motions, recorded by the International Deployment of Accelerograms (IDA), Global Digital Seismic Network (GDSN), and World-Wide Standardised Seismic Network (WWSSN). These are compared with the centroid moment tensor mechanisms presented by Dziewonski and Woodhouse, which were obtaied in a contrasting manner. In most cases, the source is well represented by a single double-couple mechanism, with good agreement of scalar moment and orientation between the two studies. Apparent mismatches for other cases may be interpreted in terms of source complexity.

We emphasize the objectivity of comparing moment tensor elements; apparent discrepancies in the moment and orientation of double-couple fault plane solutions are usually due to differences in the M_{xz} and M_{yz} moment tensor elements, which are poorly constrainted by long-period data.

References

Astiz, L., T. Lay, and H. Kanamori, A global study of intermediate-depth earthquake mechanisms, AGU Fall Meeting, San Francisco, California, December 3-7, 1984.

Scott, D. R. and H. Kanamori, On the consistency of moment tensor source mechanisms with first-motion data, *Phys. of the Earth and Planet. Int.*, *37*, 97-107, 1985.

Zhang, J. and H. Kanamori, Determination of vertical extent of faulting of larte earthquakes by inversion of surface waves, AGU Fall Meeting, San Francisco, California, December 3-7, 1984.

FAULT MECHANICS AND CHEMISTRY

9960-01485

C.-Y. King
Branch of Tectonophysics
U.S. Geological Survey
345 Middlefield Road, MS/977
Menlo Park, California 94025
(415) 323-8111, ext. 2706

Investigations

1. Water temperature and radon content were continuously monitored at two water wells in San Juan Bautista and a newly prepared well in Parkfield, California.

2. Water level was continuously recorded at six other wells.

3. Water samples were periodically taken from most of these wells for chemical analyses.

4. Radon content of ground gas was continuously monitored at two sites (Limekiln A and Cienega Winery) along the San Andreas fault in the Bear Valley area, California, and at a site in Nevada Test Site.

5. Slip events generated along a laboratory fault were studied.

Results

A continuous ground-water radon monitor was installed in February 1985 at a 350-foot-deep well in Miller's Ranch, about 1 km west of Parkfield, CA, where a moderate earthquake is expected to occur during the next few years on the basis of local seismic history. The initial radon data (Figure 1) show: (1) clear diurnal and semidiurnal variations, similar to water-level data recorded earlier at the same well (Figure 2), possibly reflecting tidal variations; (2) large spike-like increases, mostly at daily maxima, similar to some ground-water radon data recorded in China and soil-gas radon data recorded in Bear Valley, CA, area; (3) less longer-term variations than water level, possibly related to local rainfall and pumping activities.

Reports

King, C.-Y., 1984, Earthquake prediction: evaluating hydrological and geochemical anomalies: Nature, v. 312, p. 501.

King, C. Y., 1984, Earthquake hydrology and chemistry, Editor's Note: Pure and Applied Geophysics, in press.

pkf: 20:00 11 Feb 1985 042 - 19:00 23 Apr 1985 113
Parkfield radon

pkf: 20:00 11 Feb 1984 042 - 19:00 22 Apr 1984 113

Parkfield well depth(meters)
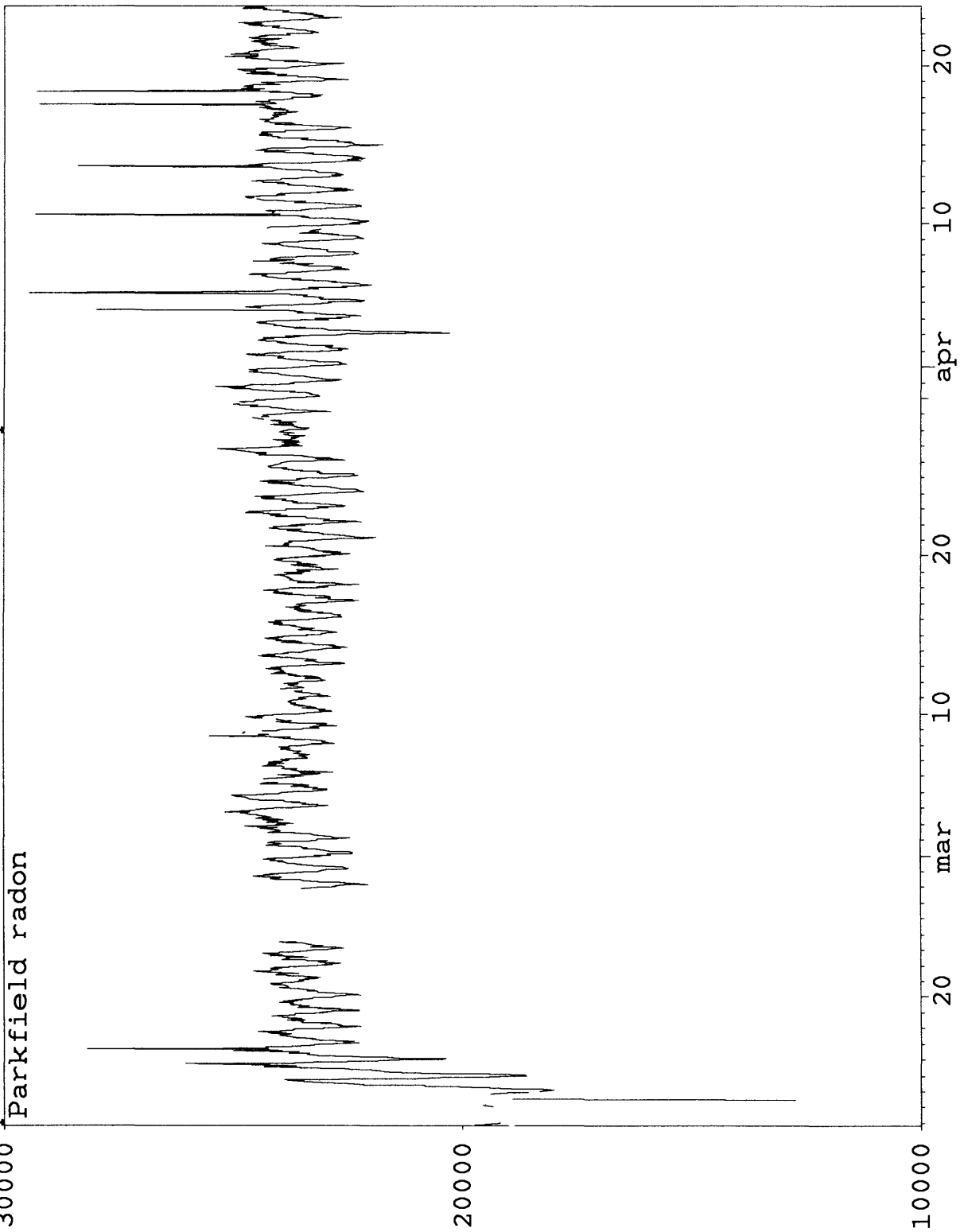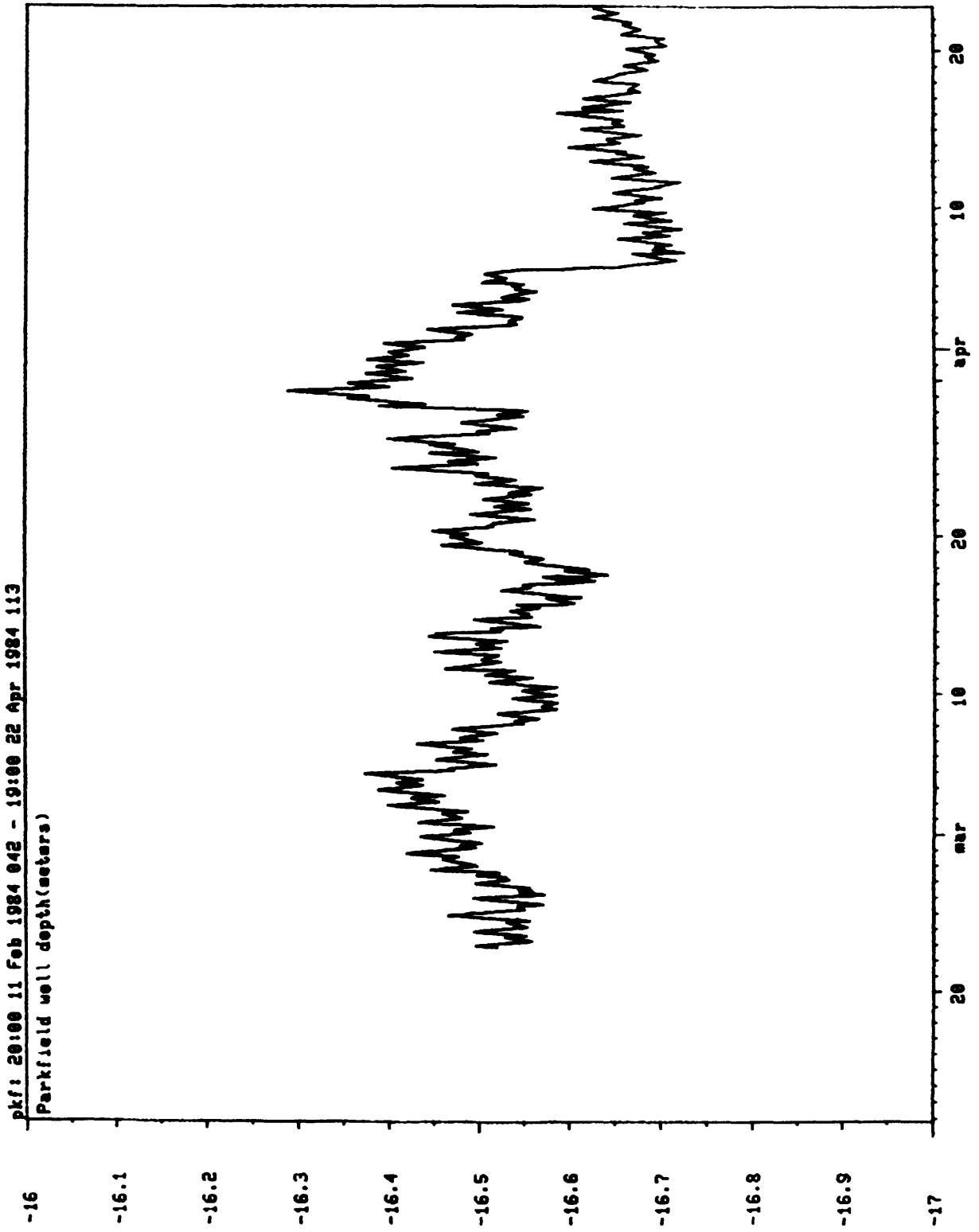
Prediction Methodology for Subduction Zone Earthquakes
Central Aleutian Islands

Grant Number 14-08-0001-G-881

Carl Kisslinger and Selena Billington
Cooperative Institute for Research in Environmental Sciences
Campus Box 449, University of Colorado
Boulder, Colorado 80309
(303) 492-8028

The research during October, 1984-March, 1985 has been focused on: 1) further development of the long-term seismic history of the Adak Seismic Zone (taken as $50°$-$53°$ N, $174°$-$179°$ W) for major earthquakes $M_s \geqslant 7$ since 1900 and time-space patterns for the past nine years shown by both microearthquakes, located by the Adak Network, and teleseismically-located events reported in the PDE, and 2) seismotectonics of the area around Adak Canyon, with emphasis on the source characteristics of microearthquakes

Seismicity of the Adak Seismic Zone

History of Strong Earthquakes. We have been observing, locating and analyzing earthquakes in the Adak Zone for more than ten years and have acquired a reliable picture of the general distribution of activity in the main thrust zone, the Benioff zone and a shallow, back-arc zone, with definition of differences east and west of Adak Canyon. We have not had a dependable history of major events, M_s 7 and greater, because of the difficulty of assembling credible catalogue information for this remote place. Because we have in effect a prediction for an earthquake in this magnitude range to occur before the end of October, 1985, we have felt it necessary to pull together data from a variety of lists, catalogues and journal articles, to evaluate the general probability of occurrence of an earthquake this strong, in a time-averaged sense, without consideration of currently observed phenomena that might be precursors. The result is shown in Figure 1 as a space-time plot since 1900. We know that the locations prior to 1957 are highly suspect, and some of the earliest events may not have even had epicenters within the zone. The suggested rupture lengths of the early events are only guesses based on magnitudes derived in various ways by others.

Keeping these uncertainties in mind, we have identified 14 strong thrust zone earthquakes, not counting 6 strong immediate aftershocks of the great 1957 event that have epicenters within the zone. The most recent major earthquake was on May 2, 1971, under Adak Canyon. Thus the average interval is six years, but the activity is clustered in three epochs, around 1910, around 1930, and around the great 1957 earthquakes. Our concept is that the 1971 event was the first in a new seismic cycle that began after the 1957 earthquake. Our conclusion is that this seismic history makes a strong event in the near future, 14 years since the last one, plausible.

Current Seismic Quiescence. Our prediction of a strong earthquake near Adak Island during this year is based mostly on the observation of pronounced seismic quiescence across the zone, beginning in September, 1982. Recent analysis of our local catalogue and the PDE reports shows that the zone of quiescence does not include the westernmost part, west of $177.8°$ W, and the rate-of-occurrence statistics are different for

the shallow, main thrust zone activity and the earthquakes at intermediate depths. Activation of subregion SW2, where the location of a m_b 5.8 event that occurred on May 6, 1984 was accurately forecast, tends to obscure the quiescence in the teleseismic events, an important lesson for activation-quiescence analysis. We are testing the hypothesis, based on these data and one well-documented cased discovered by Habermann, that a three-year long quiescence is a precursor to a magnitude 7+ event in the Adak region, with the likely site in the neighborhood of Adak Canyon.

We have used our excellent and detailed data set to examine the time dependence of seismicity rates within various ranges of focal depth. The main results, shown in Figure 2, are that the quiescence is confined to the upper 75 km. The intermediate-depth events also show fluctuations in rate of occurrence, but no deficiency of the number of events at this time in terms of the rates prior to late 1982. The geological and tectonic significance of the relative rates of shallow and intermediate events may be a clue to coupling between these two regimes, but the interpretation of these data is a task for the future.

Source Parameters of Microearthquakes in and near Adak Canyon

A study of source parameters, including associated stress values, of microearthquakes occurring within a region including Adak Canyon (Figure 3) has been completed. Spectra derived from 1897 horizontal-component records of 457 earthquakes located by the Adak Seismic Network were examined. These events occurred between January 1, 1981 and June 30, 1984, within the volume defined by 51°-51.85°N, 176.75°-177.60°W, and 0-300 km depth. No magnitude cut was made initially, but many events had to be discarded because of clipping (larger events), poor signal-to-noise ratio (smaller events), or electronic noise. The remaining 291 records of 107 events formed the data set.

Brune's source model was used to calculate seismic moment, fault radius and stress drop from each spectrum, from which the low-frequency level and the corner frequency were picked by eye. The radiated seismic energy was calculated by integrating the seismograms and apparent stresses were determined from these values. Only earthquakes for which two or more usable records were in the data set were retained. The approach and computer programs used are those employed by Scherbaum and Kisslinger (1984).

The resulting apparent stresses are plotted at the epicentral locations of the earthquakes in Figure 3. A group of events on the right margin of the region, at about 51.35°N, is the SW 2 cluster described in early work under this project. Apparent stresses range from 1 to 4 bars, with standard errors of 2-3 bars. Stress drops from less than 1 to 13 bars were observed. Figure 4 depicts these earthquakes in north-south cross-section, with events east of 177.2°W in 4a and those west of this line in 4b. This longitude marks the approximate eastern boundary of the tectonic unit associated with Adak Canyon. The main thrust zone and Benioff zone are clearly defined to the east of Adak Canyon, in contrast to the mostly shallow and diffuse distribution to the west. Higher stress events are seen to occur at various depths down to 80 km in Figure 4a, but only a few shallow higher stress events occurred to the west during this time period. Data, not shown, suggest that the number of higher stress events has increased since late 1983, but this possible trend is poorly defined. Many more events must be analyzed in order to develop fully the significance of patterns and temporal trends in the various parts of the Adak Seismic Zone.

Recent Publications Based on the Research

Scherbaum, F. and C. Kisslinger, Variations in Apparent Stress and Stress Drops prior to the Earthquake of 6 May 1984 (m_b =5.8) in the Adak Seismic Zone, *Bull. Seism. Soc. Amer.*, *74*:2577-2592, 1984.

Bowman, R., C. Kisslinger, S. Billington and M. Ando, Summary of Earthquake Prediction and Seismotectonic Research in the Central Aleutian Island Arc using Data from the Adak, Alaska Seismograph Network, *Zisin*, *37*:247-256, 1984 (in Japanese, with English abstract and figure captions).

Dewey, J.W., S. Billington, E.R. Engdahl and W. Spence, Teleseismic Search for Patterns Precursory to Large Earthquakes in Peru and near Adak, in *Earthquake Prediction: Proceedings of the International Symposium on Earthquake Prediction*, UNESCO Press, Paris, pp. 91-100, 1984.

Li, V.C. and C. Kisslinger, Stress Transfer and Nonlinear Stress Accumulation at Subductions-type Plate Boundaries - Applications to the Aleutians, *PAGEOPH*, *122*: in proof, 1984.

Bowman, J.R. and C. Kisslinger, Seismicity Associated with a Cluster of Earthquakes of $m_b \geqslant 4.5$ near Adak, Alaska: Evidence for an Asperity?, *Bull. Seism. Soc. Amer.*, *75*:223-236, 1985.

Scherbaum, F. and C. Kisslinger, Coda Q in the Adak Seismic Zone, *Bull. Seism. Soc. Amer.*, *75*:615-620, 1985.

Kisslinger, C., J.R. Bowman, F. Scherbaum, S. Billington and A.H. Silliman, Forecast of an Earthquake Location at an Activated Asperity: May 6 1984 Adak, Alaska Event, (Abstract), *EOS, 65*:987, 1984.

Silliman, A.H. and S. Billington, Seismicity Associated with an Earthquake of 4 June, 1982 beneath Adak Canyon, Central Aleutian Islands, (Abstract), *EOS, 65*: 987, 1984.
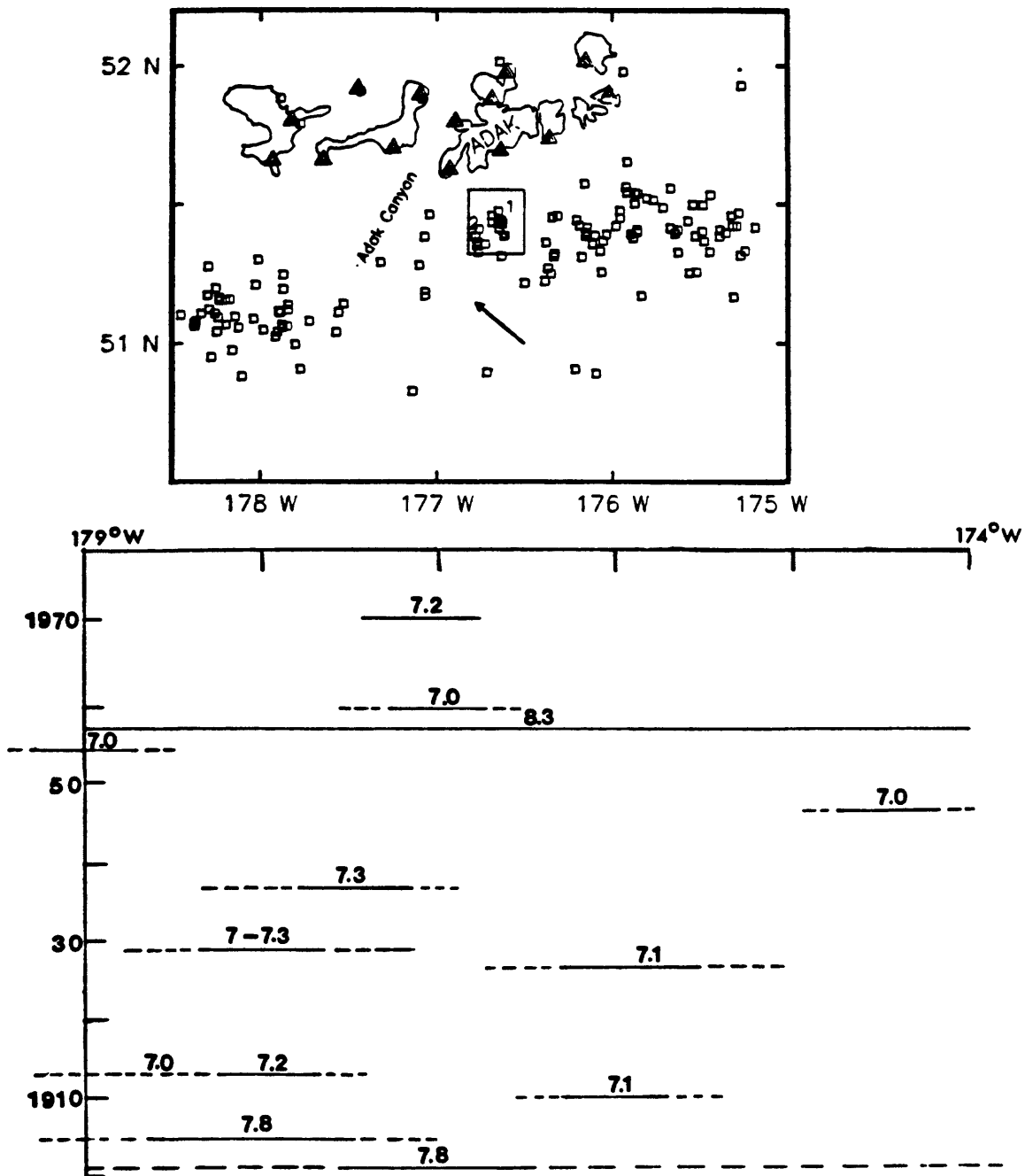
Figure 1: *Top,* Local network locations of events reported in the PDE, August 1974-June 1984. The rectangle south of Adak Island outlines the SW2 sub-region, within which the May 6, 1984 earthquake occurred, as anticipated. **B** marks the epicenter of the May 2, 1971 Adak Canyon M_s 7.2 event. *Bottom,* Time-space plot for the Adak Seismic Zone, $M_s \geqslant 7.0$, since 1900. The locations of events before 1960 are uncertain to varying degrees, the earliest ones as much as 5°. Data from various sources. The solid bars are an estimate of the rupture length, the dashed extensions indicating that the true locations of these breaks are not well fixed.
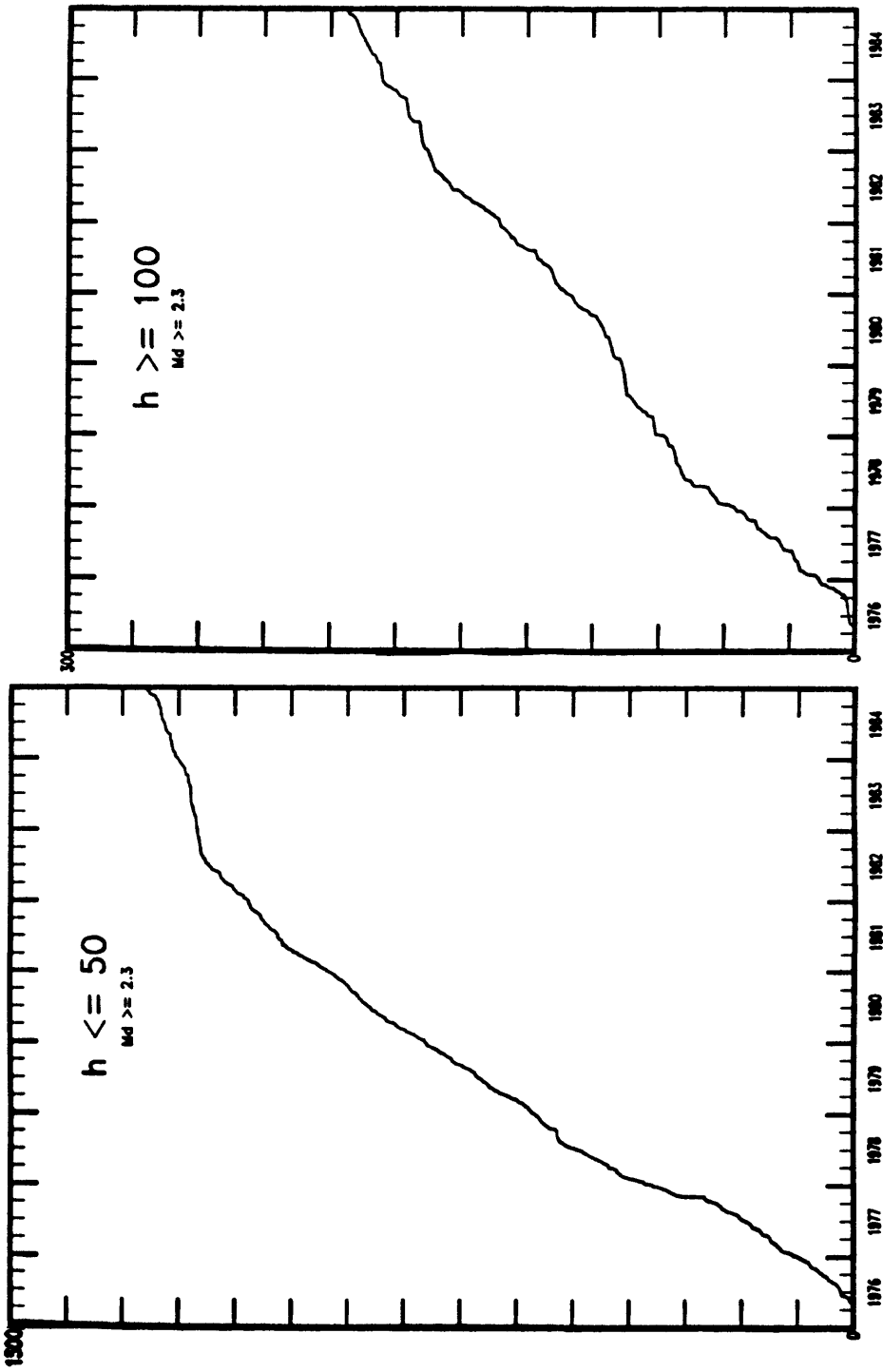
Figure 2: Seismicity rates in the Adak Seismic Zone for shallow and intermediate depths. The Adak catalogue is thought to be complete for magnitudes greater than 2.3. The sharp and persistent drop in rate of occurrence of shallow activity since late 1982 does not occur for the deeper events.
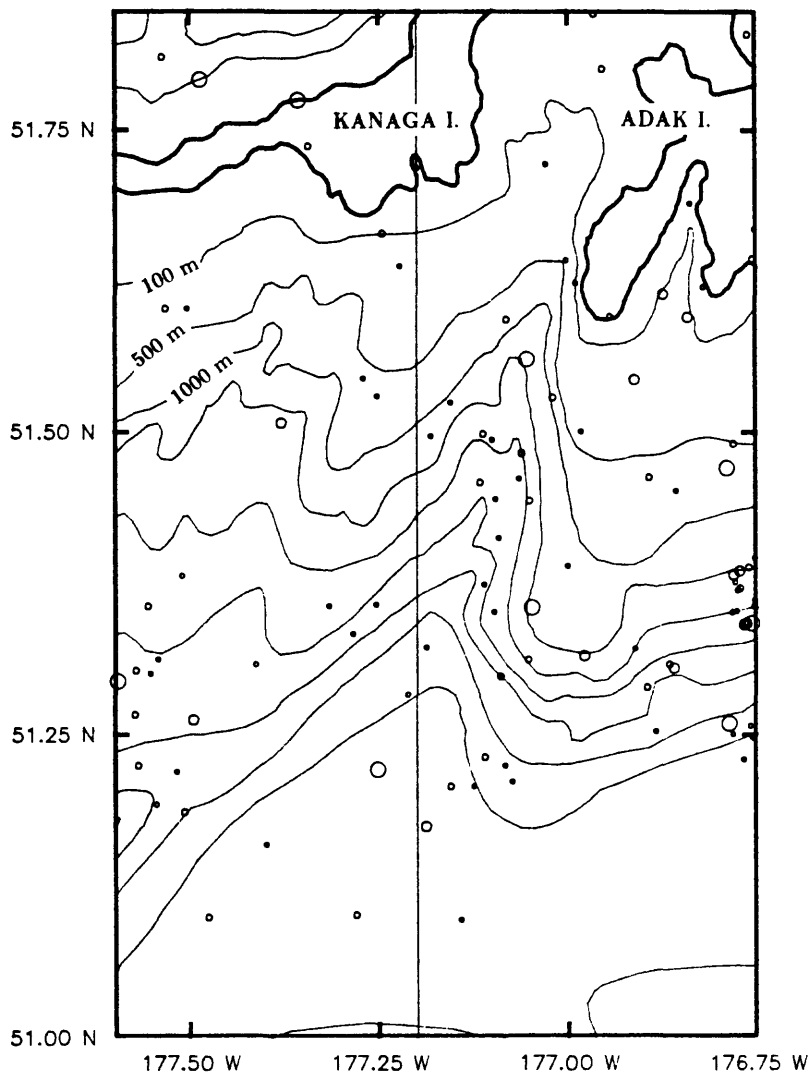
Figure 3: The region of study showing Adak Island, Kanaga Island, and Adak Canyon in between. Symbols are keyed to apparent stress, in bars (see legend below). Bathymetry in 500 meter intervals. Solid line through plot shows 177.2 ° W long. line.

LEGEND:

- $1.0 \geqslant \sigma_{app}$
- $1.0 < \sigma_{app} \leqslant 2.0$
- $2.0 < \sigma_{app} \leqslant 3.0$
- $3.0 < \sigma_{app}$
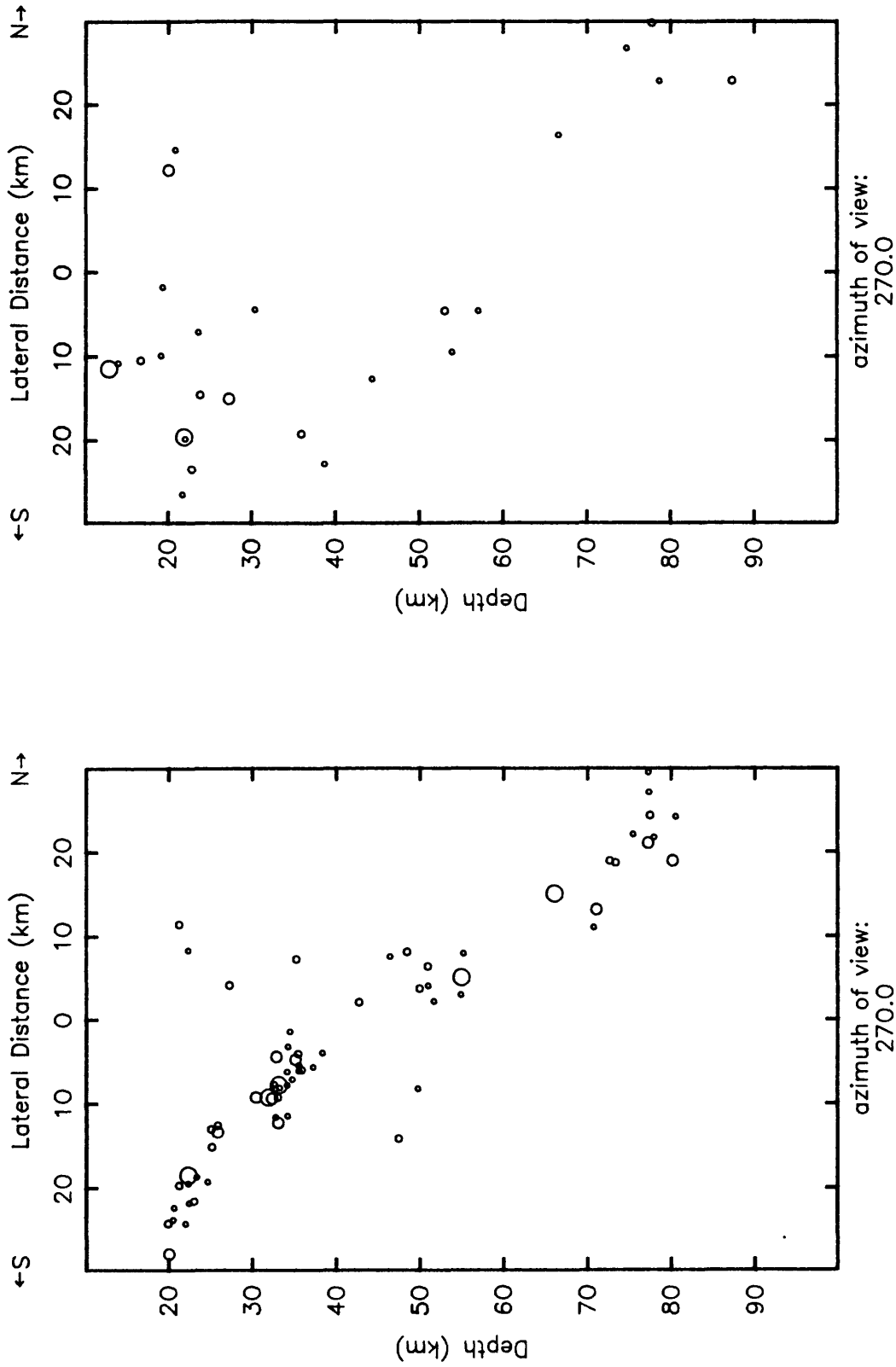
Figure 4: *(a) left,* North-south cross-section of earthquakes in the study region from 177.2° W longitude to the east; *(b) right,* same for earthquakes from 177.2° W longitude to the west. Symbol size is keyed to apparent stress, as in Figure 3.

Microearthquake Data Analysis

9930-01173

W. H. K. Lee
U. S. Geological Survey
Branch of Seismology
345 Middlefield Road, Mail Stop 977
Menlo Park, California 94025
(415) 323-8111, Ext. 2630

Investigations

The primary focus of this project is the development of state-of-the-art computation methods for analysis of data from microearthquake networks. For the past six months I have been involved mainly in studying coda decay of local earthquakes in the Mammoth Lake area, and in particular to investigate the temporal behavior of coda attenuation before and after the magnitude 5.9 event which occurred there on Nov. 23, 1984.

Results

In the previous Semi-Annual report, I discussed coda decay as a possible precursor for earthquake prediction. We have implemented an interactive coda processing and analysis program utilizing the USGS Earthquake Archiving and Processing System (see Seismic Data Library Project 9930-01501). For the past six months, we processed and analysed over 10,000 seismic records. We found large spatial variations of coda $Q(\omega)$. Stations located near the fault zones and in the Long Valley caldera have lower $Q(\omega)$ than those stations located outside. This result suggests that rocks in the fault zones and Long Valley caldera have more fractures and thus attenuate coda waves more effectively.

To investigate the temporal variation of coda $Q(\omega)$ before and after the Mammoth Lake earthquake of Nov. 23, 1984, we did a systematic analysis of earthquakes in the aftershock area and those in the adjacent area to the west for the period from April 1984 to January 1985 (easily accessible digital data from Calnet began only in April 1984). Our preliminary results indicate that there may be a coda $Q(\omega)$ anomaly a few months before the main-shock for earthquake sources in the aftershock area. For earthquake sources to the west of the aftershock area, coda $Q(\omega)$ values are very scattered and do not show any clear temporal pattern. It is also interesting to note that there was a seismicity quiescence for about two months before the main-shock.

Because USGS Calnet receives only a subset of stations operated by the University of Nevada, Reno (UNR), we need to complete our investigation by including all UNR stations. A collaboration with UNR is now underway.

Reports

(1) Lee, W. H. K., Luk, F., and Mooney, W. D., Applications of seismic
        ray-tracing techniques to the study of earthquake focal regions, in
        "Inverse Problems of Acoustic and Elastic Waves" edited by F.
        Santosa, Y. H. Pao, and W. W. Symes, SIAM, Philadelphia, p. 360-365,
        1984.

(2) Lee, W. H. K., Aki, K., Chouet, B., Newberry, J. T., and Tottingham, D.
        M., Mapping coda Q(ω) in California using the USGS Earthquake Data
        Archiving and Processing System (Abstract), Earthquake Notes, 55, p.
        15, 1985.

Determination of 'Whole Earthquake Cycle' Systematics:
Continued Studies of Large Earthquakes (M_s=7-7.5)
Along the Middle America Trench to Refine
Methodologies and Models for Earthquake Prediction

14-08-0001-G-977

Dr. Karen McNally
Charles F. Richter
Seismological Laboratory
Earth Sciences Board
University of California,
Santa Cruz, California   95064
(408) 429-4137

Objectives:

To relocate all seismicity ($M_6 > 7.0$) before and after seven large earthquakes ($M_s > 7.0$) in Mexico to determine a whole earthquake cycle model for mechanisms of loading, weakening, failure and postseismic readjustment. Determine fault mechanisms for all events $M_b > 5.5$ for interpreting relocated seismicity data. Monitor seismic quiescence near Acapulco, Mexico using WWSSN data and operate a field array in the ongoing cooperation program with Mexican scientists.

Summary of Progress:

All seismicity in central Mexico (1964-1983, $m_b > 4.0$) has been relocated using the JHD method (Dewey 1971) and WWSSN and ISC data, with well located earthquakes from portable seismograph studies for calibrations events. Fault mechanism solutions are being finalized for $M_b > 5.5$ earthquakes. The case histories of 7 large mainshocks ($7.0 < M_w < 7.6$) have been detailed for correlations relative to a whole earthquake cycle, ie, with temporal superpositions relative to the mainshocks.

As all the case histories are synthesized, distinctive patterns are emerging which suggest a systematic process of weakening and loading prior to failure. Relocated seismicity associated with (before and after, 1964-1983, $m_b > 4.0$) seven large earthquakes occurring in 1965, 1968, 1973, 1978, 1980 and 1982 span nearly an entire earthquake cycle. While local variations exist, it is remarkable that several features are persistent, indicative of common physical mechanisms. Mainshocks range within $7.0 < M_w 7.6$. For these events the patterns of seismic quiescence are consistent, with a duration of about 4 years prior to the mainshock (note that the time period might be longer for substantially larger events, but none have yet occurred). Prior to the quiescence, the downdip side of the locked zone is loaded by intense thrust faulting activity, also for about 4 years. In addition, we find that episodes of normal faulting, further downdip, appear to trigger this prefailure and loading behavior.

Following the mainshock, the normal faulting activity subsides for about one half the earthquake cycle, or about 15 years. We interpret this time dependent behavior as indicating stresses, also time dependent, caused by downdip slab pull and extension, updip loading and weakening, rupture zone locking, and mainshock failure followed by a reduction of extensional downdip stresses due to slippage in the mainshock.

A portable seismograph array is now being operated in the quiescent zone near Acapulco, Mexico in cooperation with Mexican scientists.

MAGNETIC FIELD OBSERVATIONS

9960-03814

R. J. Mueller
Branch of Tectonophysics
U.S. Geological Survey
345 Middlefield Road, MS/977
Menlo Park, CA 94025
(415) 323-8111 ext. 2533

INVESTIGATIONS

1) Investigation of total field magnetic intensity measurements and their relation to seismicity and strain observations along active faults in central and southern California.

2) Recording and processing of synchronous 10 minute magnetic field data and maintenance of the 25 station telemetered magnetometer network and its receive telemetry system for central and southern California.

3) Processing and analysis of on-site recorded data from the 64 station portable magnetometer network in California.

RESULTS

1. After successfully field testing the circuit to automatically rezero U.S.G.S. operated deep borehole dilatometers, a printed circuit board was designed to be compatible with the presently used electronic enclosures and a prototype was tested. Installation of this circuit at dilatometer stations will decrease field maintenance and protect the instruments from physical damage.

2. The circuit to convert 16 bits of parallel data to serial data compatible with the Sutron Data Collection Platforms, was layed out, a printed circuit board was built and tested, and the board is presently operating at a field station. Although commercial parallel to serial converters are available, the advantage to this design is its compatibility with the present electronic configuration. This allows conversion from the telephone line telemetry to the satellite telemetry with a minimum of wire changes and no changes in electronic enclosures.

3. Two magnetometers stations (OCHM and LSBM) in southern California were converted to satellite telemetry using Sutron Data Collection Platforms. One station is operating

in the parallel digital input mode and the other uses the serial digital input mode.

4. Software has been developed to enable plotting data, stored at Menlo Park, with battery powered portable computers via commercial telephones. This allows field maintenance personnel to assure proper operation of field stations prior to leaving remote areas.

REPORTS

Mueller, R. J., Johnston, M. J. S., Keller, V., and Silverman, S., Magnetic Field Observations in the Long Valley Caldera of Central-Eastern California, 1976-1984: EOS (Am. Geophys. Un. Trans.), v. 65, p. 1117, 1984.

Johnston, M. J. S., Silverman, S., Mueller, R. J., and Breckenridge, K. S., Secular Variation, Crustal Sources, and Tectonic Activity in California, 1976-1984 , J. Geophys. Res. (in press).

Ware, R. E., Johnston, M. J. S., and Mueller, R. J., A Comparison of Self-Calibrating Rubidium and Proton Magnetometers for Tectonic Studies, (in press).

PROBABILISTIC APPROACH TO EARTHQUAKE FORECASTING
CONTRACT NO. 14-08-0001-21916

Mansour Niazi
TERA ADVANCED SERVICES CORPORATION
2150 Shattuck Avenue
Berkeley, CA. 94704
(415) 845-5200

Investigation

Research supported under this contract is concerned with the development of a methodology for estimation of the probability jumps from the long-range estimates due to the observation of one or more potential precursory phenomena in a region. The test area for the implementation is southern California.

Results

This study led to the development of a method for combining long- and short-term probability estimates of earthquake occurrence by applying concepts of Dicision Theory. The long-term prior probability estimates derived from spatially uniform magnitude-frequency statistics are allowed to change in response to the observation of one or more precursors of known reliability and precursory time. Warning times and their associated uncertainties for a number of precursors derived as a function of magnitude and observation distance from the application of non-linear regression to an extensive set of world-wide observations are incorporated. Utilization of the distance dependency of the precursory time is a novel feature of this analysis.

The method is applied to a circular region of 200 km radius in southern California, shown in Figure 1, under equal weighing of short- and long-term predictions. An example of the modifications introduced to the long-term probability estimates for the occurrence of an earthquake of magnitude 7 due to the observation of strain anomaly, strain and ground water level anomalies or strain, groundwater level and resistivity anomalies is graphically shown in Figure 2, as a function of time. The estimated long-term probability jumps similar to those shown by the arrows of Figure 2 are summarized in Table 1 for three earthquake magnitude levels 6, 7, and 8 and three waiting periods of 100, 1,000 and 10,000 days.

Attempts are currently underway to introduce spatially variable prior probabilities within the region depending on the proximity of the observation points to potentially active faults.

Publications

Mortgat, C. P. and M. Niazi (1984). Application of Dicision Theory Models to Earthquake Forecasting, EOS, 65, 988.

Niazi, M. (1984). Regression Analysis of Reported Earthquake Precursors: I-Presentation of Data, PAGEOPH, Vol. 122.

Niazi, M. and C. P. Mortgat (1984). Application of Logistic Models to Earthquake Forecasting, Earthq. Predict. Res., 2, 221-224.

Niazi, M., C. P. Mortgat and K. N. Truong (1985). Probabilistic Approach to Short- and Intermediate-Term Earthquake Forecasting: II - Test Application to Southern California, in preparation.

TABLE I

PROBABILITY JUMPS IN SOUTHERN CALIFORNIA
FOR NEXT 100, 1,000 AND 10,000 DAYS AFTER
OBSERVATION OF ONE OR MORE POTENTIAL PRECURSORS
FOR A MAXIMUM RELIABILITY FACTOR OF 50 PERCENT.

Waiting Period	Magnitude	6	7	8
	Long-Term	0.13 (1.0)*	0.02 (1.0)	0.00 (1.0)
100 days (∼ 3 months)	Strain, Gr Water Level, Resistivity	0.46 (3.5) 0.55 (4.2) 0.56 (4.3)	0.36 (19.2) 0.48 (25.5) 0.49 (26.1)	0.31 (118.3) 0.45 (171.8) 0.46 (175.8)
	Long-Term	0.75 (1.0)	0.17 (1.0)	0.03 (1.0)
1,000 days (∼ 3 years)	Strain, Gr Water Level, Resistivity	0.87 (1.2) 0.87 (1.2) 0.87 (1.2)	0.56 (3.3) 0.59 (3.5) 0.59 (3.5)	0.47 (18.2) 0.51 (19.7) 0.51 (19.7)
	Long-Term	≃ 1.0 (1.0)	0.85 (1.0)	0.23 (1.0)
10,000 days (∼ 30 years)	Strain, Gr Water Level, Resistivity	1.0 (1.0) 1.0 (1.0) 1.0 (1.0)	0.93 (1.1) 0.93 (1.1) 0.93 (1.1)	0.62 (2.7) 0.62 (2.7) 0.62 (2.7)

* The value in parenthesis indicate probability jumps relative to long-term prediction.

TN-85-6143
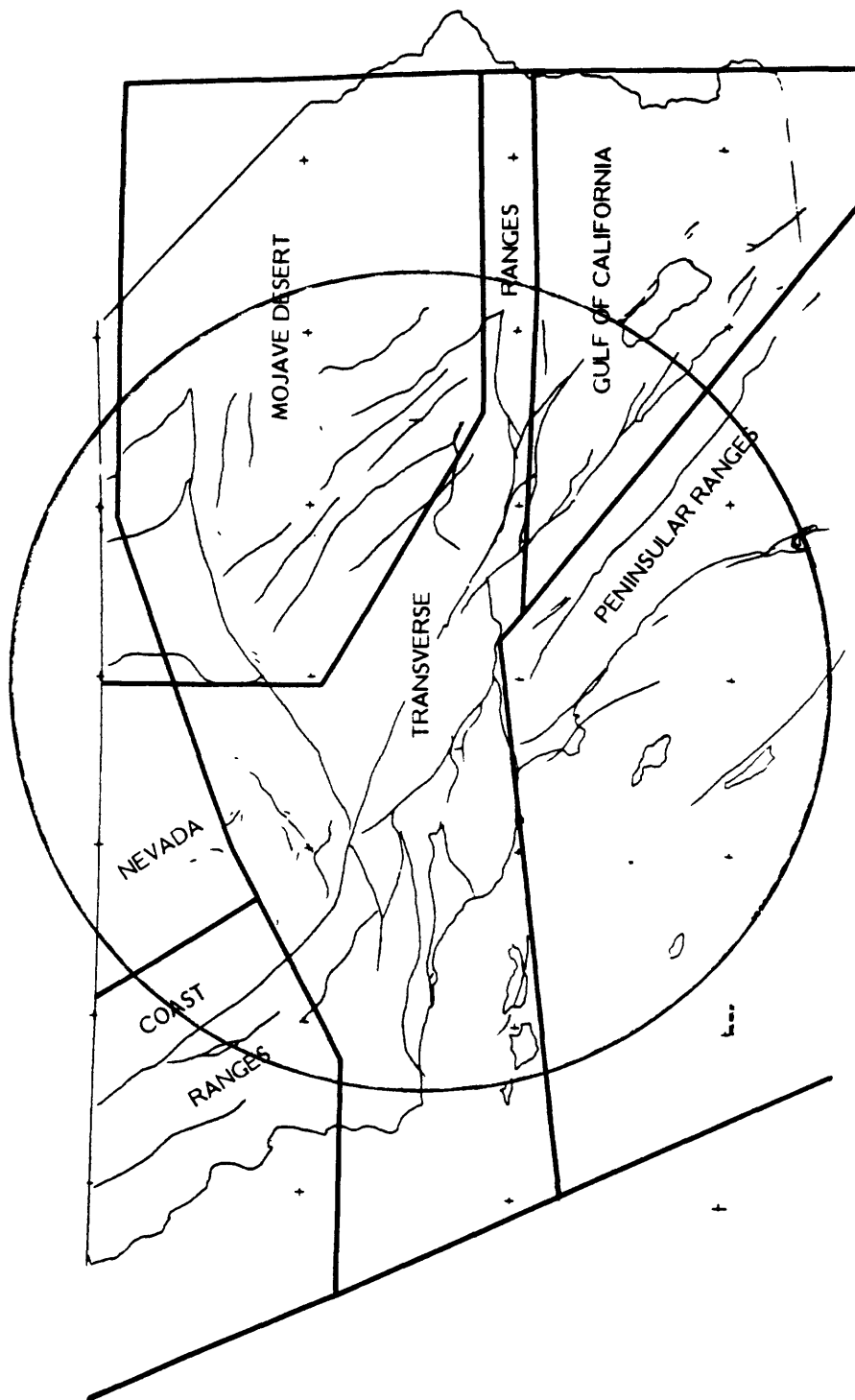
Figure 1 -- Fault map of southern California, with major seismotectonic subdivisions delineated. The circular region with a 200 km radius was studied as the test area for the estimation of earthquake occurrence probability consequent to the observation of one or more potential precursors.
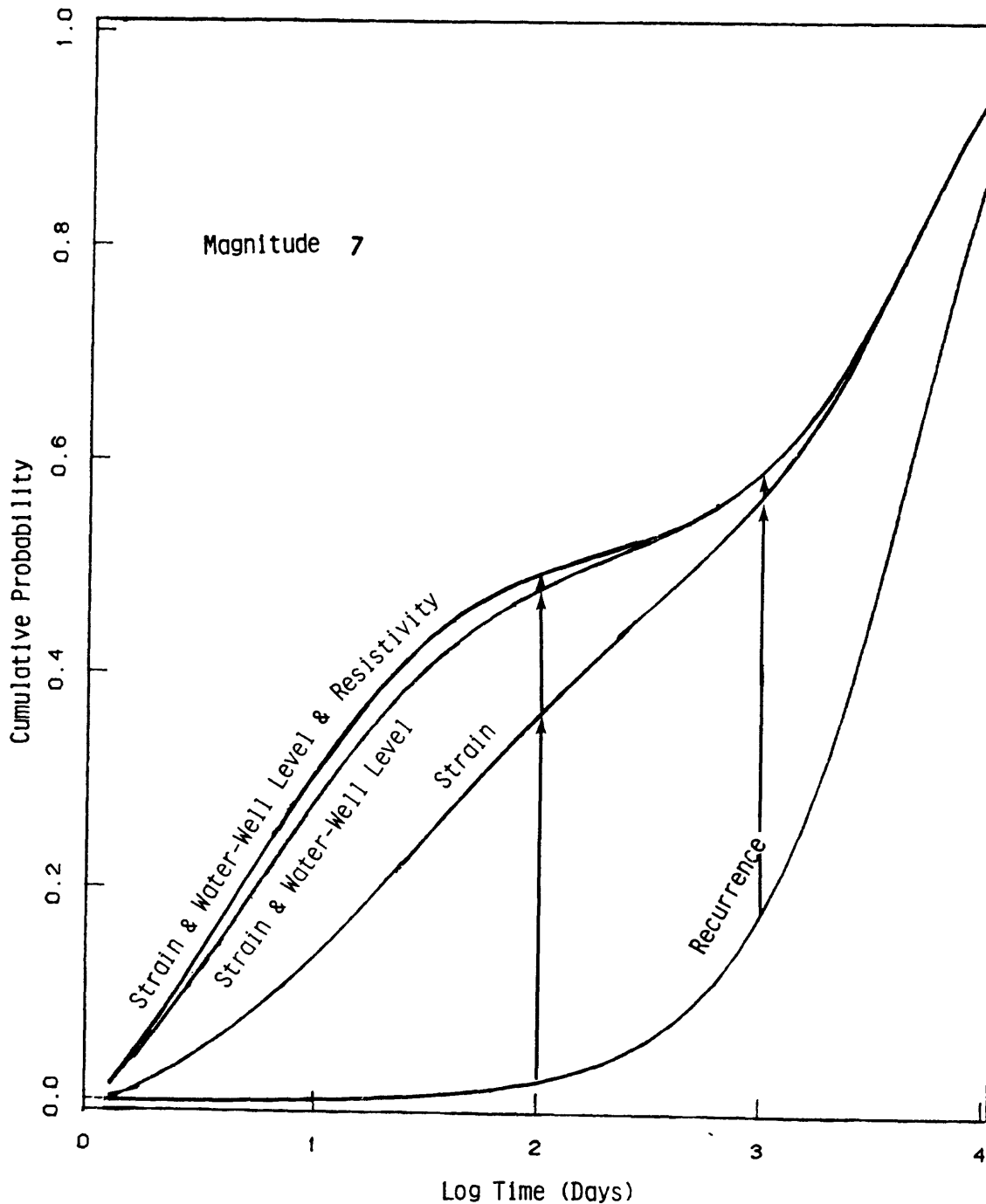
Figure 2 -- Comparison of the estimated cumulative probabilities for the occurrence of an earthquake of magnitude 7 or higher within the circular region of Figure I as a function of time. Arrows show the estimated probability jumps for 100-and 1,000-day periods resulting from the observation of one or more potential precursors.

CRUSTAL STRAIN

9960-01187

W.H. Prescott, J.C. Savage, M. Lisowski
Branch of Tectonophysics
U.S. Geological Survey
345 Middlefield Road, MS/977
Menlo Park, California 94025
(415) 323-8111, ext. 2701

Investigations

The principal subject of investigation was the analysis of deformation in a number of tectonically active areas in the United States.

1. Strain Accumulation in the Rocky Mountain States

Strain accumulation in trilateration networks in Montana, Utah, and New Mexico has been measured for over a decade. The network in New Mexico spans the Rio Grande rift near Socorro. The absence of any observed strain accumulation in that network places an upper limit (two standard deviations) of 3 mm/a on east-west spreading across the 100-km-wide rift. The network in Utah spans the Wasatch fault near Ogden. Although the 1972-1984 average rate of strain accumulation in that network is not significant at a two-standard-deviation detection threshold of 0.03 μstrain/a, short-term strain fluctuations of marginal significance have been detected in the network. The network in Montana spans the epicentral area of the 1959 Hebgen Lake earthquake (magnitude 7.1). The principal strain rates observed in that network for the 1973-1984 interval were $\dot{\varepsilon}_1$ = 0.28 ± 0.02 μstrain/a N14°E ± 1° and $\dot{\varepsilon}_2$ = -0.05 ± 0.02 μstrain/a N76°W ± 1°, extension reckoned positive. The principal extension is perpendicular to the 1959 rupture trace. The deformation of this network suggests rather rapid reloading of the 1959 rupture zone, but whether this is steady strain accumulation or still postseismic relaxation is not known. The strain rate does appear to be constant over the 1973-1984 interval.

2. Plate Flexure Approximation to Postseismic and Interseismic Deformation

The rather large postseismic deformation that is associated with two-dimensional dip-slip faulting in the lithosphere is related to the bending of a free plate generated by dip-slip faulting. In the absence of gravity, asthenosphere

relaxation eventually permits the faulted lithosphere to assume the dihedral configuration of a faulted free plate. For thrust faulting, the faulted area is depressed into the asthenosphere and the flanks of the plate slope uniformly upward. In the presence of gravity, buoyancy forces act upon the plate, and the ultimate $(t \to \infty)$ postseismic uplift is approximated $(y/\alpha > 0.2)$ by $w_1 \exp(-y/\alpha)(\cos y/\alpha - \sin y/\alpha)$ where w_1 is an explicit function of the fault parameters and lithosphere properties, y is the horizontal distance from the down-dip end of the fault, and α is the flexural parameter for the lithosphere plate. The relaxed-asthenosphere response is the sum of the coseismic deformation. The annual, steady deformation associated with strain accumulation at a subduction zone is simply the relaxed-asthenosphere response to virtual, normal slip on the main thrust zone of an amount equal to the annual plate convergence. From these relations we have estimated the deformation (strain and uplift) expected along the Pacific coast of northern Honshu. The estimated deformation is about twice the observed deformation, but the predicted geographical distribution of the deformation is similar to the observed deformation.

3. Correction of 1982 Long Valley Leveling for Magnetic Error

The U.S. Geological Survey leveling of the Long Valley monitor network in 1982 was run with a Zeiss Ni 1 level, an instrument known to be subject to a magnetic deflection of the compensator causing a systematic error in leveling. Immediately after the completion of the 1982 survey, the level was returned to Germany to have the compensator replaced. Before replacing the compensator Zeiss determined the magnetic error introduced by the old compensator. The correction at the latitude of Mammoth Lakes amounts to 1.20 mm/km in the direction of magnetic north. In 1982 not all of the leveling along Highway 395 was run by the U.S.G.S. The section from Toms Place to the crossing of Hilton Creek was run by the L.A. Department of Water and Power using a Zeiss Ni 1 level of unknown magnetic correction. However, that section trends in the direction of magnetic west, and no error would be introduced by the magnetic field. The section from June Lake Junction to Lee Vining was also run by L.A. Water and Power, but this time using a Zeiss Ni 2. The Ni 2 level is of different construction from the Ni 1 and appears to be relatively free of magnetic error. Thus, the complete 1982 survey can be corrected for the effects of the magnetic field on leveling.

The magnetic correction reduces the 1982, elevation difference over the 64 km between Toms Place and Lee Vining to

68.156 ± 0.011 m. The elevation differences in 1957, 1975, and 1983 were 68.133 ± 0.012, 68.136 ± 0.008, and 68. 128 ± 0.011 m, respectively, indicating no significant change in elevation between Toms Place and Lee Vining in the 1957-1983 interval. The elevation difference measured in 1984 was 68.050 ± 0.011 m suggesting subsidence at Toms Place. However, because of rather poor section closures in the 1984 leveling, the 1984 elevation difference is regarded as suspect.

4. **Strain Accumulation in Northwestern Washington**

Repeated triangulation across the Strait of Juan De Fuca and repeated Geodolite distance measurements across the Puget Lowlands near Seattle show maximum contraction nearly parallel to the proposed east-northeast direction of Juan de Fuca-America plate convergence. Angle changes between survey monuments common to 1892, 1913, 1942, or 1954 triangulation surveys across the Strait of Juan de Fuca give an average engineering shear strain of 0.22 ± 0.07 µradian/yr with the axis of maximum compression bearing N77°E ± 10°. If trench-parallel extension is assumed to be zero, this rate of shear implies N77°E extension at a rate of -0.22 ± 0.07 µstrain/yr. Near Seattle average principal strain rates (extension taken as positive) from repeated Geodolite surveys between 1972 and 1984 are +0.04 ± 0.03 µstrain/yr N°20°W ± 6° and -0.05 ± 0.02 µstrain/yr N70°E ± 6°. This rate of strain accumulation is smaller than that observed between 1972 and 1979, and it is not clear whether this change represents time-varying strain accumulation or contamination by larger than expected measurement errors. The east-northeast compression and the down-to-the-east crustal tilt disclosed by precise leveling over a 70-year period can be roughly reproduced by a simple dislocation model of the Cascadia subduction zone that has the shallow portion of the plate interface locked to a position near the Washington coastline. These results can also be reproduced by a more realistic two-layer coupled earth model, but the free parameters of elastic plate thickness, viscosity and earthquake recurrence interval are weakly constrained.

5. **Horizontal Deformation Across the Fairweather Fault near Yakutat, Alaska, 1967-1983**

A geodetic measurement of horizontal deformation across the northern end of the Fairweather fault near Yakutat, Alaska, shows shear strain about three to five times greater than that observed across locked portions of the San Andreas fault in California. The average rate of shear strain accumulation between 1967 and 1983 across the Nunatak

geodetic network is 1.6 ± 0.2 μrad/yr (engineering shear); distortion that is equivalent to 1.0 ± 0.1 cm/yr of relative displacement across the 6-km wide zone covered by the network. This shear is uniform across the network, which includes a subsegment that does not cross the main surface trace of the Fairweather fault. The observed deformation is consistent with a simple model of strain accumulation in which the Fairweather fault is locked to a depth of about 9 km and slipping right laterally at a rate of 5.4 cm/yr below 9 km. The depth of the postulated locked zone is only weakly constrained, as models with the fault locked to depths greater than 4 km fit the observed deformation equally well. The high rate of deformation could also be accounted for by surface slip distributed evenly between the two surface traces of the fault within the network or by transient deformation following the 1958 Lituya Bay earthquake (7.9 M_s; 8.2 M_w).

6. **Geodetic Constraints on Strain Rates in the Vicinity of the 1886 Charleston, South Carolina, Earthquake**

An analysis of triangulation data in the vicinity of the 1886 Charleston, South Carolina earthquake reveals no evidence of detectable shear strain accumulation. The resolution of the data set is such that shear strain rates as low as 0.1 μrad/yr average would have been detectable. Most of the angles were first observed in the 1930's and then reobserved between 1950 and 1970. One angle was observed prior to the 1886 earthquake. No significant change was observed in this angle. In order to improve the resolution in the data set the U.S. Geological Survey and the South Carolina Geodetic Survey have reobserved a portion of the triangulation with Global Positioning System receivers. Results of this resurvey are not available yet but the improved precision and spatial coverage should allow reduction of the shear strain rate uncertainty to about 0.04 μrad/yr at the 95% confidence level.

7. **Deformation in the Coast Range Province North of San Francisco, California**

Analysis of geodolite observations in the coast ranges of northern California indicates that relative plate motion is spread over a wide zone. Little or no deformation occurs to the southwest of the San Andreas fault itself. To the northeast of the San Andreas fault, a region transected by the parallel Rodgers Creek and Maacama faults, about 25 ± 6 mm/yr of right-lateral slip is distributed over about 60 km. There is a peak shear strain of 0.6 ± 0.1 μrad/yr near the San Andreas fault. Elsewhere in the deforming zone shear strain rates are 0.3 ± 0.4 μrad/yr. At the

northeastern boundary of the study area the strain rate is less than 0.2 µrad/yr. Except for the high strain rate near the San Andreas fault, there is no evidence of any localization of deformation to the surface traces of the faults, nor is there any evidence of creep or aseismic slip on any of the faults in the area. The data indicate that the relative motion between the Pacific and North American plate occurs primarily to the northeast of the San Andreas fault. The observations are inconsistent with models that include slip at depth on only the San Andreas fault. The data can be fit equally well by models with slip distributed on all three of the major faults or with motion distributed across the entire zone from the San Andreas fault to the Napa Valley fault. Preliminary analysis of observations to the Farallon Islands, about 40 km southwest of the San Andreas fault, suggest that little or no additional relative motion is accommodated on that side of the San Andreas fault. In particular it is unlikely that the 20 mm/yr difference between the plate motion rate (~55 mm/yr) and the San Andreas fault system rate (~35 mm/yr) can be explained by deformation between the San Andreas fault and the Farallon Islands.

8. Deformation near the Farallon Islands, Central California

Observation of deformation on the margin of the Pacific plate opposite San Francisco, California are yielding some new evidence about the distribution of relative motion along this section of the Pacific-North American plate boundary. Over the past seven years three geodetic lines from the Farallon Islands to stations near the San Andreas fault have been measured. During the period spanned by the observations, there has been very little deformation of the crust on the Pacific side of the San Andreas fault. The observed distribution of displacement is inconsistent with models of the plate boundary which have all the relative plate motion occurring on the San Andreas fault. The observations suggest that in North Central California, the difference between the slip observed along the San Andreas fault (30 ± mm/yr) and the inferred plate motion rate (55 ± mm/yr) cannot be explained by slip west of the San Andreas fault as others have recently suggested. The observations are best fit by a dislocation model with no slip (±8 mm/yr) on the San Gregorio fault and 15 mm/yr (± 2 mm/yr) on the San Andreas fault below 8 km. The absence of deformation on the Pacific side of the fault is in sharp contrast to the North American side of the fault.

9. Global Positioning System Receivers: Acquisition and Planning Stages:

Five Texas Instrument 4100/3 Global Positioning System

(GPS) receivers (often referred to as the "Tri-Agency receiver) have been ordered by the U.S. Geological Survey. Two of these receivers will go to the Office of Systems and Techniques Development of the National Mapping Division in Reston, Virginia. The other three receivers will be used by the Office of Earthquakes, Volcanoes and Engineering (OEVE) in the Earthquake Hazards Reduction Program. Two receivers are scheduled for delivery in July 1985 and the remaining three in September 1985. GPS receivers use L-band signals from a constellation of satellites at 20,000 km elevation (12 hour orbital period) to precisely locate the receiver antenna in a geocentric coordinate system. When used in pairs, the position difference obtained is accurate to a few centimeters in all three components. Initial plans for the OEVE receivers are to conduct an extensive series of frequently repeated measurements over a range of line-lengths to evaluate the precision of the instruments and to supplement the ongoing program of geodolite observations. Tests done by others so far have demonstrated that the system is more accurate than conventional high precision surveying (1 ppm), but little work has been done to evaluate repeatibility at higher precision levels.

Reports

Castle, R.O., J.E. Estrem, and J.C. Savage, Uplift across Long Valley caldera, California, J. Geophys. Res., 89, 11507-11516, 1984.

Prescott, W.H., N.E. King, and G. Gu, Preseismic, Coseismic, and Postseismic Deformation associated with the 1984 Morgan Hill, Earthquake, Cal. Div. Mines Geol., Spec. Publ., 68, 137-148, 1984.

Rymer, M.J., M. Lisowski, R.O. Burford, Structural explanation for low creep rates on the San Andreas fault near Monarch Park, Central California, Bull. Seism. Soc. Am., 74, 925-931, 1984.

Savage, J.C., M. Lisowski, J.E. Estrem, and R.O. Castle, Deformation of Long Valley caldera, eastern California, 1983-1984, U.S. Geol. Survey Open-File Report 85-41, 1985.

Stein, R.S., and M. Lisowski, The 1979 Homestead Valley earthquake sequence, California: Control of aftershocks and postseismic deformation, J. Geophys. Res., 88, 6477-6490, 1983.

G. M. Reimer
U. S. Geological Survey, MS 963
Denver Federal Center
Denver, CO 80225
(303) 236-7886

Investigations

The variations of helium in soil-gas from sample collecting stations along
the San Adreas Fault near San Benito, California continue to be observed
and related to nearby seismic activity. Soil temperature and soil moisture
measuring devices were installed in May to different depths at one site in
an effort to accumulate data so a model to understand the seasonal variations
can be developed.

Results

Figure 1 shows the plot of helium concentrations as a function of time plotted
through April, 1985. The 6-month period from the last evaluation has been
relatively devoid of helium decreases that are interpreted as precursors to
earthquakes. One decrease in October may have corresponded to the October 31,
1984 magnitude 3.8 earthquake near Lick Observatory. The decrease in late
February, 1985 appears to have no related seismic activity. Presently, there
is evidence of a decrease, in that the April helium concentrations are those
more typical of May or June, but this may be due to the unseasonably dry
conditions this year. Hopefully, the soil moisture probes that were installed
will provide information that will allow unambiguous interpretations in the
future.

Reports

Reimer, G. M., 1985, Prediction of central California earthquakes from soil-
    gas helium fluctuations: Journal of Pure and Applied Geophysics, in
   press.
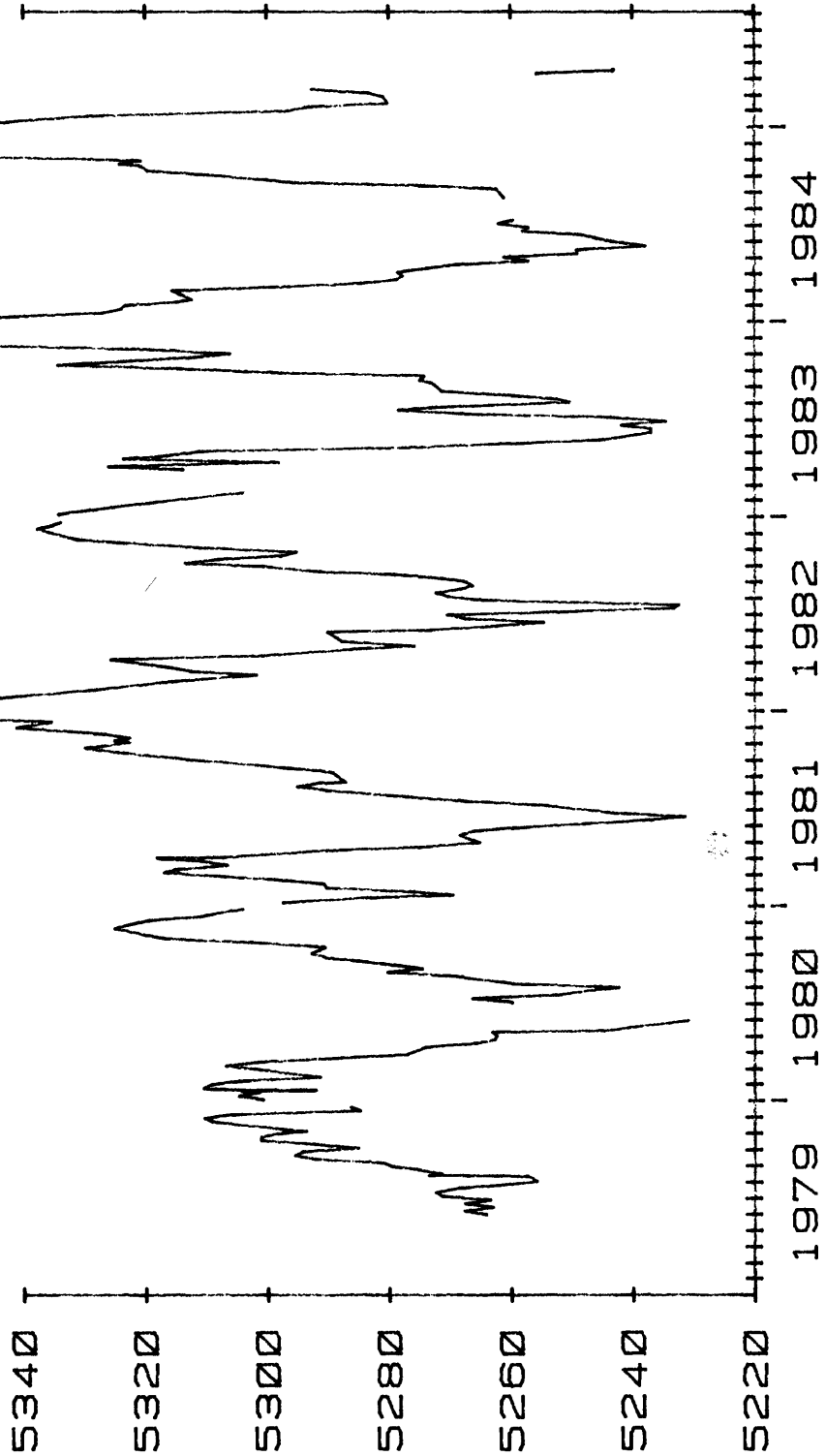
Figure 1. Helium soil-gas concentrations near San Benito, California from May, 1979 to April, 1985. Date divisions are months. Breaks in the helium record are periods when samples were not collected.

COUPLED DEFORMATION - PORE FLUID DIFFUSION EFFECTS IN FAULT RUPTURE

14-08-0001-G-978

J.W. RUDNICKI
Dept. of Civil Engineering,
Northwestern University
Evanston, Illinois 60201
(312)491-3411

Investigations

Dilatant hardening effects due to uplift and near-fault microcracking accompanying fault slip.

Results

Our results thus far are described in the following abstract submitted for presentation at the spring AGU meeting:

"Martin (GRL, 7, 1980) has observed effects of pore fluid pressure on rate of failure development in initially intact samples of Westerly granite loaded in axisymmetric compression. A recent analysis by Rudnicki (JGR, 89, 1984) suggests that duration of the transient stabilization observed by Martin is too long to be associated with the formation of a fault-like zone of concentrated deformation in the sample. Another possibility is the stabilizing effects observed by Martin are primarily associated with dilatant hardening induced by uplift and near-fault microcracking accompanying slip after a fault has formed in the sample.

"The analysis considers a slab loaded by a combination of shear and compression. The slab contains a fault with a prescribed relation between shear (friction) stress versus slip that decreases from a peak and levels off at a residual value. Analysis of this model for some simple cases suggests that dilatant hardening can actually prevent failure by stabilizing the response until the friction stress has attained its residual value. The response is, however, strongly dependent on the stiffness of the machine-sample system. The stabilizing effects are limited by saturation of dilatancy and the magnitude of the pore pressure decrease that is possible before the fluid becomes vapor-like. The latter limitation gives rise to dependence of rate of development of failure on the magnitude of the pore pressure in a reservoir connected to the sample. This feature is consistent with the observations of Martin."

The Southern Iceland Borehole Strainmeter Array:
Data Acquisition and Analysis
14-08-0001-G-961

I. Selwyn Sacks and Alan T. Linde
Department of Terrestrial Magnetism
Carnegie Institution of Washington
5241 Broad Branch Road, N.W.
Washington, D.C. 20015
202-966-0863

The location of Iceland provides an excellent opportunity to study tectonic processes associated with mid ocean spreading and transform faulting. Iceland straddles the mid-Atlantic ridge; the ridge is offset to the east on Iceland - two transform faults, one just north of Iceland and the other on land in the southern part of the country, complete the tectonic system.

From the historical seismicity of large events in Iceland, an interesting characteristic emerges: on the two transform faults large earthquakes (M > 6) occur in pairs with a time interval which varies in the range ~3 - 10 years. It appears that, as a result of spreading, stress builds up in the region of the transform faults and eventually one of these faults fails. This results in an increased load on the other fault such that it fails soon afterwards. In 1975, a sequence of tectonic events (volcanic eruptions, large extensions, intense microseismicity) culminated in a m = 6.3 earthquake on the northern transform. In light of previous seismicity, it seems probable that a similar sized earthquake will occur on the southern transform within the next few years. We therefore installed 7 borehole strainmeters in the region of the southern transform with the objective of recording changes in the strain field associated with this anticipated earthquake.

The locations of the instruments are shown in Fig. 1. These instruments have frequency response from zero frequency to several hertz and a dynamic range from 10^{-11} to 10^{-5}. The upper limit is increased by resetting the hydraulic-mechanical zero of the instrument.

A newly installed telemetry system is about to begin functioning. This is a digital system capable of sampling at rates as high as 70 samples/sec at each site. On site power limitations restrict us to 12 bit analog to digital converters, but the system can be readily upgraded when low drain 16 bit converters become available. This grant has allowed us to purchase and program a small (PDP 11/23) minicomputer for data acquisition. Delays in awarding the grant have resulted in this system not yet being ready for use. However, the programs now being developed for this system will allow us to expand our data base dramatically. Until now our only recording has been on strip charts at 1/2 inch/hr. With the new system we will record continuously (on digital tape) at a sampling rate of 1/sec and additionally retain event information at 30 samples/sec.

In addition, since 1983, we have been monitoring the micro-thermal fluctuations in the strainmeter boreholes. This is part of a collaborative program with H. Shimamura (Sapparo, Japan), Stefansson and ourselves.

Fig. 2 shows a summary plot of the data recorded since installation. The strain rates were initially high, but now are much lower. It is possible that these earlier changes are related to tectonic effects - but we believe it more likely that they are due to near-instrument perturbations resulting from the installation (Linde et al., 1982). The most important effects in this initial settling period are due to the curing of the expansive grout used to bond the instrument to the rock and to thermal perturbations resulting from changes in the aquifer system due to the drilling and installation procedures. The grout expansion effects can take about 6 months to reach equilibrium, but if the thermal environment is disturbed as a result of perturbing the aquifer system, it may take years for the strain rates to recover to the ambient value. We now have installation techniques to minimize these thermal changes.

In at least one case, SAU, the strain rates being recorded are consistent with those determined from triangulation measurements (~10 km) around the station. We anticipate that triangulation surveys will cover the other strainmeter sites in the near future.

Anomalous signals, which may be related to increased stress buildup on the southern transform, have been recorded recently on the SAU strainmeter. This site is within a few kilometers of the fault. Following installation in September 1979, SAU wrote a fairly stable and uneventful record (Fig. 2). After August 1980, small strain "bumps" (Fig. 3) began to appear in the record. These had amplitudes less than 10^{-8} and rise times of about 1 hour. The amplitudes of these bumps increased steadily with time and, near the end of 1982, reached a peak with pulse amplitudes of up to 5×10^{-7}. Since then the amplitudes have decreased somewhat to 1×10^{-7} and the rise time has lengthened to about 8 hours.

At the peak of this bump activity during Sept. - Oct. 1982, two small earthquakes (m_L 2.1, 2.7) occurred in the same region. There was also a similarly shaped pulse recorded on a nearby borehole strainmeter installed near the spreading ridge about 25 km away. A temperature change of +5°C and water level fluctuations of up to 10 m were reported from a nearby borehole, but the noise level and baseline stability of these data have yet to be determined.

In all 38 bumps were recorded during Aug. 1980 to Dec. 1983. Four of these appear to be associated with small local earthquakes. We have noted that, in other regions, similarly shaped bumps have preceded earthquakes. For example, preceding the Japan Sea earthquake (m = 8, 1983) a series of such pulses were recorded on a strainmeter about 80 km from the eventual epicenter. A similar sequence preceded the Yamanashi (southeast Honshu) m = 5.5 earthquake of June 1976. Thus it is possible that the bump occurrence in southern Iceland is an indication of enhanced stress on the transform.

Reference

Linde, A. T., I. S. Sacks, R. Stefansson, F. Wyatt, and M. Johnston, Noise in

near surface measurements of earth strain. T rans. Am. Geophys Union,

63, 1118, 1982.
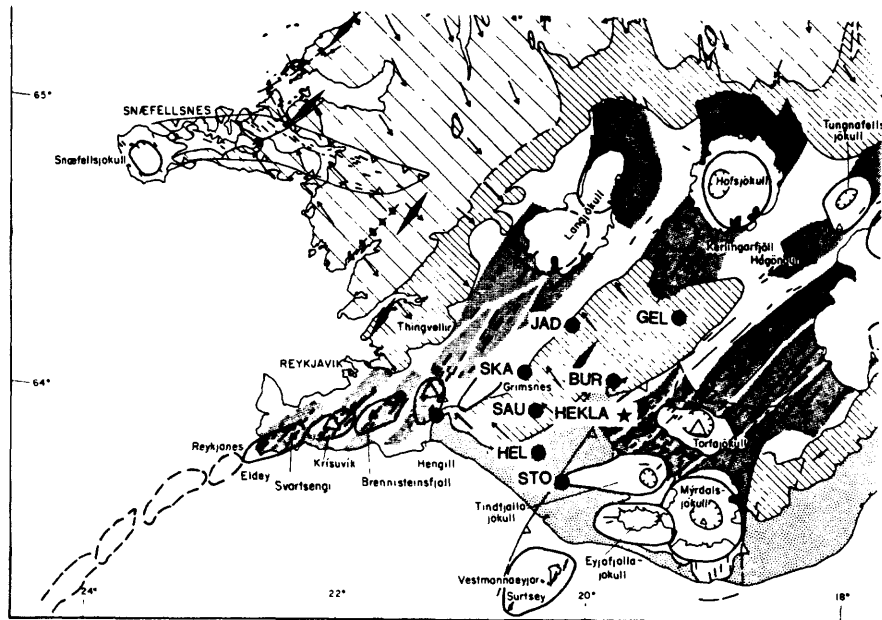
Fig. 1.   Map of southwest Iceland.   The borehole
          strainmeter sites are shown with solid circles.
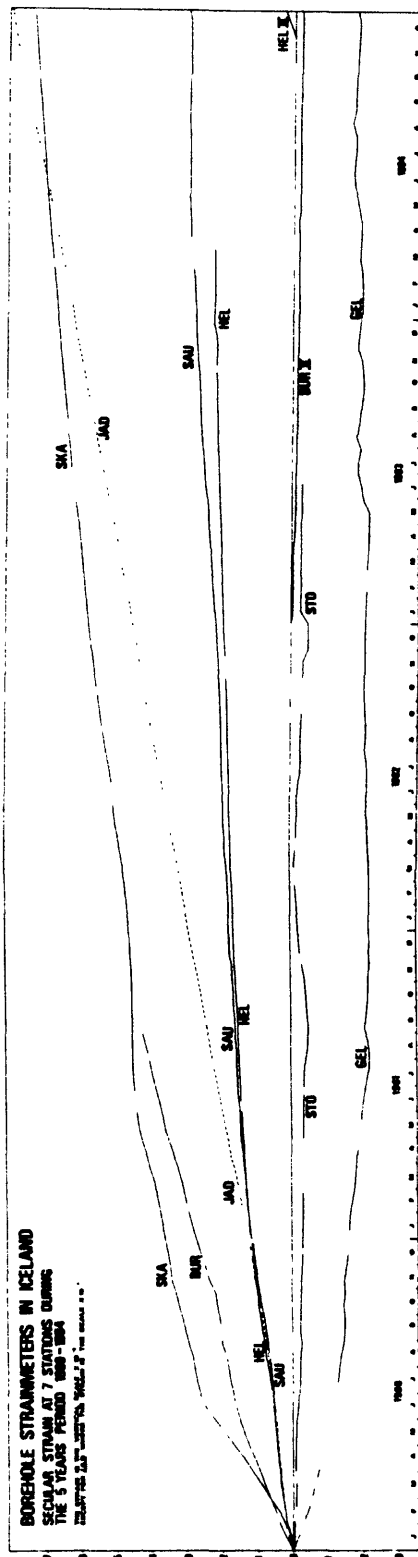
Fig. 2. Strain data from the network. Scale is in units of 10^{-5}. BUR suffered
lightning damage and HEL Lada damaged cable. Both these instruments
have been replaced; The data are labelled BUR II and HEL II.
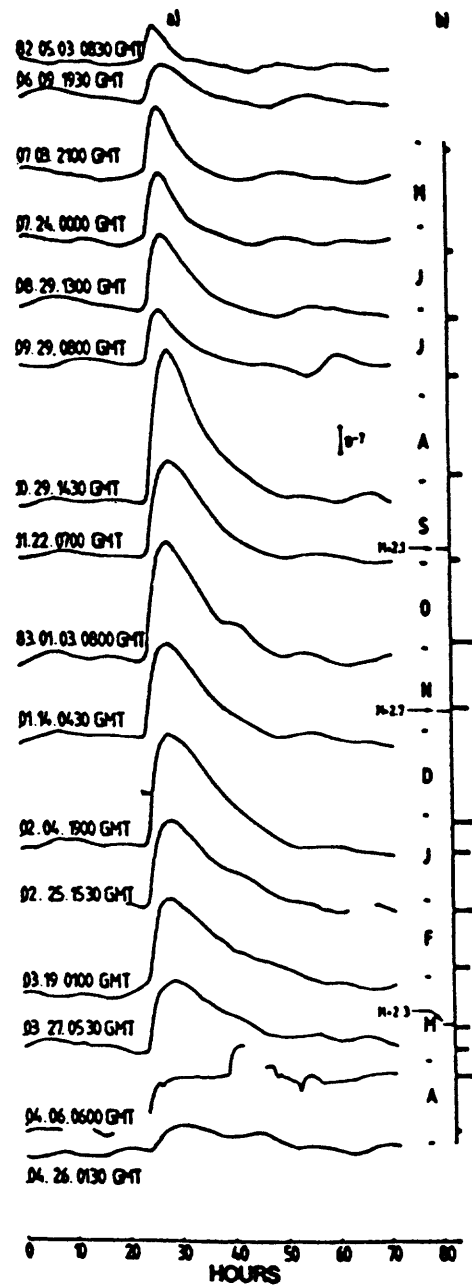
Fig. 3. Strain "bumps" recorded on the SAU station during about a 1 year interval. The amplitudes of these bumps went through a maximum in September-October 1982; also the rise times have increased. Note the occurrence of small earthquakes shown on the time scale at right.

Hydrogen Monitoring

9980-02773

Motoaki Sato, Susan Russell-Robinson, A. J. Sutton*, K. A. McGee*
Branch of Igneous and Geothermal Processes, U.S. Geological Survey
MS 959. National Center. Reston, VA 22092
(703) 860-6600
(*now at 5400 MacArthur Blvd., Vancouver, WA 98661)

Investigations

Hydrogen (H_2) concentration in soil along major seismogenic faults in central California is continuously monitored at a dozen sites (Fig. 1) by using H_2/O_2 fuel cell sensors. Efforts are directed toward the accumulation of field data, possible correlations with seismic data, understanding of mechanisms for H_2 emissions along active faults, and improvement of the monitoring method.

Results

Results obtained from 20 Jun.'84 through 8 May '85 are described in this report. Most stations were nonoperational prior to this period in 1984.

(1) Hollister area. Three monitoring sites, Coyote reservoir (H2CY), Shore Road (H2SH), and Wright Road (H2WR) are included in this area. These sites are located on the southern-most segment of the Calaveras fault.

Noteworthy changes in H_2 emission were observed at Shore Road between 16 Nov.'84 and 18 Dec.'84. These changes were characterized by a rapid increase followed by an equally rapid decrease and then a gradual increase toward the normal level (Fig. 2). During the same period, creep data at the same location showed a series of cyclic excursion events (Fig. 2), which are commonly observed after heavy rainfalls and are explainable on the basis of opening and closing of the fault plane caused by complex movements of fault blocks along intersecting faults (S.S. Schulz). There were more creep events than H_2 events events, but the start of each H_2 event coincided in time with the leading edge of a coincident creep event. The correlation may be explained as follows. Normally H_2 is escaping along the fault at a steady rate which is governed by the permeability of the fault zone. When relative movements of the fault blocks, triggered by lubrication due to increased groundwater penetration, result in the opening of the fault plane, H_2 accumulated at depth quickly escapes to the surface due to its high buoyancy. At the same time, atmospheric air ($H_2 < 1$ ppm) begins to be sucked into the ground to fill the increased volume of voids, resulting in a subsequent decrease in H_2 toward the atmospheric level. When the fault plane starts closing, the inspired air is expelled to the surface. Eventually the normal seepage rate of H_2 is restored.

Another series of events were also observed at Shore Road between 22 Feb. '85 and 25 Apr.'85 (Fig. 3). These events consisted of pronounced increases in diurnal changes and occasional deviations from the diurnal pattern. There was a large right-lateral creep event on 17 Mar.'85. Possible correlation with local seismicity is yet to be studied, but it appears that there was an increase in earthquakes in this segment of the Calaveras fault during this period.

Wright Road site had telemetry problems for over a year until 1 Mar.'85. Very small H_2 peaks were observed on 2 Feb.'85, 7 Mar.'85 and 27 Mar.'85. The 2 Feb.'85 peak was followed by an M2.8 quake that occurred on 11 Feb.'85 about

2 km NE of this site and at a depth of 8.9 km. The 7 Mar.'85 peak was accompanied by a concurrent peak at Shore Road. Coyote Reservoir site (not telemetered, had recorder failures during this period, hence no data.

(2) San Juan Bautista area. No noteworthy H_2 events were recorded at San Juan Bautista (H2SJ). Two very small increases in H_2 occurred on 30 Aug.'84 and 4 Sep.'84 at Cienega Winery (H2CW).

(3) Bear Valley area. No significant events were recorded at Melendy Ranch (H2MR). Although this site shows strong diurnal changes, large anomalous peaks have never been recorded since its installation in 1981. Perhaps the ground is too porous at this site.

Slack Canyon site was switched from the pumped air system to the tanked oxygen system on 17 Jun.'84. Small irregular peaks began to appear on 2 Nov. '84 (Fig. 4). Both the frequency and duration of the peaks increased from mid-March '85 (Fig. 5). The intensified H_2 emissions are similar to those observed at the beginning of a period of high H_2 emissions that preceded the Coalinga earthquake of 3 May '83 (previous report). Telemetry failure began on 28 Apr.'85 and the latest trend is not observable.

(4) Parkfield area. Middle Mountain site (H2MM, H2M2) has two sensors. H2MM was the only H2 station along the San Andreas fault which was operational throughout 1984 (Fig. 6). Small peaks began appearing on 8 May '84 for two weeks. Another series of minor peaks appeared from late-May to mid-June '84. The third cluster of minor peaks began on 7 Oct.'84 and lasted until 12 Nov. '84. A single minor peak, which lasted for a few hours, occurred on 25 Dec. '84. There was an abrupt offset on 4 Jan.'85, which was probably caused by bad telemetry. Another abrupt change occurred in the pattern of the signal from 21 Mar.'85 to present, but this happened after a telemetry failure and is probably an artifact. The H2M2 was down between 2 May '84 and 4 Jan.'85 because of an amplifier failure. The amplifier was removed and the sensor output was directly connected to the digital transmitter on 17 Jan.'85. The signals were frequently offset by the telemery system in 1985.

Parkfield (H2PK) station was down between 20 Jan.'84 and 18 Jun.'84. There was a sharp and large increase in H_2 emission on 8 Jul.'84 (Fig. 7). This peak amounted to an increase of about 2,600 ppm H_2. Although the high H_2 concentration dropped to 1,300 ppm by 17 Jul.'85, it stayed above 850 ppm until mid-November '84. It may be noted that a reversal of the creep direction occurred soon after the intense H_2 emission in July 1984. The magnitude of the big H_2 event is comparable to that which occurred at this site in March 1983 before the Coalinga earthquake.

No notable H_2 events were recorded at Gold Hill (H2GH) except for variations in the intensity of diurnal changes.

(5) Long Valley area. A gigantic H_2 emission event began on 13 Nov.'84 at Laurel Spring site (Fig. 8). The signal was so large at times that it saturated the analog telemery channel, hence, the maximum concentration is unknown. Ten days later, the M5.8 Round Valley earthquake struck about 30 km to SE.

Reports:

Sato M., McGee K. A., and Sutton A. J. (1984) Anomalous hydrogen emissions along seismogenic faults in California. Book of Abstracts, The 1984 International Chemical Congress of Pacific Basin Societies, Honolulu, Hawaii, p. 07B20.

McGee K. A., Sutton A. J., and Sato M. (1984) Observations of hydrogen gas events prior to volcanic seismicity. Book of Abstracts, The 1984 International Chemical Congress of Pacific Basin Societies, Honolulu, Hawaii, p. 07B18.

Sato M., Sutton A. J., and McGee K. A. (1985) Anomalous hydrogen emissions from the San Andreas fault observed at Cienega Winery, central California. Pure and Appl. Geophys., v. 122, 16 pp.(in press).

McGee K. A., Sutton A. J., and Sato M. (1985) Continuous hydrogen monitoring at Long Valley Caldera. Extended Abstracts. Workshop on Monitoring Hydrothermal System in Long Valley Caldera, Calif. (in press).
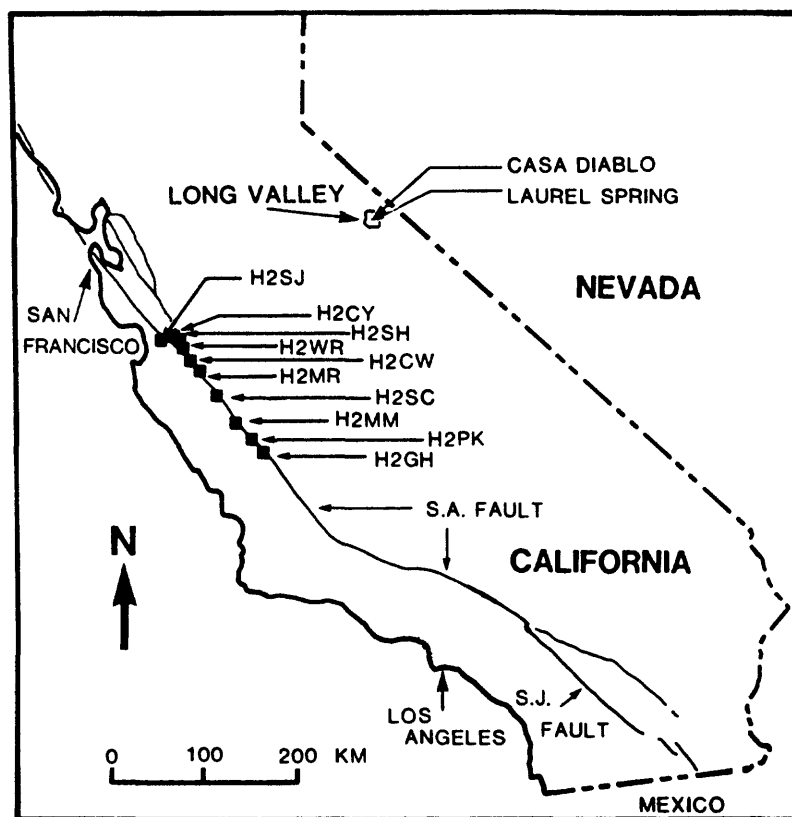
Fig. 1. Current locations of H₂ monitoring sites in central and southern California.
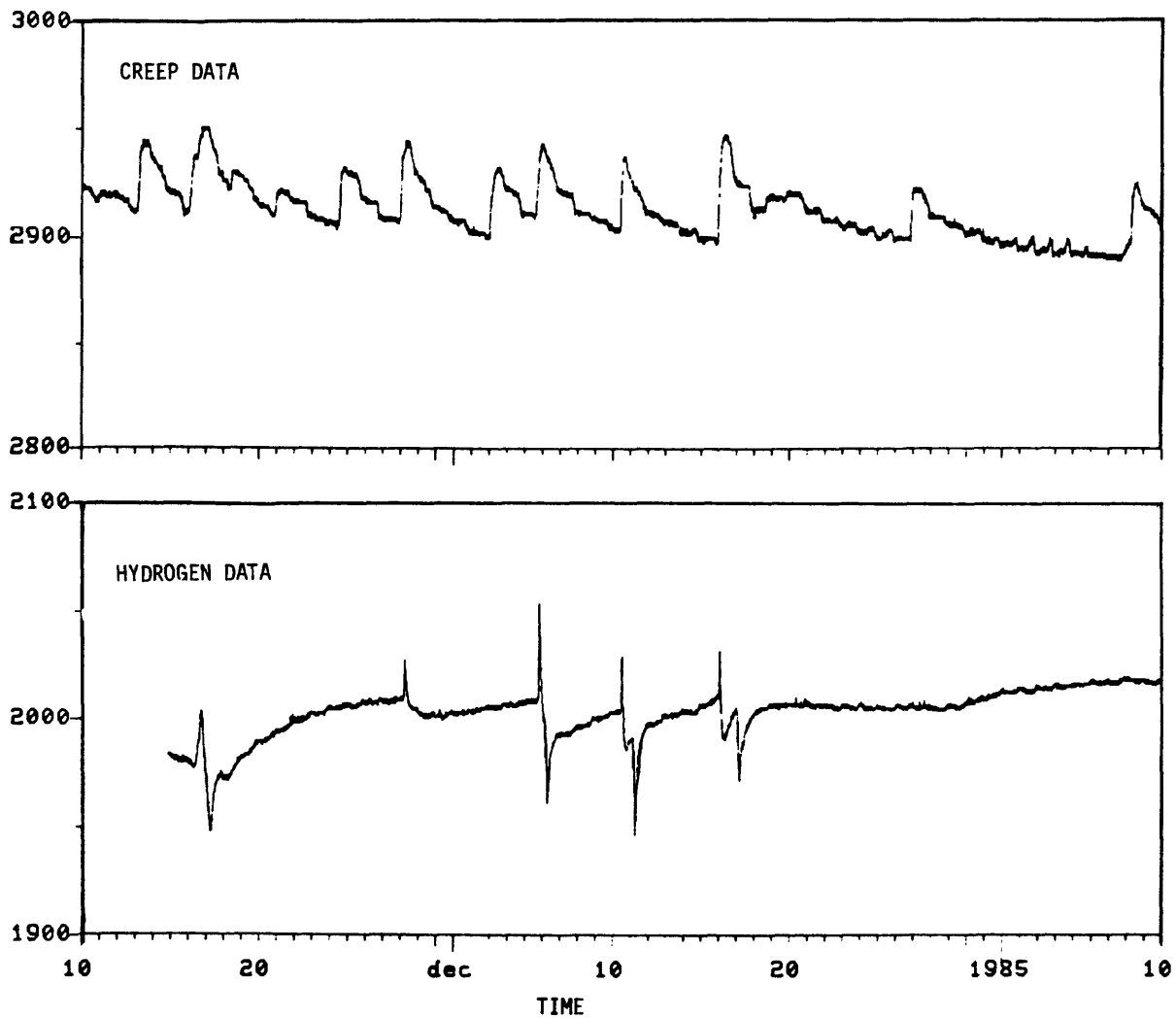
Fig. 2. Coincidence of cyclic H_2 events and creep events observed at
Shore Road (H2SH) between November 16 and December 18, 1984.
Both events are probably caused by the opening and closing
of the fault plane. Zero H_2 concentration occurs at roughly
1940 counts and 100 counts corresponds to 320 ppm.
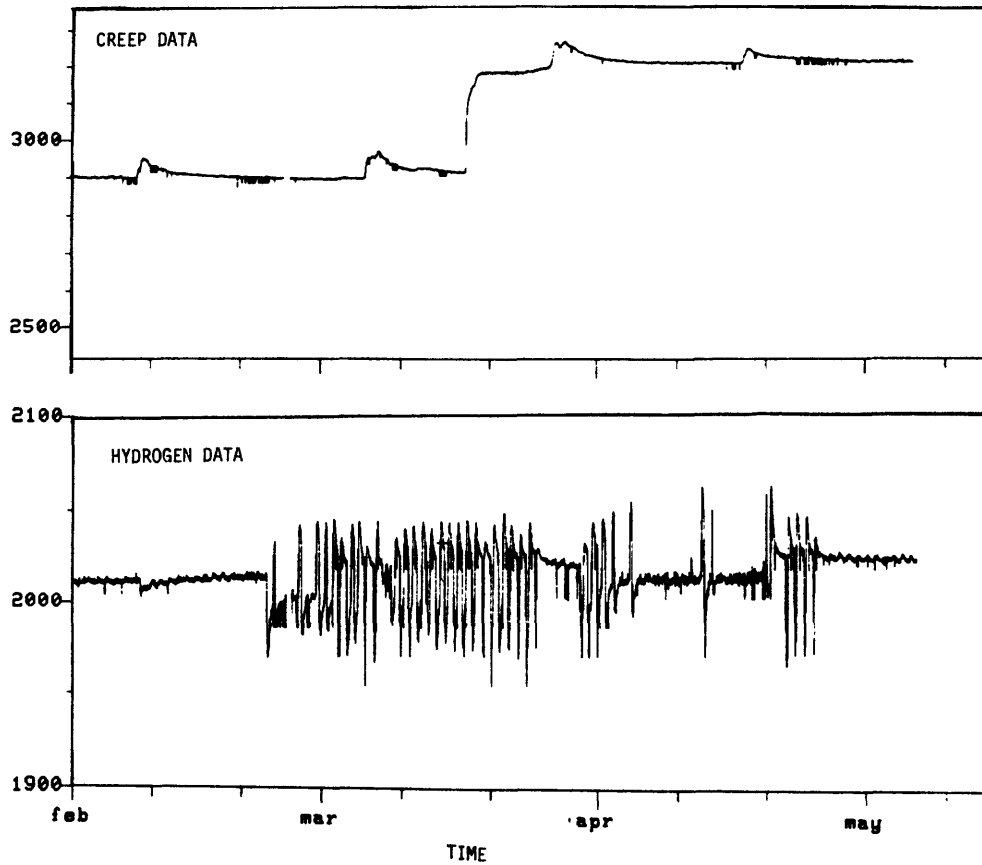
Fig. 3. Increased H_2 emission observed at Shore Road (H2SH) between February 22 and April 25, 1985. A creep event occurred on March 17, 1985.
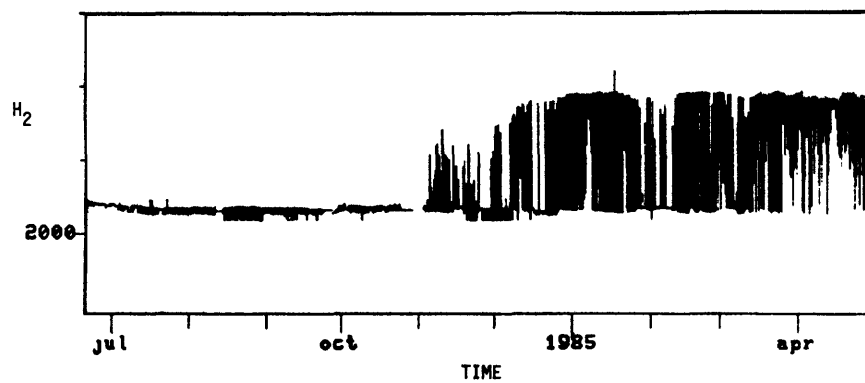
Fig. 4. H_2 record obtained at Slack Canyon (H2SC) between June 17, 1984 and April 28, 1985. Telemetry noise has been removed.
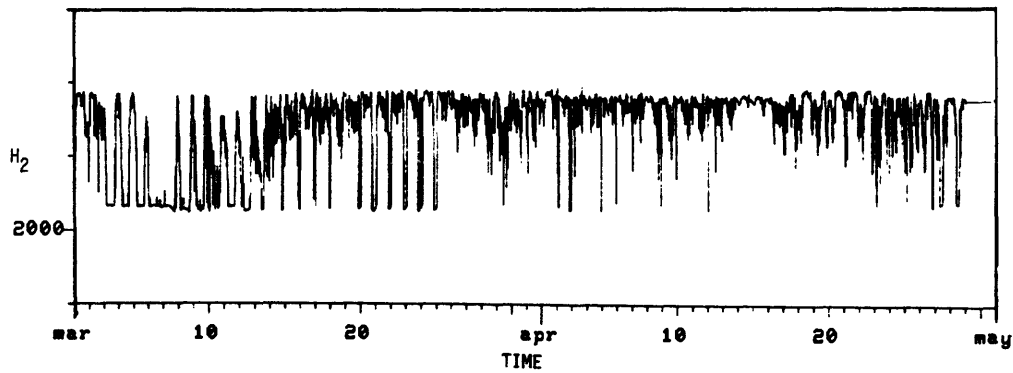
Fig. 5. H₂ record obtained at Slack Canyon (H2SC) between March and May, 1985. The expansion on the time scale shows the details of ¹a series of H₂ emission events.
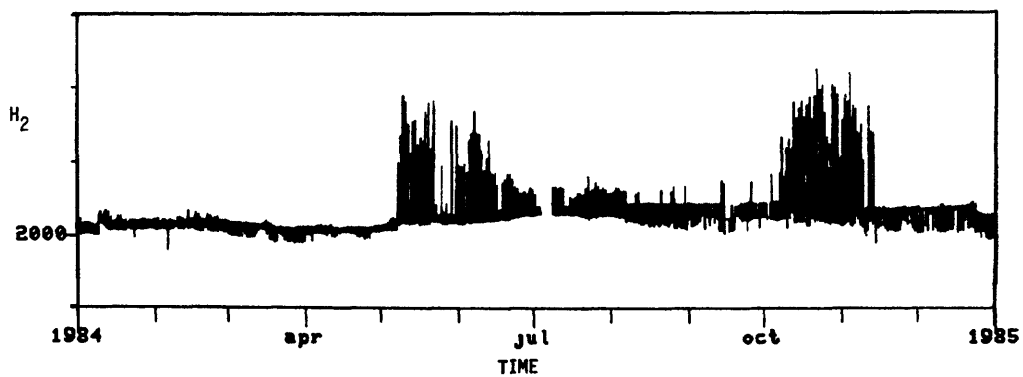
Fig. 6. H₂ record obtained at Middle Mountain (H2MM) in 1984 shows three periods of increased H₂ emissions during the year.
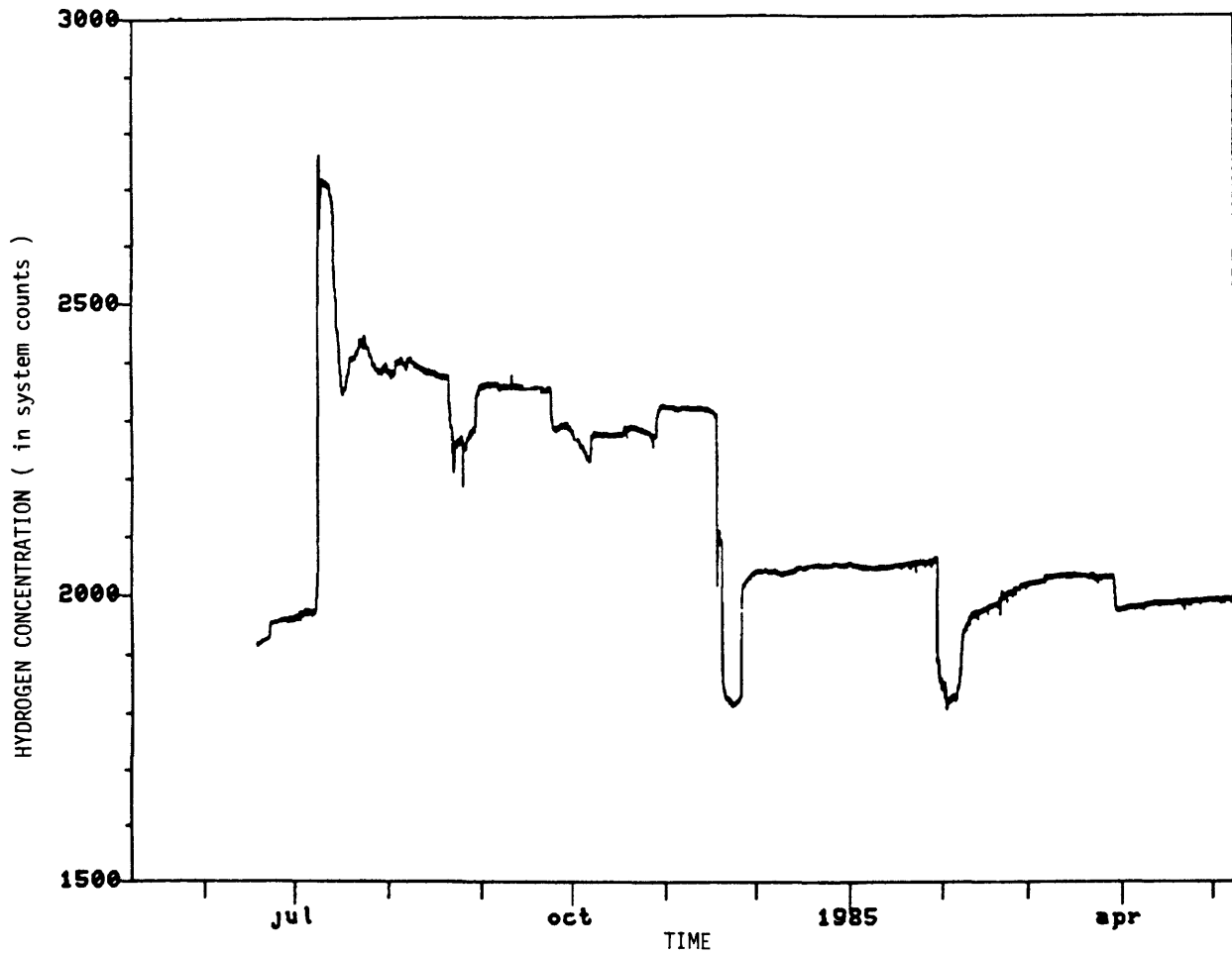
Fig. 7. Large H_2 emission events that took place during the summer and fall of 1984 at Parkfield (H2PK). Soon after the highest H_2 peak (about 2,600 ppm), the direction of creep reversed at this site.
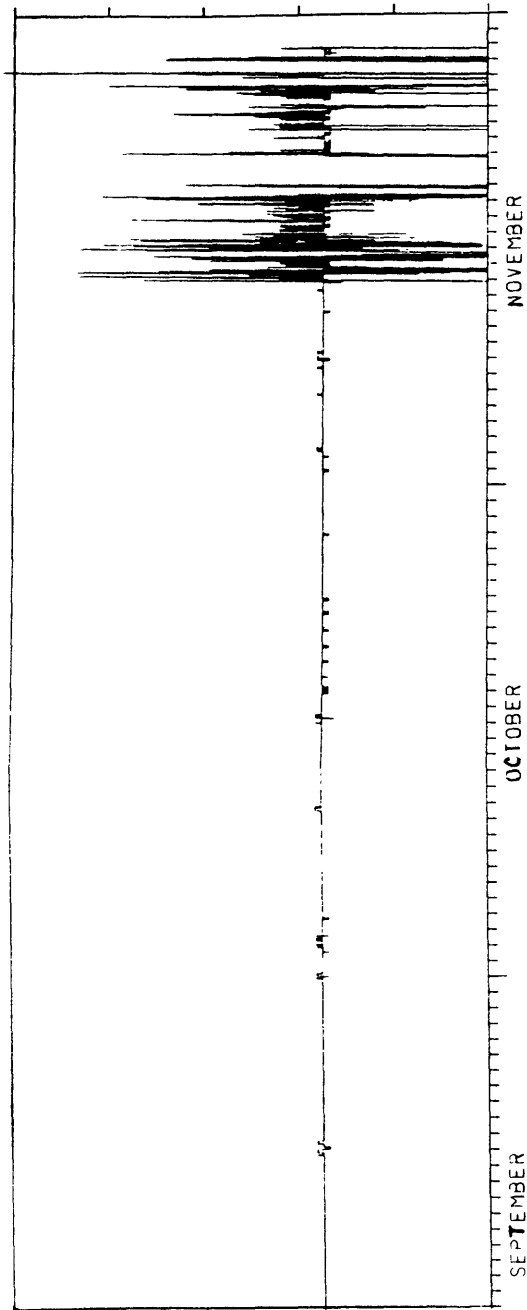
Fig. 8. An intense H$_2$ emission started November 13, 1984 at Laurel Spring site. The anomalous signals went off scale for analog telemetry band. The intensity was at least ten times greater than the largest H$_2$ event observed at this site, since its installation in 1982. Ten days later, the Round Valley earthquake (M = 5.8) struck approximately 30 km to the southeast.

Systems Analysis of Geologic Rate Processes

9980-02798

Herbert R. Shaw and Anne E. Gartner
Branch of Igneous and Geothermal Processes, U.S. Geological Survey
MS-910, 345 Middlefield Road, Menlo Park, CA 94025
(415) 323-8111, X4169, X4170

Objective: The proposed work on this project has two objectives. First to intrepret the paleoseismic parallelogram of Shaw and others (1981) in terms of the fractal geometry of Mandelbrot (1977, 1982) and Mandlebrot and others (1984). The second objective was to compare the frequency-magnitude data for earthquake activity in Japan (Wesnousky and other, 1983) for Quaternary faults with the faulting data in the conterminous U. S., as interpreted by Shaw and others (1981) in terms of a generalized branching distribution of faults of all lengths.

Results: Preliminary results indicate that fractal dimensions of earthquake phenomena vary as a function of number/length order in Shaw and others (1981) as well as with the b and c coefficients in frequency-magnitude and moment-magnitude correlations. The Japanese data plot (see figure 1) as a zig-zag trend (raw data) on the seismic parallelogram of Shaw and others (renamed a fractogram to show the relationships to the systematics of Mandelbrots fractal geometry). The trend of the Japanese data alternates between intervals roughly parallel to one or the other end-member modes of the parallelogram. Interpreted in terms of the maximum-moment model, this pattern suggests that each branch-length order defines a maximum earthquake and recurrence time each of which increases at the next lower order (longer fault branches of fewer number) according to a step-wise hierarchy. Activation of a given length-set engages longer and longer parts of segments (or complete segments having a scatter of lengths about the mean length of that order) in sucessive events, with a corresponding increase in recurrence time, until that subset reaches a characteristic moment and magnitude for that order. Activity is expressed in terms of a shift, at a constant "buildup time", to a longer branch-set order containing fewer segments. In each step, the maximum earthquake increases but the frequency decreases relative to what it would have been if the shorter branch-set orders had not reached their characteristic maximum moment. This "maximum moment" is not necessarily the ultimate theoretical maximum (in terms of potential fault length) for a given order; the latter is termed the SATURATION limit, representing activation of the longest fault segments of that order. In the case of Japanese earthquakes, the characteristic maxima seem to vary from 10 to nearly 100 percent of SATURATION values. Dynamically, these relations imply a quasi-steady chronological flow of energy from the shorter to longer branch-length orders. Complex behavior of large fault systems relates to different regimes of a general progression
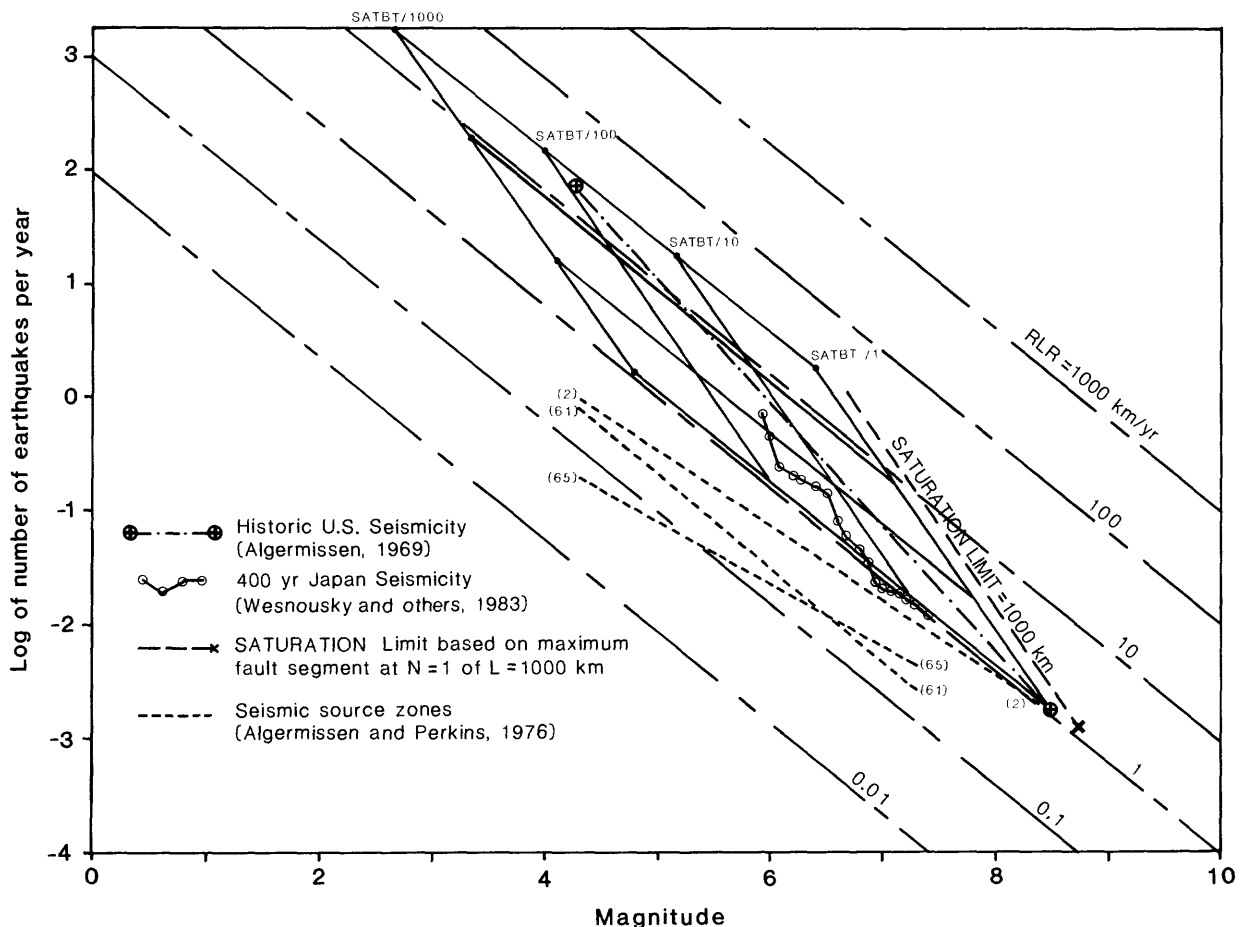
Figure 1. Frequency-magnitude diagram showing the relative positions of fractograms, fault activation rates, rupture length rate RLR, and seismic data for Japan and the U. S. Open circles indicate the raw data for historic seismicity in Japan, (replotted from Wesnousky and others, 1983). The dash-dot line represents the U. S. data (from Shaw and othes, 1981). Lines marked RLR (rupture length rate) represent the loci of frequencies and magnitudes for steady-state production of activated fault length at the rates on the curves; e. g. at a rate of 1000 km/yr, the length of activated fault produced in 100 years is 10 km which converts to a magnitude of about 6.2. The potential rate identified by the value of RLR, such as the value 10 km/yr used for the rate of activation of total length is normalized by the fraction of the length in each number/length order to give the relative distribution of frequencies and magnitudes for a given branching hierarchy. The position of the fractogram on the diagram is based on the assumption that the termination of the seismic line for the U. S. identifies the SATURATION value at order N=1; to fit that assumption, the value RLR would have to be about 40 km/yr. Saturation buildup time SATBT indicates the buildup time for SATURATION based on this assumption. The heavy dashed line shows where SATURATION limit would be if the longest first-order fault were of length 1000 km. The dashed lines and numbers in parentheses represent seismic trends within some selected Seismic Zones : (2) San Andreas system, CA, (61) vicinity of Mississippi Embayment (New Madrid system), (65) vicinity of Charleston, SC (from Algermissen and Perkins, 1976).

200

in which aseismic creep, regular intermittent earthquakes, and large unpredictable earthquakes (including concepts of seismic gaps and locked and unlocked portions of long faults) represent fractally different subsets of the same systematic seismic cycle; the possibility is explored that such cycles may represent invariant fractal structures in space and time relative to the maximum topological dimension 4. Relative to 3 spatial dimensions, fractally self-similar subsets exist over small frequency-magnitude ranges, but in general fractal dimension fluctuates from a nearly volume-filling mode (fractal dimension 3) during transitions from shorter to longer fault-length orders to "less-than-linear" (fractal dimension <1) during the approach to maximum events at the longest length orders. It is proposed that a generalized application of concepts of fractal geometry eventually may allow system-wide dynamical predictions to be made at arbitrary scales of faulting and earthquake behavior.

References Cited:

Algermissen, S. T., 1969, Seismic risk studies in the United States: World Conference on Earthquake Enginerring, 4th, Santigo, Chile, January, 13-18, 1969, Proceedings, v. 1, p. 14-27.

Algermissen, S. T., and D. M. Perkins, 1976, A probabilistic estimate of maximum acceleration in rock in the contiguous United States: U.S. Geological Survey Open-File Report 76-416, 45 p.

Shaw, H. R., A. E. Gartner, and F. Lusso, 1981, Statistical data for movements of young faults of the conterminous United States; paleoseismic implications and regional earthquake forecasting: U.S. Geological Survey Open File Report 81-946, 353 p.

Mandelbrot, B. B., 1977, Fractals form, chance, and dimension: W. H. Freeman and Company, San Francisco, 365 p.

Mandelbrot, B. B., 1982, The fractal geometry of nature: W. H. Freeman and Company, San Francisco, 460 p.

Mandelbrot, B. B., D. E. Passajo, and A. J. Paullay, 1984, Fractal character of fracture surfaces of metals: Nature, v. 308, p. 721-722.

Wesnousky, S. G., C. H. Scholz, K. Shimazaki, and T. Matsuda, 1983, Earthquake frequency distribution and the mechanics of faulting: Journal of Geophysical Research, v. 88, p. 9331-9340.

Reports

In preparation

A Study of Foreshocks to the 1960 Great Chilean Earthquake

14-08-0001-G-962

Gordon S. Stewart
Pacific Geophysics, Inc.,
170 South Chester Avenue,
Suite 20,
Pasadena, California 91106
(818)-792-9236

Objective: The foreshocks sequence of the 1960 great Chilean earthquake represents one of the most important to date. In a period of thirty-three hours prior to the mainshock, a sequence of at least forty-five foreshocks occurred, all of them located at the northern end of the future mainshock rupture zone. Of the forty-five, five had magnitude, $M \gtrsim 6.5$. Furthermore, all five of the magnitude, $M \gtrsim 7.0$ aftershocks and most of the others occurred in the same region as the foreshock activity. The objective of this research effort is to better understand the spatial relationship between these events and determine source parameters for the larger ones.

Data Collection and Analysis: Most of the events of interest in this study occurred prior to the installation of the WWSSN stations. We have, therefore, made requests to the appropriate stations for copies of their seismograms. As these data arrive they are evaluated as to suitability for analysis. We are hopeful of obtaining copies of a special collection of Chilean earthquake foreshock records in the near future. These data are important since many original station records have been lost or destroyed. Most of the analysis to date has been of a preliminary nature, preparing the data for future analysis. It includes:

1. Preparation of data as it arrives or is obtained. In particular, careful attention is given as to how best to use the data, given the available station distribution around the hypocenters. Digitizing of the records has begun.

2. Computer programs for the relocation and synthetic seismogram analysis are being prepared for the later analysis of the data.

3. Arrival-time data for the foreshocks and aftershocks have been collected and entered into the computer. Some of the preliminary relocation analysis has begun using the Joint Hypocenter Determination (JHD) method.

4. P-wave first-motion data have been read and the results plotted for the post-1963 events.

Great Earthquakes and Great Asperities, Southern California:
A Program of Data Analysis

14-08-0001-G-948

L. R. Sykes and L. Seeber
Lamont-Doherty Geological Observatory of Columbia University
Palisades, New York 10964
(914) 359-2900

Investigations

We have been conducting an examination of the seismicity, focal mechanisms, geologic evidence and other geophysical data in an attempt to resolve the pattern of deformation in time and space along the major throughgoing fault zones and some of the active secondary structures in southern California. Our procedure has been to invert arrival data time from microearthquakes to obtain local velocity structure and then to obtain accurate earthquake hypocenters. Accurate determinations of depths of events are important in obtaining high-quality focal mechanism solutions and in searching for possible premonitory changes at certain critical depth intervals. We have used data on seismicity and focal mechanisms to derive a qualitative description of the overall kinematic pattern of fault behavior and tectonic deformation in the current interseismic period between great earthquakes. We have sought to discriminate between various proposed tectonic models. In particular we are testing whether any of the larger historical events have occurred along some of the secondary structures or if those structures exhibit any precursory phenomena prior to larger earthquakes.

Results

1. We have carried out a systematic analysis of earthquake activity in the vicinity of the San Andreas fault, south of the Palm Springs, Morongo Valley area, occurring between 1980 and 1984. Of 3500 well-located earthquakes in this area, 1350 were chosen for relocation, based on their position relative to various seismicity trends. Those with at least six first motions were used to determine focal mechanism solutions. This yielded 472 earthquakes for which some determination of the faulting mechanism could be made. The dominant type of faulting observed was strike-slip along nearly vertical planes. Although control on the dips of the nodal planes is poor, the strikes are well-constrained. None of the earthquakes examined, however, could be associated with nodal planes dipping as shallow as 40°-50°, which would be necessary to place a large number of these events on the southern San Andreas. Furthermore, none exhibited a large component of thrust faulting as would be required by various kinematic models proposing large amounts of shortening in this region. Earthquakes whose focal mechanisms were not as well constrained were then compared to the individual focal mechanism solutions of the larger events within each seismic trend, thus permitting more earthquakes to be cataloged by sense of slip than would normally have been achieved if only single focal mechanisms were determined.

The data show a rather complicated pattern of deformation where strain is presently being taken up by slip on secondary structures, many of them oriented at high angles to the strike of the major throughgoing faults. Although these observations may only be valid for a limited time frame (probably that between large earthquakes), they imply that the southern San Andreas fault per se is nearly aseismic for much of its length extending from Cajon Pass to the Salton sea. In this respect, the southern San Andreas is behaving much like the 1857 earthquake rupture zone (which is also currently quiet at the microearthquake level) and much of the 1906 rupture zone.

2.   Systems of rotating blocks and faults may play an important role in the the interseismic deformation between great earthquakes on major right lateral faults in Southern California. We have now evidence for block rotation from geologic and from earthquake data. Qualitative models suggest that block rotation adjacent to a major fault strand may generate time dependent asperities that lock this fault for a time that depends on the size of the blocks and on the thickness and mechanical properties of the fractured zone along this fault. Rotating blocks are expected to interact with the adjacent active major strand by increasing normal stress across portions of this fault and locking it.

In a study of the San Bernardino-San Gorgonio Pass region, currently one of the most active areas in Southern California (Fig. 1), we could resolve many detailed features of the pattern of faulting (Nicholson et al., 1984). The results were more or less directly suggestive of a rotating block model. In general, we found the San Andreas and other major right lateral faults to be mostly aseismic. Wherever active faulting could be resolved by fault-plane solutions and hypocenter distribution, we tended to find either left-lateral northeast trending faults, or reverse faults. Crustal deformation during the interseismic period may be dominated by slip on secondary faults rather than diffuse elastic strain. Moreover, block rotations may play a particularly important role and may offer a key to the pattern of deformation leading to a great earthquake. We believe that the roles played by block rotations in the interseismic period and in the sequences of great earthquakes may be very pertinent to a earthquake prediction effort.

Fig. 1. Well-located 1975-83 hypocenters from the USGS/Caltech network and major faults from the 1:250,000 California Atlas.

50KM

Analysis of Seismic Data from the Shumagin Seismic Gap, Alaska

USGS-14-08-0001-G-946

John Taber and Klaus Jacob
Lamont-Doherty Geological Observatory of Columbia University
Palisades, New York 10964
(914) 359-2900

Investigations

Digitally recorded seismic data from the Shumagin seismic gap in the eastern Aleutian arc, Alaska, are analyzed for detecting space-time variations in seismicity, focal mechanisms, and of dynamic faulting parameters that could be precursory to a major earthquake expected in this seismic gap. The seismic results obtained from the network data are being integrated with crustal deformation data that are independently collected, with volcanicity data of nearby Aleutian volcanoes, and with teleseismic information, to identify basic tectonic processes which may be potentially precursory to a great earthquake.

Results

A detailed examination of hypocenter patterns within the Shumagin gap shows that the seismogenic zone is thicker in the western half of the region (Figure 1). Cross sections normal to the arc (Figure 2) show that the difference in thickness is due to the presence or absence of a double Benioff zone. The variation in the Benioff zone may be related to either a change in structure, a change in stress, or both. The boundary between single and double Benioff zones spatially coincides with the transition from ocean-ocean to continent-ocean subduction.

Changes in seismicity rate also seem to occur across the same boundary. Previously reported rate changes that were correlated with a temporal change in focal mechanisms appear to be limited to the eastern portion of the gap (Figure 3). Further clarification of the nature of this boundary will be necessary because we need to know whether observed seismicity patterns are related to inherent stationary differences in physical properties on the subduction zone or are temporary features related to loading before a great earthquake. Other data, such as composite focal mechanisms that show temporal changes, are not able to resolve the spatial variations. A ground tilt reversal that was coincident with the seismicity rate change (Beavan et al., 1984) was determined from level lines that are measured only in the eastern part of the network, so that the extent of the reversal along the arc is not known.

We estimate that the Shumagin region may have exceeded the long-term probability for a great earthquake. This exceedence stems from the statistically significant rate reduction of earthquake activity at the magnitude 5.5+ level, using the z statistic of Habermann (1981). In addition, Pavlof volcano did not erupt this year and McNutt and Beavan (1984) have shown that it has erupted almost yearly except before and during a deep aseismic slip event that occurred in 1978-79. If a new aseismic slip event occurs at the base of the main thrust zone, this

would cause increased stress in the locked portion of the zone.

References

Beavan, J., R. Bilham, and K. Hurst, Coherent tilt signals observed in the Shumagin seismic gap: Detection of time-dependent subduction at depth?, J. Geophys. Res., 89, 4478-4492, 1984.

Habermann, R.E., Precursory seismicity patterns: Stalking the mature seismic gap, in Earthquake Prediction, An International Review, Maurice Ewing Series, 4, edited by D.W. Simpson and P.G. Richards, pp. 29-42, AGU, Washington, D.C., 1981.

Reports and Representations

Hauksson, E., J. Armbruster, and S. Dobbs, Seismicity patterns (1963-1983) as stress indicators in the Shumagin Seismic Gap, Alaska, Bull. Seismol. Soc. Am., 74, 2541-2558, 1984.

McNutt, S.R. and R.J. Beavan, Periodic eruptions at Pavlof Volcano, Alaska: The effects of sea level and an aseismic slip event, EOS, Trans. AGU, 65, 1149, abstract V42A-087, 1984.

Taber, J.J. and S.R. McNutt, Temporal and spatial changes in seismicity associated with subduction near the Shumagin Islands, Alaska, EOS, Trans. AGU, 65, 987, abstract S11B-06, 1984.
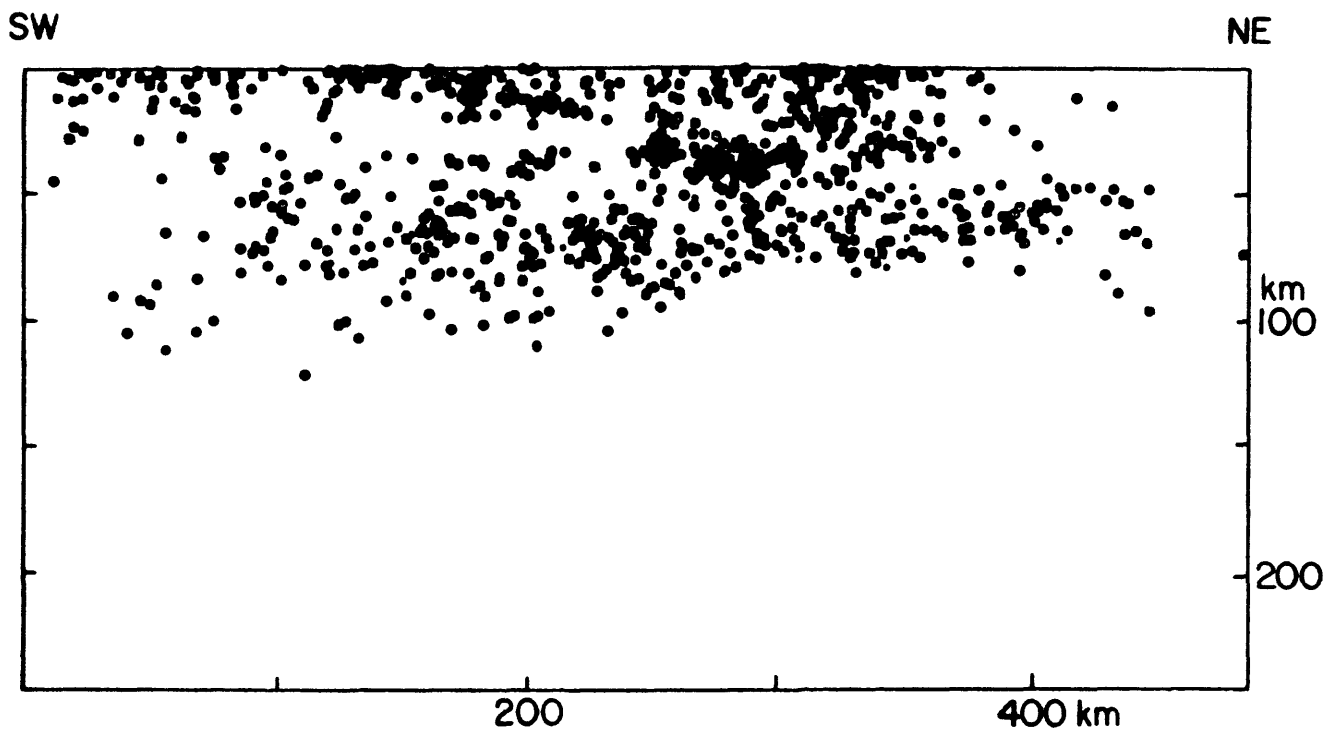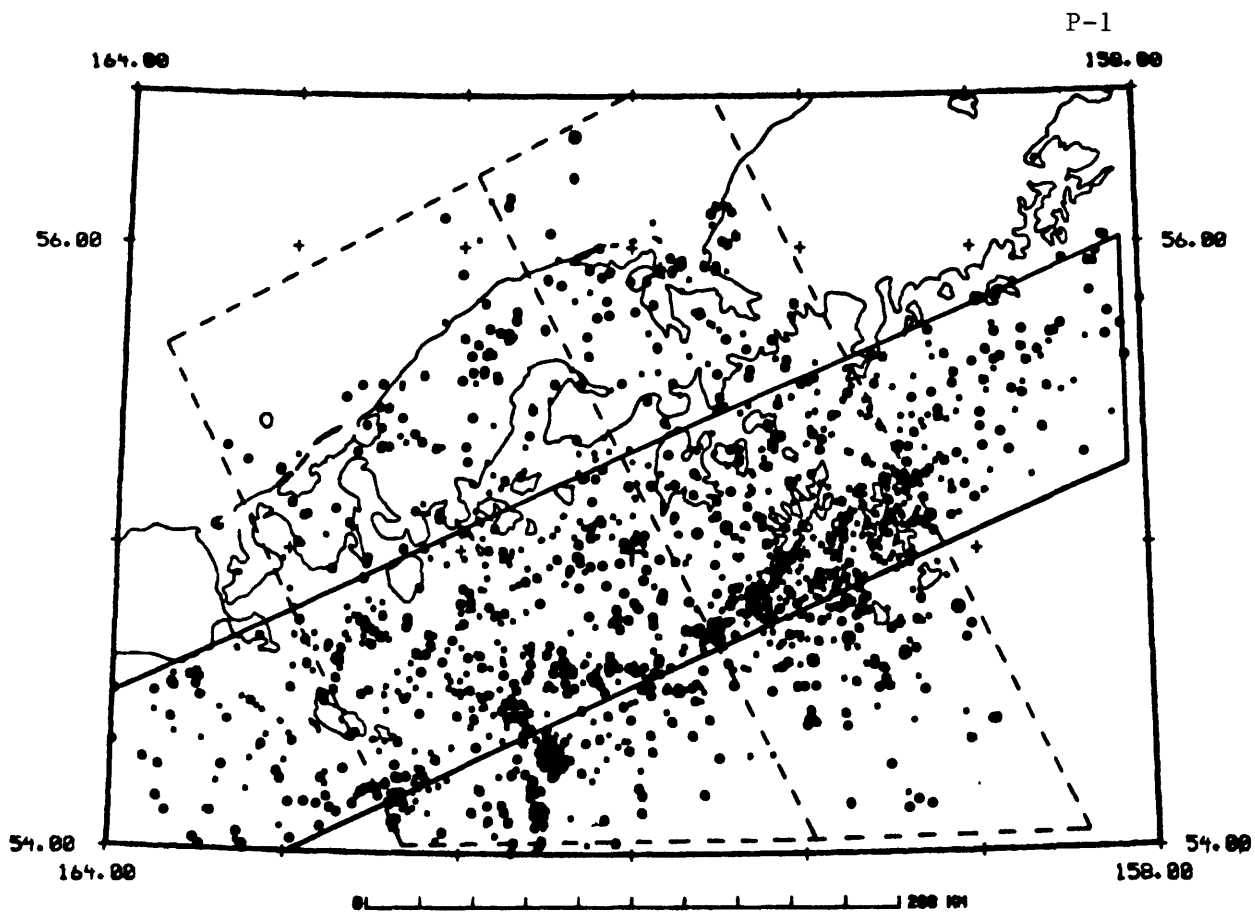
Figure 1. Top: Map showing the subregions plotted in the next 3 cross sections. The solid line encloses the events in the along strike cross section in Figure 8b. The dotted lines encloses the Shumagin east and west cross sections shown in Figure 9. The + in the center of the map is the center of the projection for all 3 cross sections. Bottom: Along strike cross section. Note the increase of seismicity at ∿50 km depth and the shallowing of the base of the seismogenic zone when moving from SW to NE.
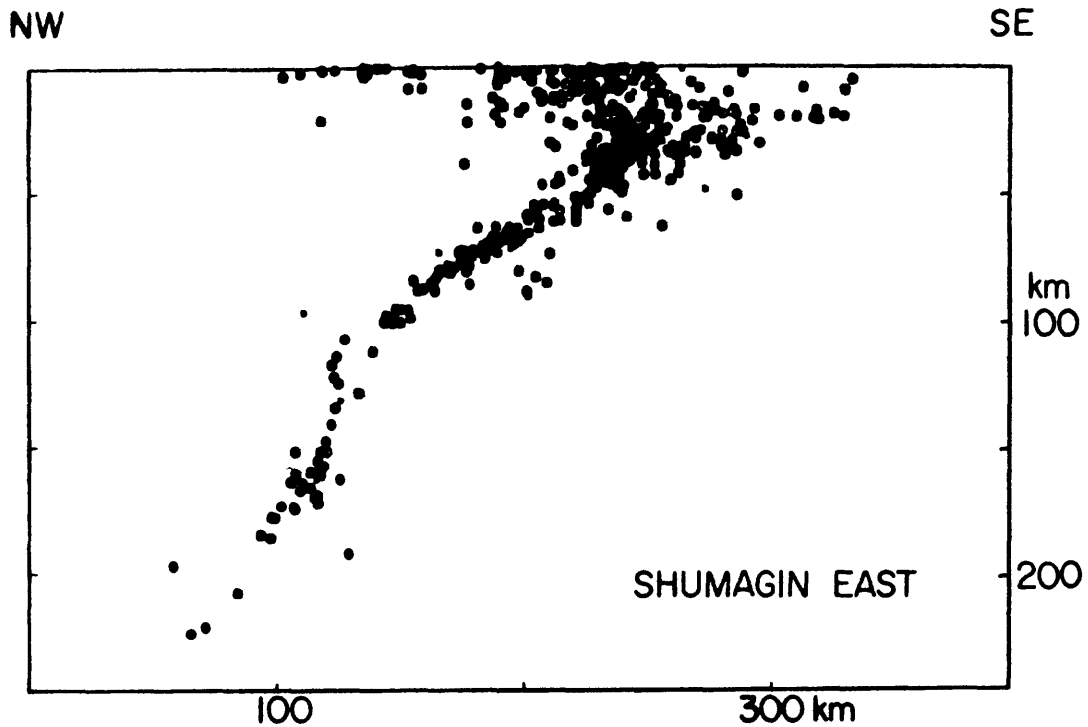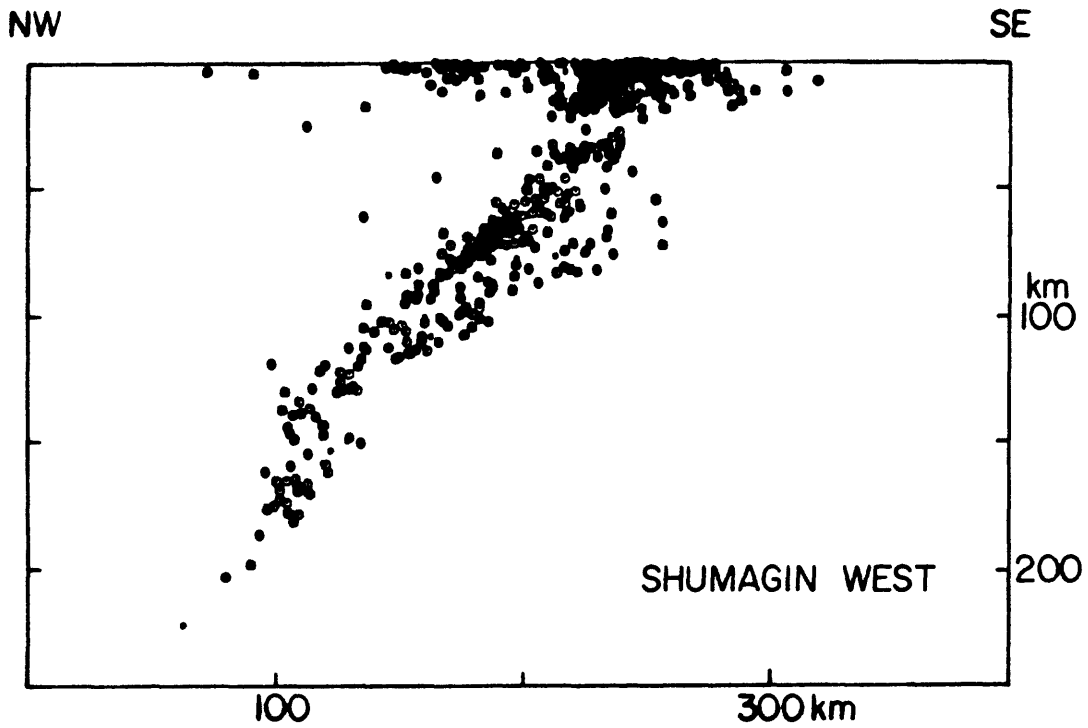
Figure 2. Perpendicular to strike cross sections for the events shown in the 2 dotted line boxes in Figure 8. Top: Shumagin west. Note clear double Benioff zone and lack of seismicity near the main thrust zone. Bottom: Shumagin east. Here there is little evidence of a double zone and there is a concentration of seismicity between 30 and 50 km.
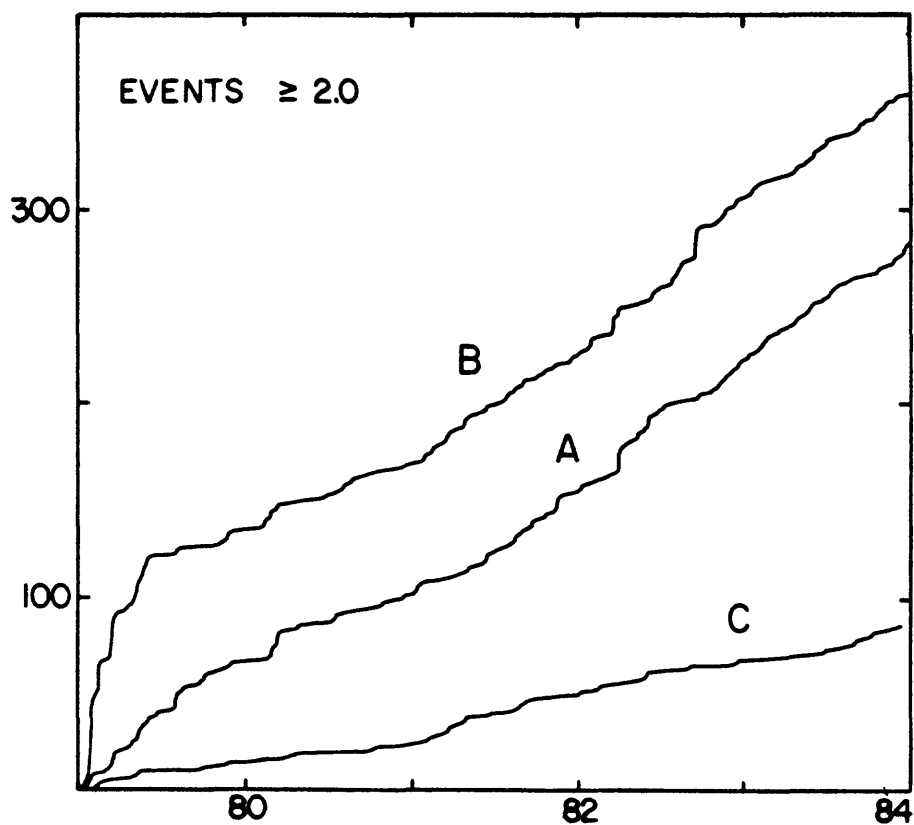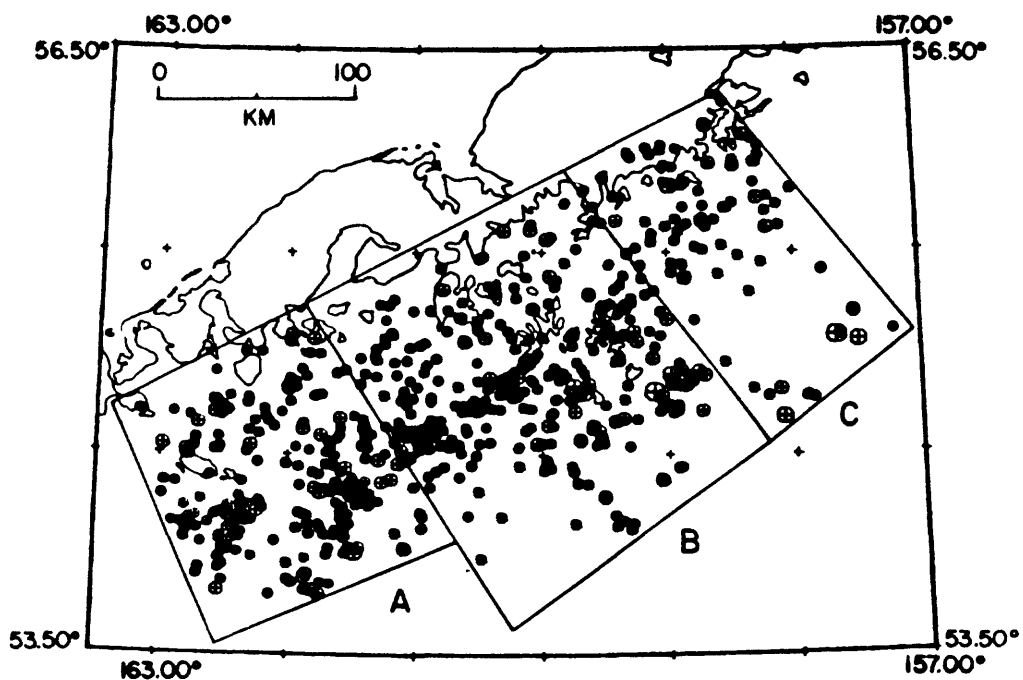
Figure 3. Top: Subdivision of the Shumagin gap into 3 subregions. Bottom: The cumulative number of events in each of the boxes in the top figure is plotted against time for the period 1979-1984. The rate decrease in 1979 in region B is not evident in regions A and C.

Earthquake Process

9930-03483

Robert L. Wesson
Branch of Seismology
U.S. Geological Survey
922 National Center
Reston, Virginia 22092
(703) 860-7481

INVESTIGATIONS

1. Analysis of theoretical and numerical models of the processes active in fault zones leading to large earthquakes.

2. Analysis of seismological and other geophysical data pertinent to understanding of the processes leading to large earthquakes.

RESULTS

A stochastic simulation of the temporal and one-dimensional spatial characteristics of an aftershock sequence has been developed for comparison with real data. The objective is to determine at least qualitatively whether the spatial expansion of aftershock zones--apparent particularly on plots of the position of aftershocks versus log time--is a real physical phenomenon or simply an artifact of the temporal sampling. In the simulation the position of an aftershock within the aftershock zone is modelled as a draw from a uniform distribution over the length of the aftershock zone. The time of occurrence of each aftershock is drawn from a distribution such that the number of aftershocks per unit time decreases as 1/t (or other power of t) from the time of the main shock. By adjusting the total number of earthquakes in a sequence, the length of the aftershock zone and the decay rate to match an observed sequence, it is then possible to generate as many synthetic sequences of aftershocks as desired which match the aggregate properties of the observed sequence. The question can then be asked, do the synthetic sequences demonstrate the kind of spatial expansion observed in real sequences? The answer for the set of California aftershock sequences studied to date is mostly no. Many California aftershock sequences, but not all, show spatial expansion that is qualitatively significant when compared with simulations generated with the corresponding aggregate characteristics. The simulations are very sobering, however, in that they show details which one might be tempted to interpret--erroneously--in terms of physical or geologic processes.

Further analysis of stress measurements made in a borehole penetrating the Cleveland Hill Fault near Oroville, California, following the 1975 Oroville earthquake lend support for the hypothesis that near surface fault movement along the Cleveland Hill fault occurred principally, if not completely, as afterslip. As previously reported (Wesson and Zoback, 1983), the measured stress profile in the borehole is consistent with a model of fault displacement of 1-2 cm extending from the surface to a depth of a few hundred meters. Geologic observations of Clark, et al. (1976) indicate most of the

surface fault displacement occurred as afterslip, suggesting that the fault zone in the near surface may have been responding in a time dependent way to the stress change associated with the main shock. Calculations show that this hypothesis is reasonable if the fault zone can slip under a stress change on the order of 10 bars or less. Analyses conducted to date suggest that for this to occur, the fault zone would have to be weaker than predicted by Mohr-Coulomb failure criteria and laboratory measurements of friction.

REFERENCES

Clark, M. M., R. V. Sharp, R. O. Castle, and P. W. Harsh, 1976, Surface faulting near Lake Oroville, California, in August 1975, Bull. Seis. Soc. Amer., 66, 1101-1110.

Zoback, M. D. and R. L. Wesson, 1983, Modelling of coseismic stress changes associated with the 1975 Oroville earthquake (abs.), EOS, Trans. Amer. Geoph. Union, 64, 834.

REPORTS

Wesson, R. L., Seismicity of the Pamir-Alai region, Soviet Central Asia, SSA Annual Meeting, Austin, Texas, April, 1985.

Wesson, R. L., A model for Aftershocks and Afterslip in California, Submitted to Symposium on "Mechanics of Earthquake Faulting" IASPEI, Tokyo, Japan, August, 1985.

Central American Seismic Studies

9930-01163

Randall A. White, David H. Harlow
Branch of Seismology
U.S. Geological Survey
345 Middlefield Road, MS/977
Menlo Park, California 94025
(415) 323-8111, ext. 2570

Investigations

We are examining the tectonic origin and the seismic characteristics of shallow (Z < 15 km), destructive earthquakes along the volcanic chain in Central America. We are focusing on these earthquakes because the historical record indicates that these earthquakes produce a greater impact than do large subduction zone earthquakes which are typically small (magnitude 7.5 to 8.0) compared to other circum-Pacific thrust zones and whose effects are mitigated by their infrequency and greater hypocentral distance. The shallow earthquakes, on the other hand, are more frequent and occur in or near major population centers which are concentrated along the volcanic chain.

Significant results of studies on recent earthquakes

Figure 1 shows all 23 magnitude 6.0 and greater, shallow damaging earthquakes that have occurred this century either within or northeast of the active volcanic chain of Central America. Isoseismal intensity maps are prepared from newspapers and other documents for those earthquakes which have no previously published intensity maps. Areas of intensity VII or greater damage, for earthquakes within a few kilometers of the active volcanic chain, are found to all be of very similar size, though some have the long axis parallel to, and others perpendicular to the volcanic chain.

We have established magnitudes for all earthquakes from a simple empirical formula $M = 0.8 \log A_{dB} + 5.5$, where A_{dB} is the amplitude at deBilt. We find that the largest earthquakes at 17 different sites along the active volcanic chain all have magnitudes between 6.0 and 6.4. Behind the volcanic chain damaging earthquakes occur much less frequently but may have magnitudes ranging up to possibly 7.5. Focal mechanisms for earthquakes along the volcanic chain show three different mechanisms: right-lateral strike-slip motion parallel to the volcanic chain, left-lateral strike-slip motion perpen-dicular to the volcanic chain, and normal motion along north and northeast trending faults.

We have obtained seismograms recorded at Guatemala City for the earth-quakes after 1930 and are able to distinguish direct P and Pn phases in some cases, and small S-P times in others to confirm the shallow origin of these earth-quakes.

Significant results of micro-seismicity studies: Figure 2 shows the epicenters of recent shallow micro-earthquakes located during cooperative projects between the USGS and Nicaragua from 1975 to 1978, Guatemala during 1982, and El Salvador during 1984. Notice that over 90 percent of the

epicenters lie along the chain of active volcanoes, at the same locations as most of the recent damaging earthquakes in the region, shown in Figure 1.

a) Along the chain of active volcanoes we have recognized at four different types of earthquakes, all of which may produce damage.

1) One type, called tectonic earthquakes, occur at the offsets in the volcanic chain and are characterized by a mainshock followed by aftershocks and b-values of about 1.0.

2) A second type, called volcanic earthquakes, occur just beneath or within active volcanoes and usually are accompanied by volcanic eruptions. These earthquakes occur in swarms characterized by a slow growth of seismic energy and later, volcanic activity, with the largest earthquakes near the middle of the period of seismic activity, preceeding or accompanying the initial eruption. B-values are probably about 2.0 or greater.

3) The third and most common type may be called tectono-volcanic earthquakes. These earthquakes occur between the volcanoes as frequent swarms of (usually) low level seismic energy. These swarms are characterized by a short period of rapidly increasing seismic energy, followed by a main-shock, followed by large numbers of small aftershocks. These swarms have b-values of 1.5-1.8 and are probably related to the subsurface movement of magma beneath these volcanoes but are never accompanied by eruptions. Occasionally a swarm will grow large enough to produce damaging earthquakes.

4) The last type is probably associated with the collapse or slumping of part of the caldera roof and are much less frequent than the others. The largest earthquake may be the last earthquake in a series, preceeded by a week or so of seismicity.

It appears that many of the damaging earthquakes of types 2 and 3 may be forecast a few days in advance because of the periods of growing precursory seismicity that usually precede the main shock. The persistent reports of foreshocks and the nature of recently recorded microearthquake swarms at the volcanoes lead to the intriguing suggestion that, at a minimum, these earthquakes could be forecast within a socially useful timeframe. Recent moderate size earthquakes in Central California, however, do not have foreshock activity that clearly broadcasts the future mainshock. Therefore, we plan to carefully evaluate these reports and to examine closely the possibility that the style of tectonic deformation along the volcanic chain creates a rupture process that is characterized by foreshock activity.

Little is known about the tectonic origin of these shallow volcanic chain earthquakes. We propose a new model in which shallow earthquakes are caused by right-lateral slip along the volcanic chain due to a subduction vector 5° to 20° oblique to the dip of the Benioff zone. The model is consistent with both seismic focal mechanisms and geologic surface features in El Salvador and Nicaragua. In Guatemala and at the Costa Rica-Panama border the data are more complex, because of interactions at triple junctions, but are not inconsistent with the proposed model.

Reports

White, Randall H., 1983. The Guatemala earthquake of 1816 on Chixy-Polochic fault: Bulletin Seismological Society of America, v. 75, pp. 455-473.

White, Randall H., Harlow, David H., and Edgar R. Quevec, 1984. Micro-seismicity of the western Motagua fault prior to the 4 February 1976 Guatemala earthquake: EOS.

McNutt, S. R., and Harlow, D. H., 1984, Seismicity at Fuego, Pacaya, Izalco, and San Cristobal Volcanoes, Central America, 1973-1974, Bull. Volcanol.

Harlow, David H., and R. A. White, 1984. Shallow earthquakes along the volcanic chain in Central America: Evidence for oblique subduction. EOS (invited paper).

SHALLOW M≥6 EARTHQUAKES SINCE 1910

Mexico

Guatemala

Honduras

El Salvador

Nicaragua

Costa Rica

Caribbean Sea

Pacific Ocean

16°N

12°N

8°N

92°W

88°W

84°W

1971

1959

1976

1918
1913
1937

1934
1915

1912
1917,

1965

1936

1951

1982

1955
1938

1955
1931,
1972

1933

1973

1955

1910

1983

0 50 100 Km

N

Areas of Damage, MM≥VII

Other Historical Damage

Volcanoes
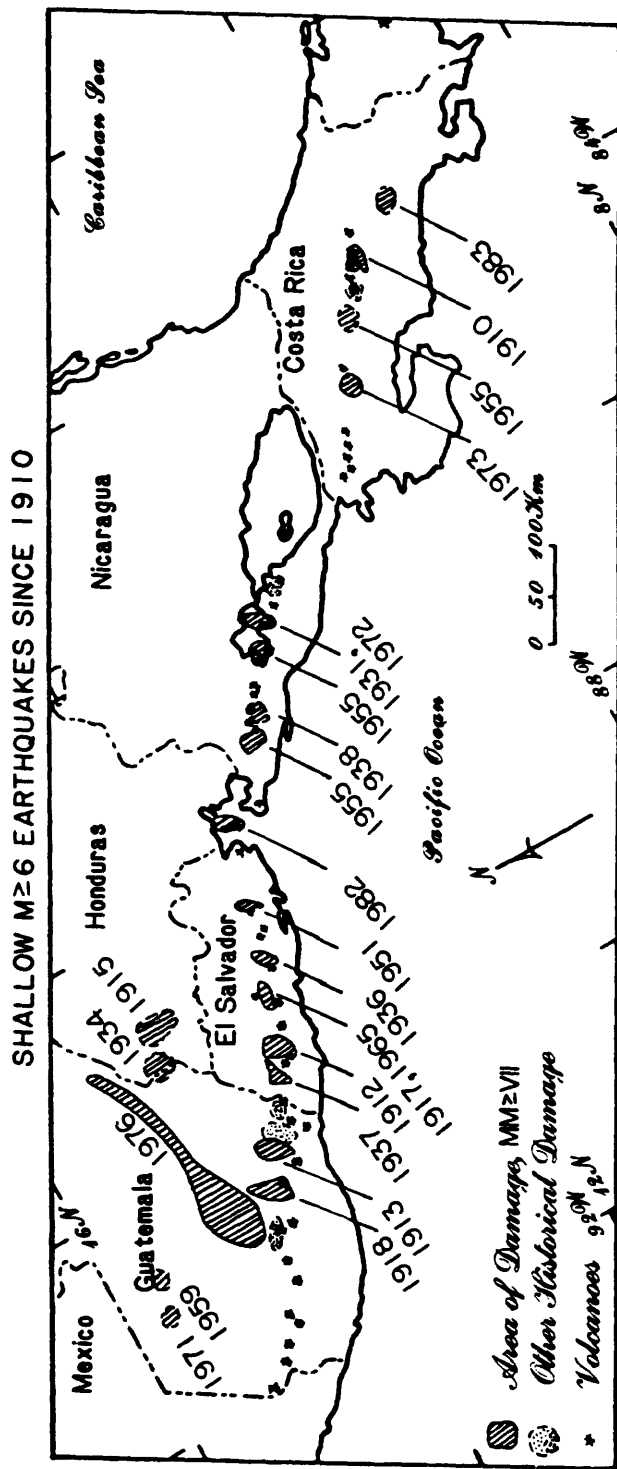
Figure 1

RECENT SHALLOW MICRO-EARTHQUAKES LOCATED DURING COOPERATIVE PROJECTS

BETWEEN THE USGS AND NICARAGUA (1975-78), GUATEMALA (1982), AND EL SALVADOR (1984)
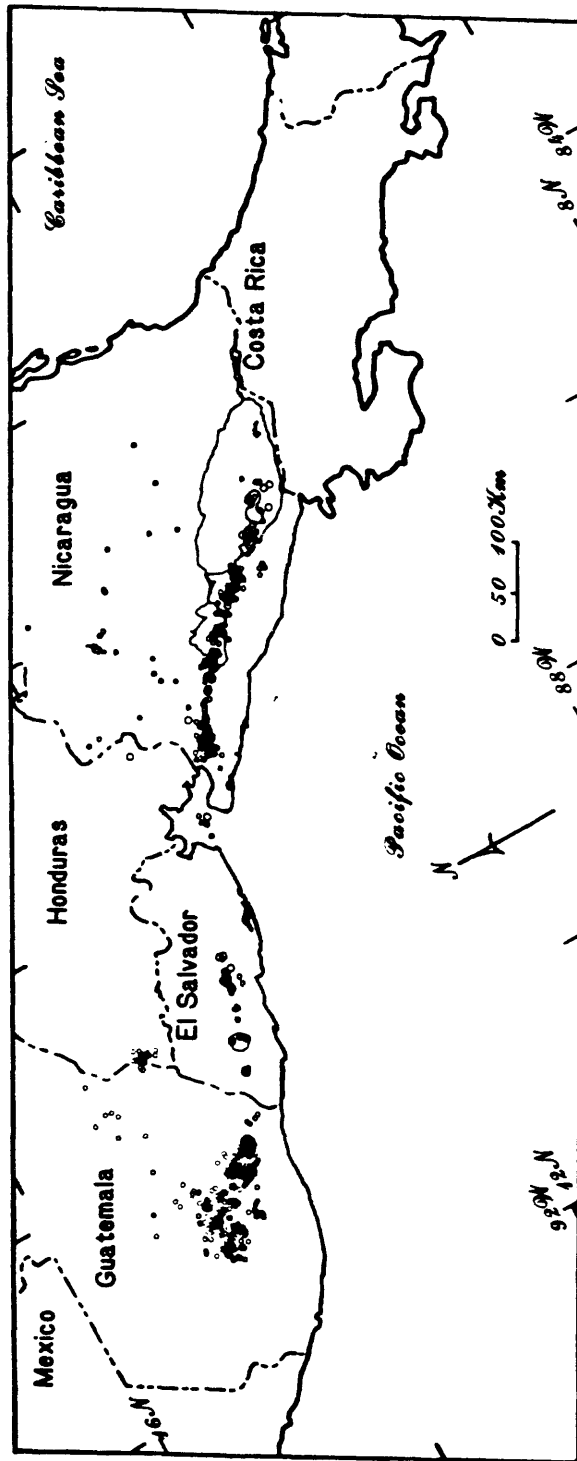

Figure 2

COOPERATIVE EARTHQUAKE PREDICTION RESEARCH WITH
INSTITUTE OF GEOPHYSICS, SSB, PRC

14-08-001-21341

Francis T. Wu
Department of Geological Sciences
Center for Study of Natural Hazards
State University of New York
Binghamton, New York 13901

Ta-liang Teng
Department of Geological Sciences
University of Southern California
Los Angeles, California 90008

Investigations

1. Augmentation of the Beijing-Tangshan-Tianjin (BTT) telemetered seismic network to lower event detection threshold and improve data acquisition system.

2. Research concerning seismicity and tectonics of the Beijing-Tangshan-Tianjin area and the use of seismicity toward earthquake prediction.

3. Fabrication and installation of water well well level monitoring instrumentation in the vicinity of Beijing and the study of data gathered from these stations.

Results

1. Level data from a 3404 meter water well shows clear response to seismic, tidal and atmospheric disturbances. Continuously recorded since September 1983, the level is shown to be steady and free from interference due to seasonal water use in the Beijing area.

2. Portable digital accelerographs deployed in the region of a magnitude 6.2 (Beijing Telemetered Network ML) earthquake in October, 1982 near the city of Lulong northeast of Tangshan yielded ample data. A study of the moment-magnitude relationship has just been completed. It shows that (a) the spectral content of seismic waves in the Beijing region is different from that in Central California -- an enrichment of high frequency is quite pronounced, (b) for events with the same moment, the Beijing magnitude is about .5 higher than Central California magnitude, and (3) simulated Wood-Anderson peak amplitudes within 5 to 25 kilometers of the source appear to fall off with distance faster than r^{-1}.

Creep and Strain Studies in Southern California

Contract No. 14-08-0001-21979

Clarence R. Allen and Kerry E. Sieh
Seismological Laboratory, California Institute of Technology
Pasadena, California 91125 (818-356-6904)

Investigations

This semi-annual report summary covers the six-month period from 1 October 1984 to 31 March 1985. The contract's purpose is to monitor creepmeters, displacement meters, and alignment arrays across active faults in the southern California region. Primary emphasis focuses on faults in the Coachella and Imperial Valleys.

During the reporting period, resurveys of theodolite alignment arrays were carried out at **Cameron, Devers Hill, Highway 80, Indio Hills,** and **Worthington Road.** New arrays were installed at **Yerxa Road** and **Thousand Palms** on the Mission Creek fault, and at **Tuttle Ranch** on the Imperial fault. In addition the arrays at **Dixieland** and **North Shore** were re-established. Nail-file arrays were resurveyed at **Anderholt, Ross Road,** and **Worthington Road.** Creepmeters were serviced and records collected at **North Shore, Mecca Beach, Superstition Hills, Harris Road, Ross Road, Heber Road,** and **Tuttle Ranch.** Both the tilt and creep instruments at **Mecca Beach** were calibrated against the telemetry system. This installation continues to be monitored at the Seismological Laboratory on a weekly basis. Periodic maintenance was also performed on the four coseismic fault displacement meters located on the San Andreas fault, at **Jack Ranch** and **Twisselman Ranch** near Cholame, **Lost Lake** north of San Bernardino, and **Mecca Beach** near the Salton Sea.

Results

The measurements of fault slip taken between October 1984 and March 1985 show few changes in the overall picture of activity. The most recently calculated linear slip rates for many alignment arrays and creepmeters for different periods are shown in the table below. The last 3 columns give the correlation of the regression, the number of separate angle measurements used, and the number of anomalous angles omitted from the regression.

Due to unfavorable weather, the January resurvey of the array at Cameron on the Garlock fault near Mojave is of poor quality (Fig. 1). Another resurvey must be done to determine if sinistral slip has continued since the disturbance of the targets by flooding between 1982 and 1983. On the Superstition Hills fault, the creepmeter record (Fig. 2) shows that 0.5 mm/year of dextral slip was taking place between 1968 and 1979. However, following the 11 mm displacement of the fault sympathetic with the 1979 Imperial Valley earthquake, the creepmeter shows to the March reading that no resolvable slip has occurred.

In re-establishing the array at Dixieland, across an unnamed fault 20 km west of El Centro, one pair of targets crossing the fault remained from the previous survey in 1979. These were measured in March and show that the 3 to 4 mm/year slip rate measured between 1970 and 1979 has apparently ceased (Fig. 1). The slip event which opened the cracks first seen in 1970, and the subsequent 10 years of slip, may well have been an isolated occurrence. A total of 25±10 mm of slip was recorded.

Calculated Slip Rates for Selected Arrays and Creepmeters						
Station	Fault	Period	Slip Rate, mm/year	cor. r	samples n	sam. omit.
Baileys Well	Coyote Creek	6/71-3/84	**5.2**	0.87	153	35
Devers Hill	Banning	10/72-11/82	**2.0**	0.64	69	0
Dillon Road	San Andreas	4/79-2/84	**0.0**	0.01	45	9
		4/70-6/77	**3.0**	0.85	18	0
Dixieland	unnamed	1/71-7/76	**4.5**	0.81	63	0
		8/70-11/79	**3.2**	0.82	99	0
Highway 80	Imperial	5/67-11/78	**5.4**	0.62	279	0
		5/74-11/78	**2.5**	0.27	99	0
Indio Hills	San Andreas	6/77-11/82	**1.8**	0.60	58	0
		4/70-2/84	**1.5**	0.74	77	6
		4/70-6/77	**1.4**	0.99	12	6
Mecca Beach	San Andreas	5/81-2/84	**0.7**	0.93	9	0
North Shore	San Andreas	11/70-3/85	**0.02**	0.10	51	0
Rand	Garlock	11/71-2/83	**0.0**	0.00	120	65
Red Canyon	San Andreas	6/77-5/83	**3.1**	0.81	44	2
		5/67-5/83	**1.7**	0.88	80	0
Sta. Ana Wash	San Andreas	1/73-12/81	**0.0**	0.02	40	4
Suprst. Hills	Suprst. Hills	5/68-8/79	**0.5**	0.91	45	0
Tuttle Ranch	Imperial	10/75-8/79	**1.4**	0.97	19	0

On the Imperial fault, the creepmeter at Heber Road recorded 1.16 ± 0.02 cm of slip between 26 and 28 December (Fig. 2). This event offset the wall of a trench at the Heber Dunes being logged by R. V. Sharp, showing that the rupture extended at least 1.5 km to the south. However, the creepmeter at Tuttle Ranch (Highway 98), 5.5 km south of Heber Road, has not detected any slip since 1982 (Fig. 2). Many other creep events having displacements less than 0.05 cm occurred throughout December and January 1985, for a total of 1.4 cm of slip between 27 November and 19 January. Events of this size have occurred many times since the 1979 Imperial Valley event. Their frequency has, however, been decreasing. The period between centimeter-sized events is now approaching 1.5 years.

The event at Heber Road was accompanied by ground fracturing in the vicinity of the instrument. Similar fracturing developed at Highway S-80 sometime between 19 January and 12 March. The alignment array there indicates that 0.84 cm of slip took place after 26 November (Fig. 1). Seismicity data from the USGS/Caltech So. Calif. Array show that a swarm of 15 events of M_L less than 2 developed around the Imperial fault in the 10 km between Heber Road and Highway S-80 in late October and November. After November seismicity data are incomplete, although no events having M_L larger than 2.5 have occurred in this period near the Imperial fault. Oddly enough, the creepmeter at Ross Road, midway between Heber Road and Highway S-80 on the fault, has not shown any slip events since 1982 (Fig. 2). On the northern part of the Imperial fault, at Worthington Road, the latest March resurvey suggests that the afterslip of the 1979 Imperial Valley event may have ceased since the previous resurvey in 1983 (Fig. 1).

The March resurvey of the array at Devers Hill across the Banning fault is inconclusive as to whether the 2 mm/year slip rate measured before 1982 is continuing (Fig. 1). On the San Andreas fault in the Coachella Valley at Indio Hills, an alignment array indicates that 1.5 mm/year of slip took place between 1971 and 1982 (Fig. 1). Recent resurveys in 1984 and March 1985 have failed, however, to confirm that slip is still occurring. More resurveys will establish whether the halt may be real or an artifact of some unstable reference targets in the array.

Farther to the southeast along the San Andreas fault at North Shore, both the newly re-established alignment array (Fig. 1) and the creepmeter (Fig. 2) confirm as of March that no slip greater than 1 mm could have occurred during the 16 years of monitoring this section of the fault. Several km southeast at Mecca Beach, the creepmeter recorded 0.7 mm/year of dextral slip

between 1981 and 1984, before the creep and tilt events in April and July, discussed in the previous semi-annual report. Since that report was submitted, the tiltmeter has been calibrated against the telemetry system, allowing us to report revised tilt values. The April creep event was accompanied by a tilt of 51.9±4 microradian with a downward-pointing gradient oriented at S26.9±2°W. The much smaller July event (Fig. 3) showed a slip of 0.055±0.025 cm, with a slip velocity of 4.7×10^{-7} cm/s during the initial 19 hours. It was accompanied by tilting at 9.8×10^{-5} μradian/s, for a total of 17.3±1.8 μradian, with the downward gradient pointing S26±3°E. From then through March no further events showing slip larger than the temperature error of 0.025 cm have been identified at Mecca Beach.
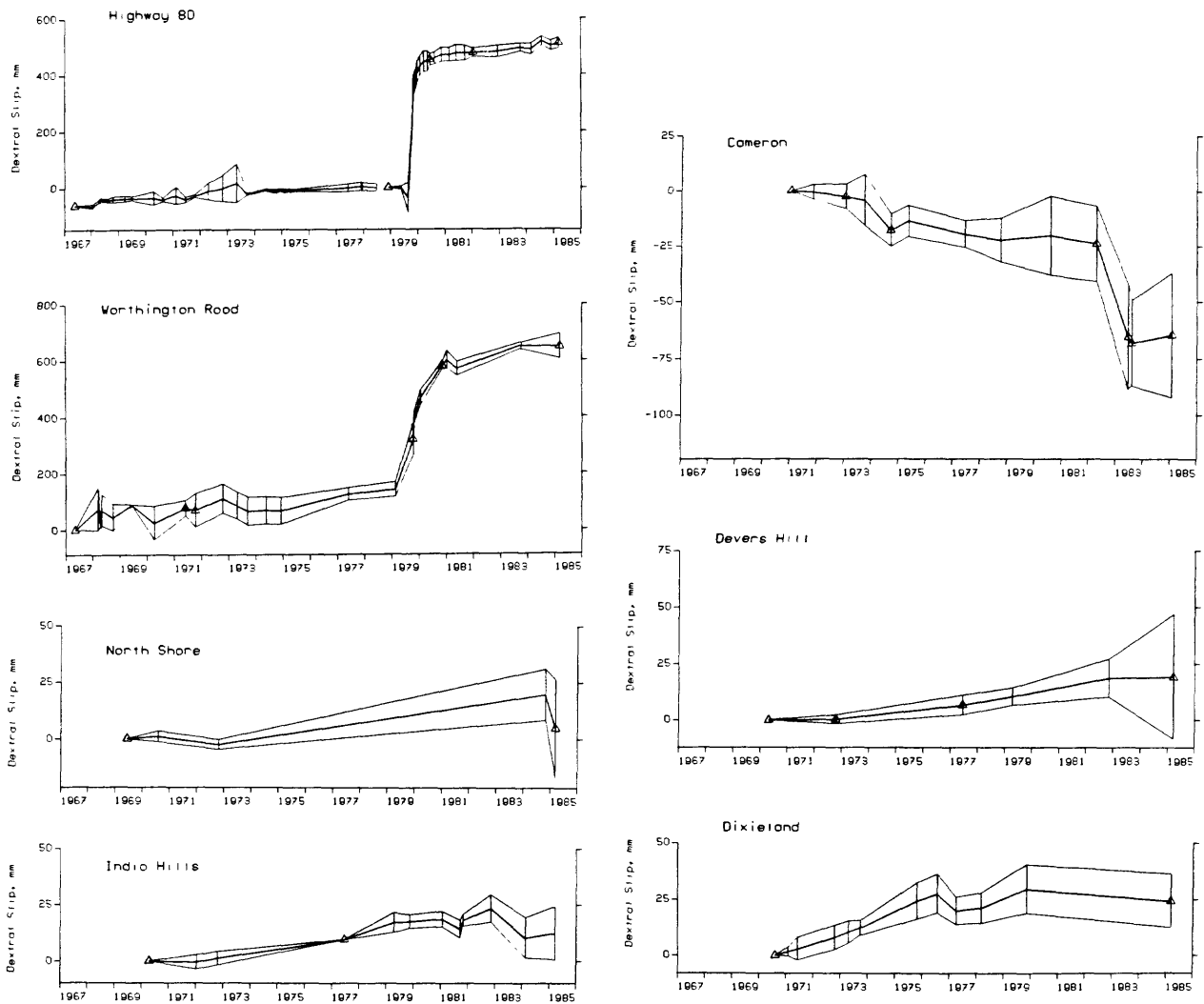
**Figure 1.** Records of cumulative parallel slip at the alignment arrays resurveyed between October 1984 and March 1985. The 3 lines represent the average and plus and minus one standard deviation of slips derived from different pairs of reference and measurement targets, with a vertical line at each resurvey. A triangle is placed where new targets were added at the average slip of existing targets.
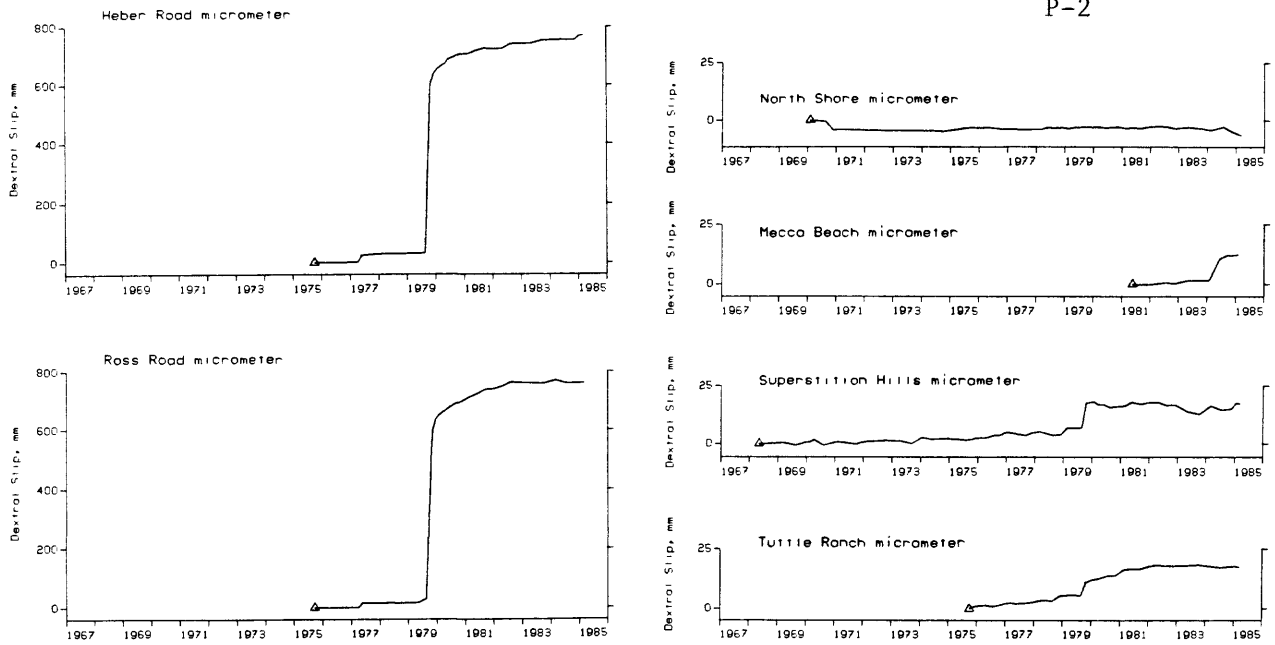
Figure 2. Records of cumulative parallel slip at creepmeters monitored on the southeastern San Andreas, Superstition Hills, and Imperial faults. The slip is derived from quarterly micrometer readings of the extension between the piers, corrected for temperature and the geometry of the instrument. The slip during the 1979 Imperial Valley event was derived from measurements of the nearby **Anderholt Road** nail array for the **Heber Road** record, and from the trilateration measurements of Crook, Mason, and Wood (U.S.G.S. Prof. Paper 1254, p. 183-191) for the **Ross Road** record.
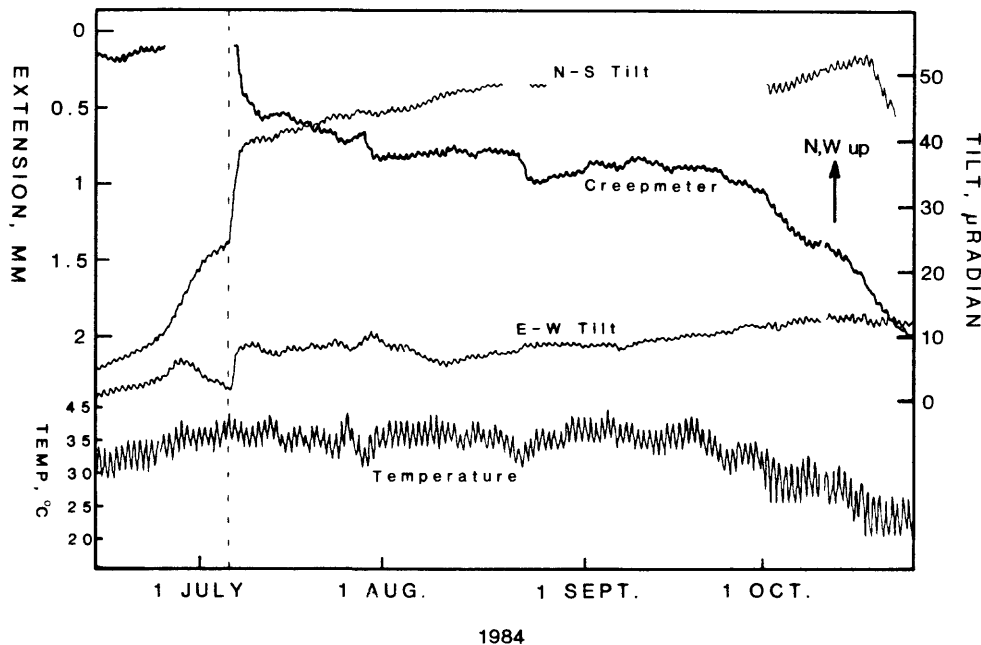
1984

Figure 3. Composite of recalibrated records from the **Mecca Beach** instruments on the San Andreas fault near the Salton Sea for the period from 13 June to 26 October 1984. The creepmeter record represents the raw extension between the piers and is corrected for temperature and instrument geometry to yield the slip. Note the apparent extension in late September and October following the fall in temperature. The dashed vertical line shows the position of 6 July 1984, when the creep and tilt events began.

On-Line Seismic Processing

9970-02940

Rex Allen
Branch of Seismology
U.S. Geological Survey
345 Middlefield Road, MS 77
Menlo Park, California 94025
(415) 323-8111 ext 2240

Investigations and Results

The Mark I real-time processors (RTP's) at Menlo Park and at the several other sites using them continue to work with little trouble. No substantial changes have been made recently.

Development of the Mark II version of the RTP using the 68010 processor has been much slower than anticipated. The FORTRAN picker is running satisfactorily, but integration with the associator developed into a major undertaking. We believe that the problems of the last few months have now been resolved and I expect to have the first of the two planned succesive prototypes in operation before July 1. (1985).

Digital Signal Processing of Seismic Data

9930-02101

W. H. Bakun
Branch of Seismology
U.S. Geological Survey
345 Middlefield Road, MS-977
Menlo Park, California 94025
(415) 323-8111, Ext. 2777

INVESTIGATIONS

Continuation of studies of seismic activity at Parkfield, California and on the Calaveras fault east of San Jose, California. Evaluation of size scales (magnitude, seismic moment) used in the Peoples Republic of China.

RESULTS

See REPORTS.

REPORTS

Bakun, W. H. and W. B. Joyner, 1984, The M_L Scale in Central California, Bulletin of the Seismological Society of America, v. 74, no. 5, pp. 1827-1843.

Bakun, W. H., 1984, Magnitudes and Moments of Duration, Bulletin of the Seismological Society of America, v. 74, no. 6, pp. 2335-2356.

Scofield, C. P., W. H. Bakun, and A. G. Lindh, 1985, The 1982 New Idria, California, earthquake sequence, in Rymer, M. J. and W. L. Ellsworth, eds., Mechanics of the May 2, 1983 Coalinga earthquake: U.S. Geological Survey Open-File Report 85-44, p. 403-429.

Bakun, W. H., and A. G. Lindh, 1985, The Parkfield, California, earthquake prediction experiment, Science, in press.

Bakun, W. H., Li, Y. Z., F. G. Fischer, and Jin, Y. F., 1985, Magnitude and seismic moment scales in western Yunnan, Peoples Republic of China, Seismological Society of America Bulletin (submitted).

Bakun, W. H., R. S. Cockerham, and G. C. P. King, 1985, Seismic slip on the Calaveras fault, California, Fifth Ewing Symposium on Earthquake Mechanics (abs.), in press.

PARKFIELD TWO-COLOR LASER STRAIN MEASUREMENTS

9960-02943

Robert Burford
Branch of Tectonophysics
U.S. Geological Survey
345 Middlefield Road, MS/977
Menlo Park, California 94025
(415) 323-8111, ext. 2574

and

Larry Slater
CIRES
University of Colorado
Boulder, Colorado 80309
(303) 492-8028

Investigations

The CIRES two-color laser ranging system has been operated at the Parkfield CAR HILL site to obtain frequent distance readings to reflector sites designated in Figure 1. Additional measurements were made occasionally to sites without permanent reflectors as well as to reference marks at the permanent sites. The effects of removing the blue laser and replacing it (after overhaul) with much higher output were tested using neutral filters to knock the power back down to a pre-overhaul value. No systematic shifts in ranges were found as a consequence of the controlled shifts in the intensity of the blue source.

Results

Currently the line-length data are recorded by hand from computer-tape printout generated at CAR HILL as the readings are conducted. Copies of data sheets are mailed weekly to Menlo Park and to Boulder, Colorado. The Menlo Park data are entered on the VAX computer into permanent files identified by abbreviated reflector-station names. Average length values composed of less than 20 ten-second samples or with standard deviations of greater than +/- 1.5 mm are not included in final plots or as input for strain analysis. Time-series displacement plots and strain results are obtained by running various programs using the files containing filtered data.

Plots of filtered data obtained during October 1984 through April 1985 for the 11 lines to permanent reflector sites are shown in Figure 2. Unfortunately, the reflector at MID

was destroyed by vandals sometime after mid-December, resulting in loss of zero reference (MID2=MID after unknown offset for new reflector). Typical errors (standard deviations) for individual data points vary between about +/-0.55 mm (4.1-km range) about +/-0.76 mm (6.2-km range). However, uncertainties in determinations of various strain trends in the data, depending on the selection of sampling period, range between about +/-0.4 and +/-0.7 microstrain/yr (1 standard deviation).

Deterioration in the system possibly due to corrosion of electrical contacts, has caused obvious instability in the range values since about mid-February. The problem is intermittent: it generally shows up on several lines as distance readings 2 to 5 mm higher than the trend. When the blue laser failed early in March (removed on 3/7 and replaced on 3/17), it was suspected that the instability had been caused by noise introduced by deterioration of the laser. However, the intermittent range errors recently returned with higher amplitudes. It is uncertain at present whether or not the problem has been eliminated by recent repairs. All entries from February 13 until replacement of the blue laser on March 17 have been removed from the filtered data files, along with high readings during April thought to be due to system instability. Length values for the lines to CREEK, HOG, MELVILLE, and TABLE show good agreement between early February and late March after replacement of the blue laser, which argues against the possibility that the laser change might have introduced a systematic offset. In contrast to apparent stability on the nearly E-W lines during the downtime, most of the N-S-trending lines show a contractional offset after the February-March gap. However, rapid contraction on the line to PITT between November and early April is due to tilt of the reflector pier. A replacement site is being considered.

From October-November 1984 through January 1985, E-W trending lines were extending (HOG, LANG, MELVILLE, and TABLE), while N-S trending lines were either stable or were extending at very low rates (BARE, CAN, CREEK, MASON, MID, and MIDE). These trends reversed during early February, indicating onset of areal contraction (negative dilatation). The details for onset of negative dilatation are obscured by gaps due to system noise and down-time in February and March, but the onset of rapid contraction along several lines in late March suggests that development of strong negative dilatation may have been delayed until that time.

A preliminary analysis of the length-change data indicates that shallow slip occurred at a high rate on the main fault NW of the network area during the summer months (about 1 cm R.L., August-October). Minor steps in the down-trend for the line CAR to MID-E during August and September correspond to the times of local creep events recorded either at XDR1 (0.8 km SE of CAR) or at XMM1 (5.6 km NW of MID-E). A uniform-strain approximation for deformation in the network area using the limited data available for this same period indicates a maximum extension rate of about +2 microstrain/yr in the direction N66E. Rates of extension normal to the fault and areal dilatation were about +1.7+/-0.5 and about +0.9+/-1.0 microstrain/yr, respectively. However, the strain pattern changed during early November such that from that time through January 1985, the rate of areal dilatation was increased to +2.2+/-0.5 microstrain/yr. Extension normal to the fault has accumulated at a nearly constant rate throughout the record through January 1985, but extension parallel to the fault reversed during October-November from -0.8+/-0.4 to +0.5+/-0.3 microstrain/yr. As of about February 1, 1985, the dilatational trend was replaced by areal contraction (Figure 2). This pattern may turn out to be related to a seasonal influence in the tectonic process.

Right-lateral slip at about 4 mm/yr on the auxiliary rupture zone 1.2 km SW of CAR Observatory may account for part of the apparent block deformation on the west side of the main fault.

Figure Captions

Figure 1. Map of the Parkfield 2-color laser network showing traces of the 1966 surface breaks within the San Andreas fault zone. Solid rays designate lines to permanent reflectors that are monitored frequently. Dotted rays designate lines to portable reflector sites that will be measured about once a month. Underlined site names indicate the 12 lines measured during 1984-85 (11 permanent sites plus BREAK). Distances from CAR to BREAK and all longer lines also were measured on October 24, 1984 with the U.S.G.S. Geodolite.

Figure 2. Line-lengths from CAR to the 11 permanent reflector sites as repeatedly resolved by the 2-color laser system during October 1984 through April 1985 (filtered data). Variations in resolved distances and error bars are plotted in millimeters.

PARKFIELD 2-COLOR NETWORK
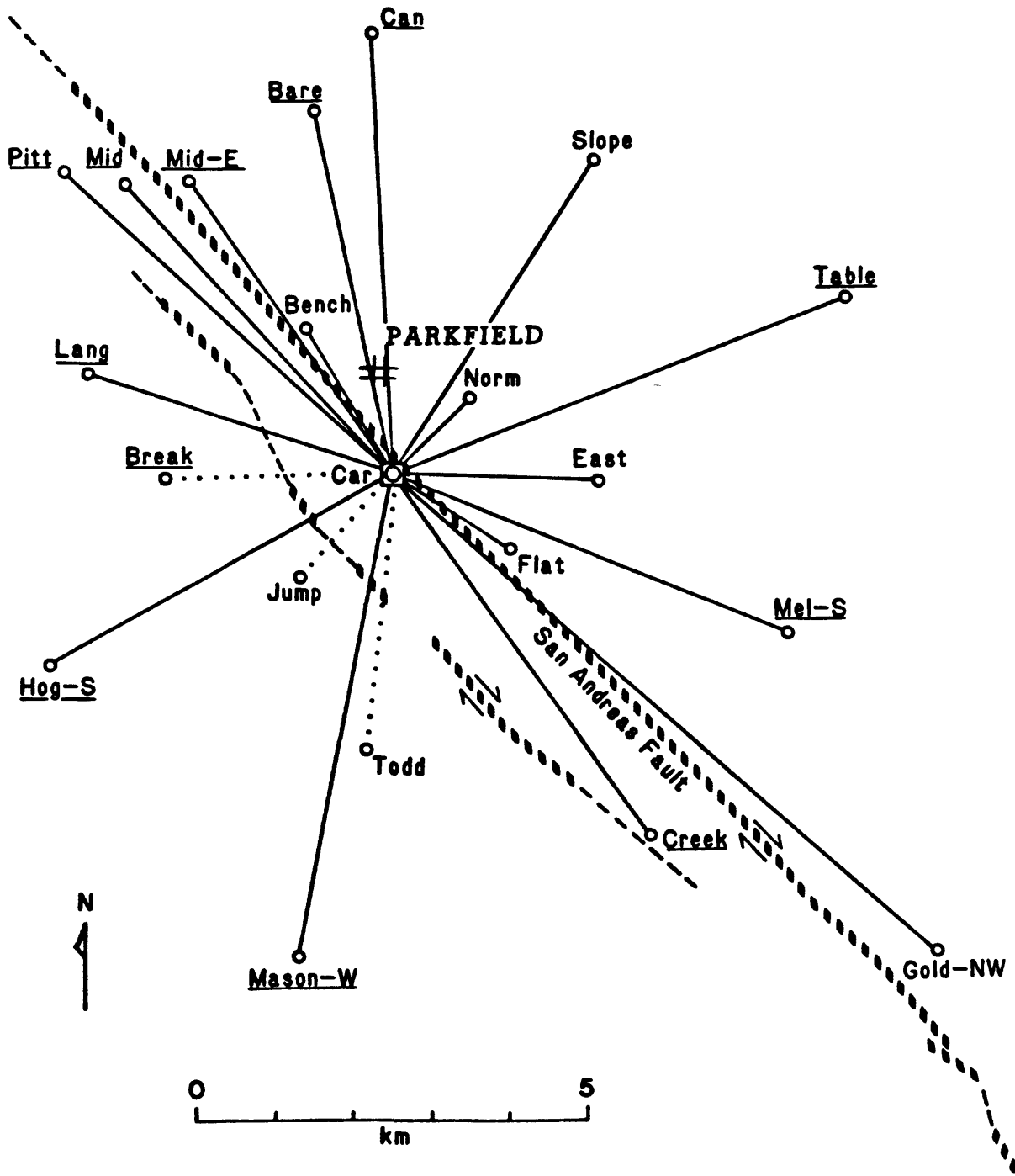
Figure 1.
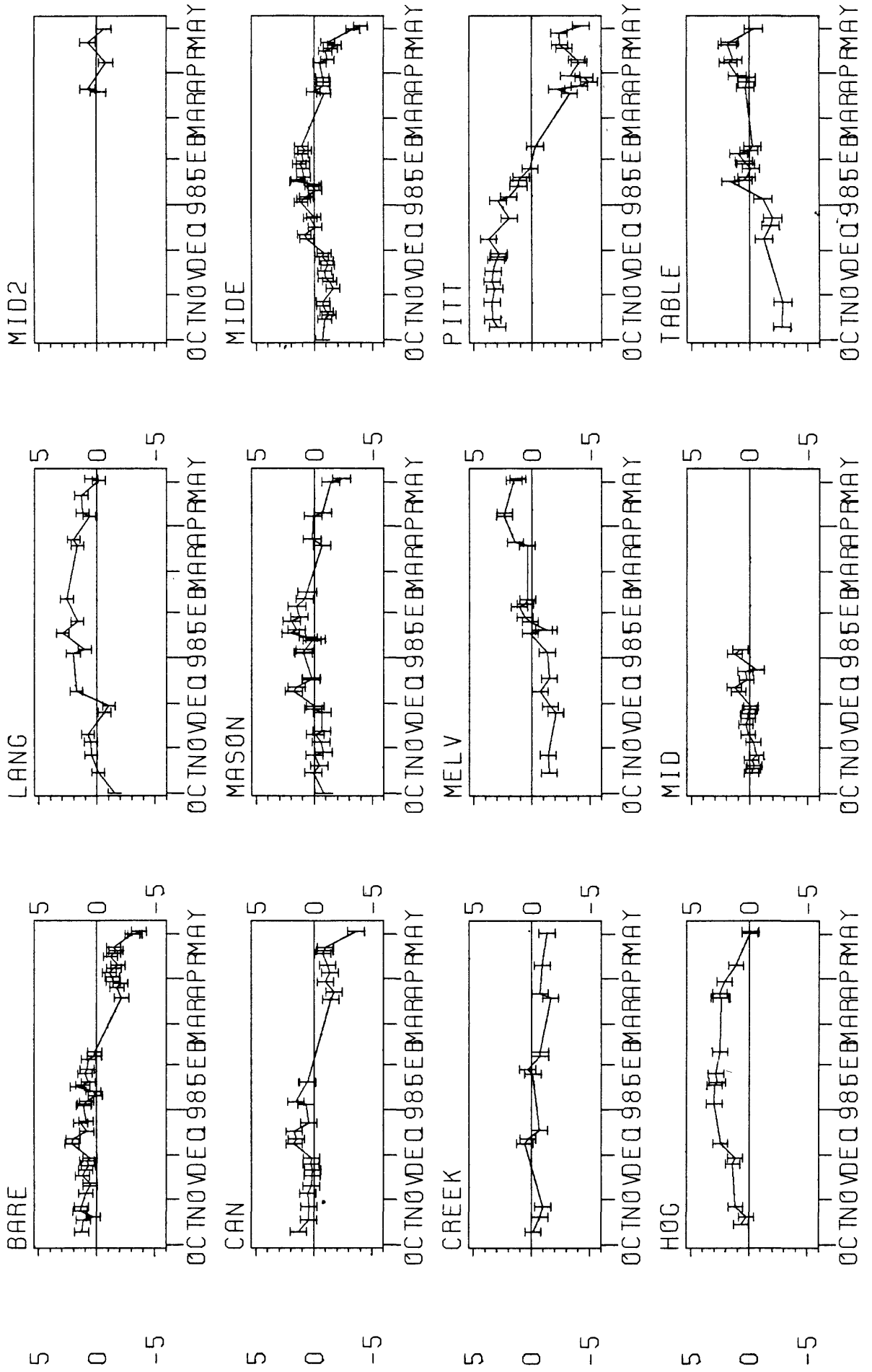
Figure 2.

Investigation of Radon and Helium as Possible
Fluid-phase Precursors to Earthquakes

14-08-0001-22003

Y. Chung
Scripps Institution of Oceanography
University of California, San Diego
La Jolla, California   92093
(619) 452-6621

Investigations:

1. Monitoring radon, helium, and other geochemical parameters in a network of thermal springs and wells along the San Andreas, San Jacinto, and Elsinore faults in southern California for possible percursory effects associated with earthquakes.

2. A general study of the relationships between these components, their origin, and variations which may be due to changes in ambient conditions, seasonal effects and meteorological factors.

3. Continuous radon monitoring at network sites with field-installed Continuous Radon Monitors (CRM's) for possible short-term anomalies that may be precursory to earthquakes.

4. Comparison study of long-term variations between the CRM and the discrete Rn data. Partition of radon between the gas and water phases.

5. Joint U.S.-Chinese geochemical studies with scientists in the Institute of Geology, State Seismological Bureau (SSB) for earthquake prediction in both countries.

Results:

1. Discrete sampling for radon and helium measurements at our southern California network sites was resumed at monthly intervals in January 1985, after a brief gap in late 1984. No major earthquakes occurred in the network region during the past six months; radon and helium at most of the sites showed no anomalous changes. New data observed at the Arrowhead site along the San Andreas fault near San Bernardino showed a local peak in January and February 1985. This is a continuation of the large-amplitude fluctuations which began in mid-1983.

2. Three of our network sites are being monitored for radon variations with the USC Continuous Radon Monitors (CRM's). At Arrowhead, the radon level observed after December 1984 has been fairly constant at a level much higher than before due to the deployment of another CRM unit which has higher counting efficiency. At Murrieta along the Elsinore fault, the 1985 data indicate a monotonic decrease toward a minimum in March before increasing probably due to extensive plumbing activities conducted by the owner during February and March. During this period, large hourly variations were often recorded, indicating high sensitivity of the CRM in detecting actual radon changes. At Hot Mineral Well near Bombay Beach by the Salton Sea, a CRM unit was installed in January 1985 after a long period of litigation. The main well which is an

artesian with a large flow rate at high temperature ($\sim 80°C$) is now used for both CRM monitoring as well as discrete sampling. The CRM was initially set up for monitoring both the gas-phase and dissolved radon using a PVC container which allows a continuous flow of the well water into its bottom and out of its top. The stripping of dissolved radon and collection of both dissolved and gas-phase radon were handled by a flushing probe which connects to an air circulation pump and the CRM. Large variations were observed, reflecting changes of flow rates of both the water and air circulation. High air circulation rate reduced radon level due to "diluting" effect. The radon concentration was diluted by the air as its carrier gas. Low water flow rate also reduced the radon level. Since abundant gas bubbles were observed, the flushing probe was removed recently and replaced by a glass funnel to collect only the gas-phase radon for monitoring. Preliminary results indicate that the radon level is now higher and more stable than that observed earlier using the probe.

3. Since all the CRM monitoring data are obtained on the gas-phase radon while all the discrete measurements are on dissolved radon, direct comparison of their temporal variations is difficult. Radon concentration in the gas-phase as determined from the CRM data is about 20 to 25 times that in the water-phase. The variation of this partition ratio is comparable to the discrete radon variation. In general the long-term CRM Rn variations are smaller than the discrete Rn variations.

4. Our joint U.S.-Chinese program is being supported by NSF. The areas designated or proposed for joint studies include part of our southern California network and Long Valley in the U.S., and Peking and S.W. Yunnan in China. Two scientists from the Institute of Geology, SSB , Peking visted our laboratory and joined our field work for one month during September and October 1984. Our field work in the designated areas in China will be carried out in May or June 1985.

Seismic Analysis of Large Earthquakes and
Special Sequences in Northern California

9930-03972

Robert S. Cockerham
Branch of Seismology
U.S. Geological Survey
345 Middlefield Road, MS 977
Menlo Park, California   94025
(415) 323-8111, ext. 2963

INVESTIGATIONS

1. Mammoth Lakes region, eastern California - investigation of the spatial
    and temporal seismicity patterns in Long Valley caldera and the Sierra
    Nevada Mountains south of the caldera.

2. Long Valley caldera - investigation on the origin of intracaldera seismic
    swarms.

3. Coalinga earthquake - investigations of (1) the regional seismic
    background prior to the M6.7 Coalinga earthquake of May 2, 1983, and
    (2) aftershock distributions and focal mechanisms.

4. Morgan Hill earthquake - investigation of the aftershocks resulting from
    the M6.1 earthquake of April 24, 1984.

RESULTS

1. A detailed analysis of approximately 2,000 well-located hypocenters within
    the Sierran block south of Long Valley caldera shows that two of the NNE
    lineations (Figure 1) are controlled by fracture systems within the Round
    Valley pluton at depths from 6 to 18 km. The third NNE lineation is, for
    the most part, an artifact of a two-dimensional projection of hypocenters
    distributed along NNW-striking planes that dip to the NE. The earthquakes
    along these NNW-striking planes are constrained to the Mt. Morrison root
    pendent. The earthquakes southwest of the Laurel-Convict fault are
    occurring along the contact between the Round Valley pluton and the roof
    pendent (Figure 1). High pressure fluids being forced along these
    contacts and fracture systems are, for the most part, believed to be
    causing the earthquakes.

2. The vast majority of earthquakes within Long Valley caldera tend to occur
    in seismic swarms of large numbers of earthquakes occurring within a small
    area over a limited time period. The caldera swarms, of which there are
    three types (S, L, and M), occur within four zones within the caldera
    (Figure 2): SW1 and SW2 in the south moat, SW3 - Hot Creek and Whitmore
    Hot Springs areas, and SW4 - Mammoth Mountain. Three features common to
    all swarms are (1) no low-frequency earthquakes, (2) no systematic
    shallowing with time of hypocenters during a swarm, and (3) the largest
    magnitude event is usually near the lower depth limit of the swarm.

3a. Seismicity in the central and southern Coast Ranges for the 11 years prior to the 1983 Coalinga earthquake is examined along with focal mechanisms of selected large recent earthquakes in the region. A preliminary model is proposed for the process that generates reverse and thrust fault earthquakes along east and west flanks of the Coast Ranges. The cause of such earthquakes appears to be a component of convergent displacement across the San Andreas transform system in the southern Coast Ranges. The earthquakes with reverse and thrust focal mechanisms are found in regions with a distinctive cluster pattern of seismicity, along the flanks of the southern Coast Ranges, that are separated from the San Andreas fault by regions of relative quiescence. The reverse and thrust fault earthquakes occur where detachment zones that lie within a ductile lower crust beneath the center of the transform system pass upward into the brittle crust along its margins. Convergence of the transform system, together with regions of unusually strong materials in the brittle upper crust flanking the San Andreas fault southeast of Cholame, may play an important role in producing such large earthquakes in that region.

3b. Analysis of the Coalinga earthquake sequence based on the Allen/Ellis RTP (real-time processor) automatic P-phase onset time and event duration measurements provides hypocentral and magnitude determinations for several thousand events from May 2, 1983, through September 30, 1983. Maps and cross sections of the nearly 800 best-located M2.5+ events show the spatial distribution and temporal evolution of the sequence and provide some clues to the nature of the faulting that produced the sequence. Focal mechanism studies of the main shock and 10 of its largest aftershocks offer two choices for the main shock fault, a thrust fault striking N 53°W and dipping 23°SW or a high-angle reverse fault striking N 53°W and dipping 67°NE, and show that the predominant focal mechanism of the larger aftershocks is reverse faulting. These materials, however, are insufficient for making a clear choice between the two possibilities for the main shock fault.

More detailed studies of the main shock and more than 100 of its M3.2 and larger aftershocks, from records played back from magnetic tape, further clarify the sequence. Maximum pressure axis orientations deduced from first-motion plots for these earthquakes vary systematically from one part of the aftershock region to another. Stereo-pair plots of the fault planes of the aftershocks permit several intersecting fault surfaces to be mapped out. The sum of the evidence strongly favors the thrust fault solution for the main shock.

4. Aftershocks (Figure 3a) of the Morgan Hill earthquake clearly outline a near-vertical fault surface that is parallel to but much simpler in structure than the mapping strands of the Calaveras Fault in the aftershock region. A central quiet zone in the aftershock pattern on the inferred fault surface marks out adjacent 3 km x 10 km and 5 km x 13 km patches that are believed to be the rupture region of the main shock (Figure 3b). The transition between these patches coincides with a 6° change in strike of the inferred fault surface. A prominent group of aftershocks southwest of the principal band of aftershocks appears to be bounded by the Calaveras Fault on the northeast and by the Silver Creek (or related, reverse) Fault below and on the southwest. These aftershocks suggest that the Morgan Hill earthquake was accompanied by, or stimulated,

movement on one or more nearby reverse faults. For aftershocks SW and NE of the Calaveras Fault, thrust faulting on NW-striking planes and right-lateral strike-slip faulting on N-striking planes, respectively, predominate. Aftershocks located on the Calaveras Fault exhibit right-lateral strike-slip movement on a NW-striking fault plane.

REPORTS

Cockerham, R. S. and Eaton, J. P., 1984, The April 24, 1984 Morgan Hill earthquake and its aftershocks: April 24 through September 30, 1984, in J. H. Bennett and R. W. Sherburne (eds.), The 1984 Morgan Hill, California Earthquake, Calif. Dept. Conservation Div. Mines Geology, Spec. Pub. 68, 215-236.

Cockerham, R. S. and Pitt, A. M., Seismic activity in Long Valley caldera, eastern California, U.S.A.: June 1982 through July 1984, in D. P. Hill, R. A. Bailey, and A. S. Ryall (eds.), Active Tectonic and Magmatic Processes beneath Long Valley caldera, eastern California, U.S. Geol. Survey Open-file Report 84-939, 493-526.

Eaton, J. P., 1985, Regional seismic background of the May 2, 1983 Coalinga earthquake, in M. J. Rymer and W. L. Ellsworth (eds.), Mechanics of the May 2, 1983 Coalinga earthquake, U.S. Geol. Survey Open-file Report 85-44, 44-60.

Eaton, J. P., 1985, The May 2, 1983 Coalinga earthquake and its aftershocks: A detailed study of the hypocenter distribution and of the focal mechanisms of the larger aftershocks, in M. J. Rymer and W. L. Ellsworth (eds.), Mechanics of the May 2, 1983 Coalinga earthquake, U.S. Geol. Survey Open-file Report 85-44, 132-201.
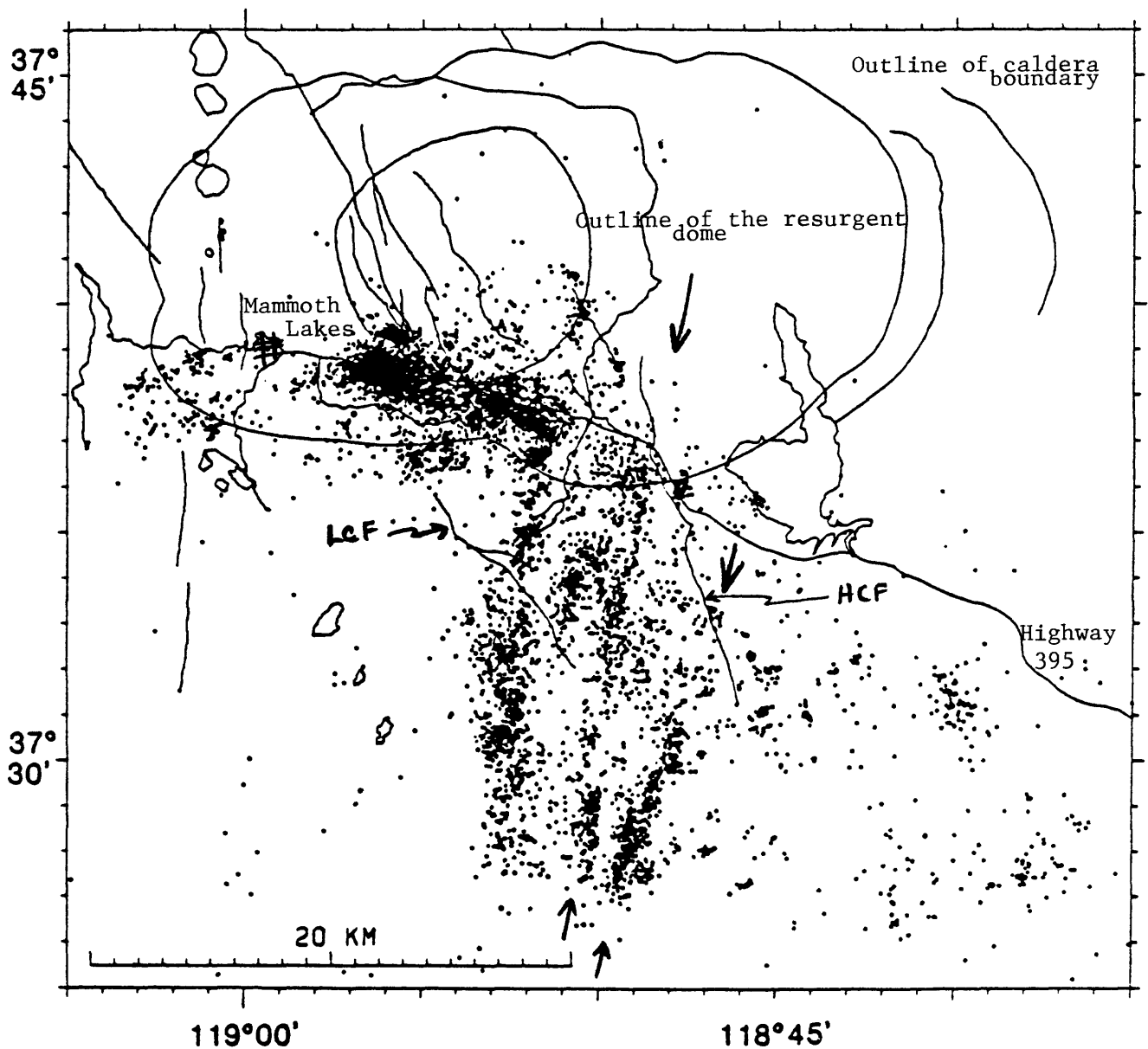
Figure 1. Map showing the locations of about 10,000 earthquakes in the Mammoth Lakes region from June 1982 through July 1984. LCF = Laurel-Convict fault. HCF = Hilton Creek fault. Arrows point to NNE lineations discussed in text.
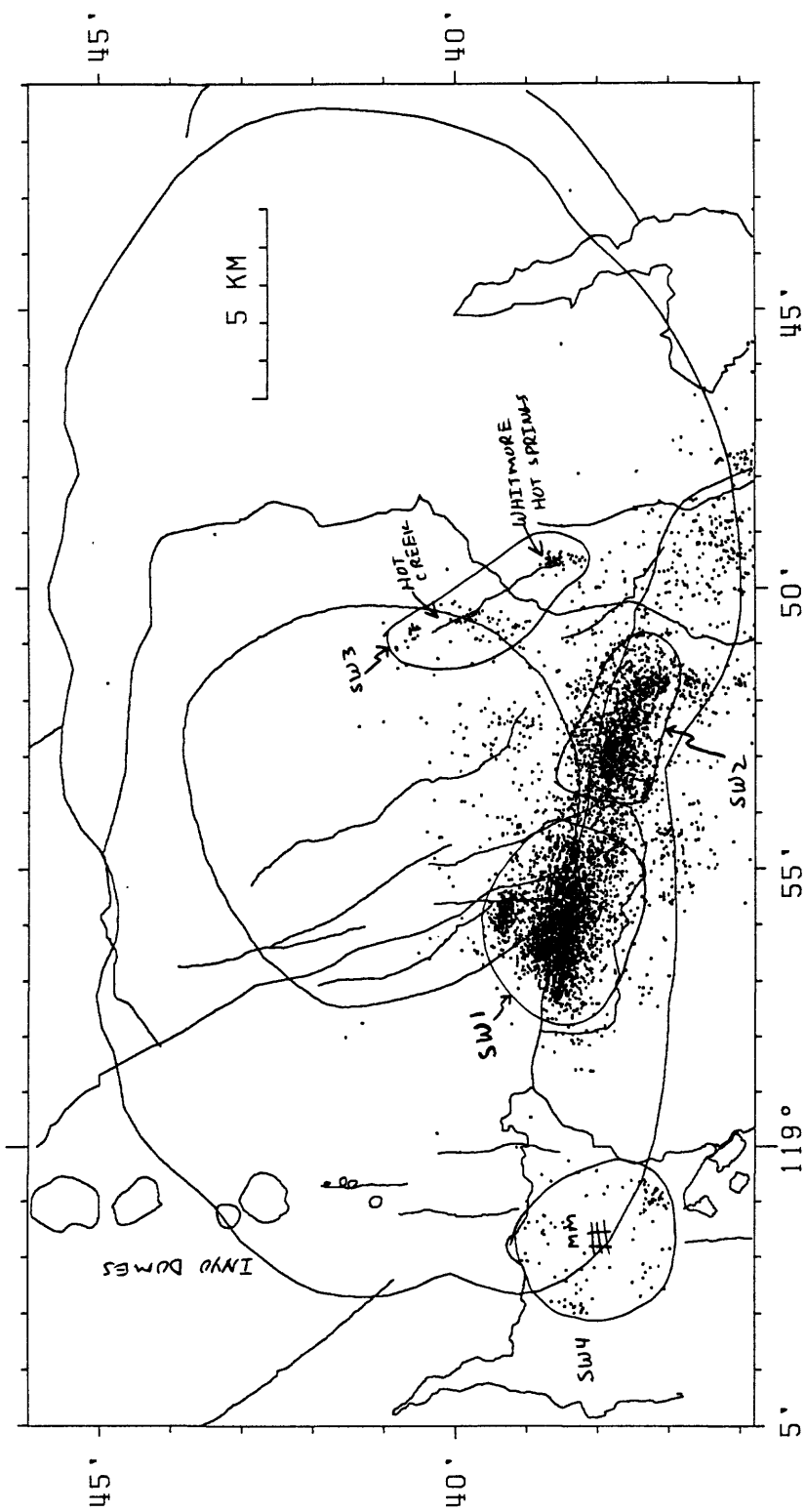
Figure 2. Map showing the epicentral locations of about 7500 earthquakes within Long Valley caldera from June 1982 through December 1984. The outlined areas are the swarm areas referred to in the text (SW1, SW2,SW3, SW4). Geographic features and physiographic features are the same as in Figure 1.
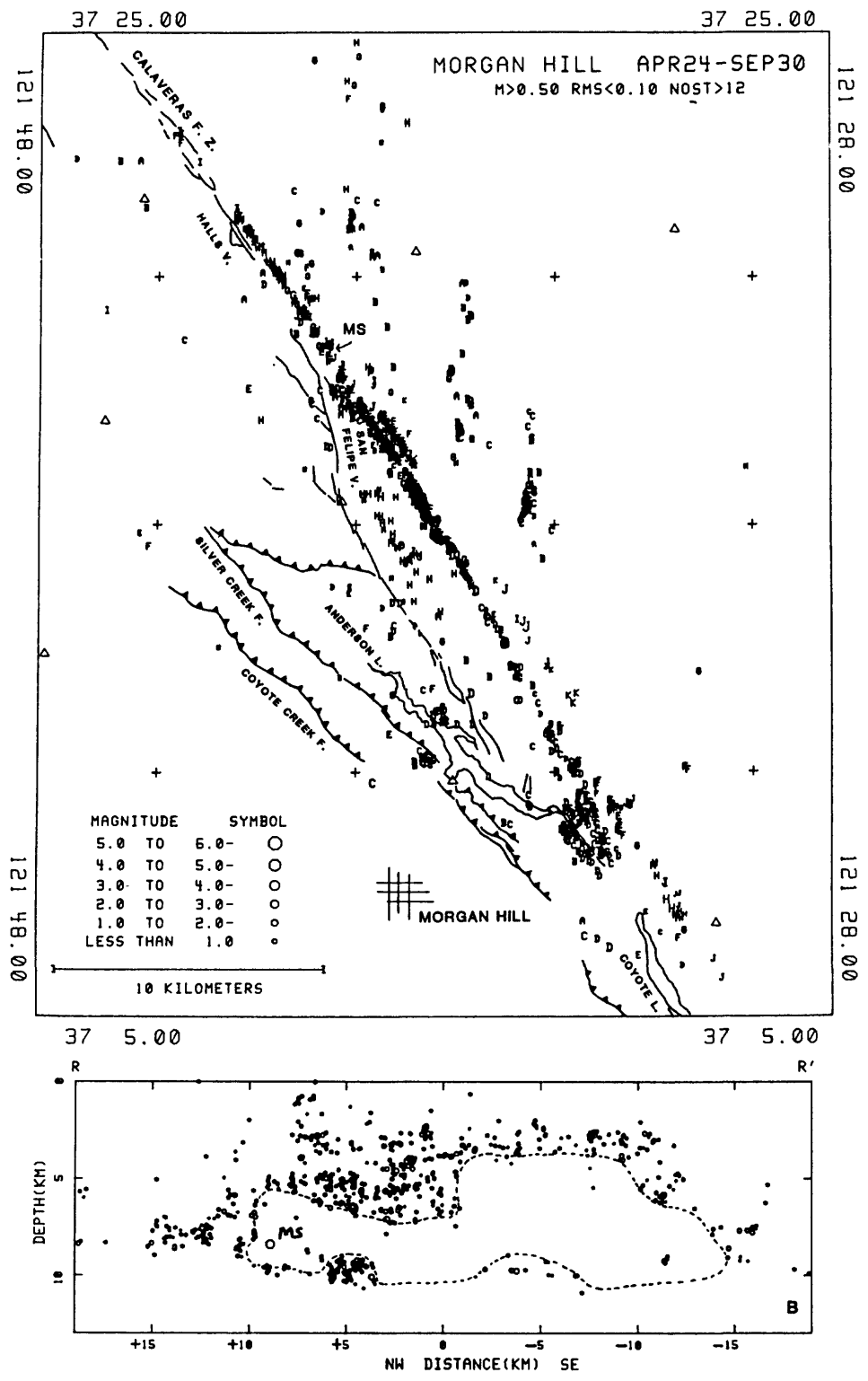
Figure 3. (A) Map of epicenters of aftershocks of the Morgan Hill earthquake of April 24, 1984 through September 30, 1984. Fault traces are from Herd (1982). (B) Longitudinal section of the aftershock distribution within a box 1.3 km NE and 0.8 km SW from a line R-R' (NW to SE) with the origin at 37° 14.39' N, 121° 37.67' W. MS = Morgan Hill main shock location.

Theodolite Measurements of Creep Rates
on San Francisco Bay Region Faults

Contract No. 14-08-0001-21988

Jon S. Galehouse
San Francisco State University
San Francisco, CA 94132
(415) 469-1204

We began measuring creep rates on San Francisco Bay region faults
in September 1979. Amount of slip is determined by noting changes in
angles between sets of measurements taken across a fault at different
times. This triangulation method uses a theodolite set up over a fixed
point used as an instrument station on one side of a fault, a traverse
target set up over another fixed point used as an orientation station
on the same side of the fault as the theodolite, and a second traverse
target set up over a fixed point on the opposite side of the fault.
The theodolite is used to measure the angle formed by the three fixed
points to the nearest tenth of a second. Each day that a measurement
set is done, the angle is measured 12 times and the average determined.
The amount of slip between measurements can be calculated trigonometri-
cally using the change in average angle.

We presently have theodolite measurement sites at 20 localities
on faults in the Bay region. Most of the distances between our fixed
points on opposite sides of the various faults range from 75-215
meters; consequently, we can monitor a much wider slip zone than can
be done using standard creepmeters. The precision of our measurement
method is such that we can detect with confidence any movement more
than a millimeter or two between successive measurement days. We re-
measure most of our sites about once every two months.

The following is a brief summary of our results thus far:

Seal Cove-San Gregorio fault - We began our measurements on the Seal Cove
fault (Site 7) in Princeton, San Mateo County, in November 1979. For the
next 5.3 years, the Seal Cove fault showed net movement at a rate of about
one millimeter per year in a right-lateral sense. However, details re-
garding the tectonic slip are difficult to ascertain because of seasonal
effects, often involving apparent left-lateral slip that tends to occur
toward the end of a calendar year.

Various logistic problems have occurred at our Site 8 across the San
Gregorio fault near Pescadero in San Mateo County. At the present time
we are unable to determine whether or not the fault is creeping.

San Andreas fault - In the five years since March 1980 when we began our
measurements across the San Andreas fault in South San Francisco (Site
10), virtually no net slip has occurred. This indicates that the San
Andreas fault is locked in the San Francisco area. We recently (February
1985) reestablished our Site 14 in Marin County, this time at the Point

16

Healdsburg-Rodgers Cr.Fault

15

West Napa Fault

20

Green Valley Fault

14

17

11

9 9A

Antioch Fault

5 3

Concord
Fault

38°00'

Hayward Fault

19

13

12

2

1

Calaveras
Fault

10

Seal Cove
Fault

7

37°30'

San Andreas Fault

8

San Gregorio
Fault

0   10   20   30

KILOMETERS

San Francisco State University

Theodolite Measurement Sites

37°00'

6
4

122°30'

122°00'
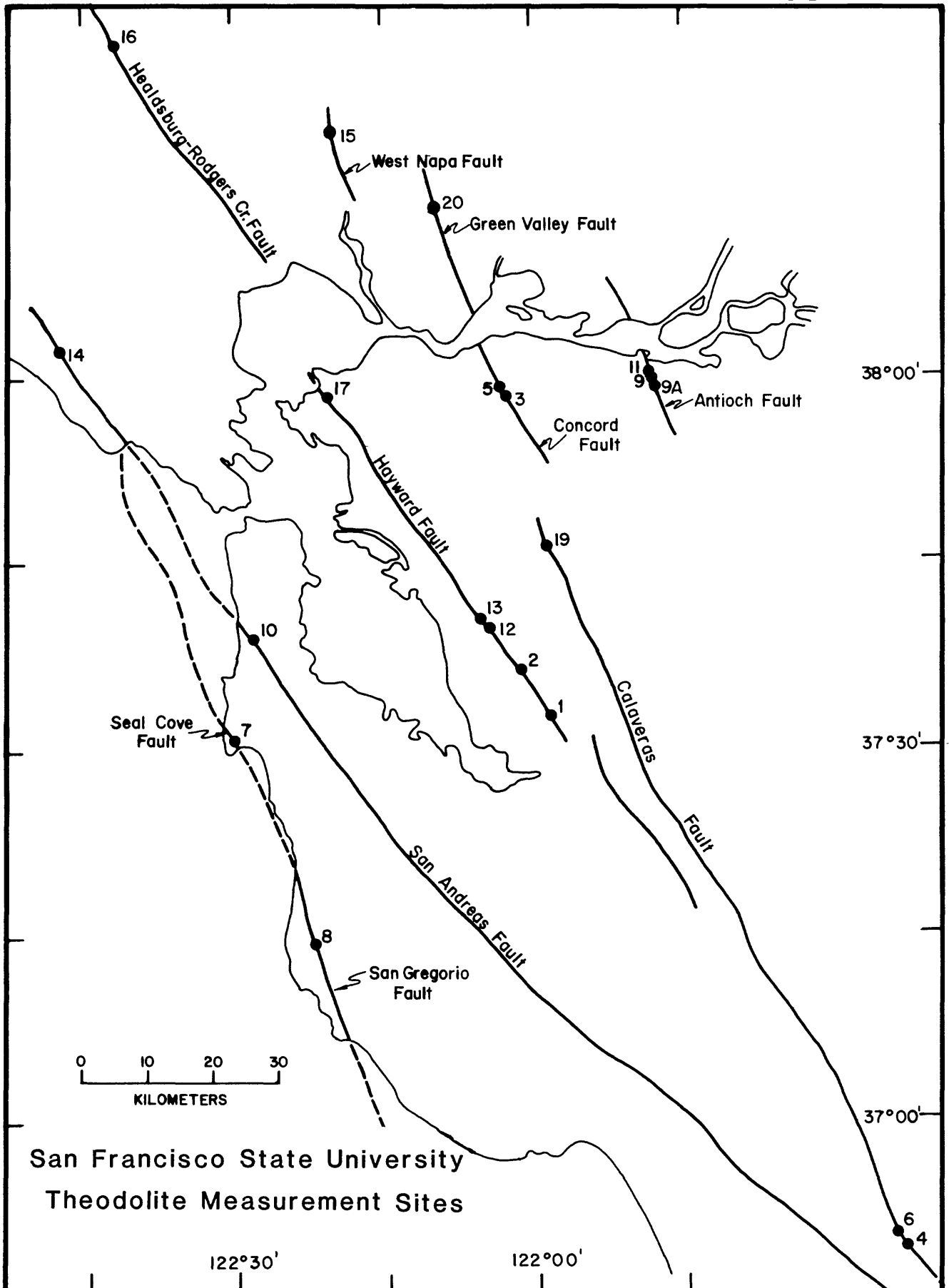
Reyes National Seashore Headquarters. Preliminary results after only one remeasurement indicate no net slip. Our Site 18 (not shown on the location map) in the Point Arena area has averaged about one millimeter per year of right-lateral slip in the four years from January 1981 to January 1985.

Rodgers Creek fault - In the 4.5 years from August 1980 to February 1985, our Site 16 on the Rodgers Creek fault in Santa Rosa has had virtually no net slip. However, our results show large variations in the amounts and directions of movement from one measurement day to another. These are probably due to seasonal and/or gravity-controlled mass movement effects, not tectonic slip.

West Napa fault - In the 4.6 years from July 1980 to February 1985, our Site 15 on the West Napa fault in the City of Napa has shown very little net slip. Similarly to our results for the Rodgers Creek fault, however, large variations up to nearly a centimeter have occurred in both a right-lateral and a left-lateral sense between measurement days. The magnitude of these nontectonic effects is obscuring any tectonic slip that may be occurring.

Green Valley fault - We recently (mid-June 1984) established a new site (Site 20) on the Green Valley fault north of Suisun Bay. Preliminary results as of mid-April 1985 indicate a few millimeters of right-lateral slip.

Hayward fault - We began our measurements on the Hayward fault in late September 1979 in Fremont (Site 1) and Union City (Site 2) During the next 5.6 years, the average rate of right-lateral slip has been about 4.6 millimeters per year in Fremont and about 4.4 millimeters per year in Union City.

We began measuring two sites within the City of Hayward in June 1980. In the 4.8 years since then, the average rate of right-lateral movement has been about 4.7 (Site 12) and about 4.9 (Site 13) millimeters per year.

We began measurements in San Pablo (Site 17) near the northwestern end of the Hayward fault in August 1980. For the past 4.7 years, the average rate of movement has been about 4.5 millimeters per year in a right-lateral sense. However, superposed on this overall slip rate are changes between some measurement days of up to nearly a centimeter in either a right-lateral or a left-lateral sense. Right-lateral slip tends to be measured during the first half of a calendar year and left-lateral during the second half.

Our theodolite triangulation results for the Hayward fault are quite comparable to those determined by U.S.G.S. creepmeters. The Hayward fault appears to be creeping at a rate of about four and one-half millimeters per year, making it the second fastest creeping fault in the San Francisco Bay region. Only the Calaveras fault in the Hollister area is moving faster.

Calaveras fault - We have three measurement sites across the Calaveras fault and the nature and amount of movement are different at all three. We began monitoring our Site 4 within the City of Hollister in September 1979. Slip along this segment of the Calaveras fault is quite episodic, with times of relatively rapid right-lateral movement alternating with times of little net movement. For the past 5.5 years, the fault moved at a rate of about 8 millimeters per year in a right-lateral sense.

At our Site 6 across the Calaveras fault on Wright Road just 2.3 kilometers northwest of our site within the City of Hollister, the slip is much more steady than episodic. In the 5.5 years from October 1979, the Calaveras fault at this site has been moving at a rate of about 14 millimeters per year in a right-lateral sense, the fastest rate of movement of any of our sites in the San Francisco Bay region.

U.S.G.S. creepmeter results in the Hollister area are quite similar to our theodolite results. Creepmeters also show a faster rate of movement at sites on the Calaveras fault just north of Hollister than at sites within the City of Hollister itself.

The rate of movement is much lower at our Site 19 in San Ramon, near the northwesterly terminus of the Calaveras fault. Only about one millimeter per year of right-lateral slip has occurred during the past 4.2 years.

The epicenter of the 24 April 1984 Morgan Hill earthquake occurred on the Calaveras fault between our Hollister area sites which are southeast of the epicenter and our San Ramon site which is northwest of it. Four papers that we published regarding our theodolite measurements and observations of surface displacement related to the earthquake are listed at the end of this summary. No unusual movement appears to have occurred prior to the Morgan Hill earthquake.

Concord fault - We began our measurements at Site 3 and Site 5 on the Concord fault in the City of Concord in September 1979. Both sites showed about a centimeter of right-lateral slip during October and November 1979, perhaps the greatest amount of movement in a short period of time on this fault in the past two decades. Following this rapid phase of movement by about two months were the late January 1980 Livermore area moderate earthquakes on the nearby Grenville fault.

After the relatively rapid slip on the Concord fault in late 1979, both sites showed relatively slow slip for the next four and one-half years at a rate of about one millimeter per year right-lateral.

However, in late Spring-early Summer 1984, both sites again moved relatively rapidly, slipping about seven millimeters in a right-lateral sense in a few months. The rate has again slowed since late August 1984 (through mid-March 1985).

The overall rate of movement on the Concord fault (combining the two periods of relatively rapid movement with those of slower movement) is about 3.7 millimeters per year (Site 3) and 3.9 millimeters per year (Site 5) of

right-lateral slip in the past 5.5 years. Only the Calaveras fault near Hollister and the Hayward fault are creeping faster in the Bay region.

Antioch fault - We began our measurements at the more southeasterly of two original sites on the Antioch fault (Site 9) in the City of Antioch in January 1980. During the next 27 months, we measured a net right-lateral displacement of nearly two centimeters. However, large changes in both a right-lateral and a left-lateral sense occurred between measurement days. Three times left-lateral displacement occurred toward the end of one calendar year and/or beginning of the next. We abandoned this site in April 1982 because of logistic problems and relocated it (Site 9A) just southeast of the City of Antioch in November 1982. In the 2.2 years until February 1985, the fault at this new site has had net movement in a right-lateral sense at a rate of about 1.6 millimeters per year.

The more northwesterly of our original sites on the Antioch fault (Site 11) is located where the fault zone appears to be less specifically delineated. In the 4.8 years from May 1980 to February 1985, we have measured an average of about 1.5 millimeters per year of left-lateral slip. Much subsidence and mass movement creep appear to be occurring both inside and outside the Antioch fault zone and it is probable that these nontectonic movements have influenced our theodolite results. However, a recent (1984) trench across the Antioch fault within the City of Antioch showed soil horizons also offset in an apparent left-lateral sense.

Reports and Publications

Galehouse, J.S., 1984, Theodolite measurements following the 24 April 1984 Morgan Hill earthquake, in U.S. Geol Survey Open-File Report 84-498, pp. 72-75.

Galehouse, J.S., and Brown, B.D., 1984, Southeastern limit of surface displacement on the Calaveras fault associated with the 24 April 1984 Morgan Hill earthquake, in U.S. Geol. Survey Open-File Report 84-498, pp. 85-91.

Galehouse, J.S., 1985, Theodolite Measurements: in Geodetic Observations section of "The Morgan Hill, California Earthquake of April 24, 1984"; U.S. Geol. Survey Bull. 1639, in press.

Galehouse, J.S. and Brown, B.D., 1985, Surface Displacement Near Hollister: in Geological Observations section of "The Morgan Hill, California Earthquake of April 24, 1984"; U.S. Geol. Survey Bull. 1639, in press.

DEEP BOREHOLE PLANE STRAIN MONITORING

14-08-0001-221228

Michael T. Gladwin
Department of Physics
University of Queensland
St. Lucia
Australia 4067.

FIELD STUDIES

An instrument capable of unattended deep borehole measurement of vector plane strain to 0.3 nanostrain has been developed and deployed at two sites in California. Response is from DC to 10 Hz on any single channel, dynamic range is approximately 10^{-4} in strain and total linearity better than 0.004%. The instrument is particularly relevant in California where shear strains dominate deformations, and provides a new dimension in continuous borehole deformation monitoring.

Normally, the instrument consists of seven independent modules of length 170 mm. Three measure strain in a plane perpendicular to the axis of the instrument. A further two measure tilt from the axis of the instrument, one component measures instrument azimuth by magnetic compass and the final component is a non-deforming reference cell. The instrument, of diameter 125mm, is cemented into 175 mm diameter boreholes at a target depth of 200 m. using expansive grout similar to that of the Sacks-Everton instrument to provide preload of the instrument. Strain is monitored using measurements of three instrument diameters spaced 120 degrees apart. The otherwise identical non-deforming reference cell is used to monitor the performance of the instrument cable and the surface electronics to guarantee the level of precision and long term stability. No tilt modules were deployed in these initial installations. The borehole is filled with the grout for some meters both sides of the instrument to produce a near homogeneous inclusion, and the hole is cemented to the surface to minimize groundwater and thermal contamination.

Operation is controlled by a microprocessor (RCA 1802), which sequences the transducers through measurement electronics common to all sensors. Gain and DC offsets for each channel are measured as a separate operation, and these parameters are used in production of a high stability data stream which is transmitted every three hours via a satellite link to the data retrieval centre at Menlo Park, California. Selected data is also printed on site for backup.

Four types of data are available from the present instrument.

1. Continuous low frequency plane-strain data for real time regional deformation mapping.
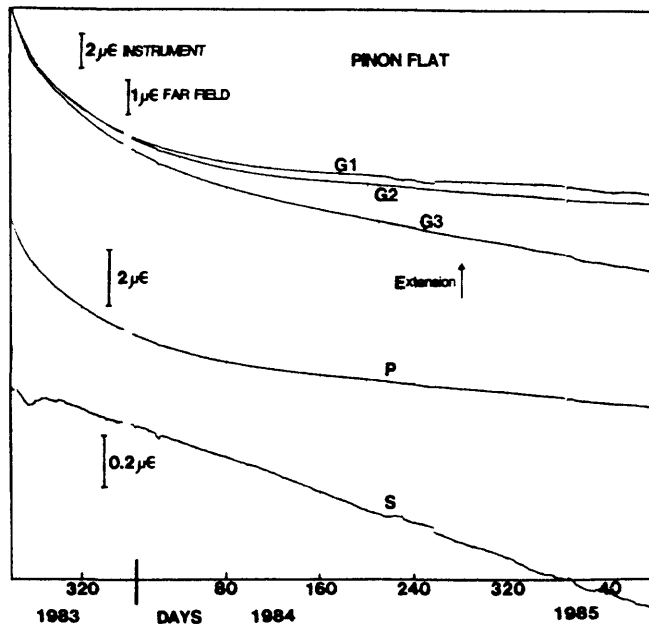
FIGURE 1. Strain measurements at Pinon Flat since installation. The upper three curves show the gauge responses, followed by the calculated hydrostatic and shear responses. Note that the scale for the shear (lower) plot indicates that the shear accumulation rate since installation has remained constant at less than 0.6 microstrain per year.
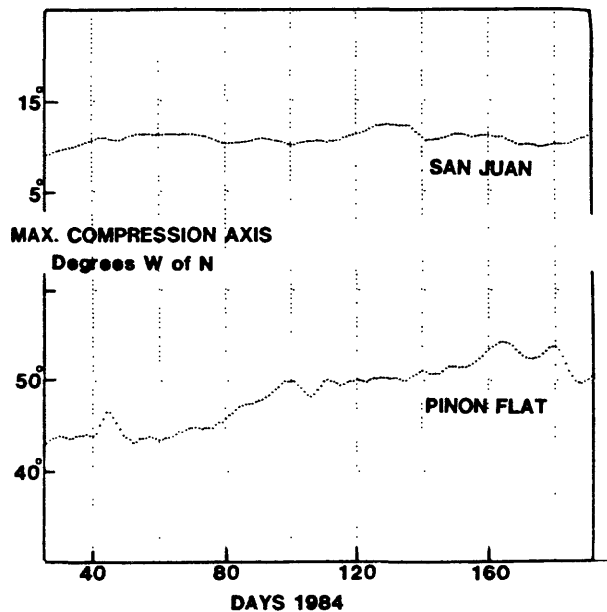

FIGURE 2. Angle of maximum compression plotted for each site. This is calculated by averaging the data from each gauge over a 25-day period, then determing the change in deformation from one period to the the next. These changes are then inverted to give the direction of the principle axes.

2. In-situ static shear field estimates when the instrument is implanted immediately after drilling.

3. Far field static offsets (elastic and plastic) related to the strain relief of nearby earthquakes and the stress redistributions which result.

4. High resolution shear strain seismology of the earthquake rupture process.

Current investigations have concentrated on the first three types of measurements.

RESULTS

One instrument was installed at the Pinon Flat Geophysical Observatory at a depth of 151m in competent granite and was operational by September 16,1983. This location was chosen for direct comparison of the strain measurements with both the long baseline interferometer spanning the site (Wyatt(1982), Berger and Lovberg(1970)), and with a pair of DTM Carnegie Institution of Washington Sacks-Everton strain meters within 100m. The axis of gauge 2 was at 5 degrees east of North, with gauge 1 at 65 degrees east of North, and gauge 3 at 125 degrees east of North.

Figure 1 shows the results of strain measurements since installation. A volumetric compression over this period of order 6 microstrain is attributed to curing of the grout, with a time constant of order 6 months. During this period a constant rate of shear of less than 0.6 microstrain per year is evident. These strains are calculated from the observed instrument response, corrected by instrument response factors as calculated in Gladwin and Hart(1984), using estimates of grout and rock properties. This rate is comparable with rates of 0.2 microstrain per year obtained with Geodolite network measurements (Prescott et al,1979,or King and Savage, 1983). It should be noted that this low strain rate was established within two months of installation. This high common mode rejection of hydrostatic noise sources associated with installation procedures is a major advantage of the present instrument design. Calculation of the angle of maximum compression for this (shown in Figure 2) indicates an axis changing from 44 degrees W of N to 50 degrees W of N.

Testing of the high resolution shear strain seismology capability of this instrumentation was carried out in December 1985, and disturbance of the strain measurements (due to additional heat input to the surrounding rock) is evident in Figure 1 for a period after that time.

The second installation was at San Juan Baptista at a depth of 146 m in close proximity to the multi-frequency laser ranging site and several USGS strain monitoring sites. The installation was completed on 1st October,1983, within five days of the completion of the drilling. For this site gauge 3 was oriented 25 degrees east of North, with gauge 2 and
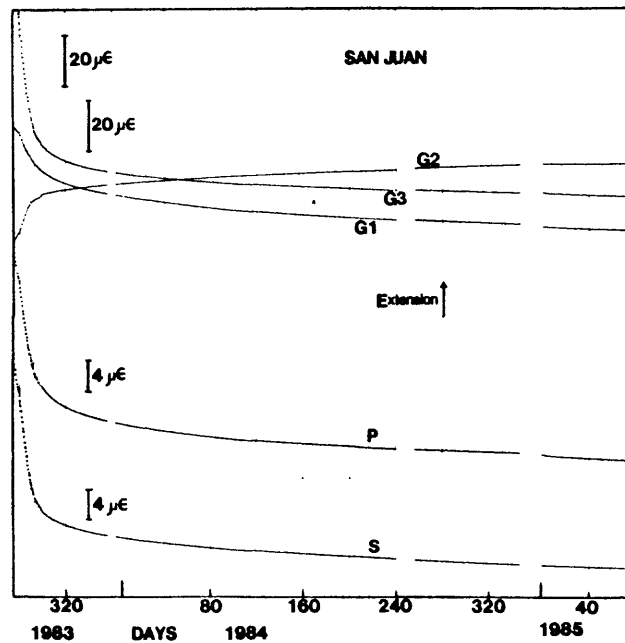
FIGURE 3. Strain measurements at San Juan Baptista since installation. The upper three curves show the gauge responses, followed by the calculated hydrostatic and shear responses.
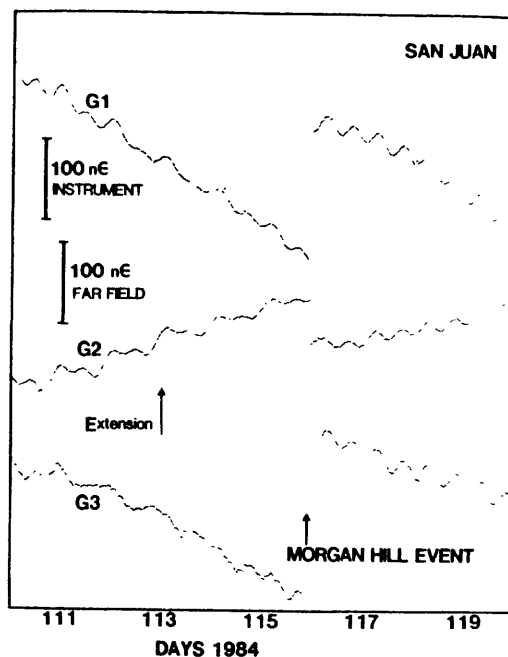

FIGURE 4. The response of the gauges of the instrument at San Juan Baptista to the Morgan Hill earthquake on 24 April,1984.

MODEL OF MORGAN HILL EARTHQUAKE (M$_L$=6.1) APRIL 24, 1984

MOMENT = 2 x 10^{25} dyne-cm
SLIP = 42 cm
LENGTH = 30 km
DEPTH = 5 → 10 km
STRIKE = N33°W
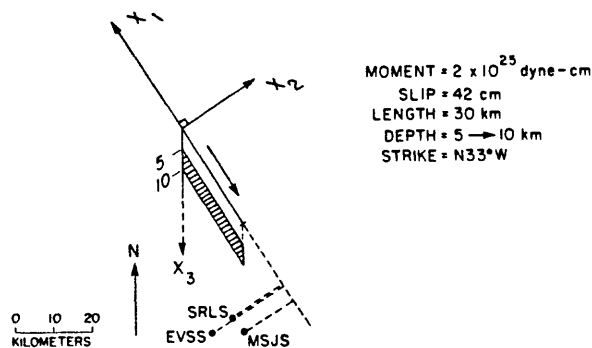
		Components		
		S$_1$(-35°)	S$_2$(-95°)	S$_3$(-155°)
Observed	(nanostrain)	242.1	-34.0	191.8
Calculated	(nanostrain)	233	-30	111

FIGURE 5. Comparison of predicted instrumental response against measured values for the elastic strain changes at San Juan (a distance of 60 km from the epicentre of the Morgan Hill event. The source parameters shown were determined seismically. The San Juan site is designated as MSJS in the figure.
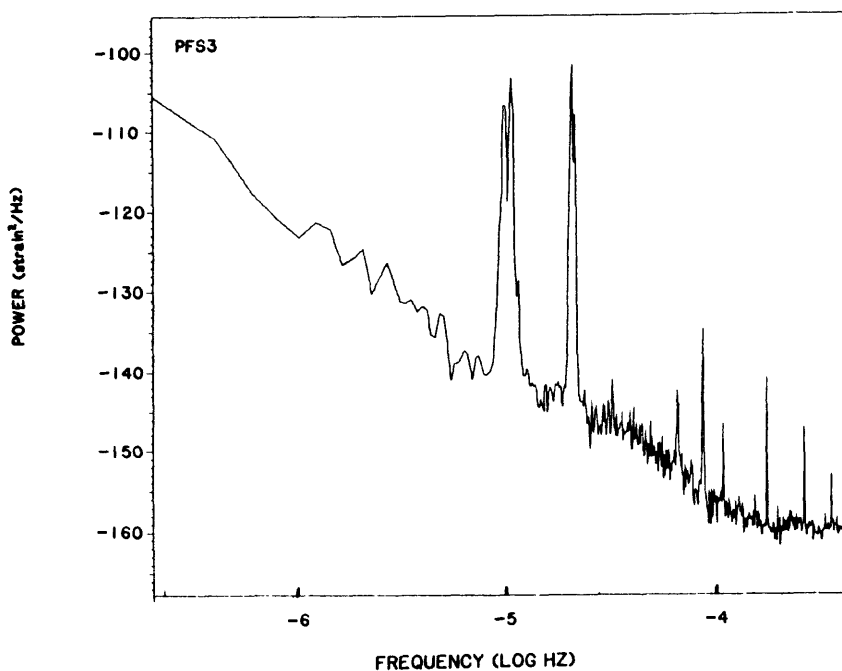
FIGURE 6. Calculated noise spectra from the Pinon Flat data. This compares favourably with analysis of data from the long baseline laser interferometer at this site.

gauge 1 at 85 and 145 degrees east of North respectively.

Figure 3 shows the response of this site, which contrasts very strongly with the post installation behaviour at Pinon Flat. The traces indicate a very normal grout curing compression, on which is superimposed a very large shear, indicating the recovery of the pre-existing shear which was stress relieved during drilling. This data gives a lower limit to the total shear strain at this site of 40 microstrain. Since the non-elastic creep recovery process is not yet complete, measurement of shear accumulation rate at San Juan is not yet possible. However the axis of maximum compression for the total shear strain is well defined (as shown in Figure 2) as 10 degrees W of N, which is in close agreement with the value of 4 degrees($\pm$10) W of N obtained by geodetic surveys (Prescott et.al.).

Response of this instrument to the Morgan Hill earthquake (24 April,1984) is shown in Figure 4. Inversion of the seismically determined source parameters for this event gives a predicted instrument response which compares very favourably with the measured instrument strains, as shown in Figure 5. An analysis of this event is now in progress and will be submitted for publication in the next two months.

Preliminary analysis of the noise spectra over the 18 month period of operation of the two sites is in progress. Figure 6 shows the spectral response for the Pinon Flat site. Noise performance is comparable with that of the laser strainmeter. Peaks at 3 hour related harmonics are an artifact of the particular measurement sequence chosen (a gain recalibration is performed at fixed 3 hour intervals, coincident with a data sample).

REFERENCES

PRESCOTT W.H., SAVAGE J.C., and KINOSHITA W.T. (1979) Strain Accumulation
        Rates in the Western United States Between 1970 and 1987.
        J. Geophysical Research, Vol.84, B10, pp 5423-5435
SAVAGE J.C., PRESCOTT W.H., LISOWSKI M., and KING N.E. (1981)
        Geododite Measurements of Deformation near Hollister,
        California, 1971-1978.
        J. Geophysical Research, Vol 86, B8, pp6991-7001.

LIST OF PUBLICATIONS

GLADWIN, M.T. (1984) High Precision Multi-Component Borehole Deformation
        Monitoring. Rev. Scientific Instruments.
        Vol 55, No 12, pp 2011-2016.
GLADWIN M.T. and GWYTHER R.L. (1985) Borehole Vector Strain Measurements
        in California. (in press)
GLADWIN, M.T. and HART, R. (1984) Design Parameters for Borehole
        Strain Instrumentation. Pure and Applied Geophysics (in press).
GLADWIN M.T. and JOHNSTON M.J.S. (1984) Strain Episodes on the San
        Andreas Fault following the April 24 Morgan Hill, California
        Earthquake.   EOS Transactions, Vol 65, No 45, p 852.

Deepwell Monitoring along the Southern San Andreas Fault

14-08-0001-22008

Thomas L. Henyey and Steve P. Lund
Department of Geological Sciences
University of Southern California
Los Angeles, CA 90089-0741
(213) 743-6123

Investigations

We have monitored the variation in water level and temperature within an array of deep wells near the southern San Andreas fault for more than five years. Our data show no variations during 1984 that might be considered related to potential seismic activity along the San Andreas fault.

Results

One goal of our study is to detect large amplitude water-level variations in the Palmdale region and define their source mechanisms. In general, water-level data sets of several years in duration are needed to assess these long-term strain changes and characterize the water level variability due to known forcing functions such as rainfall and aquifer discharge/recharge. We have previously noted long-term (several year) variations across the Palmdale array that show systematic trends indicative of either long-term strain changes or aquifer storage changes in the Palmdale region. These several-year-long trends are superposed on yearly rainfall cycles, with different wells having different ratios of the several-year to seasonal rainfall response. These long term trends are continuing through late 1984.

We have also noted in the past occasional short-term (few weeks) large-amplitude water-level fluctuations that were either unidentified or definitely co-seismic in source. The most notable cases of such anomalies have occurred in the Phelan well. In 1983, the water level in Phelan well dropped about 10 cm over several hours followed by a 3 week gradual return to its baseline (Figure 1). This occurred co-seismically with the Coalinga earthquake. No other well in the array showed a similar response and no source was defined for the anomaly. In November, 1984 the water level in Phelan again dropped about 30 cm over a few days (Figures 1, 2) and it has still not totally recovered. Three other large-amplitude anomalies have more recently occurred during January, 1985. These anomalies are shown in Figure 2. All of these anomalies have been checked independently with manual water level measurements to authenticate their reality. The anomalies are not related to any known forcing function (e.g. tides, atmospheric pressure, rainfall). Their characteristic shape - rapid onset and slower decay - is similar to anomalies reported by Johnson et al. (1973) and Lippincot et al. (1985) and ascribed to creep episodes on nearby faults (see also Wesson, 1981; and Rudnicki, 1984).

Variability in the raw water-level data, due primarily to barometric pressure changes and solid earth tides, will mask many short term anomalies due to

tectonically induced strain, unless they were abnormally large in amplitude or short in duration (~ 1 hr. or less). Furthermore, water-level variations due to longer-term changes (time constants from a few days to one year) are difficult to separate from rainfall effects. The rainfall effects include long relaxation times which can be on the order of 6 months or more (see Figure 3; also Change and Qiou, 1979; Chen et al., 1979 and Wu et al., in press) depending on the actual mechanism by which rainfall is communicated to the water table (or air/water interface in the borehole).

In order to have a chance of exposing either low-amplitude strain-induced anomalies or long-term strain induced anomalies embedded in rainfall-related effects, it will be necessary to perform time-series analyses on the raw water-level data. Data sets of several years duration may be required to adequately deal with rainfall effects (see for example Wu et al., 1984). We continue to explore various methods of time series analysis separating strain induced signals in water level from atmospheric pressure and solid-Earth tide induced signals.

An example of our recent analysis is shown in Figure 3. The water-level variations at Crystalaire (Figure 3, A) during January and February, 1984, have been broken into components (D, F, and J in Figure 3) that can be associated with the known forcing functions (atmospheric pressure - B in Figure 3; solid-Earth tides) and subtracted from the original water-level variation to remove their effects (I in Figure 3). Computer programs to aid in this processing have been kindly supplied by Duncan Agnew (U.C.-San Diego) and John Farr (U.S.G.S.-Menlo Park), and have been modified and augmented here at U.S.C. The water-level variations due to solid-Earth tidal effects (D in Figure 3) have been removed by fitting the records to the various known periodicities of the forcing function. This is the ideal method for removing such effects. We have used a more empirical method (developed at the U.S.G.S. from the work of Clark, 1967) to remove the effects of atmospheric pressure variations. This method matches trends in water level and pressure variations (even in the presence of long-term water-level trends) to calculate a transfer function for removing pressure induced water-level variations. Unfortunately, the resolution of this technique is seriously affected by white noise, and thus a 24-hr box-car filter has been used to smooth the water-level and atmospheric pressure variations (C, D, E, F in Figure 3) before use of the transfer function. The final water-level residuals that are left after removal of solid-Earth tidal, 24-hr box-car, and atmospheric pressure effects are shown in I of Figure 3.
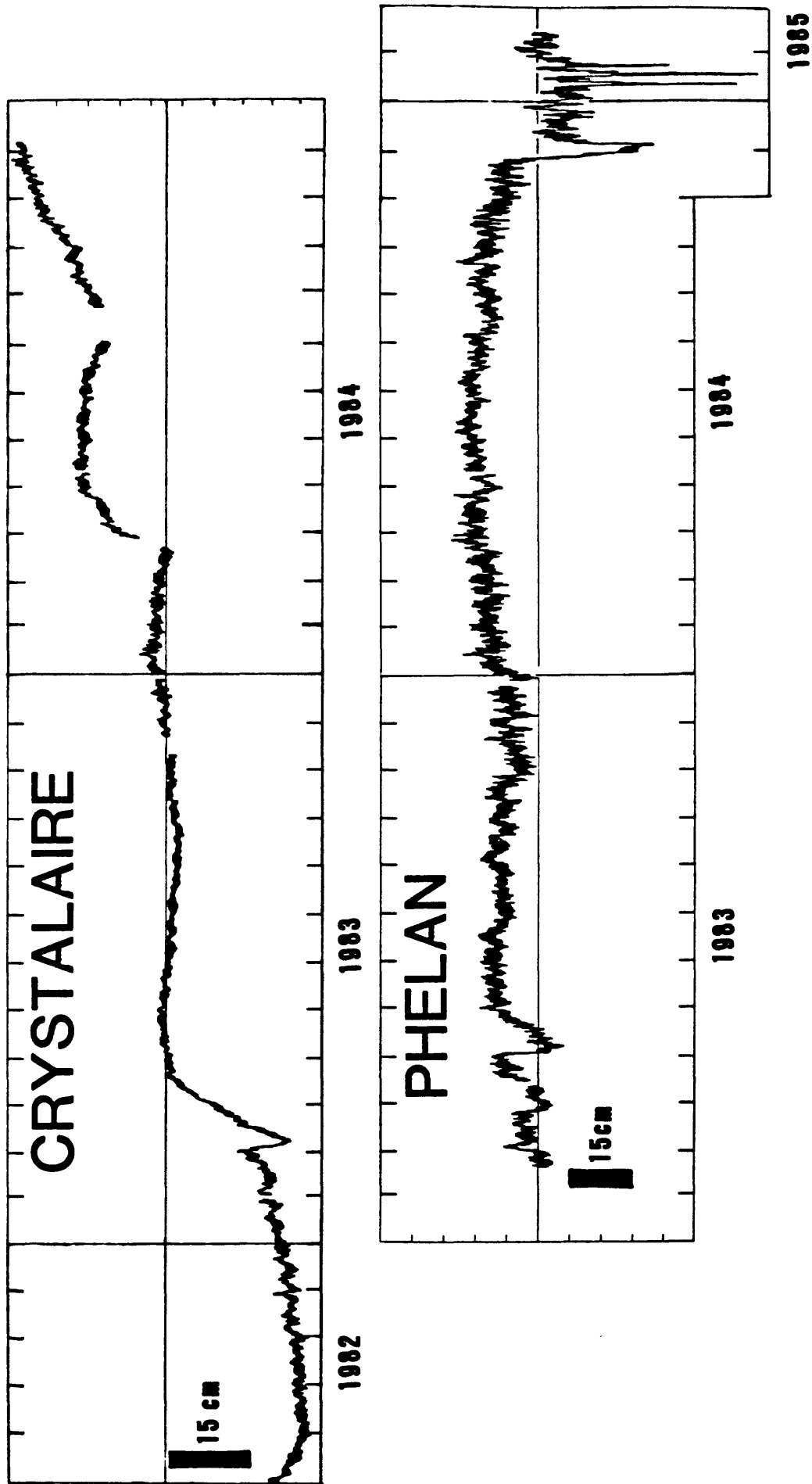
Figure 1: 1983-1984 horly-averaged water-level variation from two representative wells of the Palmdale deep-well array.

PHELAN WELL WATER LEVEL
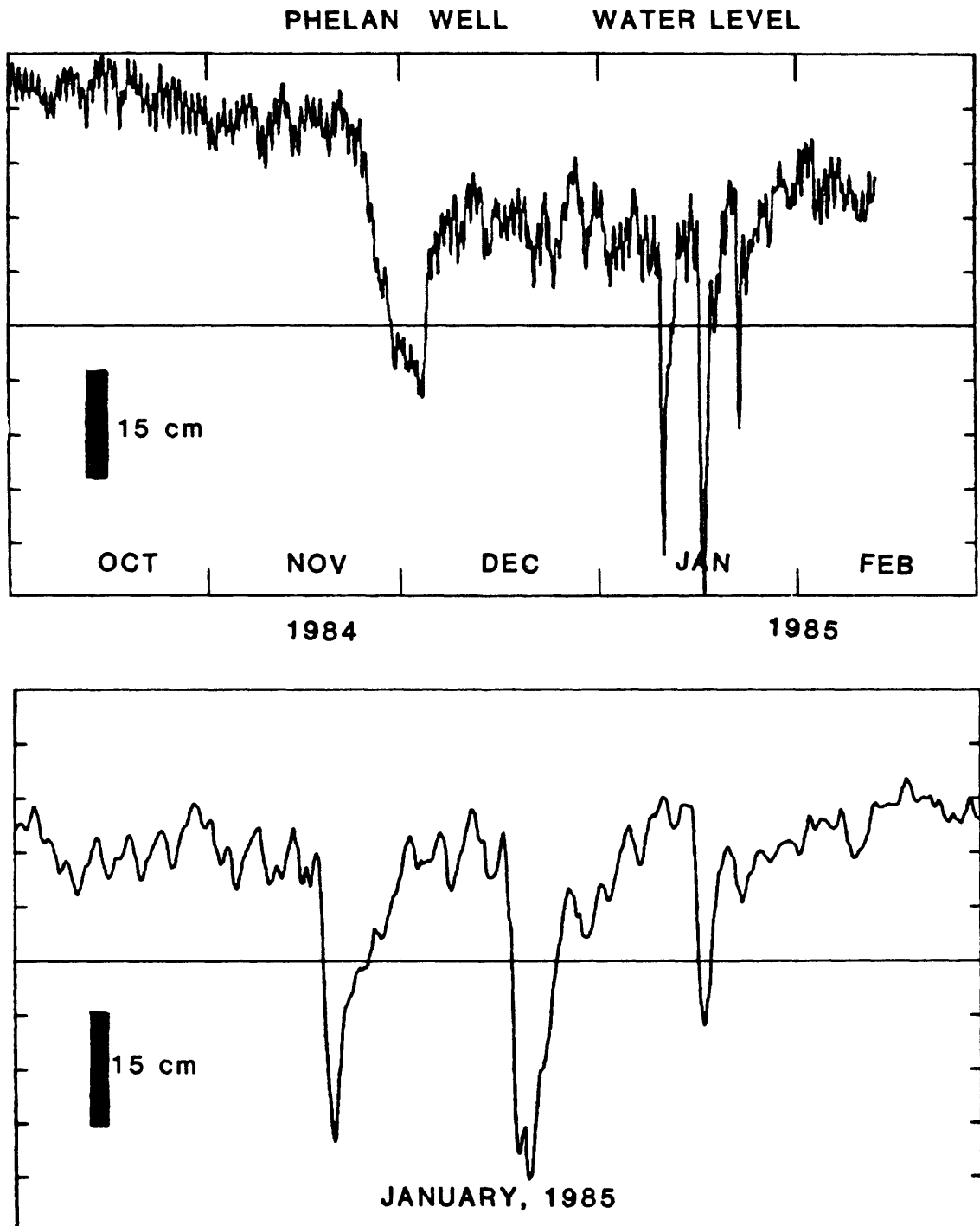
Figure 2: Anomalous water-level variations at Phelan well during late 1984 and early 1985. Four distinct short-term anomalies (one to two weeks) are supperposed on a longer-term apparent offset in the vater level.
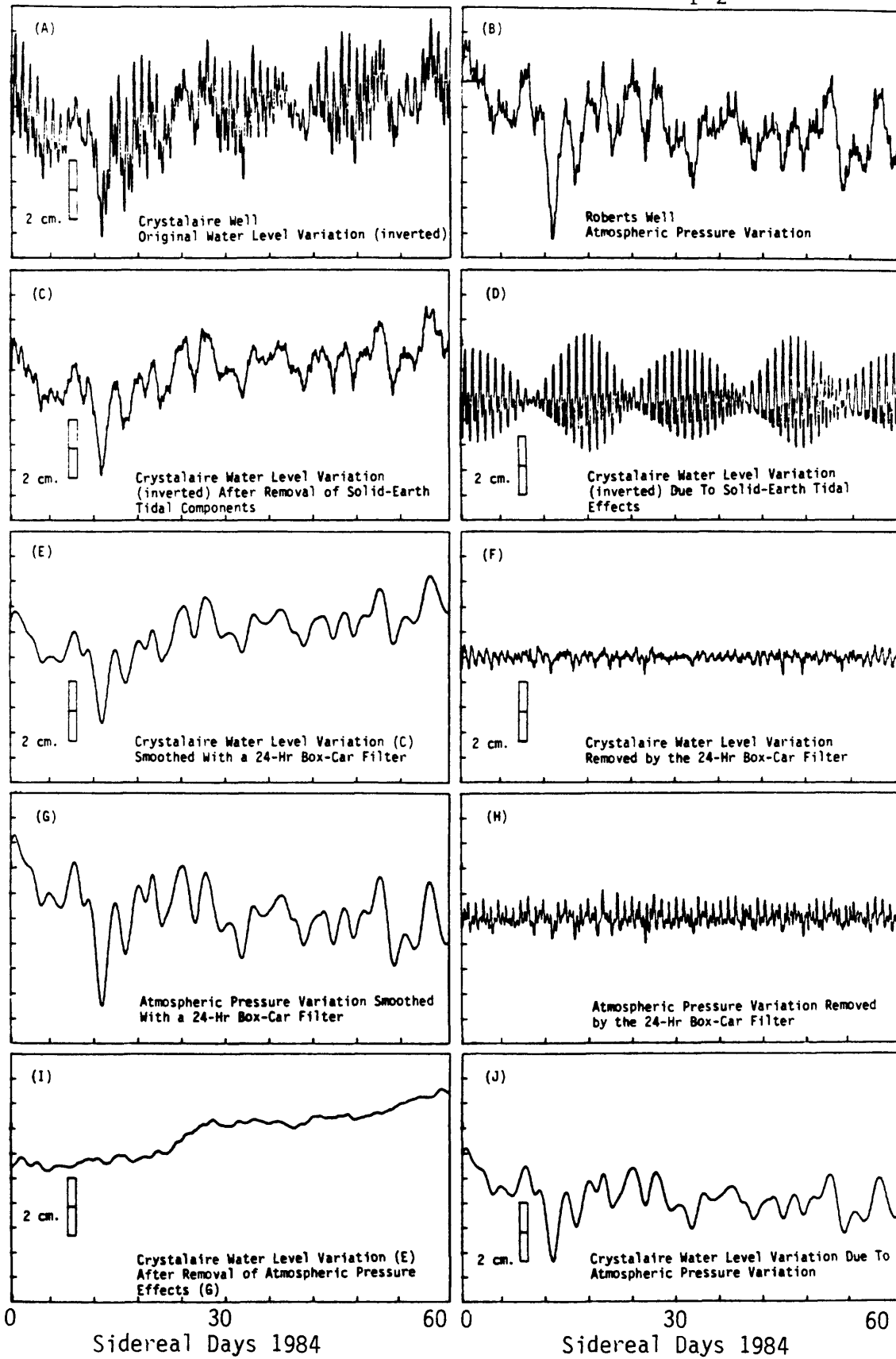
Figure 3: Time series analysis of Crystalaire water-level variations.

LOW FREQUENCY DATA NETWORK

9960-01189

J. Herriot, K. Breckenridge, S. Silverman
U.S. Geological Survey
Branch of Tectonophysics
345 Middlefield Road, MS/977
Menlo Park, California 94025
415-323-8111, ext. 2932

Investigations

1. Real-time monitoring, analysis, and interpretation of tilt, strain, creep, magnetic, and other data within the San Andreas fault system and other areas for the purpose of understanding and anticipating crustal deformation and failure.

2. Compilation and maintenance of long-term data sets free of telemetry-induced errors for each of the low frequency instruments in the network.

3. Development and implementation of graphical display systems for the purpose of monitoring seismic and surface deformation activity in real-time.

4. Installation of satellite-based telemetry system for reliable real-time reporting and archiving of crustal deformation data.

Results

1. Data from low frequency instruments in southern and central California have been collected and archived using the Low Frequency Data System. In the six months three million measurements from 125 channels have been received and subsequently transmitted on the Low Frequency 11/44 UNIX computer for archival and analysis.

2. A major effort of the project has been to provide real-time monitoring of designated suites of instruments, in particular, geographical areas. Terminals are dedicated to real-time color graphics displays of seismic data plotted in map or cross-sectional view or low frequency data plotted as a time series. During periods of high seismicity these displays are particularly helpful in watching seismic trends. This system was appreciated in the recent Morgan Hill earthquake.

3. A monitoring center continues to be maintained in Reston, Virginia. Seismic activity at Mammoth and other active areas can now be displayed directly in the Reston office.

4. Work continues on a "creep alarm" system. When finished, creep events will be detected automatically as they occur and personnel can be contacted by radio pager or "beeper".

5. New software was written to improve access to the low frequency data set for the uninitiated. Our goal is to facilitate access to the data without requiring any special training on our tools.

6. The project continues to operate a configuration of one PDP 11/44 computer running the UNIX operating system and two PDP 11/03 running real-time data collection software. This 11/44 has been operational as our analysis machine with less than 1% down time. The two 11/03 machines operate redundantly for robustness. Accordingly, our real-time collection has had 0% down time.

7. An additional IBM PC/AT or comparable computer is being added to the present configuration for the purpose of collecting satellite telemetry data. The new computer is for satellite telemetry what the 11/03 systems are for telephone-based telemetry. Once fully operational the new system will be made redundant.

8. The project continues to make use of a 5-meter satellite receiver dish which was installed in Menlo Park for retrieval of real-time surface deformation data from Alaska to California, even the South Pacific islands. The GOES-6 (GOES-4, etc.) geostationary satellite together with transmit and receive stations makes possible a greatly improved telemetry system. It is hoped that this new system will provide enhanced data quality as well as more flexibility in locating instruments over the old telephone-based telemetry system.

9. Software which was developed to control and collect data from the newly installed ground receiving station in Menlo Park is being augmented. The project has developed special purpose table-driven software which is very flexible with regard to adding and changing instrument and platform configurations while still being efficient on a small PDP 11/23 or equivalent computer. We are working on improving the time standard for time-stamping data transmissions.

10. The data from the network have been made available to investigators in real-time. Data only minutes old can be plotted. Events such as creep events can be monitored while they are still in progress.

11. The working prediction group of the Branch has made extensive use of the timely plots which are produced routinely by the project.

12. The project continues to develop color graphics and color hardcopy capabilities for use in real-time seismic displays. Using the advanced graphics software with color graphics devices we have demonstrated our real-time seismic and low frequency data monitoring ability to visiting government officials, scientific investigators, and public interest groups.

13. Jim Herriot has continued his work the Beijing Seismic Network. He is scheduled to return to China this October to continue development of real-time seismic and related software on a PDP-11/44 computer there.

Reports

Breckenridge, K., Johnston, M. J. S., 1985, Catalog of Locations: Low Frequency Instrumentation in California: U.S. Department of the Interior, U.S. Geol. Surv. Open-File Report 85-212.

Johnston, M. J. S., Silverman, S. A., and Breckenridge, K., 1984, Secular Variations and its Variations: EOS (Trans. Am. Geophys. Un.), v. 65, p. 203.

Repeat Gravity Studies
9380-03074
Robert C. Jachens and Carter W. Roberts
Branch of Geophysics
U.S. Geological Survey, MS 989
Menlo Park, CA 94025
(415) 323-8111, x 4248

Investigations

1) Remeasured southern California precision base station network in January 1985, including measurement of a station at the Holcomb Ridge 2-color geodimeter site.

2) Tied primary base station of the southern California precision gravity network to an absolute measurement site established by Mark Zumberge of U.C. San Diego. The tie was made at the same time the absolute gravity was measured.

Results

1) The latest temporal gravity surveys show that most stations continue to experience a pattern of low-amplitude, short period gravity fluctuations. However, stations at Glendale and Tejon Pass showed relatively large changes since the last measurement in May, 1984; + 39±6 and + 28±8 microgals, respectively. These stations will be remeasured in May 1985 to check whether the changes persist.

2) The primary base station tie to the absolute site was made with a precision of ±3 microgals (one computed standard error). This tie now sets the framework for establishing the stability of our Riverside base station and permits future determination of absolute gravity changes throughout the network, rather than the relative data we have worked with in the past.

Reports

1) Roberts, C. W., and Jachens, R. C., 1985, High-precision gravity stations for monitoring vertical crustal motion in southern California: U.S. Geological Survey Open-file Report 85-   , 76 p.

257

TILT, STRAIN, AND MAGNETIC MEASUREMENTS

9960-02114

M.J.S. Johnston, R. Mueller, C. Mortensen
D. Myren, A. Jones and V. Keller
Branch of Tectonophysics
U.S. Geological Survey
345 Middlefield Road, MS/977
Menlo Park, California 94025
(415) 323-8111, ext. 2132

Investigations

1. To investigate the mechanics of failure of crustal materials using deephole and surface strainmeters, tiltmeters and arrays of absolute magnetometers.

2. To investigate real-time records of these and other parameters for indications of incipient failure of the earth's crust.

Results

1. The static and dynamic strain fields have been recorded for a number of local and distant earthquakes at a sensitivity of 10E-11. An example of the records obtained at Echo Valley in central California on a borehole strainmeter installed at a depth of 400 ft (bottom) and a 3-component seismometer at the surface (top 3 traces) is shown in Figure 1.

2. Records from an array of borehole dilatometers are used to determine ground noise over eight decades of frequency (10 to 10^{-7} Hz) at diverse locations through the San Andreas fault system. The six instruments used are all installed at approximately 200 m depth. The general characteristics of power spectral density estimates obtained are similar at each of the sites. With the exception of about 10 dB of 6 second microseismic noise and 30 to 40 dB peaks at earth tidal frequencies, the spectra decrease from about -80 dB at a frequency of 10^{-7} Hz (10 megaseconds) to about -220 dB at a frequency of 10 Hz (0.1 seconds) in roughly an f^2 dependence on frequency, as expected from transient noise sources in Kelvin-Voigt or firmo-viscous materials.

3. Several strain episodes have been recorded in various ways on a cluster of borehole strain monitoring instruments near San Juan Bautista and near Parkfield at both ends of the creeping section of the San Andreas fault. If modelled as

an episode of deep slip encroaching into the locked region of the fault the slip velocities are of the order of 1 km/week.

4. High resolution strain and tilt recordings were made in the near-field of, and prior to the May, 1983, Coalinga (M_L 6.2) earthquake, the April, 1984, Morgan Hill (M_L 6.1) earthquake, and the November, 1984, Long Valley (M_L 5.2) earthquakes. These recordings were made in the first case with near surface instruments (resolution 10^{-8}), in the second case with both borehole dilatometers and a 3-component borehole strainmeter (resolution 10^{-10}), and in the last case with a borehole dilatometer (resolution 10^{-10}). While observed co-seismic offsets are generally in good agreement with expectations from elastic dislocation theory and while post-seismic deformation continued following the main event with a moment comparable to that of the main shock, pre-seismic strain or tilt perturbations from days to minutes before the main shock are not apparent above the present resolution. Precursory slip for these events, if any occurred, must have had a moment less than 1% of that of the main event. This strong constraint on the size and amount of slip triggering major rupture makes prediction of the onset times and final magnitudes of the rupture zone, for events such as these, a difficult task. These data are most easily explained by an inhomogeneous faulting model for which various areas of the fault plane to have different stress-slip constitutive laws. In terms of fracture mechanics terminology, the data would be most consistent with either small initial crack sizes or large values of V_0^*n, the product between initial crack velocity and stress-corrosion index.

5. A review of 10 years of synchronized geomagnetic field recordings from differential proton magnetometers (0.25 nT and 0.125 nT sensitivity) along the San Andreas fault has been completed. Along 600 km of the San Andreas fault as many as 27 magnetometers telemeter data in digital form once in 10-minutes to Menlo Park, California, and annual or semi-annual measurements are made at several hundred sites installed, 10 to 15 km apart, along other active faults. Since 1974, a summary of the major tectonic activity in the regions monitored includes one episode of aseismic uplift ("the Palmdale Bulge") and three moderate earthquakes. These earthquakes occurred in November, 1974 (M_L 5.2), August, 1979 (M_L 6.0), and November, 1984 (M_L 5.2). Typically, only one magnetometer was within the epicentral region for each event. Magnetic transients were recorded on two independent instruments only before the first of these earthquakes. Transients are not evident on the single magnetometers in the epicentral region before the

two other events. Calculated co-seismic offsets for all three events are below the signal resolution of the nearest magnetometer, but should have been detectable had instruments been more optimally located. The most encouraging result has been the strong correlation between changes in gravity, areal strain, and uplift during a seven-year period at Cajon, Palmdale and Cajon in southern California. This correlation is determined primarily by data taken during 1978-79 and 1981-82 when the most recent episode of the Palmdale uplift occurred.

6. A model that allows calculation of tilt, strain, and displacement time-histories through a 2 dimensional surface grid for slip on several (not necessarily connected) fault strands, has been completed and checked against known published special cases. Faults may be considered as zones of weakness (low rigidity) on which sympathetic slip may or may not occur.

Reports

Breckenridge, K. S., and M. J. S. Johnston, Catalog of Locations: Low Frequency Instrumentation in California, U.S. Geol. Surv. Open-File Report, 1985.

Borcherdt, R. D., J. B. Fletcher, E. G. Jensen, G. L. Maxwell, J. R. Van Schaack, R. E., Warrick, E. Cranswich, M. J. S. Johnston, and R. McClearn, A General Earth Observation System (GEOS), BSSA, in press.

Davis, P. M., D. R. Pierce, D. Dzurisin, M. J. S. Johnston, and R. J. Mueller, A Volcanomagnetic Observation on Mt. St. Helens, Washington, Geophys. Res. Lett., v. 11, p. 233-236, 1984.

Johnston, M. J. S., Review of Tectonomagnetic and Tectonic Activity in California, 1974-1985, Abs. I.A.S.P.E.I., Tokyo, Japan, (in press).

Johnston, M. J. S., M. T. Gladwin, and A. T. Linde, Preseismic Failure and Moderate Earthquakes in California, Abs. I.A.S.P.E.I., Tokyo, Japan, (in press)
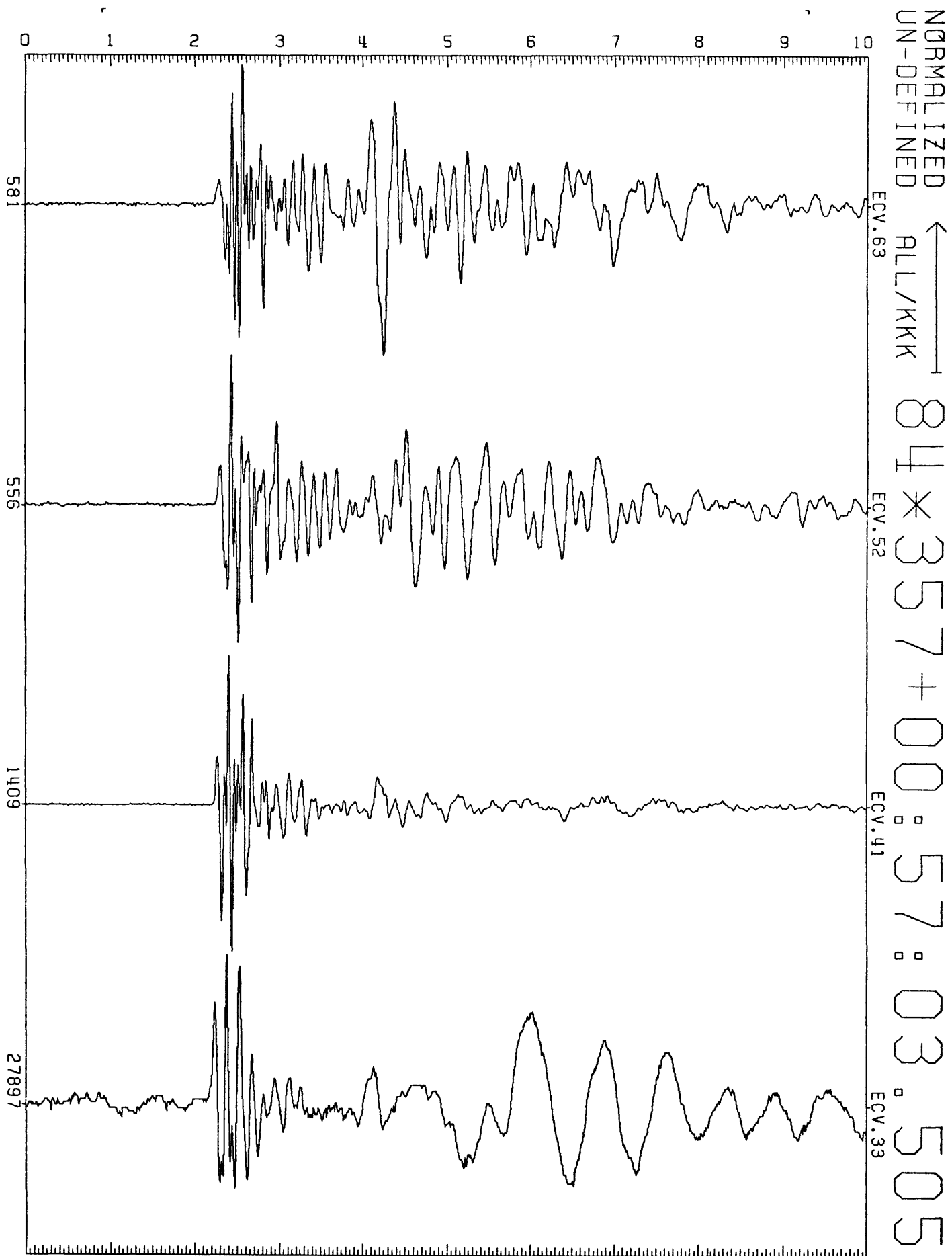
FIG 1.

Earthquake and Seismicity Research Using SCARLET and CEDAR

Contract No. 14-08-0001-21981

Hiroo Kanamori, Clarence R. Allen, Robert W. Clayton
Seismological Laboratory, California Institute of Technology
Pasadena, California 91125 (818-356-6914)

Investigations

1) Seismotectonic studies of the San Jacinto Fault.

2) Crust-mantle studies.

Results

1) Seismotectonic studies of the San Jacinto Fault.

Along the San Jacinto fault zone, in particular, large earthquakes occurred in 1937 (M_L 6.0), 1942 (M_L 6.5), 1954 (M_L 6.2), and 1968 (M_L 6.8) with only the location and rupture zone of the 1968 Borrego Mountain event known precisely. Knowledge of the time-space relationships between these large events, their individual and combined rupture patterns, and the locations of preshock and aftershock activity will provide essential insight into the variations of stress buildup and release along this major strike-slip fault.

We have begun work on this problem and have successfully obtained relatively precise epicentral locations for the 1937 and 1954 events, aftershocks, and significant preshock swarms.

In order to locate these older earthquakes using only readings from two or three distant (50-150 km) seismographs we developed a simple but effective location technique. This location method is similar to a master-event relocation technique except that the residuals from many earthquakes are averaged to obtain delay values consistent for a given small area (radius about 5 to 10 km). Time delays at stations RVR (Riverside), LJC (La Jolla), PLM (Palomar), and BAR (Barrett) were determined by averaging the travel-time residuals to these stations from small well located recent earthquakes on the various San Jacinto fault zone segments. We assume that these travel-time residuals are due to the deviation of the idealized crustal velocity model from the real velocity model between the source and receiver. The average of the residuals to a particular station becomes the delay to that station which is then used in the location routine. We have found that these delays vary somewhat in different general source locations, and thus we use different sets of delays for different segments of the fault zone.

We tested the location precision of this technique on several recent earthquakes. They were relocated, for example, using only stations RVR and LJC (distance about 100 km) with the correct delay values and were found to relocate to within two to three kilometers of their modern locations.

Since the original location uncertainties of the older events is ten to twenty kilometers or more, our relocations for these events are a significant improvement.

We relocated the 1937 (M_L 6.0) main shock, four days of aftershocks ($M_L \geq 3.0$), and a preshock swarm using this technique. The results indicate that the 1937 earthquake ruptured a 10 km segment of the Clark fault just southeast of the Anza seismic gap. Early aftershocks suggest rupture to the northwest of about 6 km with some later aftershocks extending a few kilometers southeast. In 1980 an M_L 5.5 earthquake extended from the northwest end of this rupture zone about 3 km further northwest and partially into the Anza gap. Thus a pattern of rupture toward the present seismic gap is apparent on this segment of the fault. An interesting earthquake swarm occurred 1 year

before the 1937 event. The relocated epicenters of these earthquakes are coincident with the area of Cahuilla Valley. This valley has also been the site of swarm activity recently (1980-1981) and possibly before the 1918 (M 7) Hemet earthquake but has been quiet at other times. It appears that the crust beneath Cahuilla may act as a sensitive stress meter signaling whenever high stresses are building up in the general area (radius about 40 km).

We also relocated the 1954 (M_L 6.2) main shock and large aftershocks ($M_L \geq 4.0$) and one preshock swarm. The 1954 main shock is located at the southeastern mapped termination of the Clark fault, and aftershocks extend southeast indicating a unilateral rupture of about 12 km. This is contrary to earlier assumptions that the earthquake was caused by rupture of the mapped fault segment southeast of the 1937 earthquake (Thatcher et al., 1975). In fact a 25 km long historically unbroken segment of the Clark fault is now seen to lie between the 1937 and 1954 rupture zones.

The rupture zone of the 1954 event is coincident withthe southeastward extension of the Clark fault but apparently no surface fault trace can be seen in this area despite detailed mapping (Sharp, 1967). This rupture zone raises questions about the possible extension of the Clark fault to the southeast beneath the folded young sediments in this area.

A small swarm of earthquakes preceded the 1954 earthquake by about 10 weeks (Figure 1). These preshocks have the same location as many of the 1954 aftershocks and seem to be signaling stress buildup prior to the main shock. Although preseismic swarms and foreshocks have obvious importance for short-term earthquake prediction, the occurrence of such activities is rather infrequent. There is some indication that certain faults tend to exhibit this type of precursory activity more often than others. In this regard the existence of swarm activity before the 1954 and 1937 events is significant because it suggests that other events along the San Jacinto fault may also be preceded by swarms. This swarm activity before the 1954 and 1937 events is significant because it may suggest that other events along the San Jacinto fault may also be preceded by swarms.

2) Crust-Mantle Studies.

Since most of the results of these studies are described in the previous report (p. 340, U.S.G.S. Open File Report 85-22), here we show the results in Figure 2.

References

Magistrale, Harold, Chris Sanders, and Hiroo Kanamori, The rupture patterns of large earthquakes in the San Jacinto fault zone, Abs., American Geophysical Union Fall Meeting, December 3-7, 1984, San Francisco, California.

Sanders, Chris, David Rinn and Hiroo Kanamori, Anomalous shear wave attenuation in the shallow crust beneath the Indian Wells-Coso Region, California, Abs., American Geophysical Union Fall Meeting, December 3-7, 1984, San Francisco, California.

Hearn, Thomas M., Crustal structure in southern California from array data, Ph.D. thesis, California Institute of Technology, 1985.

Webb, Terry H. and Hiroo Kanamori, Earthquake focal mechanisms in the Eastern Transverse Ranges and San Emigdio Mountains, southern California and evidence for a regional decollement, Seismo. Soc. Amer., Bull., in press.
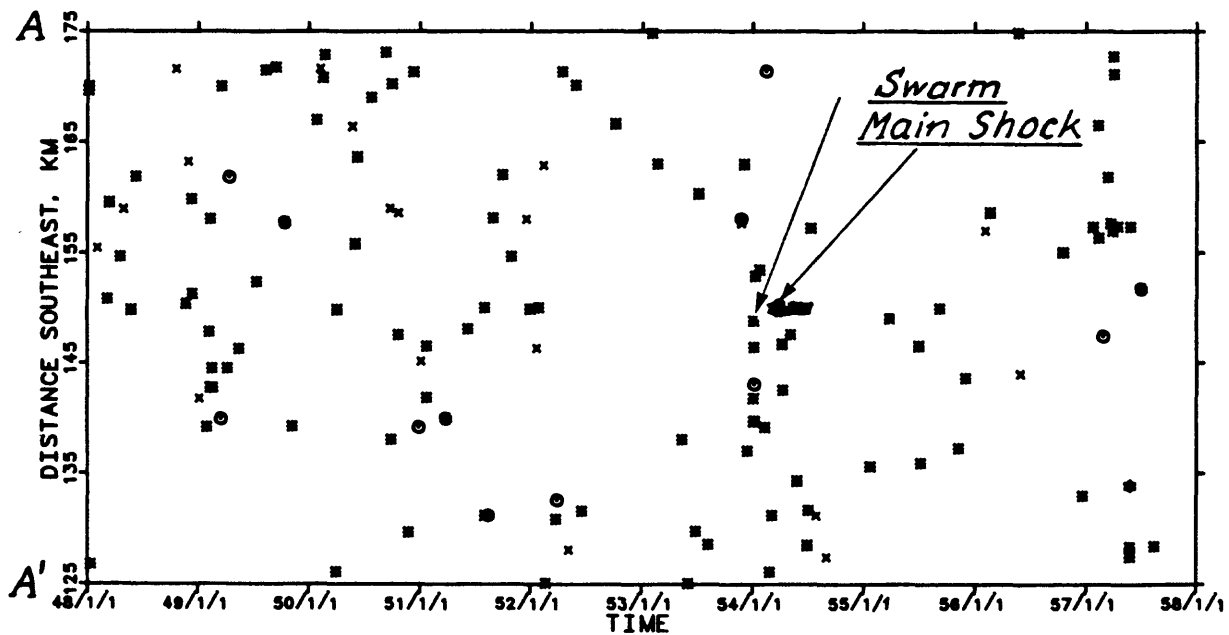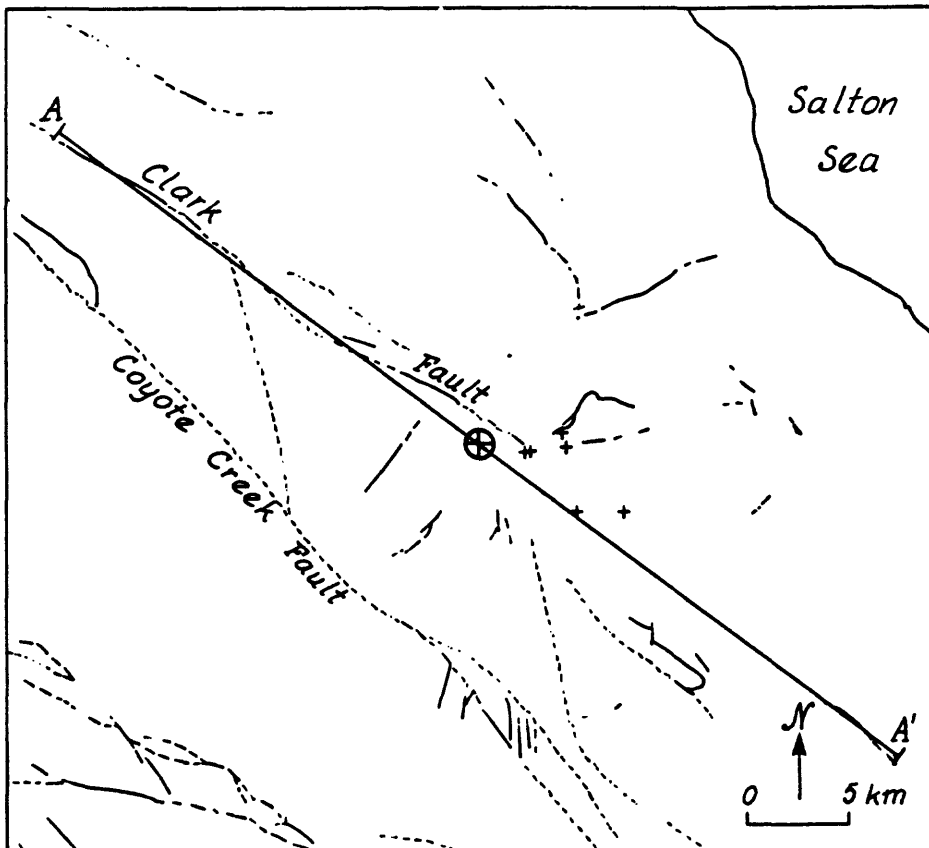
Figure 1 Top. Map view of 1954 mainshock (*) and preshock swarm of 1/4/54 (+). Line AA' indicates location of plane of Figure 1b. Scale 1:250,000. Bottom. Space-time diagram. Events from the C.I.T. catalog within 10 km on each side of the Clark fault are projected into a plane 50 km long parallel to the fault. 1954 event is at km 150. Note two year quiescence broken by the preshock swarm of 1/4/54. Grouping following mainshock is an artifact of plotting numerous aftershocks at the same location.
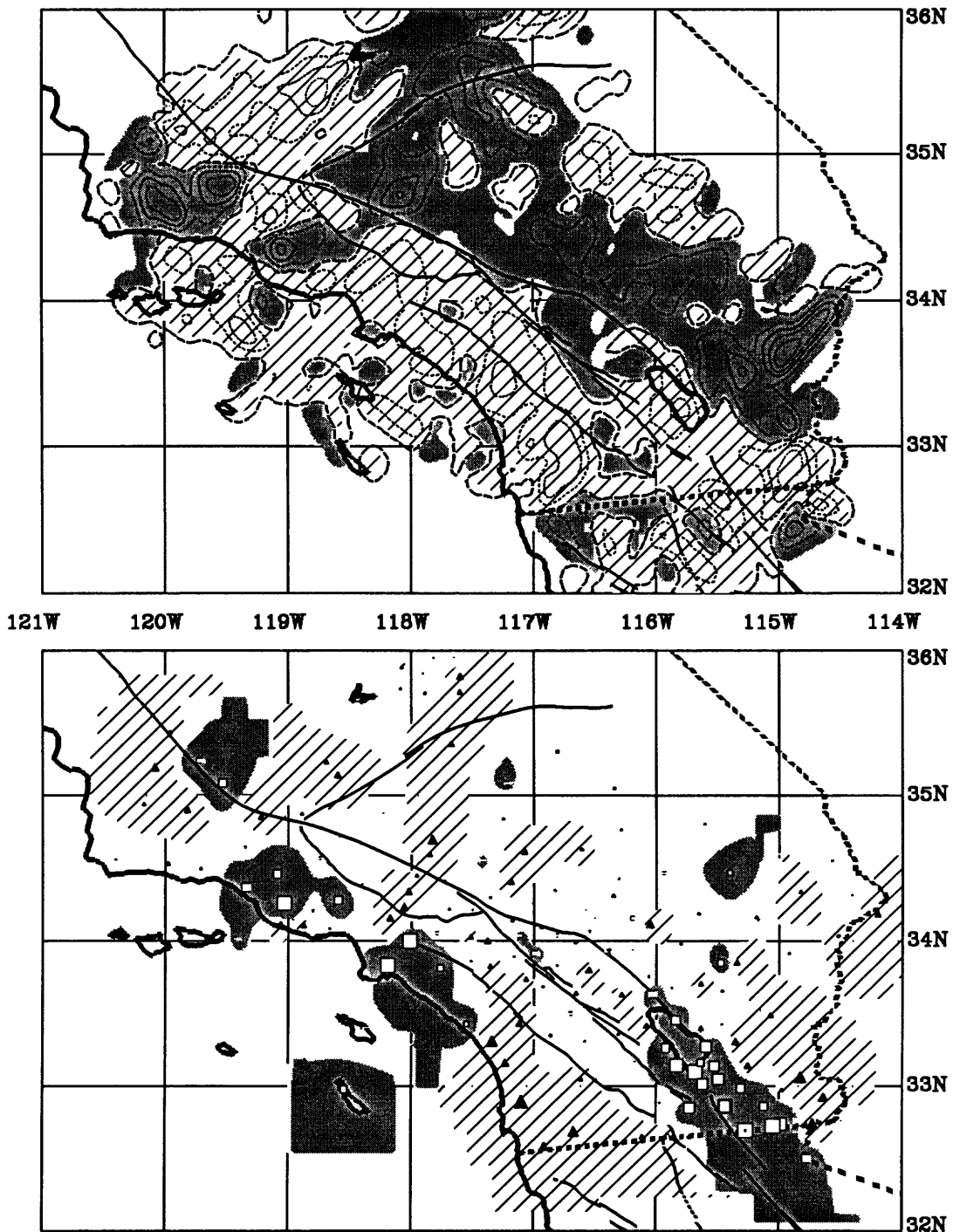
Figure 2. The upper panel shows the Pg - slowness results for southern California. The shaded areas indicate fast velocities while the striped area are slow velocities. The results are strongly correlated with surface tectonic features such as the San Andreas and Garlock Faults. The lower panel shows the Pg station delays. The shaded areas indicate positive delays and the striped regions are negative delays. The thick sediments in the L.A. and Ventura basins show up as positive delays.

HYDROLOGICAL MONITORING ALONG SAN ANDREAS
AND SAN JACINTO FAULTS, SOUTHERN CALIFORNIA,
DURING FIRST HALF OF FISCAL YEAR 1985

Contract 14-08-0001-21982

D. L. Lamar and P. M. Merifield
Lamar-Merifield Geologists, Inc.
1318 Second St., #25
Santa Monica, CA 90401

Investigations

Water levels in twenty-two wells along the San Andreas and San Jacinto fault zones were monitored during the current reporting period. Water levels and barometric pressure at one well were monitored by an Envirolabs data logger, Model DL-120-MCP, which is linked by telephone to our IBM Personal Computer. Another nine wells were monitored continuously with Stevens Type F recorders, two being maintained by Linda Woolfenden of the Geological Survey. The remaining wells were probed monthly.

Long-term water-level changes are displayed on computer-generated hydrographs for each well. Daily rainfall is plotted on the graphs for direct comparison with water levels. Long-term hydrographs of wells along the San Andreas fault typically show seasonal response to rainfall (Fig. 1). Most of the wells along the San Jacinto fault zone are in confined aquifers which are not affected by seasonal rainfall (Fig. 2). Short-term fluctuations in water level seen on the Stevens recorder charts and Envirolabs plots are caused by barometric pressure changes related to weather fronts, earth tides and solar thermal tides.

Water levels are measured every 15 minutes on the well equipped with an Envirolabs data logger. The measurements are stored on magnetic tape and data are sent to the IBM Personal Computer in our office via telephone twice a week. To date the data logger has operated without malfunction. Hydrographs are generated by a Bausch and Lomb digital plotter connected to the IBM Personal Computer.

Results

We previously suggested (Merifield and Lamar, 1981) that long-term water-level records of wells in the Palmdale-Valyermo area showed anomalous changes possibly related to the 1979 Palmdale strain event (Savage et al., 1981a, 1981b; Shapiro et al., 1980). Savage and Guohua (1984) have compared water levels in two of our observation wells (5N/12W-4H1 and 5N/10W-30L1) with strain and gravity measurements over similar periods into 1984. They find a marginal correlation and evidence for the 1979 Palmdale strain event; their analysis motivated us to re-evaluate the water-level changes by considering the longer records now available (Lamar et al., 1985).

Figure 1 is an example hydrograph showing a distinct rise during each rainfall season (September 30 to October 1) except for some seasons of

below-average rainfall. Each well appears to require a different cumulative rainfall before water levels rise during the season. Figure 3 shows a linear relationship between rainfall and water-level rise for well 5N/12W-3N1; similar plots show that the water-level rises during 1979 are all above the best fit line for nine wells in the Palmdale area.

Figure 4 is a plot of anomalous water-level rise (feet) during 1979 versus response to tides (10^{-2} feet) seen in Stevens recorder charts for the wells. The response to tides is a measure of the well's capability as a strain meter; thus a good correlation would suggest that the 1979 water-level rise was due to tectonic strain. However, the correlation coefficient between the 1979 water-level rises and the wells' response to tides is only 0.42.

The long-term observations provide background necessary for the interpretation of water-level changes which may precede a major earthquake on the San Andreas fault. Long-term records may be most valuable for the prediction of such an earthquake because Scholz et al. (1973) have suggested that the duration of earthquake precursors may be proportional to earthquake magnitude.

Short-term water-level records of wells along the San Jacinto fault have shown anomalies interpreted to be strain events in the past (Merifield and Lamar, 1983, 1985); no such anomalous water-level changes have been observed during the past six months.

REFERENCES

Lamar, D. L., S. H. Hitchcock, P. M. Merifield and R. T. Bean, 1985, Possible long-term water-level changes during the 1979 Palmdale, California, strain event reconsidered: Lamar-Merifield Technical Report 85-2, U.S. Geological Survey Contract 14-08-0001-21982, 18 p.

Merifield, P. M. and D. L. Lamar, 1981, Anomalous water-level changes and possible relation with earthquakes: Geophys. Res. Lett., v. 8, p. 437-440.

Merifield, P. M. and D. L. Lamar, 1983, Ground water anomalies along the San Andreas and San Jacinto fault zones, southern California, EOS Trans. Am. Geophys. Union, v. 64, no. 45, p. 761.

Merifield, P. M. and D. L. Lamar, 1985, Possible strain events reflected in water levels in wells along San Jacinto fault zone, southern California, Pure and Applied Geophysics, in press.

Savage, J. C., W. H. Prescott, M. Lisowski and N. E. King, 1981a, Strain on the San Andreas fault near Palmdale, California: Rapid, aseismic change, Science, v. 211, p. 56-58.

Savage, J. C., W. H. Prescott, M. Lisowski and N. E. King, 1981b, Strain accumulation in southern California, 1973-1980: J. Geophys. Res., v. 86, p. 6991-7001.

Savage, J.C. and Gu Guohua, 1984, The 1979 Palmdale, California, strain event in retrospect: unpublished manuscript, 28 p.

Scholz, C. H., L. R. Sykes and Y. P. Aggarwal, 1973, Earthquake prediction: A physical basis: Science, v. 181, p. 803-810.

Shapiro, M. H., J. D. Melvin, T. A. Tombrello, M. H. Mendenhall, P. B. Larson and J. H. Whitcomb, 1980, Relationship of the 1979 southern California radon anomaly to a possible regional strain event: California Institute of Technology, Lime Aid Preprint in Nuclear Geophysics and Cosmochemistry, LIAP-36, 16 p.

42285A
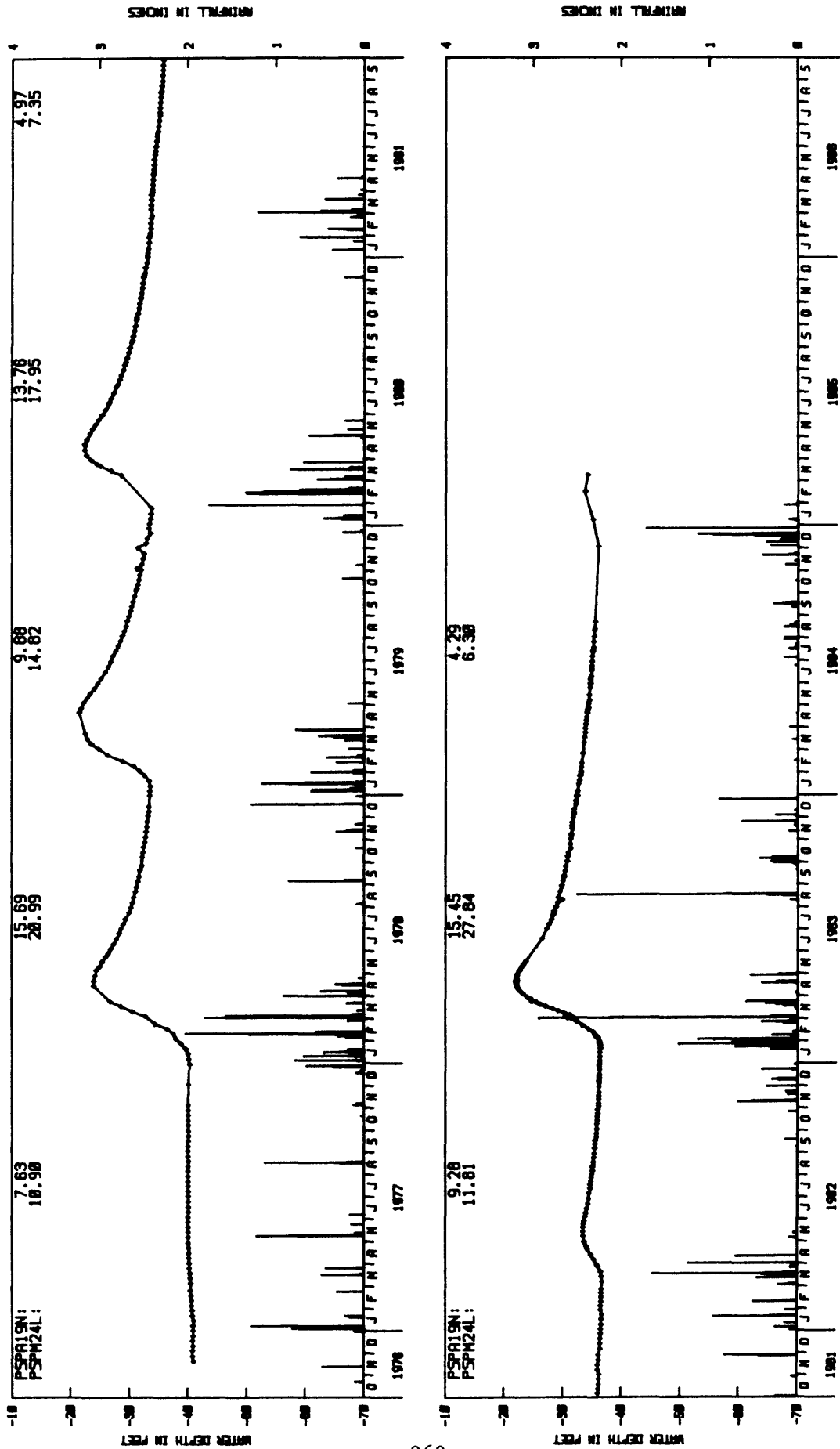
FIGURE 1 : OBSERVATIONS OF WATER LEVEL (+) AND RAINFALL (.) IN WELL 6SW/12W-14C01 DURING 1976-1986, PALMDALE AREA.
SEASONAL RAINFALL AT ADJACENT STATIONS IN INCHES ACROSS THE TOP.
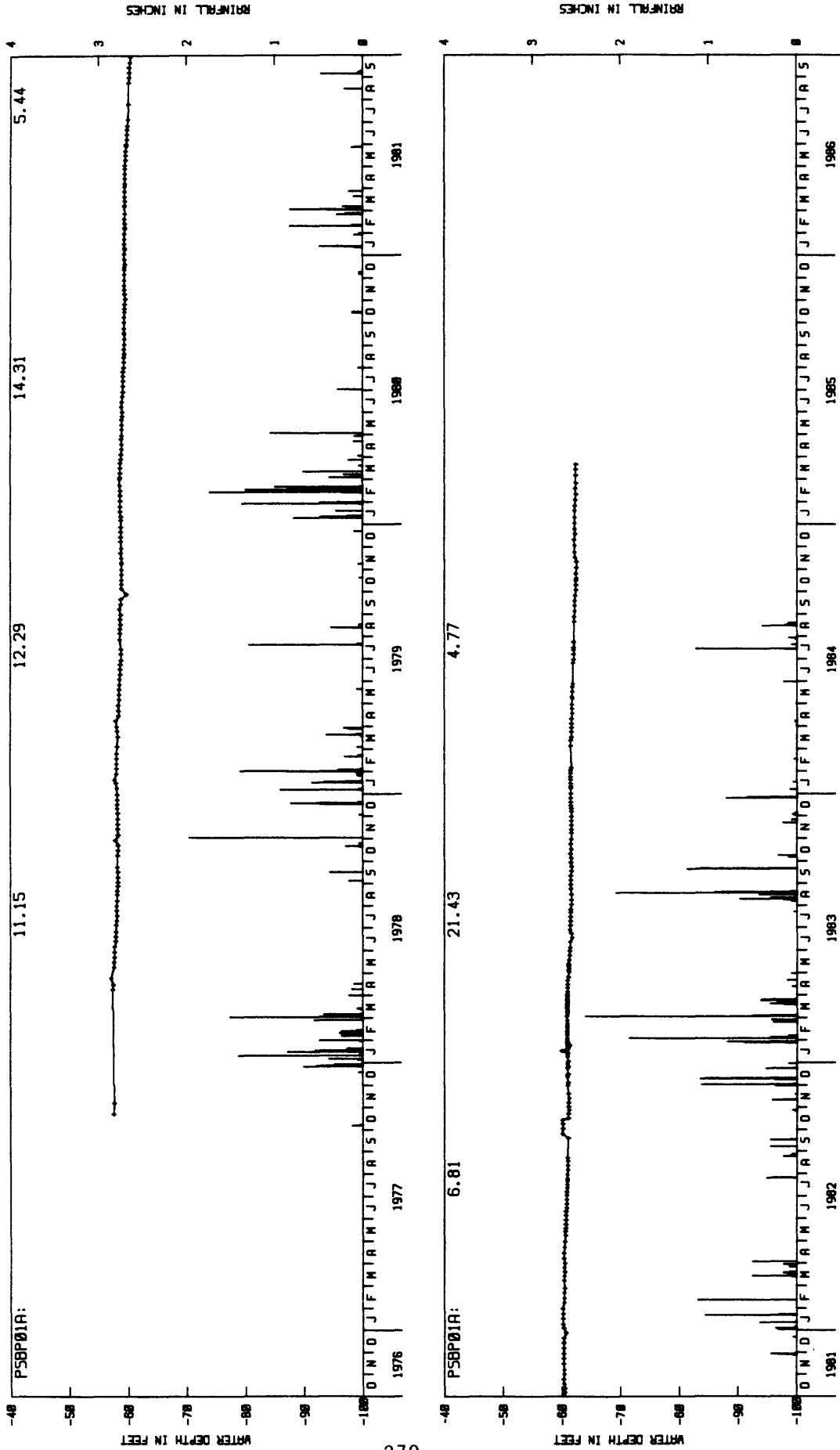
FIGURE 2 : OBSERVATIONS OF WATER LEVEL (+) AND RAINFALL (.) IN WELL 11S/06E-01C01 DURING 1976-1985, BORREGO VALLEY AREA. SEASONAL RAINFALL AT ADJACENT STATIONS IN INCHES ACROSS THE TOP.
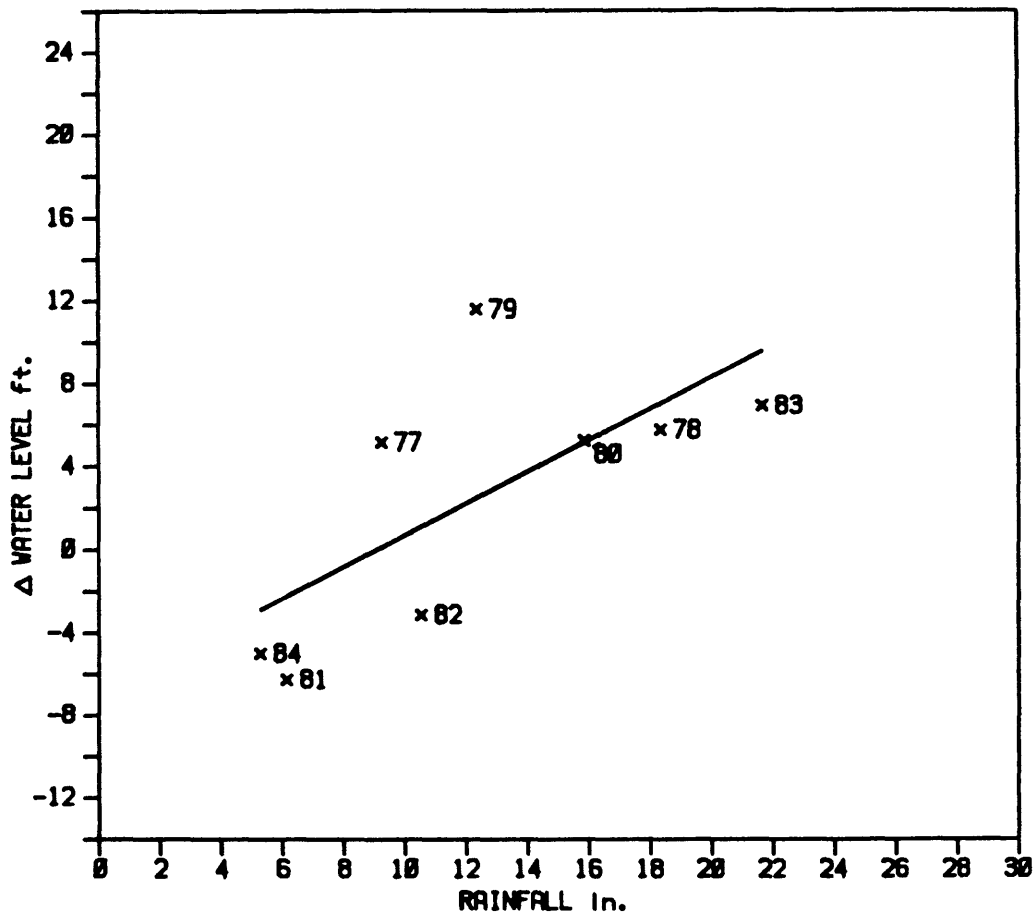
Fig. 3 - Seasonal (October 1 through September 30) rainfall versus water-level changes 1977-84 for well 5N/12W-3N1.
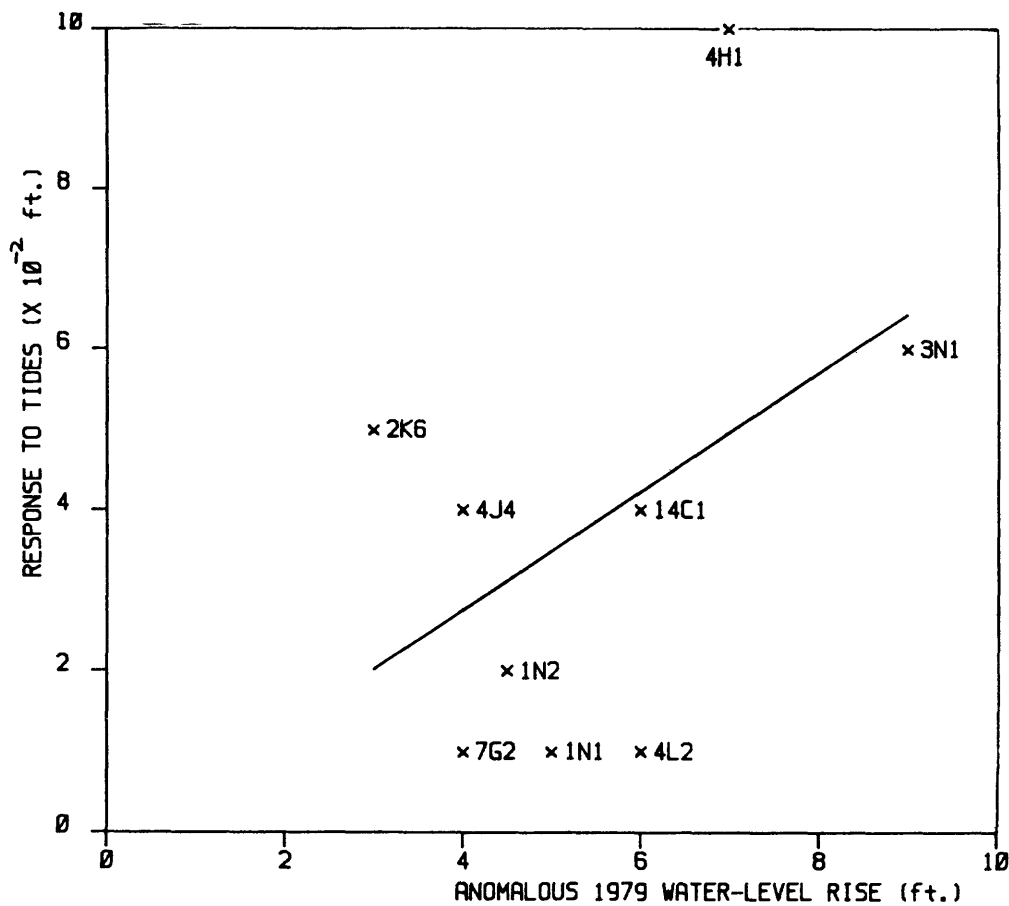

Fig. 4 - Anomalous 1979 water-level rise versus response to tides for wells in the Palmdale area.

GEODETIC STRAIN MONITORING

9960-02156

John Langbein
Branch of Tectonophysics
U.S. Geological Survey
345 Middlefield Road, MS/977
Menlo Park, California 94025
(415-323-8111, ext. 2038

Investigations

Two-color geodimeters are used to survey, repeatedly, geodetic networks within selected regions of California that are tectonically active. This distance measuring instrument has a precision of 0.1 to 0.2 ppm of the baseline length. Currently, the crustal deformation is being monitored within the south moat of the Long Valley Caldera in eastern, California, and near Pearblossom, California on a section of the San Andreas fault that is within its Big Bend section. Periodic comparisons with the proto-type, 2-color geodimeter are also conducted near Parkfield, California. These inter-comparison measurements serve as a calibration experiment to monitor the relative stabilities of the portable and proto-type geodimeters.

Results

1) Long Valley

Frequently repeated two-color laser ranging measurements (Figure 2) made within a geodetic network in the Long Valley caldera (Figure 1) during the interval June 1983 to May 1985 reveal that rapid deformation of the south moat and the resurgent dome has continued since the January 1983 earthquake swarm, the last period of notable seismicity. Although the deformation has accumulated smoothly in time, the rate of extension of many of the baselines decreased by factors of two or three from mid-1983 to mid-1984. The dominant signal has been areal dilatation with rates of extension of some baselines reaching as high as 5 ppm/a during the summer of 1983. Within the south moat shear deformation is also apparent. For the interval mid-1983 to mid-1984 the data can be adequately modeled as the result of the injection of 0.025 ± 0.003 and 0.0021 ± 0.0005 km^3 of material into two points located at respective depths of 14 and 6.5 km beneath the resurgent dome in addition to 62 ± 4 mm of shallow right lateral slip on the South Moat Fault.

The observations of line length changes through April 1985 from the 23 baseline network are shown in Figures 1 and 2. It is apparent that there was no significant deformation due to the magnitude 5.9 earthquake on November 23, 1984 in Round Valley which is approximately 30 km southeast of the center of the network.

An estimate has been determined of the precision of the portable, two-color geodimeter. Data from each baseline has been analyzed in terms of a secular rate of extension plus an acceleration term. The RMS residual of the fit to the data is then compared to a error budget of the form $\sigma = (a^2 + b^2 l^2)^{1/2}$ where l is the baseline length. From this analysis, we have determined that a = 0.7 mm and b = 0.12 ppm. This result is consistent with data that spans both 3 months and 15 months.

2. Pearblossom

Due to the high rate of deformation and our limitation of only one operating two-color geodimeter that is currently reliable and portable, the frequency of observations at Pearblossom has been significantly reduced. This network was resurveyed in November, 1984, and in January and April 1985. The strain changes from these surveys are plotted in Figure 3 along with the results from the previous measurements since October 30, 1980. The data from the past 6 months is consistent with the previous observations.

3. Instrument Inter-Comparison

The data from 3 sets of measurements taken in June, August, 1984 and January, 1985 have been analyzed in terms of the relative change in instrument length between the portable and proto-type two-color geodimeters. The data consists of nearly simultaneous measurements of distances using both instruments at a common site and approximately 6 reference monuments located between 1.6 to 6.2 km from the central site at Parkfield. From these observations, the difference in distances for each baseline using the 2 instruments is tabulated as a function of time. With this method, tectonic strain change is canceled and leaves the relative variation of instrument length as the dominant factor. The data indicates that the two instrument have changed their length relative to each other. If the prototype instrument is assumed to be stable, then the relative lengthening of the portable instrument is -0.02 ± 0.08 ppm for June, 1984, +0.21 ± 0.08 ppm for August, 1984, and -0.19 ± 0.13 ppm for January, 1985. The data unfortunately includes some measurements from each instrument that may be contaminated with blunders that have not been detected.

4. Ability of Geodetic Networks to Detect the Amount and Resolve the Location of Fault Slip

In conjunction with Ruth Harris, the current geodetic networks located near Parkfield, California have been investigated in terms of their ability to detect ground deformation due to fault slip and to determine the location of the slip. A computer code has been written to determine both the sensitivity and spacial averaging interval from postulated slip on the San Andreas fault near Parkfield. To date, only slip that varies with depth has been considered.

Reports

Harris, R. A., Langbein, J. O., 1984, The sensitivity of geodetic networks: Detecting the amount and location of slip near Parkfield, CA (abs.): EOS (American Geophysical Union Transactions), v. 65, no. 45, p. 853.

Langbein, J. O., Linker, M. F., Prescott, W. H., Jachens, R., and Slater, L. E., 1984, Strain and Gravity Changes Observed at Pearblossom, California, and Strain Changes Observed at Palmdale, California: Evidence for Correlation (abs.): EOS, v. 65, n. 45, p. 993.

Linker, M. F., Langbein, J. O,, and Estrem, J. E., 1984, Horizontal Deformation in the Southwestern Moat of the Long Valley Caldera, Eastern California for the Period 1983.5 - 1984.6 (abs.): EOS, v. 65, n. 45, p. 1117.

Figure 2. Line-length changes in mm observed using a two-color geodimeter for the baselines shown in Figure 1. Each error bar represent one standard deviation. The vertical line through the data indicates the date of the Round Valley earthquake.


Figure 1. Map showing the locations of the baselines that comprise the 2-color geodimeter network within the Long Valley Caldera near Mammoth Lakes, California.

275

CASA-SHARK

CASA-TAXI

CASA-CONVICT

CASA-TILLA

CASA-LOOKOUT

CASA-KRAK

CASA-RODGER

CASA-HOT

CASA-KNOLLS

CASA-LOMIKE

CASA-MIKE

CASA-MINER

CASA-SLIDE

CASA-SHERWIN

CASA-SEWER

1984   1985

(L — Lo) in MM
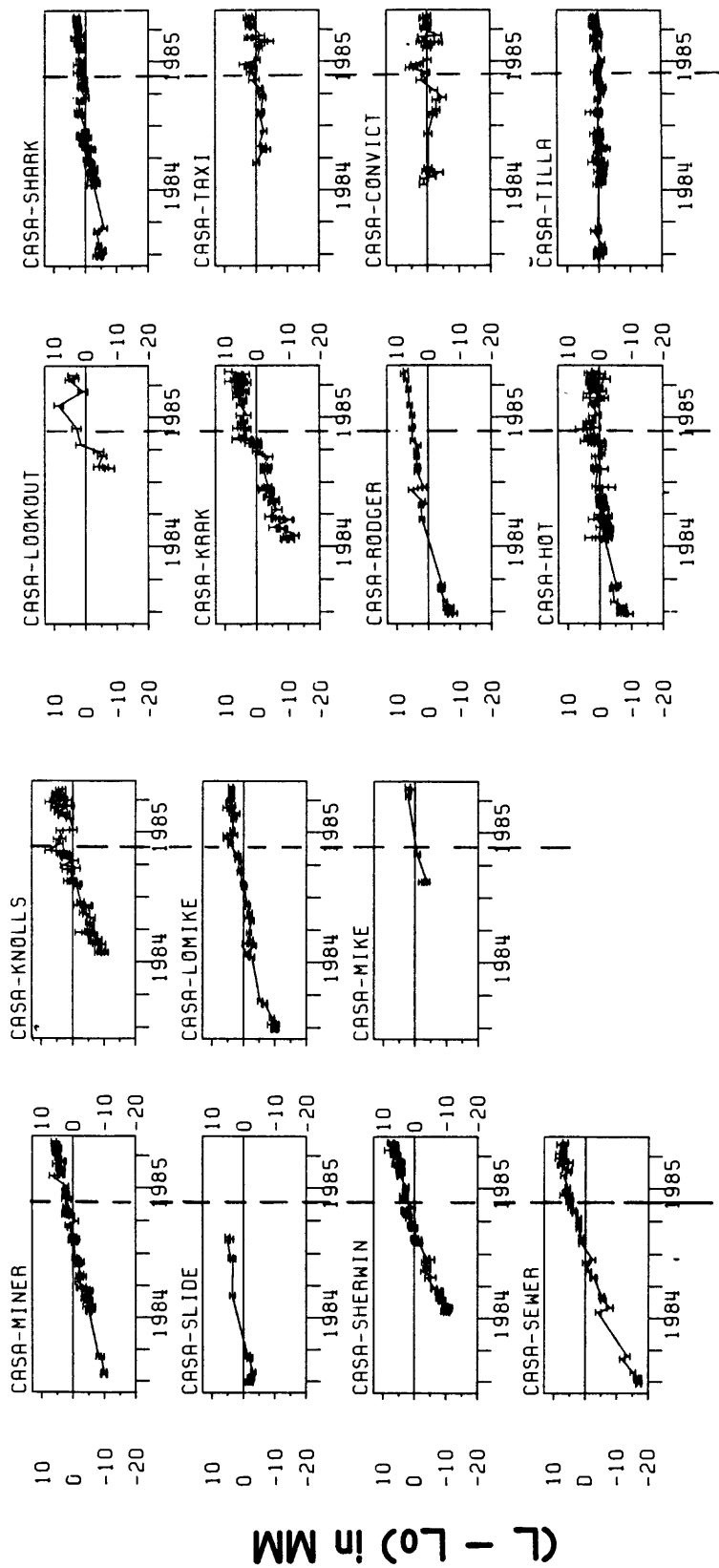
Figure 2.   (continued)

276
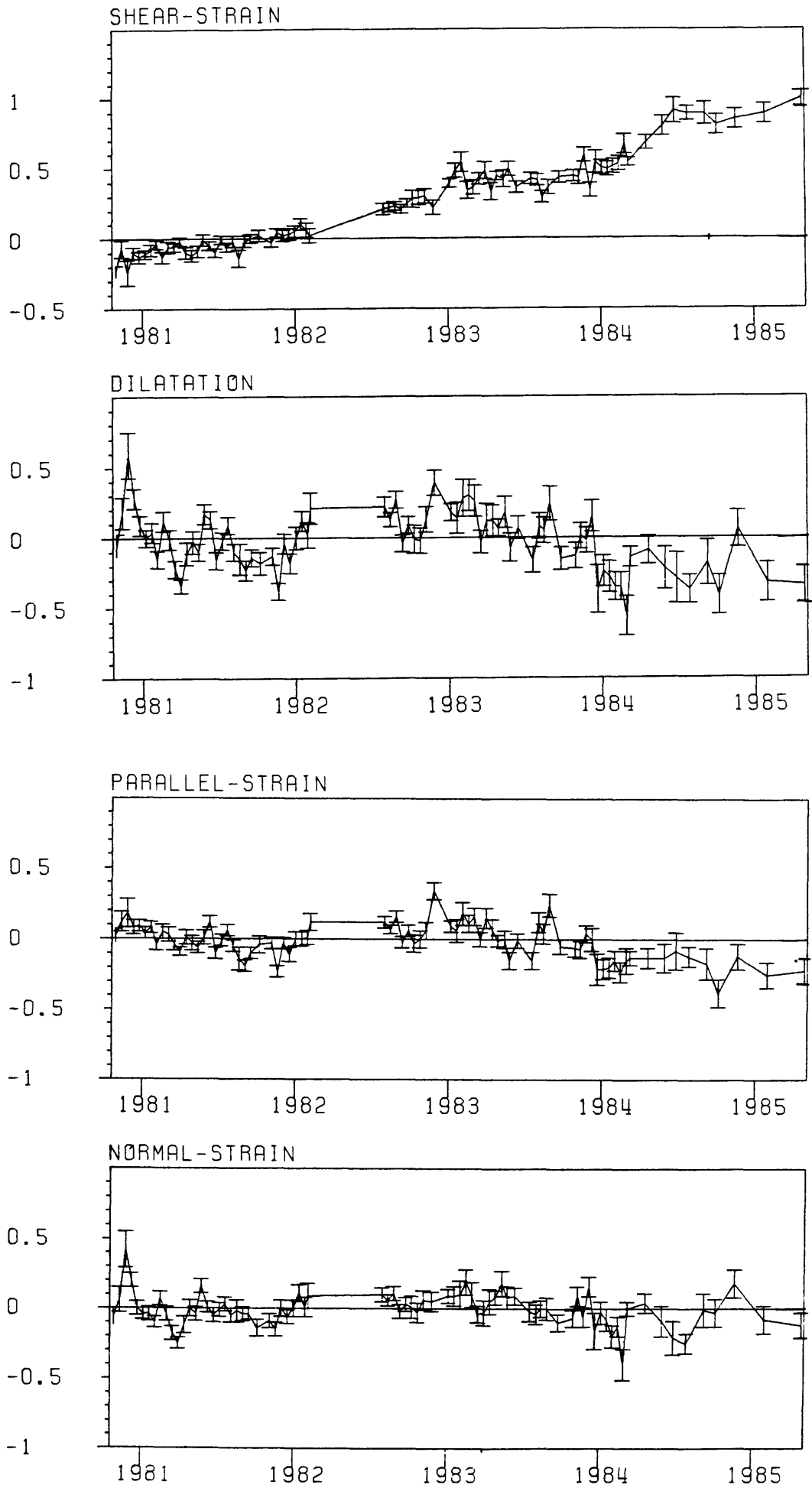
Figure 3. Extensional strain changes inferred from line-length measurements for an 11 baseline network near Pearblossom, California. The strain components are tensor quantities and have been rotated into a coordinate system that is normal and parallel to the local strike of the San Andreas fault (N65°W).

STRAIN CHANGES in PPM

277

Carbon Fiber Strainmeter Studies in Southern California

14-08-0001-21240

Peter C. Leary
Department of Geological Sciences
University of Southern California
Los Angeles, CA 90089-0741
(213) 743-8034

Objective: To monitor fault zone creep and fault block strain in the vicinity of major southern California faults.

Data Acquisition and Analysis: The unprocessed 1984 record of five tunnel-sited carbon fiber strainmeters at 3 locations in the San Gabriel Mountains and one invar steel fault zone creepmeter near Palmdale, CA are shown in Figures 1-6. The dominant registered strain is provided by overall drift (typically ~1 μstr/yr apparent contraction) and local temperature induced strain. The magnitude of instrument response to the thermal cycle is gauged by the solid earth tide amplitude retained in the trace. Rainfall is an important factor in short term strain variations in the late fall, winter, and early spring months.

The instrument records vary according to tunnel and site character. DT1 is more deeply buried in a cliff face than is DT2 and shows correspondingly reduced amplitude environmental effects. BQ1 and BQ2 are similarly situated in a tunnel in a ridge, and show similar responses to the seasonal signal at an amplitude comparable with the exposed DT2. JK1 is the driest site, and shows an annual temperature response remarkably like the shallow temperature record at the creep site (Fig. 6b). The short term temperature fluctuations at JK1 are seen at DT2, but not at DT1 and BQ1-BQ2. The reason appears to be that BQ1-2 responds to thermal driving function that is attenuated, and delayed by an incompetent "thermal blanket" of loose rock whereas at DT2 and JK1 the surrounding rock, being more competent, transmits higher frequency thermal signals. DT1 is sufficiently buried to retard and attenuate the thermal signal seen at DT2.

The creepmeter record before mid-September 1984 was subjected to thermal noise generated by a steel vault installed to facilitate record recovery. The vault was insulated from the air temperature variation resulting in a vastly improved creep stability as seen in the remaining months of 1984. The short term temperature variation is reduced [Fig. 6b], while the season temperature change continues to propagate through the soil layer. The creep signal is, however, stable against seasonal variations in temperature because the soil layer is uniform in composition.

The concurrence of increased local seismicity and strain detected by the nearby two-color laser in the spring and early summer of 1984 may be reflected in the variation of the temperature and corrected creep signal (Fig. 7). Discrete creep steps such as those reported by Leary and Malin (1984) for 1979 activity at the same creep site were not observed.

Publications: Leary, P. C. and P. C. Malin, Ground Deformation Events Preceding the Homestead Valley Earthquakes, B.S.S.A., vol. 74, p. 1799-1817, 1984.
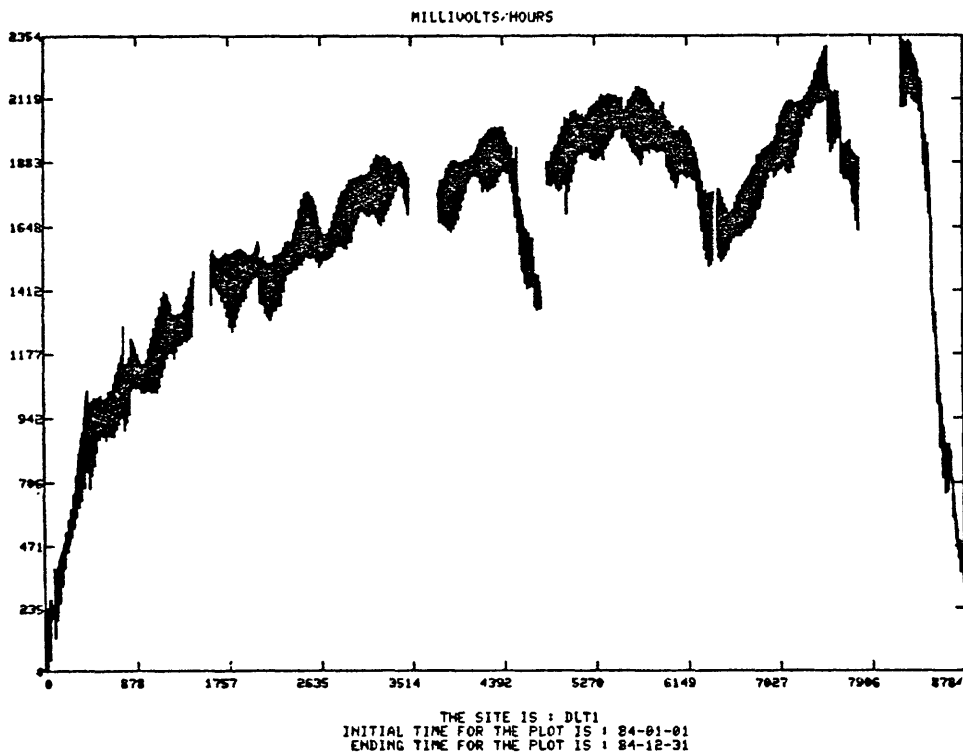
MILLIVOLTS/HOURS

THE SITE IS : DLT1
INITIAL TIME FOR THE PLOT IS : 84-01-01
ENDING TIME FOR THE PLOT IS : 84-12-31

Figure 1.   DT1-1984

MILLIVOLTS/HOURS

THE SITE IS : DLT2
INITIAL TIME FOR THE PLOT IS : 84-01-01
ENDING TIME FOR THE PLOT IS : 84-12-31

Figure 2.   DT2-1984

MILLIVOLTS/HOURS

THE SITE IS : BQT1
INITIAL TIME FOR THE PLOT IS : 84-01-01
ENDING TIME FOR THE PLOT IS : 84-12-31

Figure 3.   BQ1-1984

MILLIVOLTS/HOURS

THE SITE IS : BQR2
INITIAL TIME FOR THE PLOT IS : 84-01-01
ENDING TIME FOR THE PLOT IS : 84-12-31

Figure 4.   BQ2-1984

MILLIVOLTS/HOURS

Figure 5.   JK1-1984

MILLIVOLTS/HOURS
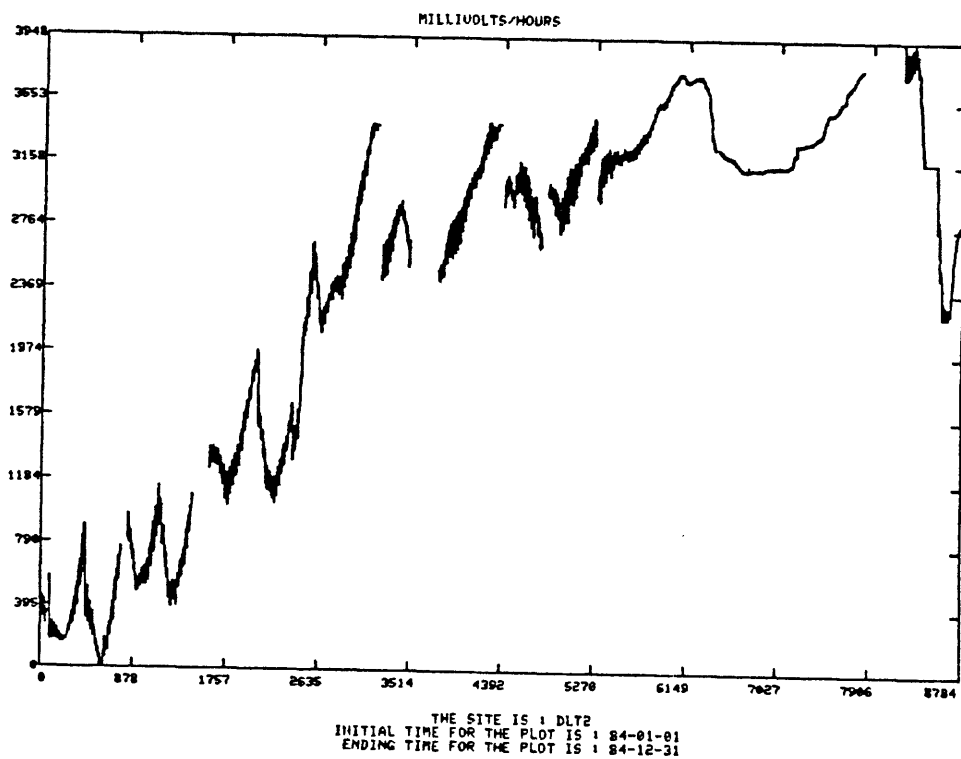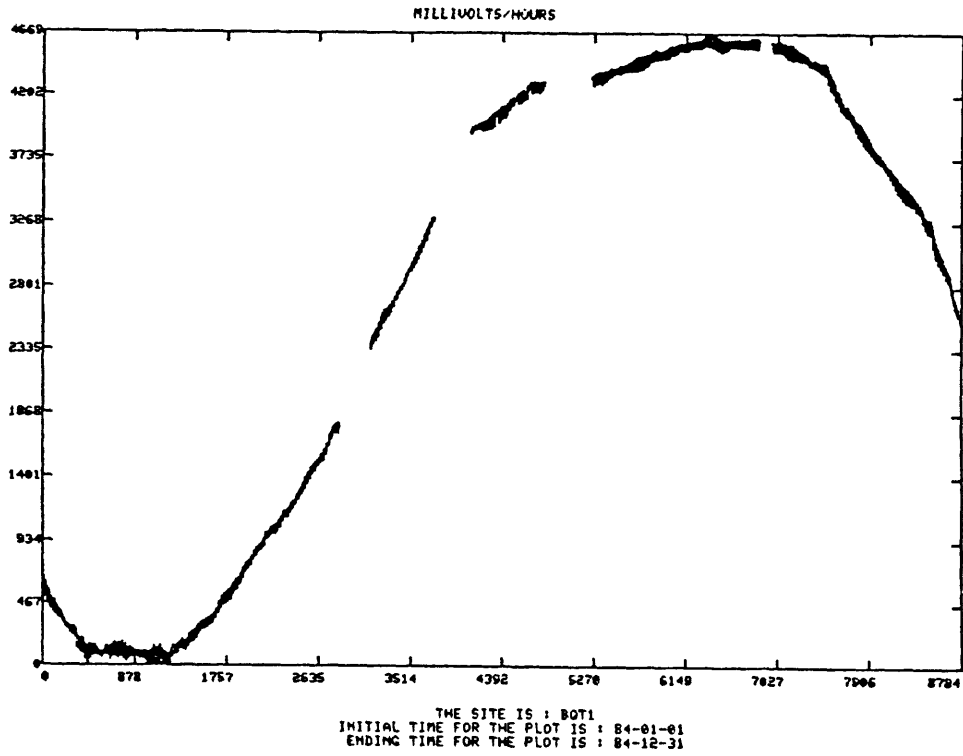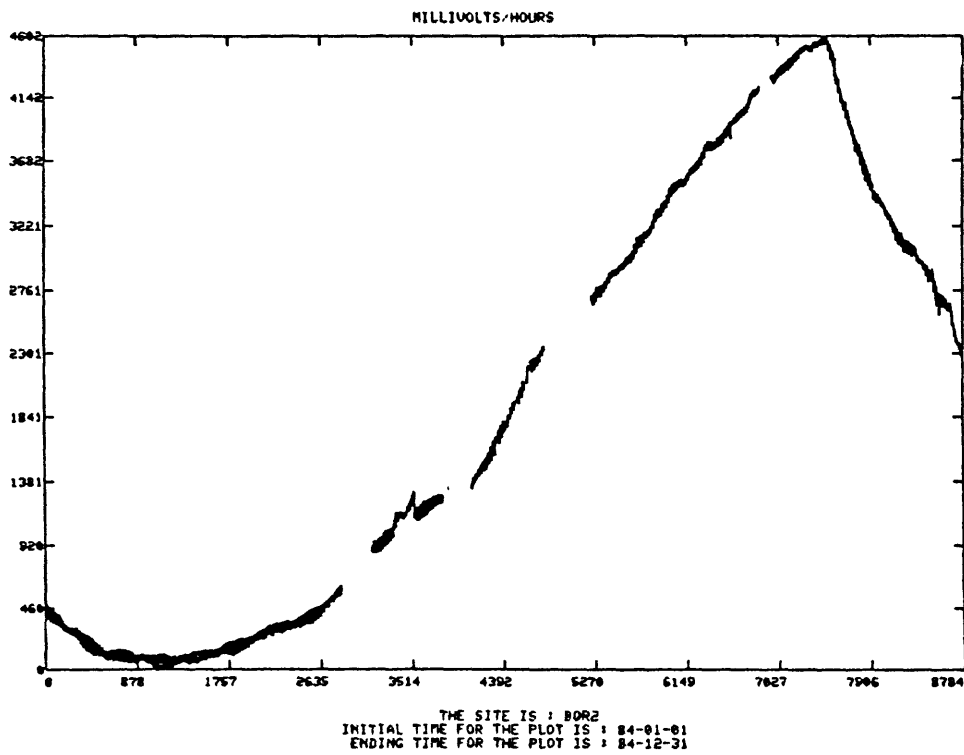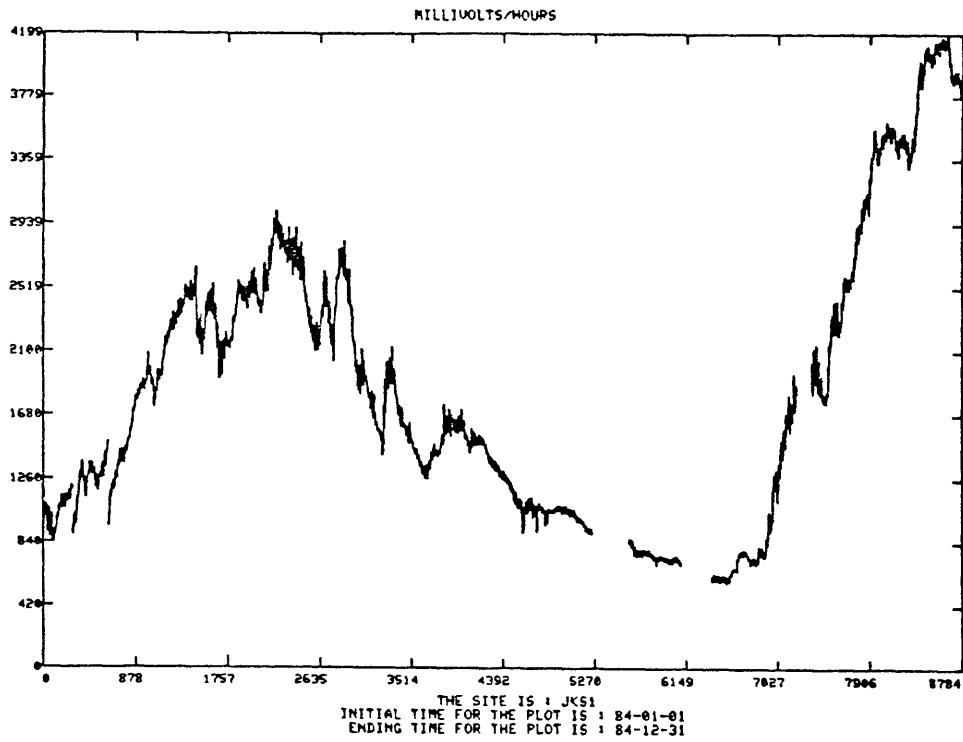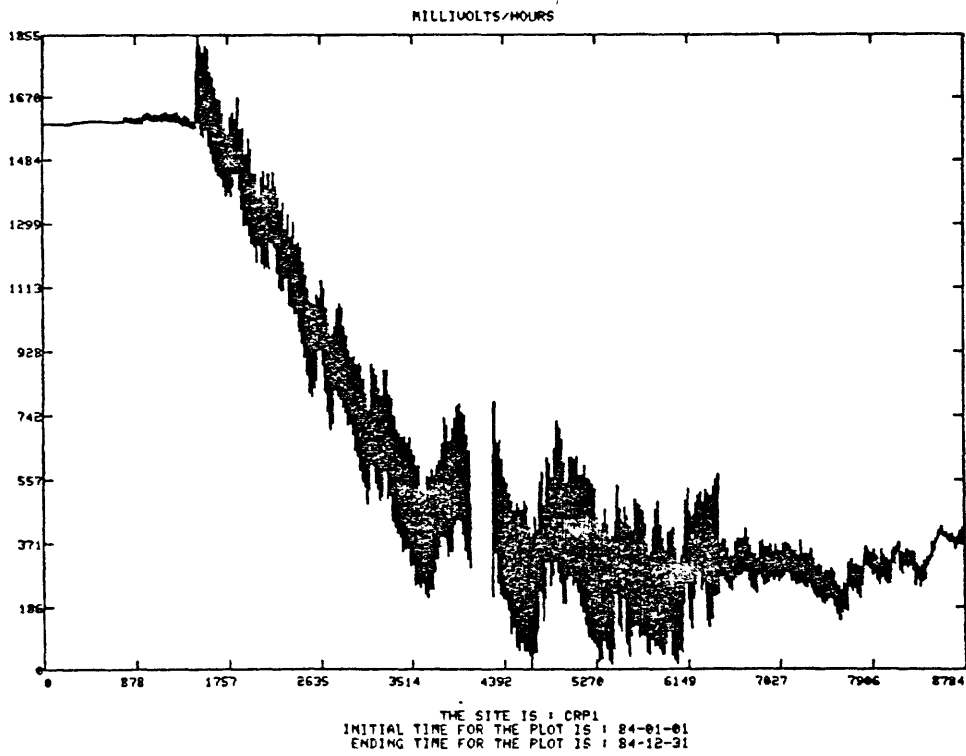
Figure 6a.   Faultzone Creepmeter.

MILLIVOLTS/HOURS
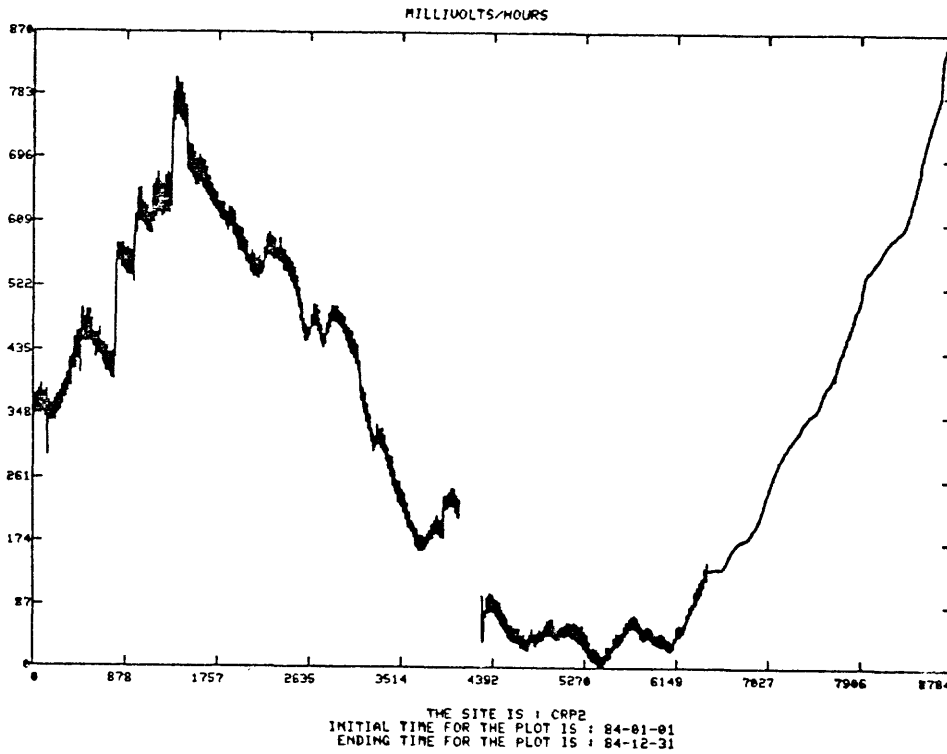
Figure 6b. Faultzone creepmeter vault temperature.

Figure 7. Expanded creep, temperature and creep residual
(temperature corrected) records for 3/84 to 8/84.

CREEP-BLU TEMPERATURE-RED RESIDUAL -BLC

CREEP

TEMPERATURE

RESIDUAL

MAR84   SEP84

TIME (MONTH)

282
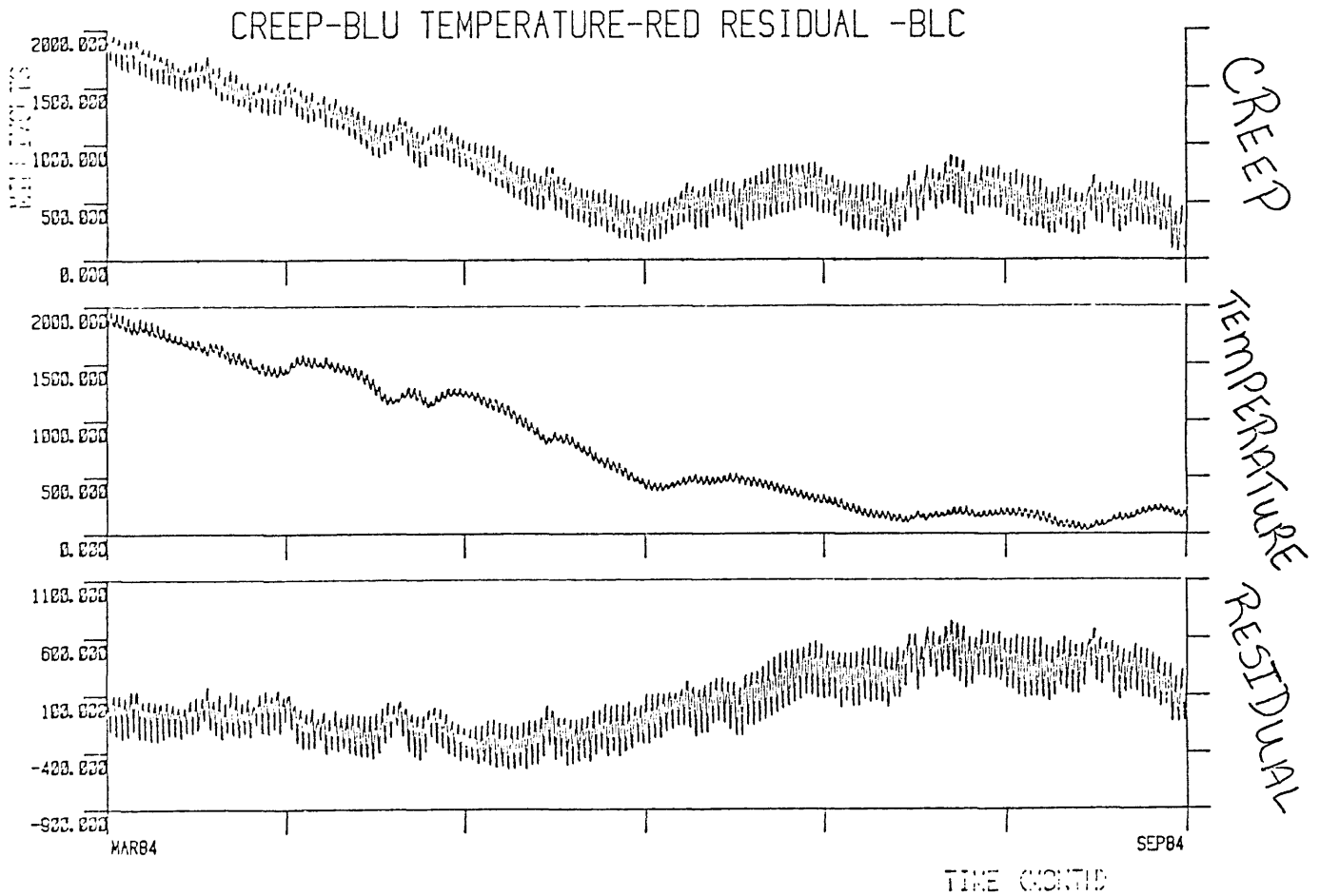
Parkfield Prediction Experiment

9930-02098

A. Lindh
Branch of Seismology
U. S. Geological Survey
345 Middlefield Road, Mail Stop 977
Menlo Park, California 94025
(415) 323-8111, Ext. 2042

Investigations

Work continued on:
1. The Parkfield Prediction Experiment, and
2. Long Term Earthquake Probabilities along the San Andreas system.

Results

Parkfield
    Prediction
    Bill Bakun and Tom McEvilly's work on Parkfield reccurence models was presented to the Fall 84 NEPEC meeting, and was endorsed as a long-term earthquake prediction; the rest is history.

    Seismicity monitoring
        Parkfield Relocations
    Katy Poley has completed relcoating all the Parkfield seismicity since 1969 with a model based on Nowack's inversion. Locations of events near the '66 hypocenter have been further refined by using a suite of well located near-by events as master events. This data set has been used to establish preliminary emperical criterian for potential Parkfield foreshocks, and Bruce Julian has implimented an improved alarm algorithem on the UNIX 11/70 that will trigger for any M1.5, or two M1 within 72 hours, within the hypocentral zone. This work is being prepared for publication and will be presented to the next NEPEC meeting.

        RTP monitoring and alarms
    Working with Rex Allen, Jim Ellis, and Sam Rodriquez, Sorsby (an SLCII monitor from Digital Pathways) has evolved to the point where he now monitors the RTP's and the 11/23 in realtime, attempts to correct faults when they occur, and calls for help when he can't. JoAnn Vinton and Gary Maxwell have upgraded the 11/23 software so it now receives the data from both RTP's. Bruce Julian has greatly improved the alarm software on the 11/70 so it now provides versatle and reliable service. The 11/70 alarm messages are passed to Sorsby, who then places the phone calls to people and/or beeper services, making that function more reliable. Barbara Bekins is looking into upgrading or replacing the 11/23 buffer function, a necessary step for long-term reliability. I have documented and improved Sorsby's software, and ordered a second unit so as to permit a more fault tolerant configuration.
    Barry Hirshorn is now reviewing all the RTP data on a daily basis, cleaning it up, and passing it to CALNET. He is also beginning to provide valuable surveillance of station and network quality on a daily basis. We had

hoped to have this operation integrated with CUSP processing on the branch 11/750 by now, but the CUSP software on the /750 is not quite ready yet, thanks largely to my footdragging on my part of it.

Station performance monitoring

Weekly to bi-weekly meetings are held on a regular basis at which the RTP station summary, Sam Stewarts CUSP station summary, and Barry's analysis of the RTP data are used to evaluate Calnet station performance. The constructive participation of people with differing perspectives on the problem has at times proven very valuable in identifying problems and finding solutions. The diligence of Wes Hall and Charles Dais in pursuing phone line and in-house problems, and Tom Burdette and John Kemp in pursuing radio and microwave problems in the field has led over the last year to steady progress in slowly reducing telemetry problems. The development by John Van Schaak, Fred Fischer, and Wes Hall of improved telemetry hardware (with a tip of the hat to Sean-Thomas Morrisey of St. Louis University) has resulted in a growing number of units in the field with honest to heaven 50-55 db dynamic ranges, and very stable VCO oscillators.

While keeping such a large net up to snuff is a never-ending process, we should not lose site of the fact that over the last year the consciencious work of these gentlemen and their cohorts has led to a significantly better quality network. In some areas, however, further progress will depend on the powers-that-be coming up with some money for investment in spares and back-up units; money is tight but it doesn't make any sense to have invaluable human expertise wasted for lack of a few spares -- sometimes it's discouraging too.

Cooperative efforts

Drilling

With monumental help from Tom Burdette, a cooperative program in downhole instrumentation at Parkfield is making significant progress. Collaboration between Peter Malin of UC Santa Barbara, Tom McEvilly and Rich Clymer of UC Berkeley, John Brederhoft and John Singer of Water Resources, and John Sims of the Branch of Faulting and Strong Ground Motion, has led to the selection of several sites for downhole seismic instrumentation and deep water wells. John Brederhoft currently has three instrumented wells in the area that are drawing solid earth tides, and Peter has just completed installation at two sites of three-component seismometer packages at depths between 500 and 1000 feet. More drilling is planned in the coming months. Peter and John Singer "discovered" granite at 500' depth at the top of the hill on Vineyard Canyon (west of the San Andreas, about 3 km SE of the '66 epicenter), opening up new possibilities for down-hole strain instrumentation near Middle Mountain.

Leveling

John Estrem of the USGS, and Art Sylvester of UCSB are cooperating in efforts to frequently measure 1-3km long level lines situated normal to the fault at Parkfield. Preliminary analysis of the three to five years of data available for two of these lines -- one crossing the fault at Parkfield and one on the Pomona property on the west flank of Middle Mountain -- shows tilt down to the southwest at rates of 1 to 3 micro-radians per year. Comparison with the 15 km long crossing line through Parkfield put in by Bob Wilson suggests that most of this tilt is confined to within a few km of the San Andreas. Back of the envelope calculations indicate that these results are consistent with a shallow dislocation pile-up to the northwest of Parkfield beneath Middle Mountain, something which is also strongly indicated by the

creep and geodetic data. We hope to get one or two additional short crossing lines installed this summer, one along the Turkey Flat Road and another near Gold Hill. Measurement schedules of 3-4 repeats per year may be possible.

Ross Stein has initiated a leveling program at Parkfield including a longer line (10-15 km) that loops around Middle Mountain. The encouraging results on the shorter lines lend hope that this line will contribute to understanding the slip regime in this critical transition zone.

Tilt meters

Tom Burdette is helping Sean-Thomas Morrisey with planning and site investigations for two or three clusters of his improved bubble tilt-meters at Parkfield. Frank Wyatt has proposed to the external program development of a long-base-line tiltmeter suitable for installation at Parkfield. In light of the encouraging results obtained on short level lines in the Parkfield area, this would be a very desirable addition to the experiment, but the logistical difficulties associated with such a development, and the relativley short time available before 1988, are formidable difficulties.

Structural Studies

Bob Jachens and Andy Griscom of Branch of Regional Geophysics have started working on unraveling the complex three-dimensional configuration of crustal blocks in the Parkfield area, and John Estrem and Carter Roberts have started collecting additional gravity and magnetic data where detail is needed. In my opinion it is absolutely vital that this effort be encouraged AND adequately funded; it is absolute madness to consider going ahead with very expensive refraction, reflection, or deep-drilling efforts at Parkfield without first extracting all the information that can be gleaned from potential measurements. Many of the juxtaposed terraines at Parkfield have distinct gravity and/or magnetic signatures, and already vital information concerning the Gold Hill block has been obtained.

John Sims is continuing with detailed geologic mapping along a 1-2km wide swath flanking the fault at Parkfield, and has provided critical insight toward decisions concerning drill hole and instrument siting. John and Bob Jachens are beginning to bring together their various data sets in an effort to better understand the deep structure.

Earthquake Probabilities

Work continues with Bill Ellsworth on long-term recurrence rates and probabilities along the San Andreas system. The probabilites in our long overdue paper on that subject are being redone to reflect recent progress in formulating the conditional probability problem. In most work to date on the problem the standard deviation of the probability density function has been treated as a constant fraction of the recurrence interval; this sometimes results in logical conundrums when comparing segments for which we have extensive information, with those where little is known. We are now treating the standard deviation as a variable which DECREASES as the amount of significant information on a segment INCREASES, this results in sharply peaked probability functions (ie. long-term predictions) when the information is good. When the information on a segment is limited, the standard deviation is increased to reflect the resulting uncertainity, and the conditional probabilites asymtotically approach the unconditional Poisson estimate. This approach leads to smoother conditional probability maps which merge with traditional (ie. unconditional) hazard maps in areas where only approximate

recurrence intervals, and/or b-slope type information is available.

Reports

Bakun, W. H. and A. G. Lindh, 1985, The Parkfield, California, earthquake prediction experiment, Science, in press.

High Sensitivity Monitoring of Resistivity and Self-Potential Variations in the Hollister and Palmdale Areas for Earthquake Prediction Studies

14-08-0001-21235

Theodore R. Madden
Massachusetts Institute of Technology
Cambridge, Massachusetts 02139

We are attempting to understand the nature of the noise in our telluric signal comparisons in order to find ways of improving our sensitivity. It seems we have bottomed out in our analysis using purely statistical data analysis methods. In this effort, we are making extensive use of the graphics capabilities of our new computer facilities. It appears that some of the residuals are signal related, which is a hopeful sign for improving the analysis, but the exact cause of these residuals has not yet been determined. Possible candidates include source field gradient effects, phase shifts across the array, and diurnal or semi-diurnal near-surface resistivity variations. Equipment limitations such as phone line leakage and non-linearities in the recording are also possible factors. We are also seeking to identify electrode noise and to reduce its effects using the redundancy in our array.

The long period telluric signals from our arrays have been analyzed using magnetic observatory data for earth conductivity structure. The E/H amplitudes and phases at the long period (24 hours and over) are quite anomalous and seem to require a high resistivity barrier going to considerable depths. These results apply to both the Palmdale and Hollister data.

Seismicity Studies for Earthquake Prediction in
Southern California

14-08-0001-22000

Dr. Karen McNally
Charles F. Richter
Seismological Laboratory
Earth Sciences Board
University of California,
Santa Cruz
Santa Cruz, California   95064
(408) 429-4137

Objectives:

To determine the statiscal correlation of earthquake
clusters (excluding aftershocks) with subsequent moderate and
large mainshock events in southern California.   We determine the
number of earthquake clusters that are followed by large
mainshocks compared with those that are not. Similarly, the
number of mainshocks that are preceded by clusters, and those
that are not, must be ascertained. These correlations will be
determined as a function of (1) the magnitude of the mainshock,
(2) the minimum magnitude threshold of the seismicity that
constitutes a cluster (clustering increases with decreasing
magnitude threshold of the seismicity data), (3) the time between
the clustering and the mainshock, and (4) the distance (up to ~50
km) between the cluster and the mainshock. The results will be
formulated as probabilities for intermediate term (few weeks to
few years) prediction applications, with appropriate scaling for
compatability with probabilities that may be used for long term
(few years to few decades) predictions. A computer program for
automated seismicity monitoring and probability determinations
will be written.

Progress Summary:

Computer programs and data are now being synthesized and
augmented. New statistical tests for monitoring cluster behavior
are being implemented to supplement existing algorithms. The
database from the Long Valley, California region is being analyzed
for calibration of results from southern California. (The
intense Long Valley clustering is consistent with, and
supplements, the sparser southern California clustering dataset,
for establishing statistical monitoring criteria.) Grant funding
for this project began only 3 months ago, thus more information
will be available for the next summary.

Tiltmeter and Earthquake Prediction Program in S. California and at Adak, AK

14-08-0001-21244

Sean-Thomas Morrissey
Saint Louis University
Department of Earth and Atmospheric Sciences
P.O. Box 8099 - Laclede Station
St. Louis, MO 63156
(314) 658-3129

I: Task 1: The Tiltmeter System

Objective: To continue to improve the performance of bubble sensor tiltmeter systems and to investigate other sensor systems for use in moderate depth boreholes, seeking relatively low-cost, readily deployed instrumentation.

Accomplishments: In assembling and testing the new tiltmeter electronics systems for a related project, a study was made of the residual thermal noise of the system, which has been about 5 nano-radians $(10^{-9})/^{\circ}C$ for most systems. It was found that a small frequency drift of the excitation oscillator was the major cause of the thermal errors, mostly due to variations in the reactance of numerous circuit elements that would be thermally caused and frequency sensitive. The crustal stabilized digital sine excitation oscillator that was modified for the prototype variable-inductance pendulum sensor was tried, with remarkable results. So the other C-MOS oscillators were converted, and the tiltmeter systems re-tested. Now the thermal drift is less than 0.5 nano-radian $/^{\circ}C$, and most of this is due to thermal changes in the reference bridge resistors used in the substitute bubble sensor.

Little has been done on the new pendulum transducer development. A borehole-sized (28 mm diameter) biaxial transducer was built, and its' linearity was verified over a range of 100 microns to be as good as the differential micrometer used. The output, using the bubble sensor electronics, is 100 mv/micron. We hope to have a complete prototype completed soon, since field qualification will take some time, and the supply of working bubble sensors is insufficient for the number of installations planned. In other developments, the new auto-zeroing electronics has been fully qualified and new zeroing systems provided for all the Palmdale tiltmeters.

II: Task 2: The Installation Method

Objective: To improve the installation methods for borehole instruments with a goal of installing them as deep as 100 meters.

Accomplishments: The Palmdale tiltmeters still await installation, which has been further delayed by other committments and obligations making demands of the available manpower. Hopefully, they will be installed in late spring or early summer. The portable winch/headframe system designed for handling the pre-leveling installation tool was not

completed before winter set in, so installation tests at the CCMO test site will be done this spring. No major problems are anticipated, since the prototype systems functioned well.

III: Task 3: The Digital Data System

Objective: To continue to develop and operate a digital data acquisition system to acquire geodetic data and to thoroughly monitor the environment of the instrument installations.

Accomplishments: The Adak digital system continues to function well, with floppy disks arriving every 8 days from Adak with multiplexed data from the five remote 14-channel digitizers. We have continued to have problems repairing these remote units when they are damaged by lightning or otherwise fail. (Spontaneous failure has been rare, though, with only about 1 unit/year.) They are 1978 vintage electronics, and parts are not available, so four of the 12 on hand have become donors for the others. Major progress has been made on the replacement remote digitizer, built around an RCA COSMAC (1802 microprocessor) system. A fully operational prototype has been assembled and programmed (in E-Prom) to exactly emulate the behavior and output format of the older units. However, a 16-bit digitizer is used, allowing an order of magnitude increase in dynamic range. Standby power is 22 ma at 7.5 volts. Field testing should begin shortly. Hardware problems are expected to be minimal, since all the complexities have been kept in the firmware programming.

IV: Task 4: Data Interpretation

Objective: To process the digital data and make efforts to remove the environmental noise from the data, so as to establish the intrinsic long term stability of the tiltmeters. Various analysis techniques are then utilized to present the data in meaningful formats such that any precursory tilt events would become evident.

Accomplishments: The post-doctoral research assistance is no longer available to this program, so data interpretation has not progressed as expected. However, the Adak data has continued to be processed within a week of its being recorded, and the data file systems maintained.

A further effort was made to analyze the Adak data for any possible long-term secular tilts. Since the data has a predominant annual cycle, the study focused on fitting this by least squares processing to the borehole and surface temperature data. This process quite successfully removed the annual cycles from the data, leaving shorter (approximately monthly) cycles related to barometric pressure and storms. This data was then fitted to linear regression lines that show some coherent long-term secular behavior between tiltmeters at the same site. Figure 1 shows the raw data for a 20 month segment of the Adak west site instruments, East-West data; notice that the annual thermal cycles are not necessarily of the same polarity. Figure 2 shows the thermal data that has been smoothed (by cubic spline) and de-meaned before fitting to the tilt data. Figure 3 shows the residuals after this process. There are still some remnants of the annual cycle, probably due to expected

phase differences that would be better handled by deconvolution in the frequency domain. Nonetheless, remarkable agreement between the data is evident. Figure 4 is the linear regression lines fit to the data. These show that the west site hill is tilting down to the west at about 2.9 ppm/year.

A preliminary special technical report was written on this study of secular tilting at Adak, covering all the data for the last four years. While the results so far are encouraging, much additional work needs to be done.

Reports:

"An Estimate of Secular Tilt from the Adak, Alaska, Tiltmeters," a preliminary draft, February 1985, not published.

"Recent Developments in Shallow to Intermediate Depth Tiltmeter Instrumentation," Abstract for Fall AGU, EOS, November 6, 1984.

Proposal Submitted:

In response to RFP 1586, a proposal to continue this effort was submitted to the U.S. Geological Survey.

S.T. Morrissey
Senior Research Scientist
21 April 1985

Adak Tilt Data, 20 Mo.
West Site, East-West Data
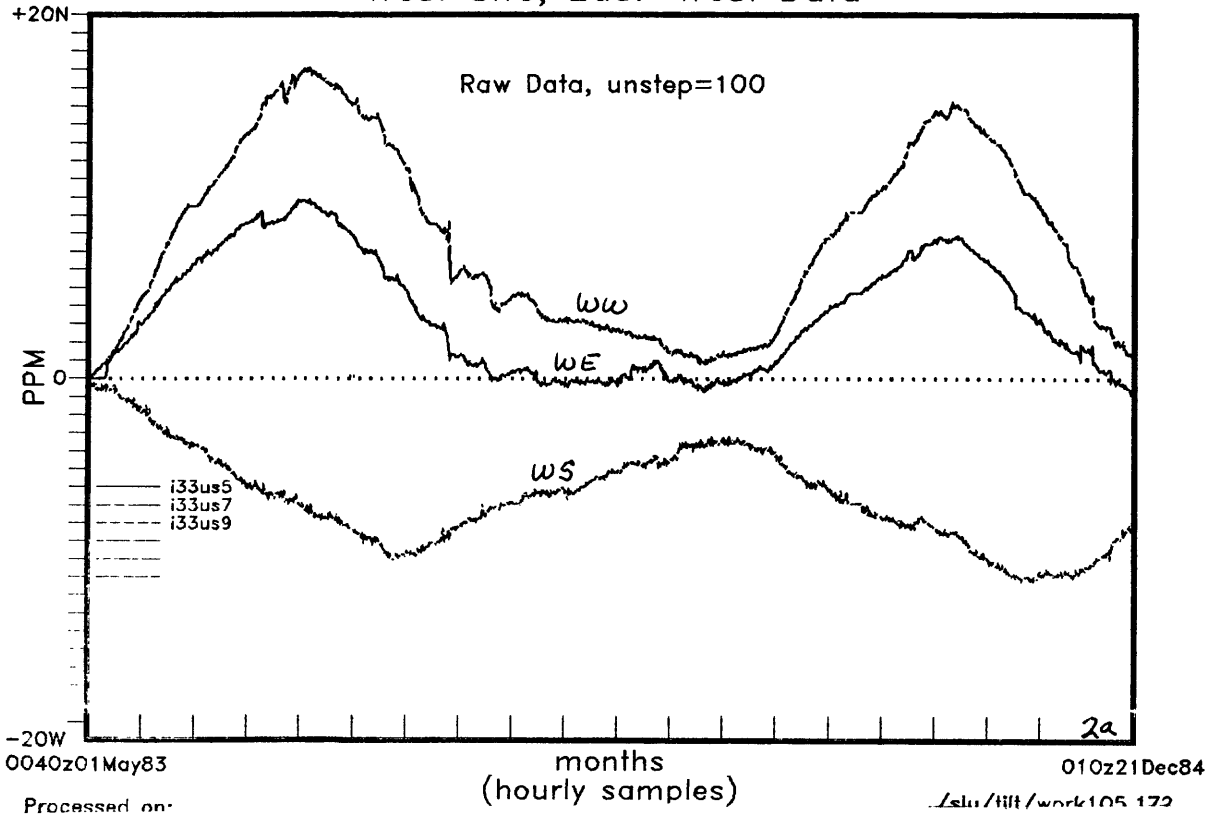
Raw Data, unstep=100

WW

WE

WS

i33us5
i33us7
i33us9

+20N

PPM

0

-20W

0040z01May83

months
(hourly samples)

010z21Dec84

2a

Processed on:

/slu/tilt/work105.172

Adak Thermal Data, 20 Mo.   *Figure 2*
Borehole and Surface temps

initial offsets removed

Borehole

Surface

iusthrmb
iusthrms

+10

degC

0

-10

0040z01May83

months
(hourly samples)

010z21Dec84

292

Adak Tilt Data, 20 mo. P-2 figure 3
West Site, East West data

Residual Tilt after thermal corrections

months
(hourly samples)

010z21Dec84

/slu/tilt/work105,172
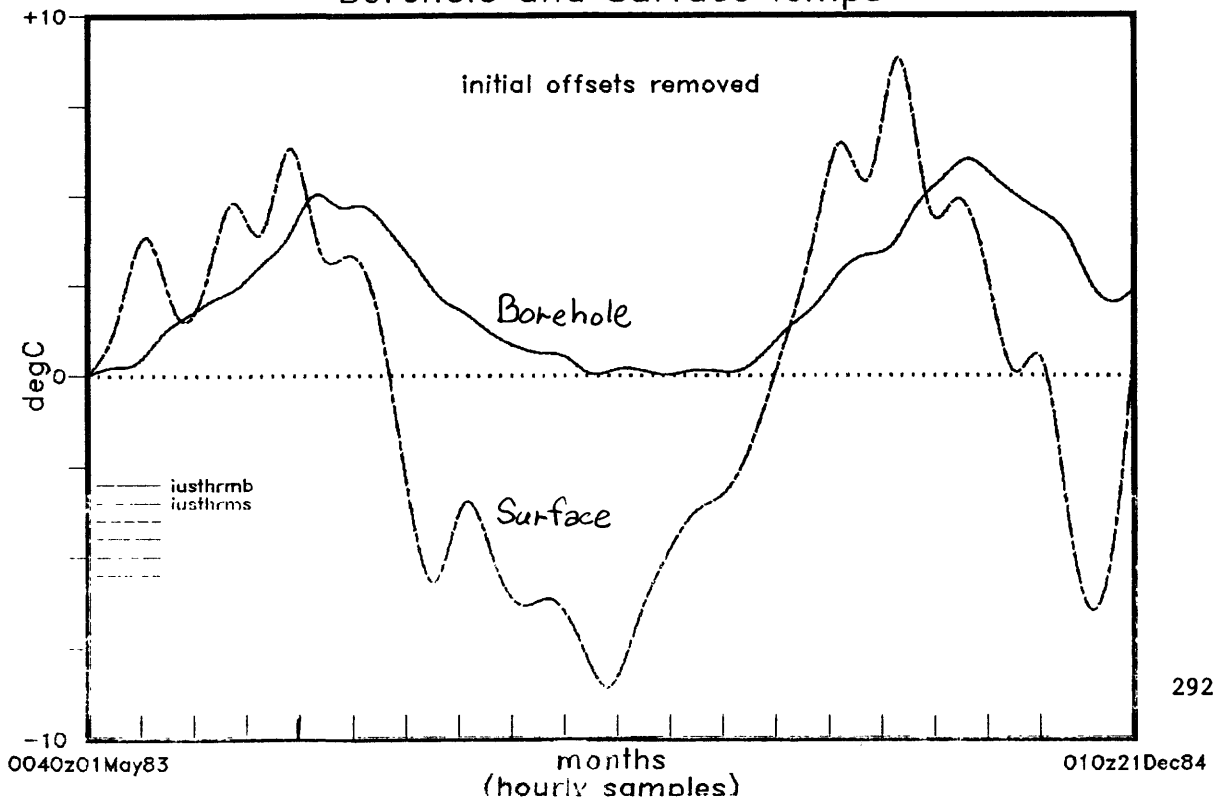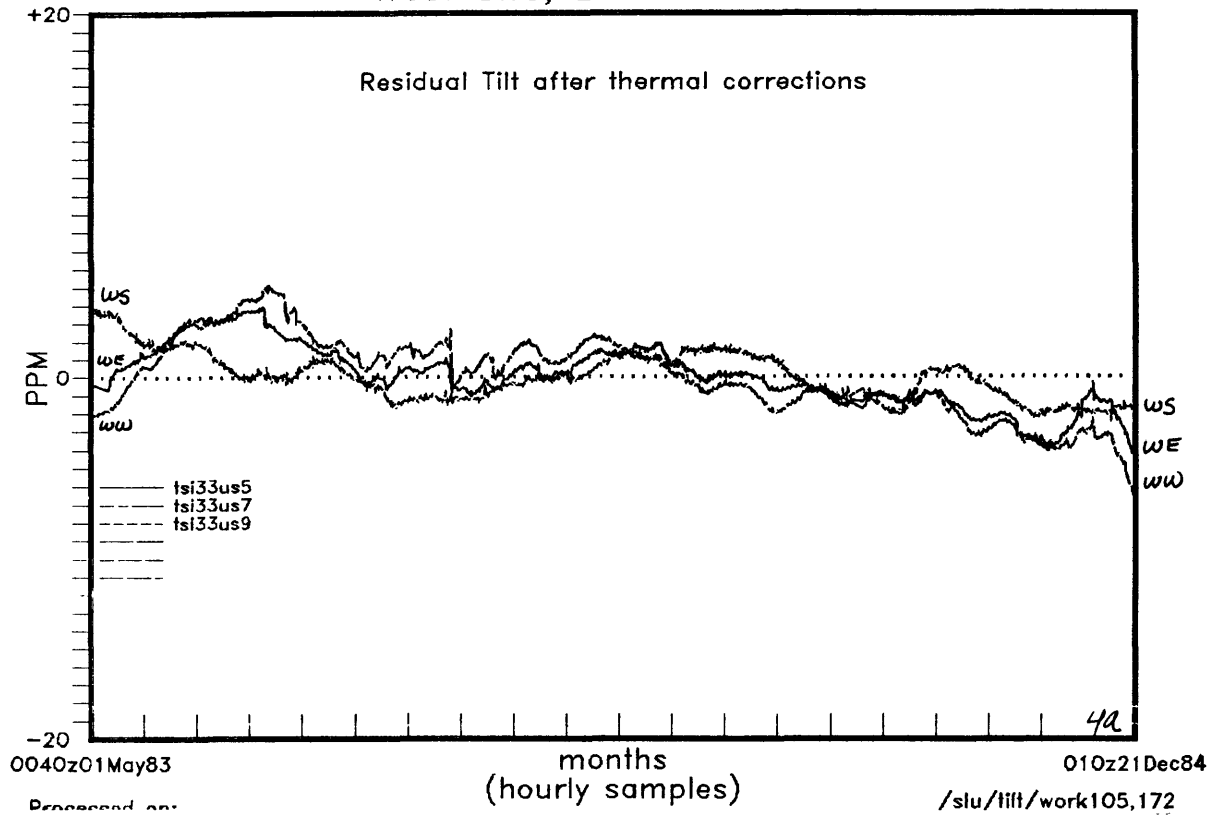
Adak Tilt Data, 20 mo. figure 4
East–West data, West site, X2

Least squares linear fit of residual tilt

293

0040z01May83

months
(hourly samples)

010z21Dec84
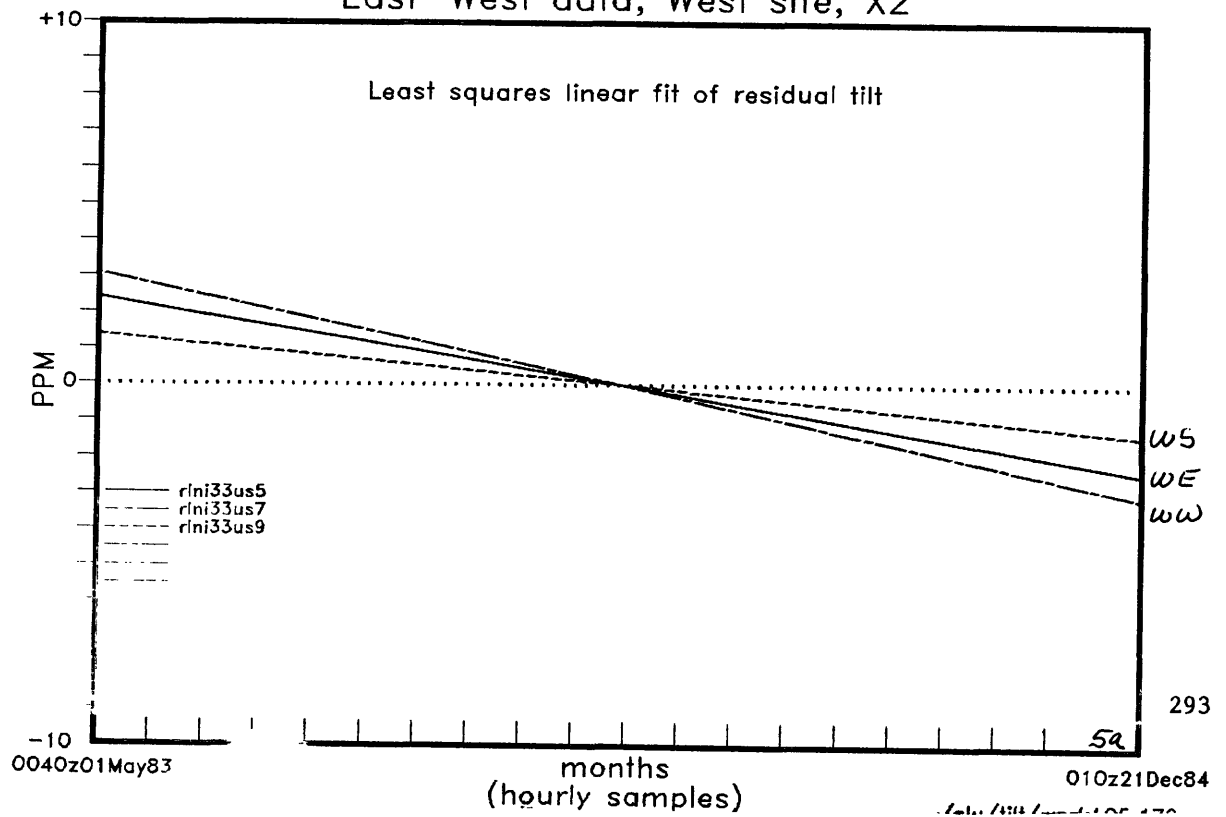
EXPERIMENTAL TILT AND STRAIN INSTRUMENTATION

9960-01801

C.E. Mortensen
Branch of Tectonophysics
U.S. Geological Survey
345 Middlefield Road, MS/977
Menlo Park, California 94025
(415) 323-8111, ext. 2583

Investigations

1. Implementation of the GOES satellite telemetry system for the acquisition of low frequency data suffered a major setback from August, 1984, through March, 1985, as all 25 of the Sutron Data Collection Platforms (DCPs) failed due to a common, malfunctioning component. All DCPs were returned to Sutron for warranty repair. Twenty-two DCPs have been returned from repair and, on retesting, 19 of those were accepted as operational within specifications. The DCPs are currently being installed in the field following the testing. To date DCPs are operating at the following locations:

REGION	LOCATION	INSTRUMENT
Central CA	Slack Canyon	creepmeter/hydrogen
Parkfield, CA	Middle Mountain	creepmeter/hydrogen
Parkfield, CA	Work Ranch	creepmeter
Parkfield, CA	Gold Hill	creepmeter/hydrogen
Parkfield, CA	Gold Hill	tiltmeter/cluster
So. CA, Morongo Valley	Old Canyon House	magnetometer
S. CA., Morongo Valley	Little San Bernardino	magnetometer

Eight DCPs having 16-bit A-to-D converters have been received from Sutron and are being tested. These DCPs actually have 17-bit resolution (16-bit plus sign). These units seem to be operating well and should provide exceptional dynamic range for broad-band sensors once some critical omissions in the software menu are corrected by Sutron.

A True Time radio clock has been installed by Grey Jensen and interfacing software has been written by Jim Herriot and Stan Silverman to merge exact time with the incoming data from the satellite receiver. Some bugs that appear to originate in the receiver remain to be rectified by Sutron.

2. Networks of tiltmeters, creepmeters and shallow strain-meters have been maintained in various regions of interest in California. A network of 14 tiltmeters located at seven sites monitor crustal deformation within the Long Valley caldera. Other tiltmeters are located in the San Juan Bautista and Parkfield regions. Creepmeters are located along the Hayward, Calaveras and San Andreas faults from Berkeley to Parkfield and shallow strainmeters are located in the Parkfield region. Observatory type tiltmeters and strainmeters are located at the Presidio in San Francisco and a tiltmeter is installed in the Byerley Seismographic Vault at Berkeley. Data from all these instruments are telemetered using 12-bit digital telemetry via phonelines and radio links to Menlo Park.

Results

1. The tiltmeters at Casa Diablo (CA1&2), in the Long Valley caldera, recorded an episode of deformation, between September 18, and October 4, 1984, apparently associated with a blowout of a nearby steam well that occurred on September 29. This episode resulted in a net tilt offset of 9.5 microradians downward in a southwesterly direction. This result was supported by nearby levelling measurements that showed a net tilt of 9.1 microradians downward in a southerly direction. A subsequent deformation event was associated with an unprecedented increase in water dis-charge recorded at a nearby gaging station within the geothermal field. The first episode was recorded by the CA1 instrument and by the EW component of the CA2 instru-ment. By the time of the second event, both components of the CA2 instrument had failed. These tilt episodes probably represent localized deformational responses to changes in the geothermal system at shallow depths.

Reports

Mortensen, C. E., J. E. Estrem, R. P. Liechti and J. A. Westphal, 1985, Changes in ground tilt at the Casa Diablo geothermal field in the Long Valley caldera, California, EOS, abs., Trans. Amer. Geophys. Union, v. 66, n. 18, p. 411.

Crustal Deformation Observatory, Part (i):

Shallow Borehole Tiltmeters

14-08-0001-21939

Sean-Thomas Morrissey
Saint Louis University
Department of Earth and Atmospheric Sciences
P.O. Box 8099 - Laclede Station
St. Louis, MO 63156
(314) 658-3129

Objective: To apply the latest innovations and technology of instrumentation and installation methods to the shallow borehole tiltmeters at Pinon Flat such that their performance, particularly with regard to longterm stability, will compare more favorably with the data from the long baseline tiltmeters.

Accomplishments: We have completed procurement of components and assembly of the new tiltmeter electronics systems and temperature sensor units for the reinstallations at CDO. Unexpected delays were, as usual, encountered, such as the on-site Rustrak recorders being shipped with the wrong meter movement and chart drive gears, but the four new systems are in the final testing stages. Three of the four CDO units will be reinstalled in late spring, utilizing the present bubble sensors (but with the new bubble sensor housing). Special gain levels have been provided so as to accomodate the CDO digital data system.

Funding for continuation for a second year has been provided, including provisions for testing installations at a depth of 30 meters. A new pre-leveling installation tool that will provide hydraulic tamping of the sand pack is in the design stage. The present system is limited to 10 meters, since the sand tamping is done by hand from the surface. Drilling of the 30 meter holes will be delayed until late in the yer so as to coincide with other drilling at CDO.

In testing the CDO electronics systems for thermal stability, the expected low thermal noise level was found at about 3 nano-radians/$^{\circ}$C. However, a study of the source of the residual thermal noise was made, and found to be a drift of a few hertz of the excitation oscillator. It also produced a change in sensitivity of about 10% over the -40° to $+60^{\circ}$C range. The errors were found to be reactive (frequency dependent) changes in circuit elements that were directly sensitive to temperature. When excitation was produced by the crystal stabilized oscillator designed for the new variable reluctance sensor, remarkable improvement resulted. The thermal noise decreased from an average of $3 \times 10^{-9}/^{\circ}$C to $5 \times 10^{-10}/^{\circ}$C, or less than 0.5 nano-radian per degree Centigrade over the conceivable operating temperature range. Consequently, all the units were modified with the Statek programmable crystal oscillator, which easily replaces the CD4047 device previously used.

Results of two of the thermal tests are shown in the attached figure. The high range (centered at +20°C) and low range (centered at 0°C) temperature data has been extrapolated past the built-in limiters, and a coarse fit of the drift of the data has been estimated. Such data is routinely obtained for all the tiltmeter systems since it is automatically digitized during the thermal test cycle activity, where the thermal warm-up ramp is preceeded by a 24 hour "cold soak" at -40°C.

A proposal was submitted in response to RFP 1586 of the U.S. Geological Survey for continuation of this effort.

S.T. Morrissey
Senior Research Scientist
21 April 1985

Tiltmeter Thermal Test Data
Crustal Deformation Observatory

ALPHA tiltmeter electronics

+1ppm→
Calibration

+40°C

t+20 °C

X °C

Ambient, °C

Y data

X data

i85hr5
i85hr7
i85hr10
i85hr11
i85hr12

−1ppm
Calibration

−40°C

0000z26Mar85   hours   2350z26Mar85
                      (ten minute samples)

Processed on:
Fri Mar 29 15:18:41 CST 1985

/slu/tech/morr/cdo.data
28566

Tiltmeter Thermal Test Data
Crustal Deformation Observatory

BETA tiltmeter electronics

+40°C

Y data

t+20 °C

X °C

Ambient, °C

X data

174hr5
174hr7
174hr10
174hr11
174hr12

+1ppm
Calibration

−40°C

0000z15Mar85   hours   2350z15Mar85
                      (ten minute samples)

Processed on:
Wed Apr 3 16:48:51   5

/slu/tech/morr/cdo.data
87

298

Cooperative Tiltmeter Program at Parkfield, California

14-08-0001-22017

Sean-Thomas Morrissey
Saint Louis University
Department of Earth and Atmospheric Sciences
P.O. Box 8099 - Laclede Station
St. Louis, MO 63156
(314) 658-3129

Objective: To apply the latest state-of-the-art technology to shallow borehole tiltmeter installations and data acquisition in the Parkfield area, which is forecast to be the locale of a moderate earthquake in the near (3-8 years) future. Considerations of the current failure model, based on known creep data and fault-constituitive models, allows locating the tiltmeters such that probability of acquiring large coherent signals during the precursory stages is enhanced. The cooperative aspect involves the assistance of the U.S. Geological Survey in site selection, preparation, maintenance, and data acquisition.

Accomplishments: The program began 1 January 1985, so the effort to date is one of procurement of hardware and assembly of electronics systems for the five additional tiltmeters. (Three of the Palmdale systems have been diverted to the Parkfield program.) The availability of operating bubble sensors may limit further expansion of this effort until the new pendulum sensor has been proven. A detailed research of the available literature on Parkfield has also been completed, including a review of previous strain/tilt instrumentation efforts. This current effort is a completely new approach to tilt instrumentation, beginning with very careful screening of prospective sites prior to drilling the 10 meter installation holes. The sites were inspected in December 1984, and shallow refraction for near surface structural detail will be done in late spring. Drilling will probably be done in the fall.

A recent paper by Stuart et al., "Forecast Model for Moderate Earthquakes Near Parkfield, California," (JGR 90, 592-604) has proposed a detailed model of the eventual Parkfield earthquake, including some estimates of the theoretical uplift of the ground during three phases of the pre-earthquake process. This has thus allowed us to determine exactly where the tiltmeters should be installed, as indicated on the schematic map of Figure 1 where, following the figures of the referenced paper, distances are measured in km southeast of the 1966 epicenter. The current funding provides for two tiltmeter sites, each with three tiltmeters (and a spare), at the Gold Hill site (km 14) and the site southeast of the Lasar Geodimeter hill (km 11). A proposal in response to RFP 1586 of the U.S. Geological Survey requested funding for additional tiltmeters at the southeast end of Middle Mountain (km 5), and at the southern end of the 1966 break where it reached the southwest side of the Cholame Valley (km 24). These additional sites would provide much better constraints and/or support of the stress law and fault failure mechanism parameters used in the forecast model.

The latest issue of "Science News" (vol. 127, no. 15, 225-240, 13 April 1985) has a note that the National Earthquake Prediction Evaluation Council has endorsed a prediction of an earthquake for Parkfield within the next 8 years, along with qualified support for a suggestion that the Parkfield earthquake might initiate or extend itself into a rupture of the locked portion of the fault to the southeast that broke in the 1857 Ft. Tejon event.

Problems: Details of the digital data acquisition system have yet to be resolved. Early plans were to use the Menlo Park DCP system via the GOES satellite, but the hardware seems to have serious shortcomings. We will probably use our own 16-bit digital system, recording on weekly floppy disks at the lasar geodimeter building (or nearby), with a dial-up capability for Menlo Park to access the data.

S.T. Morrissey
Senior Research Scientist
21 April 1985

San Andreas Fault zone in the vicinity of Parkfield, CA., showing locations of active deformation monitoring experiments.

120°15'
36°00'

Creeping
San Andreas Fault zone
inactive

Xmm1

1966 epicenter, reference for distance figures
Tilt(?), Dilat.

Middle Mountain...x

(new) Tilt(?) ...→x 5 km

(Table Mountain)

(Cholame Hills)

8 Xpk1

Parkfield

10km Tilt(3), Dilat.

Lasar Geodim. creeping

inactive 15km.. Xwkr1

(Turkey Flat)

...cracked pipe, pre 1966

Xcrr1....→ Tilt(3), Dilat.

Gold Hill... ....Xhg1 (20km)

Cholame

1966 break...

Valley

locked trace

(new) Tilt(3)...→x

Xwt1→

highway 41

120°30'

Instrumentation,N. to S.
km
-1 Creep,XMM1
 0 1966 Epicenter
   Dilatometer, Tilt(?)
 5 New Tilt, 3 units
 8 Creep, XPK1
10 Lasar Geodimeter
11 Dilatometer,
   Tilt (1985), 3 units
15 Creep,WXR1
18 Creep,CRR1
19 Gold Hill
   Dilatometer,
   Tilt (1985), 3 units
20 Creep, XHG1
24 New Tilt, 3 units
25 Creep, XWT1

(Cholame Hills)

35°45'

0   5
kilometers

to US 466

Note that most of the instrumentation is east of the fault zone, in the competent formations of the North American plate. The surface structure west of the fault is mostly north-west bound rubble.

Dilatometer Operations

9960-03815

G. Douglas Myren
Branch of Tectonophysics
U.S. Geological Survey
345 Middlefield Road, MS/977
Menlo Park, California 94025
415-323-8111, ext. 2705

Investigations and Results

This project is involved with the installation and maintenance of dilatometers (volumetric strainmeters).

Since October of 1984 our effort has been concentrated in Parkfield, California. In September the Tectonics Branch Drilling Project began to drill a series of holes in this region. Under the direction of Tom Moses a hole was drilled on the Eade property (formerly Durham Ranch) approximately 3/4 of a mile southeast of Parkfield. The hole was cased to a depth of 700 feet and casing cemented. The hole was then drilled to 900 feet; caliper, s.p., resistivity, natural gamma, and televiewer logs were run. Based on this information a site was picked and the dilatometer was installed at 875 feet in early October of 1984. One inch pvc pipe was installed from 850 feet to the surface for heat flow measurement.

In early November a second hole was begun at Middle Mountain approximately 4 miles northwest of Parkfield on the Varian Ranch. This hole was drilled to 700 feet cased and casing cemented. It was then drilled to 800, 900, and 1000 feet. The forementioned logs were run each successive interval in search of a suitable site; none was found and the hole was cemented back to the casing with heat flow black pipe installed to 1000 feet.

A third hole was drilled 2-1/2 miles west-northwest of Parkfield on the Frohlich property opposite Pitt Ranch off Vineyard Canyon Road. This was started in February of 1985. It was drilled to 800 feet and casing cemented to that depth. Cores were attempted from 813 to 833 with 14 feet of recovery, 833 to 853 with 4 feet of recovery, 853-873 with no recovery. Logs, as mentioned previously, were taken at each interval with the exception of televiewer. Based on the core caliper and other logs no acceptable section was found for instrument installation. Drilling was continued to 1013 feet and a televiewer log was taken. A good section was found near 1013 feet.

Another core was taken from 1013 to 1033 with 4 feet of recovery. The hole was cemented back to target depth and preparation was made for instrument installation. At this time no instrument is in this hole due to a possible clay pinch at 905 feet. We anticipate another attempt at installation.

Along with these three installation operations at Park-field, continued maintenance of existing dilatometers in central and southern California proceded as required.

See accompanying maps for installation locations.

CALIFORNIA

PARKFIELD,CA

VARIAN ×

FROHLICH×

× EADES

▲ GOLD HILL
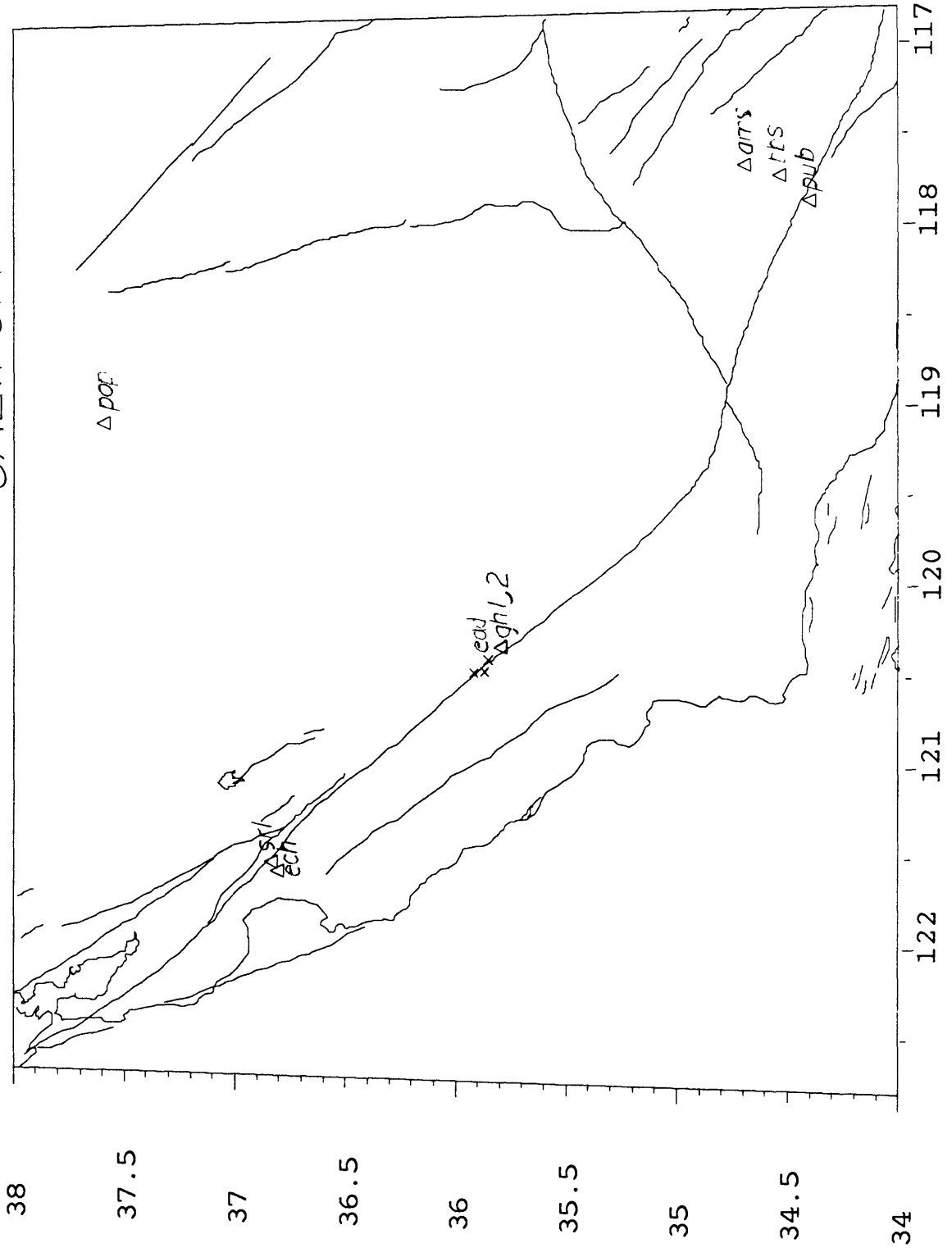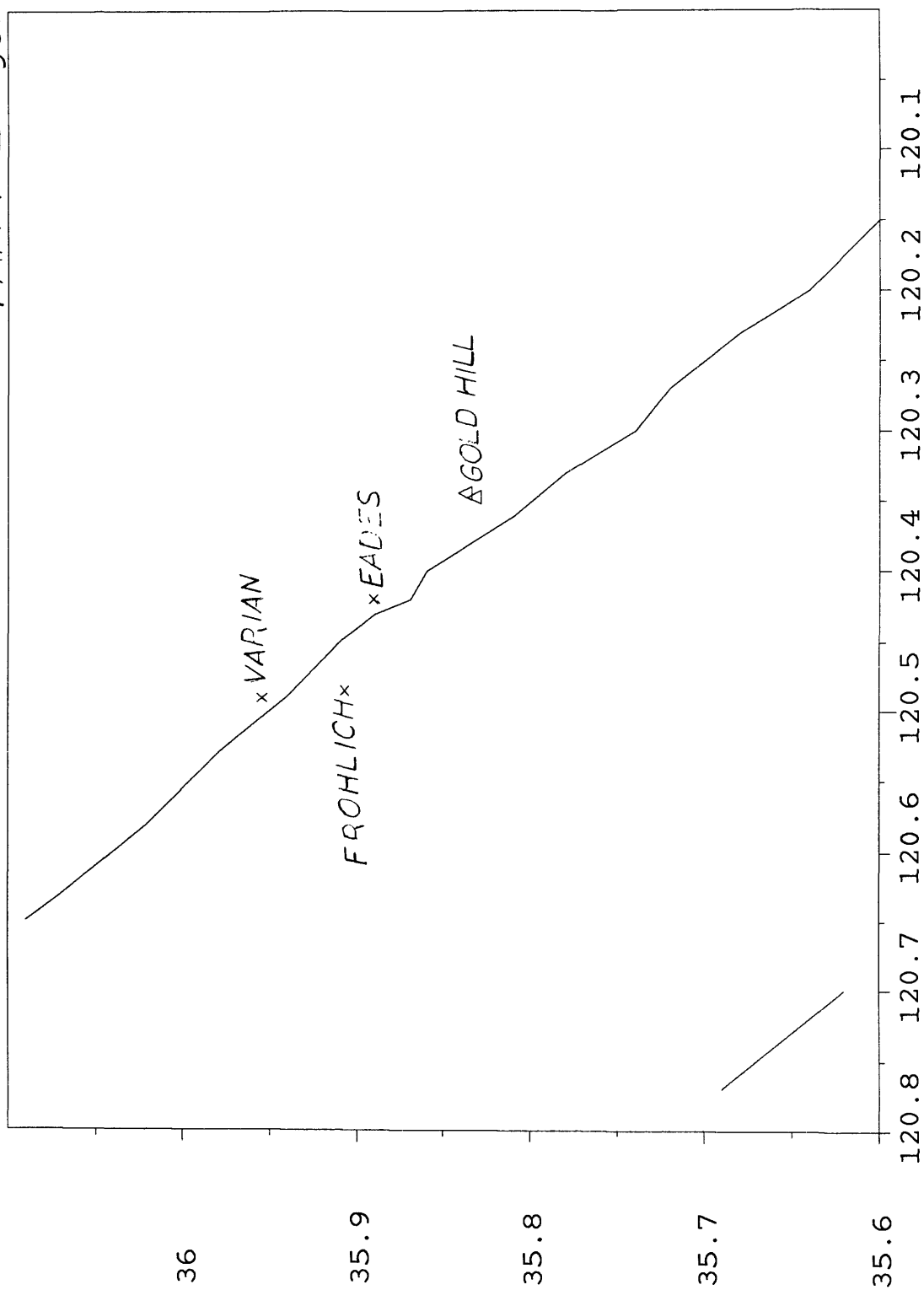
FAULT ZONE TECTONICS

9960-01188

Sandra S. Schulz, Beth D. Brown
Branch of Tectonophysics
U.S. Geological Survey
345 Middlefield Road, MS/977
Menlo Park, California 94025
(415) 323-8111 x 2763

Investigations

1. Directed maintenance of creepmeter network in California.

2. Updated archived creep data on PDP 11/44 computer.

3. Designed and fabricated prototype strong-motion creepmeter for Parkfield area.

4. Continued to establish and survey alinement array network on California faults.

5. Requested proposals from private sector to survey selected alinement arrays in Imperial Valley and Parkfield.

6. Monitored creepmeter and alinement array data for retardations or other possible earthquake precursors.

Results

1. Currently 28 extension creepmeters operate; 20 of the 28 have on-site strip chart recorders, and 18 of the 20 are telemetered to Menlo Park. A computer program continues to check Parkfield telemetry data once each hour and alert Project personnel via 'beeper' whenever unusual fault movement occurs.

2. Fault creep data from all USGS creepmeter sites along the San Andreas, Hayward and Calaveras faults have been updated through January 1985, and stored in digital form (1 sample/day). Telemetry data covering the period between January 1985 and the present are stored in digital form (1 sample/hour), updated every 10 minutes, and merged with the daily-sample data files to produce complete plots when needed.

3. A strong-motion creepmeter utilizing an existing water-level recorder design was fabricated for installation in Parkfield creepmeter vaults, in order to record coseismic and immediate post-seismic slip from the next Parkfield

earthquake. The device consists of a pulley arrangement and braided stainless steel cable, installed so as not to interfere with the existing creepmeter. The new instrument will have a range of 30+ cm, compared to 25 mm for the regular creepmeter, and fault movement as small as 1 mm will be discernible on the telemetry signal. An on-site chart recorder provides a permanent record.

4. Currently 30 alinement arrays are surveyed across five (5) active faults in California (San Andreas, Hayward, Calaveras, Nunez, and Imperial). Three new arrays were installed in the Parkfield area. Two were placed across the southwest trace of the 1966 surface rupture zone. The most northerly is Parkfield Kester West (PKW4), the other is Ranchita Canyon West (RCW4). One line, Parkfield North (XPN4) near creepmeter (XPK1), was installed to verify whether the creepmeter spans the most active trace of the San Andreas fault. Alinement arrays are remeasured every 90-120 days and are used to guide emplacement of creep-meters, check creepmeter measurements, and monitor fault movement where creepmeters are logistically impractical.

5. Received inquiries from private surveyors in response to a Request for Proposals to survey selected alinement arrays. Following issuance of specifications and Statement of Work, proposals were received, evaluated, and results returned to Contracts Section for financial evaluation. Final award of contract was pending at the end of March.

6. a. As shown in Figure 2, five of eight Parkfield area creepmeters continue to record decreased creep rates since the Coalinga earthquake of May, 1983. If retardation is a trusty precursor, this creep lag at Parkfield may indicate the predicted earthquake will occur closer to the beginning of the prediction window than to the end.

   b. An unusually slow creep rate is now being recorded at XSJ2, near San Juan Bautista in central California (arrow, Figure 3a), suggesting the possibility of creep retardation like that seen at SHR1 (Shore Road) near Hollister prior to the 1979 Coyote Lake and the 1984 Morgan Hill earthquakes (Figure 3b).

Reports

Mavko, Gerald M., Sandra Schulz, and Beth D. Brown, 1985, Effects of the 1983 Coalinga, California, earthquake on creep along the San Andreas fault: Bulletin of the Seismological Society of America, v. 75, no. 2, April, 1985, pp. 475-489.

Figure 1a
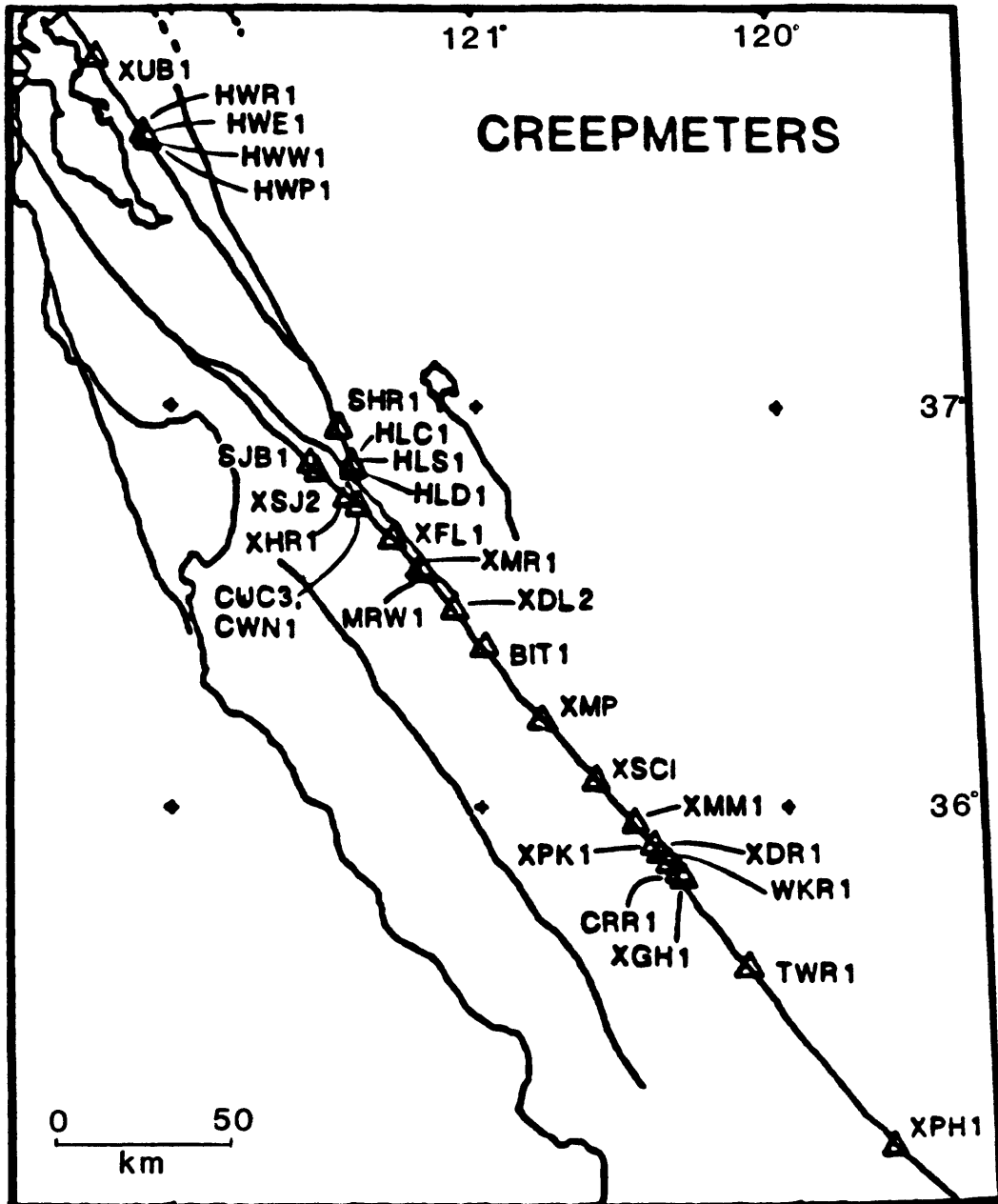
CREEP PROJECT :
Theodolite Alinement Arrays
(Northern and Central California)
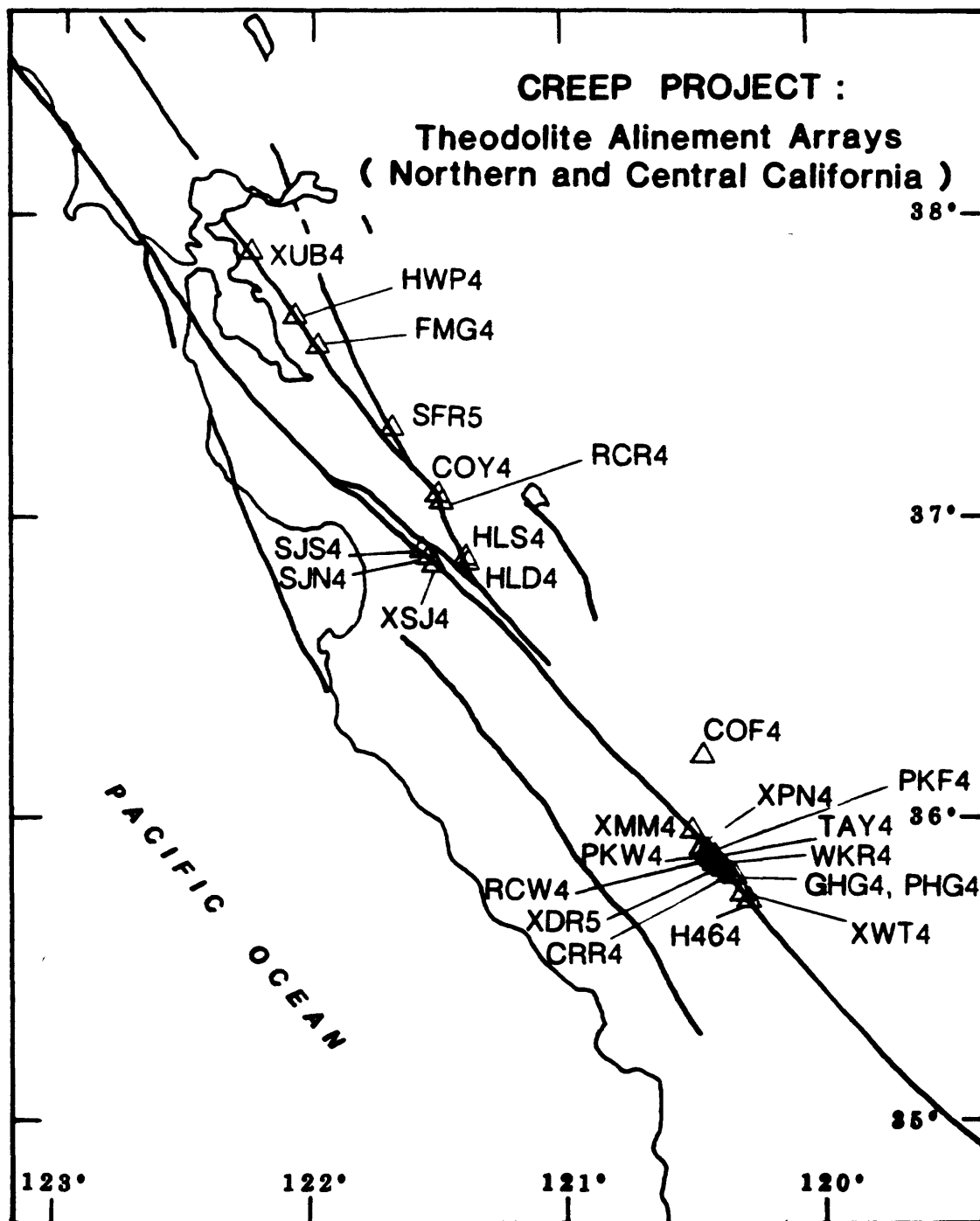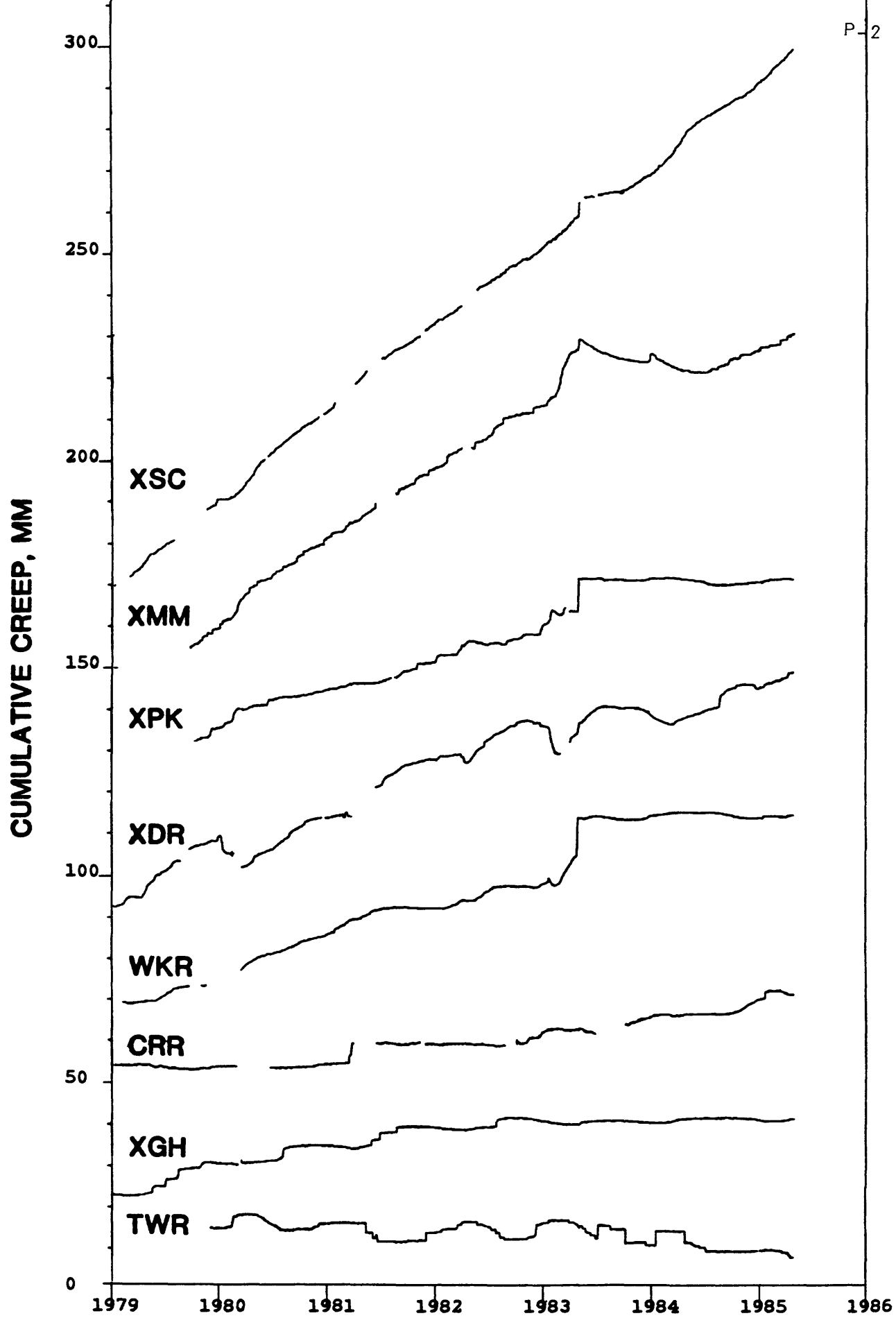
Figure 1b

Figure 2

PARKFIELD CREEPMETERS

xsj2: 01 Jan 1968 001 - 01 Apr 1985 091
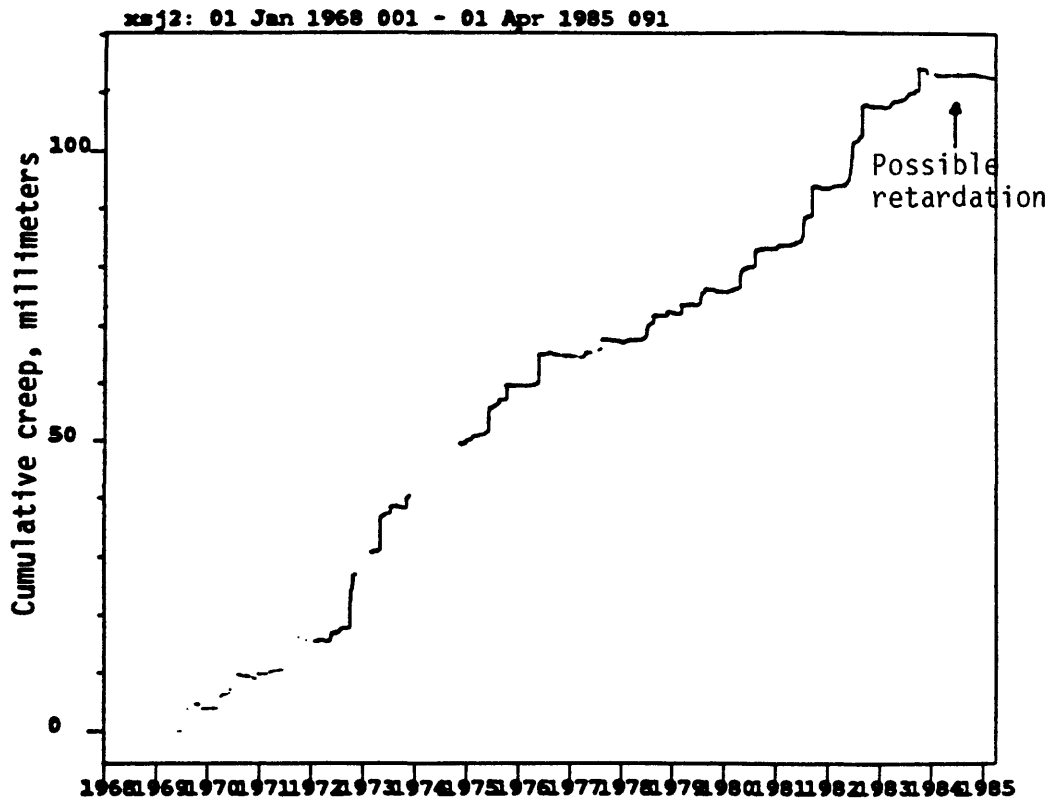
Figure 3a.   Cumulative creep at XSJ2
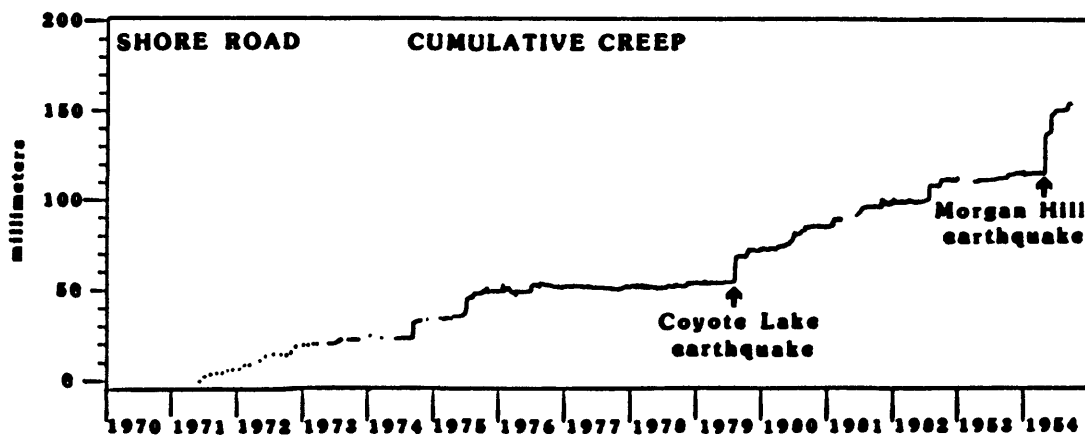
Figure 3b.   Cumulative creep at SHR1

Acquisition and Analysis of Data from
Sacks-Evertson Borehole Strainmeters in California
14-08-0001-G-960

I. Sewlyn Sacks and Alan T. Linde
Department of Terrestrial Magnetism
Carnegie Institution of Washington
5241 Broad Branch Road, N.W.
Washington, D.C. 20015
202-966-0863

This is a collaborative program in which we make continuous strain measurements in moderate depth (~200 m) boreholes. Together with the Geological Survey, we have installed 10 Sacks-Evertson borehole strainmeters: 4 near Palmdale in the Mojave Desert; 2 near San Juan Bautista; 3 in the Parkfield area, and one at Devils Postpile near Long Valley (see Fig. 1). Additionally 3 instruments (200 m apart) were installed at the Pinon Flat Observatory in cooperation with F. Wyatt and D. Agnew of U.C.S.D.

Long term drift of the instruments which have been in operation for several years is now decreasing to values which are more comparable with generally accepted thought on tectonic strain rates (Figs. 2, 3). The initial drift rates observed have been high due to compromises in the installations resulting from poor rock quality and various logistical problems. (Most of these difficulties should be substantially reduced in future installations.)

At shorter periods the data are reliable. For example Fig. 4 shows similar variations in the strain at several widely spaced stations. These correlated changes are almost certainly due to atmospheric pressure changes rather than tectonic effects, but nevertheless demonstrate that the installation provides good data at those periods. The stability of these installations at even shorter periods is well illustrated by Fig. 5. This demonstrates that the ratio of observed to theoretical tidal amplitude has remained constant over a time span of years.

Our colleagues in the Geological Survey have been able to obtain temporary use of some high frequency triggered recorders which have provided some valuable data. Fig. 6 shows a recording of a nuclear blast on a strainmeter and a seismometer at the same site and Fig. 7 shows a natural event. The strain record shows a small but definite coseismic step and the frequency domain plot indicates the relative richness in low frequency data obtained compared with the seismic record. Determination of seismic moment or corner frequency using broad band frequency data (50 sec to 10 Hz in the example shown) is obviously more reliable. A more distant earthquake is recorded in Fig. 8. There is of course no detectable strain step but the record is again rich in long periods. A manuscript on the analyses of these data is currently in preparation.

An intriguing record has been obtained from the instrument at Devils Postpile near Long Valley. There is a clear record (Fig. 9) of a long period precursor around 20 minutes before a magnitude 5.7 quake about 50 km distant. The event caused unusual large and slow (duration ~1 hr) strain strains at the station. Are these effects caused by changes near the instrument (aquifer effects, perhaps) or are they symptomatic of larger scale processes?

Clearly we need a densification of sites and other types of data before we are able to address these questions in a meaningful manner. What is clear is that we do need to understand the nature of these perturbations and to evaluate their significance in terms of tectonic processes.

BOREHOLE DILATOMETER STRAIN ARRAY
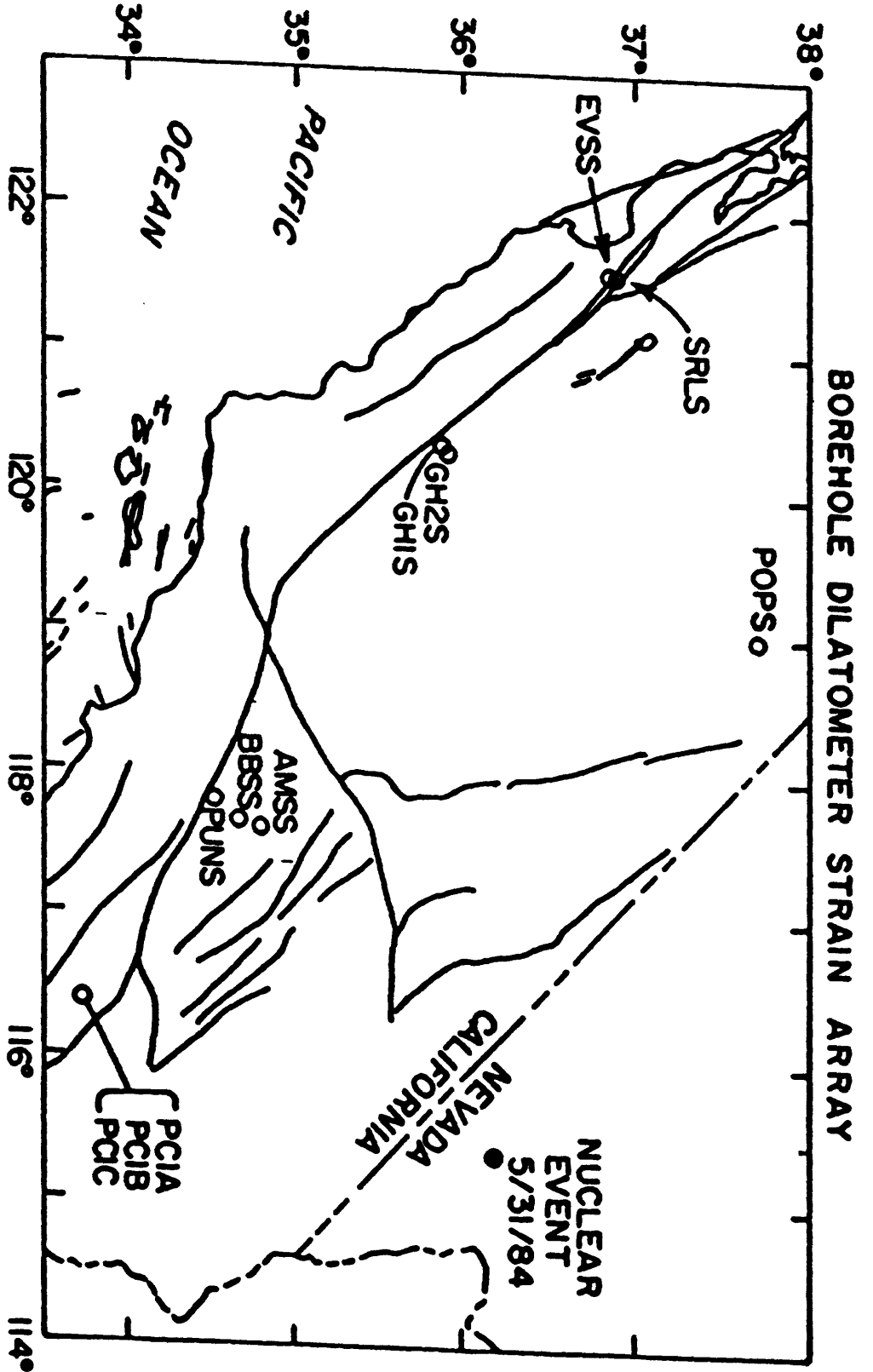
Fig. 1. Map showing locations of borehole strainmeters in California. The location of a nuclear test event is also shown.

Carnegie Volume Strainmeters
Piñon Flat Observatory

5 microstrain/div

1982:86 — 1984:285

Extension positive

CIA

CIB

CIC

Time, yr

1982.5   1983.0   1983.5   1984.0   1984.5
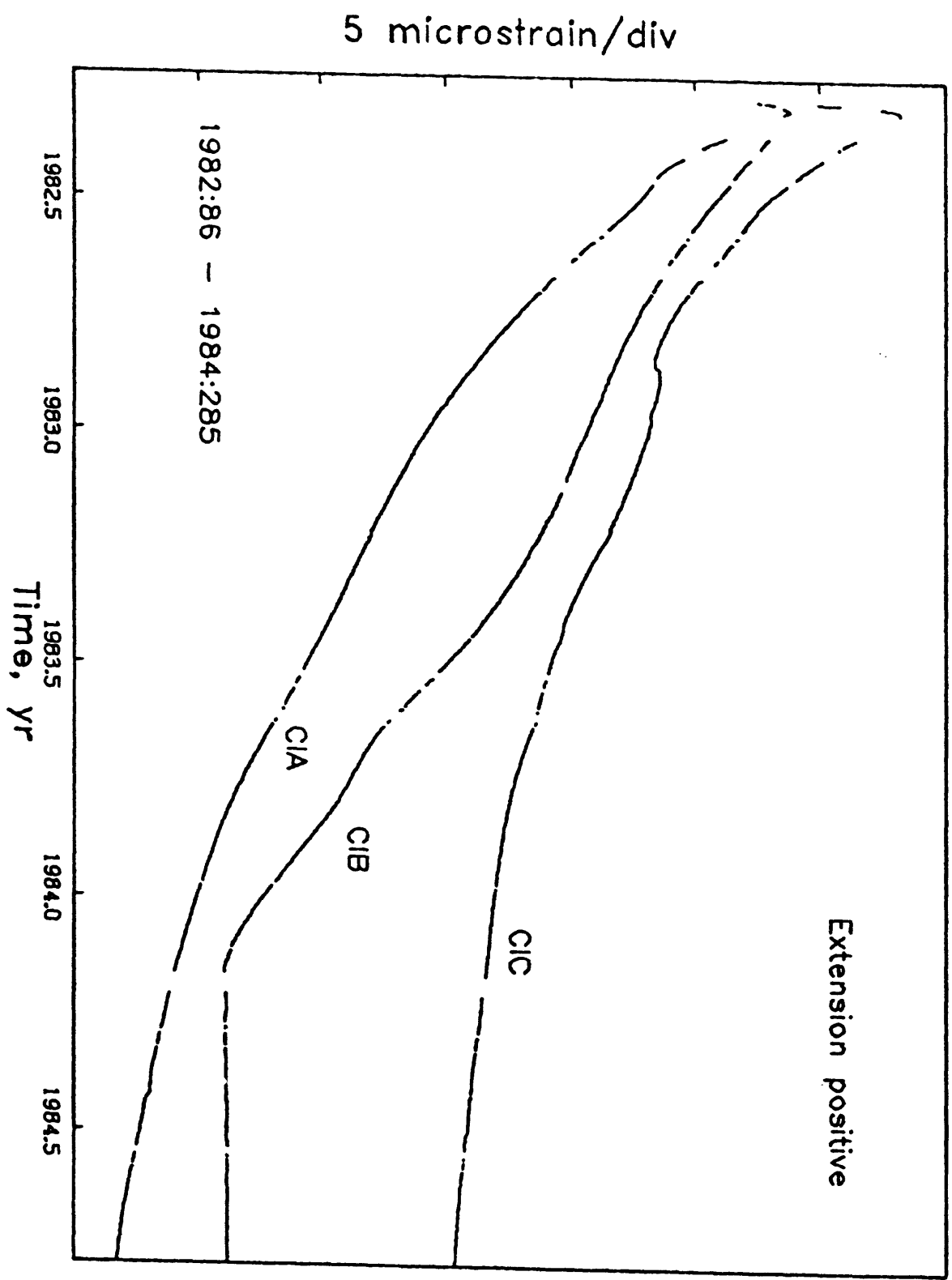
Fig. 2. Data from the instruments installed at Piñon Flat Observatory. In general, the strain rates are continuing to decrease with time.
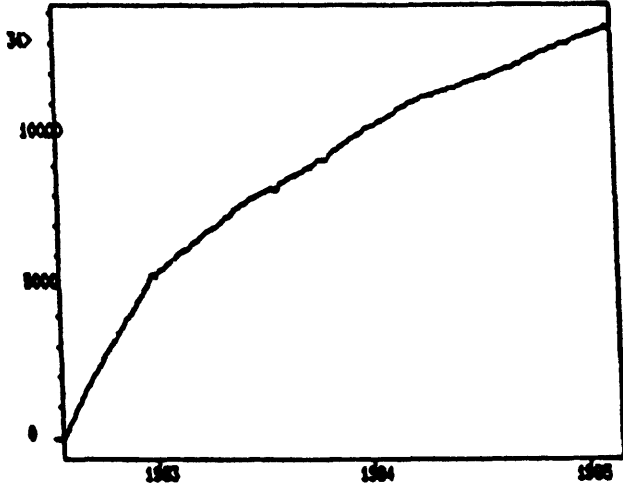
Fig. 3. Data from AMSS, BBSS and EVSS, all of which are showing lower strain rates with increasing time.
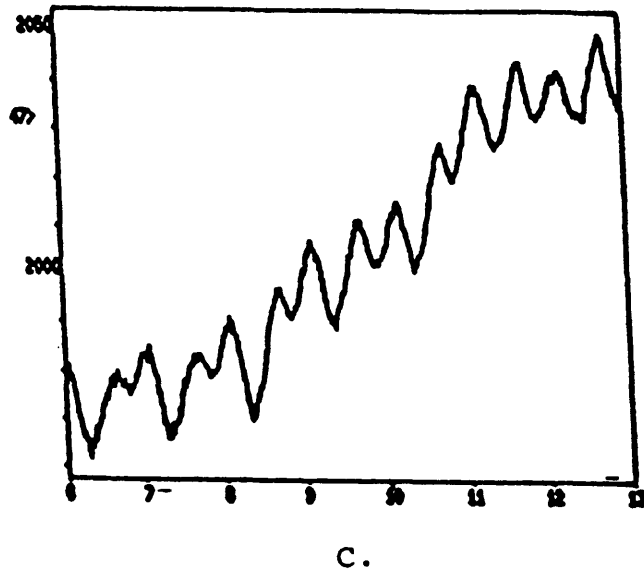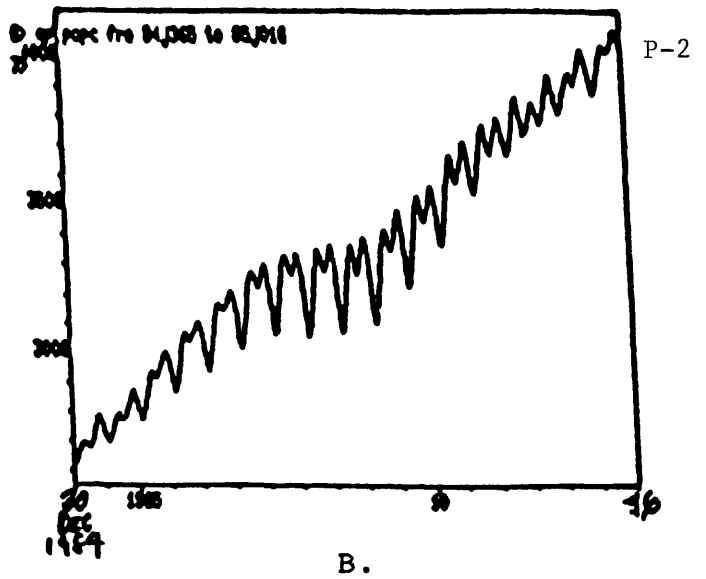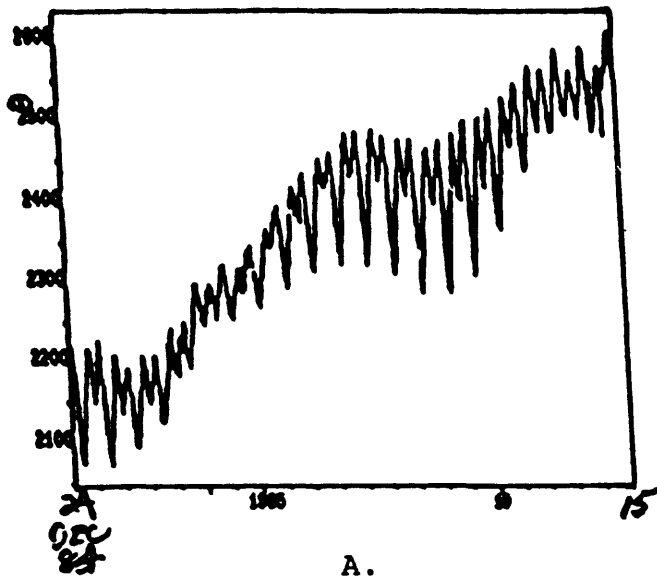
Fig. 4. Short sections of data for similar intervals for
BBSS (A), POPS (B) and GH2S (C). Tidal signals
are well recorded. Also there is similar short
period variation (∿10 day period) on all records.

Time Variation of M₂ Tide
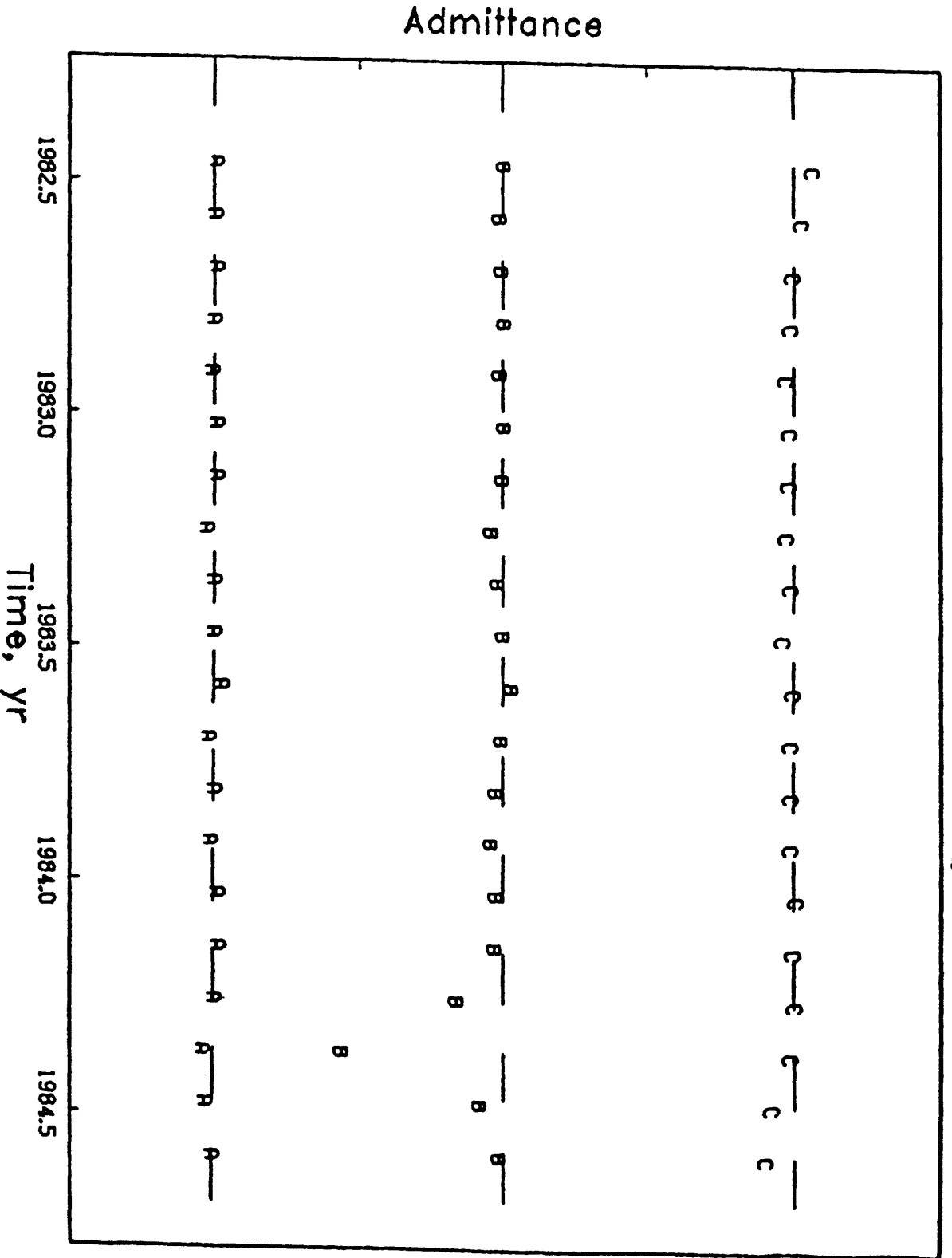
Fig. 5. Ratio of observed to calculated tidal amplitudes for the three Pinon Flat instruments. Instrument B has erratic behavior recently, probably due to water penetrating the cable. Otherwise the constancy of the values indicate very good stability at tidal periods.

TIDAL and NUCLEAR STRAIN
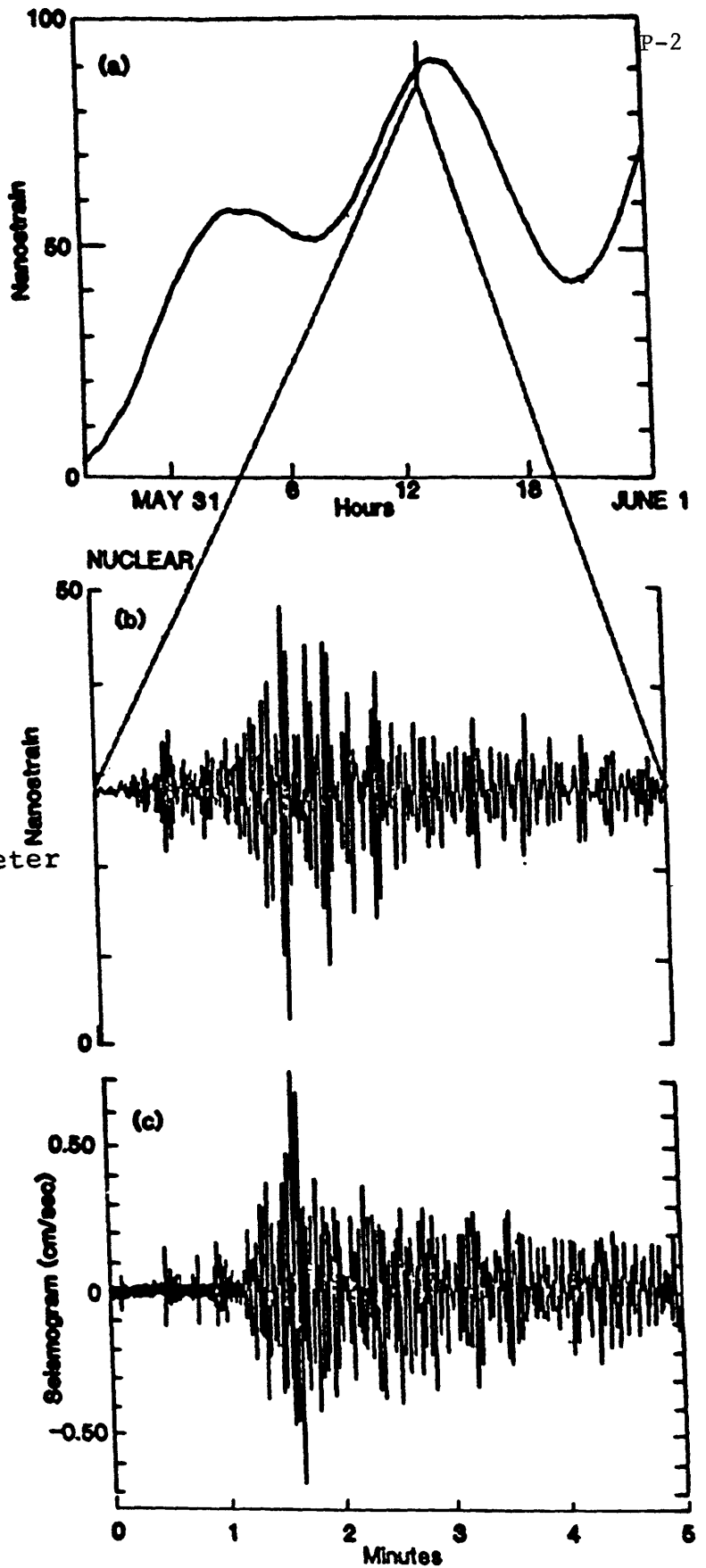
Fig. 6 . A nuclear test blast recorded on the strainmeter (top 2 traces) and on a seismometer at the same site.

319
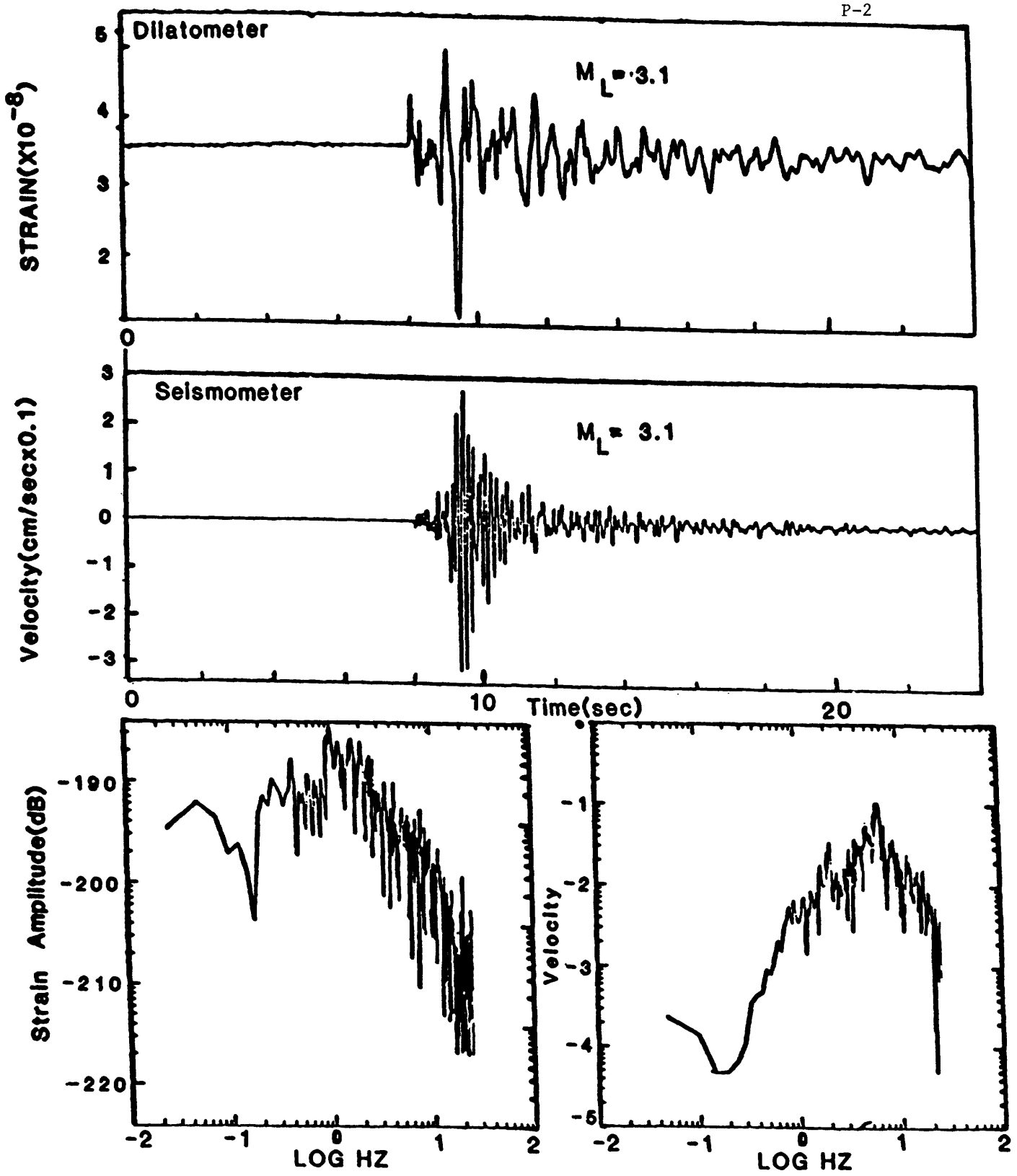
Fig. 7 . A nearby 3·1 quake recorded on a strainmeter and a seismometer at the same site. A small strain offset is discernable in the strain-gram. Frequency plots demonstrate the enhanced long period character of the strain record.
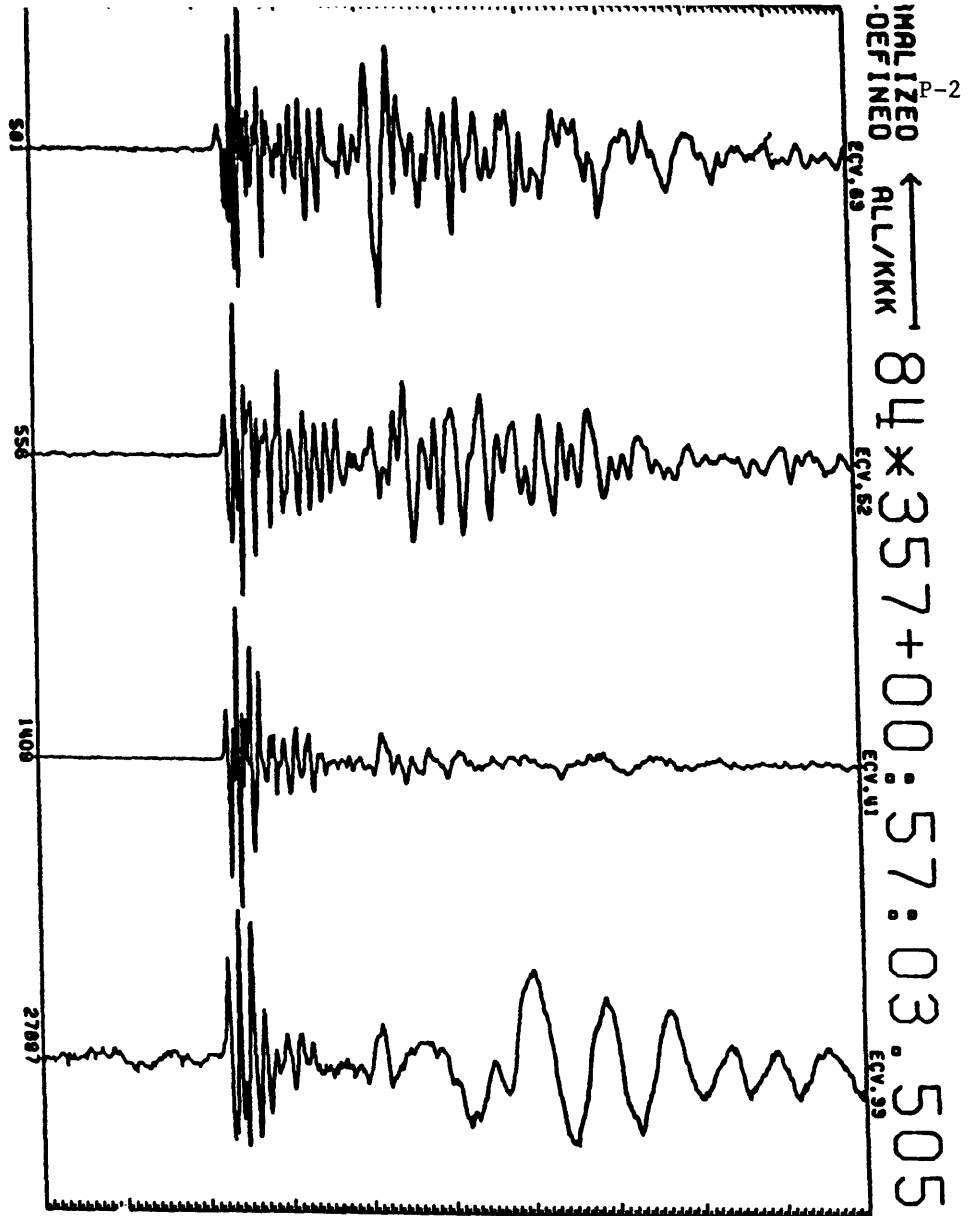
Fig. 8. Records from a three component seismograph (NS, EW, V) and a strainmeter (bottom trace) at the same site. Time scale is in seconds. Note the high quality of the strain record and its excellent wide frequency range response.
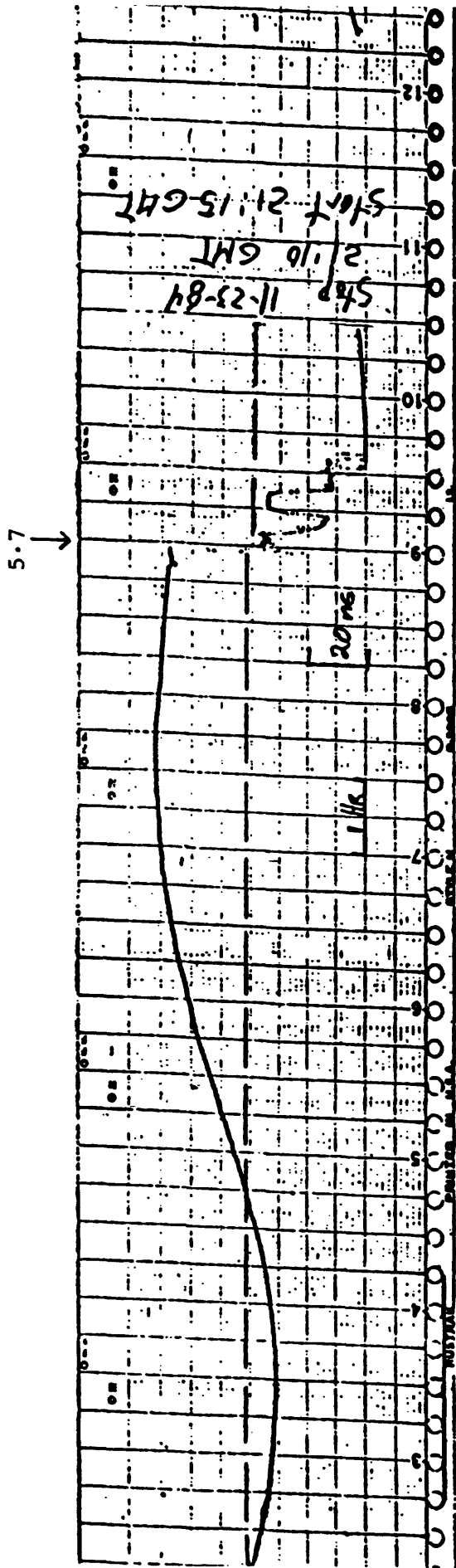
Fig. 9. Strain record at POPS at time of m 5.7 quake about 50 km away. Apparent precursory strain changes occurred ~20 min before the quake and following it there are large slow strain changes. This station normally draws a very quiet record as can be seen by the tidal record shown.

THE EXTENSION AND OPERATION OF A COMPUTER-CONTROLLED MONITORING NETWORK FOR RADON AND OTHER GEOCHEMICAL PRECURSORS, AND LABORATORY STUDIES ON SEISMO-GEOCHEMICAL PRECURSORS

14-08-0001-21268

M.H. Shapiro, A. Rice, S. Stryker, and T.A. Tombrello
Div. of Physics, Mathematics, and Astronomy - Caltech
Pasadena, CA 91125
(818) 356-4277

INVESTIGATIONS

During the past six months both laboratory and field experiments were carried to compare the performance of the Caltech radon-thoron monitors with the USC continuous radon monitor. The field experiment at our Ft. Tejon site is still underway.

Owing to funding limitations field monitoring of radon and geochemical variables has been terminated at Pinyon Flat. Monitoring at Lake Hughes and Anza also will be terminated shortly. It likely will be necessary to terminate a fourth site to keep the project within budget.

RESULTS

A detailed report of the comparison experiments was presented at the last data review meeting. In general the USC device is more sensitive and responds more quickly to changes in radon level. However, it was found to be more sensitive to flow variations, and to the build up of radioactive contaminants. The older Caltech instrument appeared to perform better in the field test than in the lab test. As normally installed the Caltech instrument measured combined water and gas phase radon, while the USC instrument usually just measures water phase radon.

Generally all network monitoring sites have recorded radon data within normal limits during the past six months. The new plumbing associated with the comparison experiment at Ft. Tejon has caused some problems (a check valve occasionally fails to open fully). This accounts for a few periods of relatively low radon in the recent Ft. Tejon record. The carbon dioxide driven spiking at both Lake Hughes and Lytle Creek terminated with the recovery of the water levels at both sites. However, the carbon dioxide driven spiking at Alandale has continued although the water level now has risen substantially. This may be a cause for some concern.

Additional insulation was added to the water holding tank at Anza. However, this failed to eliminate the temperature driven spiking that occurs during the warmer months.

Water level and radon data from all sites in operation during the past six months are shown in figures 1 and 2.

CALTECH WATER LEVEL NOV 1984 to MAY 1985

324
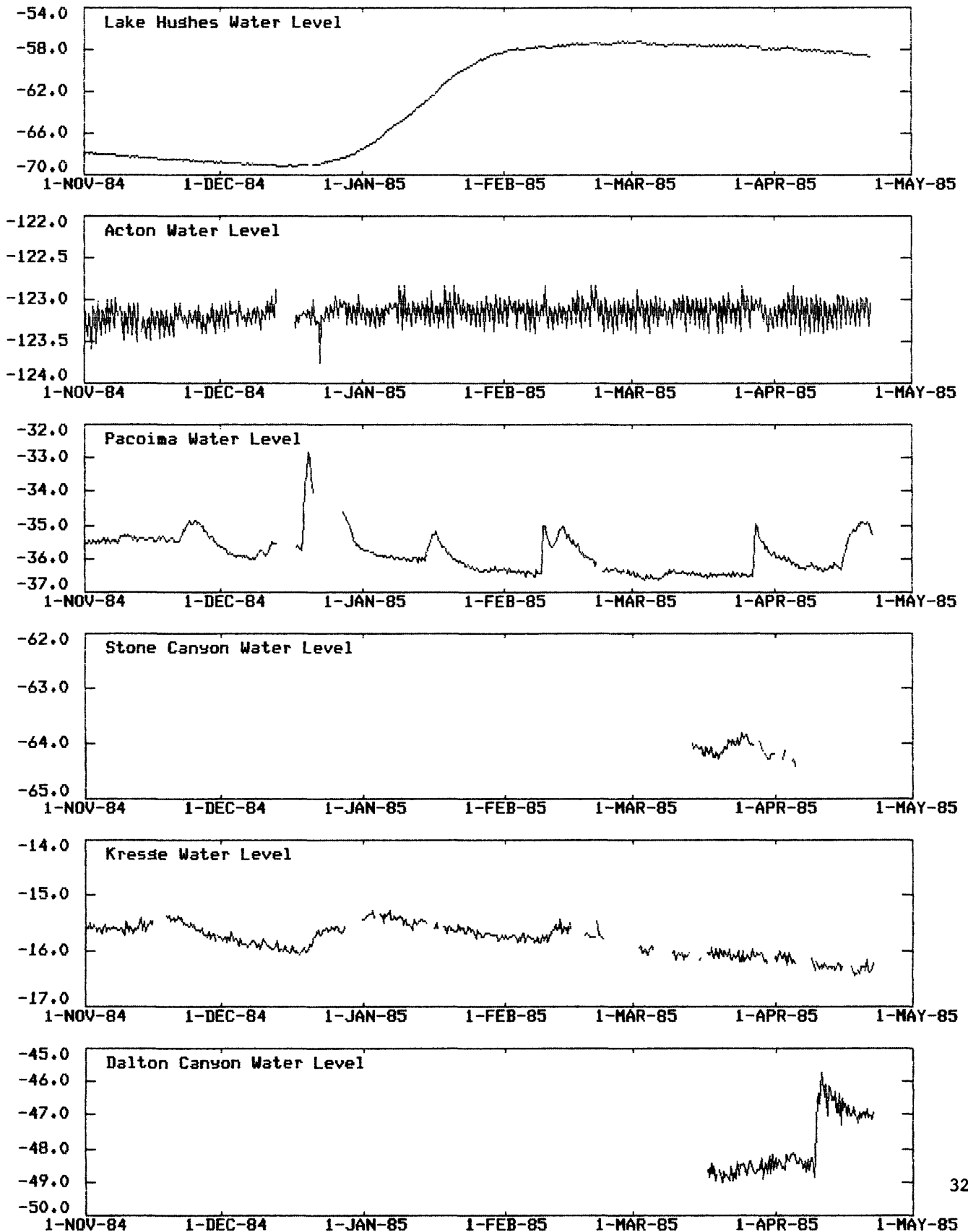
CALTECH WATER LEVEL NOV 1984 to MAY 1985
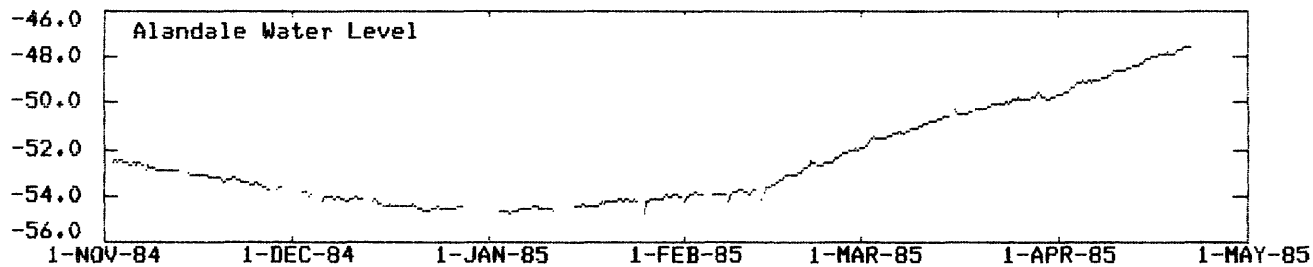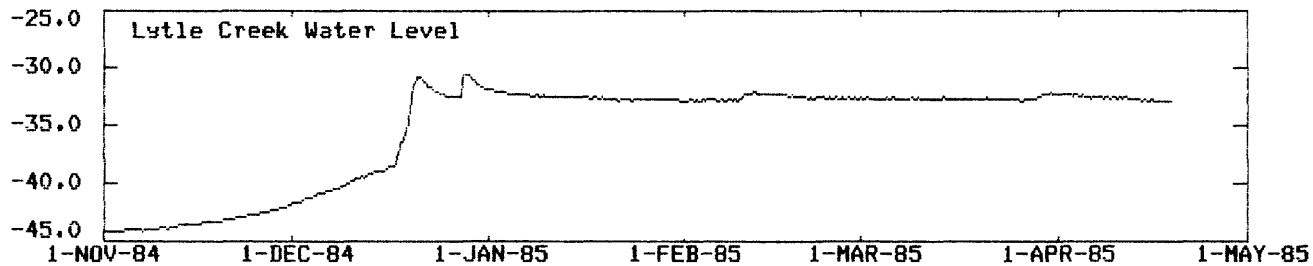
CALTECH RADON DATA NOV 84 to MAY 85
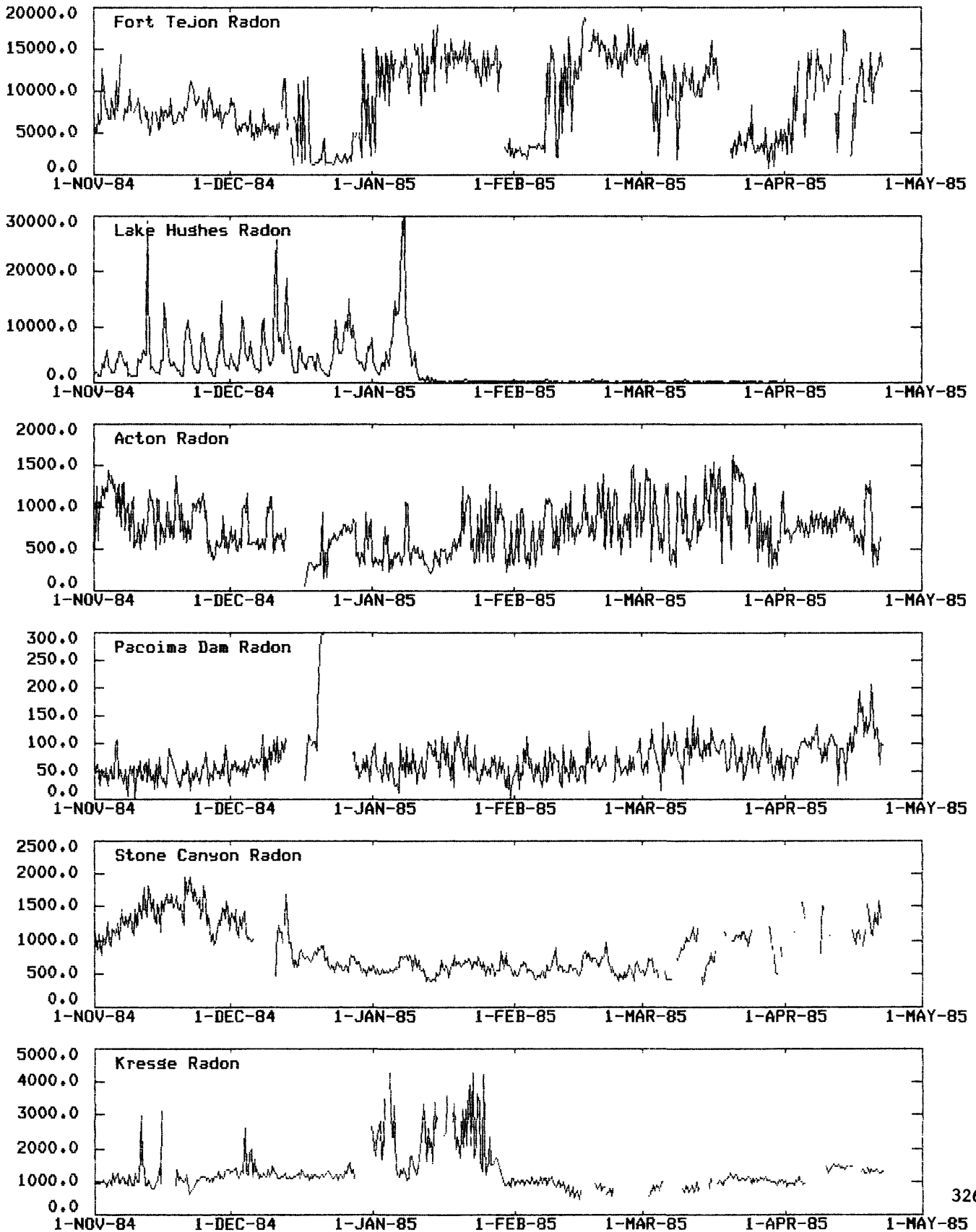
Figure 2b.

CALTECH RADON DATA NOV 84 to MAY 85

327
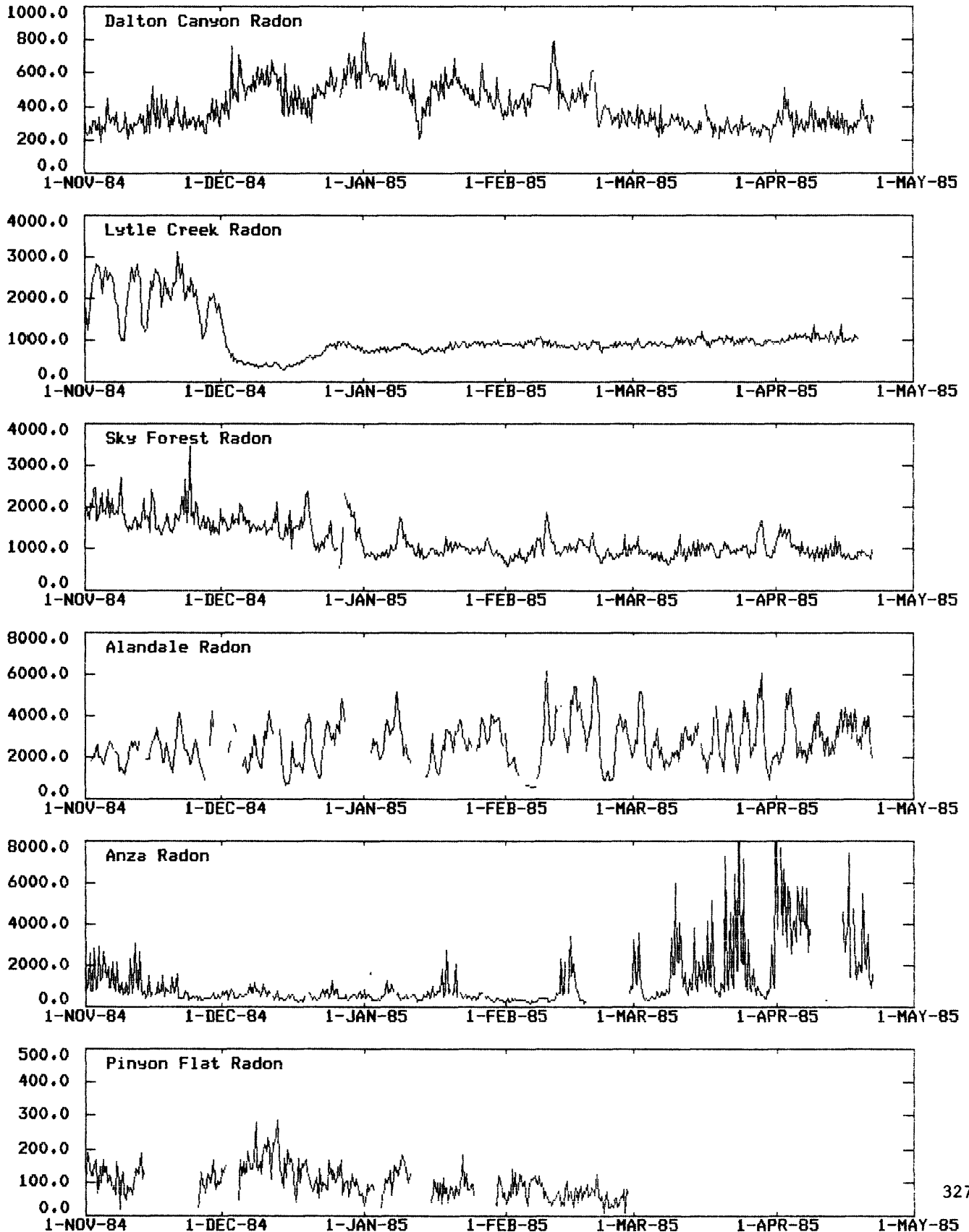
A Crustal Deformation Observatory in Central California
Near the San Andreas Fault

14-08-0001-21300

Larry E. Slater
CIRES
Campus Box 449
University of Colorado
Boulder, Colorado   80309
(303) 492-8028

Objective: A portion of the San Andreas fault in Central California near
Parkfield has been subject to repeated earthquakes in the historical past.
These earthquakes are typically of magnitude 6 and occur approximately
every 20 - 25 years. The last in the series of these events occurred in
1966. Several researchers have suggested that a high probability exists
that the next in the series will occur within 5 years. Because of those
studies and the expectation that the location is also known we have in-
stalled a multiwavelength distance measuring instrument (the C-meter)
in the region. The instrument site is located near the center of the
1966 break and the array spans a considerable amount of the fault trace
that showed ground breakage during the 1966 event. The goal of this
project is to monitor crustal deformation in this region and attempt to
detect any premonitory deformation events.

Results: A radial geodetic array has been established near Parkfield,
California. The array consists of approximately a dozen primary lines
that are measured several times a week and several secondary lines that
are measured approximately every month. The C-meter is located at the
hub of the array and measures the lines to a precision of approximately
1 part in 10 million.

The C-meter is located approximately 1 km south of Parkfield in a pro-
tective shelter on Carr Hill. At the other end of each of the primary
lines is a smaller protective shelter housing the retro-reflectors.
Each retro-reflector is mounted on a pier whose horizontal stability
can be evaluated by independent measurements. Much of the installation
and daily measurements have been assisted by local field personnel.

Most of the primary lines have been monitored for over six months. Many
of these line length data sets are beginning to show changes of length
consistant with the expected deformation patterns.

Because of the importance of rapid availability the line length
measurements are transmitted weekly to the U.S. Geological Survey.

Crustal Deformation Observatory - Part G

14-08-0001-21302

Larry E. Slater
CIRES
Campus Box 449
University of Colorado
Boulder, Colorado   80309
(303) 492-8028

Objective: Evidence of large scale crustal uplift in several regions prompted the design and development of several types of long-baseline fluid tiltmeters a few years ago. One of those, the 2-fluid tiltmeter, utilized 2 different fluids to correct thermally induced errors. Laboratory evaluation and short term tests verified the concept but long term stability tests were needed. A site in Southern California, Pinon Flat Observatory, was selected because of the numerous other deformation studies ongoing there.

Results: The 2-fluid tiltmeter was installed along side 3 other long-baseline tiltmeters at Pinon Flat Observatory. The length of the fluid path was approximately 500 meters and closely followed a contour across a gently sloping grade. The position of the fluid path proved to be a considerable problem, the nearly level path with gentle undulations and the small diameter of the fluid tubing (approx. 2 cm) provided many locations for bubbles to form and occlude the fluid along the path. The elimination of bubbles required a considerable effort. An earlier field test was conducted across a small v-shaped valley where any bubbles that formed tended to migrate to one end or the other of the tiltmeter where they were easily vented.

Another major problem with the 2-fluid tiltmeter has been frequent, re-occurring problems with the electronics. The system was designed around early CMOS components that are now very difficult to find replacements for. These early CMOS components are not well protected and have been subject to frequent failure. The design originally specified a typical fluid path of 1 km, however, the system was never capable of path lengths greater than 250 meters because of the inability of the electronics to drive the longer signal lines.

This effort has failed to produce the long term stability test that was desired. A further complication occurred a few months ago when we were unable to conclusively convince ourselves that a small fluid leak did not exist. We decided to purge the fluid lines so that we would not jeopardize the other tiltmeters in the immediate area.

The concept remains valid but further instrumental development needs to be undertaken before further field tests are initiated.

MODELING AND MONITORING CRUSTAL DEFORMATION

9960-01488

Ross S. Stein, Wayne Thatcher
Branch of Tectonophysics
U.S. Geological Survey
345 Middlefield Road, MS/977
Menlo Park, California 94025
(415) 323-8111, ext. 2120

Investigations

Analysis and interpretation of repeated geodetic survey measurements relevant to earthquake-related deformation processes at or near major plate boundaries. Principal recent activities have been:

1. Investigation of the role of geodetic survey measurements in the study of active tectonic processes, earthquake repeat times, and the relation of these present-day measurements to geological measures of recent deformation and the earthquake cycle.

2. Study of deformation accompanying and following dip-slip faulting in regions of compressional tectonics (1983 M_s 6.7 Coalinga, CA, earthquake), and in regions of extensional tectonics (1983 M_s 7.3 Borah Peak, ID, earthquake).

Results

1. Geodetic Measurement of Active Tectonic Processes

Repeated geodetic observations are sufficiently precise to detect the growth of mountains, the relative movements of the great lithospheric plates, and present-day rates of fault slip and earthquake strain accumulation. The cyclic buildup and release of strain across major faults can be monitored over the short-term (~years or less) using ultra-precise modern techniques, and longer term movements can frequently be determined by utilizing the historic record of measurements, which in many active regions extend back into the late 19th century. Since about 1970, annual laser ranging surveys in the western U.S. and southern Alaska have delineated the pattern and current rates of deformation in these seismically active regions and begun to provide accurate fault slip rates to compare with late Holocene geological estimates. The imperfect balance between interseismic strain buildup and coseismic strain

release introduces a component of permanent deformation into the earthquake cycle that under favorable conditions can be estimated geodetically, providing another link between present-day movements and those preserved in the recent geologic record. Examples include tectonically elevated former shore-lines related to great interplate thrust earthquakes and deformed river terraces observed in intraplate reverse faulting environments. Despite the relative uniformity of longer term deformation rates, accumulating evidence indicates considerable short-term irregularity, at least in some regions. Perhaps the best-documented example comes from southern California, where rapid, correlated changes among gravity, elevation, and horizontal strain measurements have recently been observed. (Thatcher)

2. The Coalinga Earthquake: Concealed Reverse Faulting

The Coalinga earthquake (M_l = 6.7) uplifted Anticline Ridge 0.5 m, depressed adjacent Pleasant Valley syncline 0.25 m, but caused no fault rupture at the ground surface. A steeply dipping reverse fault is well fit by the geodetic and seismic data, whereas a gently dipping thrust fault is less compatible with the leveling and the location and depth of the mainshock. Using the N53°W strike and a 67°NE dip of the mainshock, the best-fit earthquake parameters are: 1.7 ± 0.5 m of dominantly reverse dip slip on a fault extending from a hypocentral depth of 12 ± 1.5 km to within 4 ± 1 km from the ground; M_o = 6-7 x 10^{25} dyne-cm. Because the geodetic and seismically determined moments are nearly equivalent, most of the slip was released seismically. The deformation caused by the 1983 earthquake strikingly resembles the structural contours of the Pleistocene Tulare Formation on Anticline Ridge. About 2 km of cumulative concealed fault slip would account for this similarity, yielding a slip rate of 1-4 mm/yr. Well documented examples of anticlinal uplift associated with larger thrust earthquakes, and similarities between Anticline Ridge and adjacent structures, argues that the earthquake potential along the eastern Coast Ranges is larger than previously recognized. (Stein)

3. The Borah Peak, ID, Earthquake: Planar High-Angle Faulting

Geodetic elevation changes record the broad-scale deformation associated with the M 7.0 28 October 1983 Borah Peak, Idaho, earthquake on the Lost River fault. The crest of the Lost River Range rose 0.2 m and adjacent Thousand Springs Valley subsided 1.0 m, relative to reference points 45 km from the mainshock epicenter. The deformation was modeled by dislocations in an elastic half-space. A planar

fault with uniform dip slip of 2.05 ± 0.10 m, dipping 47 ± 2°SW and extending to a depth of 13.3 ± 1.2 km fits the geodetic data best, and is also consistent with the mainshock hypocenter and fault plane solution. The geodetic moment is 2.6 ± 0.5 x 10^{19} Nm [2.6 ± 0.5 x 10^{26} dyne-cm], and the estimated static stress drop is 2.9 ± 4 bar]. Tests for coseismic slip on listric faults (which flatten with depth) and on detachments (horizontal faults or shear zones) showed fits to the geodetic data that are inferior to those for planar high-angle faults. No detectable coseismic slip occurred on the Mesozoic White Knob thrust fault, although the low-angle thrust sheet intersects the south end of Lost River fault near the 1983 mainshock epicenter. If the high-angle Lost River fault abuts a flat-lying detachment fault or shear zone, such a structure must lie at depths > 12 km, near the brittle-ductile transition, where stick-slip behavior gives way to creep. The depth and geometry of faulting at Borah Peak is similar to that inferred from seismic and geodetic evidence for the 1975 M = 7.2 Fairview Peak, Nevada, and the 1959 M = 7.3 Hebgen Lake, Montana, events, suggesting that if detachments are active at these localities, they are deep and most likely slip by creep. (Stein and Barrientos)

4. **Postseismic Deformation Associated with Large Intraplate Earthquakes**

Leveling surveys carried out following the 1983 Coalinga (M_s = 6.5) and 1983 Borah Peak (M_s = 7.2) earthquakes, supplemented by less complete results from other intraplate dip-slip shocks, are used to determine the pattern and mechanism of short-term (~1 year) postseismic intraplate deformation. Movements differ notably from those observed following large plate boundary thrust events. Although the postseismic deformation is discernible, it is small, averaging only ~5% of the coseismic movements and having nearly the same spatial pattern. Clearly, such motions are best explained by continued minor slip on the same fault that ruptured during the earthquake itself. In contrast, short-term movements following intraplate thrust events are large (~20% coseismic), differ markedly from coseismic deformation, and are conveniently explained by transient slip downdip of the coseismic rupture plane. However, limited evidence from intraplate shocks indicates a temporal broadening of the movement profile, suggesting a deepening of slip or ductile deformation. Resurveys at Coalinga and Borah Peak planned for the spring of 1985 should provide better detail. Meanwhile, the results in hand indicate significant differences between intraplate and plate boundary environments, both in the rheological properties beneath the seismogenic zone and consequently in

the mechanics of strain accumulation and release in these regions. (Thatcher and Stein)

Reports

Atwater, B. F., J. C. Tinsley, R. S. Stein, D. A. Trumm, A. B. Tucker, D. J. Donahue, A. J. T. Tull, L. A. Payden, 1985, Alluvial stratigraphy across the Coalinga anticline suggests average repeat time of at least 250 years for major fold-building earthquakes of the late Holocene, submitted to U.S. Geol. Surv. Prof. Pap. on the Coalinga Earthquake, 45 pp.

Barrientos, S., S. N. Ward, J. R. Gonzalez-Ruiz, and R. S. Stein, 1985, Inversion for moment as a function of depth from geodetic observations and long period body waves of the 1983 Borah Peak, ID, earthquake, in Proceedings of Workshop XXVIII on the Borah Peak, Idaho, earthquake, U.S. Geol. Surv. Open-File Rep. 85-290, 485-518.

Stein, R. S., 1985, Evidence for surface folding and subsurface fault slip from geodetic elevation changes associated with the 1983 Coalinga, California, Earthquake, submitted to the U.S.G.S. Professional Paper on the Coalinga Earthquake, 45 pp. [Also published in Rymer, M. J., and Ellsworth, W. F., eds., Mechanics of the May 2, 1983 Coalinga, California, earthquake, U.S. Geol. Surv. Open-File Rep. 85-44, 225-253].

Stein, R. S., 1985, Role of the North American vertical datum for earthquake research and prediction: An example from the Great Basin, Proceed. 3rd Int. Symp. on No. Amer. Vert. Datum, National Geodetic Survey, 10 pp., in press.

Stein, R. S., and S. E. Barrientos, 1985, Planar high-angle normal-faulting in the Basin and Range: Geodetic analysis of the 1983 Borah Peak, Idaho, earthquake, J. Geophys. Res., in press.

Stein, R. S., and S. E. Barrientos, 1985, The 1983 Borah Peak, Idaho, earthquake: Geodetic evidence for deep rupture on a planar fault, in Proceedings of Workshop XXVIII on the Borah Peak, Idaho, earthquake, U.S. Geol. Suv. Open-File Rep. 85-290, 459-484.

Stein, R. S., and R. C. Bucknam, eds., 1985, Proceedings of Workshop XXVIII on the Borah Peak, Idaho, earthquake, U.S. Geol. Surv. Open-File Rep. 85-290A (Introduction and 40 research papers) and 85-290B (field guide and maps), 720 pp.

Stein, R. S., and R. C. Bucknam, 1985, Basin and Range viewed from Borah Peak (News article and cover), EOS, Trans. Amer. Geophys. Un., 66, in press.

Stein, R. S., 1984, Coalinga's Caveat (News article and cover), EOS, Trans Amer. Geophys. Union, 65, 791-795.

Thatcher, W., and R. S. Stein, 1985, Postseismic deformation from intraplate earthquakes: Comparison with plate boundary events, submitted to the 5th Ewing Symposium, Lamont-Doherty Geol. Obs., 19-23 May.

Thatcher, W., 1985, Geodetic measurement of active tectonic processes, in Active Tectonics - Impact on Society, National Research Council, Washington, D.C., in press.

Thatcher, W., 1985, Cyclic deformation related to great earthquakes at plate boundaries: Models and observations, Proc. Int'l Symp. on Recent Crustal Movements, Wellington, New Zealand, in press.

Abstracts

Atwater, B. F., J. C. Tinsley, R. S. Stein, D. A. Trumm, and S. L. Wert, 1985, Late Holocene floodplains as structural datums across the Coalinga Nose-Guijarral Hills anticline, Fresno County, California, Rymer, M. J., and Ellsworth, W. L., eds., Mechanics of the May 2, 1983 Coalinga, California, earthquake, U.S. Geol. Surv. Open-File Rep. 85-44, 437-438.

Barrientos, S. E., S. N. Ward, and R. S., Stein, 1985, Inversion for fault geometry and slip distribution of the 1983 Borah Peak, Idaho, earthquake from geodetic data, G.S.A. Abs. with Programs, Rocky Mountain Sec., 17, 207.

Barrientos, S. E., S. N. Ward, K. C. McNally, and R. S. Stein, 1984, Inversion of moment distribution with depth for the Lost River fault: 1983 Borah Peak, Idaho, earthquake, EOS, 65, 989.

King, G. C. P., and R. S. Stein, 1984, Earthquake potential of active faults, EOS, 65, 1113.

Stein, R. S., and S. E. Barrientos, 1985, High-angle normal-faulting in the Intermountain seismic belt: geodetic investigation of the 1983 Borah Peak earthquake, Idaho, G.S.A. Abs. with Programs, Rocky Mountain Sec., 17, 266.

Stein, R. S., 1984, Strategies for modeling coseismic deformation, AGU Chapman Conference on Vertical Crustal Motion, 22-26 October 1984.

Stein R. S., and S. E. Barrientos, 1984, Planar fault-slip associated with the Borah Peak, ID, earthquake, EOS, 65, 989.

Thatcher, W., 1984, Cyclic deformation related to great earthquakes in plate boundaries, 21st Annual Mtg., Society of Engineering Science, Blacksburg, VA, 15-17 October 1984.

Tucker, A. B., J. C. Tinsley, B. F. Atwater, D. A. Trumm, S. W. Robinson, R. S. Stein, D. J. Donahue, and A. J. T. Tull, 1985, Accelerator dating of detrital and burned-in-place charcoal from the alluvium of Los Gatos Creek, Fresno County, USA, 12th International Radiocarbon Conference, Trondheim, Norway.

GROUNDWATER RADON STUDIES FOR EARTHQUAKE PRECURSORS IN SOUTHERN CALIFORNIA

14-08-0001-21193

Ta-liang Teng
Center for Earth Science
University of Southern California
Los Angeles, CA 90089-0741

Investigations

We are investigating the relationship between groundwater radon content and earthquakes across the Central Tranverse Ranges of southern California.

Results

This is a six-month update of groundwater radon monitoring in the study area. The reporting period is from September, 1984 to February, 1985. The most important accomplishments are:

A. Satisfactory operation of seven continuous radon monitors (CRMs) at six sites.

      1. Haskell Ranch - This is also a test site with two CRM units for calibration.
      2. Warm Springs
      3. Seminole Hotsprings
      4. Arrowhead #2
      5. Arrowhead #4
      6. Encino Park (warm spring)

Results from the past six months of CRM operation show no anomalous measurements. All instruments have performed well except for a few short data gaps caused by battery problems. Seismicity in the monitoring region has been quiet, no moderate event has been recorded.

B. Completion of an instrument comparison experiment between USC's CRM and Caltech's RTM.

Following the experience of the calibration test on several types of tiltmeters recently carried out at Pinon Flat, the USGS adopted the recommendation from the 1984 NEHRP Review Panel and suggested that a calibration test be conducted between USC's CRM and Caltech's RTM. Principal investigators from the two research groups thus met in November, 1984, and planned a comprehensive test of the two instruments that included both a laboratory controlled test and a test carried out at an actual field site. Both tests lasted at least two months each with results summarized in Figure 1 for the lab test and Figure 2 for the field test. Details of this experiment are given in an extensive paper submitted to the USGS for an Open-File Report. A brief summary of these results and findings on these two instruments is given below.

a. The CRM and RTM have significant differences in addition to their basic counting methods (alpha scintillation vs. beta geiger counting). The CRM with its counter-flow stripping chamber is very sensitive to water phase radon. The RTM with its large air pump and closed or semi-closed radon path counts the combined effects of gas phase and water phase radon; the combined effects are basically responsible for the strong temperature dependence of the RTM output.

b. The CRM responds rapidly to changes in the radon activity in the water phase, and has a high sensitivity. Because of its high sensitivity, a low stripping efficiency at near equilibrium state can be tolerated with this instrument. Use of a low efficiency system for stripping reduces, but does not eliminate flow dependence. 25% loss of signal was experienced by the CRM in the field test owing to an order of magnitude drop in water flow rate. Changes in flow rate such as occurred when the RTM holding tank was filled produced measurable noise in the CRM signal.

c. The RTM responds more slowly to changes in radon activity than the CRM. In its usual borehole mode of operation the RTM can respond within one run (8 hours), but when used with a holding tank up to 24 hours can be required for full response. Because it is intended to measure the combined gas and water phase radon, the RTM is more sensitive to changes in water temperature that can affect radon partitioning. Changes of temperature of a few degrees C may result in as much as 50% fluctuations of the RTM output.

d. The CRM employs newer electronics and requires much less power for basic instrument operation. It does not need AC power or telephone lines provided its water supply can be obtained from an artesian well or natural spring. However, it presently has no telemetry system installed. Although the basic response of the instrument is fast (about 1 hour), appropriate telemetry is needed if and when radon monitoring is going into operation with respect to earthquake prediction. This will make use of the information it produces in a timely fashion.

e. Both instruments are useful for radon monitoring. The USC CRM is more useful in situations where there is a steadily flowing water supply (artesian well or natural spring). The Caltech RTM is more useful for monitoring from static boreholes or pumped wells, particularly if a significant gas phase is present.

f. The tests have identified features of both instruments that need improvement. At present, the CRM does not record important engineering data, and it does not automatically record background. For field installations involving waterflows, it is desirable for both CRM and RTM to monitor the flow rate. Provisions for CRM to measure cell background periodically should be included in order to check for contamination. The RTM, particularly when used with a holding tank is sensitive to water temperature. Provisions should be made to keep the water temperature in the holding tanks close to groundwater temperature at all times.

337

Figure 1a

338

1984.12.14-28 RADON-DATA * USC *

84.12.29-85.1.12 RADON-DATA * USC *

Figure 1b

339
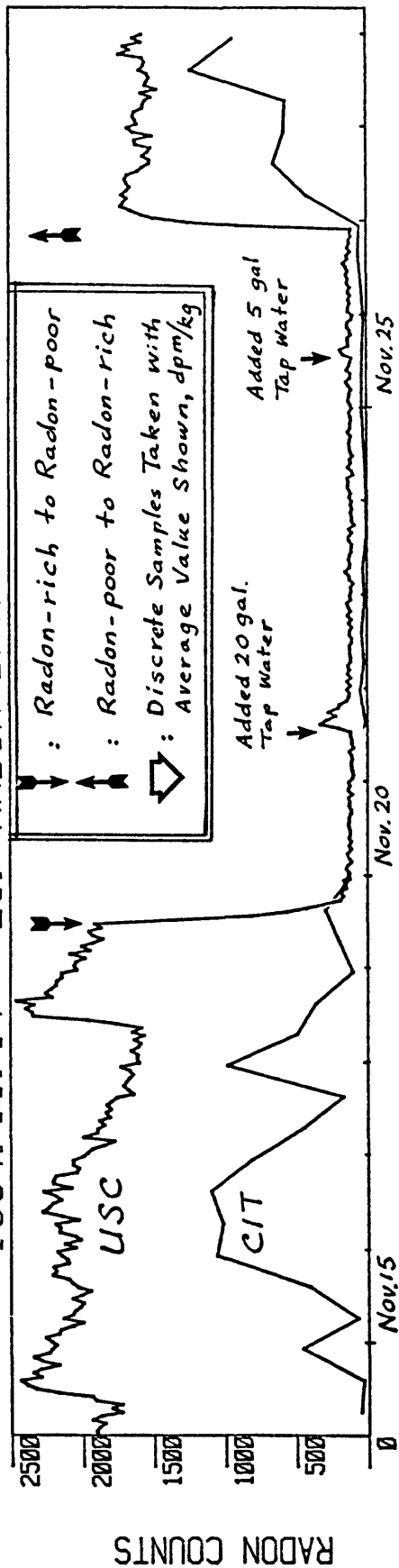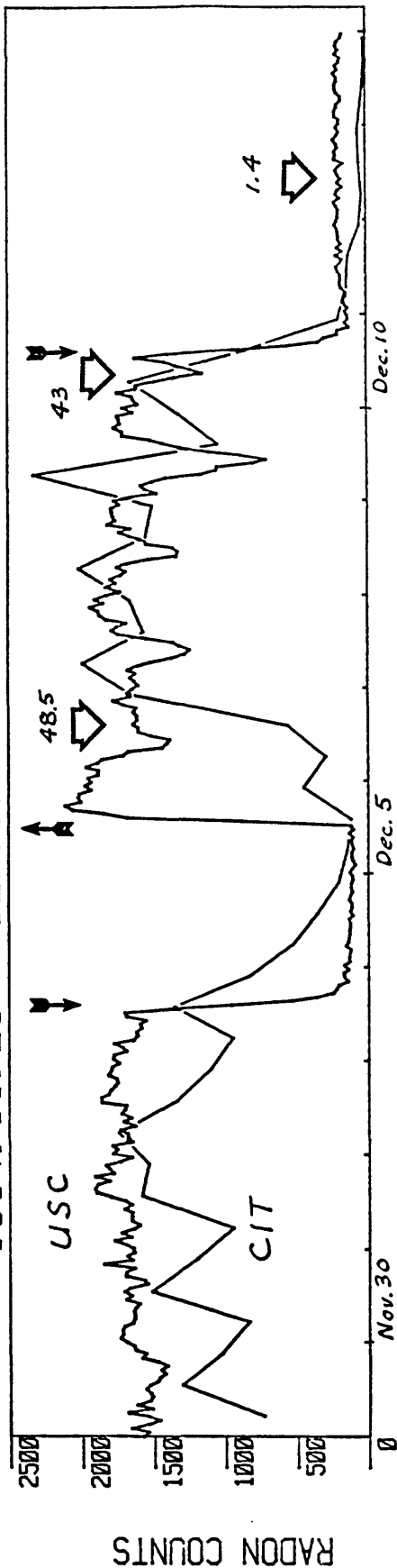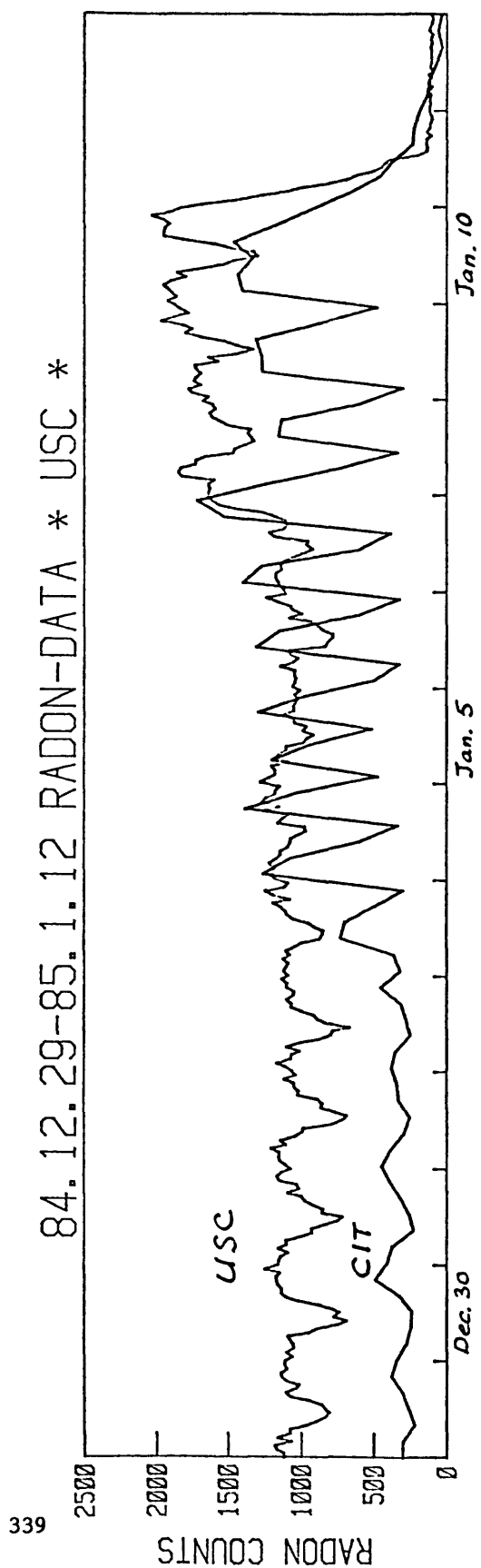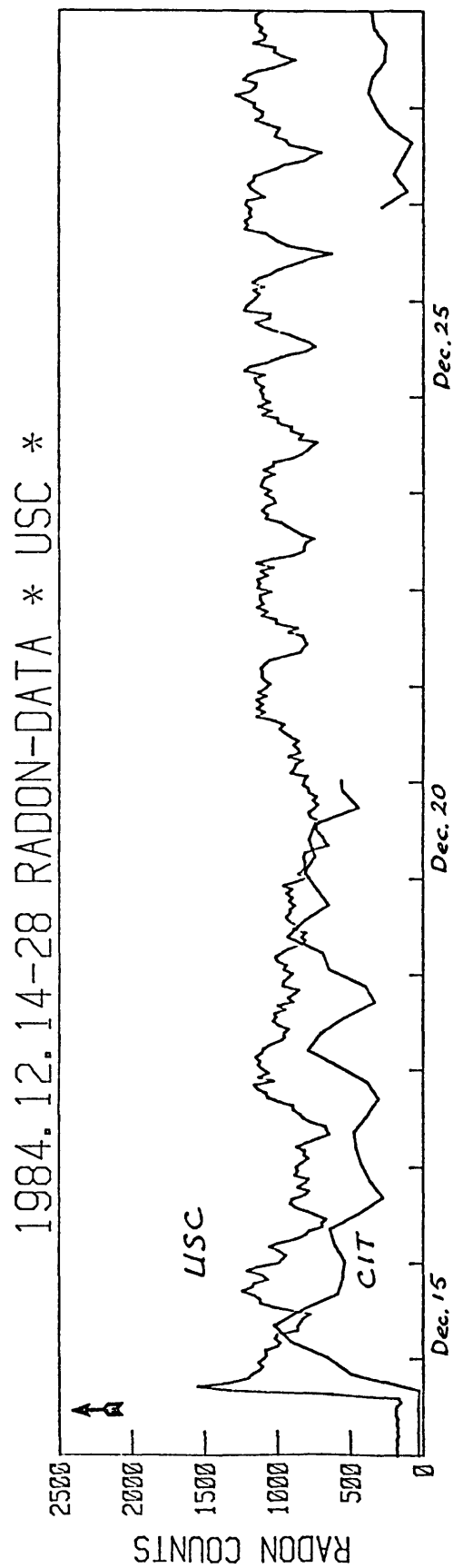
1984.12.12 - 26. RADON-DATA * FORT TEJON

P: Pumping (Note: Small downward dips record the activation of CIT's pump sensor)
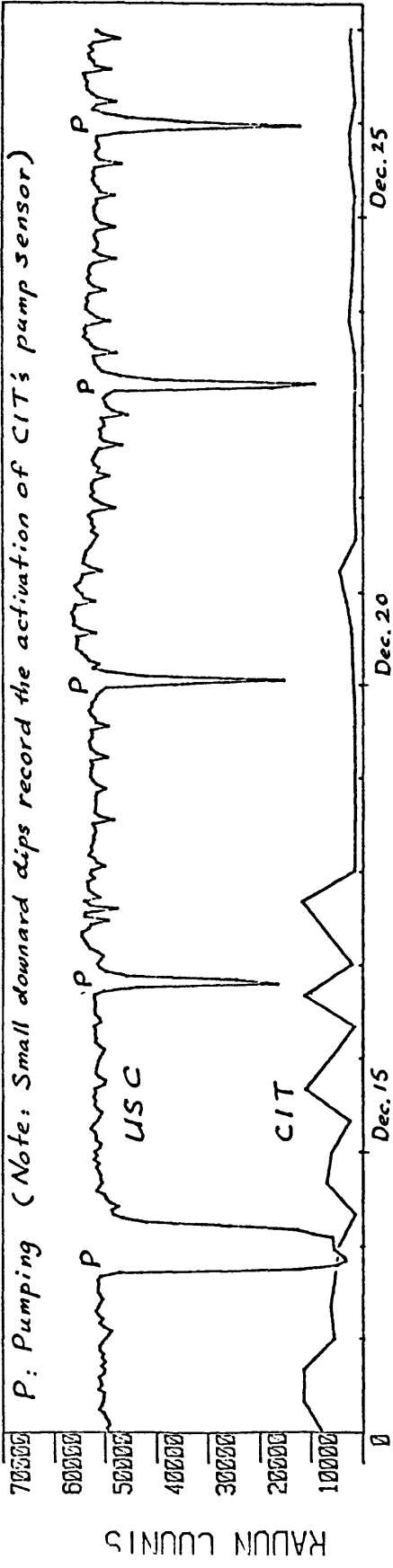
1984.12.27 - 1985.1.10.

Figure 2a

340

Figure 2b

341
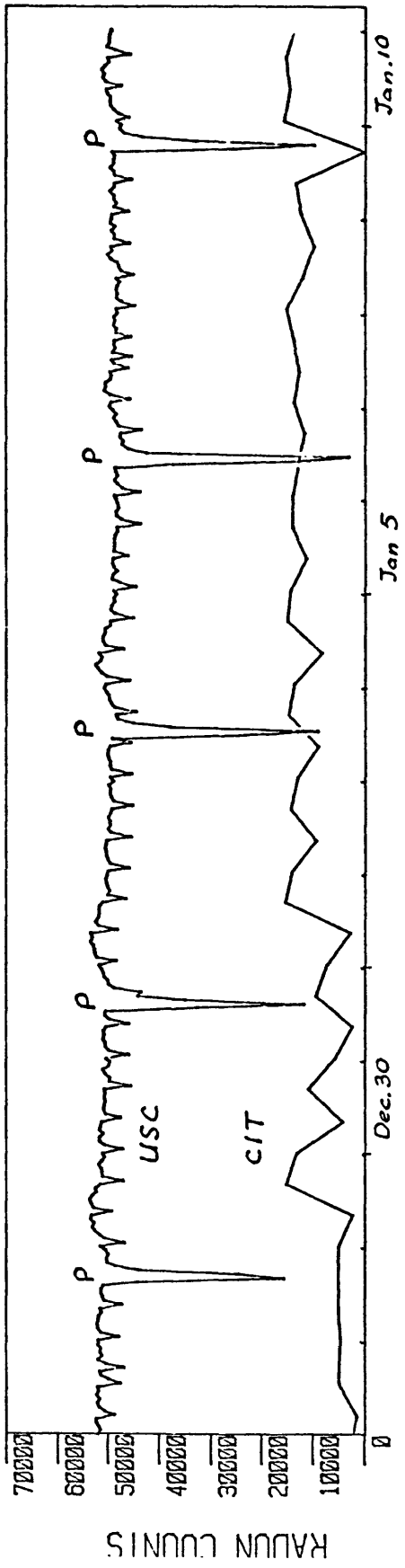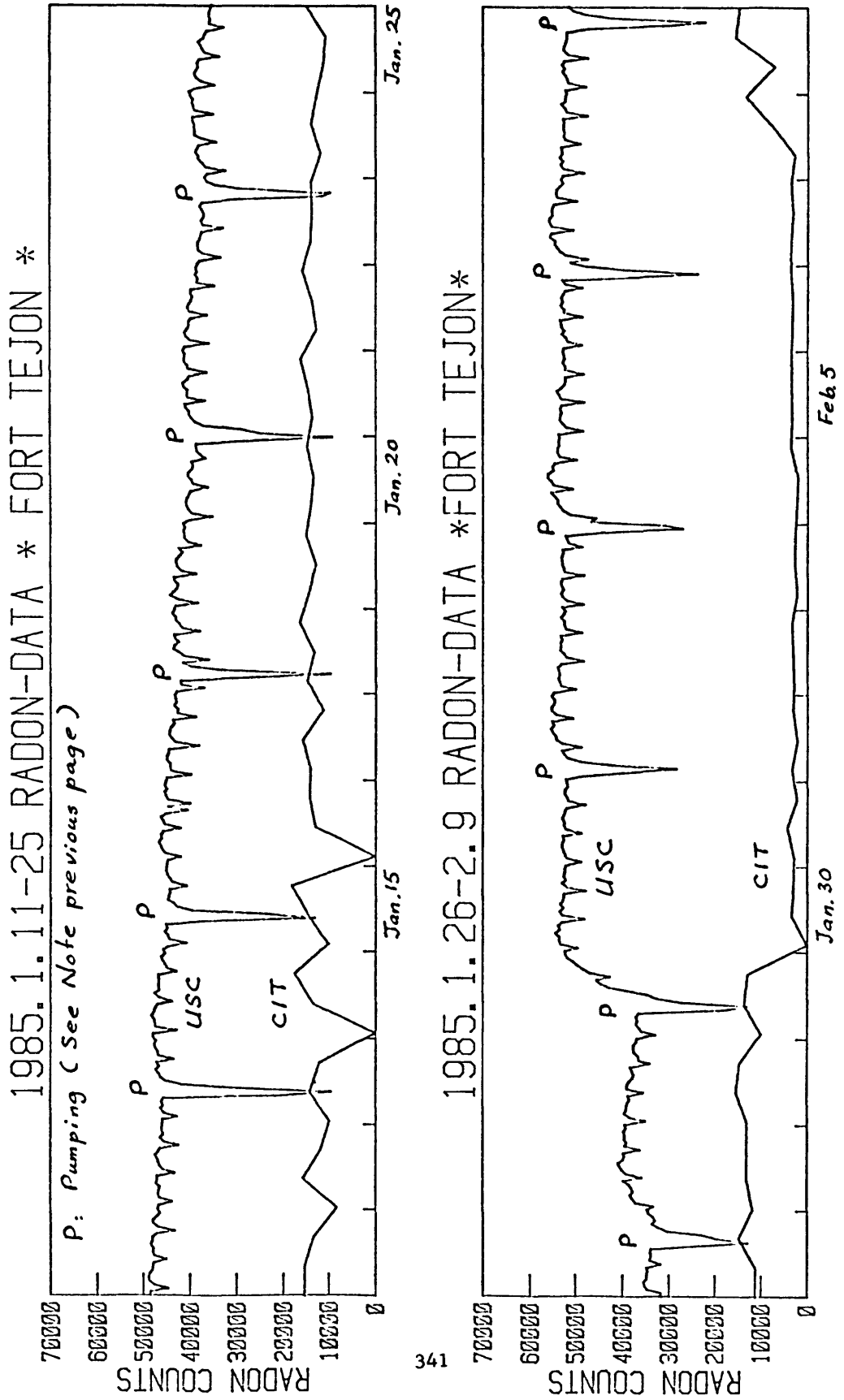
Analysis and Interpretation of Releveling
and Other Geodetic Observations in Seismically
Active Areas in the Western U.S.:
Implications for Earthquake Prediction

14-08-0001-21998

M. N. Toksöz and R. E. Reilinger
Earth Resources Laboratory
Massachusetts Institute of Technology
Cambridge, Massachusetts 02142
(617) 253-7852

INVESTIGATIONS

Analyzed and interpreted evidence for historic crustal deformation in: (1) Hebgen Lake-Yellowstone region, (2) Imperial Valley, California, (3) Rio Grande Rift, New Mexico.

RESULTS

1. *Postseismic Viscoelastic Relaxation Following the 1959 M = 7.5 Hebgen Lake, Montana Earthquake.* A 1983 releveling survey conducted by the National Geodetic Survey provides evidence for ongoing vertical deformation of a broad region (diameter $\sim$ 150 km) surrounding the site of the 1959 Hebgen Lake earthquake. Deformation consists of relative uplift centered roughtly on the coseismic fault and a smaller amplitude zone of relative subsidence south of the fault. Maximum observed elevation change during the postseismic period (1960 to 1983) exceeds 30 cm. The rate of vertical deformation appears to be decreasing exponentially with a characteristic decay time of about ten years. The spatial pattern and time behavior of the observed movements are consistent with simple models of postseismic deformation following normal faulting in an elastic layer (thickness $\sim$ 30-40 km) overlying a viscoelastic half-space (viscosity $\sim 10^{20}$ poise). This model may also account for the anomalously large horizontal strain around the Hebgen Lake region measured by repeated trilateration surveys during the period 1973 to 1984. The 1983 M = 7.3 Borah Peak, Idaho earthquake occurred in a similar tectonic setting as the Hebgen Lake event (Northern Basin and Range) and the geometry of the coseismic faults are quite similar. If the amplitude of postseismic viscoelastic deformation is linearly related to fault slip as suggested by the model used for the Hebgen Lake event, then a minimum of 6 cm of relative elevation change over a distance of about 50 km should occur during the ten-year period following the Borah Peak earthquake. This should be easily detected with modern geodetic techniques. The releveling and trilateration measurements in the Hebgen Lake region appear to provide the first observations of viscoelastic relaxation in the asthenosphere following an intraplate earthquake in the U.S.

2. *A Strain Anomaly Near the Southern End of the San Andreas Fault, Imperial Valley, California.* Repeated first-order leveling surveys conducted by the National Geodetic Survey in 1972, 1974, 1976, 1978, and 1981 provide evidence of contemporary relative uplift near the junction of the San Andreas fault and the Brawley seismic zone. Uplift, which extends over a distance of about 5 km where crossed by the leveling line, apparently developed progressively between

1972 (possibly before) and 1978. Maximum relative uplift during this period reached 58 ± 4 mm. This spatially and temporally coherent pattern of uplift was interrupted between 1978 and 1981 possibly as a result of the 1979, M6.6 Imperial Valley earthquake. While the cause of the observed uplift is unknown, given the location, one interpretation is that it represents a zone of concentrated strain possibly associated with fault activity.

3. *Evidence of Ongoing Crustal Deformation Related to Magmatic Activity Near Socorro, New Mexico*. Recent leveling conducted by the National Geodetic Survey in central New Mexico provide new evidence of ongoing tectonic deformation associated with the Rio Grande rift. A 1980-81 resurvey over suspected mid-crustal and shallow magma bodies near Socorro, New Mexico indicate continued uplift averaging 0.18 cm/yr between 1951 and 1980. Although this rate is somewhat smaller than that reported between 1912 and 1951 (0.34 cm/yr, Reilinger *et al.*, 1980), the new observations suggest possible systematic errors in the earlier surveys. Reanalysis of the earlier data suggests an average rate of only 0.23 cm/yr from 1912 to 1951, consistent not only with the new observations, but with geomorphic evidence which indicates an average uplift rate of 0.18 cm/yr over the past 20,000 years. Thus the rate of uplift may have been relatively constant with time. The new measurements also confirm prominent zones of subsidence flanking the central uplift. Modeling the deformation, together with other geophysical observations, suggests that the movements in the Socorro area are likely associated with the 19 km deep Socorro magma body. Although the details of magma movements are not well constrained, plausible models include flow of magma from the periphery towards the central magma chamber, and flow from sources in the lower crust into the mid-crust. Horizontal deformation calculated from these models is more consistent with available trilateration measurements than previous models. The Rio Grande rift is clearly an important site for future monitoring of crustal deformation.

4. *The Earthquake Deformation Cycle: Implications for the North American Vertical Datum (NAVD)*. A particularly detailed set of releveling observations in the vicinity of an intraplate, thrust earthquake (M 7.4) in Argentina, indicate a cyclic pattern of deformation very similar to that reported previously for interplate earthquakes. This deformation cycle, which may be characteristic of many seismically active areas, consists of: (1) steady strain accumulation, possibly punctuated by strain reversals; (2) coseismic strain release, (3) a period of continued strain release due to after-slip (persisting for perhaps a year or so), (4) rapid postseismic strain accumulation which decreases exponentially and grades into steady strain accumulation. Permanent deformation results when strain accumulation is not exactly balanced by strain release. Vertical deformations associated with three earthquakes in the U.S. (1940, M 7.1 Imperial Valley, California; 1964, M 8.4 Alaska; 1959, M 7.5 Hebgen Lake, Montana) are used to demonstrate that: (1) significant vertical movements can occur in association with coseismic faulting in purely strike-slip environments; (2) large postseismic vertical movements can occur for strike-slip, thrust, and normal fault events; and (3) viscoelastic relaxation must be incorporated in models of earthquake related deformation.

PUBLICATIONS

Reilinger, R.E., Vertical movements associated with the 1959, M=7.5 Hebgen Lake, Montana earthquake, *U.S. Geol. Surv. Open File Rept., 85-290*, 519-530, 1985.

Reilinger, R.E., Postseismic viscoelastic relaxation following the 1959 M=7.5 Hebgen Lake, Montana earthquake, *EOS, Trans. Am. Geophys. Union*, *66*, 383, 1985.

Reilinger, R.E., The earthquake deformation cycle: implications for the North American vertical datum (NAVD), *Proceedings of the 1985 NAVD Symposium*, in press, 1985.

Larsen, S., R.E. Reilinger, and L.D. Brown, Evidence of ongoing crustal deformation related to magmatic activity near Socorro, New Mexico, *J. Geophys. Res.*, in press, 1985.

Reilinger, R.E., A strain anomaly near the southern end of the San Andreas Fault, Imperial Valley, California, *Geophys. Res. Lett.*, submitted, 1985.

Crustal Deformation Observatory Part J:
Askania Borehole Tiltmeter

14-08-0001-21990

Frank Wyatt, Duncan Carr Agnew
Institute of Geophysics & Planetary Physics
Scripps Institution of Oceanography
University of California, San Diego
La Jolla, CA   92093
(619) 452-2019

This contract supports the installation and operation of an Askania borehole tiltmeter at Piñon Flat Observatory (PFO) and analysis of data from it. This work is part of the Crustal Deformation Observatory (CDO) program, as a cooperative enterprise with Dr. Walter Zürn of Karlsruhe University (West Germany), who is providing the instrument on loan. The goals of this project are to:

1. Establish techniques for emplacing and orienting a removable borehole tiltmeter in holes of various depths, and determine the costs of such installations.

2. Compare these borehole tilt measurements with those from adjacent long-base surface tiltmeters to establish both the sources of instability and noise, and the accuracy of the different techniques.

3. Use a commercially available transducer in an attempt to accurately monitor tilt in a tectonically active area.

We received the tiltmeter from Dr. Zurn in February 1985 (at about the same time as our initial funding), and have built a test stand for it so that we may make a preliminary installation in the basement seismic vault of IGPP. Because this is very near the shore the tidal tilts are very large, (4 μrad P-P) so that the purpose of this setup is to familiarize ourselves with the operation (the control panel and manual are in German). We have also prepared a shallow vault at Piñon Flat Observatory for a possible test setup, and laid out and installed the wiring for the borehole installation planned for this summer (location KUA, in NE corner of Figure 1).

PIÑON FLAT OBSERVATORY
PLAN VIEW OF INSTRUMENTATION
N.W. CORNER

FEBRUARY 1985
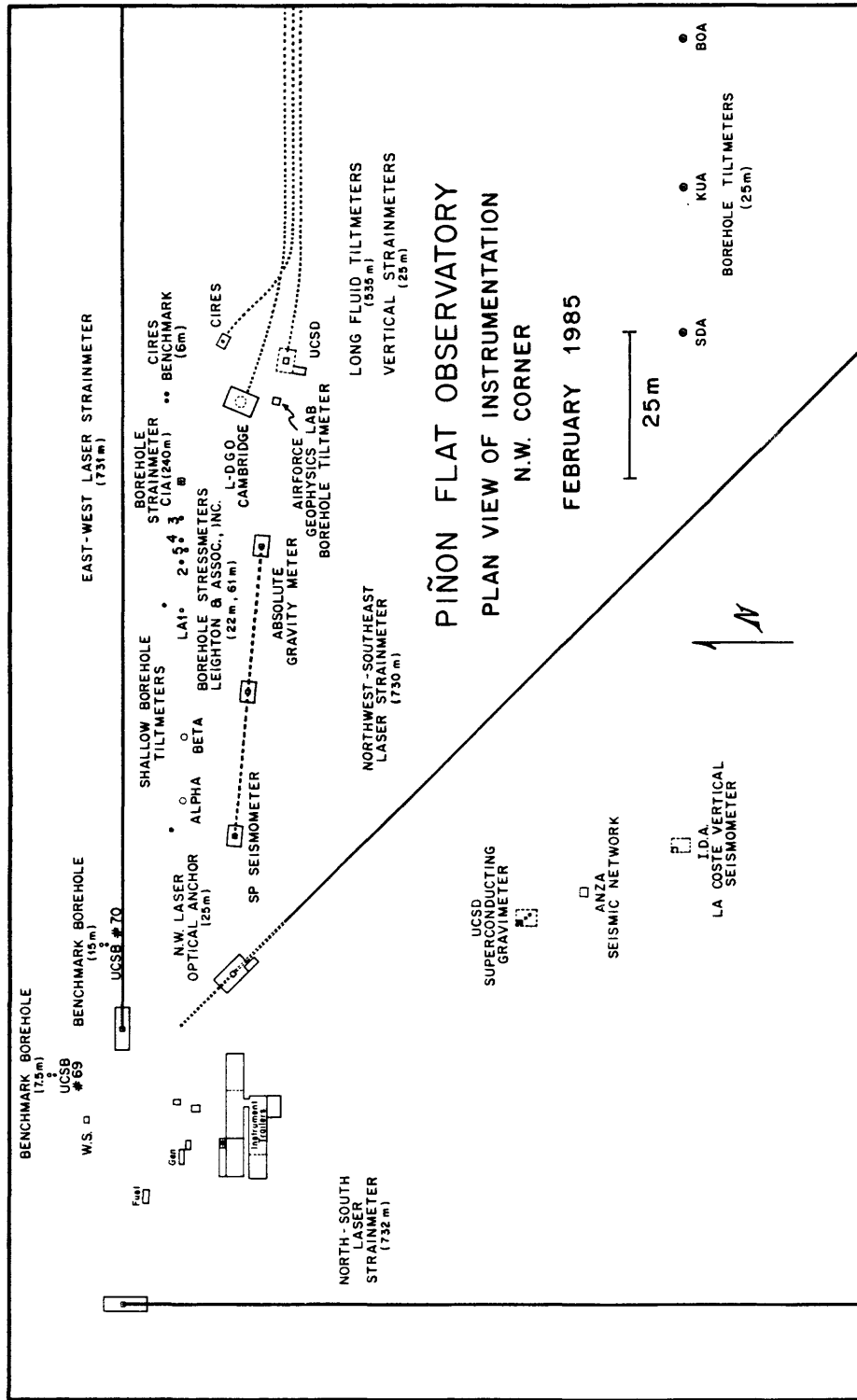
Figure 1.

Crustal Deformation Observatory Program
and Related Studies
at Piñon Flat Observatory

14-08-0001-21987

Frank Wyatt and Duncan Carr Agnew
Institute of Geophysics & Planetary Physics
Scripps Institution of Oceanography
University of California, San Diego
La Jolla, CA   92093
(619) 452-2019

This contract aids research by independent investigators working at Piñon Flat Observatory (PFO) under the sponsorship of the U.S. Geological Survey. The aid includes research coordination, instrument operation and testing, data recording, preliminary data reduction, and collaborative data analysis. This is part of a cooperative effort to evaluate instrumentation for measuring long period (days to years) ground deformation in a tectonically active area. The evaluation of these different techniques involves understanding and reducing sources of noise in the instruments as well as developing improved methods to describe the errors of the measurements.

Recent activity at Piñon Flat Observatory has includes:

1. <u>Air Force Geophysics Laboratory</u>. The A. D. Little borehole tiltmeter (BBT #2), installed March 1984, has continued in operation, although electronic problems in the downhole package have made the NS records noisy; those from the EW component (parallel to the long-base tiltmeters) have been quite good.

2. <u>Cooperative Institute for Research in the Environmental Sciences</u>. In 1984, Larry Slater made several trips to PFO in order to work on his his two-fluid tiltmeter. The beginning of measurements was delayed by problems with the acoustic transducers. Some evidence also developed that fluids were leaking from the tubing, and the decision was made to drain them completely. This was done in late 1984.

3. <u>Lamont-Doherty Geological Observatory</u>. The Lamont-Doherty tiltmeter has continued to produce good data during this period, requiring relatively little maintenance (Figure 1).

4. <u>University of California, Los Angeles</u>. Dave Jackson has continued in his role as the independent referee of the comparative tiltmeter studies at PFO. Under his supervision Michael Rogers edited CDO

data for the period of 1983:82-1984:135 and presented the results at the 1984 Fall AGU Meeting (Rogers et al., 1984). Two undergraduate UCLA students also visited PFO during the summer of 1984 to make frequent micrometer readings on the Lamont and UCSD tiltmeters as a check on the continuous sensors.

5. University of California, Santa Barbara. The UCSB surveying team measured the benchmark array at PFO in January and August 1984, for a total of 15 surveys. Results from earlier surveys were published in September 1984 (Sylvester 1984). As a test of improved benchmark construction methods, six special deep-hole rod marks were added to the existing benchmark array in August.

6. California Institute of Technology. Drs. Mark Shapiro and Jonathan Melvin have continued to operate a continuously recording radon gauge at borehole CIB; transmiting data daily, via telephone, to their lab in Pasadena. A measurement of the water height was added in March 1984.

7. Carnegie Institution of Washington. The three Sacks-Evertson strainmeters have continued to operate well during the past year, though the records were again interrupted over the summer by frequent thunderstorms, during which times the instruments were disconnected. Unhappily, one of the instruments (CIB), eight months after abruptly changing to a "zero" drift rate, began to drift rapidly in December 1984, and now appears to be inoperable. The strain rates on the other two are gradually decreasing, and the high-frequency "glitches" on them have become less frequent.

8. Leighton & Associates. Recording of the two shallow borehole stressmeters installed by Bruce Clark in 1981 has continued. A version modified for greater sensitivity was installed at 60 m depth in October 1983, a second in June 1984, and a third in October 1984.

9. NGS/JPL. The MV-3 VLBI antenna made measurements at PFO in November 1984. Measurements with a GPS receiver are planned at the VLBI mark and at the absolute gravity pier during 1985.

10. U.S. Geological Survey - Crustal Deformation. In July 1984, Doug Myren visited PFO to record (on several GEOS recorders) an NTS explosion measured by the Carnegie volumetric strainmeters. This (along with the records from the laser strainmeters) was also recorded on a datalogger at IGPP using the recently upgraded telemetry link to the site provided by Sandia National Laboratories.

11. U.S. Geological Survey - Water Resources Division. The Stevens water- level gauge in borehole CIC has continued to operate well. This record has proven extremely valuable in our attempts to understand the hydrology at PFO. Figure 2 shows the

measurements from the CIC gauge and from our electronic pressure gauge in borehole CIA.

12. <u>University of Queensland</u>. The three-component borehole strainmeter installed by Dr. M. T. Gladwin (Gladwin, 1984) in borehole UQB has operated extremely well during 1984, requiring only one visit by us (simply to reset its clock). Dr. Gladwin visited in December 1984 both to compare data and to test the seismic recording capability of the instrument.

13. <u>University of California, San Diego</u>. We prepared a preliminary comparison of the long-base tiltmeters at PFO, which was published in October 1984 (Wyatt <u>et al.</u> 1984). The main conclusion from this comparison was that even long-base instruments must be anchored to depth if the noise from soil motion is not to overwhelm the tectonic signal. For the first time we have seen some coherence outside the tidal bands between two low-noise tiltmeters (UCSD and Lamont), though the exact cause of this is not yet established.

REFERENCES

Gladwin, M. T. (1984). High-precision multicomponent borehole deformation monitoring, <u>Rev. Sci. Instr., 55</u>, 2011-2016.

Rogers, M., F. Wyatt, A. Sylvester, T. Owen, R. Bilham, C. Macdonald, and D.D. Jackson (1984). Tilt at Piñon Flat Observatory, California, <u>EOS, Trans. Am. Geophys. Union, 65</u>, 854.

Sylvester, A. G. (1984). Leveling precision and benchmark motions, Piñon Flat Observatory, California, <u>J. Geophys. Res., 89</u>, 7949-7956.

Wyatt, F., R. Bilham, J. Beavan, A. Sylvester, T. Owen, A. Harvey, C. Macdonald, D. Jackson, and D. Agnew (1984). Comparing tiltmeters for crustal deformation measurement - a preliminary report, <u>Geophys. Res. Letters, 11</u>, 963-966.
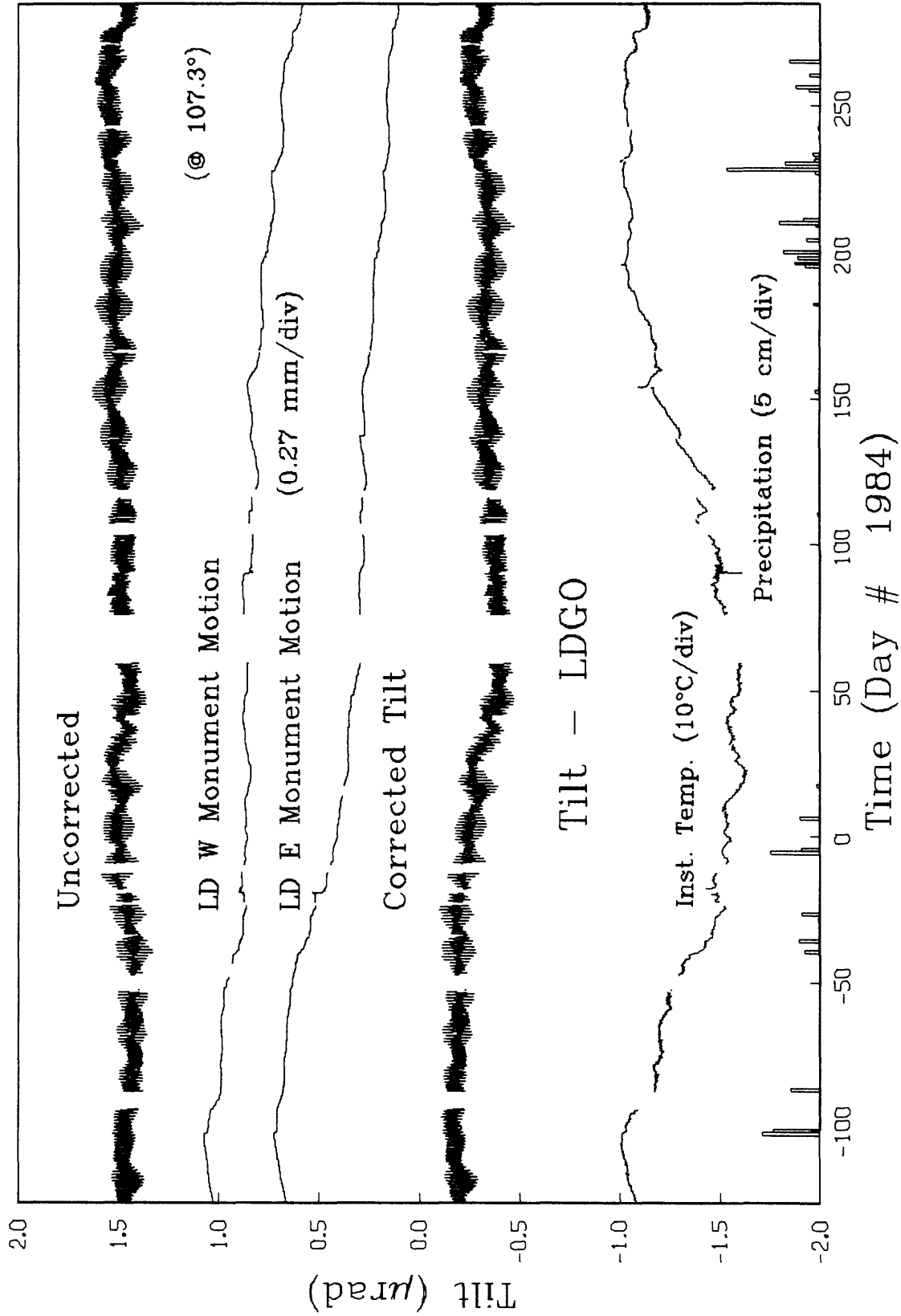
Figure 1.
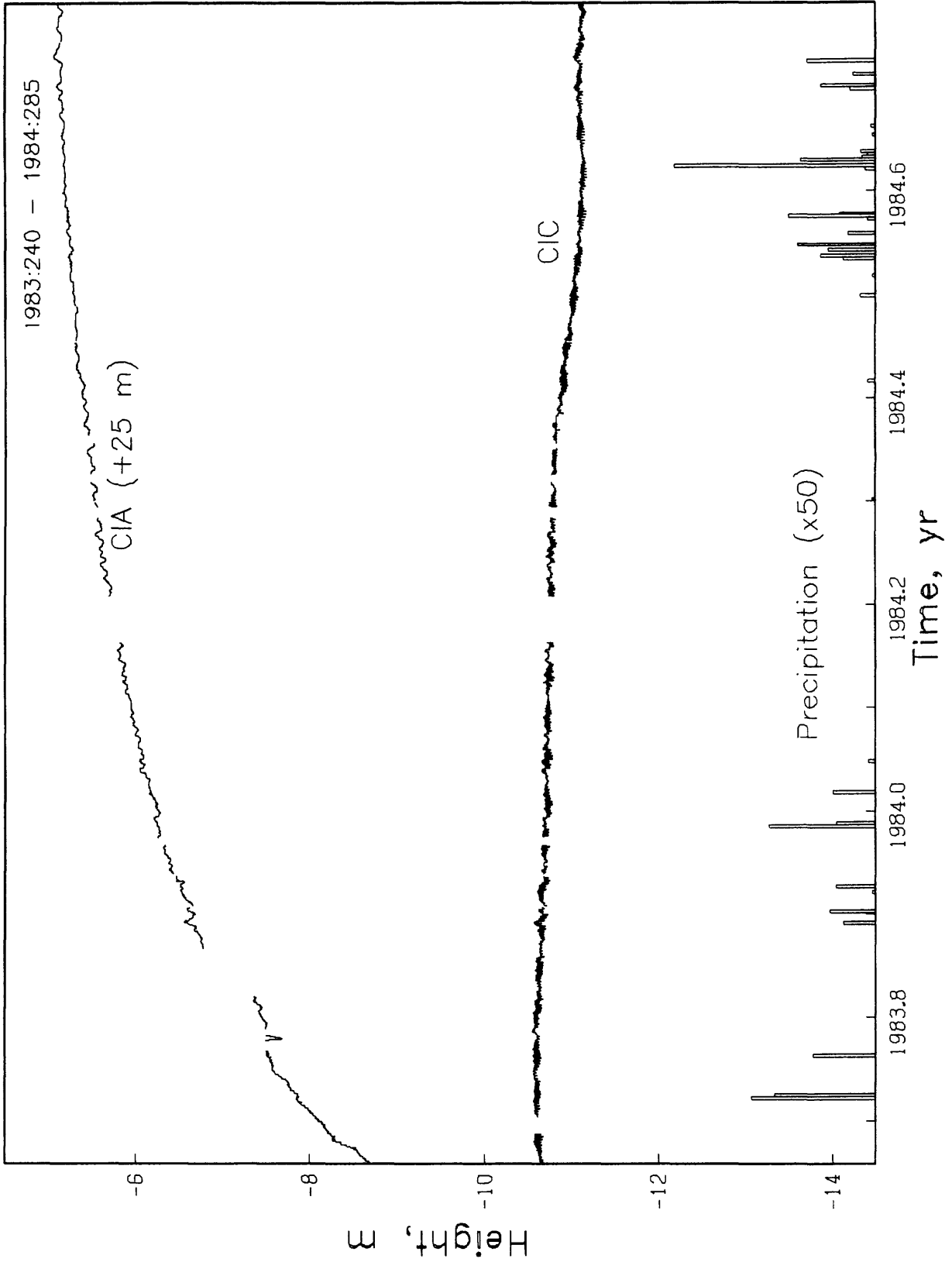
Figure 2.

Piñon Flat Observatory:
A Facility for Studies of Crustal Deformation

14-08-0001-21996

Frank Wyatt and Duncan Carr Agnew
Institute of Geophysics & Planetary Physics
Scripps Institution of Oceanography
University of California, San Diego
La Jolla, CA 92093
(619) 452-2019

Introduction

This contract provides funds for the ongoing program at Piñon Flat Observatory (PFO) by supporting a common site, with shared facilities, for improving precision geophysical instruments. The work done there includes establishing the accuracy of instruments in measuring various geophysical quantities (primarily tilt and strain) by comparing results with data from the best instruments available (the so-called reference standard instruments). This comparison also allows reliable monitoring of strain and tilt changes in the region near the observatory, between the San Jacinto and southern San Andreas faults.

This report summarizes results from the reference-standard instruments for the 410 days from 28 August 1983 through 12 October 1984.

Laser Strainmeter Observations

The longest running instruments at (PFO) are the three 732 m laser strainmeters. At all but the longest periods these strainmeters produce very quiet data and thus give useful bounds on the state of strain at Pinyon Flat. The recent records are shown in Figure 1.

Continuing efforts to identify noise sources has led to a number of refinements to all three instruments. For the true aficionados (only) we describe the details. At this time, the least reliable instrument is the North-South strainmeter; the south end- monument is subject to extreme tilting about its base (for which we correct) and, we assume, associated displacements. These cyclical signals are definitely correlated with the weather, with apparent extension of the instrument during the dry months followed by rapid compression when the soil is wet. The East-West strainmeter behaves similarly, though adding an awning in 1984 has reduced its response to rainfall. Since 1979, extensive work has been done on the Northwest-Southeast instrument to eliminate sensitivity to near-surface conditions. Optical anchors that measure horizontal motions of the end-monuments became operational at both ends of this strainmeter in late

1983. Until day 200 of 1984 applying the optical anchor corrections worked quite well, yielding (as Figure 1 shows) a remarkably flat and noise-free strain series. The storms following day 200 rather rudely reminded us of another problem. The laser beam for this stainmeter actually travels along a slightly bent path, passing through a small-angle steering prism (2.2 degrees deviation) at its midpoint. Small vertical movements of this prism (1 mm) can cause relatively large apparent strains (50 nanostrain). As this prism is not well coupled to the earth, such motions are bound to occur; we have begun an effort to cement the prism stage to the ground properly and to divert rainwater away from the area.

Long-Base Tiltmeter Observations

In contrast to the laser strainmeters, the latest results from the UCSD long fluid tiltmeter do not show any obvious response to the environment. These data are also corrected for monument motions, in this case vertical motions recorded by vertical laser strainmeters, one at each end of the tiltmeter. Applying the corrections yields the results presented in Figure 2 (both with and without the tidal signals). For this 1.1 year period the tilt is of the order of 40 nrad/a (down to the east) with variation of no greater than this about the linear trend. The origins of the 60 nrad bump beginning about day 130 of 1984 are unknown, but probably instrumental. Much of the shorter-term signal (days-weeks) is associated with a barometric response of 12 prad/Pa. The overall stability of this quantity in an area of active tectonic deformation is surprising, perhaps an artifact of the particular instrument azimuth.
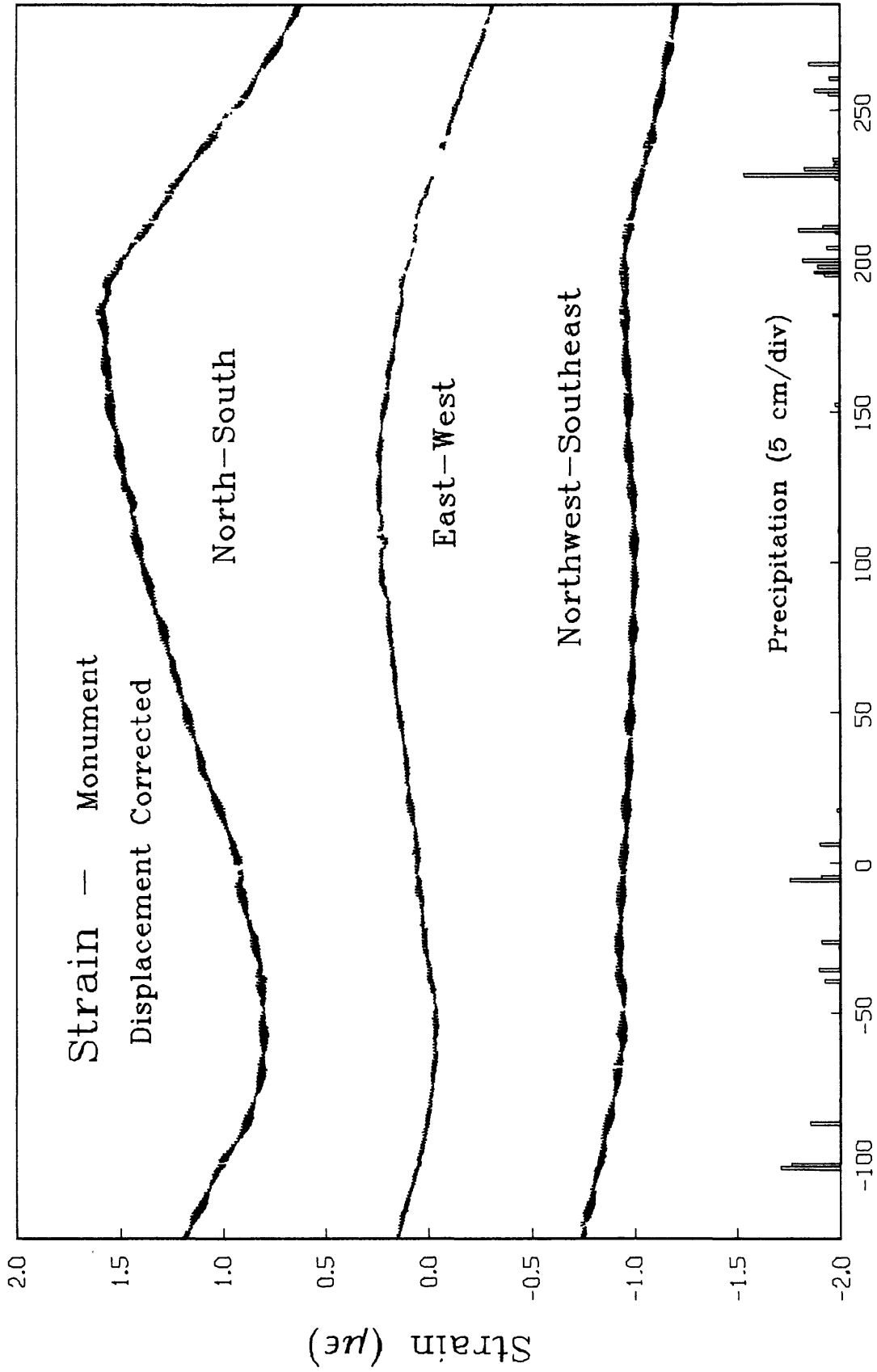
Piñon Flat Observatory   1983:240 — 1984:285

Strain — Monument Displacement Corrected

North-South

East-West

Northwest-Southeast

Precipitation (5 cm/div)

Strain ($\mu\varepsilon$)

Time (Day # 1984)
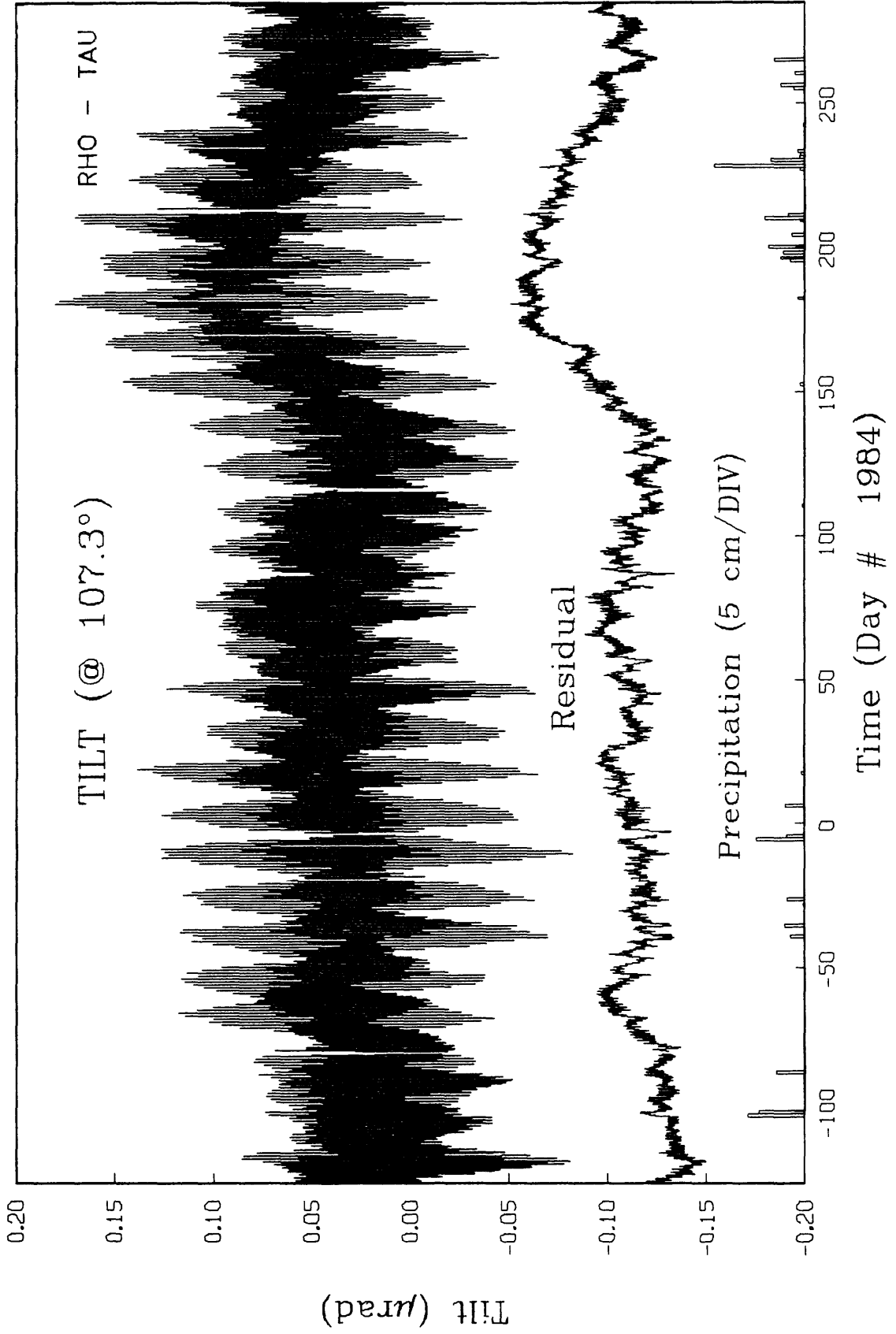
Figure 1.

Figure 2.

THERMAL, MECHANICAL, AND CHEMICAL HISTORY OF WASATCH FAULT CATACLASITE AND PHYLLONITE TRAVERSE MOUNTAINS AREA, SALT LAKE CITY, UTAH

14-08-001-G-886

R. L. Bruhn and W. T. Parry
Department of Geology and Geophysics
University of Utah
Salt Lake City, UT 84112
(801) 581-6619

INTRODUCTION

Observation of fluid inclusions on a heating-freezing microscope stage and of the mineral assemblages and fabric in the fault rock on the Wasatch fault have provided an estimate of fluid pressure, temperature, and composition on which to base estimates of the rheological behaviour of faulting, and the depth of the quasi-plastic/frictional transition in the Wasatch fault zone.

FAULT ROCK MINERALOGY AND FABRIC

Near the Wasatch Fault, footwall rock has been subjected to multiple alteration and deformation episodes with progressive displacement of the footwall. Successively younger, lower temperature, lower pressure mineral assemblages are superimposed upon older, higher temperature, higher pressure assemblages. Mechanical deformation is ductile to brittle in character in the early alteration stages and becomes successively more brittle with later lower temperature alteration.

Mechanical deformation and hydrothermal alteration of the quartz monzonite in the Wasatch fault zone has produced striking textural changes. Two textural rock types are evident – a phyllonite, containing cleavage with mineral stretching lineation, and a later cataclasite. Phyllonite is locally preserved, with the largest outcrops along the east-trending part of the Wasatch fault in Fort Canyon where the phyllonite forms a carapace about 30 m thick on the southern margin of the Little Cottonwood stock. The boundary between the undeformed quartz monzonite and phyllonite dips about 40° south, and in one area the lineation on the foliation plane was horizontal indicating dextral shear (Figure 1). The mesoscopic fabric of the phyllonite is also characterized by S-C bands, with S band thickness varying from a few millimeters to several centimeters in width. The orientation and geometry of the S-C bands indicates dextral oblique-normal shear, with an average slip vector trending about 220° (Figure 2). At one outcrop the slip direction was 150° based on S-C band geometry, but this seemed to be a local phenomenon.

The cleavage and stretching lineation is defined by flattened and stretched quartz grains, highly fractured relic feldspar augen, fractured epidote grains, and aligned sericite and chlorite grains. Axial ratios (long dimension/short dimension) of stretched

quartz grains in thin sections cut parallel to the extension lineation and perpendicular to the cleavage plane range from 1.7:1 to 5:1 with an average of 3.1:1. S-C bands and asymmetric feldspar augen indicate the phyllonite fabric developed during progressive simple shear, based on the criteria of Simpson and Schmidt (1983). Deformation of the phyllonite at the scale of mineral grains varied from quasi-plastic flow caused by dislocation processes in quartz to extensive microfracturing of feldspar concomitant with recrystallization of feldspar to phyllosilicates. Elongated quartz grains are highly undulatory under polarized light contain numerous deformation bands, and have undergone partial syntectonic recrystallization, particularly around the margins of grains. Feldspar grains, on the other hand, containing abundant microfractures and trails of comminuted feldspar are observed extending outward from feldspar augen into the foliation planes. Feldspar grains are altered to assemblages of sericite, chlorite and epidote, with the amount of relic feldspar decreasing with increasing phyllosilicate content in the phyllonite.

Cataclasite is the dominant textural rock type within the Wasatch fault zone and footwall. The cataclastic texture is marked by extensive grain size reduction of original igneous minerals and syndeformational hydrothermal minerals. The cataclasite occurs as large, tabular and lensoidal bodies forming a partly preserved carapace ten's of meters thick on the western and southern margins of the Little Cottonwood stock, and as discrete meter to millimeter thick zones associated with individual normal faults in the interior of the footwall. The cataclastic fabric has been superimposed on the remnant phyllonite fabric, demonstrating that cataclasis followed development of the mesoscopically ductile phyllonite fabric. Two periods of hydrothermal alteration can be identified as developing during cataclasis - an early high temperature assemblage of chlorite-sericite-epidote, and a later, lower temperature laumontite-prehnite assemblage.

The remnants of the catalastic carapace are characterized by penetrative systems of mesoscopic faults. These faults form populations defined by two or more fault sets with different orientations and slip vectors. Often, these mesoscopic faults permeate the rock down to centimeter scale. Numerous fault surfaces have grooves and scratch marks indicative of frictional sliding during deformation. These slicken-sided surfaces are commonly coated with finely comminuted alteration minerals, such as epidote, chlorite, and sericite.

The cataclasite is characterized by marked grain size reduction of the original igneous quartz and feldspar grains. Reduction in feldspar grain size and content in the cataclasite was accomplished by two primary means - grain size reduction by fracturing and recrystallization of feldspar to phyllosilicates. Quartz, on the other hand, appears to have been reduced in grain size solely by fracturing. Reduction in quartz grain size by fracturing was limited to a grain diameter of about 5 to 6 microns.

FLUID INCLUSIONS

Primary fluid inclusions are present in vein quartz and secondary fluid inclusions are present in igneous quartz of the quartz monzonite. Vein quartz in chlorite-sericite-quartz veins contains primary fluid inclusions consisting of carbon dioxide and a solution of water and salt. These inclusions are generally smaller than 1 or 2 micrometers and phase changes on the heating stage could not be reliably observed. Igneous quartz which

shows pronounced undulatory extinction and deformation lamellae contains abundant trains of secondary fluid inclusions that decorate healed fractures. In some cases solid inclusions of chlorite, sericite, or calcite accompany trains of fluid inclusions and sericite veinlets mark the extension of the fluid inclusion trains into surrounding feldspar. The linear trains of fluid inclusions often bisect the angle between zones of undulatory extinction (subparallel to c) and the deformation lamellae (subperpendicular to c). The trains of fluid inclusions thus coincide approximately with the maximum principal stress in the grain (Carter and Raleigh, 1969). The relationship between fluid inclusion trains, the stress system, and alteration mineral assemblage establishes their syndeformational origin. These inclusions are similar in content to smaller, primary inclusions in quartz veins; they contain a carbon dioxide vapor bubble, often surrounded by liquid carbon dioxide and an aqueous salt solution, and reach 10 micrometers in size permitting observation of phase changes on a heating-freezing microscope stage discussed below.

Careful observation of thin sections from widely spaced localities in the Little Cottonwood stock shows that no part of the stock is completely free of hydrothermal effects, and fluid inclusions are not uncommon. However, the presence of carbon-dioxide-rich inclusions in highly deformed quartz grains and in veins is uniquely restricted to the vicinity of the footwall of the Wasatch fault in the Corner Creek-Traverse Mountain locality, and the abundance of inclusions is directly related to proximity to the fault and abundance of alteration minerals.

MICROTHERMOMETRY

Identity and characteristics of fluid-inclusion contents were determined by observation of phase changes on a Chaix-Meca heating-freezing microscope stage. Phase changes which characterize the fluid are the carbon dioxide triple point at -56.6° C (disappearance of solid CO_2 on slow heating), melting of clathrate ($CO_2 \cdot 5.75H_2O$) in equilibrium with liquid and vapor CO_2 at +10 to -1.7° C depending on salinity of the aqueous phase, CO_2 liquid-vapor homogenization, and homogenization of CO_2 fluid and aqueous salt solution. An additional phase change, melting of ice in the aqueous salt solution, could not be reliably observed.

Carbon dioxide triple point temperatures are tightly grouped around -56.6° C confirming the identity of CO_2 with undetectable concentrations of methane. Above this temperature a clathrate forms in the inclusions. Melting temperatures of the clathrate have been converted to equivalent weight percent NaCl (Table 1) using the data of Bozzo et al. (1973). The average weight percent NaCl of the data displayed in Table 1 is 8.2 relative to H_2O.

Homogenization of liquid and vapor CO_2 takes place at 7.0° to 30.5° C as shown in Table 1. These temperatures define the density of the carbon dioxide portion of each fluid inclusion and are used in subsequent calculations of inclusion composition and pressure.

Finally, the temperatures of homogenization of CO_2 with the aqueous phase are shown in Table 1. Approximately two-thirds of the inclusions decrepitated before this temperature could be reached due to the high pressures within the inclusions. Fluid inclusions in the 5-10 micrometer size range can be expected to decrepitate with internal

pressures of 1 to 3 kb. (Hollister et al., 1981). The mean homogenization temperature for inclusions that did not decrepitate is 266° C.

FLUID INCLUSION COMPOSITION

The microthermometry data were interpreted in terms of entrapment temperatures and pressures. The mole fraction CO_2, NaCl, and H_2O in each inclusion were estimated using the procedures outlined by Burrus (1981) which are based on an estimate of the salinity of the aqueous phase from clathrate melting temperatures, the density of the CO_2 phase from CO_2 liquid-vapor homogenization and an estimate of the relative volume of CO_2 and aqueous phases at 40° C. Density of the CO_2 phase was calculated from the data of Angus et al. (1973), density of the aqueous phase was calculated from Potter and Brown (1977) and mole fractions of each component were then computed from volumetric and density estimates.

Fluid inclusion microthermometry is used to estimate densities of inclusion fluids. The liquid-vapor homogenization temperature of CO_2 defines CO_2 density, and salinity estimated from clathrate melting temperature defines water density. The overall fluid inclusion density, D_I, is obtained from an initial estimate for XCO_2 from microscope observation of vapor bubble size and fluid inclusion size, and an initial estimate of pressure at T_H (overall homogenization temperature) using the two phase boundary curves of Bowers and Helgeson (1983b). The overall density of the inclusion contents is then computed at T_H and pressure using the modified Redlich-Kwong coefficients of Bowers and Helgeson (1983a). Generally, the estimate of volume will differ from the initial estimate made from microscope measurements probably due to errors in estimation of the third dimension for inclusions with irregular geometries. An erroneous estimate of XCO_2 will result that will lead to an incorrect pressure estimate and an incorrect density. A new estimate of XCO_2 is made from the calculated volume and the calculation is repeated until a consistent set of pressure, density, and volume are obtained. Estimated uncertainties are: T_H ($\pm 5^\circ$C), P ($\pm$ 200 b), weight percent NaCl ($\pm$ 1).

Pore fluid pressures, temperatures, and compositions are shown in Table 1. The pressure on the two-phase boundary for each fluid inclusion has been estimated and is shown in Figure 3, which also shows the P-T projection of the two phase region for 10 mole percent CO_2 and 6.7 weight percent NaCl. Fluid pressures range from a maximum of 2800 b to the minimum observed pressure of 1150 b. These estimated temperatures and pressures are minima and the true entrapment P-T conditions must lie along isochores in the single phase region for each fluid inclusion composition. Fluid inclusions show a range in vapor bubble proportions, mole fraction carbon dioxide and density of carbon dioxide suggesting that pressure reduction has resulted in separation of carbon dioxide rich vapor and that entrapment is near the two phase boundary. Maximum pressure is near lithostatic pressure and minimum pressure is near hydrostatic pressure. A broad trend is evident from higher pressures and higher temperatures to lower pressures, lower temperatures, and decreasing X_{CO_2} consistent with displacement of the footwall block of the fault.

DEPTH OF FAULTING

Our estimates of temperatures and pressures of pore fluids lead naturally to estimates of other parameters of the Wasatch fault including depth of formation of the fault rock, minimum throw on the fault, minimum age, and displacement rate. The maximum fluid pressure of 2800 b is equal to lithostatic pressure at a depth of 11 km for a rock density of 2.6 g/cm^3. The temperature at this pressure is 337°C (Table 1) which is consistent with a thermal gradient of 30°C per km. Other high pressures in Table 1 plot near a lithostat defined by a thermal gradient of 30°C per km and a rock density of 2.6 g/cm^3 (Figure 3). The present-day geothermal gradient in this portion of the Western United States is near 30° C/km (Lachenbruch and Sass, 1977) placing the minimum fluid inclusion entrapment temperature of 223° C at a depth of 7.2 km and the maximum temperature of 353° at a depth of 11.4 km. Fluid pressures in fluid inclusions of 2800 b to 1150 b (Table 1) are between a lithostatic and hydrostatic geotherm for a thermal gradient of 30°C/km (Figure 3). A higher thermal gradient would place the highest fluid pressures above the lithostatic geotherm, and a lower thermal gradient leads to geologically unreasonable depths and displacement rates.

A minimum uplift rate required to bring alteration mineral assemblages and fluid inclusions formed at 300°C to the surface on the footwall of the fault is 0.5 mm/yr. Fission track dating of apatite from the Archean Farmington Canyon complex 50 km north of Corner Creek suggests uplift rates of 0.012 mm/yr. from 90 m. y. to 10 m. y. and accelerated uplift of 0.4 mm/yr from 10 m. y. to the present (Naeser et al., 1980). If uplift of the CO_2 rich fluid inclusions began 10 m. y. ago then the slip rate must be at least 1.0 mm/yr in good agreement with rates of 0.8+0.6 or -0.2 mm/yr reported by Swan et al. (1981) for the last 19,000 years.

SEISMOGENIC CHARACTERISTICS OF THE FAULT ZONE

Understanding the seismogenic characteristics of the Wasatch fault zone is a primary objective of our research. The transition depth from frictional to quasi-plastic deformation within the fault zone is particularly important, because this depth should represent the peak shear strength in the crust, and consequently, the depth at which large characteristic earthquakes nucleate (Sibson, 1977, 1982, 1984; Meissner and Streahlau, 1982). The quartz monzonite protolith exposed at Traverse Mountain is similar in composition to the quartzo-feldspathic gneiss, schist and igneous rock that forms the crystalline basement throughout northern Utah. Therefore, estimates of the depth to the frictional/quasi-plastic transition at Traverse Mountain may have regional implications for the seismogenic characteristics of the entire Wasatch fault zone.

Structural fabrics, mineral assemblages, and pressure/temperature characteristics of fluid inclusions at Traverse Mountain indicate that fault rock originally located at the frictional/quasi-plastic transition has been preserved in the footwall during uplift caused by normal faulting. The phyllonite fabric is highly ordered, with flattened and aligned mineral grains defining the cleavage and lineation. This type of fabric develops as the result of aseismic creep according to Sibson (1977). The cataclastic fabrics, which were superimposed on the phyllonite during uplift, are poorly ordered, and presumably developed as the result of seismic slip at depths above the frictional/quasi-plastic transition in the fault zone. Quartz monzonite in the footwall immediately adjacent to

the phyllonite is essentially undeformed and in particular, shows no evidence for quasi-plastic flow of quartz. Consequently, quasi-plastic deformation was confined to the fault zone at depths below 11 km and was not pervasively distributed throughout the crystalline basement.

Thermo-mechanical modelling of the transition from frictional to quasi-plastic deformation in the crust has been applied by several authors in studies of crustal seismicity (Meissner and Strehlau, 1982; Sibson, 1982, 1984; Chen and Molnar, 1983; Smith and Bruhn, 1984). The models have been based on experimentally calibrated creep and frictional sliding laws for different lithologies at various combinations of temperature and strain-rate. Meissner and Strehlau (1982) and Smith and Bruhn (1984) predicted the depth to the frictional/quasi-plastic transition in the eastern Basin-Range Province as 8-10 kilometers by using rheological parameters for quasi-plastic flow of westerly granite published by Hansen and Carter (1982) and assuming hydrostatic fluid pressure, a contemporary heat flow of 90 mW/m^2 and an extensional strain rate of 10^{-13} to 10^{-15} sec^{-1}. This depth is located below 80% of recorded earthquakes in the crust, indicating that the modelled transition is near, but not at, the base of the seismogenic zone. We have plotted the frictional/quasi-plastic transition depth for westerly granite as a function of strain-rate in Figure 4 for hydrostatic fluid pressure and for fluid pressure equal to 90% of lithostatic pressure.

Westerly granite is a reasonable material for modelling the behavior of Little Cottonwood quartz monzonite. Our fabric data from the Wasatch fault zone indicates that the transition from quasi-plastic to frictional deformation in quartz monzonite was marked by a change from dislocation-dominated flow to extensive cracking in quartz. Feldspar, on the other hand, behaved brittley in both the phyllonite and cataclasite, deforming by cracking and altering to phyllosilicates. Therefore, quartz was apparently the dominant mineral controlling the change from ductile to brittle behavior -- a similar situation to that observed in laboratory rock deformation experiments on westerly granite.

The frictional/quasi-plastic transition in the quartz monzonite in the Corner Creek area occurred at temperatures near $350^\circ C$, at depths in excess of 11 km, and at fluid pressures between hydrostatic and lithostatic. These temperatures and depths are consistent with a regional geotherm of about $30^\circ C/km$ and with a modelled transition depth for Westerly granite at strain-rates of about 10^{-12} to 10^{-13} sec^{-1} and fluid pressures at or above hydrostatic values. These strain-rates are 2 to 3 orders of magnitude greater than those estimated for the eastern Basin-Range and Wasatch fault zone from geodetic and seismic moment tensor inversion (Dozer and Smith, 1982; Snay and others, 1984). This discrepency could result from errors in extrapolating laboratory flow laws to geological strain-rates. Alternatively, strain rates of 10^{-11} to 10^{-13} sec^{-1} are probably representative of crustal fault zones (Sibson, 1984), and there are some data supporting this contention from the Wasatch fault zone. A minimum average uplift rate to exhume the fault rock at Traverse Mountain is about 0.5 mm/year. If displacement is concentrated in a zone between 1m and 100m wide, which is reasonable based on our mapping, then shear strain rates would be between 10^{-11} and 10^{-13}/sec in the fault zone. Further testing of this hypothesis is underway using fission track data to refine the uplift history of the footwall in the Traverse Mountain area.

Our geological mapping of the fault dip and our estimate of the depth to the frictional/quasi-plastic transition can be used to estimate the maximum expectable earthquake magnitude in the Salt Lake segment using the fault area-magnitude relation-

ships of Wyss (1979). The fault zone dips about 40°-45° west along the edge of the Little Cottonwood stock in the southern part of the Salt Lake segment. The down-dip, seismogenic length of the fault zone is estimated as about 17 km -- the depth to the frictional/quasi-plastic transition divided by the sine of the dip angle. This value, when multiplied by the strike length of the Salt lake segment (35 km) yields an estimated seismogenic fault area of 600 km^2, a fault area capable of generating magnitude 6.9 earthquakes. This result is consistent with the characteristic earthquake magnitudes of 7 to 7.5 estimated from surface faulting displacements (Schwartz and Coppersmith, 1984).

REFERENCES

Angus, S., B. Armstrong, K. M. de Reuk, V. V. Altunin, O. G. Gadetskii, G. A. Chapale, and J. S. Rowlinson, International Thermodynamic Tables of the Fluid State: Carbon Dioxide, Pergamon Press, New York, 1973.

Bowers, T. S., and H. C. Helgeson, Calculation of the thermodynamic and geochemical consequences of nonideal mixing in the system H_2O-CO_2-NaCl on phase relations in geologic systems: Equation of state for H_2O-CO_2-NaCl fluids at high pressures and temperatures, Geochim. et Cosmochim. Acta, 47, 1247-1275, 1983a.

Bowers, T. S., and H. C. Helgeson, Calculation of the thermodynamic and geochemical consequences of nonideal mixing in the system $H_2 O-CO_2 -NaCl$ on phase relations in geologic systems: Metamorphic euilibria at high pressures and temperatures, Am. Mineralogist, 68, 1059-1075, 1983b.

Bozzo, A. T., J. R. Chen, and A. J. Barduhu, The properties of the hydrates of chlorine and carbon dioxide. In: Delyannis, A. and Delyannis, E. Eds. 4th Int. Symposium on Freshwater from the Sea vol. 3, 437-451, 1973.

Burruss, R. C., Analysis of phase equilibria in C-O-H-S Fluid inclusions: in Mineralogical Association of Canada Short Course in Fluid Inclusions: Applications to Petrology, editors L. S. Hollister and M. L. Crawford, 39-74, 1981.

Carter, N. L. and C. B. Raleigh, Principal stress directions from plastic flow in crystals, Geol. Soc. Am. Bull., 80, 1231-1264, 1969.

Chen, W., and W. P. Molnar, Focal depths of intracontinental and intraplate earthquakes and its implications for the thermal and mechanical properties of the lithosphere, J. Geophys. Res., 88, 4183-4214, 1983.

Hansen, F. D. and N. L. Carter, Creep of selected crustal rocks at 1000 MPa (abstract), EOS Trans. AGU, 63, 437, 1982.

Hollister, L. S., M. L. Crawford, E. Roedder, R. C. Burruss, E. T. C. Spooner, and J. Tournet, Practical aspects of microthermometry in Hollister, L.S. and Crawford, M. L., editors, Short Course on Fluid Inclusions: Applications to Petrology, Mineralogical Association of Canada Short Course Handbook Vol. 6, 278-304, 1981.

Lachenbruch, A. A., and J. H. Sass, Heatflow in the United States and the thermal regime of the crust, in The Earth's Crust, Geophys. Monogr. Ser., Vol. 20, edited by J. G. Heacock, pp. 626-675, AGU, Washington, D. C., 1977.

Meissneer, R., and J. Strehlau, Limits of stresses in continental crusts and their relationship to the depth-freequency distribution of shallow earthquakes, Tectoncis, 1, 73-89, 1982.

Naeser, C. W., B. R. Bryant, M. D. Crittenden, and M. L. Sorenson, Fission-track dating in the Wasatch Mountains, Utah: an uplift study, Proceedings of Conference X, Earthquake hazards along the Wasatch and Sierra Nevada Frontal Fault Zones, U. S. Geol. Surv. Open-File Rept. 80-801, 634-646, 1980.

Potter, R. W., II, and D. L. Brown, The volumetric properties of aqueous sodium chloride solutions from 0° to 500° C at pressures up to 2000 bars based on a regression of available data in the literature, U. S. Geol. Survey Bulletin, 1421-C, 36p, 1977.

Schwartz, D. L., and K. J. Coppersmith, Fault behavior and characteristic earthquakes: examples from the Wasatch and San Andreas fault zones, J. Geophys. Res., 89, 5681-5698, 1984.

Sibson, R. H., Fault rocks and fault mechanisms, J. Geol. Soc.. London, 133, 741-767, 1977.

Sibson, R. H., Fault zone models, heat flow, and the depth distribution of earthquakes in the continental crust of the United States, Bull. Seismol. Soc. Am., 72, 151-163, 1982.

Sibson, R. H., Roughness at the base of the seismogenic zone, contributing factors, J. Geophys. Res., 89, 5791-5800, 1984.

Simpson, C., and S. M. Schmidt, An evaluation of criteria to deduce the sense of movement in sheared rocks, Bull. Gol. Soc. Amer., 94, 1281-1288, 1983.

Smith, R. B., and R. L. Bruhn, Intra-plate extensional tectonics of the eastern Basin-Range: inferences on structural style from seismic reflection data, regional tectonics, and thermal-mechanical models of brittle-ductile deformation, J. Geophys. Res., 89, 5733-5762, 1984.

Swan, F. H., III, K. L. Hanson, D. P. Schwartz, and P. L. Kneupfer, Study of earthquake recurrence intervals on the Wasatch fault at the Little Cottonwood site, Utah, U. S. Geol. Survey, Open-File Report No. 81-450, 30 p, 1981.

Wyss, M., Estimating maximum expectable magnitude of earthquakes from fault dimensions, Geology, 7, 336-340, 1979.

Table 1. Fluid inclusion characteristics in Wasatch Fault cataclasites

Sample	Inclusion Number	Tcm	Tlv	TH	WNaCl	XCO_2	P (b)
CHC-1	2	5.8	19.0	303	7.5	.13	2150
CHC-6	1	4.4	26.0	330	9.7	.14	2350
	4	7.0	27.1	307	5.5	.14	1800
	5	7.5	25.7	292	4.6	.18	1450
	7	5.9	28.2	289	7.3	.10	1500
	8	6.0	30.5	288	7.2	.08	1300
	9	5.6	29.0	250	7.8	.05	1100
	11	5.0	25.5	271	7.0	.09	1350
	12	6.1	26.5	302	8.8	.13	1800
	13	7.0	26.0	272	5.5	.11	1475
	14	6.8	26.1	272	5.8	.12	1750
	16	4.5	23.3	279	9.5	.09	1750
	17	3.5	26.5	268	11.0	.07	1425
	21	4.2	29.6	288	10.0	.08	1400
	22	5.0	30.0	292	8.8	.09	1300
CHC-10	1	5.8	27.3	288	7.5	.11	1500
	3	6.5	19.1	283	6.3	.11	2100
	6	4.0	22.4	353	8.0	.17	2200
	8	6.0	25.5	262	7.2	.09	1700
	10	3.7	25.5	273	10.7	.09	1900
	14	5.2	25.7	244	8.5	.07	1450
	15	4.3	25.2	248	9.8	.06	1400
	16	2.0	22.9	270	12.9	.08	1900
S3-2	8	-1.7	26.7	282	16.8	.08	2300
S3-3	1	4.4	16.0	304	9.8	.13	2400
	6	7.3	7.3	306	4.9	.28	2300
	7	7.0	9.6	300	5.5	.22	2500
	9	6.3	7.0	337	6.7	.28	2800
	11	6.5	11.3	300	6.3	.16	2600
	13	7.2	10.3	324	5.1	.35	2300
	15	7.3	10.2	296	4.9	.24	2100
	16	7.2	9.0	295	5.1	.18	2450
	17	7.7	9.7	317	4.2	.31	2300
CHC-7	2	1.0	17.3	254	14.1	.09	1700
	4	3.3	26.2	227	11.3	.04	1150
	5	3.0	26.9	239	11.7	.05	1500
	6	3.3	26.6	223	11.3	.04	1150
MEAN				266	8.2	.13	

Tcm = clathrate melting temperature, Tlv = CO_2 liquid-vapor homogenization temperature, TH = homogenization temperature, WNaCl = weight percent NaCl relative to H_2O, XCO_2 = mole fraction CO_2, P = fluid pressure in bars.
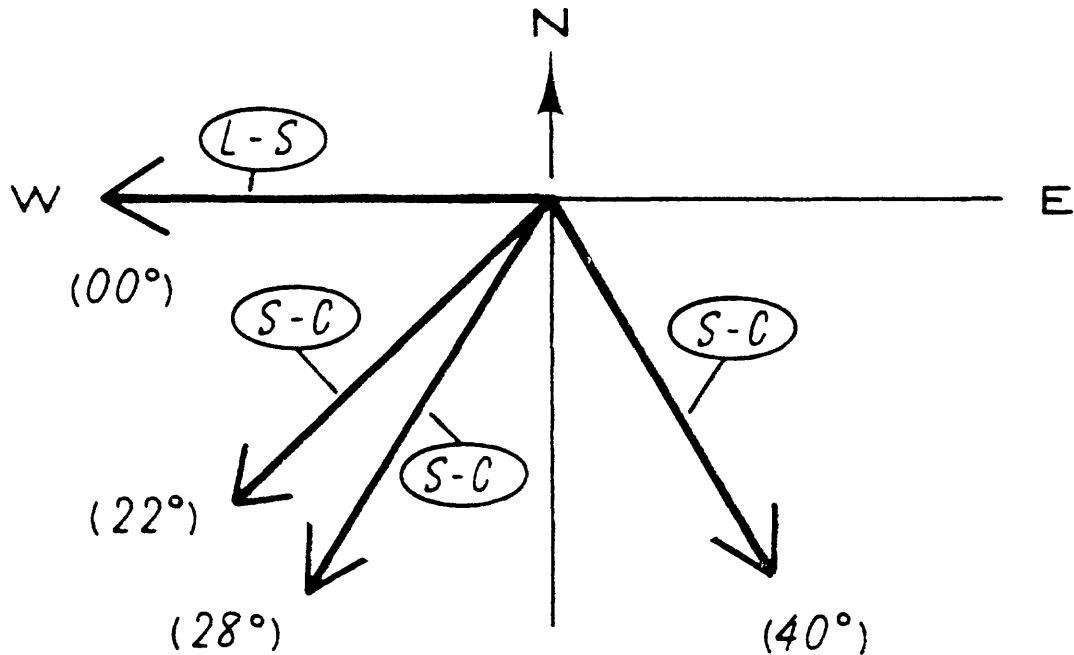
S-C   Slip determined by geometry of s-c bands

L-S   Slip determined using geometry of lineation, foliation plane and shear zone boundary

Trend and plunge of slip vector
(22°)

Figure 1.   Slip direction for shearing during formation of phyllonite in Fort Canyon area. Slip directions were determined using methods of Ramsay and Graham (1970) for L-S fabrics and method of Simpson and Schmidt (1983) for S-C fabrics. The L-S and S-C band measurements come from two outcrops in Fort Canyon with surface areas of 500 m^2. Each measurement represents an average for an outcrop area of 100 m^2 as determined by visual inspection of the fabrics within the rock. West to southwest slip directions are most representative. The results are discussed in the text.
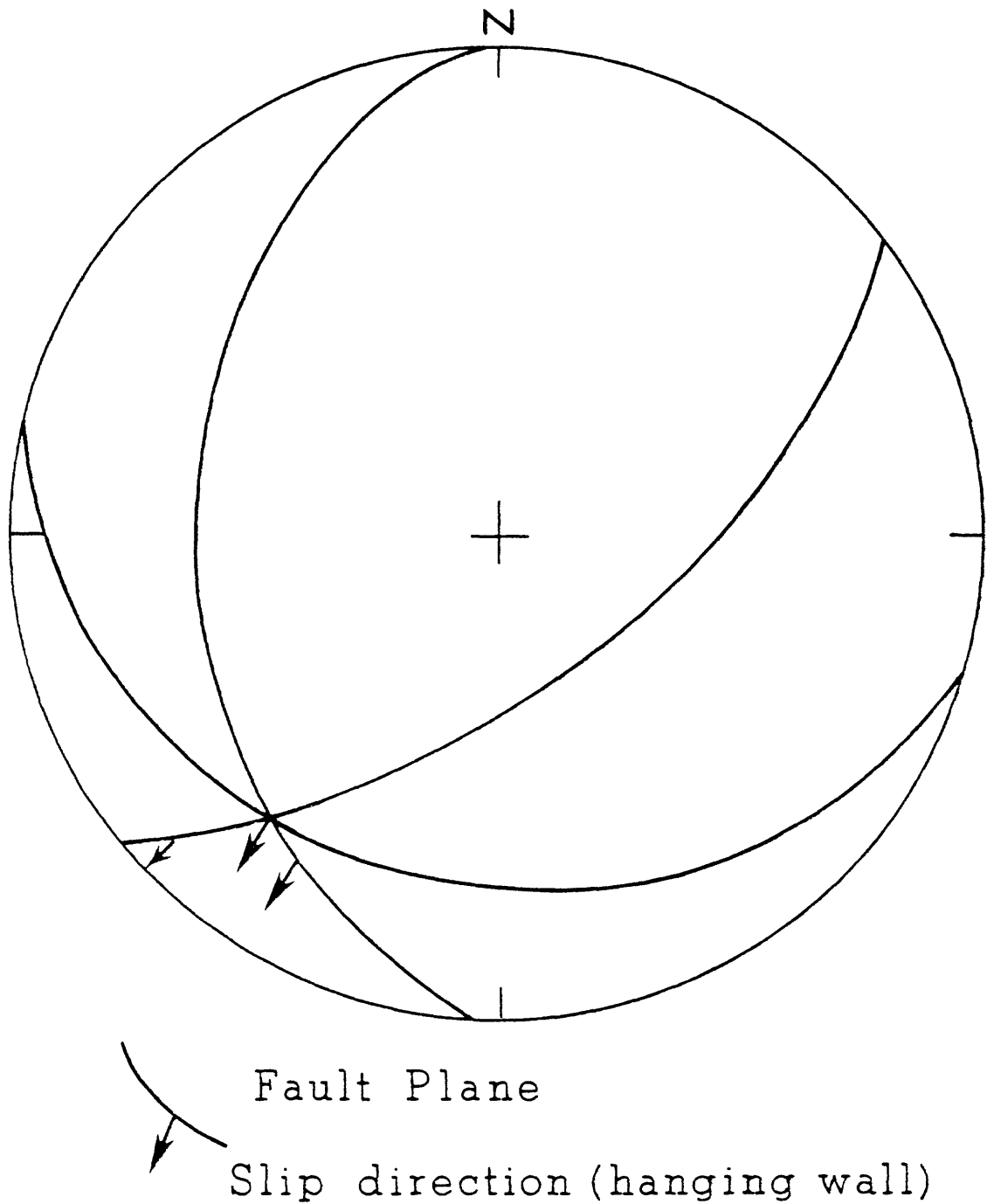
Figure 2. Stereographic plot showing the representative orientations of major mescocopic fault sets in the footwall of the Wasatch fault. The data come from the western margin of the Little Cottonwood stock. The fault sets are representative of more than 100 fault plane measurements by R. L. Bruhn and P. R. Gibler. Data are plotted on a lower hemisphere, equal area projection.
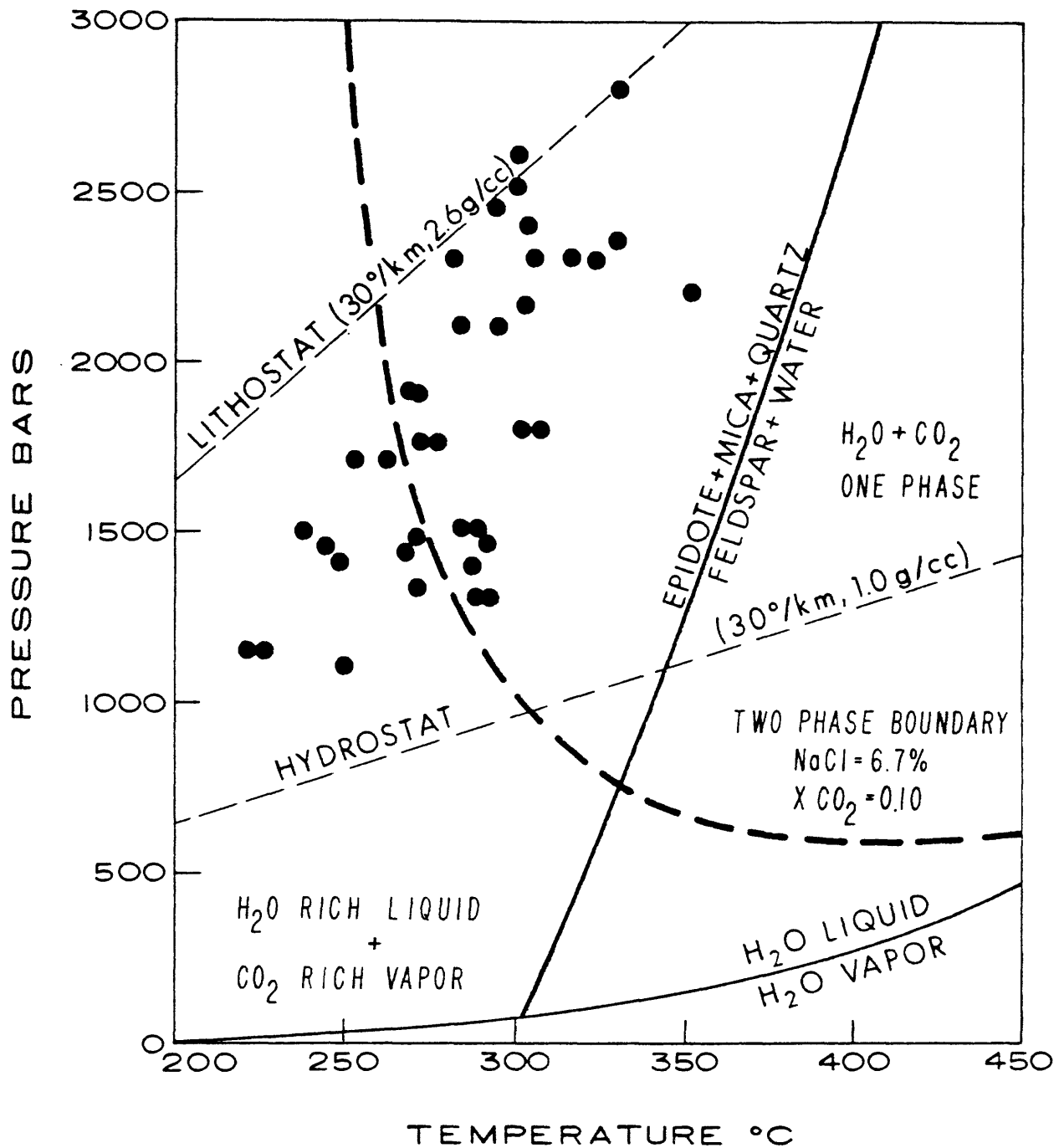
Figure 3. Fluid pressures and temperatures estimated from fluid inclusions in the Wasatch Fault rocks. Also shown are the boiling curve for water with 8% NaCl, the two-phase boundary for 6.76% NaCl, and 10 mole % CO_2, a univariant equilibrium curve for the reaction epidote + mica + quartz = feldspar + water, hydrostatic and lithostatic pressure gradients.
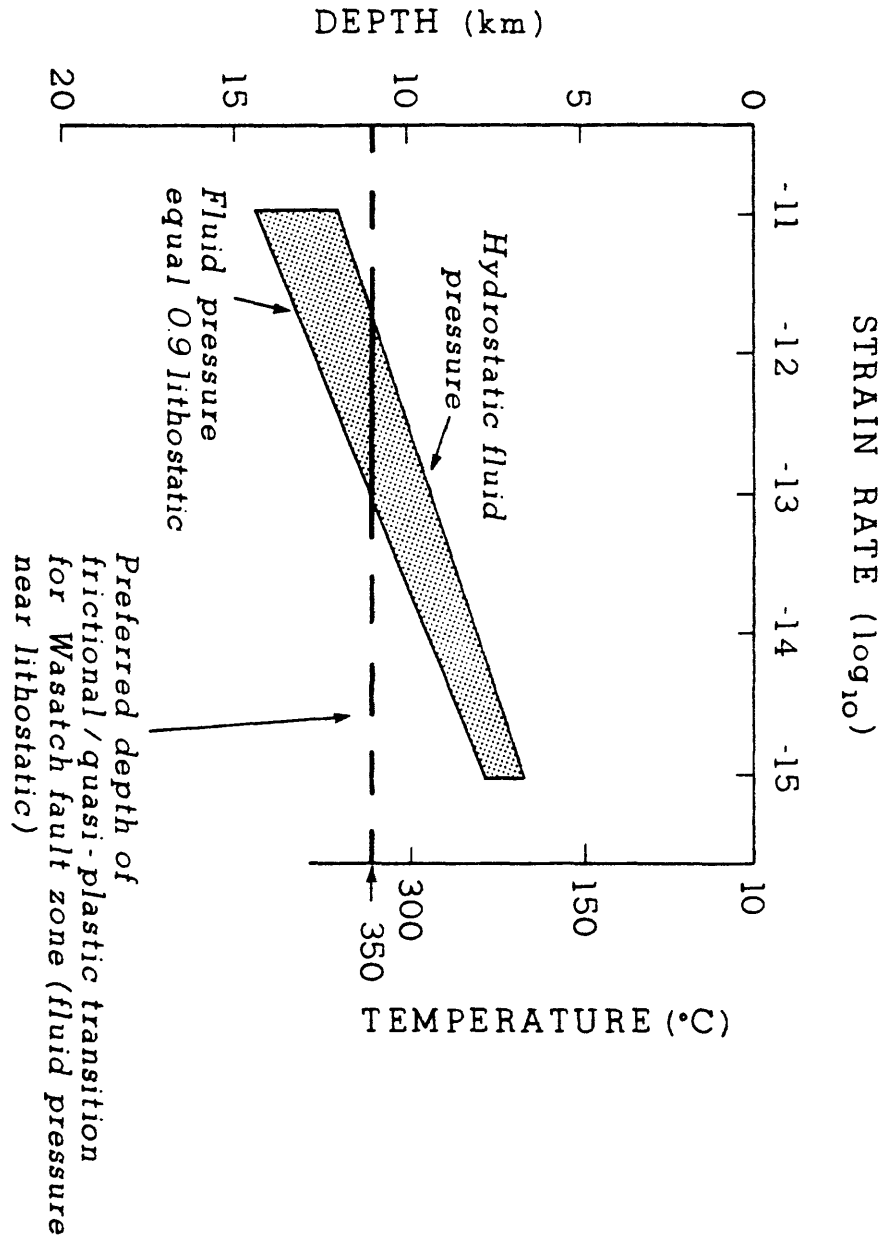
Figure 4. Frictional/quasi-plastic transition depth for Wasatch fault zone compared with calculated depths for westerly granite. Dotted box represents range of frictional/quasi-plastic trasnition depths for westerly granite in a normal faulting regime with Basin-Range heat flow, strain-rates from 10^{-11} to 10^{-15} s^{-1}, and hydrostatic to 90% lithostatic fluid pressure.

ROCK MECHANICS

9960-01179

James Byerlee
U.S. Geological Survey
Branch of Tectonophysics
345 Middlefield Road, MS/977
Menlo Park, California 94025
(415) 323-8111, ext. 2453

Investigations

Laboratory experiments are being carried out to study the physical properties of rocks at elevated confining pressure, pore pressure and temperature. The goal is to obtain data that will help us to determine what causes earthquakes and whether we can predict or control them.

Results

The coefficient of friction μ, observed in sliding experiments on rocks, generally varies with changes in sliding rate. To measure such changes, the quantity, $B = \Delta\mu/\log_{10} (v_2/v_1)$, has been defined as the slip rate sensitivity of the friction coefficient. B is positive if μ increases with increasing slip rate. Both positive and negative values of B have been observed in different types of experiments. However, it is not clear what specific experimental variables may account for these differences in the sign of B. We have conducted several sliding experiments on sawcut samples of Westerly Granite in a triaxial apparatus. The samples were initially water-saturated and a pore water pressure of 0.5 MPa was maintained constant during each experiment. A layer of crushed Westerly Granite, 1 mm thick, was placed along the sawcut to simulate a layer of fault gouge. Two experiments were conducted at each of three confining pressures (3.5, 30 and 300 MPa). The slip rates varied from 7.33×10^{-3} μm/sec to 7.33 μm/sec in one decade increments. The average value of B was $0.007\pm.006$ for all six experiments. B values did not appear to correlate with either normal stress or amount of slip. The changes in μ resulting from slip rate changes were frequently superimposed on longer term variations in μ. Thus, in these cases, we extrapolated the linear strain hardening from one slip rate increment to the next in order to obtain B. A positive value of B was also obtained in an experiment on a dried sample in which the normal stress was maintained constant rather than confining pressure. Rapid slip events occurred in most experiments, but these were not specifically associated with velocity changes.

Reports

D. Lockner and J. Byerlee, 1985, Complex resistivity of fault gouge and its significance for earthquake lights and induced polarization, Geophys. Res. Lett., v. 12, no. 4, p. 211-214.

D. Lockner and J. Byerlee, 1984, Complex resistivity measurements of fault gouge and implications for earthquake lights, E.O.S. Trans. Am. Geophys. Union, v. 65, no. 45, p. 1078.

J. Byerlee and P. Vaughan, 1984, Dependence of friction in water saturated granite with added gouge, E.O.S., Trans. Am. Geophys. Union, v. 65, no. 45, p. 1078.

D. Moore, Ma Jin, R. Summers, and J. Byerlee, 1984, The affect of strain rate and pore pressure on the strength of heated fault gouge, E.O.S. Trans. Am. Geophys. Union, v. 65, no. 45, p. 1078.

J. Byerlee, Ma Jin, and D. Moore, 1984, Frictional strength and mode of sliding of fault zones within the crust, I.A.S.P.E.I., p. 210.

In Situ Stress Measurements

9960-01184

John Healy
Branch of Tectonophysics
U.S. Geological Survey
345 Middlefield Road   MS 977
Menlo Park, CA   94025
415/323-8111, ext. 2535

Activities

We are in the process of preparing new sets of hydrofrac equipment to work at pressures up to 10,000 psi. We plan to use this equipment in August 1985 in the Cajon Pass hole to depths of about 6,000'.

Reports

Hickman, S. H., Healy, J. H., and Zoback M. D., 1984, In situ stress, natural fracture distribution, and borehole elongation in the Auburn geothermal well, Auburn, New York.

Mooney, W. D., Fuis, G. S, and Healy, J. H., 1984, Seismic refraction studies of a sedimentary basin, southern California, USA: Methods and results: submitted to Journal of the Association of Exploration Geophysicists.

Healy, J. H., Hickman, S. H., Zoback, M. D., and Ellis, W. L., 1984, Report on televiewer log and stress measurements in core hole USW-G1, Nevada Test Site, December 13-22, 1981: U.S. Geological Survey Open-File Report 84-15, 51 pp.

Stock, J. M., Healy, J. H., and Hickman, S. H., 1984, Report on televiewer log and stress measurements in core hole USW-G2, Nevada Test Site, U.S. Geological Survey Open-File Report 84-172, 48 pp.

Zoback, M. D., Healy, J., Lachenbruch, A., and Henyey, T., 1984, In situ stress, heat flow, and fault zone monitoring in a deep well near the San Andreas fault at Cajon Pass (abs.): EOS, Transactions of the American Geophysical Union, v.   , no.   , p.   .

372

Tilt at Pinon Flat, California

David D. Jackson and Michael Rogers
Department of Earth and Space Science
University of California
Los Angeles, California 90024

OBJECTIVES

The Crustal Deformation Observatory is a cooperative project whose goal is to develop and test advanced methods for observing crustal deformation, and to compile an accurate record of such deformation at one site in southern California. The UCLA role is primarily data analysis. The site is the Pinon Flat Observatory (PFO), located between the San Andreas and San Jacinto faults near Palm Desert, CA. PFO is operated by the University of California at San Diego (UCSD).

We have measured tilt at PFO using both continuously recording tiltmeters and geodetic leveling. No tectonic tilt has occurred there since 1981, to within an uncertainty of about 100 nanorad/yr.

CONTINUOUS TILTMETER OBSERVATIONS

We have now analysed 2.98 years of tilt data from three long baseline fluid tiltmeters at Pinon Flat Observatory, California. The tiltmeters operate on the same 535m baseline oriented N107E. There are two fluid level tiltmeters which use Michaelson interferometers to measure the water level at each end. These were built by UCSD and the Lamont Doherty Geological Observatory, and they will be referred to as 'UCSD' and 'LDGO' respectively. Cambridge University have built a fluid pressure tiltmeter (called 'CAMB') with a pressure transducer at the center. The CAMB and LDGO instruments share the same end piers, so any differences represent experimental error. The UCSD tiltmeter is only 10 m away, so it should be geophysically equivalent to the others, but local soil motions might cause differences. The LDGO is a relative instrument, in that any arbitrary tilts would go undetected whenever the instrument is out of service.

The tiltmeter data are shown in Figure 1. These data have been filtered to remove tides. The most stable tilt record is UCSD while the other tiltmeters contain transients as large as a few hundred nanorads over a few months. This may be due to tilting or instrumental drift or a combination of both.

Figure 2 shows a subset of the data collected after some problems with the lasers on the LDGO instrument were resolved, and after corrections for vertical strain in the upper 25 m below each endpoint were implemented. The upper curve shows LDGO, while the lower curve shows UCSD. The straight lines are least squares fit linear trends through both datasets. The estimated trends are 130 +/- 6 and 19 +/- 2 nanorad/yr, respectively. The error estimates are not very meaningful, because the data are far from being statistically independent, but they do serve as a guide to the deviations about the linear trends. We do not associate the estimated trends with tectonic activity; rather we believe that the observed trends are approximate upper limits to the magnitude of secular tectonic tilting at Pinon Flat. It is interesting that the deviations from the secular trends are of the same sign for both instruments during much of the time period. These similarities suggest that the variations are caused by true tilt, rather than instrumental problems. However, these tilts might well be surficial effects rather than tectonic.

We looked for evidence of temperature and rainfall effects on the corrected tilt data by regressing tilt on temperature, rainfall, and ten tidal components. The temperature was measured at 1 m depth, and the rainfall was a 40 day running mean of recorded daily values. Results are as shown in Table 1.

Table 1

Inst	Effects	Temp Sens (nrad/deg)	Prob (%)	Rain Sens (nrad/mm)	Prob (%)
LDGO	Temp only	11 +/- 1.	0	-	-	-
LDGO	Rain only	-	-	-	23. +/- 2.	0
LDGO	Both	21 +/- 2	0	4.4 +/- 2.5	8
UCSD	Temp only	1.9 +/- 0.3	0	-	-	-
UCSD	Rain only	-	-	-	39. +/- 2.3	0
UCSD	Both	0.3 +/- 1.0	76	0.15 +/- 1.40	92

In this table, '-' means that the value was constrained to zero, and 'Prob' is the probability that the estimated regression coefficient, or a larger one, would occur at random if the true value were zero. Thus any coefficient having a 'Prob' of 5 or less is significant at the 95% confidence level. From the table, it is clear that the tilts are significantly correlated with some linear combination of temperature and rainfall, but the specific effects of temperature and rainfall cannot be resolved. The temperature coefficients are not of serious concern, because the temperature variations are only a few degrees. However, the rainfall coefficients may indicate a significant problem: rainfall averaged over 40 days might reach 10 mm or more, causing up to 400 nrad of tilt during a particularly rainy season, if the 'Rain only' models were correct.

A possible source of error for the LDGO tiltmeter is the lack of an absolute measurement of water heights at the ends. For this instrument, changes in water height are measured by counting interferometer fringes, but the absolute fringe count is lost when the instrument is out of service because of power failures, etc. For short service breaks the fringe count may be reconstructed with little error, but for longer breaks the error may be substantial, and even smaller errors may accumulate to serious levels over time. For this reason, the LDGO has mechanical micrometers installed to measure the water level independently of the laser interferometers. The UCSD tiltmeter uses a white-light interferometer, which provides a more nearly absolute measurement, so it is not affected as much by service breaks. However, the UCSD tiltmeter also has micrometers at either end, adjusted automatically by a servomotor to track water height. To test the precision of the micrometers, and thus the degree to which electronic drift could be reduced by using the micrometer measurements, we conducted a controlled experiment. The micrometers were read four times per day over a 14 day period. Tilts estimated from the UCSD micrometers are compared with the electronically read values in Figure 3. Because the micrometers are adjusted automatically by servomotor, the values read by the observers are not independent of the electronic values, and the excellent agreement is not surprising. Similar values for the LDGO tiltmeter are plotted in Figure 4. Here the electronic and micrometer

values are quite independent, and agreement is not guaranteed. There were many power failures during the first week of the experiment, and the LDGO tilt data required extensive editing which was performed without reference to the micrometer data. Algae in the water at the East end of the tiltmeter caused serious errors in the micrometer readings. We now believe that drift in the electronics can be reduced well below the level of drift caused by residual soil motions and errors in the vertical strain measurements.

LEVELING

UCSB has carried out 14 leveling surveys at PFO since 13 Oct 79. 7 of these surveys, from 25 Jan 81 to 26 Jul 84, have included the end points of the UCSD tiltmeter as monuments. The inferred tilt rate is 150 +/- 190 nanorad/yr, consistent with a lack of tectonic tilt. For the other monuments, random benchmark motions of up to 1mm cause the dominant errors in the leveling data. Therefore, we established several special benchmarks anchored at about 10m depth. Using these monuments, we can estimate the tilt rate to within about 500 nanorad per year.

CONCLUSIONS

Tilt records at Pinon Flat for the last 3 years are among the most accurate and stable observed anywhere. Secular tilting has not exceeded 100 nanorad/year during this time period. Any episodic tilting greater than 100 nanorad in a few months would have been detected on both the UCSD and the LDGO tiltmeters. No such episodic tilts occurred.

The Pinon Flat experiment has been exceptionally successful in achieving high accuracy tilt measurements that lead to unambiguous geophysical conclusions. This rare success is due to several factors, including the creativity and strenuous effort of the experimenters; the existence of a secure, well maintained site; a philosophy of doing things properly rather than cheaply; and especially the tender loving care provided to the instruments at Pinon Flat by Leo Wueve.

TILTMETER DATA FROM PINON FLAT, CALIFORNIA
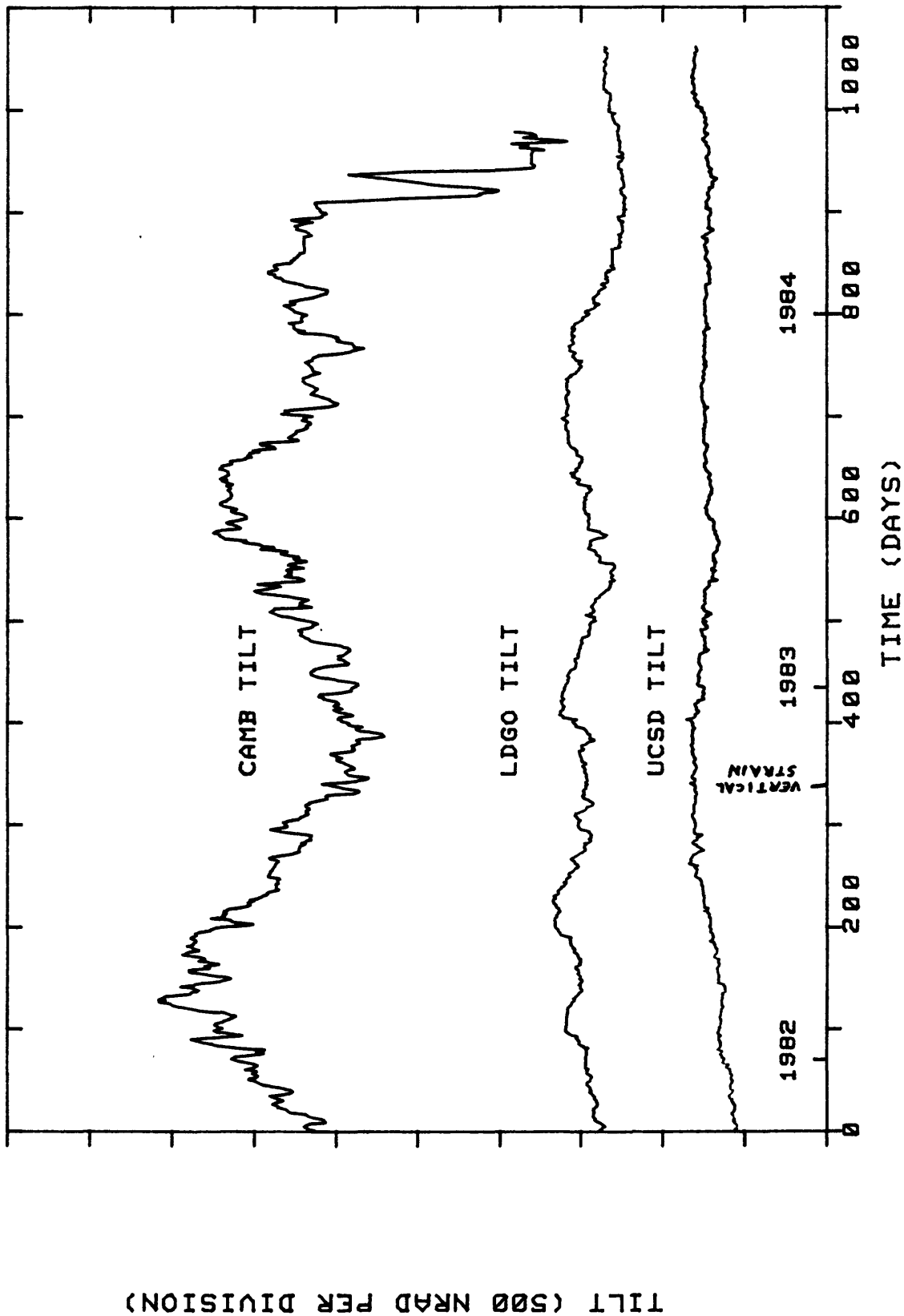
Figure 1. Tilt variations at Pinon Flat, CA, measured on three adjacent long-baseline tiltmeters. Record starts on 21 Oct 81 and ends 11 Oct 84. After 27 Sep 82, the LDGO and UCSD records have been corrected for near surface soil motions.
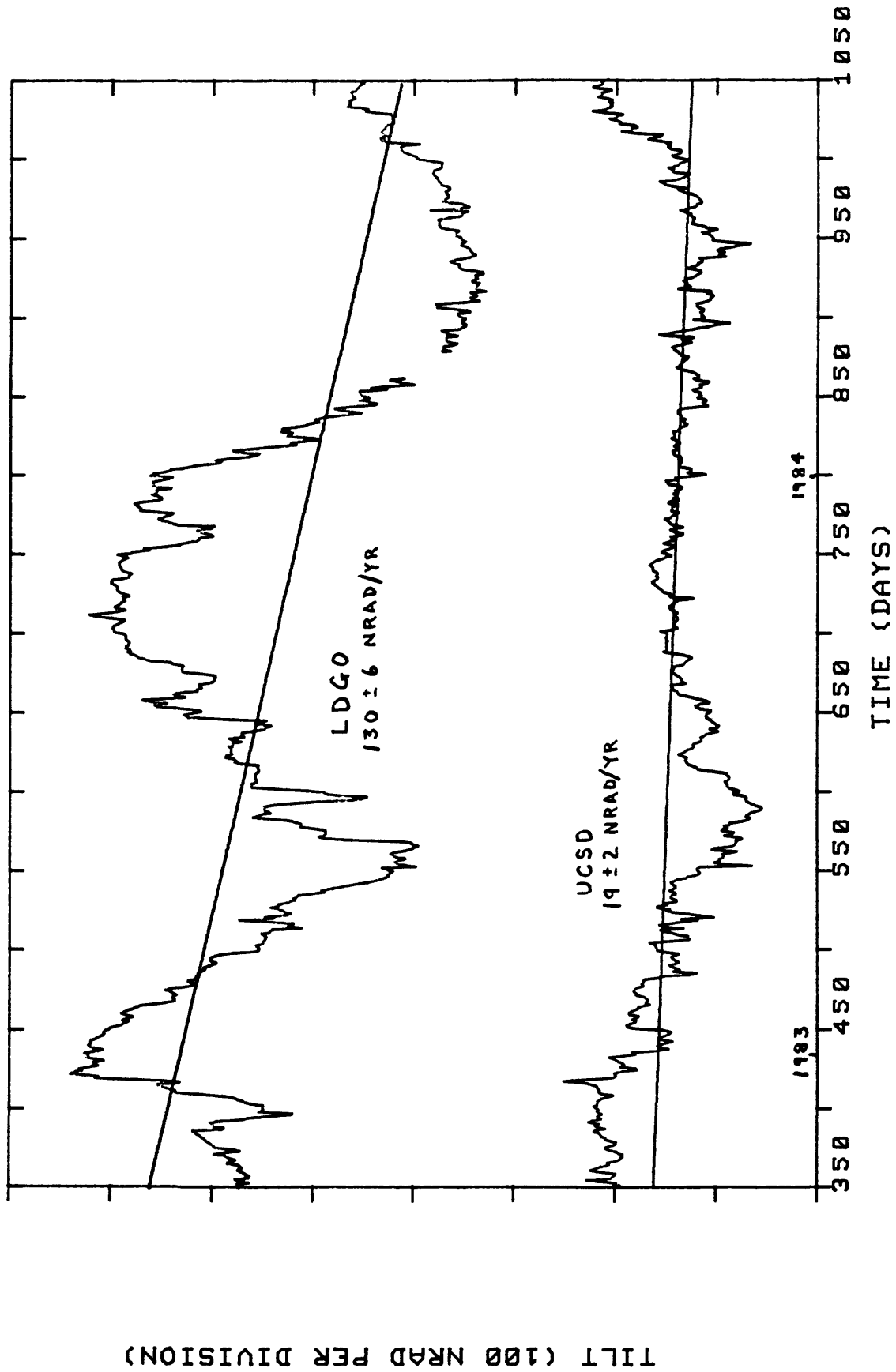
Figure 2. Subset of tilt data for LDGO and UCSD, beginning 27 Sep 82 when both were corrected for near surface soil motion. Straight lines are linear trends estimated by least squares.

# UCSD MICROMETER AND LASER TILT
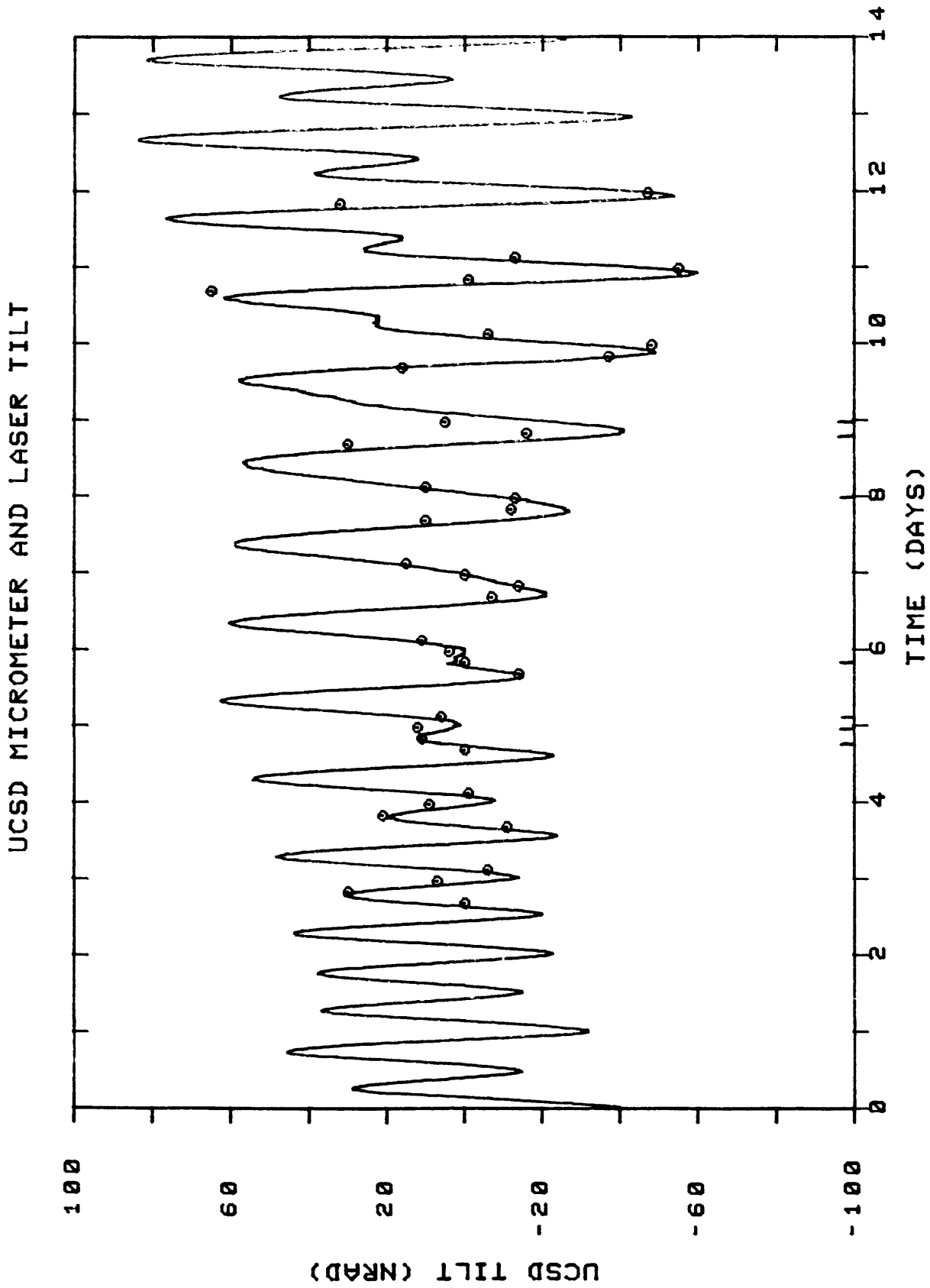
Figure 3. Tilt estimated using visible readings of micrometer scales (dots) and electronic readings (curve) for UCSD tiltmeter. Values should be totally redundant, and they agree well.
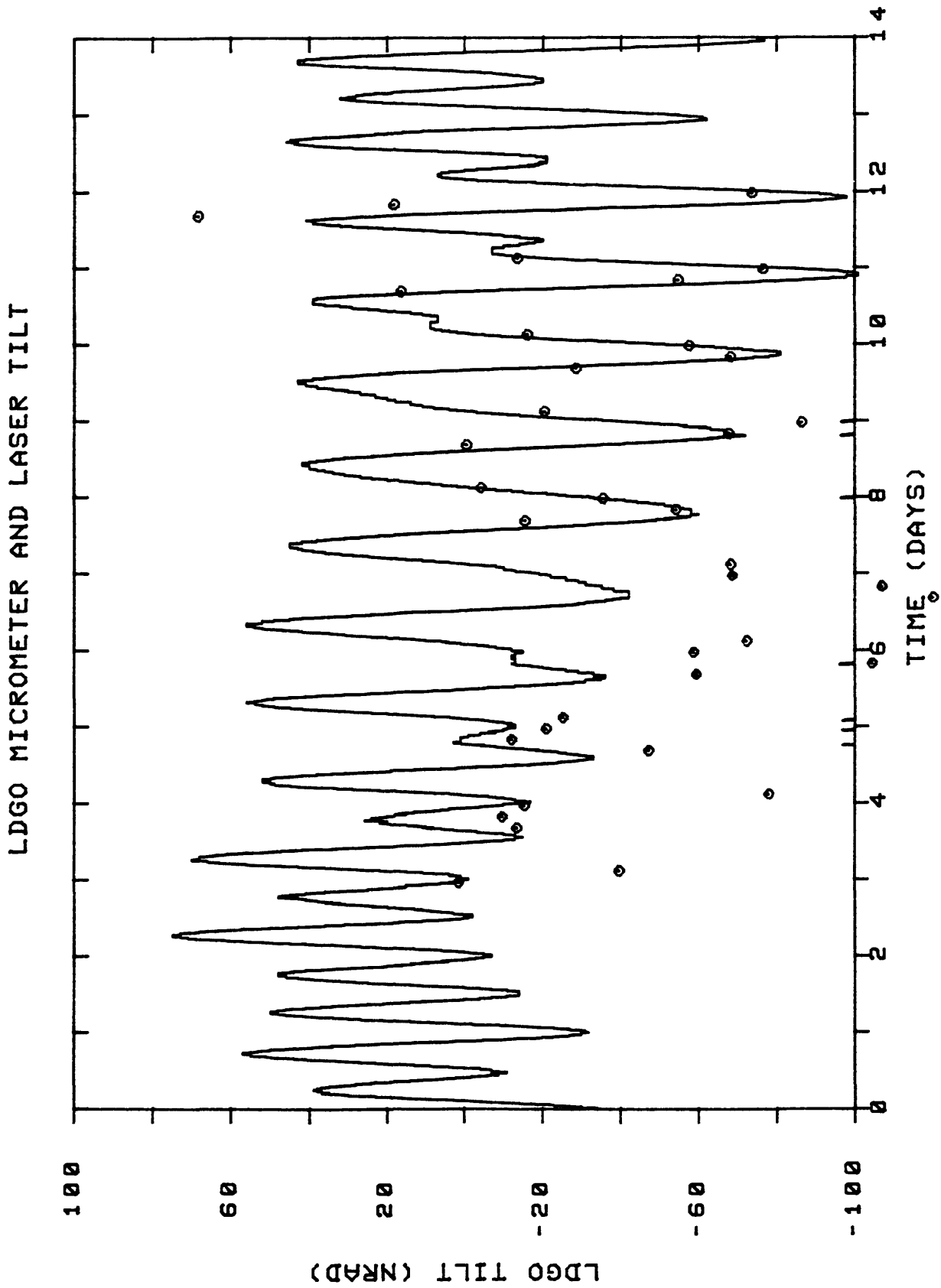
Figure 4. Tilt estimated using visible readings of micrometer scales (dots) and laser interferometer readings (curve) for LDGO tiltmeter. Micrometer and laser readings are independent. Disagreement in record is caused by algae growth at east end of the tiltmeter.

New Model of Earthquake Faulting

Contract No. 21803

Victor C. Li
Department of Civil Engineering
Joseph B. Walsh
Department Earth, Atmosphere & Planetary Science
Massachusetts Institute of Technology
Cambridge, MA 02139
(617) 253-7142

In the last funding period, we formulated a simple model of surface displacements, strains, and gravity changes associated with aseismic slip in a horizontal detachment surface. While acceptable correlation between observed and calculated values of uplift and strain for the Palmdale region was obtained, the average slip rate on the detachment surface is unsatisfactorily large compared to relative plate movement for this region (Ho et al, 1983, 1984).

Our current focus on surface deformation, particularly on horizontal surface strain rate, is based on a two dimensional Elsasser model in which the lithospheric plate is coupled to a viscoelastic asthenosphere. Relaxation of the asthenosphere produces an aseismic horizontal detachment-like movement at the base of the lithosphere, in addition to aseismic slip on the fault zone below a locked seismogenic layer. Loading of the fault is due to tectonic plate motion and is incorporated as a periodic seismic slip with magnitude consistent with remote plate velocity $V_{p\ell}$. Parameters of the model are chosen to fit the apparent time-dependence, throughout the earthquake cycle, of surface strain rates along presently locked traces of the 1857 and 1906 San Andreas ruptures (Thatcher, 1983). We also fit data assembled by King et al on variations of contemporary surface strain and displacement rates as a function of distance from the 1857 trace, by Yu and Prescott (1983) for the 1906 trace and by Savage (1983) for the Salton Sea area. Using $V_{p\ell}$ = 40-50 mm yr, T_{cy} = 160 yr and H = 45 km, reasonable fits are given with a 10 yr relaxation time for the Elsasser model and with ℓ = 8 to 15 km. Fitting contemporary strain rates from King et al suggests the possibility of some upward penetration of slip into the locked zone near Carrizo Plain (Fig. 1). This work has just been submitted to J. Geophys. Res. for publication by Li and Rice (1985).

While the surface strain rates appear to be well fitted, the vertical deformation cannot be captured by such 2-D models (which also produces no gravity changes). We are currently investigating surface deformation patterns associated with along-strike strength inhomogeneity, such as creep zones or asperity zones. Some of these results will be presented at the 5th Maurice Ewing Symposium in New York in May, 1985 by Li and Fares (1985).

Reports and Publications

Ho, S.C., V. C. Li and J.B. Walsh, Surface deformation associated with aseismic slippages on detachment surfaces, EOS, Trans. Am. Geophys. Union 64 (45), 1983.

Ho, S.C., V.C. Li and J.B. Walsh, Surface deformation associated with aseismic slippages on detachment surfaces, Research Report R84-03, MIT, Dept. of Civil Engineering, 1984.

Li, V.C. and J.R. Rice, Crustal deformation in great California earthquake cycles, submitted to J. Geophys. Res., March, 1985.

Li, V.C. and N. Fares, Control of rupture processes by asperities and creep zones, submitted, 5th Maurice Ewing Symposium on Earthquake Source Mechanics, May, 1985.
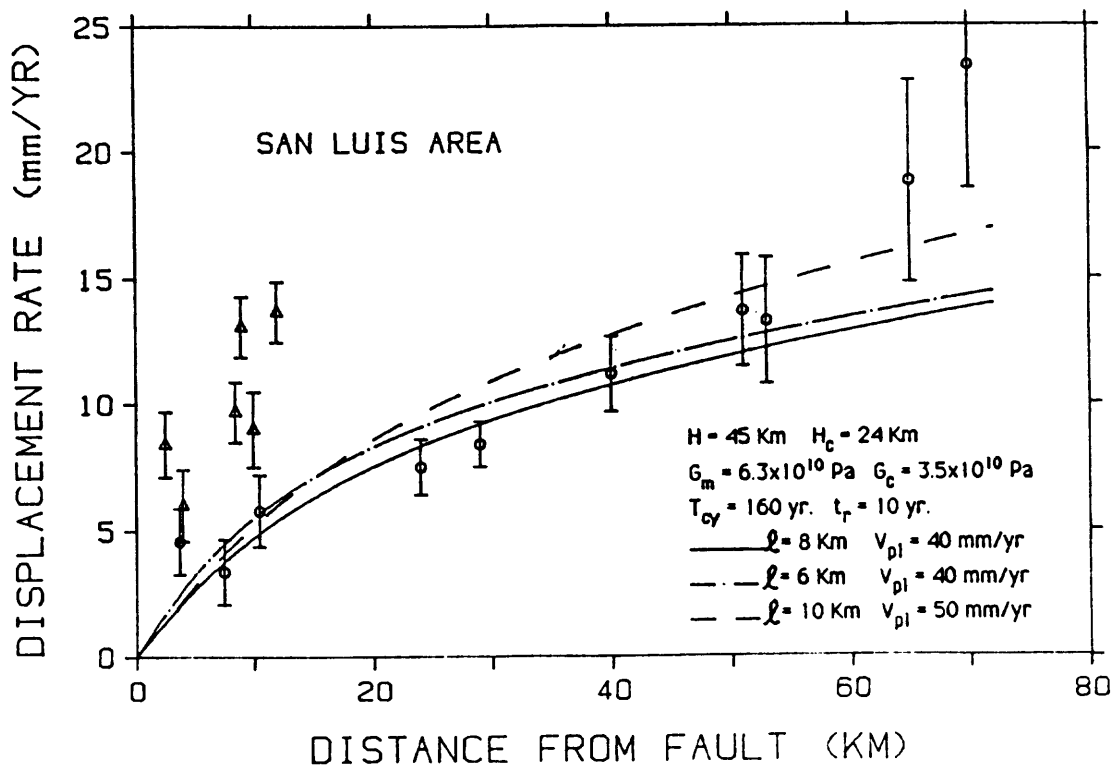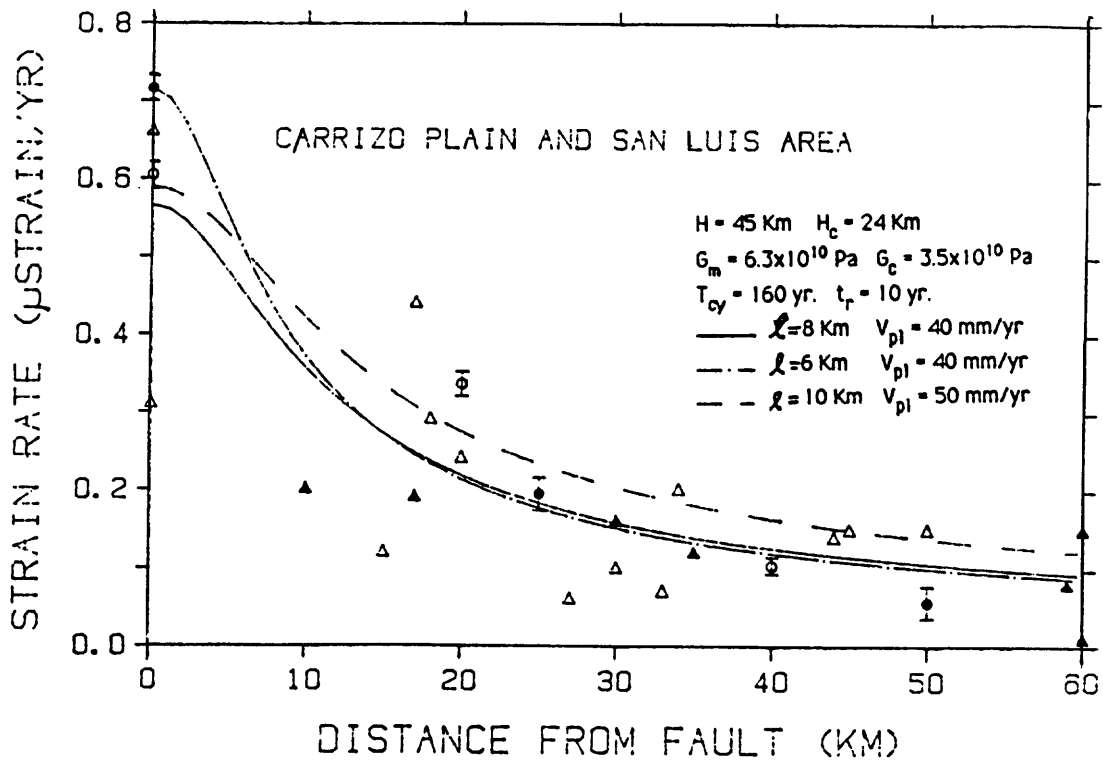
Fig. 1

PRECISE VELOCITY AND ATTENUATION MEASUREMENTS
IN ENGINEERING SEISMOLOGY

9910-02413

Hsi-Ping Liu
Branch of Engineering Seismology and Geology
U. S. Geological Survey
345 Middlefield Road, Mail Stop 977
Menlo Park, California 94025
(415) 323-8111, ext. 2731

Investigations

1. Data analysis of the results obtained for dynamic testing of Monticello dam, Lake Berryessa, California. The test was conducted for the purpose of improving upon the current methods of dynamic dam testing by firing a 656 cm^3 volume air gun fired at pressures up to 13.8 MPa in the reservoir as the excitation source and recording the dam response at various locations on the dam with three-component 1 Hz electromagnetic geophones.

2. Design and construction of a pneumatically driven shear wave generation device. The objective is to develop a horizontally polarized seismic shear wave source in order to measure seismic wave attenuation in shallow crust to a depth of 500 m. The near-surface shear wave attenuation data are needed for seismic safety site evaluation of engineering structures and for determination of earthquake source parameters from records obtained at the earth's surface.

3. Effect of tidal stress on seismic travel times in glaciated and exfoliated granite. The stress-induced seismic velocity variation in crustal rocks could be a valuable tool for measuring stress changes and for earthquake precursor studies by measuring the velocity changes in the seismogenic zones prior to an earthquake.

Results

1. The Fourier analysis of every geophone record of the dam motion excited by the air gun source shows more than ten resonance peaks; some of the lower frequency peaks agree with the vibration frequencies determined by Rouse and Bouwkamp (1967). The most striking feature of the vibration records is the very slowly decaying 23.1 Hz resonance vibrations in the vertical-component motions; its damping coefficient is at least 10 times less than those of the flexural modes. This vertical resonance mode is interpreted as a result of interference of elastic waves propagating vertically in the dam and reflected at the dam top surface and at the base. Bycroft (1980) has recorded ground accelerations during the 1979 M_S = 6.9 Imperial Valley earthquake at a distance of 6 km from the ruptured Imperial Fault. The upper cut-off frequency of the vertical acceleration spectrum is 25 Hz. Some arch dams may experience similar accelerations during future earthquakes. The observed vertical vibration mode provides a magnifying mechanism for vertical ground motions, and implies a need for additional field tests, numerical analysis,

and material testing in the interest of dam safety evaluation.

2. In collaboration with Richard E. Warrick, a shear wave generation device based on the horizontal traction principle (Warrick, 1974) has been designed. The improvement over the existing shear wave generator are increased seismc energy output and improved repeatability of the source characteristics. This device is now under construction at the U. S. Geological Survey.

3. A paper describing the results of our Massachusetts experiment has been completed during this report period. Using improved methods, we have conducted a seismic survey at a Massachusetts granite quarry. The survey was conducted in the intervals (230d23h, 231d11h) and (231d22h, 233d10h), 1983 (U.T.) along a 148 m baseline situated in nearly flat topography. The source for the present experiment was an air gun placed in an mud-filled pit. Travel times for the first five body wave extrema were analyzed. The results are: I. The 1st, 2nd, 4th, and 5th extrema show travel time variations; the 3rd extremum remains constant throughout the experiment. The magnitude of the fractional travel time variation, $\Delta t/t$, ranges from 0.5 to 0.9 percent. II. Changes in travel times of the 1st and 2nd extrema correspond to opposite changes in travel times of the 4th and 5th extrema. III. Two sets of nearly orthogonal joint systems are observed in the granite; the theoretical tidal strain variation in the direction perpendicular to the nearly vertical joints matches the travel time variations of the 1st and 2nd extrema whereas the tidal strain variation in the direction perpendicular to the nearly horizontal sheets matches the travel time variations of the 4th and 5th extrema, when a 4-hr delay is introduced for all the tidal strains. These results are interpreted in terms of the velocity changes of seismic rays as the two joint systems open and close due to the tidal stress.

Reference Cited

Bycroft, G. N., El Centro California differential ground motion array, Open File Rept. 80-919, Geological Survey, U. S. Department of the Interior, Washington, D. C., 1980.

Rouse, G. C., and J. G. Bouwkamp, Vibration studies of Monticello dam, Research Rept. No. 9, Bureau of Reclamation, U. S. Department of Interior, Washington, D. C., 1967.

Warrick, R. E., Seismic investigation of a San Francisco Bay mud site, Bull. Seism. Soc. Am., 64, 375 - 385, 1974.

Reports

H.-P. Liu, E. D. Sembera, R. E. Westerlund, J. B. Fletcher, P. Reasenberg, and D. C. Agnew, Tidal variation of seismic travel times in a Massachusetts granite quarry, Geopys. Res. Lett., in press, 1985.

H.-P. Liu and L. Peselnick, Improved phase-ellipse method for in-situ geophone calibration, Geophysical Prospecting, in press, 1985.

Laboratory and Field Studies of Constitutive Relations of Fault Zones

G-981

John M. Logan
Center for Tectonophysics
Texas A&M University
College Station, TX   77843
(409) 845-3251

Objectives:

The occurrence of major earthquakes along fault zones has made the physical and mechanical properties of such features of considerable interest. To this end we have continued our program of laboratory and field studies to attempt to determine constitutive relations that will accurately characterize the mechanical behavior of fault zones. The objective is to utilize such relations in theoretical models that will aid predictive efforts. It is our belief, that however appealing laboratory results of such investigations, they must be assessed through field studies before they can be utilized with confidence in any theoretical model.

Results:

1. Velocity-Dependent Behavior in Halite Simulated Fault Gouge: An Analog for Silicates.

Recent laboratory experiments on simulated fault gouge of halite have demonstrated a much wider spectrum of velocity dependence than found or envisioned by other workers. Halite is selected as an appropriate analog for natural fault-gouge material because it provides a spectrum of mechanical behavior at tractable laboratory conditions. Experiments at velocities from 10^{-3} to 10^4 μm/sec have been conducted in triaxial compression at pressures which span the spectrum of behavior from dominately brittle (Pc = 10 MPa) to clearly ductile (Pc = 250 MPa). Although previous workers have concentrated their efforts on the nuances of negative velocity dependence, a necessary condition for instability (e.g., Rice, 1983), our present results demonstrate many previously unreported changes in the velocity relationship (Figure 1). (1) A negative velocity dependency present at low to moderate normal stress, changes to positive dependency, at low velocities; (2) this negative-velocity-dependency also changes with increasing velocity to a region of no dependence and subsequently to one of positive dependence; (3) the region of negative velocity dependence shrinks at increasing confining pressures, until at Pc = 250 MPa, the behavior over the entire spectrum of velocities is one of positive dependency; (4) a method of predicting the critical velocity where the change from negative to positive occurs with decreasing velocities is offered for other fault gouge material; (5) the largest degree of negative dependency is found not in the brittle regime as suggested by others, but in the transitional region of behavior, suggesting a possible reason why major seismic events nucleate in the lower portion of the crust; (6) the transition to positive dependency with increasing confining pressure ($\approx$ increasing depth) suggests the inhabitation of instability propagation in this region; (7) a plot of shear stress versus normal stress clearly shows departures from "Byerlee's Law" at pressures outside of the brittle regime. This departure

increases with decreasing velocity. Thus, normal stress is found to be a
prominent factor of semi-brittle behavior. (8) The semi-brittle field fault-
zone behavior emerges as the primary area of interest in determining constitu-
tive reslations, not the brittle domain as previously suggested; (9) this
semi-brittle field in shear environments is shown to be much larger than
previously suggested from conventional triaxial tests; (10) as an analog for
other fault-zone compositions the spectrum of anticipated velocity-dependency,
although broader than previously expected, offers an explanation of a variety
of laboratory, theoretical and field observations, and a guide to future
experimental efforts.

Figure 1.

FRICTONAL & FLOW REGIMES

log (SLIP RATE) ⟶
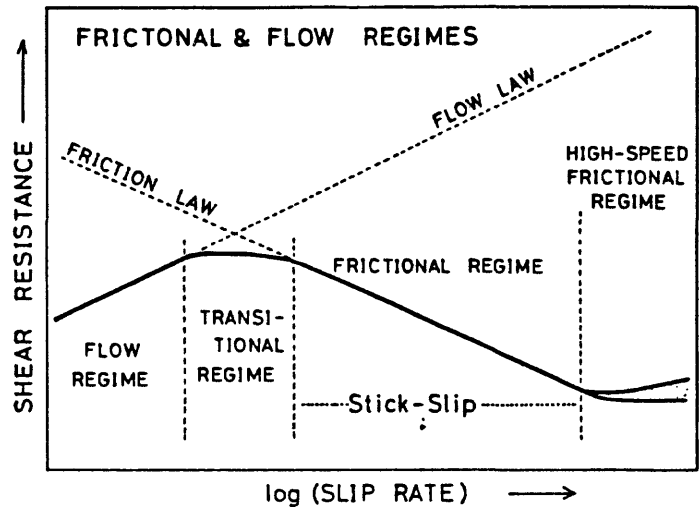
2. Velocity and Time-Dependent Behavior of Dimineralic Fault Gouge.

Constitutive relations of fault gouge are an important part of accurate
models for earthquake prediction. Fundamental work has been accomplished by
Dieterich (1972, 1976, 1981) and recently enhanced by Ruina (1983) and Tullis
(1984). The demonstration by Shimamoto (1985) of the broad range of mechani-
cal changes with velocity and the importance of the semi-brittle field on
monomineralic gouge has provided an important framework for investigating
polymineralic fault gouge. In an attempt to understand simple compositions so
that the behavior of more complex material may be predicted mixtures of mont-
morillonite and quartz have been deformed in triaxial shear experiments.
Confining pressures of 50 MPa, velocities from 3×10^{-3} m/sec to 3×10^{3} m/sec and
saturated mixtures have been investigated. Simulated gouge thickness was 1 mm
and precompacted at 70 MPa confining pressure to facilitate steady-state
conditions. Mixtures of 100% montmorillonite show only stable behavior under
these conditions with shear stresses of about 7 to 9.5 MPa. A slight positive
velocity dependence exists. A clear evolution of the gouge is found as a
function of shear strain and is reflected by increasing values of the shear
stress until steady state is achieved. The increase in shear stress is
apparently retarded at higher velocities, presumably by high pore pressures
(and thus lower normal stresses) that are produced at the higher displacement
rates. The low permeability of the clay would preclude dissipation of the
fluid pressures to achieve equilibrium at these rates. The other end member--
quartz--generally shows stick-slip behavior at intermediate and fast veloci-
ties, with larger stress drops at the faster rates. Shear stress values range
from 43 to 48 MPa. It appears that a transition from negative to positive
velocity dependence occurs at about .03 m/sec, in agreement with data of
Shimamoto. All mixtures of montmorillonite and quartz show stable behavior,

even with as little as 5% montmorillonite. These gouges show positive velocity dependency. The values of the shear stress in the steady-state regime varies directly but not linearly, as the quartz content. A dramatic difference from the end members occurs with mixture between 85 and 50% quartz. Displacement hardening is marked, with steady state sliding difficult to achieve. Examination of thin sections of the deformed gouge clearly shows that the quartz grains are only slightly deformed, in contrast to the totally crushed character of the 100% quartz gouge. Displacement is accommodated by deformation within the clay, shielding the quartz. This apparently (1) precludes compaction, (2) attaining more homogenous although still localized deformation and (3) delaying steady-state behavior. Thus, although the fabrics of monomineralic gouges are quite regular, those of the 50 to 80% quartz are quite chaotic. The displacement is accommodated at the country rock interface.

Extensive work needs to be done to extend the behavior to natural gouge mixtures. Although the behavior is more complex than anticipated, the considerable progress to date is encouraging.

Reports:

Shimamoto, T. and Logan, J. M., 1984, Laboratory friction experiments and natural earthquakes: An argument for long-term tests: Tectonophysics, v. 109, p. 165-175.

Chester, F. M., Friedman, M., and Logan, J. M., 1985, Foliated cataclastics: Tectonophysics, v. 111, p. 134-146.

Logan, J. M., 1985, Frictional properties of fault zones: Present research and future trends, in N. L. Carter and S. Uyeda eds., Tectonophysics, in press.

Logan, J. M., 1985, Microstructure and mechanics of gouge zones in the seismogenic regime (Abstract): Seismological Society of America Annual Meeting.

Shimamoto, T. and Logan, J. M., 1985, Velocity-dependent behavior in halite simulated fault gouge: An analog for silicates: Ewing Symposium.

Active Seismology in Fault Zones

9930-02102

Walter D. Mooney
Gary S. Fuis
U.S. Geological Survey
Branch of Seismology
345 Middlefield Road, Mail Stop 977
Menlo Park, California 94025
(415) 323-8111, Ext. 2569

Investigations

1. Continuation of analysis of seismic-refraction data in southern Alaska. This is part of the Trans-Alaska Crustal Transect (TACT) (Fuis, Ambos, Mooney, Page).

2. Continued analysis of the crustal structure of the Central Valley of California (Walter, Mooney).

3. Interpretation of seismic-refraction data from a cooperative program in Yunnan Province, southwestern China (Mooney).

4. Continued analysis of seismic refraction and reflection data from central California, including the region of the May 2, 1983, Coalinga earthquake (Walter); completion of a manuscript on tectonic wedging associated with emplacement of the Franciscan assemblage (Walter, C. Wentworth and others).

5. Continued analysis of seismic refraction data from the Columbia Plateau, eastern Washington State (Catchings and Mooney).

6. Initiation of analysis of seismic refraction data from Maine and Quebec (Luetgert).

Results

1. The U.S. Geological Survey has undertaken a multi-year program to investigate in detail the continental lithosphere across the state of Alaska following the north-south route of the trans-Alaska oil pipeline and extending offshore to the edges of the Pacific and Arctic continental margins. Seismic refraction, gravity, magnetics, and geologic data were collected in the first year of the TACT (Trans-Alaska Crustal Transect) program in the southern portion of the state. These provide new information on the crustal structure in the Jurassic-Cretaceous Chugach terrane (CGT), and in the Paleozoic-Mesozoic Peninsular-Wrangellia (PNT/WRT) composite terrane to the north. An east-west seismic refraction profile in the CGT reveals a relatively thin (2-5 km) layer of metamorphosed pelitic and volcanic rocks (Vp=5.8 km/s), a layer of mafic rocks (Vp-6.8 km/s), and an alternating series of low-velocity zones (LVZ's) and ultramafic layers (Vp 7.6 km/s). The first ultramafic layers occur at 20, 27, and 35 km depth. This alternating series of high and low velocity zones may be imbricated fossil subduction complexes.

A north-south refraction line was shot perpendicular to the structural trend of the CGT and PNT/WRT. This line indicates a shallow crustal LVZ (6-8 km depth) in both terranes that cross-cuts the deep projection of the major terrane boundary, the Border Range fault (BRF). An underlying ultramafic layer dips 3 to 5 degrees northward from the CGT to the BRF, then deepens suddenly, assuming a dip of 12 degrees.

2. Application of synthetic seismogram modeling of seismic refraction data from the Great Valley, central California reveals a complex one dimensional structure. The first layer has a high velocity gradient which begins with a Vp = 1.6 km/sec and Vs = .2 km/sec which increases linearly to a depth of 2.93 km to velocities of 4.1 km/sec and 0.90 km/sec respectively. The Q structure appears to be simple with an average Q=100 for the first layer. Q for the remainder of the model was not studied.

The second layer, a gradient with velocity of 4.25-4.40 km/sec is truncated by a low velocity zone which extends from a depth of 4.8 km to 6.20 km and has a velocity of 4.23 km/sec. Previous models ruled out phase E as a multiple or converted phase. Thus, it must be a primary reflection from the bottom of the low velocity zone.

Layers 3 and 4 are simple gradients extending from 6.20-8.00 km and velocity of 5.70-5.95 km/sec, and 8.00-12.10 km, 5.95-6.3 km/sec respectively. The remainder of the crust and upper mantle can be modeled as either simple steps or complexly as alternating high and low velocity zones depending on the travel time interpretation. The simple model interprets two phases as primary reflections from the top of each layer. The complex model interprets these phases as delayed reflected branches from the bottom of low velocity zones. Despite the differences between the models in certain regions, both models are strikingly similar to the data and neither of them can be ruled out as a possible structure for the crust-moho transition zone. Future two-dimensional modeling will help to distinguish between the two models.

3. Yunnan Province, in southwestern China, is located at the eastern end of the Himalaya-Burma Arc, just southeast of the Tibetan Plateau. Tectonically active, with major through-going faults, the region is highly seismic. The prominent Red River Fault, for example, shows substantial recent movement and is considered to be a boundary between major crustal blocks. Historical records yield evidence for some forty major earthquakes (probably of magnitude six or greater) in the last 400 years. This century such earthquakes have occurred at a rate of about three every ten years. The largest recent shock in western Yunnan, of magnitude 7, severely damaged the old town of Dali in 1925. Chinese scientists have estimated a 120-year recurrence interval for the 1925-type earthquake.

The first seismic refraction profiles in Yunnan Province, southwestern China, define the crustal structure in an area of active tectonics on the southern end of the Himalaya-Burma Arc. The crust ranges in thickness from 38-46 km, and is described seismologically by three layers. Seismicity is confined generally to the upper layer, whose base appears to constitute the brittle-ductile transition. The mean crustal velocity is less than 6.4 km/s, allowing for a crustal composition compatible with

normal continental crust and consisting mainly of meta-sedimentary and silicic intrusive rocks, with little mafic or ultra-mafic rocks. This suggests a crustal evolution involving sedimentary processes on the flank of the Yangtze Platform and possibly the accretion of oceanic plateaus, rather than the accretion of oceanic island arcs, as previously proposed. An anomalously low upper mantle velocity (7.7 km/s) is observed on one profile but not another at right angles to it. This may be indicative of active tectonic processes in the mantle, or of seismic anisotropy.

4. The May 2, 1983 Coalinga earthquake ($M_1 = 6.7$) was unusual in that it was a large non-strike-slip earthquake located 35 km east of the San Andreas fault at the structural transition between the southern Diablo Range and the San Joaquin Valley, a part of the 500-km long Coast Range-Great Valley boundary. Since 1981 the USGS has been acquiring both seismic reflection and refraction data along several profiles across the Coast Range-Great Valley boundary. The occurrence of the Coalinga earthquakes provided an additional opportunity to acquire seismic reflection and refraction data across this structural transition with the goal of understanding the structural relationships responsible for the unusual seismicity. Such an understanding is needed to assess the probability of large earthquakes occurring elsewhere along the Coast Range-Great Valley boundary.

Seismic refraction data were collected using 120 vertical-component seismographs deployed along two profiles that intersect in the hypocentral region of the 1983 Coalinga earthquakes. A 83-km long E-W profile extended from the San Joaquin Valley to the Diablo Range across Anticline Ridge, 1-km south of the $M_1 = 6.7$ main shock epicenter. A 102-km long NW-SE profile extended sub-parallel to the Diablo Range front along the syncline west of Anticline Ridge. In the San Joaquin Valley the velocity of the Quaternary and Tertiary strata increases from 1.6 km/s near the surface to about 3.6 km/s at 3.6 km depth. Close to the base of the Tertiary section or at top of the Cretaceous Great Valley Sequence (GVS), the velocity increases abruptly to 4.0-4.3 km/s and with increasing depth of burial the velocity of the GVS in the valley increases to over 5.0 km/s. On the western flank of the valley, velocity inversions within the GVS section indicate high formation pore pressures. The velocity inversions do not extend into the Diablo Range. At equivalent depths of burial, the velocities of the lower GVS units in the Diablo Range (4.8-4.9 km/s) are higher than those found for the GVS farther east in the San Joaquin Valley (4.0-4.3 km/s).

In the San Joaquin Valley, the GVS units overlie a basement with a velocity of 6.3-6.4 km/s, indicative of a mafic composition. The dip of the basement increases westward of the valley axis from less than 5o to about 10o-10o. The basement plunges to an estimated 14-15 km depth at the front of the Diablo Range where a wedge of 5.7-6.1 km/s Franciscan rocks lies between the GVS exposed at the surface and the mafic basement layer. The depth of the boundary separating the GVS and Franciscan wedge beneath increases eastward to a junction with the mafic basement under the upturned western flank of the San Joaquin Valley. East of the Franciscan wedge the San Joaquin Valley is underlain by a basin containing several additional kilometers of sedimentary strata associated with the GVS.

Unreversed refraction data support a deeper layer within the mafic basement with velocities over 7 km/s and a Moho depth of 28-30 km near the front of the Diablo Range. Comparison of the refraction velocity models to the located seismicity reveals that the source region for the M_l = 6.7 main shock and larger shocks is within the Franciscan wedge and that the seismicity extends upward into the folded GVS section.

5. In August 1984, the USGS, in conjunction with DOE/Rockwell Hanford Operations conducted a seismic-refraction survey over the Columbia Plateau of east-central Washington and northeast Oregon. The 260-km-long profile, centered on the Pasco Basin (within the Hanford Property), trended N 50o E from 30 km south of Wasco, OR, to 50 km northeast of Warden, WA. The Survey consisted of 8 shots (900 to 2300 kg), 4 shotpoints, and 240 station locations (930-m spatial sampling interval between shots).

Our interpretation suggests that the Columbia River Basalt Group (CRBG) (V_p=approx. 6 km/s) is variable in thickness but is generally less than 7 km deep and is interbedded with sediment at depth. Underlying the (CRBG) are thick sediment accumulations (as deep as 12 km) beneath some of the basins. Atypically high velocity basement rocks (V_p = 6.5 km/s) underlie the sediments within basins, but basement velocities outside the basins are more typical (V_p = 6.1 km/s). Normal faulting is observed near the basin edges. Low-velocity zones exist in the intermediate crust (about 25 km) and near the Moho (38 km). A thick high-velocity lower crust (V_p = 7.5 km/s), relief on the Moho, and a high-velocity upper mantle (possibly as high as V_p = 8.4 km/s), combined with the above observations, suggest that this area of Columbia Plateau resulted from continental rifting.

6. In the fall of 1984, the USGS in collaboration with the Earth Physics Branch of Canada, conducted a seismic refraction experiment in the State of Maine and the Province of Quebec. This experiment included a 400 km transect of the northern Appalachians from the Atlantic coast to the St. Lawrence River paralleling existing reflection profiles, three cross profiles in Maine, and a profile within the coast volcanic terrane of southeastern Maine. Shots were fired at 30-40 km intervals and recording instruments were placed at 800 meter intervals providing high-density coverage. Preliminary results show a thick crust with upper crustal velocities ranging from 5.7-6.3 km/sec with localized regions of low velocity within the upper crust. Secondary arrivals provide evidence for a higher velocity lower crust (6.8-7.2 km/sec). Clear Pn arrivals are observed, but the uniform lack of mantle reflections suggests a gradational crust-upper mantle interface. In addition to the shots fired along each profile, several off-axis shots were fired. These "pseudo-fans" provide us with a measure of the amount of out-of-profile structural variability and show that there are significant variations in the velocity depth function along the strike of the northern Appalachians.

Reports

Catchings, R., and Mooney, W. D., 1985, Crustal structure of the Columbia Plateau, Earthquake Notes, v. 55, no. 1, p. 22.

Fuis, G. S., and Zucca, J. J., 1985, A geologic cross section of northeastern California from seismic refraction results, in, Nilsen, T. H., ed., Geology of the Upper Cretaceous Hornbrook Formation, Oregon and California: Society of Economic Paleontologists and Mineralogists, Pacific Section, v. 42.

Fuis, G. S., Ambos, E. L., Mooney, W. D., Page, R. A., and Campbell, D. L., 1985, Crustal structure of southern Alaska - Preliminary results of the TACT 1984 seismic refraction experiment (abstr), Earthquake Notes, v. 55, p. 23.

Plafker, G., Nokleberg, W. J., Fuis, G. S., Mooney, W. D., Ambos, E. L. and Campbell, D. L., 1985, 1984 results of the Trans-Alaska crustal transect in the Chugach Mountains and Copper River Basin, Alaska (abstr), Geol. Soc. Am. Abstracts, in press.

Fuis, G. S., Ambos, E. L., Mooney, W. D., Page, R. A., and Campbell, D. L., Preliminary results of TACT 1984 seismic-refraction survey of southern Alaska, U.S. Geol. Survey Circular "Branch of Alaskan Geology, 1984 accomplishments", in press.

Kohler, W. M., and Fuis, G. S., Travel-time, time-term, and basement depth maps for the Imperial Valley region, California, from explosions: in review for Bulletin Seismological Society of America.

Luetgert, J. H., and Mooney, W. D., 1985, Earthquake profiling at Mammoth Lakes, California: Bulletin Seismological Society of America, v. 75, pp. 211-221.

McMechan, G. A., Luetgert, J. H., and Mooney, W. D., 1985, Imaging of earthquake sources in Long Valley caldera, California, 1983: Bulletin Seismological Society of America, v. 75, no. 4.

Mooney, W. D., 1985, Crustal structure in the vicinity of the Morgan Hill earthquake, in Tucker, B., ed., The 1984 Morgan Hill, California, earthquakes: California Division of Mines and Geology, in press.

Mooney, W. D., and Colburn, R. H., 1985, A seismic refraction profile across the San Andreas, Sargent, and Calaveras faults, west-central, California, Bull. Seis. Soc. Am., v. 75, pp. 175-191.

Page, R. A., Fuis, G. S., Mooney, W. D., Nokleberg, W. J., and Plafker, G., Crustal transect of accreted tectonostratigraphic terranes in the Chugach Mountains and Copper River Basin, Alaska: initial results of TACT (abs.): EOS Transactions American Geophysical Union, Fall 1984.

Walter, A. W., Velocity Structure near Coalinga, California, in Rymer, M. J., and Ellsworth, W. L., eds., Mechanics of the May 2, 1983, Coalinga, California, earthquake: U.S. Geological Survey Open-File Report 85-44, p. 10-18.

Wentworth, C.M., Blake, M.C., Jones, D.L., Walter, A.W., and Zoback, M.D., 1984, Tectonic wedging associated with emplacement of the Franciscan assemblage, California Coast Ranges, in Blake, M.C., ed., Franciscan Geology of No. CA: Soc. of Economic Paleontologists and Mineralogists, Pacific Section, pp. 163-174.

Fault Mechanics and Earthquake Precursory Processes

14-08-0001-G-823

J.R. Rice (P.I.) and R. Dmowska
Division of Applied Sciences
Harvard University
Cambridge, MA   02138
(617) 495-3445

and

V.C. Li
Department of Civil Engineering
Massachusetts Institute of Technology
Cambridge, MA   02139
(617) 253-7142

Investigations

1. The temperature dependence of laboratory-based frictional slip constitutive parameters for Westerly granite and a Lachenbruch-Sass San Andreas fault geotherm are used to develop a depth-variable description of a strike slip fault surface.

2. Stressing and rupture of slip-deficient zones along transform plate boundaries is studied. The results are being used to model the stressing of seismic gaps of first kind, as well as to simulate slip and stressing along some parts of San Andreas fault in California, with more detailed analysis of the Parkfield area.

3. Crustal deformation associated with strike-slip earthquakes is being computed and compared to geodetic data, based on a thick lithosphere model locked between earthquakes at shallow depth at the plate margin but slipping below, and riding on a viscoelastic asthenosphere.

Results

1.1 The constitutive relations that we use for fault instability modelling is the slip rate and slip history dependent friction law developed experimentally by Dieterich, Ruina and others. At a fixed normal stress σ_n and environment (temperature, surface roughness, etc.), the frictional resistance τ can be expressed in terms of (i) an instantaneous "viscosity" parameter $A = A(\tau,V)$ where V is slip velocity and (ii) a steady state strength level $\tau^{ss}(V)$ towards which τ evolves exponentially over a characteristic decay distance $L(V)$. That is,

$$d\tau/dt - [A(\tau,V)/V]dV/dt = -[V/L(V)][\tau - \tau^{ss}(V)]$$

In most of our numerical studies we have used $L = $ constant, $A = $ constant dependent on normal stress and temperature and

$$\tau^{ss}(V) = \tau_* + (B-A)\ln(V_*/V + e^{-n})$$

where V_* is a reference speed and B and τ_* likewise depend on a normal stress and temperature. n is a constant chosen such that the steady state stress

becomes independent at high speed. We use $n = 10$ so that $\tau^{ss}(V)$ begins to
level off above about 0.1 mm/sec for $V_* = 30$ mm/yr. From the room temperature
experiments by Dieterich [1981] and Tullis and Weeks [1984] and high temperature
(from 300°C up to 700°C) experiments by Stesky [1975,1978] on Westerly granite
and the geotherm determined by Lachenbruch and Sass [1973] for the San Andreas
fault, A and B are found to vary with depth as shown in Fig. 1. As seen in
Fig. 1, the friction response changes from velocity weakening at shallow depth
(above 11 km) to velocity strengthening at greater depth. This change of fric-
tional slip property is thought to be responsible for the shallow depth confine-
ment of seismicity.

1.2 We have developed a crustal scale model which simulates a uniform strike
slip fault by two oppositely sliding elastic plates. The bottom and top surfaces
are stress free. Remote stress is applied at the plate boundaries in such a way
that the relative plate velocity is 30 mm/yr had there been uniform slip throughout
the depth. Fig. 2 shows a typical plot of slip vs depth throughout a time history
of two earthquake cycles with $L = 80$ mm, $e^{-n} = 0$, A and B as shown in Fig. 1.
Each line represents a constant time but the time spacing between any two lines
are not uniform. Line A to line H corresponds to a complete earthquake cycle with
recurrence time equal to about 128 years in this case. The earthquake is initiated
at about 9 km depth and the instability lasts for about 1 minute (line E to F).
The coseismic surface slip is about 2.5 m. As predicted earlier, the earthquake
is confined to the upper 12 km which roughly corresponds to the depth at which the
frictional slip property changes from velocity weakening at shallow depth to
velocity strengthening at greater depth. Rapid post-seismic slip also occurs and
seems to penetrate down to about 17 km (line F to H) in a few years after the
earthquake. After that, the seismogenic layer which has experienced an earthquake
begins to slow down and forms a locked or slip-retarded patch to prepare for the
next cycle. As the tectonic loading increases, this locked region is gradually
eroded from below leading to accelerating pre-seismic slip (line B to D) and
finally earthquake instability again.

2. An analysis is presented of the stressing of locked patches along a fault zone
which is creeping elsewhere. The model consists of strike-slip faulted elastic
lithospheric plates loaded in a manner equivalent to imposition of a remotely uni-
form tectonic shear stress. The fault zone has an inhomogeneous strength distri-
bution both depthwise and along strike. It is modelled as being composed of locked
patches and freely slipping parts treated as cracks. The solution is given with
the use of the "line-spring" model which analyses the problem by thickness averaged
plane stress theory for lithospheric plates which slip along a discontinuity cut
at the plate boundary. As a boundary condition, thickness averaged stress and slip
at each local section along the cut are related to one another by the result of an
antiplane strain analysis of slip for the crack or crack pair which describes the
slipping and locked depth ranges at that section. The analysis indicates that the
slip distribution along creeping parts of the fault, as well as the stress distri-
bution along locked patches, depends strongly on the geometry of these zones. The
model is used to examine stress concentrations associated with a slip-deficient
seismic gap along strike and to study the effect of local irregularities in the
margin of a locked region.

It is also used to simulate slip and stressing processes associated with the
creeping portion of the San Andreas fault in central California, between the
presently locked zones of the great 1906 and 1857 ruptures, and to constrain the
nature of an apparently locked zone at the southeastern end which ruptures in
characteristic Parkfield earthquakes. Near fault creep and broadscale displacement

data along the fault since the 1966 Parkfield earthquake and inferences from seismicity distributions are used. Limitations of the modelling procedure at short spatial wavelengths prohibit an accurate description of the Parkfield locked patch, but results suggest that it may be localized and occupy a small fraction of area of the normal seismogenic zone. An effective remote stressing rate of order $0.3 \times 10^{-6} \times$ shear modulus/year is inferred, together with a less well constrained 30 to 40 km lithospheric thickness, for consistency with the displacement data. Results enable estimates of stress accumulation along the locked 1857 rupture zone and of the build-up of fracture energy release capability (of order 10^7 J/m^2 in 150 yr) at its lower margin.

The work has been submitted to *Bull. Seism. Soc. Am.*

3.   Periodic crustal deformation associated with repeated strike slip earthquakes is being computed for the following model: A depth ℓ ($\leqslant$ H) extending downward from the Earth's surface at a transform boundary between elastic lithospheric plates of thickness H is locked between earthquakes, but slips an amount consistent with remote plate velocity V after each lapse of earthquake cycle time T. Lower portions of the plate boundary slip continuously under constant stress throughout the cycle, and the plates are coupled to a Maxwellian viscoelastic asthenosphere. Parameters of the model are chosen to fit the apparent time-dependence throughout the earthquake cycle, shown by Thatcher in 1983, of surface strain rates along presently locked traces of the 1857 and 1906 San Andreas ruptures. We also fit data assembled by King *et al.* on variations of contemporary strain rates as a function of distance from the 1857 trace, and by Prescott *et al.* for the 1906 trace. Using V = 40 to 50 mm/yr, T = 160 yr, for a generalized Elsasser foundation model, reasonable but not yet optimized fits are given with a 10 yr relaxation time for that model and with ℓ = 8 to 15 km in a lithosphere with H = 45 km. Fitting contemporary strain rates from King *et al.* suggests some upward penetration of slip into the locked zone near Carrizo Plain.

References

Dieterich, J.H., Constitutive properties of faults with simulated gouge, in *Mechanical Behavior of Crustal Rocks (the Handin Volume)*, edited by N.L. Carter, M. Friedman, J.M. Logan, and D.W. Stearns, Geophys. Monogr. Ser., No. 24, AGU, 103-120, 1981.

Lachenbruch, A.H. and J.H. Sass, Thermo-mechanical aspects of the San Andreas fault system, Proc. Conf. Tectonic Probl. San Andreas Fault System, Stanford Univ. Publ. Geol. Sci., Vol. 13, 192-205, 1973.

Tullis, T.E. and J.D. Weeks, Constitutive behavior and stability of frictional sliding of granite, draft manuscript, intended for *J. Geophys. Res.*, 1984.

Publications (including "in press" items, updated when possible, from previous report)

Dmowska, R., W. Bielski, and R. Teisseyre, Electromechanical and magnetomechanical coupling, in *Continuum Theories in Solid Earth Physics*, ed. R. Teisseyre, pp. 399-475, Elsevier, in press, 1985.

Dmowska, R. and J.R. Rice, Fracture theory and its seismological applications, in *Continuum Theories in Solid Earth Physics*, ed. R. Teisseyre, pp. 187-255, Elsevier, in press, 1985.

Dmowska, R., S.T. Tse, and J.R. Rice, Stressing of locked zones along a creeping fault (abstract), *EOS, Trans. Am. Geophys. Union,* 65, N. 45, p. 993, 1984.

Li, V.C., Estimation of *in situ* diffusivity, *Pure Appl. Geophys.*, Special issue on Earthquake Hydrology and Chemistry, ed. C.Y. King, 122, N. 2/4, 1984.

Li, V.C. and S. Hull, Control of time and spatial distribution of aftershocks by fluid flow, in preparation, 1985.

Li, V.C. and C. Kisslinger, Stress transfer and nonlinear stress accumulation at subduction-type plate boundaries, applications to the Aleutians, *Pure Appl. Geophys.*, Special issue on Earthquake Prediction, ed. K. Shimazaki and W.D. Stuart, 122, N. 6, 1984.

Li, V.C. and J.R. Rice, Crustal deformation in great California earthquake cycles (abstract), *EOS, Trans. Am. Geophys. Union,* 65, N. 45, p. 993, 1984.

Rice, J.R., First order variation in elastic fields due to variation in location of a planar crack front, *J. Appl. Mechanics*, in press, 1985.

Rice, J.R., Discussors report on shear localization, faulting and frictional slip, in Mechanics of Geomaterials, ed. Z. Bazant, Wiley and Sons, pp. 211-216, in press, 1984.

Rice, J.R., Constitutive relations for fault slip and earthquake instabilities, *Pure Appl. Geophys.*, Special issue on Instabilities in Continuous Media, 121, N. 3, pp. 443-475, 1983 (issued 1984).

Rice, J.R., Relation of surface deformation to pre-instability slip on crustal faults (abstract), *EOS, Trans. Am. Geophys. Union,* 65, N. 45, p. 851, 1984.

Tse, S.T., R. Dmowska, and J.R. Rice, Stressing of locked patches along a creeping fault, submitted to *Bull. Seism. Soc. Amer.*, Sept. 1984.

Tse, S.T. and J.R. Rice, Stick-slip confinement to upper crust by temperature dependent frictional slip response (abstract), *EOS, Trans. Am. Geophys. Union* 65, N. 45, p. 993, 1984.

FIG. 1.

$$\tau^{ss}(V) = \tau_\ast - (B-A)\ln\frac{V}{V_\ast}^{P-3}$$

A, B (bars)

$\dfrac{d\tau^{ss}}{dV} < 0$

velocity weakening; possibly unstable sliding

$\dfrac{d\tau^{ss}}{dV} > 0$

velocity strengthening; stable sliding

A

B

DEPTH (km)

200°C   300°C   400°C

FIG. 2.

SLIP (m)

1 m

A B C D, E   F G H

time intervals:

A to B , 97 years

B to C , 26 years

C to D , 1 year

D to E , 9 minutes

E to F , 1 minute

F to G , 3 hours

G to H , 4 years

cycle time

128 years

DEPTH (km)
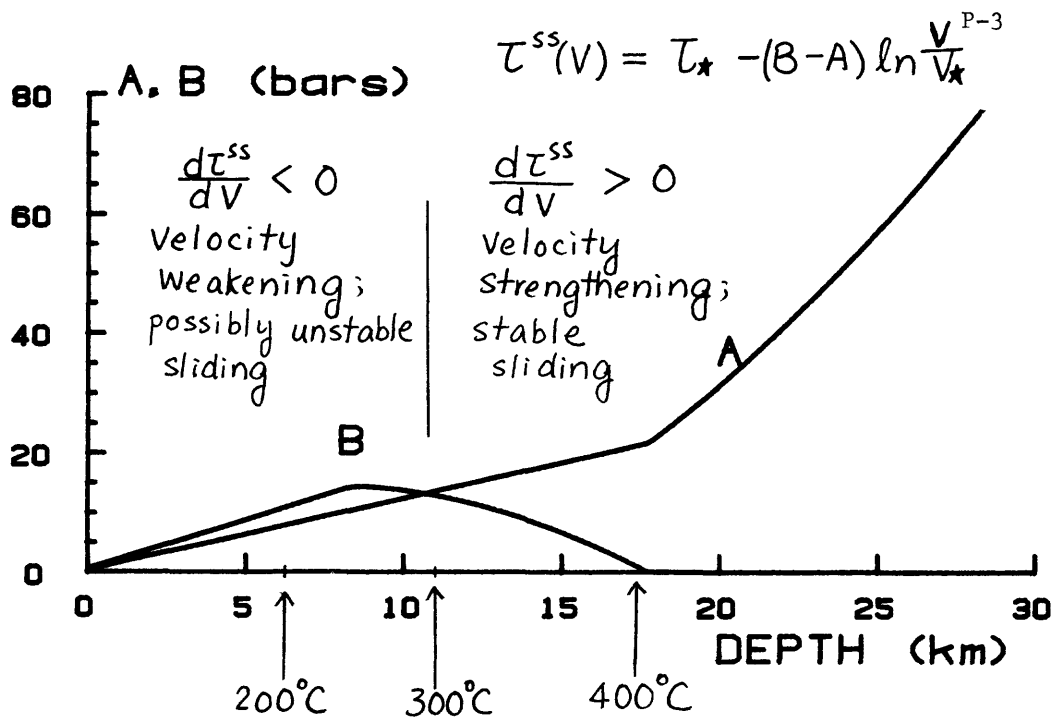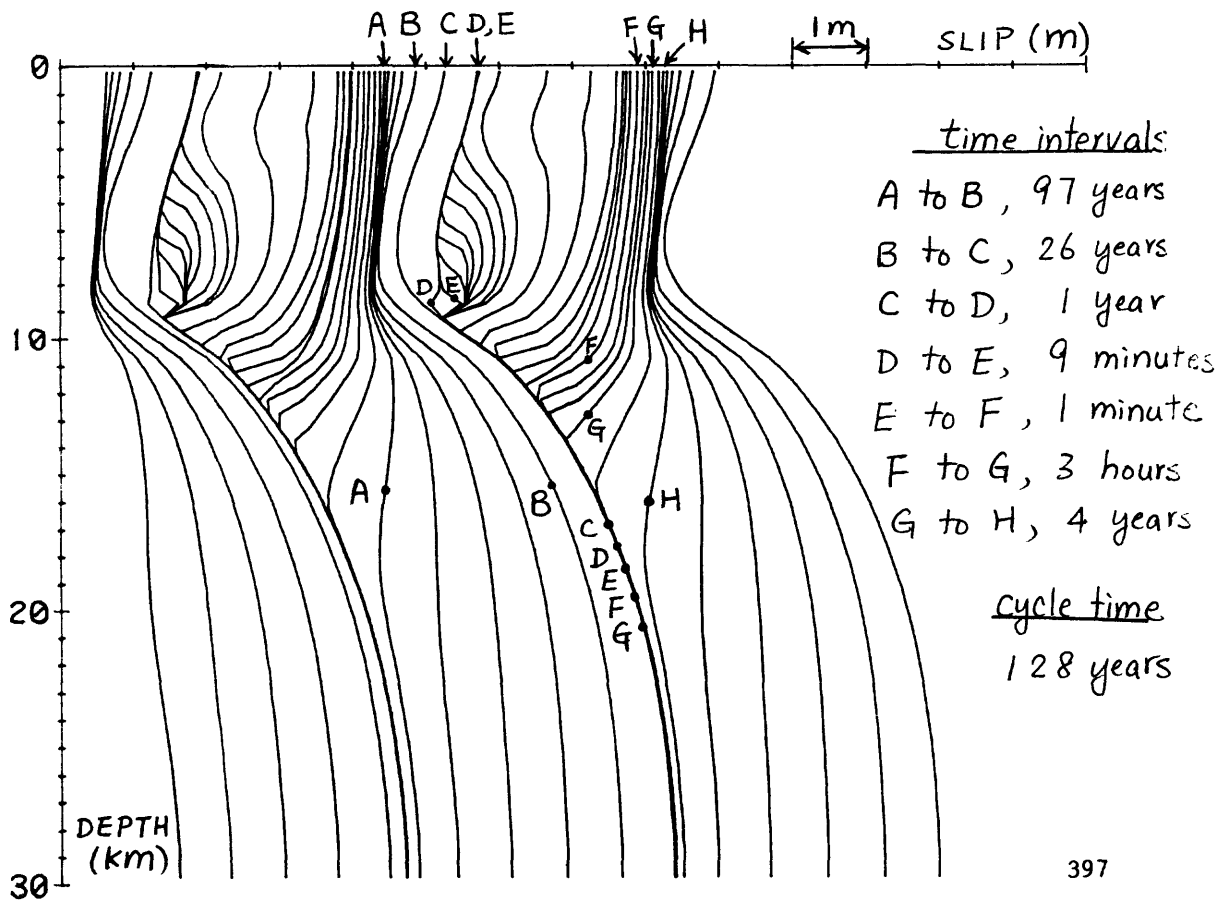
Rock Deformation

9950-00409

Eugene C. Robertson
Branch of Engineering Geology and Tectonics
U. S. Geological Survey
922 National Center
Reston, VA 22092
(703) 860-7404

Investigations

The anelastic properties of rocks tested at a seismic frequency of 5 Hz and under strains of 10^{-5} to 10^{-3} have been studied in the laboratory. The changes in attenuation and in shear modulus with increasing torsional strain to failure were measured.

Results

Preliminary results have been obtained from anelasticity tests on gneissic granite from the Idaho Springs formation in Colorado, basalt from the Wachung flows in New Jersey, and limestone from the Solenhofen district in Bavaria. The rocks all have low porosity, are reasonably homogeneous and isotropic, and were tested at room temperature and in a dry state. The apparatus was an inverted torsion pendulum; an initial rotary deflection was applied to a rod of rock, 16.5 cm long by 0.65 cm dia., which was then allowed to decay to rest in subsequent free oscillations. Energy for the restoring force and the damping are determined by the rock sample properties. Angular displacements (10^{-4} to 10^{-2} radians) and peak energy voltages were measured with a small motor converted for the purpose and appropriate electronic circuitry. Signal data were stored in a PDP 1103 microcimputer and processed after each experiment to obtain frequency, strain, and amplitude. Resistance strain gages placed on several rock samples were used to check the dynamic transducer signals. Most samples were run at increasing initial-deflection steps to failure. Pure aluminum, copper, and nickel, and steel, pyrex, lucite, and polystryrene were the principal standards used for calibrating rigidity from frequency.

The lowest values of attenuation and the highest values of rigidity were observed at the lowest strain (less than 10^{-5}) and after total decay of the initial strain. Fully elastic behavior was observed only at the lowest strains; at higher strains a nonlinear anelastic behavior was seen. Perhaps the most significant result of these tests was that the nonlinear strain was fully recovered; after each run, the attenuation and rigidity both recovered to their original low-strain values.

The following table of data shows the difference in behavior of the three rocks studied. The granite is more rigid and fails at a lower total strain than the limestone or basalt, but all three have about the same decrease in rigidity, from low to failure strain, about 3 %. The effect of increasing strain (above 10^{-5}) is to cause an exponential change in attenuation; at the maximum strain (just before failure) the limestone attenuation is 4 times its low-strain elastic value.

Representative Results on Torsion Experiments

Rock Type	Strain at failure (10^{-4} units)	Attenuation (nepers/cm)		Rigidity (Mb)	
		Low strain	Max. strain	Low strain	Max. strain
granite	7	.065	.190	.427	.414
basalt	12	.075	.147	.361	.350
limestone	9	.041	.161	.274	.262

The measurements of frequency and rigidity and of strain and peak voltage had estimated precisions of 0.1 and 1.0 % respectively, and had estimated accuracies of 1.0 and 5 % respectively.

The frequency of the pendulum can be reduced by adding weights to the oscillating mass, and they are currently being installed. The effect of the lower frequency on attenuation is expected to provide information on the problem of linear versus quadratic damping behavior of rock.

Heat Flow and Tectonic Studies

9960-01177

John H. Sass
Branch of Tectonophysics
U.S. Geological Survey
2255 N. Gemini Drive
Flagstaff, AZ. 86001
(602) 527-7726
FTS: 765-7226

Arthur H. Lachenbruch
Branch of Tectonophysics
U.S. Geological Survey
345 Middlefield Road
Menlo Park, CA. 94025
(415) 323-8111, ext. 2272
FTS: 467-2272

Investigations:

1. Heat Flow and Tectonics of the Western United States
     Some additional mathematical modeling has been done to help clarify the implications of our heat flow measurements for the evolution of the Salton Trough.

     In response to questions that arose in connection with proposals for deep drilling in the San Andreas fault, we investigated the temperature rise accompanying frictional heating by an earthquake. We resumed long-term stability testing on a refined version of a precision temperature-monitoring device for use in bore holes.

     We measured thermal conductivities on 50 samples of preserved core from hole VC-1, drilled by LANL in the Valles Caldera. From these and a temperature log, a preliminary value of heat flow was calculated.

     Investigations on the thermal and hydrologic state of the southwestern Colorado Plateau continued.

2. Heat Flow and Tectonics of Alaska:
     We continued reduction and analysis of temperature and thermal conductivity data from the National Petroleum Reserve -- Alaska.

     Some simple modeling studies are being undertaken to help explain the implications of our geothermal data for recent climatic change in arctic Alaska.

Results:

1. Heat Flow and Tectonics of the Western United States
     We have found that one-dimensional and thermo-mechanical models of distributed extension, sedimentation, and intrusion account fairly well for observation in the Salton Trough. They imply that if the Trough evolved as a pull-apart-basin during opening of the Gulf of California, the spreading could not have

all taken place in the present narrow zones of active seismicity without massive melting of the crust in the Imperial Valley. However, as the conclusion was based on one-dimensional models, it neglected heat lost horizontally to the crust from the "spreading" seismic region. We have adapted a two-dimensional analytical model to the problem, and found that it supports the previous conclusion; extension velocities required by plate tectonic models are, in order of magnitude, greater than the minimum required by heat balance for crustal melting.

A summary of simple models of frictional heating by an earthquake provides rules of thumb for estimating co-seismic and post-seismic temperature rise in terms of fault-width, friction, particle velocity, and slip. It provides a simple basis for examining the feasibility of schemes to evaluate fault friction from temperature observations in bore holes.

In borehole VC-1, drilled in the Valles Caldera by LANL, a temperature profile obtained only 24 hours after completion of drilling indicates a conductive thermal gradient of about $230°$ C km $^{-1}$ within the Madera Limestone between depths of 425 and 800 meters. Twenty four measurements yield a mean thermal conductivity of 2.83 ± 0.08 W m $^{-1}$ K $^{-1}$ at $25°$ C. When corrected for the mean in situ temperature of $110°$ C, this number is reduced to 2.4 W m $^{-1}$ K $^{-1}$, yielding a heat flow estimate of 552 mW m $^{-2}$ or 13 HFU.

In the San Francisco Volcanic field near Flagstaff, Arizona, there is volcanism younger than 1000 years, and studies by Doug Stauber indicate the probable existence of molten magma or hot rock beneath the volcanic field; yet there are no surface manifestations of hydrothermal or magmatic activity, nor is the heat flow high. The area is also one in which the transition in the stress field between east-west horizontal extension characteristic of the Basin and Range Province, and east-west compression characteristic of the interior of the Colorado Plateau occurs. The lack of surface or near-surface thermal waters and the apparent decoupling of the near-surface and deeper thermal regimes has rendered exploration for and evaluation of possible geothermal resources extremely difficult using conventional surface geophysical-geochemical techniques and shallow thermal gradients. At present there are indications of vertical mixing between the regional acquifer (Coconino Sandstone) and thermal waters, but there exist no hard numbers of the type usually used for regional evaluation of geothermal potential. Data on the magnitude of regional stresses and horizontal stress gradients are lacking. These and reliable heat-flow data are essential to understanding the tectonic transition from the Sonoran Desert Region of the Basin and Range Province to the Colorado Plateau as well as to evaluation of the geothermal potential of the region. We have proposed to DOSECC the drilling of 2 coreholes to depths of between 2 and 2.5 km on the Colorado Plateau to investigate the coupled stress, heat flow and hydrologic problems, and to provide a preliminary evaluation of the geothermal resource (if

indeed it exists) associated with the San Francisco volcanic field.

2. Heat flow and Tectonics of Alaska

Thermal data from 25 wells in the National Petroleum Reserve -- Alaska (NPRA) yield heat-flow estimates of variable, but generally high, quality. Within NPRA, heat flow generally increases from south to north and from west to east from values in the range 45-60 mW m^{-2} to values of from 70 to 100 mW m^{-2}. The increases correspond in general (but not in detail) to thinning of the Mississippian through Tertiary sedimentary sequence, suggesting some association with deep lateral circulation of groundwater.

Reports:

Bills, D.J., and Sass, J.H., 1985, Hydrologic and near-surface thermal regimes of the San Francisco volcanic field: U.S. Geological Survey Professional Paper, in press.

Lachenbruch, A.H., Sass, J.H., and Galanis, S.P., Jr., 1985, Heat flow in southernmost California and the origin of the Salton Trough: J. Geophys. Res., in press.

Lachenbruch, A.H., 1985, Simple models of Frictional Heating by an Earthquake: U.S. Geological Survey Open-File Report 85-31, 8 pp.

Lachenbruch, A.H., Sass, J.H., Lawver, L.A., Brewer, M.C., and Moses, T.H., Jr., 1985, Depth and temperature of permafrost on the Alaskan Arctic Slope: U.S. Geological Survey Professional Paper, in press.

Pollack, H.N., and Sass, J.H., 1985, Thermal regime of the lithosphere, in Haenel, R., Rybach, L., and Stegena, L., eds., Handbook of Terrestrial Heat-flow Density Determination (Guidelines and recommendations of the International Heat Flow Commission), in press.

Sass, J.H., Lachenbruch, A.H., and Silver, L.T., 1984, Exploratory crustal drilling near the southern margin of the Colorado Plateau and in the San Francisco volcanic field (abstract): EOS, v. 65, p. 1096.

Sass, J.H., Lawver, L.A., and Munroe, R.J., 1985, A heat-flow reconnaissance of southeastern Alaska: Canadian Journal of Earth Sciences, v. 22, p. 416-421.

Zoback, M.D., Healy, J., Lachenbruch, A.H., and Henyey, T., 1984, In situ stress, heat flow, and fault zone monitoring in a deep well near the San Andreas fault at Cajon Pass (abstract): EOS, v. 65, p. 1097.

Fault Patterns and Strain Budgets

9960-02178

Robert W. Simpson
U.S. Geological Survey
Branch of Tectonophysics
345 Middlefield Road, MS/977
Menlo Park, California 94025
415-323-8111, ext. 4256

Investigations

Purpose is to investigate the effect of fault geometries upon the distribution of stress and strain in an attempt to determine the relative importances of geometry and mechanical properties in defining strain budgets.

Results

The displacement-discontinuity program obtained from Gary Mavko has been modified so that stress and strain fields can be plotted in color on an Envision terminal. Tests with simple fault geometries to check the proper functioning of the program show that long straight model faults with nearly uniform friction from end to end have very simple earthquake cycles, consisting of single large events breaking the entire fault. To obtain more varied earthquake histories for the model faults, the distribution of frictions assigned to the fault segments needs to be heavily skewed, with many segments having lower frictions.

Earthquake Forecast Models

9960-03419

William D. Stuart
Branch of Tectonophysics
U.S. Geological Survey
Pasadena, California   91106
(818) 356-6883

Investigations

Develop and test a procedure for predicting earthquakes using an earthquake instability model and repeated measurements of fault slip and ground deformation.

Results

The current model represents the San Andreas, Imperial, Cerro Prieto, and San Jacinto faults by flat vertical planes in an elastic half space. The fault is divided into 551 rectangular cells, each of uniform slip. In most of the cells, slip and stress are computed results and vary with position and time. In the remaining cells, which occupy steadily creeping areas, fault slip rate is imposed as a boundary condition.

The main free parameter in the problem is the variation of brittle fault strength along strike. The fault is assumed to be brittle from the ground surface to about 12 km depth between Parkfield and the Salton Sea. The strength of the brittle zone has been adjusted by trial until slips and times of instabilities (the earthquake analogs) agree with measured fault offsets since 1080 reported by Sieh and others. The brittle zone is found to be made of five contiguous sections of alternately low and high strength. The sections from north to south are : 1 - Parkfield to Bitterwater Valley, 2 - Bitterwater Valley to Lake Hughes, 3 - Lake Hughes to San Bernardino, 4 - San Bernardino to Palm Springs, and 5 - Palm Springs to the Salton Sea. Sections 1, 3, and 5 have low strength, and sections 2 and 4 have high strength.

The figure is a space-time diagram showing lengths of computed unstable slips as solid horizontal lines. Instability names, such as X and Z, and dates in parentheses refer to earthquake offsets reported by Sieh and others. Dates without parentheses are instability times. Dashed lines are for reference and are not instabilities. In this simulation the next future instabilities are on patch sections 1 and 5 in 1993. The uncertainty of instability dates is hard to estimate, but is likely to be at least a few decades. Preliminary calculations show that lengthening rates of certain hypothetical trilateration lines have pre-instability changes starting several years to several decades before instabilities. The changes appear to be large enough to detect by existing survey techniques.

Reports

Stuart, W.D., Instability model for recurring large and great earthquakes in southern California, Pure Appl. Geophys., 122, 1984, in press.

Stuart, W. D., R. J. Archuleta, and A. G. Lindh, Forecast model for moderate earthquakes near Parkfield, California, J. Geophys. Res., 90, 592-604, 1985.

Stuart, W.D., Theoretical line length changes before great earthquakes in southern California (abs.), EOS Trans. Am. Geophys. Un., 66, 1985, in press.
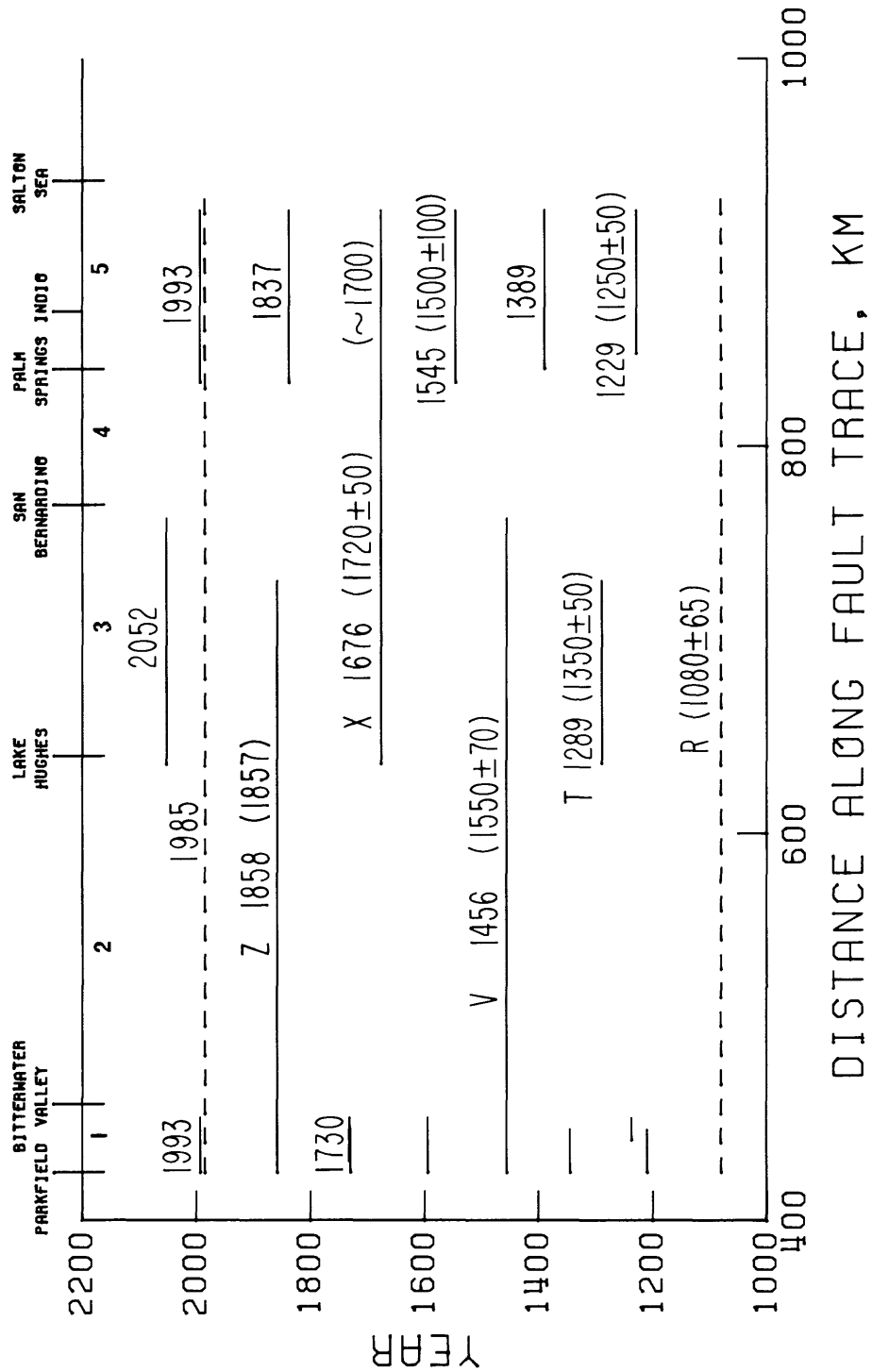
EXPERIMENTS OF ROCK FRICTION CONSTITUTIVE LAWS
APPLIED TO EARTHQUAKE INSTABILITY ANALYSIS

Terry E. Tullis
John D. Weeks
Department of Geological Sciences
Brown University
Providence, Rhode Island 02912
(401) 863-3829

Investigations

1. We have continued our investigation of the dependence of the frictional strength of dolomite marble on velocity. Previously, we had determined that the frictional constitutive behavior departed from that used in Gu et al. (1984). We have been developing a constitutive law that describes the behavior of dolomite better.

2. We have attempted to understand the physical explanation for the existence of characteristic sliding distances in experimentally based constitutive descriptions of frictional sliding. This is important in order to scale laboratory results to natural faults.

3. We have continued our theoretical investigation of the stability of a spring-and-slider block frictional system, using the theories developed by Gu, et al. (1984). Since our modeling of experimental data has shown that two state variables are needed to match our experimental results, we are examining how changes of the values of the constitutive constants affects the stability of a frictional system characterized by two state variables.

Results

1. Previously, we reported that the frictional strength of dolomite marble did not follow a linear dependance of coefficient of friction on log velocity, in contrast with results for granite. Subsequent modelling using the techniques of Gu, et al. (1984) shows that if a state variable constitutive law is used to model our results, the constitutive parameters are not constant with velocity. In particular, the the distance over which the state variables evolve with sliding is not constant with velocity, in contrast with results for granite obtained by us and others. Figure 1 shows the results of modelling for several changes in load point velocity during two experiments. For the standard friction law with constant parameters, behavior depends only on the size of the velocity change. In Figure 1 the size of the velocity change is constant, so that the varying behavior must be caused by changing constitutive parameters. For the modelling shown in Figure 1, the longer-term state variable was modelled with a constant characteristic evolution distance while the shorter one has been modelled with characteristic distance that changes in proportion to the load point velocity. The success of the modelling suggests that the explanation for the changing evolution distance is that the shorter state variable evolved in a characteristic time, rather than in a characteristic distance. Consequently, we have developed a constitutive law having a state variable that evolves in time rather than distance and we are now using it to interpret our results for dolomite. Work on this constitutive law continues.

2. Dieterich (1979) found a qualitative correlation between the roughness of sliding surfaces and the sliding distance d_r required for frictional resistance to reach a new steady state value following an abrupt change in sliding velocity. He speculated that d_r might represent the amount of sliding

required to totally change the population of contact spots which represent the true area of contact between the sliding surfaces. In order to test this we have calculated the expected size of the average contact spot for three surfaces of different roughness and compared the calculated spot radii with observed d_r.

The calculations are based upon contact theory for nominally flat surfaces characterized by Fourier analysis; the input data come from profilimeter measurements made by Paul Okubo. The d_r measurements were reported previously by Dietrich and Okubo and Dietrich. We prepared the profiled surfaces in a manner similar to theirs and used the same rock material. Figure 2 shows good agreement between the predicted spot size and the observed d_r. These results must be regarded as preliminary because of the many assumptions invloved in the calculating the spot radii, but the good agreement suggests the essential correctness of the physicl explanation for d_r proposed by Dietrich.

3. We have investigated numerically how changes of various constitutive parameters effect the stability of a frictional system in which two state variables describe the frictional response of the sliding surface. Our experiments have shown that these parameters vary between rock types, but are nearly constant for a single rock type over limited ranges of sliding velocity. Here we present results showing how changes of b_2, the coefficient giving the magnitude of frictional change associated with the more slowly evolving state variable ψ_2 affect frictional stability when all other constitutive parameters are held constant.

Frictional behavior may be represented on three-dimensional plots with axes of frictional resistance μ, log sliding velocity V, and ψ_2 (Figures 3a, b, c). Evolution of the system with time can be represented as trajectories in this phase space. On these plots, a stability surface separates a region of stability below from one of instability above. Steady state behavior is represented by the heavy diagonal line.

The central figure (3b) uses the stiffness of our rotary shear apparatus and constitutive parameters we have found experimentally to describe the sliding of granite. Figure 3a was constructed using a b_2 value 1/2 that in 3b, and Figure 3c was constructed using a b_2 value 4 times that in 3b. We find that lowering b_2 (Figure 3a) decreases the slope of the stability surface in the ψ_2, μ plane and increases the volume of the stable region above the origin (the steady state point towards which all stable trajectories spiral). In addition, the region at low velocity and high ψ_2 is expanded, allowing stable sliding after larger velocity jumps. Negative values for b_2 change the sign of the slope in the ψ_2, μ plane but a stability surface still exists, even for values of b_2 so negative that steady state velocity strengthening occurs. Raising b_2 (Figure 3c), conversely, steepens the stability surface, severely restricts the region of stability above the origin, and allows only extremely small load point velocity jumps to result in stability.

Reference

Gu, J. C., Rice, J. R., Ruina, A. L., and Tse., S., Stability of frictional slip for a single degree of freedom elastic system with non-linear rate and state dependent friction, manuscript in preparation, 1984.

Reports

Tullis, T. E., J. D. Weeks, and M. Blanpied, Constitutive behavior and stability of frictional sliding of granite. To be submitted to 5th Maurice Ewing Symposium, Earthquake Source Mechanics, *AGU Monograph*, 1985.

Weeks, J. D. and Tullis, T. E., Frictional sliding of dolomite: a variation in constitutive behavior, *J. Geophys. Res.*, in press, 1985.
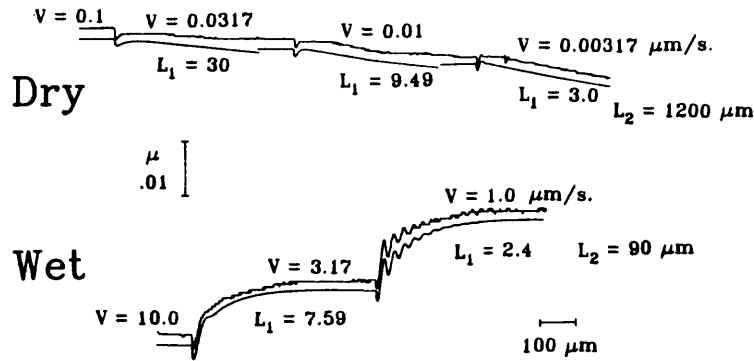
Figure 1. Modelling of friction of dolomite following decreases in load point velocity. Experimental observations of friction versus displacement are shown in the top curve of each pair, while the results of numerical modelling are shown by the bottom curve. The lower pair shows data from an experiment in which free pore water was present at the beginning of the experiment (but pore pressure was zero) and the upper pair is for a sample that was dried prior to the experiment. Modelling was done using a two state variable constitutive law. The decay distance of the longer term state variable, L_2, was held constant for each experiment. The shorter one, L_1, was set to a value proportional to load point velocity.
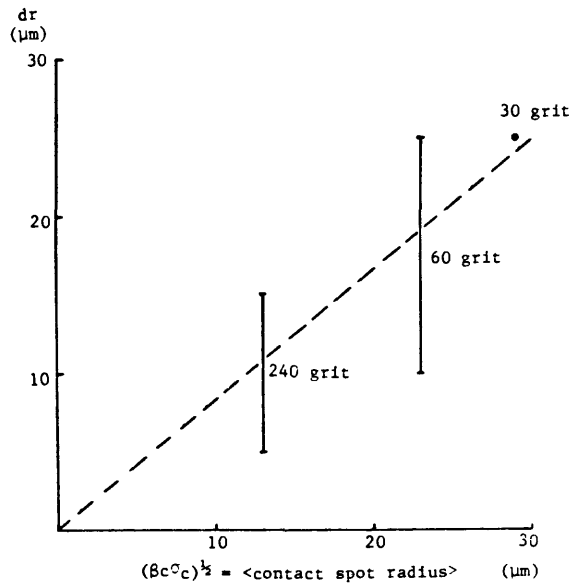
Figure 2. Plot of measured d_r versus calculated average radius of contact spot. Horizontal and vertical scales are the same. The contact spot sizes were calculated using the moments of the power spectral density from measured roughness profiles. The fact that the two quantities are similar in size and apparently linearly correlated supports the model of Dieterich (1979) for the origin of the characteristic decay distance, d_r.
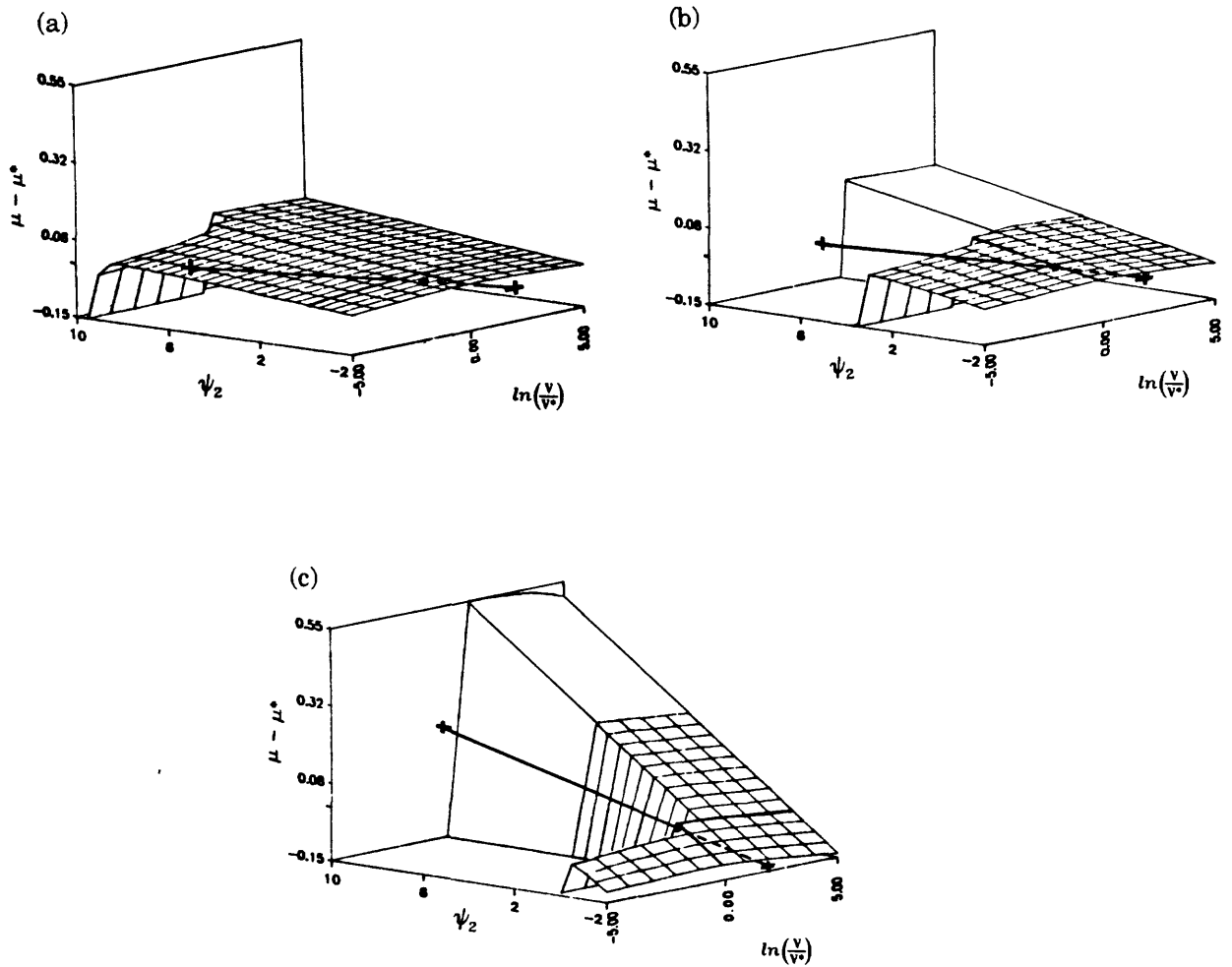
Figure 3. Stability for a frictional system described by a law having two state variables, showing the effect of changing the parameter b_2 while holding all other parameters constant. The heavy diagonal line is the steady state line, its ends showing where it cuts the bounding planes of the diagram and the dot along it marking the origin. The darkened line in the surface is in the plane $\psi_2 = 0$, and helps to show how far the surface is above the origin. The normalized critical stiffness K_{cr} also changes as result of changing b_2 and so the ratio of the normalized stiffness K to K_{cr} changes. In all cases the parameter values are $a = 0.004$, $b_1 = 0.0075$, $L_1 = 8$ μm, $L_2 = 150$ μm, and the normalized stiffness $K = 17.38$. (a) $b_2 = 0.00727$ and the critical stiffness $K_{cr} = 9.65$ so $K/K_{cr} = 1.80$. (b) $b_2 = 0.01454$ and $K_{cr} = 10.66$, the experimentally determined values for granite. In this case $K/K_{cr} = 1.63$. (c)Here $b_2 = .05816$, $K_{cr} = 16.70$ and so $K/K_{cr} = 1.04$.

New Model of Earthquake Faulting

Contract No. 14-08-0001-21803

Joseph B. Walsh
Dept. of Earth, Atmospheric and Planetary Sciences
Victor C. Li
Dept. of Civil Engineering

Massachusetts Institute of Technology
Cambridge, Massachusetts 02139
607-253-5731

Investigations

We have been studying a model for faulting in which an earthquake
is triggered by aseismic slip on a "detachment zone" at the interface
between the lithosphere and the underlying viscous strata. The detachment
zone is a consequence of spatially and temporally non-uniform viscous
forces as the lithosphere is dragged over the asthenosphere. Slip
on the detachment zone loads a fault in the elastic lithosphere, and,
if frictional resistance on the fault is sufficiently low, an earth-
quake ensues.

Our studies so far have been directed toward calculating surface
displacements, strains, and gravity changes associated with slip on the
detachment zone. A graduate student, Steven C. Ho, developed a computer
program which allowed him to find these parameters quickly for arbitrary
dislocation distributions over the detachment zone, and he applied his
results to uplift and strain data for the Palmdale (Cal.) region during
an episode (1959-1977) of aseismic tectonic deformation. Preliminary
results of the analysis were presented at the Fall Meeting of the AGU
and at an informal meeting with R.O. Castle, J.C. Savage, and William
Stuart at the U.S.G.S. Office of Earthquake Studies in Menlo Park, Cal.

Results

Ho found acceptable correlation between observed and calculated
values of uplift and strain for his model. One difficulty with this
tentative model is that the average slip rate over the detachment
zone is about an order of magnitude larger than the estimated relative
tectonic movement for this region. We examined two modifications of
the model in an exploratory way: in one, the detachment zone is
tilted 5° rather than horizontal, and in the other, slip on a vertical
at depth plane is allowed, simulating aseismic creep on the San Andreas,
the upper portion remaining fixed. Both modifications reduce the
average slip required for agreement with observed values without
changing the overall pattern.

Present Status

The principal investigators have completed a rough draft of a manuscript which summarizes the results of this research. We will complete this manuscript under the continuation contract and submit it for publication in the open literature.

Reports

Ho, S.C., V.C. Li, and J.B. Walsh, Surface deformation associated with aseismic slippages on detachment surfaces, EOS, Trans. Am. Geophys. Union, 64(45), 1983.

Ho, S.C., V.C. Li, and J.B. Walsh, Surface deformation associated with aseismic slippages on detachment surfaces, Research rept. R84-03, order no. 763, M.I.T. Department of Civil Eng., Feb. 1984.

Ho, S.C., Surface deformation associated with aseismic slippages on detachment surfaces, M.Sc. Thesis, M.I.T. Dept. Civil Eng., Cambridge Mass., Feb. 1984

PERMEABILITY OF FAULT ZONES

9960-02733

James Byerlee
Branch of Tectonophysics
U.S. Geological Survey
345 Middlefield Road, MS/977
Menlo Park, California 94025
(415) 323-8111, ext. 2453

Investigations

Laboratory studies of the permeability of fault gouges were carried out to provide information that will assist us in evaluating whether in a given region, fluid can migrate to a sufficient depth during the life-time of a reservoir to trigger a large destructive earthquake.

Results

Both laboratory and in situ studies indicate that pore pressure can lower the strength and sliding stability of fault materials. In addition to the increase in hydrostatic pressure with depth, excess fluid pressures are generated in the seismogenic zone by compaction of gouges, by fluid expansion during heating, and by metamorphic reactions that affect the volume and hydration state of the gouge minerals. Excess pore pressures can be maintained for long periods of time if the permeability of the gouge layer is low, or the gouge zone is thick. Recent friction studies on gouges deformed at elevated temperatures suggest that temperature may have a significant effect on the permeability of the gouge. Clay particles become welded together during sliding, particularly when both pore pressure and temperature are high. The originally friable gouge resembles slate after deformation, and the frictional strength is increased due to the grain welding. This behavior is accompanied by an "apparent" departure from the effective stress law, which can be explained simply by the decreasing permeability of the gouge, preventing the fluid pressure from equilibrating quickly. Thus, not only can metamorphic processes affect the pore pressure by the dewatering of minerals, but the accompanying permeability changes can affect the ability of the gouge to maintain excess pressures. These processes may also occur in the seismogenic zone, where temperature effects are important.

Reports

D. Moore, C. Morrow, and J. Byerlee, 1985, Permeability and fluid chemistry studies of the Topopah Spring member of the Paintbrush Tuff, Nevada Test Site Part II, U.S.G.S. Open-File Report 84-848.

C. Morrow, Zhang Bo Chong, and J. Byerlee, 1984, The effective pressure and cubic root law for the permeability of Westerly Granite, E.O.S., Trans. Am. Geophys. Union, v. 65, p. 1078.

P. Vaughan and J. Byerlee, 1984, Mechanism of permeability reduction during flow of hot aqueous solutions through Westerly Granite, E.O.S., Trans. Am. Geophys. Union, v. 65, no. 45, p. 1126.

Stress Measurements at the Jordanelle Dam Site, Central Utah, Using Wireline Hydrofracturing

14-08-0001-21890

Bezalel C. Haimson
University of Wisconsin, Madison
1509 University Ave.
Madison, Wisconsin 53706
(608) 262-2563

Investigations

1. Stress measurements at Jordanelle dam site, central Utah, utilizing our wireline-hydrofracturing technique.

2. Comparison of results with regional tectonics, fault plane solutions, and other stress measurements, and an evaluation of the stability of the Jordanelle site.

Results: We have conducted in situ stress measurements employing our own wireline-hydrofracturig technique in a 300 m borehole adjacent to the planned Jordanelle Dam site in the seismically active Wasatch Hinterland of central Utah. This marks probably the first time that stress measurements to determine the stability of the rock under a planned dam and reservoir were undertaken before construction and impoundment. Tests results in the generally fractured andesite prophyry of the test hole reveal a transition from high near-surface horizontal stress (σ_H and σ_h) exceeding the vertical stress magnitude (σ_v), to low σ_H and σ_h of the order of $\sigma_v/2$ toward the bottom of the hole. This stress configuration seems to persist with depth over an extended area as evidenced from our previous measurements in another drill hole situated some 50 km south of Jordanelle. Figure 1 shows the results of our present tests (140-300 m depth) together with the earlier measurements (450-600 m). It suggests a state of stress potentially condusive to normal faulting ($\sigma_v > \sigma_H > \sigma_h$) along fault planes striking to the northwest. The measured stress magnitudes suggest a stress regime close to the limit of stability based on a simple model of frictional sliding on properly oriented preexisting faults (see Brace and Kohlstedt, 1980). The results are compatible with the extensional tectonics of the Wasatch Hinterland and its active seismicity, and correlate well with many fault plane solutions of recent earthquakes in the region.

Reports

Haimson, B. C., Hydrofracturing studies - drillhole DH101, Report to U. S. Bureau of Reclamation, p. 29, 1981.

Haimson, B. C. , Stress measurements in the Wasatch Hinterland complement existing tectonic and seismic data, EOS Trans. AGU, 65, p. 1118-1119, 1984.

Haimson, B. C. and M. Y. Lee, Stress measurements at the Jordanelle Dam Site, Central Utah, Final Report to U.S. Geological Survey, p. 34, 1985.
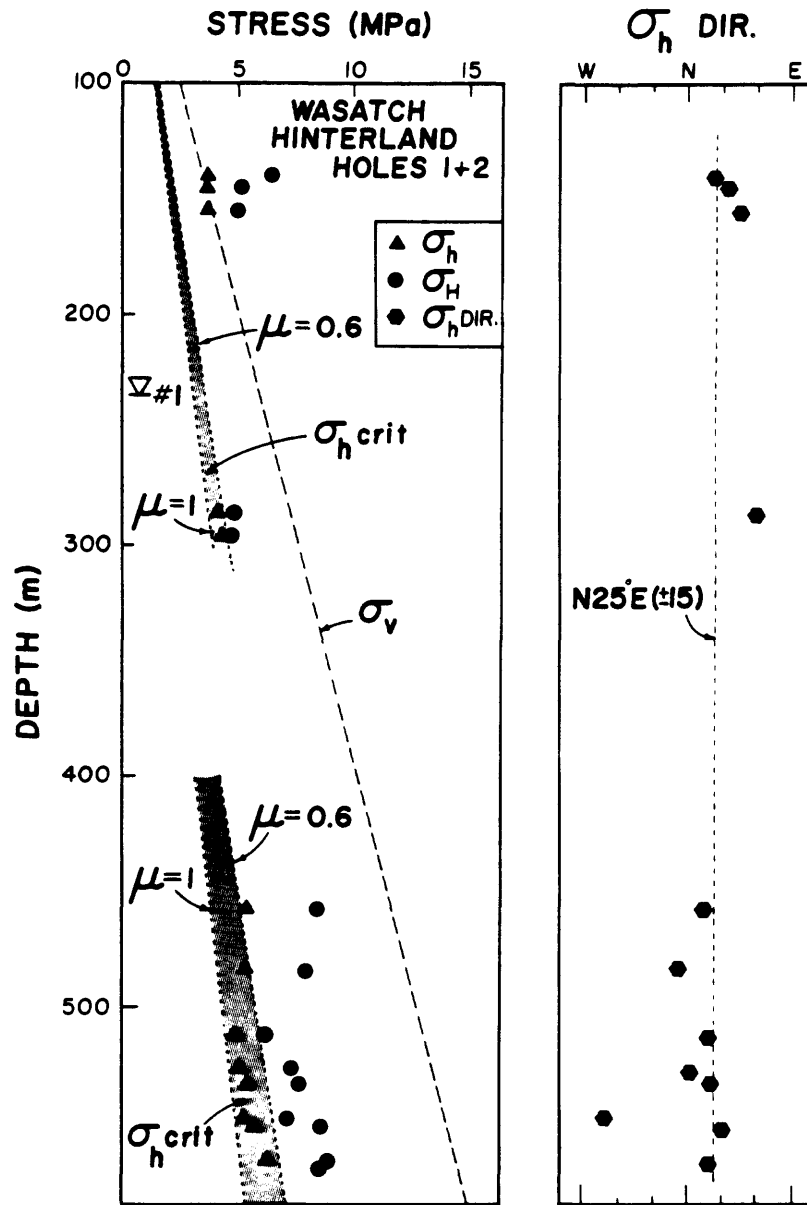
Figure 1. Variation of stress magnitudes and directions with depth in the Jordanelle test hole (0-300 m) and in another hole 50 km to the south. The shaded bands delineate the zone of minimum allowable σ_h based on Byerlee's (1978) frictional sliding criterion for a coefficient of friction μ between 0.6 and 1.0 (also see Brace and and Kohlstedt, 1980).

Array Studies of Seismicity

9930-02106

David H. Oppenheimer
Branch of Seismology
U.S. Geological Survey
345 Middlefield Road - Mail Stop 977
Menlo Park, California 94025
(415) 323-8111, Ext. 2791

Investigations

1. Devise computer algorithms to compute and display earthquake fault-plane solutions.

2. Investigate fault-plane solutions at The Geysers for inferences on state of stress and mechanism of induced seismicity.

3. Continue monitoring of induced seismicity at The Geysers.

4. Continue investigations into frequency-wavenumber spectra of near-field strong motion array data for detection of rupture front position.

Results

1. Algorithms to compute and display double-couple earthquake fault plane solutions from first motion polarities were developed and tested. The inversion is accomplished through a two-stage grid-search procedure that finds the source model minimizing a normalized, weighted sum of first-motion polarity discrepancies. Two weighting factors are incorporated in the minimization: one reflecting the estimated variance of the data, and one based on the absolute value of the theoretical P wave radiation amplitude. The latter weighting gives greater (lesser) weight to observations near radiation lobes (nodal planes). In addition to finding the best double-couple source model, the program estimates the uncertainty in the model parameters (strike, dip, and rake). An Open-file report is in preparation which describes the inversion and lists the source code.

2. Over 170 fault plane solutions were computed for earthquake data recorded at The Geysers, California geothermal field for the period 1/84-1/85. The results provide several constraints on the mechanism for inducing earthquakes in the steam field. The orientation of the fault planes are random, which prevents identification of the failure plane from the auxilliary. The random orientation of the fault planes, coupled with the small magnitudes of the earthquakes (M<4.0) suggest that failure is occurring on randomly oriented, pre-existing fractures which are reactivated due to the current state of stress in the field. The distribution of P and T axes show a depth dependency whereby earthquakes at depths less than 1.0 km exhibit strike slip to reverse mechanisms, and for greater depths range from strike-slip to normal.

Comparison of the orientation of P and T axes with regional geodetic

observations indicates that the regional stress field is predominant at The Geysers. However, the magnitude of the maximum and intermediate principal stress components are nearly equal, suggesting that The Geysers geothermal field is undergoing uniaxial extension. The orientations of the T axes are normal to the orientation of Quaternary basalt-andesite vents near Clear Lake, which also indicates that the tectonic extension deduced from focal mechanisms at The Geysers controls the process of volcanic eruptions throughout the region between the Rogers Creek-Healdsburg-Maacama and Green Valley-Bartlett Springs faults.

The inducing mechanism is likely due to the mass of fluid withdrawn from the reservoir which causes localized contraction in the vicinity of the steam wells. This contraction results in small stress perturbations to the regional stress field which exceed the frictional strength on favorably oriented existing fractures. The subsidence and contraction observed at the surface is the elastically integrated effect of volumetric contraction at depth and explains the strike-slip to reverse fault-plane solutions for the shallow events.

3. Microearthquake activity continues to be monitored at The Geysers. All geothermal power plants now exhibit induced seismicity, although the level of seismic activity is not directly proportional to the amount of power generated at each unit (a measure of the volume of steam withdrawn from the supply wells). We now observe that seismicity near P.G.&E. Unit 15 is abating concurrent with the declining production statistics at this unit. The yearly amount of power generated summed over all the operating geothermal power units at The Geysers correlates with the number of earthquakes of M>1.2 within the field, indicating that even earthquakes in the vicinity of the older power units are also induced. Thus, we now believe that all the earthquakes at The Geysers are induced, and that the region was generally aseismic prior to extraction of steam. We expect seismicity to continue at The Geysers and expand into regions of new production.

4. In a hypothetical test, synthetic ground velocity seismograms from an irregularly expanding rupture on a horizontal fault were calculated for a proposed 26 element array in the Parkfield region. Wavenumber axes were adjusted during computation of high resolution frequency-wavenumber (f-k) spectra so as to maintain constant slowness axes over varying frequencies. The f-k spectra were converted to frequency-slowness (f-s) spectra and stacked over frequency to enhance stable spectral peaks. Computations were performed for sequential time windows and projected back onto the fault plane via ray-tracing to yield an image of power radiated from the rupturing fault as a function of time. The expanding rupture can be seen in the sequence of f-s images, but is complicated due to source factors such as directivity as well as spectral amplitudes for various frequences which dominate the stack.

Reports

Oppenheimer, D. H., 1985, Induced seismicity at The Geysers, California, Earthquake Notes, v. 55, p. 17.

Cockerham, R., Eaton, J. P., Reasenberg, P., and Oppenheimer, D., 1985, The April 24, 1984 Morgan Hill earthquake and its aftershocks, Trans. Am. Geophys. Union, v. 66, p. 307.

Bostwick, T. K., Spudich, P. A., and Oppenheimer, D. H., 1985, Suppressing aliases and side lobes in frequency/wavenumber transformations through slowness and frequency stacking, Trans. Am. Geophys. Union, v. 66, p. 313.

Spudich, P., and Oppenheimer, D., 1985, Dense seismograph array observations of earthquake rupture dynamics, submitted to 5th Maurice Ewing Symposium.

Mechanics of Faulting and Fracturing

9960-02112

Paul Segall
Branch of Tectonophysics
U.S. Geological Survey
345 Middlefield Road, MS/977
Menlo Park, California 94025

Investigations

1. Continued study of deformation and seismicity induced by subsurface fluid extraction and injection.

2. Inversion of trilateration data to determine slip distribution on the Parkfield-Cholame section of the San Andreas fault.

3. Field and microstructural investigation of fault and shear zone formation in granitic rocks.

Results

1. Extraction of large volumes of fluid from the Earth's crust is known to induce subsidence, horizontal strain, and, in some places, faulting and seismicity. Extraction causes horizontal contraction in the zone of peak subsidence and extension at the flanks of the subsiding region. We have found general solutions for the changes in stress and pore pressure resulting from injection or extraction of fluid into confined permeable strata. The analysis predicts stress and pore pressure changes even in regions where there are no flow induced changes in pore-fluid content. These stresses arise because changes in pore-fluid content induce solid volume changes, and these strains, in turn, generate stresses. These effects are not predicted by simple application of the effective stress principle. Surface displacements and strain calculated for fluid extraction from a single permeable layer embedded in an impermeable matrix are qualitatively similar to those for observed profiles. The analysis predicts subsidence, a central zone of horizontal contraction, and flanking zones of extension. The stresses induced by extraction immediately above and below the producing layer are compressive, parallel to the layer. The model thus predicts reverse faulting in the central region near the producing layer and normal faulting in the flanking zones of extension. The method has been used to assess the possibility that the 1983 Coalinga earthquake was induced by fluid extraction

from the overlying oil fields. The sign and magnitude of the calculated stress change, <0.05 MPa at hypocentral depths, does not support the hypothesis that the earthquake was induced. The model has been corroborated by comparing the calculated subsidence rate of 3 mm/yr with the observed rate, from releveling, of 3.3 ± 0.7 mm/yr.

2. Trilateration data from the Parkfield-Cholame section of the San Andreas is being inverted to determine the spatial distribution of slip-rate along the fault. The interseismic distribution of slip deficit, relative to the slip rate in the creeping zone north of Parkfield will be compared to the geodetically and seismically determined coseismic slip during the 1966 earthquake. The goal of this study is to determine whether all of the strain which has accumulated following the 1966 earthquake is released in characteristic Parkfield events.

3. Small shear zones in granitic rocks of the Sierra Nevada, California, and near Roses, NE Spain, display features which indicate that dilatant fracturing preceded the localization of deformation within the zones, the majority of which exhibit ductile textures and microstructures. Many of the zones have sharp, nearly planar, boundaries between their highly deformed interiors and undeformed, or nearly undeformed, wall rock. The Roses shear zones narrow continuously to hairline fractures at their distal ends. Mineralized microcracks, which parallel the shear zones, are found adjacent to the zone boundaries in both areas, and are interpreted as relicts of an earlier fracturing episode. Ductile deformation of minerals filling these microcracks and macroscopic fractures in the Sierra Nevada demonstrate that fracturing predated the ductile deformation. Deformation appears to spread laterally into the wall rocks following nucleation of the shear zones. We suggest that cracks enhance the wall rock ductility by increasing local fluid fluxes, thereby promoting chemical alteration and/or hydrolytic weakening.

Reports

Segall, P., Stress and subsidence resulting from subsurface fluid withdrawal in the epicentral region of the 1983 Coalinga earthquake, J. Geophys. Res., in press.

Segall, P., The mechanics of induced seismicity resulting from subsurface fluid extraction, Abstracts with Programs, Geol. Soc. America, v. 16, p. 650, 1984.

Segall, P., and J. W. Rudnicki, Stress and pore pressure changes resulting from fluid extraction and injection: Application to the 1983 Coalinga, California, earthquake, Earthquake Notes, v. 55, no. 1, p. 17.

Simpson, C. and P. Segall, The role of fractures in the nucleation and propagation of shear zones in granite (abstract), Abstracts with Progams, Geol. Soc. Amer., v. 16, p. 657, 1984.

McTigue, D. F., and P. Segall, Vertical displacements from a dip slip fault beneath surface topography (abstract), E.O.S., Trans. Amer. Geophys. Union, v. 65, p. 1113, 1984.

Kronenberg, A. K., G. H. Wolf, and P. Segall, Variations in intragranular water within a strain gradient: FTIR traverse across a ductile shear zone (abstract), E.O.S., Trans. Amer. Geophys. Union, v. 65, p. 1098, 1984.

"Earthquake prediction and induced seismicity in Soviet Central Asia"

14-08-0001-22002

David W. Simpson, William Leith and Daniel Davis
Lamont-Doherty Geological Observatory of Columbia University
Palisades, New York, 10964

Background

Our work is part of a continuing study of induced seismicity at Nurek and Toktogul reservoirs in Soviet Central Asia. As part of the induced seismicity studies, we have also compiled data on the regional seismicity and geology that we are using to reevaluate the Soviet prediction efforts in Central Asia. Our program includes the continued monitoring of induced seismicity, theoretical modelling of induced seismicity, geological mapping and Quaternary fault offset studies, and earthquake source mechanism determinations.

Results of Current Investigations

1. Induced Seismicity: Seismicity and water-level data collected during 1983 and 1984 at Toktogul reservoir indicate a gradual increase in the seismicity of the reservoir area in general and along the Talas-Fergana fault in particular, while the concentrated seismicity that marked the immediate dam area in earlier years has dispersed. Some of the increase in seismicity comes from the region below the dam, where a second reservoir, Kurupsai, has recently been filled. Comparing seismicity and water level data for Kurupsai, we have found preliminary evidence for a positive correlation of reservoir water-level with seismicity. We have also detected an increase in seismicity along the segment of the Talas-Fergana fault southeast of Toktogul reservoir. This seismicity is generally deeper than that of the dam area; also, it lies mostly southwest of the mapped fault trace. Preliminary mapping of the Talas-Fergana fault drainages and fault offsets has been completed.

2. Mechanics of induced seismicity: Further study of the seismicity of Kariba reservoir support our hypothesis that the seismicity at any given reservoir may very between two extremes: an early phase due purely to the consolidation effect and a later phase reflecting reservoir water diffusion. Several reservoirs are now seen to have shown this variation, and we are concerned that the recent changes in seismicity at Toktogul reservoir may be indicative of a gradual change to the second type, which is potentially more hazardous (see Simpson et al., 1984).

3. Geology and tectonics of the Garm, Tadjikistan region: Fieldwork in the Peter-the-First range has documented the existence of at least four salt peircements lying in a line just to the north of the crest of the range. Although a fault was been mapped by earlier workers in some segments, there is no evidence for a fault between individual piercements. Instead, they may mark the position of a buried basement block fault, the "Vakhsh flexure," which may localize the flow of salt at depth. One of these piercements is located along the Runou river, a few hundred meters south of the Runou long-baseline tiltmeter. The long-term northward tilt measured on that instrument can therefore be tentatively explained by upward salt protrusion.

4. Earthquake Prediction studies: Focal mechanism solutions for earthquakes in the Gissar range in the Garm area indicate two preferred orientations for p-axes: N-S and NW-SE. These solutions therefore contain nodal planes that correspond to the two predominant azimuths of faults in the Gissar range: NW-SE and E-W, respectively. However, the east-west trending faults are older (and are inherited from the Mesozoic) and have most of the structural displacement, while the NW-SE set has more the character of fractures. Thus, we suggest that the two directions reflect either rock mass failure in the ~N-S compressional field (NW-SE) or fault failure along the older major planes of weakness (E-W). All of the largest earthquakes in this area have occurred on E-W trends.

Recent Publications

Leith, W., Structural mapping from satellite images: An example from Central Asia (abstract), *in* Proceedings, Conference on Landsat Thematic Mapper Applications for the Study of Sedimentary Basins, Denver, Jan. 10-11, 1985.

Leith, W., A mid-Mesozoic extension across Central Asia?, Nature, v. 313, p. 567-570, 1985.

Leith, W. and D. W. Simpson, Seismic domains within the Gissar-Kokshal seismic zone, Soviet Central Asia, submitted to J. Geophys. Res., 1985.

Simpson, D. W., W. Leith and C. H. Scholz, Two types of reservoir-induced seismicity (abstract), *in* Proceedings, Regional Assembly of IASPEI, Oct. 31-Nov. 7, Hyderabad, India, 1984.

Simpson, D., Induced seismicity at Kariba reservoir--A reexamination (abstract), paper to be presented at the Spring meeting of the American Geophysical Union, 1985.

INDUCED SEISMICITY AT ASWAN RESERVOIR

USGS-14-08-0001-22006

David W. Simpson and William Leith
Lamont-Doherty Geological Observatory of Columbia University
Palisades, New York 10964
914-359-2900

In cooperation with the Helwan Institute of Astronomy and Geophysics, a 13-station telemetered seismic network is being used to monitor seismicity near the northern end of Aswan reservoir, in the area of a magnitude 5 1/2 earthquake on November 14, 1981. There is no indication in the historical or instrumental record for an earthquake of this size in the Aswan area prior to 1981. The seismicity is concentrated along the Kalabsha fault, an E-W trendig strike-slip fault that extends west from the reservoir. Focal mechanisms and fault offsets indicate right-lateral motion. The highest level of seismicity following the November 1981 earthquake was at 12-25 km depth. More recent activity has extended east and north of the mainshock are, but at considerably shallower depths (0-8 km).

The November 1981 earthquake occurred immediately following the seasonal peak in water level in the reservoir and increases in activity have followed each of the seasonal maxima in 1982-84. A magnitude 4.8 earthquake and numerous aftershocks also followed the seasonal minimum in August 1982. Because of the African drought, the water level in the reservoir has been generally decreasing (with seasonal fluctuations) since 1981, so that it is now lower than it has been since 1974. The overall level of seismicity has also decreased.

The maximum depth of water in the reservoir at the time of the November 1981 earthquake was 70 m, but in the epicenteral area, 30 km west of the Nile River channel, the water depth was less than 10 m. The reservoir is underlain by a westward thickening wedge of porous Nubian sandstone, which is up to 400 m thick in the epicentral area. Flooding of the sandstone has raised the water table by at least 60 m. The influence of the reservoir is thus significantly greater than that of the water in the reservoir alone and extends to include the changes in the water content of the sandstone as well.

Deep Hole Desalinization of the Dolores River

9920-03464

William Spence
Branch of Global Seismology and Geomagnetism
U.S. Geological Survey
Denver, Federal Center, MS 967
Denver, Colorado 80225
(303) 236-1506

Investigations

This project relates to monitoring of the seismicity of the region of the intersection of the Delores River and Paradox Valley, southwest Colorado. This project is a part of the Paradox Valley Unit of the Colorado River Basin Salinity Control Project and is being performed for the U.S. Bureau of Reclamation with support from the Induced Seismicity program of the USGS. In this desalinization project it is proposed to pump approximately 30,000 barrels/day from brine-saturated rocks beneath the Dolores River through a borehole to the Madison-Leadville limestone formation of Mississippian age, some 15,000 feet below the surface. There is a possibility of seismicity being induced, especially in the long term, by this desalinization procedure. The project objectives are to establish a pre-pumping seismicity baseline and, during the pumping phase, to closely monitor the discharge zone for possible induced seismicity. If induced seismicity does occur it should be possible to relate it to formation characteristics and to the pumping pressure and discharge rates.

Results

A ten-station seismograph network has been installed, centered on the location of the proposed injection well. This high-gain network has a diameter of about 80 kilometers. Final installation of the network was complete in September, 1983. Seismic data are presently being brought to Golden, Colorado, via microwave and phone line transmission. These data are fed through an A/D converter and then through an event detection algorithm. The network has operated at high quality, except for a period in Spring, 1984 when the network was decommissioned by a lighting strike. While 32 probable earthquakes have been identified in the region of the network there has been a general absence of earthquake activity within about 25 km of the network. Analysis procedures have been considerably complicated by a high rate of blasting activity in the region but means have been developed to distinguish the occurrence of natural earthquakes to good reliability. Notable regional earthquake activity occurred with a swarm of shallow events (maximum magnitude 3.2) near Carbondale, Colorado, a magnitude 3.4 shallow earthquake near Blue Mesa Reservoir, Colorado, and a 54-km-deep earthquake located about 25 km northwest of the network. These early results, combined with a lack of historical seismicity at the zone of the Paradox Valley seismic network, indicate that any seismicity induced by deep-well injection near Paradox Valley should be identifiable as such.

Report

Spence, W., and Jacobs, W., 1984, Seismic monitoring in the region of the Paradox Valley, Colorado (Annual report, July 1983 – June 1984, U.S. Bureau of Reclamation, Deep well injection site, Paradox Valley Unit, Colorado River Basin Salinity Control Project), 45 p.

INDUCED SEISMICITY IN THE SLEEPY HOLLOW OIL FIELD,
RED WILLOW COUNTY, NEBRASKA

14-08-0001-21880

Don W. Steeples
Kansas Geological Survey
University of Kansas
Lawrence, Kansas 66046
(913) 864-3965

Investigations

1. Continue to monitor the spatial and temporal distribution of earth-
    quakes in the vicinity of the Sleepy Hollow oil field, southwestern
    Nebraska.

2. Examine possible correlations between earthquake activity and fluid
    injection.

3. Investigate why earthquakes occur in the Sleepy Hollow field, but
    not in other, nearby fields.

Results

Earthquake hypocenters in the vicinity of the Sleepy Hollow oil
field show considerable scatter in both map view and cross section
(Figure 1). The scatter seems to be real and may occur because the
earthquakes are activated in a set of faults rather than on a single
structure. A set of intersection faults have been independently mapped
in the basement rock. The earthquakes are shallow (generally less than
5 km), although most occur in the crystalline basement rock (Figure 1b).

The first motion data from these earthquakes represent two major
faulting mechanisms near the oil field. Well constrained composite
fault plane solutions yield both reverse and normal faulting mechanisms
(Figure 2). The strikes of fault planes inferred from these focal
mechanisms nearly parallel the strikes of mapped faults in the oil
field.

There are two producing units in the Sleepy Hollow field: the
Lansing Limestone Group (1050-1130 m deep) and the Reagan Sandstone
Group (1150-1170 m deep), which is the basal sedimentary unit. Both
units are being injected with water for enhanced recovery. The permea-
bility of the Reagan Sandstone is exceptionally high (about 2.9 darcies)
so the fluid and pressure can be easily transmitted to the basement
rock.

Injection pressures in the oil field have been nearly constant
throughout this study. In May and June 1983, however, ten production

wells were converted to injection wells for the Reagan Sandstone unit. This conversion was followed by six months of significantly increased seismic activity.

Many oil fields in Kansas and Nebraska are injected for enhanced recovery purposes. The Sleepy Hollow field, however, is the only major field in which the basal sandstone unit (viz. the Reagan in this locale) is injected. Earthquakes in the Sleepy Hollow oil field may occur because of the unusual circumstance of injection into a unit of high permeability directly above the crystalline basement.

Reports

Evans, D.G., and Steeples, D.W., Microearthquakes and fluid injection in the Sleepy Hollow oil field, southwestern Nebraska, (in review): Submitted to J. Geophys. Res.
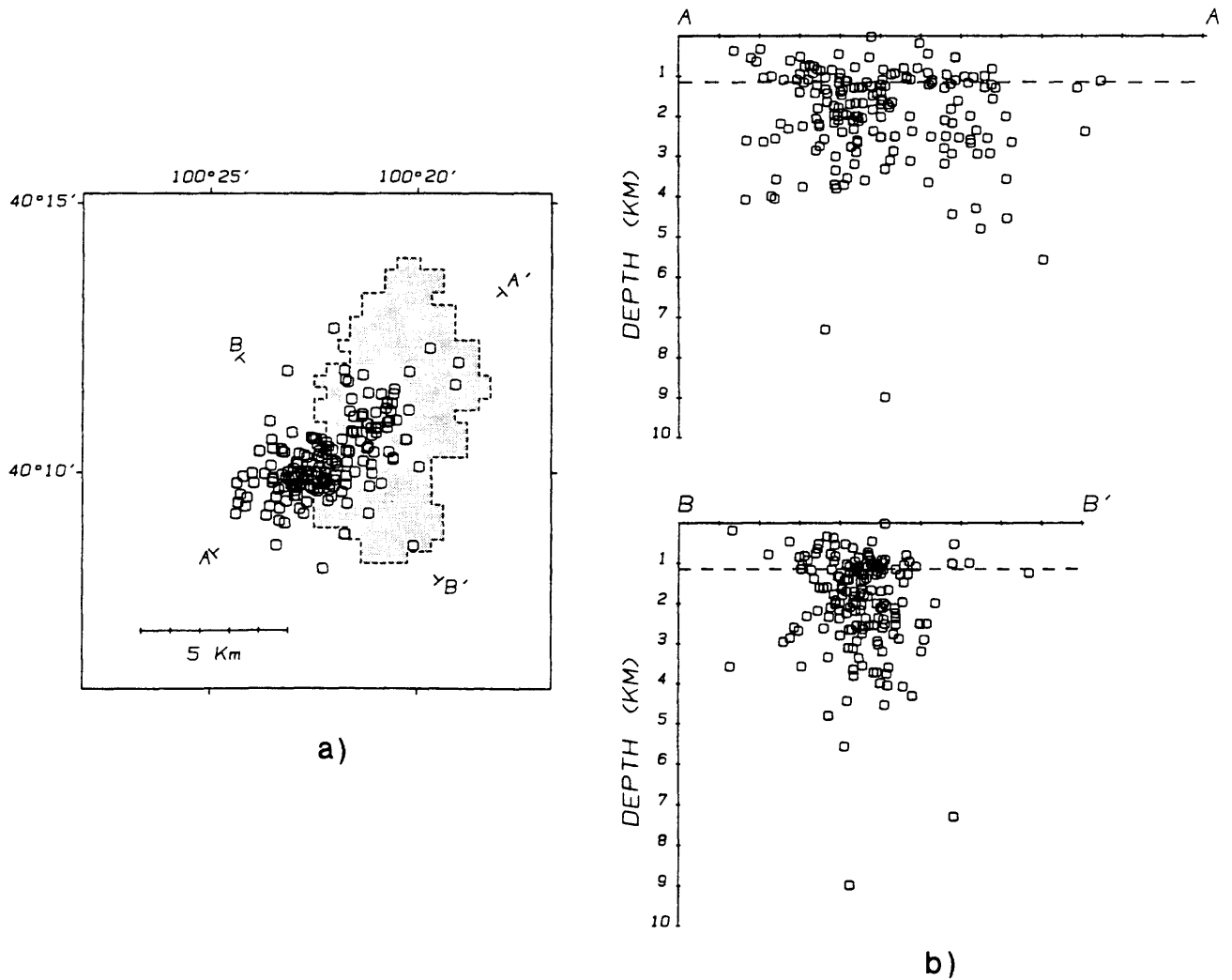
Figure 1. a) Epicentral distribution of earthquakes in the vicinity of the Sleepy Hollow oil field. The shaded region indicates the lease boundaries for the Reagan Sandstone unit.

b) Cross section of earthquake hypocenters. The broken line represents the top of the basement rock.

a)

b)
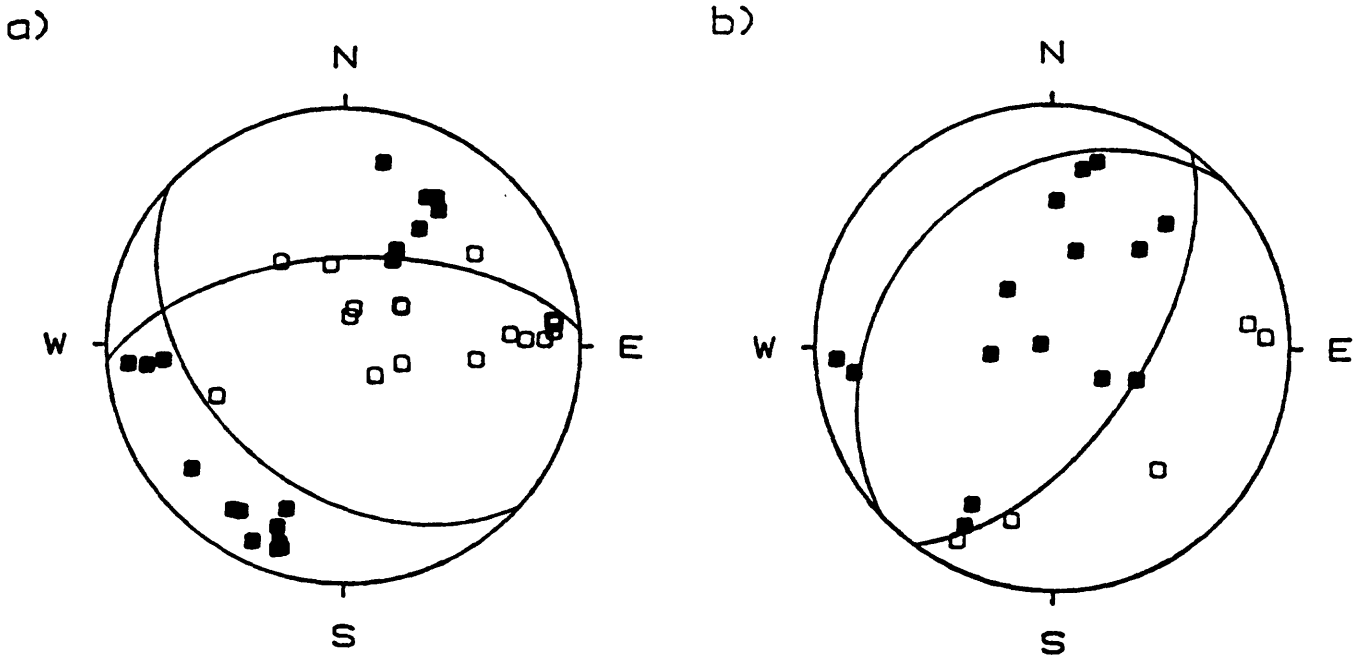
Figure 2. Fault plane solutions for a spatial cluster of earthquakes near the western limits of the oil field.
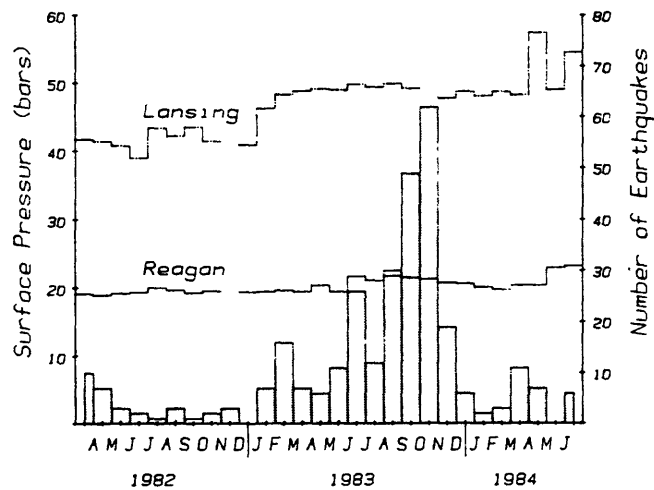
Figure 3. Average monthly pressures for both the Lansing and Reagan units, and a monthly histogram of earthquakes recorded. Ten injection wells were added to the Reagan unit in May and June 1983, followed by six months of increased seismic activity. The apparent low level of activity in 1982 is probably due to long periods of network failure during that time.

Study of Reservoir Induced Seismicity and
Earthquake Prediction in South Carolina

Contract No. 14-08-0001-22010

Pradeep Talwani
Geology Department
University of South Carolina
Columbia, S.C. 29208
(803) 777-6449

Investigations

1. Monitor seismicity near Monticello Reservoir, Newberry, S.C.,
    and Lake Jocassee.

2. Develop a theoretical model for RIS.

Results

1. We are continuing to actively monitor seismicity near Monti-
    cello Reservoir, and Lake Jocassee, South Carolina. We have
    analyzed the temporal pattern of the distribution of hypocen-
    tral depths at Monticello Reservoir from its inception in
    1977 to the present. Seismicity migrated downward from 1978
    through 1982 (Figure 1). Approximately 84% of the events
    were located within 2 km of the surface in 1978 compared with
    51% in 1982. This trend subsequently reversed and by the end
    of 1984, 86% of the events were again located within the top
    2 km. The data suggest the presence of a depth range suppor-
    ting an anomalously high density of events, i.e. fractures.
    Field mapping and a detailed gravity survey indicate this
    horizon may be associated with the lower limits of migmatitic
    granite plutons.

    Seismicity fell to a low of approximately 3 events per week
    in 1984, compared with a pre-impoundment level of 1 event per
    week and a peak of 81 events per week in 1978. Epicenters
    during the last half of 1984 were generally located in an
    east-west band stretching across the central portion of the
    reservoir (Figure 2).

    Seismicity near Newberry, South Carolina continued at about
    one event per two weeks during the last six months of 1984.
    We have refined a velocity model for the area and relocation
    of the events indicates their occurrence at shallow depths
    (< 3.0 km) on the flank of a granitic pluton which may be
    sheared near that depth.

    Lake Jocassee seismicity has been monitored since 1975, first
    with portable instruments, currently with three permanent
    stations. Activity for the last six months of 1984 was low
    (< 3 events per week) and the magnitudes were small (<2.0).

Epicentral locations (Figure 3) are scattered throughout the reservoir area. The cluster of activity in the northwest corner of the figure is predominantly blasting from the construction at the Bad Creek Dam site. As the lake level is expected to fluctuate up to 160 feet per day, studies are being conducted to determine preimpoundment levels of seismicity.

2. A Fortran program is being developed to model the pore pressure increase at depth associated with reservoir filling. The program calculates the diffusion of a pressure pulse along a two dimensional fracture. Fracture length, orientation, and coefficient of diffusivity are chosen within geological and seismological constraints. The algorithm calculates pressures along the fracture with each rise in reservoir level. Data from this program will be used to help interpret the patterns of observed RIS.

Publications

Rastogi, B.K. and Talwani, P., Reservoir-Induced Seismicity at Lake Jocassee in South Carolina, USA in Proc. Indo-German Workshop on Rock Mechanics, eds. T.N. Gowd and F. Rummel, Publ. by National Geophysical Research Inst., Hyderabad, India, 225-232, 1983. (Book appeared in 1984.)

Talwani, P. and Acree, S. Pore Pressure Diffusion and the Mechanism of Reservoir Induced Seismicity, to appear in Pure and Applied Geophysics, 1985.

Presentation

Invited Keynote Paper. Induced Seismicity - a review. International Association of Seismology and Physics of the Earth's Interior, Hyderabad, India, November 1984.

DEPTH DISTRIBUTION 1978 (A AND B QUALITY)
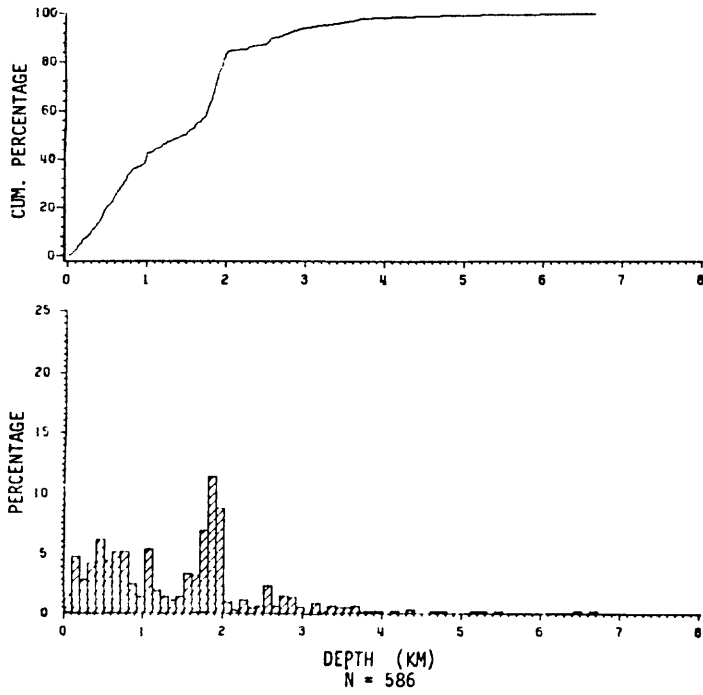
DEPTH DISTRIBUTION 1979 (A AND B QUALITY)
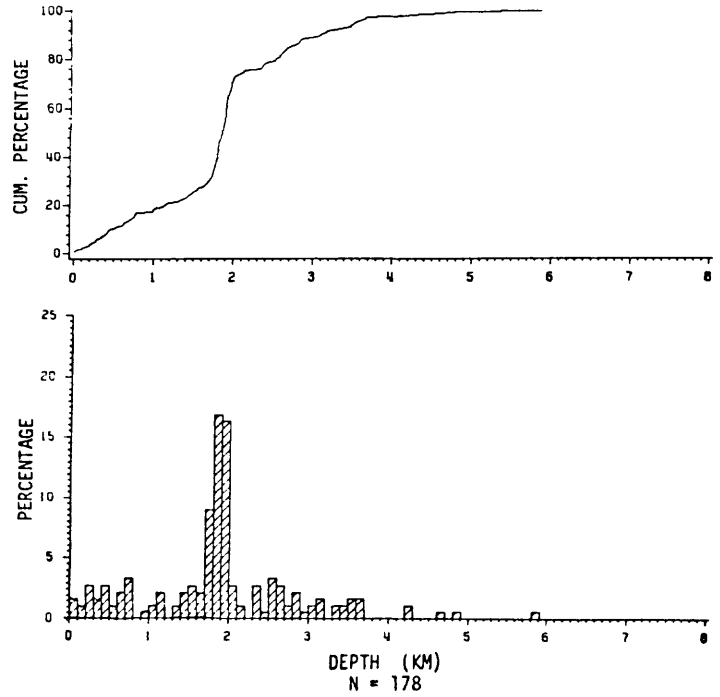
DEPTH DISTRIBUTION 1980 (A AND B QUALITY)
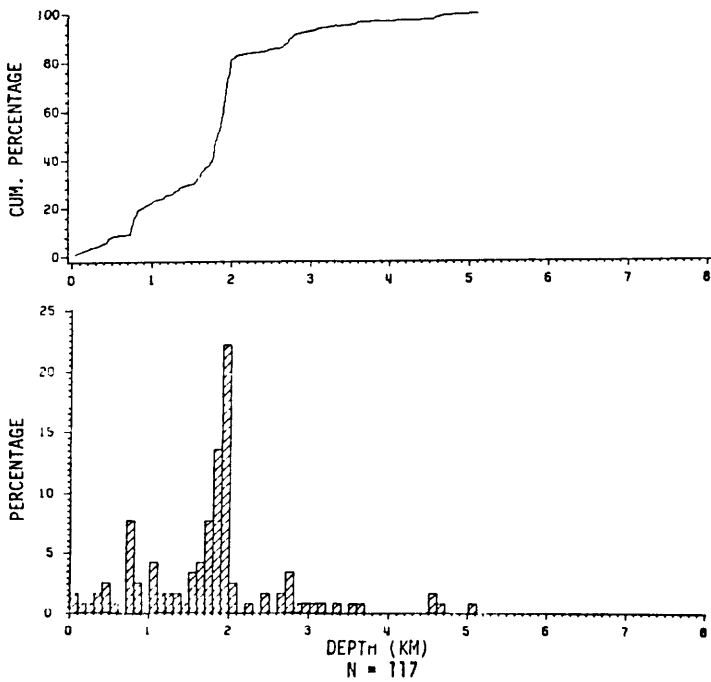
DEPTH DISTRIBUTION 1981 (A AND B QUALITY)

Figure 1

435
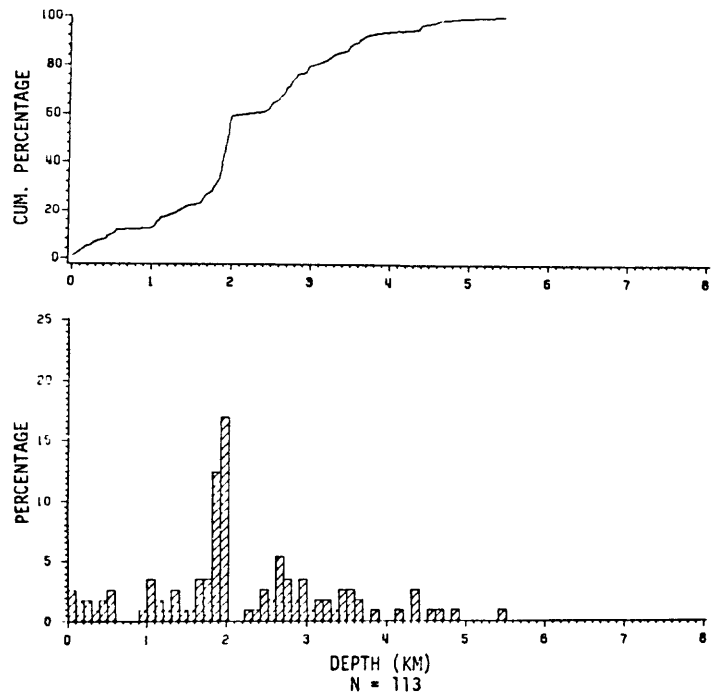
DEPTH DISTRIBUTION 1982 (A AND B QUALITY)
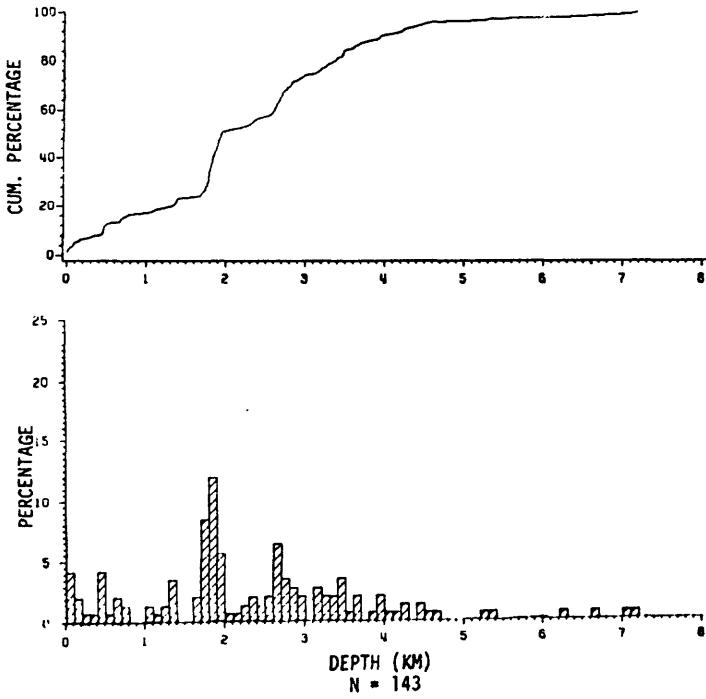
DEPTH DISTRIBUTION 1983 (A AND B QUALITY)
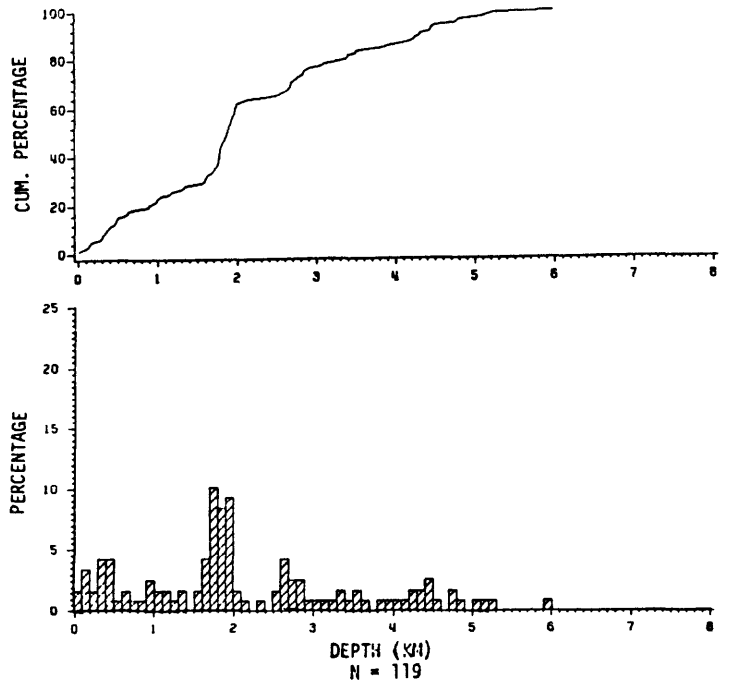
DEPTH DISTRIBUTION 1984 (A AND B QUALITY)

Figure 1 (Continued)

JOCASSEE EARTHQUAKES
JULY – DECEMBER 1984

Figure 3

MONTICELLO EARTHQUAKES
JULY – DECEMBER 1984
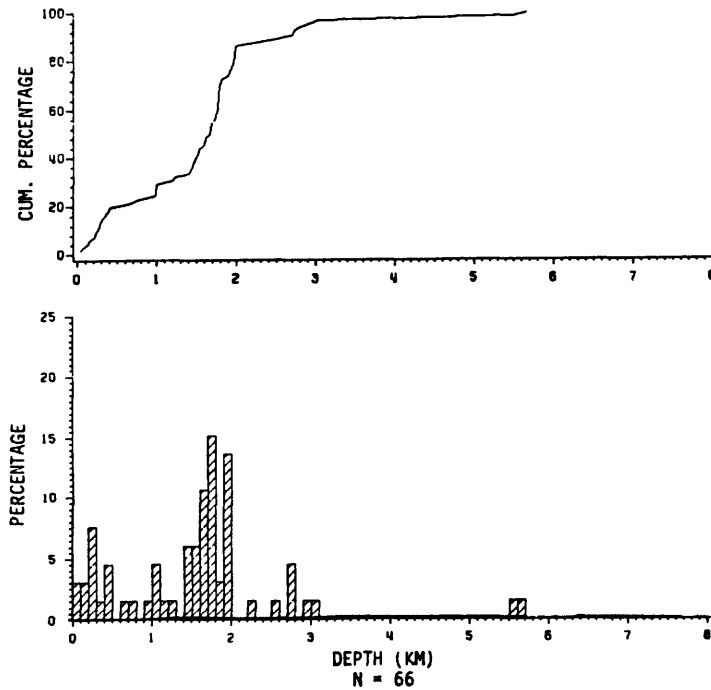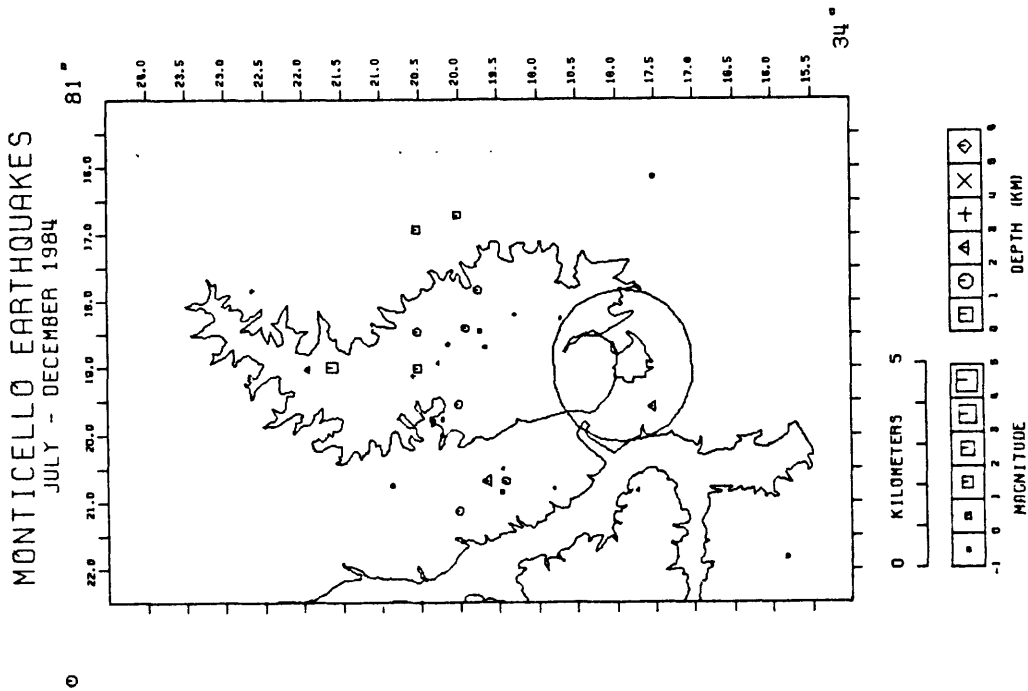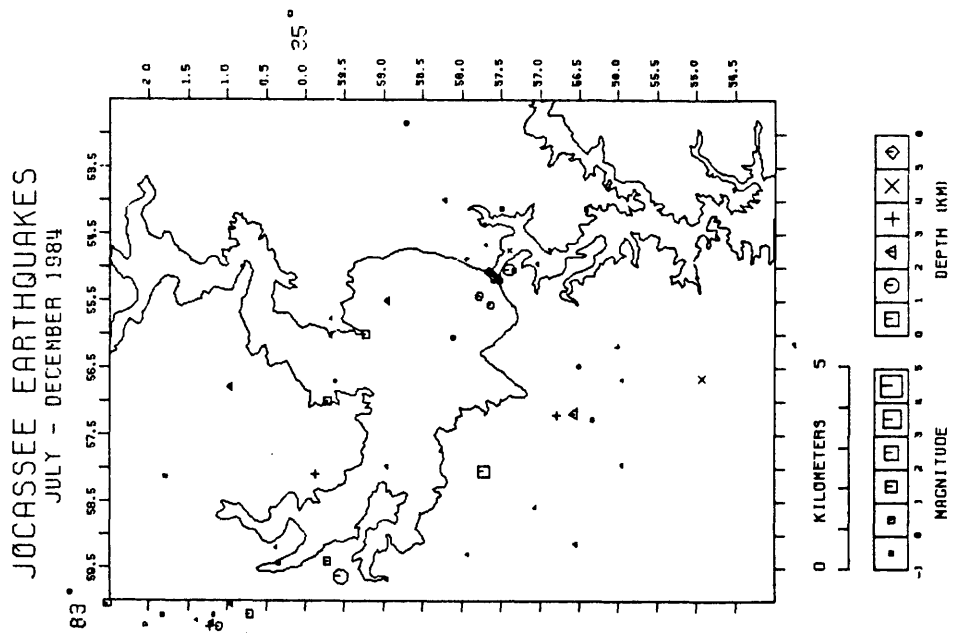
Figure 2

Worldwide Standardized Seismograph Network (WWSSN)

5-9920-01201

O. J. Britton
Branch of Global Seismology and Geomagnetism
U.S. Geological Survey
Albuquerque Seismological Laboratory
Building 10002, Kirtland AFB-East
Albuquerque, New Mexico 87115-5000
(505) 844-4637

Investigations

1. Technical and operational support were provided to each station in the Worldwide Standardized Seismograph Network (WWSSN) as needed and required.

2. One hundred and eighty-seven (187) modules and components were repaired, and three hundred and sixty-nine (369) separate items were shipped to support the network during this period. Several shipments of photographic paper and chemicals were made to the stations requiring these supplies. All routine paper shipments have now been made. Emergency shipments have been minimized.

3. During the month of October 1984, three weeks training was provided to Mr. Russ Grout of Denver, Colorado and Mr. Scott Lawson of Reston, Virginia. They were trained in the operation and maintenance of the WWSSN system. They are presently operating the South Pole Station.

Results

A continuous flow of high quality seismic data from the cooperating stations within the network is provided to the users in the seismological community.

National Strong Motion Data Center

9910-02085

Howard Bundock
Branch of Engineering Seismology and Geology
U. S. Geological Survey
345 Middlefield Road, MS 977
Menlo Park, California   94025
(415) 323-8111, ext. 2982

Investigations

The goals of the National Strong Motion Data Center are to:

1) Maintain a strong capability for the processing, analysis and dissemination of all strong motion data collected on the National Strong Motion Network and portable arrays;

2) Support research projects in the Branch of Engineering Seismology and Geology by providing programming and computer support for computation of numerical models;

3) Provide digitizing, processing, graphics and plotting capabilities rapidly in the event of an earthquake as an aid to earthquake investigations.

Project personnel have studied and investigated advanced technologies for data storage, such as optical disks, processing, digitizing, data retrieval, hardcopy output for text and graphics and data communications networks.

Results

The Center's facilities include a VAX 11/750 computer operating under VMS, a PDP 11/70 and two LSI 11/73 computers running RSX-11M+. The Center's computers are connected to other OEVE computers as well as ISD's VAX 11/780 and Marine Geology's VAX 11/780.

During the first six months of FY85, the project has installed a 3D graphics workstation with digitizing tablet, a color camera system for making slides, prints and transparencies for presentations, and a 456Mb disk for increased data processing capability. The Center has also provided a Data Base Management System to Branch scientists for the organization, archiving, and retrieval of data. Project personnel have participated in the planning of a Survey-wide data communications system and have maintained our local computer network.

Data collected during this six month period were from Anza-Borrego and from the Chile aftershock sequence.

Reports

None.

Seismic Data Library

9930-01501

W. H. K. Lee
U.S. Geological Survey
Branch of Seismology
345 Middlefield Road, Mail Stop 977
Menlo Park, California 94025
(415) 323-8111, Ext. 2630

This is a non-research project and its main objective is to provide access of seismic data to the seismological community. This Seismic Data Library was started by Jack Pfluke at the Earthquake Mechanism Laboratory before they joined the Geological Survey. Over the past ten years, we have built up one of the world's largest collections of seismograms (almost all on microfilm) and related materials. Our collection includes approximately 4.5 million WWNSS seismograms (1962 - present), 1 million USGS local earthquake seismograms (1966-1979), 0.5 million historical seismograms (1900-1962), and 20,000 earthquake bulletins, reports and reprints.

In February, 1985, we received a large collection of seismic station bulletins from the St. Louis University. We plan to merge these materials with our holdings and keep only those we don't have already.

In conjunction with the Microearthquake Data Analysis Project (9930-01173), we completed documentation on a general earthquake data management system called "USGS Earthquake Archiving and Retrieval System". This system allows rapid development and implementation of data processing and analysis programs on the archived data.

Reports

Crane, C. R., Lee, W. H. K., and Newberry, J. T., USGS Earthquake Data Archiving and Retrieval System: Reference Manual, USGS Open-file Report 84-840, 159 pp., 1984.

Crane, C. R., Lee, W. H. K., and O'Neill, M. E., USGS Earthquake Data Archiving and Retrieval System: User's Manual, USGS Open-file Report 85-xxx, 24 pp., 1985.

Source Properties of Great Basin Earthquakes

9950-03835

Arthur C. Tarr
Branch of Engineering Geology and Tectonics
U.S. Geological Survey
Box 25046, MS 966, Denver Federal Center
Denver, CO 80225
(303) 236-1605; 776-1605 (FTS)

Investigations

Two investigations, begun in FY 1984, continued during the first two quarters of FY 1985. These investigations are:

1. Analysis of digital data recorded by DR-100 portable seismic systems at the Nevada Test Site in 1981.

2. Information systems element of the Wasatch Front Regional and Urban Hazards Evaluation.

Two new investigations were begun during the reporting period:

3. Analysis of digital data recorded by MCR-600 portable seismic systems in the epicentral area of the October 18, 1984 Laramie Peak, Wyoming earthquake.

4. Analysis of digital data recorded by DR-200 seismic systems in Provo, Utah of an NTS nuclear shot on March 23, 1985.

An investigation on digital data analysis software development will be discussed in the report for new project 9950-03874, Seismic Data Processing and Shallow Structures:

The objective of the first investigation was to analyze digital seismic data that had been recorded at the Nevada Test Site in 1981 (Figure 1). Preliminary results, discussed last reporting period, suggested low levels of ambient stress in the area of the recorded earthquakes because the calculated values of stress drop and apparent stress were low. The values of magnitude determined from seismic moment determinations were consistent with coda duration magnitude determined from the Southern Great Basin Seismic Network. The determination of source parameters was made using several convenient but possibly overly simplistic assumptions. The investigation was continued using more refined methods, including accounting for the effect of whole-path attenuation on corner frequency determination.

The objective of the second investigation was to provide the mechanism for an information delivery system for the Wasatch Front Regional and Urban Hazards Evaluation study. That system was described in the last Semi-Annual Technical Report for this project. Implementation of elements of that system are to be completed next fiscal year.

The objective of the third investigation was to determine source parameters of aftershocks of the October 18, 1984 Laramie Peak, Wyoming earthquake recorded by MCR-600 digital field systems. This investigation is in support of Charley Langer's Seismic Field Investigations project (9950-01539).

The objective of the fourth investigation was to assist in the analysis of the first data (other than test and calibration data) acquired by new DR-200 digital field systems. The data were acquired in Provo, Utah recording a nuclear shot at NTS on March 23, 1985. This investigation is in support of Ken King's Urban Hazards Seismic Field Investigations project (9950-01919).

Results

The source parameters of the events recorded at NTS in 1981 were recomputed using more accurate formulas for seismic moment and more representative constants for correcting for whole-path attenuation. In addition, the digital velocity time series were numerically integrated and converted to records of equivalent Wood-Anderson response so that ML could be computed directly. The result of the recomputations was that stress drops, in the range 0.02 to 4.4 bars, were generally two to four times larger than stress drops cited in the last report. Moment magnitude was an average of 0.3 units lower than the corresponding coda duration magnitude (Md) while equivalent Wood-Anderson magnitude was an average of 0.3 units lower than Md (Figure 2). When plotted against coda duration magnitude, moment magnitude showed less scatter than did Wood-Anderson magnitude. Except for one event at a distance of about 180 km, the correction for whole-path attenuation was insignificant in raising the corner frequency. The phenomenon of fmax, although apparent on some spectra, did not affect the picking of the corner frequency.

Activity in the second investigation consisted principally of contributing material to the "Wasatch Front Forum" in the form of summaries of Semi-Annual Technical Reports appropriate to the Wasatch Front studies and of solicited articles on specific topics, such as the importance of the Borah Peak, Idaho earthquake to the Wasatch Front earthquake hazard. Consultation with Don Mabey of the Utah Geological and Mineral Survey resulted in improvements to the UGMS's in-house computer system.

The third investigation came about as a result of the need to analyze digital data recordings of aftershocks of the magnitude 5.5 October 18, 1984 Laramie Peak, Wyoming earthquake. The earthquake is interesting because it was deep (24 km), widely-felt, and located in an area of low heat flow. After methods were devised for playing back the data into the Golden VAX/VMS computer, the digital data were converted into a format appropriate for the digital data analysis software used to analyze the NTS data. Preliminary results show that the largest aftershocks are characterized by relatively high stress drops (200-800 bars). If one uses the Oroville stress drop gradient of 16.2 bars/km of Fletcher and others(1984), maximum stress drops of about 390 bars would be expected at the 24 km hypocentral depth of the aftershocks.

Six newly-acquired DR-200 digital field systems were deployed by Ken King and David Carver on a variety of ground conditions in Provo, Utah for the purpose of recording a large nuclear shot at NTS. Relative ground amplification curves can be constructed from the spectral ratios derived from the digital data analysis. During the report period, I have been involved in coordinating

the software tasks required to convert the DR-200 data into a format compatible with the data analysis software. Following tests with calibration data, conversion of one Provo tape was completed successfully at the end of the reporting period.

Reports

None.

References Cited

Fletcher,J., Boatwright, J., Haar, L., Hanks, T., and McGarr, A, 1984, Source parameters for aftershocks of the Oroville, California, earthquake: Bulletin Seismological Society of America, v. 74, p. 1101-1123.
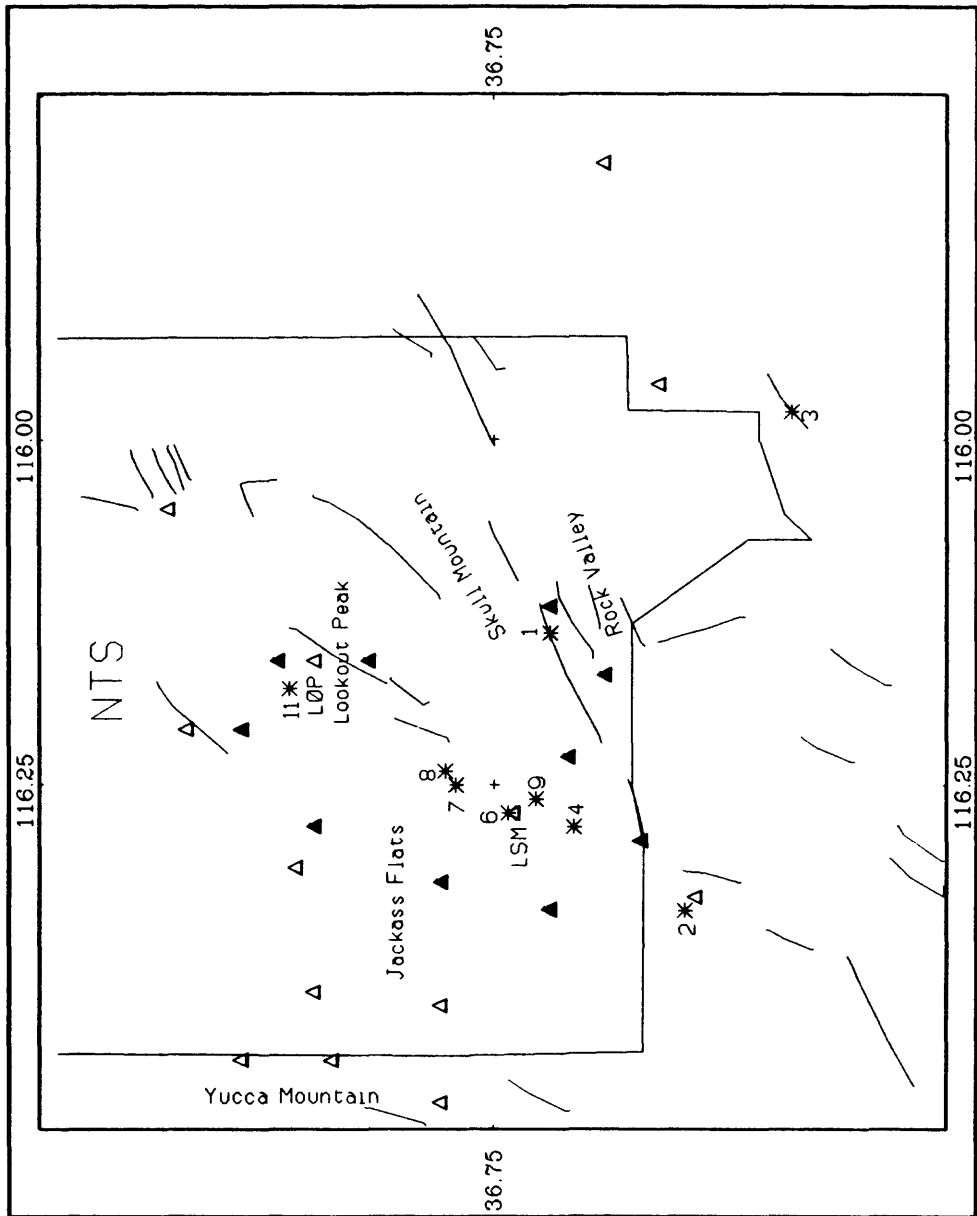
Figure 1.--Map of southern NTS showing locations of seismic stations and earthquakes. Faults are shown as line segments. The period of operation of digital seismic stations (filled triangles) was April 26, 1981 through June 28, 1981; earthquakes recorded by the digital stations and SGBSN stations (open triangles) during the time period are designated by asterixes.
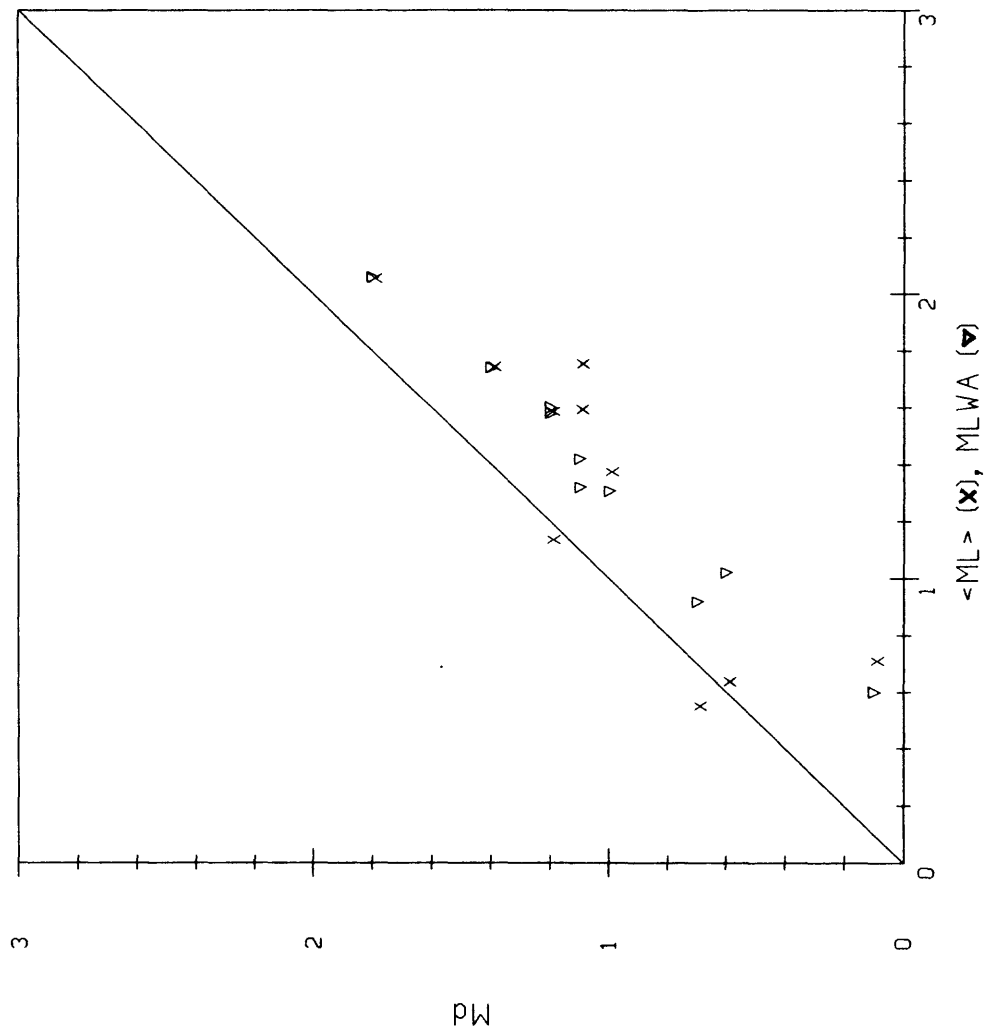
Figure 2.—Graph showing comparison of moment magnitude <ML> (crosses) and equivalent Wood-Anderson local magnitude MLWA (triangles) with coda duration magnitude Md.

Regional and National Seismic Hazard and Risk Assessment

9950-01207

S. T. Algermissen
Branch of Engineering Geology and Tectonics
U.S. Geological Survey
Denver Federal Center, MS 966
Denver, CO 80225
(303) 236-1611

Investigations:

1. Development of near-source scaling relations for peak horizontal acceleration (PHA) from 300 freefield recordings of earthquakes ranging in magnitude from 2.5 to 5.5 M_L.

2. Continued study and development of probabilistic seismic source zone boundaries in modeling seismicity for probabilistic ground motion hazard maps. Initial testing of a preferred technique and the associated computer software modeled a line of 40 sites traversing several seismic source zones in the source zone model of the national seismic hazard maps (Open-File 82-1033) for the central interior region. A manuscript entitled "Source Zone Fuzzing in Seismic Hazard Analysis" has been submitted for journal review.

3. Continued statistical analysis of pattern recognition techniques. A manuscript entitled "Usefulness of Pattern Recognition Techniques for Identifying Earthquake Prone Areas" is in review.

Results:

1. One of the significant findings of this attenuation study was that predictions of PHA for M_L = 5.5 and distances of 0 to 25 km were remarkably similar to predictions based on a scaling relation previously developed for $M_L \geq 5.0$ earthquakes. Thus, we are pursuing the development of a single near-source scaling relation for the entire range of recorded magnitudes in our data base (2.5 M_L to 7.5 M_s).

We have found focal depth to be an important parameter in the prediction of PHA for $M_L > 5.0$ earthquakes, but there is evidence to suggest that this observed dependence may be the result of a systematic bias in the computation of focal depths. Multiple recordings at individual accelerograph sites has allowed a statistical analysis of site effects. As a whole, we find that sites situated on basement rock or in basements of buildings founded on alluvium have peak accelerations substantially smaller than the standard 1-2 story, non-embedded buildings. Sites founded on sedimentary rock have only marginally smaller PHA's than the standard site. The largest accelerations were found to occur at sites where shallow soils overlie rock, especially basement rock. We find that individual sites can deviate substantially from the global behavior of a particular classification, suggesting that individual sites should be investigated if a site-specific estimate of PHA is required.

Predictions based on our M_L < 5.0 scaling relation have been compared with peak accelerations recorded near-source in the eastern United States to test whether California data could be used to predict eastern U.S. accelerations. Preliminary results suggest that we can adequately predict eastern U.S. accelerations providing we use m_b as an estimate of M_L and that we correct for site conditions. The majority of recordings available in the East have been obtained at sites founded on shallow soils. This gives the appearance that near-source PHA in the East is significantly higher than in the West at comparable magnitudes and distances. Correcting for this bias makes the eastern and western accelerations similar in amplitude.

2. For many seismic source zones used in probabilistic ground motion hazard assessment, descrete line boundaries are not a strictly accurate representation of either the geological premises upon which the source zone is defined nor the certainty with which seismicity can be associated with geological structure within the seismic sources. Quantifying these uncertainties through probabilistic boundary locations can significantly affect ground motion hazard estimates for locations either side of the zone boundary. Return periods of moderate to high ground motion values could decrease by as high a factor as eight for locations near zone boundaries.

3. Pattern recognition techniques seek to distinguish earthquake prone areas from nonearthquake prone areas. However, these techniques can give misleading results if the questions asked are correlated and/or if the sample points are not properly selected. In many cases, using a maximum likelihood technique gives better results than using a pattern recognition technique.

Reports:

Algermissen, S. T., 1984, Interpretation, analysis and evaluation of hazard data, in, Williams, M. E., ed., Proceedings of the Geologic and Hydrologic Training Program, March 5-30, 1984, Denver, Colorado: U.S. Geological Survey Open-File Report 84-760, p. 1-27.

Barnhard, L. M., Stover, C. W., Hopper, M. G., Thenhaus, Paul C., and Algermissen, S. T., 1985, Intensity studies of the May 2, 1983, Coalinga, California, earthquake: U.S. Geological Survey Professional Paper, in press.

Campbell, K. W., 1984, The selection and development of strong motion scaling relationships for seismic hazard studies, in, Williams, M. E., ed., Proceedings of the Geologic and Hydrologic Hazards Training Program, March 5-30, 1984, Denver, Colorado: U.S. Geological Survey Open-File Report 84-760, p. 28-82.

_____1984, Strong ground motion data and its use in earthquake engineering, in, Pathways and Future directions for Environmental Data and Information Users, Denver, Colorado, Proceedings: National Oceanic and Atmospheric Administration, p. 240-261.

_____1985, Preliminary analysis of peak acceleration scaling relations for small-to-moderate (M_L < 5.5) earthquakes [abs.]: Earthquake Notes, v. 55, no. 1, p. 5.

Hopper, M. G., 1984, Historical evidence of earthquake activity, in, Williams, M. E., ed., Proceedings of the Geologic and Hydrologic Training Program, March 5-30, 1984, Denver, Colorado: U.S. Geological Survey Open-File Report 84-760, p. 125-152.

Oaks, S. D., Hopper, M. G., Barnhard, L. M., and Algermissen, S. T., 1985, November 7, 1882, Colorado earthquake reinterpreted in light of the October 18, 1984, Wyoming earthquake [abs.]: Earthquake Notes, v. 55, no. 1, p. 24.

Thenhaus, P. C., 1984, Geologic evidence of earthquakes: some geologic studies and applications in estimating the seismic hazard, in, Williams, M. E., ed., Proceedings of the Geologic and Hydrologic Hazards Training Program, March 5-30, 1984, Denver, Colorado: U.S. Geological Survey Open-File Report 84-760, p. 107-124.

Thenhaus, P. C., Ziony, J. I., Diment, W. H., Hopper, M. G., Perkins, D. M., Hanson, S. L., and Algermissen, S. T., 1985, Probabilistic estimates of maximum seismic horizontal ground acceleration on rock in Alaska and the adjacent continental shelf: Earthquake Spectra, Journal of the Earthquake Engineering Research Institute, v. 1, no. 2, p. 285-306.

Regional and Local Hazards Mapping in the Eastern Great Basin

9950-01738

R. Ernest Anderson
Branch of Engineering Geology and Tectonics
U.S. Geological Survey
Box 25046, MS 966, Denver Federal Center
Denver, CO 80225
(303) 236-1684

Investigations

1. Continued analysis of data pertaining to hazards mapping along the Wastach fault (Machette and Personius).

2. Continued analysis of data bases pertaining to the segmentation of the Wasatch fault zone (Wheeler).

3. Continued analysis of paleostress data from south of the Wasatch fault in the central Sevier Valley area (Anderson and Barnhard).

4. Continued analysis of surface-rupture data and other effects of the 1983 Borah Peak, Idaho earthquake (Crone).

5. Continued processing of high-resolution reflection seismic data from faults in the eastern Great Basin (Crone and Harding).

6. Conducted 2-day course on paleostress determinations and 1-day field trip on data-collection procedures (Anderson and Angelier).

Results

1. Four conclusions are drawn by Personius from detailed mapping of Quaternary deposits, soil studies, and measurement of topographic profiles across Quaternary fault scarps along a portion of the northern Wasatch fault (WFZ) near Brigham City (BC), Utah:

   (a) Late Quaternary offset decreases both north and south of BC. Maximum offset on scarps in Provo-age deposits just east of BC.

   (b) Offset data suggest that late Quaternary slip rates may have culminated in latest Pleistocene time, during the final stages of Lake Bonneville. A pre-Bonneville (200 ka) alluvial-fan deposit 16 km north of BC is offset 30 m by the WFZ, yielding a slip rate of 0.15 m/ka. Nearby Provo-age (13 ka) alluvial-fan deposits are offset about 4 m, yielding a slip rate of 0.3 m/ka. Just east of BC, Provo-age lacustrine gravels are offset 12-15 m, yielding a slip rate of 1.0 m/ka. Adjacent post-Provo (10 ka) alluvial-fan deposits are offset 4-6 m, yielding a slip rate of 0.5 m/ka.

(c) The youngest materials offset by the WFZ in the BC area are early to middle(?) Holocene alluvial-fan deposits; soil studies of these deposits, and analysis of scarp profiles indicates that most-recent movement probably occurred no later than 5-6 ka.

(d) The boundary between the Collinston and Ogden segments of the WFZ may be located near the reentrant in the mountain front 2 km northeast of Honeyville, Utah. Offset of similar pre-Bonneville alluvial-fan deposits decreases markedly here, from 30 m near Two Jump Canyon (Ogden? segment) to 15 m near Jim May Canyon (Collinston? segment). Between these two canyons, the surface trend of the WFZ abruptly changes from northeast to northwest.

2. Fault-slip studies by Anderson and Barnhard in the central Sevier Valley area south of the Wasatch fault show that strike-slip faulting is common. In fact, in part of the area, the Pliocene-Pleistocene structural fabric is dominated by strike-slip faults and associated folds. The folds, with amplitudes of 200 m and wavelengths of 1 km, and the strike-slip faults, with displacements of as much as a few kilometers, suggest significant amounts of north-south horizontal shortening. Stress axes orientations computed from hundreds of mapped and unmapped strike-slip, oblique-slip, and dip-slip faults, and microfaults in the area show consistent east-west orientations of least compressive stress (σ_3) and variably oriented maximum compressive stress (σ_1), which is north-south for strike-slip faults and vertical for dip-slip faults. The faults with predominantly strike-slip motion divide into sinistral and dextral groups of differing strike and true conjugate behavior and are thus mechanically compatible with the north-south shortening indicated by the mapped fault and fold patterns. Fault-plane solutions from 17 of 25 microearthquakes are also compatible with north-south shortening, suggesting that the stress field responsible for the mapped patterns still exists. Some of the strike-slip faults are as large and young as the largest and youngest normal faults in the area and must therefore be considered in earthquake-hazards evaluations and resource appraisals.

Reports

Barnhard, T. P., 1985, Map of fault scarps formed in unconsolidated sediments, Elko 1° x 2° quadrangle, Nevada and Utah: U.S. Geological Survey Miscellaneous Field Studies Map, 24 p., 1 sheet, scale 1:250,000. (in press)

Personius, S. F., 1985, Preliminary assessment of late-Quaternary displacement along the Wasatch fault zone near Brigham City, Utah [abs.]: Geological Society of America Abstracts with Programs, v. 17, no. 4, p. 261.

South Carolina Reflection Studies

9950-90017

John C. Behrendt
Branch of Engineering Geology and Tectonics
U.S. Geological Survey
Box 25046, MS 966, Denver Federal Center
Denver, CO 80225
(303) 236-1136

Investigation

During the reporting period, two reports were prepared on deep crustal
multichannel seismic profiles collected earlier across South Carolina and
Georgia. These results are summarized in the following abstract:

Results

In 1981, the U.S. Geological Survey acquired 1350 km of 96-channel, 24-fold,
multichannel seismic-reflection data along three profiles (S4, S6, and S8),
recorded to 6 s and 8 s, extending across South Carolina and Georgia from the
Appalachians to the Atlantic Coast. Previously, in 1979, a 6-line grid
(CH 1 - CH 6) comprising 650 km of 64-channel, 31-fold data recorded to 12 s
was surveyed over the continental shelf near Charleston, S.C. The offshore
grid is tied to line S4 onshore and to the regional survey of the Atlantic
continental margin. The result is a transect of four lines (including
published COCORP data for Tennessee-Georgia) across the southeastern United
States, extending, on a number of offshore deep-reflection lines, to oceanic
crust.

The Appalachian decollement can be seen discontinuously on S6 and S8 from the
Appalachian Mountains southeastward as far as the Carolina Slate Belt; it is
not appareltly continuous to the surface interpreted as the Charleston
decollement offshore. A series of reflections on lines S4, S6, and S8 and on
the COCORP line is interpreted as evidence of southeastward-dipping imbricate
faults, from the Brevard fault on the northwest to beyond the Augusta fault,
which marks the southeastern extent of the Eastern Piedmont fault zone. The
Carolina Slate Belt is characterized on the four seismic profiles by a complex
series of diffractions and reflections extending from less than 1 s to 8 s. A
number of Triassic(?) basins are apparent in the reflection data for the
rifted Charleston terrane identified from low-gradient magnetic anomalies.
These basins are bounded by normal faults reactivated in the meizoseismal area
of the Charleston earthquake of 1886 and, elsewhere, in a compressional
reverse or strike-slip sense during the Late Cretaceous and Cenozoic time. It
appears probably that the seismicity in the Charleston terrane is related to
movement on these fault zones bounding the basins; movement on the faults
identified at depth in the eastern Piedmont fault zone may be related to
seismicity there. Good reflections from the Moho are observed in the 6 CH
lines offshore of Charleston in the range of 8 to 11 s, which is consistent
with COCORP reflection data for land surveys.

Other Investigations

Completed processing (mainly by Annette Yuan) of high-resolution multichannel reflection survey over the Helena Banks fault (HBF) offshore of Charleston, S.C. These data are being interpreted and a report is in the writing stage. Main results show that HBF is 110 km long and has been displacing Coastal Plain sedimentary rock since Late Cretaceous time to probably the present in a left-lateral strike-slip sense with about 70 m of reverse displacement.

References

Behrendt, J. C., 1985, Structural interpretation of multichannel seismic-reflection profiles crossing the southeastern United States and the adjacent continental margin—decollements, faults, Triassic(?) basins, and Moho reflections: American Geophysical Union Special Volume, Geodynamics Series, Deep Structure of the Continental Crust. (in press)

_____1985, Interpretations from multichannel seismic-reflection profiles of the deep crust crossing South Carolina and Georgia from the Appalachian Mountains to the Atlantic Coast: U.S. Geological Survey Miscellaneous Field Studies Map MF-1656, 3 sheets.

Seismic Hazards of the Hilo 7 1/2' Quadrangle

9950-02430

Jane M. Buchanan-Banks
Branch of Engineering Geology and Tectonics
U.S. Geological Survey
Hawaiian Volcano Observatory, Box 51
Hawaii Volcanoes National Park
Hawaii 96718
(808) 967-7982

Investigations

1. Completed paper on structural damage and ground failures from the November 1983 Kao'iki earthquake.

2. Continued geologic mapping of Hilo quadrangle, and began compilation of geologic map and explanation.

3. Continued to computerize field and office data.

Results

1. Prepared a chapter for inclusion in Professional Paper 1350: "Volcanism in Hawaii," describing the structural damage and ground failures associated with the M 6.6 Kao'iki earthquake, and sent it out for peer review.

Damage to structures was greatest in the epicentral area, with the foundations under some houses moving as much as 1.2 m laterally away from the house. Structures with post-and-pier foundations were more severely damaged in this earthquake than those with concrete slab foundations. Lithology and topography also seemed to affect the location and degree of structural damage. More houses were damaged where ash deposits were at or near the surface and were 0.5 m or more thick. Houses built across breaks in slope, on uneven terrain, or near the edges of unsupported embankments sustained greater damage than those on flat ground.

Most ground failures occurred in the epicentral area in the extensively cracked and jointed lava flows that form steep slopes. They were predominantly shallow rock slides and falls. Small soil failures and extensional cracks also occurred in the thick ash deposits in the epicentral area and in Hilo. The threshold intensity for triggering small rock falls and soil slumps was a MMI of IV to V.

2. The geology of the Hilo quadrangle was transferred from photos to a stable topographic base, and an outline of the map units has been completed. Geologic mapping was curtailed due to preparation of the professional paper contribution and to consistently rainy weather. Some mapping and field checking were accomplished, but more remains to be done.

3. A catalogue of photos taken in the Hilo and adjacent quadangles was put in the computer to make future retrieval of slides for specific locations and/or subjects more efficient.

Analytical Investigation of Soil Liquefaction

9910-03390

Albert T. F. Chen
Branch of Engineering Seismology and Geology
U.S. Geological Survey, MS-974
345 Middlefield Road
Menlo Park, CA 94025
(415) 323-8111, Ext. 2605

Investigations

(1). Updated computer programs on liquefaction potential assessment.

(2). Continued the study and report preparation of the liquefaction hazards of the debris dams north of Mt. St. Helens, Washington.

(3). Initiated an investigation on the liquefaction of gravelly soils.

Reports

Tinsley, J.C., Youd, T.L., Perkins, D.M., and Chen, A.T.F., 1985 (in press), Evaluating liquefaction potential, in Ziony, J.I., ed., Earthquake hazards in the Los Angeles region: U.S. Geological Survey Professional Paper 1360.

Investigations of Intraplate Seismic-Source Zones

9950-01504

W. H. Diment
Branch of Engineering Geology and Tectonics
U.S. Geological Survey
Box 25046, MS 966, Denver Federal Center
Denver, CO   80225

Investigations

1. Interpretation of 320 km of seismic-reflection profile data in the upper Mississippi embayment.

2. Preliminary reprocessing of seismic-reflection data to investigate deep structure.

3. Quantitative geomorphic study of stream profiles in the southeastern part of the Ozark Mountain.

4. Processing and interpretation of seismic-reflection data recorded on the Mississippi River.

5. Analysis of level line data in the upper Mississippi embayment and environs.

6. Logging and interpretation of two trenches excavated across the scarp of the Meers Fault in Comanche County, Okla., in conjunction with personnel from the Oklahoma Geological Survey.

7. Interpretation of trench excavated near Blytheville, Ark., in 1982.

8. Analysis of high-resolution reflection data obtained across the Meers Fault.

9. Effects of earthquakes on two perennially boiling wells in the Long Valley caldera, Mono County , Calif.

Results

1. A report by A. J. Crone, F. A. McKeown, S. T. Harding, R. M. Hamilton, D. P. Russ, and M. D. Zoback describing a structurally disrupted zone along the axis of the Reelfoot Rift was submitted to Geology. The disrupted zone is coincident with the northeast-trending zone of epicenters between Caruthersville, Mo., and Marked Tree, Ark., and underlies the area with the greatest number of sandblows in the New Madrid region. On seismic-reflection profiles, the disrupted zone is characterized by loss of coherent reflectors below an antiform of Cambro-Ordovician rocks. The reflectors in the antiform diverge from a reflector identified as magnetic basement, suggesting that tha antiform is the result of intruded material. The origin of the antiform and disrupted zone is unknown but is important because they are associated with a major seismogenic zone.

2. Reprocessing of field tape records of seismic-reflection profiles to 11 s two-way traveltime has begun and shows discontinuous but strong deep reflectors, particularly at depths of about 15 and 30 km. Preliminary interpretation of these zones (Dwyer and Harding, 1985) suggests that they may correlate with the tops of crustal layers with velocities of 6.60 and 7.30 km/s shown on refraction data by Mooney and others (1983) and that they extend below the earthquake zone.

3. A draft report entitled "Analysis of stream-profile data for the eastern Ozark Mountains region and their geologic implications," by F. A. McKeown, M. J. Cecil, B. L. Askew, and M. B. McGrath, has been prepared and is nearly ready for technical review. The report describes the use and results of calculating stream-gradient indices, slopes, and two-dimensional hypsometric values to detect evidence suggestive of tectonic uplift of large (thousands of square kilometers) areas. The fluvial geomorphic evidence, however, is not definitive and must be integrated with other information on the tectonic history of a region. A principal conclusion of this report is that the Salem Plateau section of the Ozarks has been uplifted relative to the Boston Mountains and Arkansas Valley section since late Pliocene or early Pleistocene.

4. Progress on the interpretation of the seismic-reflection data recorded on the Mississippi River has been slow because of unanticipated redirection of the work of the investigators.

5. Compilation and analysis of level line data for the upper Mississippi embayment and vicinity was completed by Richard Dart. Compilation and analysis of breakout zones in drill holes for Mark and Mary Lou Zoback has precluded timely preparation of an open-file report planned for the level line data.

6. The two trenches across the Meers fault indicate that the scarp was formed by a reverse fault that dips to the northeast in the shallow subsurface. Nearly all of the deformation in the alluvium is accomplished by warping and flexing with only a small component of brittle deformation. Stratigraphic units in the trenches have a net vertical throw of more than 3 m. Preliminary interpretation of the trenches indicates one surface-faulting event since late Pleistocene time; however, this surface faulting is probably mid-Holocene or younger. There is no evidence in the trenches that supports a large component of lateral slip.

7. The trench, excavated across prominent linear features in the Blytheville, Ark., area of the New Madrid seismic zone, failed to expose any near-surface faults but did reveal numerous liquefaction-induced sandblows that were probably produced by the 1811-1812 earthquakes. An unusual feature observed in this trench was liquefied sand that rose toward the surface through the soil until it encountered the root-bound turf in the A horizon. The turf of the A horizon delaminated from the underlying parts of the soil and a lens of sand was injected laterally beneath the A horizon. Eventually the pressure accumulated in the lens-ruptured turf and the sand and water flowed onto the ground, burying the soil. A more detailed description of the results of this study has been technically reviewed for publication as a U.S. Geological Survey Miscellaneous Field Studies Map.

8. A short, high-resolution seismic-reflection line was conducted across the Meers fault in Oklahoma. This data has been processed and shows a fault at approximately 271 m in depth which can be connected to the surface faulting. This fault has a displacement of about 30 m (Harding, 1985).

9. Temperature logs obtained in Chance No. 1 (south moat of the Long Valley caldera, Mono County, Calif.) in 1976, 1982, 1983, and 1985 show a progressive cooling in the uncased part of the hole. Examination of the rate of change suggests that the cooling began to accelerate about the time of the strong earthquakes of May 1985 (Diment and Urban, 1985). Temperature logs from Mammoth No. 1 (near Casa Diablo Hot Springs, 3 km west of Chance No. 1) obtained in 1979, 1982, and 1983 are also being processed and examined for seismically induced phenomena (Urban and Diment, 1984; 1985).

Reports

Crone, A. J., McKeown, F. A., Harding, S. T., Hamilton, R. M., Russ, D. P., and Zoback, M. D., 1985, Structure of the New Madrid seismic source zone in southeastern Missouri and northeastern Arkansas: Geology, v. 13. (in press)

Diment, W. H., 1984, Earthquake hazards in northeastern United States, in Management of earthquake hazards in New England—a regional conference: Federal Emergency Mangement Agency, Region I and New England Governor's Conference, Inc., Boston, Massachusetts, p. 19.

Diment, W. H., and Urban, T. C., 1985, Temperature variations with time in a perennially boiling well in the Long Valley caldera, Mono County, California: Observations in Change No. 1 (1976-83): Geothermal Resources Council Transactions, v. 9. (in press)

Dwyer, R. A., and Harding, S. T., 1985, Mid-crustal seismic reflections from part of the New Madrid seismic zone: Earthquake Notes, v. 55, p. 26.

Harding, S. T., 1985, Preliminary results of a high-resolution reflection survey across the Meers Fault, Comanche County, Oklahoma: Earthquake Notes, v. 55, p. 2.

McKeown, F. A., 1984, New Madrid seismic zone, Part I, Historical review of studies; Part II, Contemporary studies by the U.S. Geological Survey, in Proceedings of the New Madrid seismic zone symposium, Cape Girardeau, Missouri, April 27-28, 1984: U.S. Geological Survey Open-File Report 84-770, p. 6-32.

Thenhaus, P. C., Ziony, J. I., Diment, W. H., Hopper, M. G., Perkins, D. M., Hanson, S. L., Algermissen, S. T., 1985, Probabilistic estimates of maximum seismic horizontal ground acceleration of rock in Alaska and the adjacent outer Continental Shelf: Earthquake Spectra, v. 1, p. 285-306.

Urban, T. C., and Diment, W. H., 1984, Precision temperature measurements in a deep geothermal well in the Long Valley caldera, Mono County, California: EOS [American Geophysical Union Transactions], v. 65, p. 1084-1085.

Urban, T. C., and Diment, W. H., 1985, Convection in boreholes: limits on interpretation of temperature logs and methods for determining anomalous fluid flow, in Proceedings National Water Well Association Conference on surface and borehole geophysical methods in ground-water investigations: National Water Well Association, Worthington, Ohio. (in press)

References Cited

Mooney, W. D., Andrews, M. C., Ginzburg, A., Peters, D. A., and Hamilton, R. M., 1983, Crustal structure of the northern Mississippi embayment and a comparison with other continental rift zones: Tectonophysics, v. 94, p. 327-348.

Seismic Hazard Studies, Anchorage, Alaska

9950-03643

A. F. Espinosa
Branch of Engineering Geology and Tectonics
U.S. Geological Survey
Box 25046, MS 966, Denver Federal Center
Denver, CO 80225
(303) 236-1597

Investigations

1. A suite of seismicity maps and depth cross sections for the Anchorage and vicinity region in Alaska are being prepared. A technique has been developed to map the subducting lithospheric plate on a three-dimensional finite-element display for Anchorage and vicinity. ISC, USGS, and Menlo Park's local seismicity data files are used to perform the geometrical mapping of the lithosphere in this region.

2. A "completeness" of the seismicity catalogue is being investigated in order to use lower magnitude thresholds in (a) spatial and magnitude-temporal distribution of shallow ($h \leq 33$ km) and intermediate ($33 < h \leq 100$ km) seismicity ($M_s \geq 5.5$) occurring within a specified area in the period of time which uses (a) historical and (b) instrumentally recorded earthquakes. This effort is part of the seismicity study being carried out in this project for the Anchorage and vicinity region in Alaska.

3. A suite of surficial geologic maps of the northeastern, southeastern, and western part of Anchorage and vicinity are being prepared. Geologic field data are also being collected and mapped.

4. Two geological cross section maps for the City of Anchorage are being prepared which are contiguous to the east-west geologic cross section along the DeBarr line (84-791).

5. A damage evaluation for the City of Anchorage, sustained from the 1964 Alaskan earthquake, is in preparation with damage data that have not been published previously. This information and local surficial geological data is planned to be used in order to evaluate transfer-function amplification curves in Anchorage and to ascertain any existing correlation between damage and soil conditions in the area.

Reports

Bartsch-Winkler, Susan, and Schmoll, H. R., 1984, Bedding types in Holocene tidal channel sequences, Knik Arm, upper Cook Inlet, Alaska: Journal of Sedimentary Petrology, v. 54, no. 4, p. 1239-1250.

Espinosa. A. F., 1984, Seismicity of Alaska and the Aleutian Islands, 1960-1983: U.S. Geological Survey Map 84-855.

Espinosa, A. F., and Michael, J. A., 1984, Seismicity of the Arctic and adjoining regions, 1960-1983: U.S. Geological Survey Map 84-376.

Odum, J. K., Gardner, C. A., Yehle, L. A., and Schmoll, H. R., 1985, Strength and durability properties of Tyonek Formation core, Cook Inlet region, Alaska: American Association of Petroleum Geologists Bulletin, v. 69, no. 4, p. 674.

Nichols, D. R., and Yehle, L. A., 1985, Volcanic debris flows, Copper River basin, Alaska: Japan Landslide Institute Bulletin, 8 p.

Seismic Slope Stability
9950-03391

Edwin L. Harp
Branch of Engineering Geology and Tectonics
U.S. Geological Survey
345 Middlefield Road, MS 998
Menlo Park, CA 94025
(415) 856-7124

Investigations

1. Conducted a reconnaissance of seismic-induced landslides from the September 14, 1984, Nagano-ken-Seibu earthquake in Japan.

2. Compiled data from the Mt. Borah, Idaho and Mammoth Lakes, California earthquakes on the movement and trajectories of boulders from seismic-induced rock falls. The data obtained from numerous boulders and boulder tracks serve as constraints for computer simulations of boulder movement down steep slopes and out across flatter slopes at their bases commonly subject to development.

3. Completed analysis of data on landslides from the May 2, 1983, Coalinga, California earthquake.

Results

1. The September 14, 1984, Nagano-ken-Seibu earthquake (M 6.8) triggered several hundred small rock falls and four destructive, high velocity landslides. These destructive landslides included three soil flows and one of the largest rock avalanches in history generated by an earthquake. The rock avalanche originated on the flank of an active volcano in andesitic volcanic deposits underlain by a weathered rhyolitic tuff that served as the intial sliding surface. The avalanche was 36×10^6 m^3 and travelled 13.1 km from its source on an average slope of 7^0 and at an average speed of 80 kph. Fifteen people perished in the avalanche. Upon failure, the avalanche rapidly disaggregated and flowed along a stream course overtopping several ridges of up to 100 m local relief.

The soil flows were all $1-5 \times 10^5$ m^3 and occurred in unconsolidated to weakly cemented colluvium and alluvium, weathered rhyolitic tuff, and ash. One of the flows was reported by an eyewitness to have travelled at 20 to 60 kph. Another destroyed 14 houses and accounted for 13 fatalities. Geologic conditions under which the rock avalanche and soil flows occurred are similar to conditions producing other such landslides in historic earthquakes.

2. Measurement of precise tracks and impact marks of boulders from seismic-induced rock-fall deposits have served as data to generate a computer program modeling the movement of rocks from cliffs down steep slopes and out onto relatively flat-lying areas

commonly occupied by dwellings. The program takes into account the type of surface the boulder collides with, the mass and shape of the boulder, its angular momentum as it collides with the slope, and its frictional rolling resistance when not bouncing. The goal of the study is to eventually produce a general method to predict the outrun of rocks dislodged by earthquakes and therefore the degree of hazard that exists on slopes below cliffs where rock falls are likely.

3. The distribution of all landslides produced by the May 2, 1983, Coalinga earthquake shows that rock falls and rock slides predominated. They extended up to 36 km from the epicenter and occurred mainly from weakly cemented upper Cretaceous and Tertiary age sandstone cliffs that form ridge crests in the Coalinga and Joaquin Ridge anticlines. The largest rock falls, however, formed from steep cliffs in serpentinous shale and mudstone of the Big Blue Formation just west of the Coalinga oil field. Other shales and fine-grained units produced rock falls and rock slides only where incision by ephemeral streams have cut steep cliffs. At such places, rock falls and rock slides are as numerous as those from sandstone cliffs. The distribution of all types of landslides from this earthquake shows that the maximum distances from the epicenter are lower than the average for other historic earthquakes of equal magnitude.

Reports

Harp, E.L., and Keefer, D.K., 1985 (in press), Landsliding (Section) in Predicted geologic effects of a postulated earthquake along the northern part of the Newport-Inglewood zone, Chapter, in Ziony, J.I., ed., Earthquake hazards in the Los Angeles region: U.S. Geological Survey Professional Paper.

Wilson, R.C., and Keefer, D.K., 1985 (in press), Predicting earthquake-induced landslides, in Ziony, J.I., ed., Earthquake hazards in the Los Angeles region: U.S. Geological Survey Professional Paper.

Harp, E.L., Wilson, R.C., Keefer, D.K., and Wieczorek, G.F., 1985 (in press), Current research on seismically induced landslides by the U.S. Geological Survey (abs.): submitted to International Association of Engineering Geology, symposium on Engineering Geology Problems In Seismic Areas, Bari, Italy.

Experimental Investigation of Liquefaction Potential

9910-01629

Thomas L. Holzer
Branch of Engineering Seismology and Geology
U.S. Geological Survey
345 Middlefield Road, MS 977
Menlo Park, California 94025
(415) 323-8111, ext. 2760

Investigations

1. Preliminary exploration to find a site at Parkfield, California, to install pore-water pressure transducers and borehole accelerometers for observation of pore pressures caused by strong ground motion.

2. Analysis of the lateral spread at the San Fernando Juvenile Hall caused by the February 1971 San Fernando earthquake.

3. Evaluation of the dependency of liquefaction during strong ground motion on earthquake magnitude and crustal stress state.

Results

1. The high probability of an earthquake greater than magnitude 5.5 in the Parkfield-Cholame area may provide an unusually good opportunity to record pore-water pressures in sediment undergoing liquefaction during an earthquake. Field reconnaissance was conducted to determine the possibility of finding an adequate thickness of liquefiable material near enough to the San Andreas that peak accelerations in a future earthquake would be high enough to liquefy the material. An area directly south of the Jack Ranch has such potential and will be explored in more detail.

2. The liquefaction susceptibility of deposits beneath a lateral spread caused by the February 1971 San Fernando earthquake was determined by the Seed-Idriss simplified procedure. Standard penetration tests and core sample analysis indicated a Holocene loose sandy silt that had been deposited in an alluvial-fan environment was susceptible to liquefaction and it had probably formed the base of the lateral spread.

3. The empirical correlation of peak accelerations during strong ground motion with liquefaction forms the basis for both site specific and regional evaluations of liquefaction susceptibility. The observed dependency of peak accelerations on crustal stress state as well as magnitude suggests that the state-of-the-art for liquefaction prediction could be improved by distinguishing between earthquakes of the same magnitude but in regions with different crustal stress states. Field observations are being compiled to determine if this effect is apparent in these records.

Strong Ground Motion Studies
Application to Puget Sound

Contract No. 14-08-0001-21306

Steven M. Ihnen and David M. Hadley
Sierra Geophysics, Inc.
15446 Bell-Red Road
Redmond, WA 98052
(206) 881-8833

Investigations

Seismic intensity patterns during earthquakes in the Puget Sound region show large spatial variations which cannot be attributed to surface geology. The purpose of this project is to use seismic raytracing techniques on a three-dimensional model of the subsurface structure to determine if this spatial variation can be predicted and, if so, to incorporate that knowledge into seismic risk maps of the area.

Results

A raytracing simulation of the 1965 Seattle earthquake (M=6.5) was performed. Synthetic accelerograms were computed at 1600 locations on the surface of a 3-D velocity model which incorporated extensive geological, geophysical, and geotechnical information. The simulation correctly predicted the ratio of peak ground accelerations at the Seattle and Tacoma strong-motion stations and accurately modeled the observed variations in seismic intensity. Results indicate that focusing of rays within sedimentary basins can substantially increase the PGA at a site compared to the same site with a flat velocity structure. These results are described in detail in Ihnen and Hadley (1985).

We are preparing to incorporate these results into a series of seismic risk maps for the Puget Sound region. In order that these maps be most useful to the engineering community, we will map that acceleration for which there is a 90% probability that it will not be exceeded in 100 years. A second map will express the same quantity for a 1000 year time period. Peak velocity maps may be constructed in the same way.

The unique character of Puget Sound seismicity complicates the assessment of seismic risk for this area. Most computer programs for risk assessment break down the seismicity into a number of discrete sources. However, Puget Sound seismicity consists of a very diffuse shallow seismic zone which cannot be associated with known faults and an important, but ill-defined deeper seismic zone associated with the subducted Juan de Fuca plate. Several authors, including Heaton and Kanamori (1984) have suggested that this plate interface may be capable of generating a great (M>8) earthquake. The most appropriate way to include this possibility in the risk calculations is being studied.

References

Heaton, T.H. and H. Kanamori, 1984, Seismic potential associated with the subduction in the northwestern United States, J. Geophys. Res., 74, pp. 933-941.

Ihnen, S.M. and D.M. Hadley, 1985, Prediction of strong ground motion in the Puget Sound region: the 1965 Seattle earthquake, to be published in Bull. Seism. Soc. Amer.

Socorro Magma Bodies

9920-03379

Lawrence H. Jaksha
U.S. Geological Survey
Geoscience Dept.
New Mexico Tech.
Socorro, New Mexico   87801
(505) 835-5501

Investigations

1. Albuquerque basin seismicity.

2. Crustal structure

3. Magma

4. NM Seismicity

5. Instrumentation

Results

1. A paper summarizing the results of the Albuquerque basin study has been submitted to the JGR. An open-file report covering the data used in the study is in preparation.

2. Two field trips were made to the Jemez lineament on the NM-AZ border. A preliminary analysis of data recorded suggests a Pn volocity of about 7.94 km/s for the study area.

3. Grant Goodyear is studying the relationship between P-wave rise-time and crustal Q using local microearthquakes as energy sources. Q_p for the weathered section beneath each station in the USGS-NMT seismic network is being estimated along with an average Qp for the basement rocks.

4. Scott Phelps has completed an open-file report covering New Mexico seismicity for 1982. The study was limited to earthquakes with magnitude $\geq$ 1.5. The data set consisted of 83 shocks, the largest (M=2.9) being felt at Socorro on September 20.

5. Frequency response curves and magnification were determined for 6 of the stations in the Array. Work continues on obtaining this information for the remainder. A substantial amount of time has been spent working on long-period amplifiers this report period.

Reports

Wong, I. G., Cash, D. J., and Jaksha, L. H., 1984, The Crownpoint, New Mexico earthquakes of 1976 and 1977: Bulletin of the Seismological Society of America, v. 74, no. 6, p. 2435-2449.

Phelps, S., Sanford, A., Ake, J., and Jaksha, L., 1985, Earthquakes in New Mexico, 1982: Geophysics Open-File Report 51, New Mexico Institute of Mining and Technology, 11 p.

Jaksha, L. H., 1985, Earthquakes near Albuquerque new Mexico, 1976-1981: Journal of Geophysical Research (submitted).

Jaksha, L. H., 1985, Pn velocity beneath western New Mexico and eastern Arizona: Lunar and Planetary Institute, Houston (submitted).

Urban Hazards Seismic Field Investigations

9950-01919

Kenneth W. King
Branch of Engineering Geology and Tectonics
U.S. Geological Survey
Box 25046, MS 966, Denver Federal Center
Denver, CO   80225
(303) 236-1591; 776-1591 (FTS)

Investigations

The basic objective of this project is to improve the fundamental knowledge on how the ground response is affected by local geology. The investigations are presently concentrating in the LA/Wasatch areas.

An investigation of the feasibility of using a high resolution reflection method to identify soil parameters and shallow displacements (faults?) is now in progress. Part of the reflection investigations are in cooperation with the Kansas Geological Survey.

Shallow reflection profiles have been made at all the Salt Lake City urban hazards strong-motion sites. The data will be processed in the near future. Shallow reflection profiles were made at a high, medium and low response site in the Los Angeles area. The data were recorded on rock, thin, medium and thick sections of unconsolidated alluviums. Shallow reflection profiles have been made at similar sites in the Springfield-Provo, Utah area. The data are being processed at this time.

A Wasatch strong-motion instrumentation program is now in progress in cooperation with the Utah Geological and Mineral Survey.

A seismic field investigation at the Hovenweep National Park is near completion. The program investigated the seismic effects on archeological sites caused by nearby industrial activities.

Results

1. Several field methods are being evolved from the on-going field efforts in high-resolution shallow reflection methods. The best energy sources found to date are a 12 gauge slug or a 50 cal slug impact for compression waves and a hydraulic plate system for shear waves. Frequencies from 150 to 250 Hz have been found to be the most useful to map beds in the 20 to 50 foot depth range.

2. Tailoring the in-put software to the Disco programs to process the shallow reflection data is in progress. The normal data entry methods had to be modified to achieve the desired resolution for the shallow targets.

3. Preliminary reflection data from the Denver Federal Center indicate a feasibility of mapping beds in unconsolidated sediments with a shallow water table in the 20 to 100 foot depth ranges. A report is in progress.

469

4. A seven instrument seismoscope array has been installed in the Salt Lake City area to supplement the existing SMA-1 array.

5. Reports on the national park seismic investigations are in progress.

References

Hays, W. W., and King, K. W., 1985, Evaluation of the ground shaking hazard in Utah urban areas [abs.]: Seismological Society of America, Eastern Section, Austin, Texas.

Determining Landslide Ages and Recurrence Intervals

9950-03789

Richard F. Madole
Branch of Engineering Geology and Tectonics
U.S. Geological Survey
Box 25046, DFC, M.S. 966
Denver, Colorado 80225
(303) 236-1617

Investigations

Fossil mollusks and related sediments were studied as part of a test of the applicability of amino-acid racemization (slow, spontaneous structural rearrangement of L- and D-amino acids in fossil material) to dating earthquake-induced landslides and to determining landslide recurrence intervals. Fossil mollusks, chiefly snails, are common in landslide deposits on the west flank of the Wasatch Plateau, much more so than other materials suitable for radiocarbon dating. Hence, if fossil mollusks can be used for amino-acid dating, it should be possible to determine the ages of a large percentage of the older landslide deposits in central Utah.

Results

Amino-acid dating does not require large sample sizes, generally a few shells will suffice. However, the method does require knowing the genus and species of the specimen dated and a capacity for reconstructing or estimating the temperature history of that specimen. Consequently, the widespread occurrence of taxa that can be identified to species level by shell morphology alone, rather than by soft-part anatomy, is desirable. It is also desirable that these taxa be found in stratigraphic sections that can be related to a regional Quaternary history, and that at least a few stratigraphic sections contain material capable of providing age determinations by an independent dating technique. The fossil mollusks in the landslide deposits on the west flank of the Wasatch Plateau meet these requirements exceptionally well.

Four fossil fauna of different ages were collected from deposits on the Manti landslide in Manti Canyon and one recent fauna was collected from a pond on the Twin Lake landslide in the canyon of Twelvemile Creek. Stagnicola elodes, a relatively large, high-spired aquatic snail dominates the fossil assemblages, composing 75-100 percent of the fauna in most of the units sampled (Table 1). Approximately 14 kg of sediment, collected from three sample sites, yielded 1,701 specimens of this snail. Stagnicola elodes is large enough, as much as 2-3 cm tall by 1-1.5 cm wide, that a single specimen would be sufficient for an amino-acid age determination. Moreover, this species can be identified by shell morphology alone and occupies a broad range of life zones from the foothills to the subalpine.

The temperature history of samples of <u>Stagnicola elodes</u> can be estimated from modern weather data and from correlation with the Quaternary paleoclimatic record. Three of the four sample sites in Manti Canyon contain a sufficient amount of organic matter to obtain ^{14}C ages. These ages will allow correlation of the stratigraphic sections at the sample sites with the Quaternary paleoclimatic record; they will also permit a calibration of amino-acid ratios (ages) in terms of radiocarbon years. Two assumptions are made in estimating temperature history: (1) localities with the same altitude and aspect are assumed to have had similar temperature histories and (2) temperature differences between localities at different altitudes are assumed to have been about the same in the past as they are at the present.

The widespread distribution and abundance of <u>Stagnicola elodes</u> in the translocated-pond deposits on the Manti landslide provide an opportunity to calculate landslide recurrence intervals by means of amino-acid dating. Translocated pond deposits have been moved laterally downslope by flow or slide from the sites where they accumulated, and they are now high, dry, and exposed for study. On slides like the Manti landslide, there has been a tendency for pond-forming depressions to remain in relatively the same position, even though the material beneath them, including pond sediment, has periodically moved downslope. Thus, repetitive slope failure gives rise to a series of spatially separate pond deposits that have the potential for recording the number of mass movement events, as well as providing dates for the events.

The age limits of amino-acid dating vary with temperature and/or latitude; racemization is faster where temperatures are higher. Amino-acid racemization is complete (stops) when the two forms, L- and D-amino acids, exist in equal amounts. The method is applicable to fossil material of Pleistocene age and has been applied successfully to shell material as old as the Lava Creek volcanic ash (620,000 ka). Whether or not the method will be useful on materials collected from landslide deposits in central Utah that are as young as Holocene remains to be seen. The amino-acid age determinations have not been completed yet. They are being done at the Amino-Acid Dating Laboratory, Institute of Arctic and Alpine Research, University of Colorado.

Reports

As yet, no reports on this work have been submitted for publication.

Table 1.--Fossil gastropods from four sites on landslide deposits in Manti Canyon, Sanpete County, Utah

Sample site	Taxon[1]	Habitat	Number	Fauna (percentage)
Upper Manti landslide				
Unit 6	Stagnicola elodes (Say)	Freshwater	4	100.0
Unit 4	Stagnicola elodes (Say)	Freshwater	468	89.3
	Gyraulus (Armiger) crista (Linnaeus)	--do-------	51	9.7
	Vallonia cyclophorella Sterki	Terrestrial	3	0.6
	Vertigo ventricosa (Morse)	--do-------	1	0.2
	Zonitoides arboreus (Say)	--do-------	1	0.2
Unit 4, lower 4 cm	Stagnicola elodes (Say)	Freshwater	55	98.2
	Gyraulus (Armiger) crista (Linnaeus)	--do-------	1	1.8
Unit 4, basal contact	Stagnicola elodes (Say)	Freshwater	56	93.3
	Vallonia sp.	Terrestrial	1	1.7
	Pupilla sp.	--do-------	1	1.7
	Vertigo ventricosa (Morse)	--do-------	1	1.7
	Euconulus fulvus (Muller)	--do-------	1	1.7
Middle Manti landslide	Stagnicola elodes (Say)	Freshwater	447	74.5
	Gyraulus (Armiger) crista (Linnaeus)	--do-------	97	16.2
	Gyraulus (Torquis) parvus (Say)	--do-------	50	8.3
	Oreohelix sp.	Terrestrial	4	0.7
	Vallonia gracilicosta Reinhardt	--do-------	2	0.3

Table 1.--Fossil gastropods from four sites on landslide deposits in Manti Canyon, Sanpete County, Utah--(Continued)

Sample site	Taxon[1]	Habitat	Number	Fauna (percentage)
Lower Manti landslide				
Unit 5	Stagnicola elodes (Say)	Freshwater	671	91.8
	Gyraulus (Armiger) crista (Linnaeus)	--do------	55	7.5
	Gyraulus (Torquis) sp.	--do------	1	0.1
	Vallonia gracilicosta Reinhardt	Terrestrial	4	0.5
Unit 2	Oreohelix sp.	Terrestrial	12	37.5
	Vallonia albula Sterki	--do------	15	46.9
	Zonitoides arboreus (Say)	--do------	4	12.5
	Microphysula ingersollii (Bland)	--do------	1	3.1
Landslide-dammed lake, Cottonwood Creek	Oreohelix sp.	Terrestrial	2	5.0
	Pupillidae	--do------	1	2.0
	Catinella sp.	--do------	38	93.0

[1]A few hundred specimens of fingernail clams Pisidium casertanum, P. milium, P. nitidum, and Musculium lacustre were collected at the three sites on the Manti landslide.

Analysis of Earthquake Ground-Shaking Hazard
For the Salt Lake City-Ogden-Provo Region

21914

M.S. Power [*], R.R. Youngs [*], D.P. Schwartz
F.H. Swan III [*], R.K. Green
Woodward-Clyde Consultants
100 Pringle Ave
Walnut Creek, CA 94596
(405) 945-3000

Objectives: We are completing an assessment of ground motion hazard for the Ogden-Salt Lake City-Provo urban corridor using a probabilistic approach, often termed a probabilistic seismic hazard analysis. The seismic hazard is expressed as levels of a ground motion parameter, such as peak acceleration, having certain probabilities of being exceeded during a specified time period. The results of this study will be shown on regional maps as contours of peak ground acceleration for selected probabilities of exceedance. Also, acceleration response spectra corresponding to selected probabilities of exceedance will be presented for representative locations in the study region for use in further establishing the damage potential of ground motions to buildings.

The basic approach for probabilistic seismic hazard analyses incorporates the inherent uncertainties in the location, time of occurence and size of future earthquakes and the uncertainties in the resulting ground motions at a site in the evaluation of the probability of exceeding a specified ground motion level in a specified time period. Specifically, these factors are incorporated in three probability functions:

1. A probability distribution for the distance from a site to the earthquake rupture surface is developed from the geometry of the identified seismic sources and a relationship between earthquake magnitude and rupture size.

2. A probability distribution for the rate of occurrence of earthquakes of various sizes (magnitudes) is developed from a recurrence relationship for each seismic source.

3. A probability distribution for the resulting ground motion levels at a site a specified distance from a specified size earthquake is developed from appropriate attenuation relationships.

---

[*] present adress Geomatrix Consultants, One Market Plaza
San Francisco, CA 94105 (415) 957-9557

In a basic seismic exposure analysis, it is assumed that the source characterization parameters required to develop the above probability distributions (fault length , dip and width, maximum earthquake magnitude, and earthquake recurrence rate) are known with certainty. In fact, there usually is uncertainty in these parameters arrising from less than complete knowledge of the seismogenic processes at work. These uncertainties can significanty affect the estimated seismic hazard levels. In the present study, the uncertainties in characterizing the potential sources of future seismicity are explicity incorporated in the analysis in order to express the uncertainty in the estimated seismic hazard levels in the study region.

Results: Two types of seismic sources have been characterized for use in the seismic hazard analyses: known faults and distributed areal sources of seismicity. Geologic studies by numerious investigators have identified a number of active or potentially active faults in the region. The locations of faults significant to the study are shown in Figure 1. These faults are believed to be capable of generating moderate to large magnitude earthquakes, and the Wasatch fault and East Cache fault have evidence of Holocene surface rupture. The maximum earthquake magnitudes and recurrence rates for large magnitude events on these faults are being characterized based on geologic and paleoseismic data as summarized in Table 1.

Evaluations of the historical and instrumental seismicity catalog for Utah (for the years 1850 to 1984) have been used to characterize the recurrence rates for smaller magnitude earthquakes. These evaluations, together with the results of other published studies indicate that much of the smaller magnitude seismicity cannot be directly associated with mapped faults. Consequently distributed area sources of small to moderate magnitude earthquakes are being included in the model of the regional seismicity.

At the present time, there is uncertainty as to the appropriate attenuation characteristics for the study region. Examination of the various published studies indicates there are arguments for both a somewhat higher rate of attenuation and a somewhat lower rate of attenuation than that observed in California. There are very few strong ground motion recordings of earthquakes in the study region to use in evaluating attenuation relationships. Therefore, the approach taken in this study is to use several attenuation relationships and test the sensitivity of the computed hazard levels to these relationships. Preliminary results indicate that the computed hazard levels are not overly sensitive to variations in the rate of attenuation within a reasonable range.

Reports: Power, M.S. ,Schwartz, D.P., Youngs, R.R, and Swan, F.H. III, Analysis of earthquake ground-shaking hazard for the Salt Lake-Ogden-Provo region: Paper presented at the Workshop on Evaluation of Regional and Urban Earthquake Hazards and Risk in Utah, Salt Lake City, August 14-16, 1984.

TABLE 1

FAULT BEHAVIOR DATA
WASATCH FAULT ZONE

Segment	Site	Slip Rate (mm a^{-1})[a]	Displacement per Event (m)		Recurrence		Elapsed Time (yr)[c]	Reference
			Measured	Average[b]	Interval	Average (yr)		
Collinston	-	≥ 0 (13,500)	-	-	-	-	≥ 13,500	Schwartz and others (1983)
Ogden	Kaysville	1.3 (+0.5, -0.2)[e] (8,000; +1000, -2000)	1.6 1.7	- -	2 (after 1580)[d]	2000	≤ 500	Swan and others (1980)
Salt Lake City	Little Cottonwood Canyon	0.76 (+0.6, -0.2) (19,000 ± 2000)	-	2 (2)	-	2400-3000	-	Swan and others (1981); Schwartz and Coppersmith (1984)
Provo	Hobble Creek	0.85 - 1.0[e] (13,500)	2.7	1.6-2.3 (6-7)	6-7 (after 13,500)	1700-2600	> 1000	Swan and others (1980)
Nephi	North Creek	1.27-1.36 (± 0.1) (4580)[d]	2.0-2.2 2.0-2.5 2.6	2.3 (3) -	2 (between 4580 and 3640)[d] 1 (after 1100)[d]	1700-2700	300-500	Schwartz and Coppersmith (1984)
Levan	Deep Creek	≤ 0.35 ± 0.05 (7300)[d]	2.5	-	1 (after 7300)[d]	-	<1750[d]	Schwartz and Coppersmith (1984)
East Cache	Logan	0.1-0.2 (14,000-15,000)	1.35 1.4	- -	1 (between 15,000 and 13,500) 1 (after 13,500)	-	6000-10,000	Swan and others (1982)

a Age of displaced datum (years B.P.) on which slip rate is based is shown in parentheses.
b Number of events on which average is based is shown in parentheses.
c Time in years since the most recent surface faulting earthquake.
d Age in ^{14}C yr B.P.
e Modified from Swan et al. (1980).

113° IDAHO 112°

Collinston

WYOMING

1 Logan 7

Brigham City

Ogden 2

11 41°

Salt Lake City

10 3

Tooele

9 Provo

4

8

40°

5

Nephi

Levan

6

1. Collinston
2. Ogden
3. Salt Lake City
4. Provo
5. Nephi
6. Levan
7. East Cache
8. Strawberry Valley
9. Oquirrh-Boulter-Tintic
10. Oquirrh Marginal
11. Great Salt Lake

0   25   50
kilometers
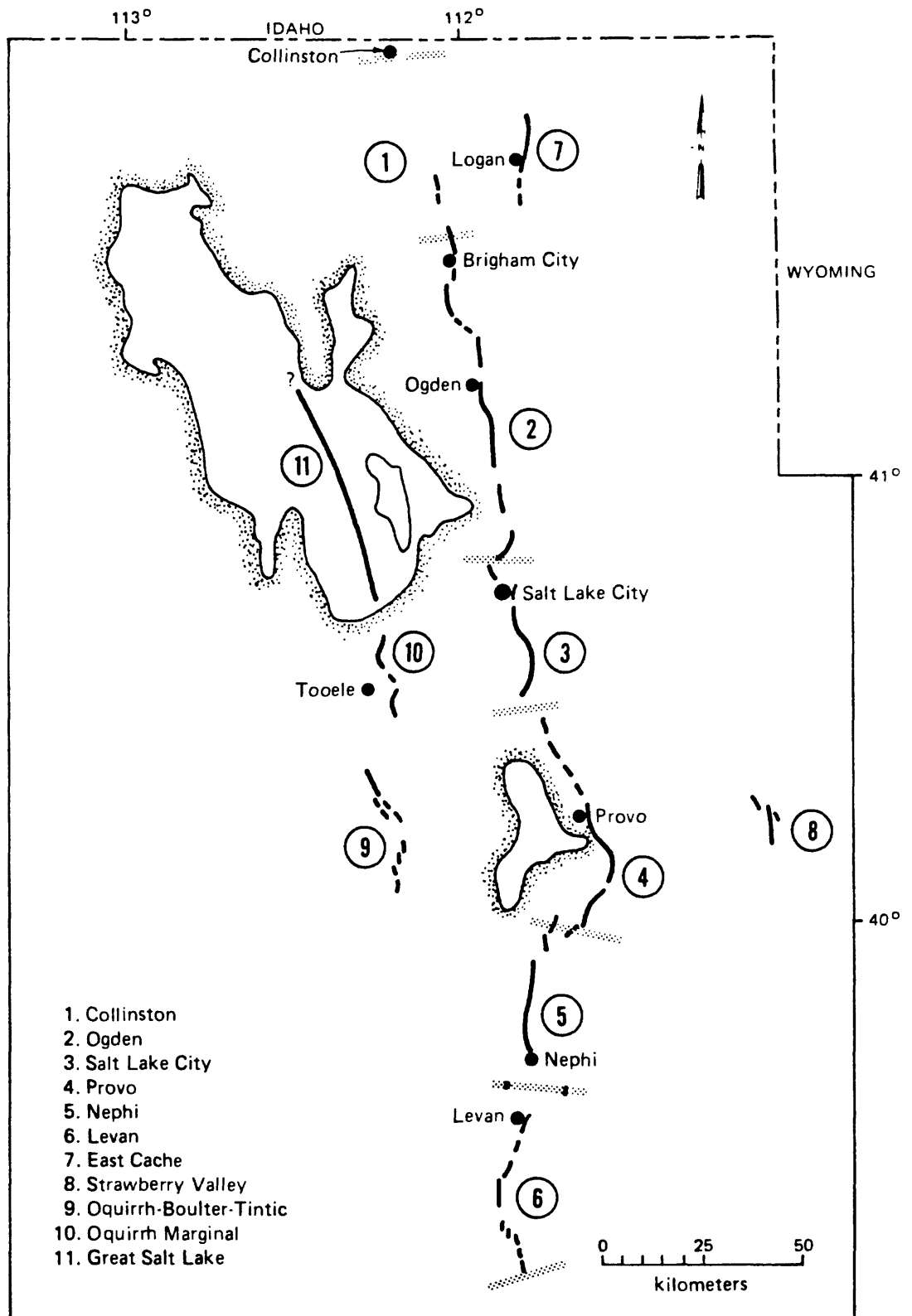
Figure 1. Map of Proposed Sources (faults and fault segments) for
Seismic Exposure Analysis of Ogden-Salt Lake-Provo Corridor.
Wasatch Fault Zone Segments Are from Schwartz and
Coppersmith (1984)

Source and Path Effects for Northeastern US Earthquakes -
Implications for Earthquake Hazards

Contract No. 14-08-0001-21284

M. Nafi Toksöz and Jay J. Pulli
Earth Resources Laboratory, M.I.T.
42 Carleton St., Cambridge, MA 02142
(617) 253-7852

Investigations:

1) Study the spectral source parameters of microearthquakes in the northeastern U.S. and combine these results with our studies of moderate events to develop spectral scaling relations.

2) Use synthetic seismograms to estimate ground displacements, velocities, and accelerations for northeastern U.S. earthquakes.

Results:

1) Our earlier studies of the 1982 New Brunswick and 1983 Goodnow, NY earthquakes have shown that these events were of relatively high stress drop for their seismic moments. We are now extending our studies to smaller events to determine if the spectral scaling relationship in the northeastern U.S. changes with seismic moment. To accomplish this task, we are examining the displacement spectra of local earthquakes recorded digitally on the M.I.T. Seismic Network. The first step is to confirm the instrument responses, especially at high frequencies. Step function calibration signals are input to the seismometers on a daily basis. Generally, five response pulses are stacked after high pass filtering to improve the signal to noise ratio. The stacked pulses are then Fourier transformed and multiplied by ω^3 to obtain the displacement response. Fourier transformed seismograms are then corrected for this instrument response, and additional corrections are made for geometrical spreading and attenuation. Figure 1 shows some sample spectra. We are now experimenting with the effects of window length and smoothing on the spectra. Any conclusions or generalizations about the spectra must await the analysis of many events.

2) We have begun to use synthetic seismograms to study source and path effects of northeastern U.S. earthquakes. A sample calculation is shown in Figure 2. These synthetics were calculated using the discrete wavenumber method of Bouchon and Aki (1977). (Instrument responses are not included in the displays.) For the New England case, a three layer crustal model with a total crustal depth of 40 km was used. The source depth was 7 km. The calculation is for a thrust fault dipping at 55° with an irregular source time function of 0.6 sec duration. The

azimuth of observation is 20° from the fault plane strike. For the California case, a four layer crustal model of total depth 33 km was used. The source is a strike slip event at 4 km depth and 4.0 sec duration. The differences in the results are readily apparent. The New England seismograms are of short duration and high frequency, whereas the California seismograms have low frequency surface wave trains due to the slow top crustal layer and longer source duration. By calculating synthetics at varying distances, we can develop ground motion attenuation models for displacement, velocity, and acceleration.

Reference

Bouchon, M. and Aki, K. (1977), Discrete wavenumber representation of seismic source wavefields, *Bull. Seis. Soc. Amer.*, *67*, 259-277.

Figure 1

480

New England Seismograms

Vertical displacement   Vertical velocity   Vertical acceleration

California Seismograms

Vertical displacement   Vertical velocity   Vertical acceleration
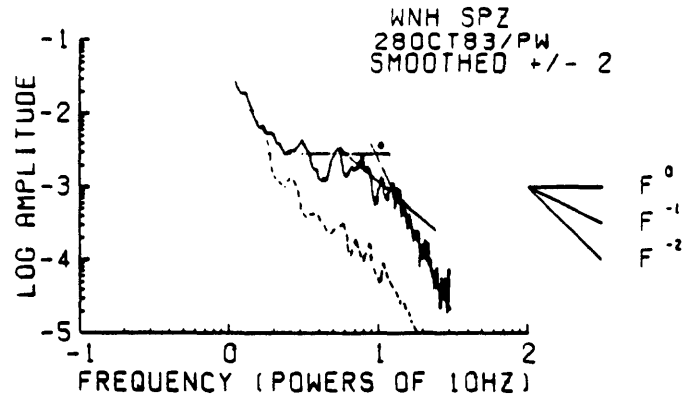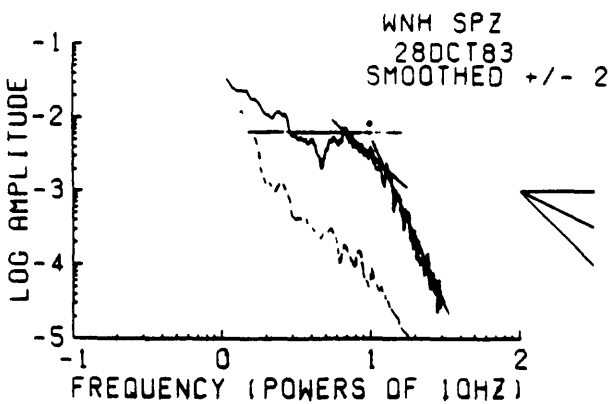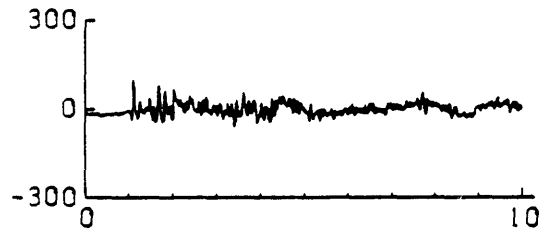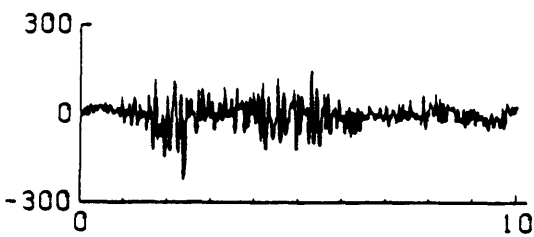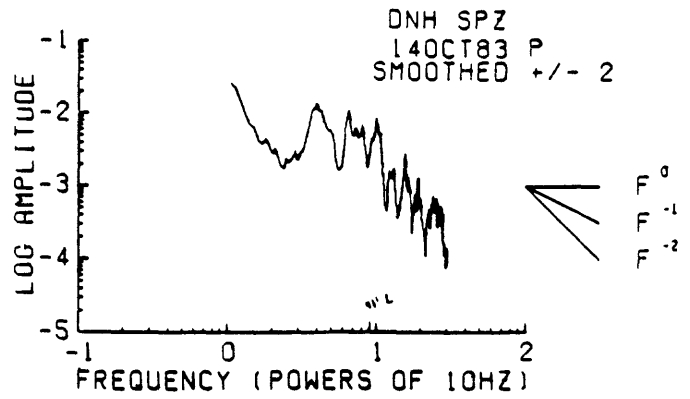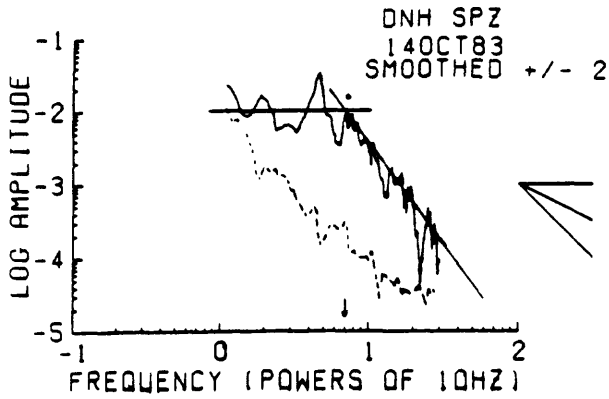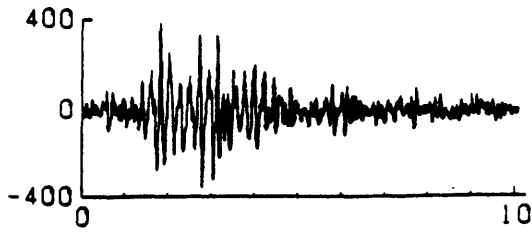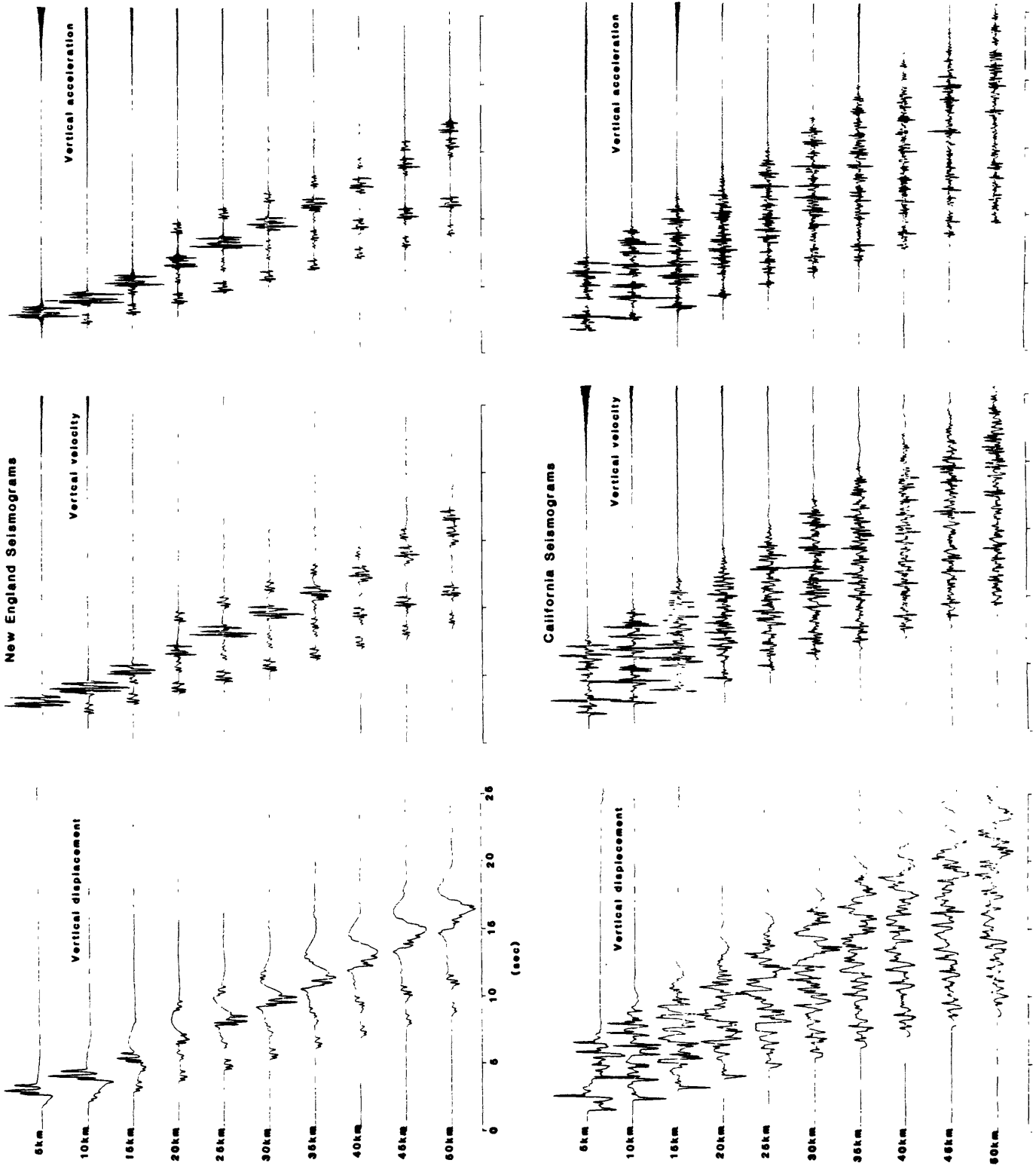
Figure 2

Tectonic Analysis of Active Faults

9900-01270

Robert E. Wallace
Office of Earthquakes, Volcanoes and Engineering
345 Middlefield Road, MS 977
Menlo Park, California 94025
(415) 323-8111, ext. 2751

Investigations

1. Evaluation of fault scarps and tectonics of the central Nevada and eastern California seismic belts.

2. Active Tectonics--Impact on Society. A project under the auspices of the Geophysics Study Group, National Research Council, National Academy of Sciences. Serve as chairman of study group.

3. International Geological Correlation Program - Active Faults of the World.

4. Investigations of active faults in Ningxia and Gansu Province, PRC. Cooperative program in earthquake studies: U.S. Geological Survey/State Seismological Bureau, People's Republic of China.

Results

1. Completed manuscripts for two entries in the Geological Society of America Field Guide Project; one for the site on the 1915 Pleasant Valley, Nevada fault scarp, the second as co-author with Kerry Sieh on a site along the San Andreas fault in the Carrizo Plain, California.

2. The NRC volume on Active Tectonics--Impact on Society is near completion with sixteen chapters finished including one by me on Overview and Recommendations.

3. First drafts of the following manuscripts were completed and sent to Chinese co-authors for review. The preliminary titles and abstracts of the papers are as follows:

Zhang Buchun, Lia Yuhua, Guo Shunmin, Robert E. Wallace, Robert C. Bucknam and Thomas C. Hanks, 1985, Fault scarps related to the 1739 earthquake and seismicity of the Yinchuan Graben, Ningxia, Huizu Zizhiqu, China

ABSTRACT: Surface faulting accompanying the great earthquake of 1739 in Ningxia Huizu Zizhiqu produced two sections of fault scarps 3.5 and 11 km long and separated by 65 km along strike. The scarps are on the west side of the Yinchuan graben within a few kilometers of or at the base of the Helan Shan. The east side of the faults is downthrown and vertical displacements are as much as 4.3 m on the Honggonzigou section, and nearly 8 m on the Suyukou section. Near the north end the Great Wall is offset by about 2.6 m vertically and about 3 m right laterally. A free face several meters high has persisted for the 245 years since the scarps were formed in 1739.

The 1739 fault displacement occurred along an older fault scarp that is estimated from profile analysis to be about 12,000 years old.

The historical record of destructive earthquakes in the Yinchuan graben since 1010 AD includes only one near M 8 in 1739, and only two of approximately M 6.5, one in 1143 and the other in 1774.

Zhang, Buchun, Li Yulong, Guo Shunmin, Robert E. Wallace, Robert C. Bucknam and Thomas C. Hanks, 1985, Ancient canals in Gaotai County, Gansu Province, China

ABSTRACT: A set of ancient canals in Gaotai County, Gansu province head at the Dasha River, trend N°60-65°W for about 65 km, and have their lower, northwest ends near the walled City of Camels and Xusanway Village. The average gradient of the canals is between 1.2-1.4 m/km. From one to four closely spaced parallel canals make up the set, and the canals are from 20-50 m wide and from 3-5 m deep. Berms of spoil are on the uphill side of each.

The age of the canals is not known, but some may be as old as Han dynasty.

The canals are believed to have been built primarily for the transport of water, but may also have served as a defensive military barrier.

Reports

Wallace, R. E., 1985, Variations in slip rates, migration and grouping of slip events on faults in the Great Basin Province: Proceedings of conference on the Borah Peak, Idaho 1983 earthquake, Stein, R., and Bucknam, R. [eds.], U.S. Geological Survey Open File Report 85-290.

Wallace, R. E., 1985, Fault scarps formed during the earthquakes of October 2, 1915, Pleasant Valley, Nevada: Geological Society of America Field Guide (in press).

Bull, William and Wallace, R. E., 1985, Penrose Conference on Tectonic Geomorphology: Geology, v. 13, n 3, p. 216.

Hanks, T. C. and Wallace, R. E., 1985, Morphological analysis of the Lake Lahontan shoreline and Beachfront fault scarps, Pershing County, Nevada: Bulletin of the Seismological Society of America (in press).

Regional Syntheses of Earthquake Hazards in Southern California

9910-03012

Joseph I. Ziony
Branch of Engineering Seismology and Geology
U.S. Geological Survey
345 Middlefield Road, MS 977
Menlo Park, CA 94025
(415) 323-8111, ext. 2944

Investigations

For the reporting period, our efforts primarily were devoted to final revisions of the USGS Professional Paper 1360 manuscript and to corrections of the galley proofs. We thus temporarily deferred our field studies on determining late Quaternary slip rates and styles along the northern Elsinore fault zone. However, USGS-supported Quaternary geologic mapping and analysis of soil-profile development was continued by Douglas Millman (San Diego State University) in Temescal Valley, and by Patrick Vaughan (University of Colorado) in Pala Valley. We also began planning for a workshop on earthquake-hazards evaluation for scientists, engineers, and planners in southern California.

Results

1. Galley proofs of Professional Paper 1360, Evaluating Earthquake Hazards in the Los Angeles region, were corrected and returned to the Office of Scientific Publications. Printing of this 16-chapter, 400+ page volume is anticipated for July or August 1985.

2. From the surficial geologic character of the numerous late Quaternary faults of the Los Angeles region, we identified 87 distinctive fault segments that we consider capable of producing "characteristic" earthquakes. Rupture lengths of these segments were digitized and provided to J.F. Evernden as the basis for 87 postulated earthquakes using his intensity-prediction method. The resulting 1:250,000-scale maps (parts of the Los Angeles, Long Beach, San Bernardino, and Santa Ana 1° x 2° sheets) depict the cumulative maximum predicted intensities for the region and thus highlight those areas having the greatest long-term potential for damaging seismic intensities.

3. A workshop on Future Directions in Evaluating Earthquake Hazards of Southern California has been organized by J.I. Ziony and W.J. Kockelman for November 12-13, 1985 at U.S.C. in Los Angeles. Cosponsors will include NSF, FEMA, and five State agencies. The workshop will summarize recent results of earth-science research on hazards-prediction methods, will present examples of applying them for hazard reduction, and will identify the needs for additional scientific and technical information.

Reports

Ziony, J.I., and Tinsley, J.C., 1984, Mapping the earthquake hazards of the Los Angeles region, in Petak, W.J., and Mittler, E., eds., Earthquake forecasting, preparedness, and response: Proceedings of First International Earthquake Conference, Los Angeles, California, February 1983, p. 108-115.

Harms, K.K., Clark, M.M., Rymer, M.J., Bonilla, M.G., Harp, E.L., Herd, D.G., Lajoie, K.R., Lienkaemper, J.J., Mathieson, S.A., Perkins, J.A., Wallace, R.E., and Ziony, J.I., 1984, The April 24, 1984 Morgan Hill, California earthquake: The search for surface faulting, in Bennett, J.H., and Sherburne, R.W., eds., The 1984 Morgan Hill, California earthquake: California Division of Mines and Geology Special Publication 68, p. 149-160.

Thenhaus, P.C., Ziony, J.I., Diment, W.H., Hopper, M.G., Perkins, D.M., Hanson, S.L., and Algermissen, S.T., 1985, Probabilistic estimates of maximum seismic horizontal ground acceleration on rock in Alaska and the adjacent continental shelf: Earthquake Spectra, v. 1, no. 2, p. 285-306.

Millman, D.E., and Rockwell, T.K., 1985, Lateral offset of mid and late Quaternary deposits along the northern Elsinore fault, southern California (abs.): Geological Society of America Abstracts with Programs 1985, Cordilleran Section, v. 17, no. 6, p. 370.

Geophysical and Tectonic Investigations
of the Intermountain Seismic Belt

9930-02669

Mary Lou Zoback
U.S. Geological Survey
Branch of Seismology
345 Middlefield Road, Mail Stop 977
Menlo Park, California 94025
(415) 323-8111, Ext 2367

Investigations:

1) Compilation of available Utah gravity data. The data were obtained from a variety of sources and were merged and reduced to a common datum (that used for the DOD gravity data set). Data sources include: DOD gravity file, Utah Geologic and Mineral Survey (UGMS) contract data obtained from geothermal areas, UGMS file data, several University of Utah master theses, and data collected by the author.

2) Analysis of wellbore elongations ("breakouts") from three exploration fields on the continental shelf of the eastern United States these data are used to infer principal horizontal stress orientations.

3) Compilation of stress data for the entire Circum-Pacific area.

Results:

1) The gravity data for the entire state of Utah were successfully merged to a single large gravity file and were then terrain corrected from 0 to 167 km using the digital terrain data set. Inner zone terrain corrections were done with the 30 sec digitization data because the 15 sec data set is not complete for the entire state. Several preliminary gravity maps have been prepared: a complete Bouguer map of the entire state at 1:1,000,000 (previous maps have all been simple Bouguer) and three complete Bouguer maps at 1:100,000 designed to overlay the new Wasatch Front geological maps being published by UGMS.

2) Breakout data were obtained from three areas on the continental shelf: Baltimore Canyon, southeast Georgia embayment, and Georges Bank. To date we have analyzed data from both industry and government (COST) wells. Results are as follows:

   a) Georges Bank - 6 wells with total depths ranging from 9,655 to 21,711 feet. All wells gave consistent orientations and suggest approximately E-W compression.

   b) Baltimore Canyon - 13 wells, most between 13,000 and 17,000 feet deep. Nine of the 13 wells yielded well-defined, consistent breakouts and suggested a compressive stress orientation between N55° E and N 70° E.

c) SE Georgia embayment - 4 wells, 3 are between 6,000 and 7,000 feet deep, one is 12,800 feet deep. Good data was obtained from only one of the shallower wells and suggests a maximum horizontal compression about N 40° E.

These data together with new data collected by workers in other areas suggest that the state of stress along the Atlantic seaboard is characterized by NE- to ENE-compression, (possibly closer to E-W compression in the New England area), not NW-compression as previously proposed. This NE- to ENE-compressive stress orientation is the same as that in the mid-Continent region, suggesting that much of the mid-plate region of the North American plate is characterized by a relatively uniform stress field.

3) A map of lithospheric stress for the entire Circum-Pacific region was prepared as part of the Circum-Pacific Geodynamic map series.

4) Megan Lacey Zoback, Jan. 20, 1985, 9 lbs. 3 oz., 22 1/2 in.

Reports:

Dart, R., 1985, Horizontal stress directions in the Denver and Illinois Basins from the orientations of borehole breakouts: U.S. Geological Survey Open-File Report, 85- , 37 p.

Zoback, M. L., 1985, Lithospheric stress: American Association of Petroleum Geologists, Geodynamic Map, Circum-Pacific Map Series, Pacific Basin sheet, 1:17,000,000.

Estimating Strong Ground Motion for Engineering
Design and Seismic Zonation

9910-01168

W. B. Joyner
D. M. Boore

Branch of Engineering Seismology and Geology
U. S. Geological Survey
345 Middlefield Road, MS 977
Menlo Park, California 94025
(415) 323-8111, Ext. 2754, 2698

Investigations

1. Analysis of strong-motion data leading to the development of predictive
    equations for strong-motion parameters and development of methodology for
    making predictive maps of strong ground motion.

2. Cooperation with professional groups in the development of code provisions
    for earthquake resistance.

3. Study of the scaling of earthquake spectra.

4. Measurement of shear-wave velocity at seismic recording sites in the
    Coalinga earthquake sequence to assist in the determination of seismic
    source parameters.

Results

Using spectral scaling laws we have derived constraints applicable to the
currently popular method for simulating ground motion from large earth-
quakes by the Green's function addition of smaller earthquakes.

Reports

Joyner, W. B. and Boore, D. M., 1985, On simulating large earthquakes by
Green's function addition of smaller earthquakes, Proceedings, 5th
Maurice Ewing Symposium on Earthquake Source Mechanics, Harriman, NY,
May 19-23, 1985.

Development Of A
Seismic Slope Stability Map
Of The Urban Corridor Of
Davis And Salt Lake Counties, Utah

14-08-0001-21913

Jeffrey R. Keaton
Dames & Moore
250 East Broadway, Suite 200
Salt Lake City, Utah 84111
(801) 521-9255

Loren R. Anderson
Department of Civil & Environmental Engineering
Utah State University
Logan, Utah 84322
(801) 750-2780

INVESTIGATIONS

1. Began parametric analyses to identify ranges of critical slope angle as a function material strength for several values of slope height for two horizontal ground acceleration values and dry and fully saturated ground water conditions.

2. Began compiling map of existing landslides.

3. Have nearly completed arrangements to acquire digital topographic data for 7-1/2-minute quadranges covering about 75 percent of the study area.

4. Began assessment of area for uniformity of geotechnical and geologic conditions affecting slope stability.

RESULTS

1. Rather than construct a slope map with arbitrary ranges of slope gradient, we are conducting parametric analyses to calculate critical slope angles for two key acceleration values and ground water conditions and for a range of slope heights and strength parameters. Figure 1 illustrates the typical curve relating critical acceleration and slope angle for a specific set of geotechnical parameters (geoproperties). Based on lique-faction studies of Davis County (Anderson and others, 1982) and Salt Lake County (Anderson and others, 1985), the upper bound ground acceleration (10 percent probability in 100 years) is 0.23 g for the study area, while the lower bound ground acceleration (50 percent probability in 100 years) is 0.13 g. These are average values representative of the study area.

The term 'critical acceleration' in the context of liquefaction ananlyses (Anderson and others, 1982 and 1985) refers to the minimum horizontal ground acceleration required to induce liquefaction. In the context of seismic slope stability studies, 'critical acceleration' refers to the minimum horizontal ground acceleration required to reduce the computed Factor of Safety to unity, a value which is interpreted to represent the
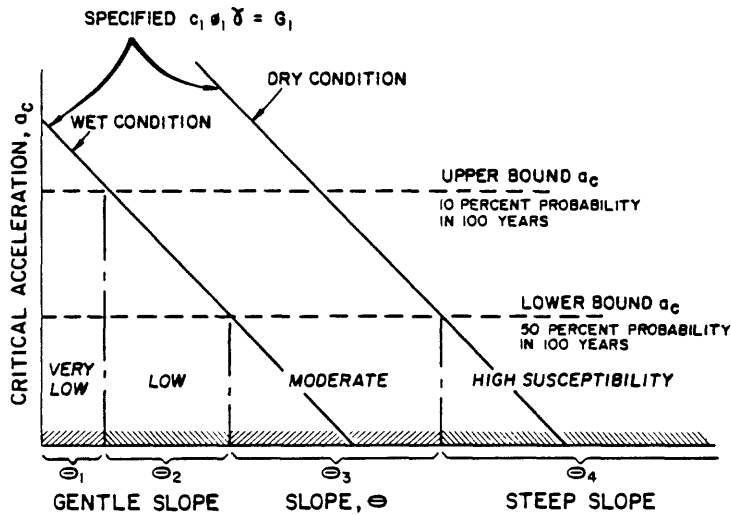
FIGURE 1. TYPICAL CRITICAL ACCELERATION VERSUS SLOPE CURVE
FOR A SPECIFIC GEOPROPERTY UNIT

threshold of 'failure.' Therefore, as used in this seismic slope stability research, the accelerations on Figure 1 represent critical accelerations.

2. Data on existing landslides are being compiled from the liquefaction analyses of the two counties comprising the study area (Anderson and others, 1982 and 1985). In addition, areas of instability contributing to the disaster in the Salt Lake City region in May and June of 1983 are also being shown (Anderson and others, 1984, and Pack, 1985, personal communication).

3. At the time our proposal was submitted, no regional digital topographic data was available in the Salt Lake City area. As a result of research in progress at Utah State University (Jadkowski, 1985, personal communication), arrangements are being made to acquire digital topographic data from the Geometronics Service Center (U.S. Department of Agriculture, Forest Service). This will eliminate the requirement to create slope maps by manually overlaying a transparent template on USGS 7-1/2-minute topographic quadrangles. Approximately 75 percent of the study area (17 quadrangles) will be digitized under the current plan.

4. Typical analyses of dynamic slope stability follow the method developed by Newmark (1965). This method is used to calculate displacement of slopes based on a critical acceleration value and an acceleration time-history. Newmark (1965) showed that the critical acceleration is a function of conventional static factor of safety and slope angle:

$$a_c = (FS-1) \sin \Theta$$

where a_c = critical acceleration; FS = static factor of safety; Θ = slope angle. Displacements are then determined by performing double

490

integration of that part of the acceleration time-history in which $a(t) > a_c$.

Wilson and Keefer (1983) used the Newmark method to predict displacement of a preexisting slump which was displaced during the 6 August, 1979 Coyote Lake, California earthquake. They found excellent agreement between predicted (27 mm) and measured (21 mm) displacements using one component of a nearby strong-motion record but no agreement using the other component of the same record.

The results of Wilson and Keefer's (1983) analysis demonstrates the general validity of the Newmark method and significant local variations in intensity of seismic shaking. Only one strong-motion record exists in Utah (1962 Logan earthquake) and only a few at distances of about 60 miles from the 1983 Borah Peak, Idaho earthquake (Reaveley, 1985, personal communication). Other available strong motion records represent compressional tectonics unlike the extensional tectonics of Salt Lake City. Therefore, using acceleration-scaled time-history records to compute displacements is not justified for the study area and would result in an artificial basis for indexing relative slope stability hazards. We believe that the critical acceleration values themselves represent the best relative slope stability index.

The seismic slope stability map will differentiate slope failure hazards with the qualitative terms of very low, low, moderate and high, as shown on Figure 1. Those slopes which have critical accelerations under fully saturated (wet) conditions that are higher than the acceleration which has a 10 percent probability of occurring in 100 years (0.23 g for the study area) are considered to have a very low potential for seismic slope failure. Similarly, those slopes which have critical accelerations under dry conditions that are lower than the acceleration which has a 50 percent probability of occurring in 100 years (0.13 g) are considered to have a high potential for seismic slope failure. The range of slopes corresponding to moderate and low potentials is shown on Figure 1.

By comparing critical acceleration values required to induce slope 'failure' with the 100-year 50 percent and 10 percent probable acceleration values for the study area, a rational perspective of regional seismic slope stability can be developed. Additionally, this method is identical to the one used to develop liquefaction potential maps of the study area (Anderson and others, 1982 and 1985). Consequently, the results of the two hazard evaluations can be readily combined for a more complete assessment of ground failure potential related to earthquake shaking.

REFERENCES

Anderson, L.R., Keaton, J.R., Aubry, Keven, and Ellis, S.J., 1982, Liquefaction potential map for Davis County, Utah: Final report submitted to U.S. Geological Survey Earthquake Hazards Reduction Program, Contract No. 14-08-0001-19127, 49 p.

Anderson, L.R., Keaton, J.R., Saarinen, T.F., and Wells, W.G., II, 1984, The Utah Landslides, Debris Flows and Floods, May and June, 1983: Committee on Natural Disasters, National Research Council, National Academy of Sciences, Washington, D.C., 96 p.

Anderson, L.R., Keaton, J.R., and Spitzley, J.E., 1985, Liquefaction potential map for Salt Lake County, Utah: Final report submitted to U.S. Geological Survey Earthquake Hazards Reduction Program, Contract No. 14-08-0001-19910 (in press).

Jadkowsky, Mark, 1985, Research Assistant, Department of Civil and Environmental Engineering, Utah State University, Logan, Utah, personal communication.

Newmark, N.M., 1965, Effects of earthquakes on dams and embankments: Geotechnique volume 15, number 2, p. 139-160.

Pack, R.T., 1985, Research Assistant, Department of Civil and Environmental Engineering, Utah State University, Logan, Utah, personal communication.

Wilson, R.C., and Keefer, D.K., 1983, Dynamic analysis of a slope failure from the 6 August, 1979 Coyote Lake, California Earthquake: Seismological Society of America, volume 73, number 3, p. 863-877.

Reaveley, L.D., 1985, President, Reaveley Engineers and Associates, Salt Lake City, Utah, personal communication.

Effects of Site Geology on Ground Shaking
in the Wasatch Front Urban Area

9950-03788

Albert M. Rogers
Branch of Engineering Geology and Tectonics
U.S. Geological Survey
Box 25046, MS 966, Denver Federal Center
Denver, CO 80225
(303) 236-1585; 776-1585 (FTS)

Investigations

In order to supplement previous data sets in this region, we recorded Nevada Test Site nuclear event ground motions at six sites in the Wasatch Front region. The recording sites were located south of Provo, UT near Springville, UT. The sites were selected to represent different surficial materials and depths to bedrock. One site near Utah Lake had been previously occupied by King and others, 1983. For this site and others located on deep Quaternary deposits, they calculated spectral ratios greater than 10 in the period of 0.7 to 1.0 seconds. A site near Hobble Creek was occupied where considerable shallow seismic reflection and drill hole data were available. Other sites were occupied to increase the amount of data in certain geologic condition categories.

Analog playbacks of the digital data recorded near Springville indicate that all six seismographs operated properly and that on-scale recordings were made. Good progress is being made in developing a system to play the tapes into the computer and to reformat the data. The reformatted data will be processed using preexisting software.

We have also begun to collect well logs in the Salt Lake City area. The goal of this effort is to correlate geotechnical information with ground response data. A meeting with Don Mabey of the Utah Geological and Mineral Survey revealed that the UGMS has already cataloged data from deep drill holes along the Wasatch Front. We are planning a trip to retrieve that and other well-log data from the city, county, and the State Highway Department. Reconnaissance work has been done to determine sites in Salt Lake City where we will need to drill additional holes.

Results

Results shown in the last semiannual report are being published in open-file report

Rogers, A. M., Carver, D. L., Hays, W. W., King, K. W., Miller, R. D., 1985, Preliminary estimates of geographic variation in relative ground shaking in the Wasatch Front urban corridor in Proceedings of Conference 26 "A workshop on evaluation of regional and urban earthquake hazards and risk in Utah," U.S. Geological Survey Open-File Report 84-763.

Seismic Data Processing and Shallow Structures

9950-03874

Arthur C. Tarr
Branch of Engineering Geology and Tectonics
U.S. Geological Survey
Box 25046, MS 966, Denver Federal Center
Denver, CO 80225
(303) 236-1605; FTS 776-1605

Investigations

Estimates of probability of exceeding a given level of ground motion in an earthquake-prone urban area are required by various Federal, State, and local workers in earthquake hazards studies. Precise estimates of ground motion amplification are frequently not established in an urban area because estimating ground motion amplification requires (1) precise measurements of actual ground motion and (2) knowing physical parameters of shallow geological structure, among them being lithology and depth of unconsolidated sediments. The Branch owns several types of portable digital seismic systems (Mini-Sosie, DR-200, MCR-600, and Bison) which can be used (1) to record seismic events opportunistically and (2) to determine shallow structures to depths of 1000 meters, using reflection, refraction, and spectral methods in urban areas where conventional methods (such as Vibroseis) may be inappropriate, prohibitively expensive, or unfeasible. The problem is that large areas need to be surveyed and optimizing such surveys (by varying size and spacing of spreads, for example) requires rapid processing of data (as opposed to processing later in a distant computer center) of each test shot or run to recover usable data. Further, software to analyze shallow reflections and refractions either does not exist or existing programs are inappropriate, expensive, or not implemented on large Branch computers. Finally, every system records and plays back seismic data differently so, without standardization during data processing, comparison of records recorded of different systems may be clumsy and inconvenient. Ideally, the needed software should ultimately be designed to execute a standard set of programs on a field computer so that results are obtained in nearly real time to optimize production of usable results. In addition, the software package should incorporate standardization of formats and integration of function for the several kinds of seismic systems available.

The objectives of this new project are to develop a seismic data analysis package on the Golden VAX/VMS that will analyze the effects of shallow geologic structures on ground motion based on reflection, refraction, and other digital data acquired in seismic surveys, determine the feasibility of transferring the software to a field computer, and implement the seismic data analysis package on the field computer.

Results

Software development activities that had formerly been conducted under the Source Properties of Great Basin Earthquakes project (9950-03835) are incorporated in this new project. The implementation of a Seismic Data

Analysis Package (SDAP) in that project forms the nucleus of software to be used in this project. The programs of SDAP operate on digital data written in a standard format used in Menlo Park for GEOS and DR-100 digital systems. Digital data written by DR-200, MCR-600, and Bison field systems can be converted into the standard format and thus analyzed with the SDAP programs. Data written by the Mini-Sosie system are currently analyzed by the DISCO software system at the Denver Federal Center.

A feasibilty study has established that MC68000-based microcomputers exist in the marketplace for the application desired here. Several manufacturers sell systems that can accomodate up to 4 megabytes of addressable memory and allow expansion options that include fast floating-point operation and permit array-processing.

Investigations will continue into converting existing software that is used in analysing refraction and portable digital using this technology. For example, Hunter and colleagues of the Geological Survey of Canada have had impressive success in analyzing seismic data using the "optimum window technique" employing an Apple II microcomputer. Their results will be examined for applicability to this project.

Implementation of Research Results
and Information Systems for Regional
and Urban Earthquake Hazards Evaluation, Wasatch Front, Utah

9950-03836

William M. Brown III
Branch of Engineering Geology and Tectonics
345 Middlefield Road, MS 998
Menlo Park, California 94025
(415) 856-7112/7119

Investigations:

This project is a part of the three-year program on Regional and Urban Earthquake Hazards Evaluation, Wasatch Front, Utah, directed by the U.S. Geological Survey. The goal is to foster creation and implementation of hazard-reduction measures in the Salt Lake City-Provo-Ogden urban corridor. We attempt this by providing high-quality scientific information and interpretations thereof that can readily be used by decisionmakers as a basis for changing and upgrading regulations, ordinances, and other measures of earthquake hazard reduction.

Results:

1. Quarterly publication of Wasatch Front Forum, a newsletter for timely dissemination of information regarding the program to participants and to interested persons affiliated with the program. This newsletter was published in June and September, 1984, and March and June, 1985.

2. Upgrading of State of Utah programs for comprehensive emergency management through recommendations of Federal Interagency Hazard Mitigation Team. This team was formed in response to landslide, flood, and debris-flow disasters in Utah during 1983-84, and oversaw preparation of the State of Utah Hazard Mitigation Plan. The plan, cited below, lists mitigation measures for a broad spectrum of geologic hazards in addition to those related to the 1983-84 disasters.

3. Support of a new cooperative program between USGS and Utah Geological and Mineral Survey begun in January, 1985 to provide funding and technical assistance to counties so they can employ geologists to work on geologic hazards in the five most populous Wasatch Front counties. Funding of all salaries and benefits will be paid initially by a grant of $92,500 from the USGS to the UGMS. The total grant over the three-year period will approach $300,000. The UGMS will provide technical assistance, technical supervision, and specialized equipment. The counties will provide office space, vehicles, and secretarial support. The County Hazards Geologists will compile information on geologic hazards and pull together in a single location all the hazard-related investigations already completed for each county. An end product of the three-year program will be maps and reports describing the geologic hazards in the counties. These final products will be published by UGMS.

<u>Reports:</u>

Federal Emergency Management Agency, 1984, Interagency Hazard Mitigation
Report FEMA-720-DR-UTAH (Federal Disaster Declaration for the State of Utah
due to Severe Storms, Flooding, Mudslides, and Landslides for the period April
1, 1984 to July 1, 1984): Federal Emergency Management Agency Region VIII,
Denver, Colorado, 22p. plus appendices.

Federal Emergency Management Agency, 1984, Post-Flood Recovery Progress Report
FEMA-720-DR-UTAH: Federal Emergency Management Agency Region VIII, Denver,
Colorado, 16p. plus appendices.

Utah Department of Public Safety, 1984, Hazard Mitigation Plan, Utah 1984:
Utah Department of Public Safety, Division of Comprehensive Emergency
Management, Salt Lake City, Utah, 92p.

Digital Data Analysis

9920-01788

Ray Buland
Branch of Global Seismology and Geomagnetism
U.S. Geological Survey
Denver Federal Center, MS 967
Denver, Colorado 80225
(303) 236-1506

Investigations

1. Moment Tensor Inversion. Apply methods for inverting body phase wave-forms for the best point source description to research problems.

2. Computation of Free Oscillations. Study the effects of anelasticity on free oscillation eigenfrequencies and eigenfunctions.

3. Earthquake Location Technology. Study techniques for improving the robustness, honesty, and portability of earthquake location algorithms.

4. Real Time Earthquake Location. Experiment with real time signal detection, arrival time estimation, and event location for regional earthquakes.

5. ScS Studies. Use multiple ScS phases to study lateral heterogeneity, attenuation, and scattering in the Western Pacific.

6. Detection Capabilities. Study the seismic event detection capability of each proposed station in the Southern Hemisphere Seismic Net (SHSN) now under development.

7. Network Day/Event Tapes. Support and enhance portable software for retrieving data from the Global Digital Seismograph "Network Day Tapes." Create and distribute Network "Event Tapes."

8. NEIS Monthly Listing. Contribute both fault plane solutions (using first- motion direction) and moment tensors (using long-period body-phase waveforms) for all events of magnitude 5.8 or greater when sufficient data exist. Contribute waveform/focal sphere figures of selected events.

Results

1. Moment Tensor Inversion. The catalogue of moment tensors for all sufficiently large events in 1981-1983 has been redone allowing for a source depth computed by the moment tensor algorithm. This catalogue is being prepared for publication. A comparative study between this and other source-parameter catalogues is under way using a vector representation of the moment tensor.

2. <u>Computation of Free Oscillations</u>. The complete theory for anelastic free oscillations predicts an observable source phase which cannot be modeled by perturbation theory. This could result in the destructive interference of modes forming long period body phases which could be interpreted as an attenuation or a scattering effect. A journal article describing this phenomenon is being prepared.

3. <u>Earthquake Location Technology</u>. The behavior of least squares, outlier truncation, M-estimators, and R-estimators were studied by means of Monte-Carlo experiments using realistic models of the teleseismic travel-time residual probability density function. Least squares, the 1-norm, the best R-estimator, and the best M-estimator were found to have asymptotic efficiencies of .16, .75, .95, and 1.00, respectively. Outlier truncation cannot be easily analysed because of its ad hoc nature. Outlier truncation and typical implementations of M-estimators performed poorly for small samples. R-estimators and properly applied M-estimators were equally good for small samples. The best M-estimators are non-unique. The best unique M-estimator is asymptotically equivalent to the best R-estimator.

4. <u>Real-time Earthquake Location</u>. The real-time system developed in cooperation with the Instituto Nazionale di Geofisica (Italian Government) is being implemented in Golden, Colorado, for the United States' seismic network. The system is being generalized to handle both digital and analogue telemetry, different sample rates, and asynchronous channel timing. Dedicated microcomputer hardware is being procured for the near-real-time back end system. Software for regional and teleseismic on-line event location is being tested. The current prototype is processing 64 analogue channels.

5. <u>ScS Studies</u>. The Tonga-Fiji to Hawaii path has been chosen for study, a suite of deep focus events have been selected, and digital seismic waveform and gravity anomaly data have been collected. Software for waveform processing and synthetic seismogram generation are being developed.

6. <u>Detection Capabilities</u>. The new Quick Epicenter Determination (QED) bulletin, prepared by the NEIS 3 to 5 days behind real time, has been compared with the weekly PDE (30 days behind real time) and with a Committee on Disarmament, Group of Scientific Experts (GSE) monitoring experiment (14 days behind real time). Despite being more timely, the QED's results were found to be more accurate and reliable, but less complete than the GSE results. Some difficulties with the GSE processing were found.

7. <u>Network Day/Event Tapes</u>. Event tapes are being routinely produced and distributed to 16 data centers. Production and distribution is complete for the current (1984) tapes. Historical tapes have been produced for January 1980-December 1983 and distributed for 1980-1982. The distribution of the historical tapes should be completed by the end of this summer. Software is being developed to add data from Graefenberg, USSR, NARS, and Geoscope stations to the event tapes.

8. <u>NEIS Monthly Listing</u>. Since May 1981, fault plane solutions for large events have been contributed to the Monthly Listing. Beginning in November 1982, moment tensors and waveform/focal sphere plots are also being contributed. In the last six months the fault plane solutions and moment tensors of approximately 80 events were published. A catalogue of all fault plane solutions along with first motions data is being prepared for publication as a U.S. Geological Survey Bulletin.

<u>Reports</u>

Buland, R. P., Yuen, D. A., Widmer, R., and Konstanty, K., 1984, Effects of a stratified anelastic earth on toroidal free oscillations and seismic excitation: EOS, v. 65, p. 1002.

Buland, R., 1985, Uniform reduction error analysis: Bulletin of the Seismological Society of America, submitted.

McDermott, P. N., Hansen, C. J., Van Horn, H. M., and Buland, R., 1985, The non-radial oscillations of neutron stars: Astrophysical Journal, submitted.

Presgrave, B., and Buland, R., 1985, The use of later phases in catalogue preparation, <u>in</u> Abstracts, 23rd IASPEI General Assembly, Tokyo, Japan, in press.

Needham, R. E., 1985, <u>Evaluation of the National Earthquake Information Center's Quick Epicenter Determinations</u>: U.S. Geological Survey Open-File Report, 85-278.

Sipkin, S. A., 1984, Interpretation of non-double-couple earthquake mechanisms derived from moment tensor inversion: EOS (American Geophysical Union, Transactions), v. 65, no. 45, p. 990.

Sipkin, S. A., and Silver, P. G., 1985, Current research projects using teleseismic array data: EOS (American Geophysical Union, Transactions), v. 66, no. 18, p. 303.

Silver, P. G., and Sipkin, S. A., 1985, Seismic imaging of the "rest of the Earth": EOS (American Geophysical Union, Transactions), v. 66, no. 18, p. 303.

Sipkin, S. A., 1985, Estimation of earthquake source parameters by the inversion of waveform data using optimal filter theory, <u>in</u> Abstracts, 23rd IASPEI General Assembly, Tokyo, Japan, in press.

_____ 1985, Moment tensor solutions estimated using optimal filter theory, <u>in</u> Abstracts, 23rd IASPEI General Assembly, Tokyo, Japan, in press.

Zirbes, M. D., and Moon, B. J., 1985, <u>Waveform Catalogue for IASPEI Events</u>: U.S. Geological Survey Open-File Report, 85-218.

U.S. Seismic Network

9920-01899

Marvin A. Carlson
Branch of Global Seismology and Geomagnetism
U.S. Geological Survey
Denver Federal Center, MS 967
Denver, Colorado 80225
(303) 236-1506

Investigations

U.S. Seismicity. Data from the U.S. Seismic Network are used to obtain a preliminary location and magnitude of significant earthquakes throughout the United States and the world.

Results

As an operational program, the U.S. Seismic Network operated normally throughout the report period. Data were recorded continuously in real time at the NEIS main office in Golden, Colorado. At the present time, 100 channels of SPZ data are being recorded at Golden on develocorder film. This includes data telemetered to Golden via satellite from both the Alaska Tsunami Warning Center, Palmer, Alaska, and the Pacific Tsunami Warning Center, Ewa Beach, Hawaii. A representative number of SPZ channels are also recorded on Helicorders to give NEIS real time monitoring capability of the more active seismic areas of the United States. In addition, 15 channels of LPZ data are recorded in real time on multiple pen Helicorders.

Data from the U.S. Seismic Network are interpreted by record analysts and the seismic readings are entered into the NEIS data base. The data are also used by NEIS standby personnel to monitor seismic activity in the United States and worldwide on a real time basis. Additionally, the data are used to support the Alaska Tsunami Warning Center and the Pacific Tsunami Warning Service. At the present time, all earthquakes large enough to be recorded on several stations are worked up using the "Quick Quake" program to obtain a provisional solution as rapidly as possible. Finally, the data are used in such NEIS publications as the "Preliminary Determination of Epicenters" and the "Earthquake Data Report."

Development is continuing on an Event Detect and Earthquake Location System to process data generated by the U.S. Seismic Network. We expect the new system to be ready for routine operational use by early next fiscal year. At that time, the use of develocorders for data storage will be discontinued. Ray Buland and David Ketchum have been doing most of the developmental programming for the new system.

Earth Structure and its Effects upon Seismic Wave Propagation

9920-01736

George L. Choy
Branch of Global Seismology and Geomagnetism
U.S. Geological Survey
Denver Federal Center, MS 967
Denver, Colorado 80225
(303) 236-1506

Investigations

1. **Shear wave interaction with the Earth's mantle.** We are seeking constraints on the frequency dependence of shear wave attenuation in the Earth's mantle by synthesizing broadband P- and S-type body waves with frequency content from tens of seconds to several Hz.

2. **Source parameters from GDSN data.** We are developing methods to extract more accurate source parameters from digitally recorded data of the GDSN by determining corrections to waveforms for propagation effects, especially frequency dependent attenuation.

Results

1. We have obtained broadband records of displacement and velocity from deep earthquakes recorded by stations of the GDSN and the GRF array. Using a method of seismogram synthesis that can model frequency dependent effects from source directivity and attenuation, we have derived constraints on attenuation for midband (0.1-1 Hz) frequencies. Differences in S and ScS body waves provide strong constraints on differential attenuation in the Earth. The mid-mantle between depths of 400 and 1600 km contributes primarily to attenuation of low frequencies (0.01 to 0.1 Hz). P- and S- waveforms suggest that below mantle depths of 1600-1800 km little or no attenuation exists in the band of 0.01 to 5 Hz.

2. In the computation of radiated energy, it is important that spectral information about and above the corner frequency is corrected for attenuation. The frequency-dependent attenuation models that we have been developing are being incorporated in a scheme to automate the computation of energy using digitally recorded data of the GDSN.

Reports

Boatwright, J., and Choy, G. L., 1984, Teleseismic estimates of the energy radiated by shallow earthquakes: Journal of Geophysical Research, in press.

Choy, G. L., and Boatwright, J., 1985, Estimates of teleseismic source parameters of shallow earthquakes from broadband waveforms [abs.]: To be presented at the 23rd General Assembly of IASPEI, Tokyo, Japan.

Choy, G. L., and Cormier, V. F., 1985, Direct Measurement of the Mantle Attenuation Operator from Broadband P and S Waveforms [abs.]: To be presented at the Spring Meeting of the American Geophysical Union, Baltimore, Maryland.

Systems Engineering

5-9920-01262

Harold E. Clark, Jr.
Branch of Global Seismology and Geomagnetism
U.S. Geological Survey
Albuquerque Seismological Laboratory
Building 10002, Kirtland AFB-East
Albuquerque, New Mexico 87115-5000
(505) 844-4637

Investigations

Design, develop, and test microprocessor based seismic instrumentation.

Design, develop, procure, and test special electronic systems required by seismic facilities.

Design, develop, and test microprocessor/computer software programs for seismic instrumentation and seismic recording systems.

Results

The China Digital Seismic Network (CDSN) power systems were assembled and shipped to the People's Republic of China. These power systems will be installed at each of the field recording sites.

The CDSN Depot Repair Facility equipment and test systems were also shipped. This CDSN Depot Repair Facility will provide maintenance and repair for the CDSN field recording systems. Major test analysis and repair diagnostics can be run on all CDSN field recording system units. Repair capabilities are provided for all units with the exception of the HCD-75 tape drive systems. The HCD-75's are too complex, and it is not cost effective to provide complete repair facilities.

The CDSN system software is being upgraded to provide read-after-write verify for the digital data being written on the magnetic tape.

Final design and assembly of the remaining CDSN units are in the process of being completed.

Reanalysis of Instrumentally-Recorded U.S. Earthquakes

9920-01901

J. W. Dewey
Branch of Global Seismology and Geomagnetism
U.S. Geological Survey
Denver Federal Center,MS 967
Denver, Colorado 80225
(303)236-1506

Investigations

1. Relocate instrumentally recorded U.S. earthquakes using the method of joint hypocenter determination (JHD) or the master event method, using subsidiary phases (Pg, S, Lg) in addition to first arriving P-waves, using regional travel-time tables, and expressing the uncertainty of the computed hypocenter in terms of confidence ellipsoids on the hypocentral coordinates.

2. Evaluate the implications of the revised hypocenters on regional tectonics and seismic risk.

Results

1. Jim Dewey has completed analysis of regionally recorded earthquakes that occurred in central Idaho from 1944 through March 1984, including the early aftershock sequence of the M_s=7.3 Borah Peak earthquake of October 28, 1983. The distribution of epicenters of the Borah Peak main shock and early aftershocks suggest that the fault segment that ruptured in the main shock was approximately a parallelogram with one pair of sides parallel to the zone of surface fault scarps associated with the earthquake and with the other pair of sides parallel to the slip vector of the earthquake. Such a main-shock rupture shape would be expected on geometrical grounds if the 1983 rupture zone were terminated on the north and south by intersection with adjacent segments of the Lost River fault that have the same slip vector as the 1983 rupture. Epicenters of earthquakes occurring before 1983 define a seismic zone, the White Cloud Peaks zone, that is approximately parallel to the Lost River fault and situated about 30 km west of the Borah Peak aftershock zone. The relocated epicenters may also be interpreted as defining a north-northeast trending seismic zone near Seafoam and a north-northeast trending seismic zone that is situated north and west of Challis. The Seafoam zone includes the epicenter of the largest instrumentally recorded central Idaho earthquake prior to the Borah Peak earthquake, the magnitude 6.1 shock of July 12, 1944. The region within 25 km of the epicenter of the Borah Peak main shock was quiescent for at least two decades before the main shock for magnitudes of 3.5 and greater.

2. At a symposium on the Meers fault, one of the sessions of the April Seismological Society of America meeting at Austin, Texas, Dave Gordon interpreted earthquake activity in southern Oklahoma within the context of regional seismicity, the available focal mechanisms, basement tectonics, and the contemporary stress regime.

Southern Oklahoma lies along a previously recognized, linear seismic zone, the Wichita-Ouachita Zone, that extends east-southeasterly from the Texas Panhandle to Mississippi. Although the historic record is comparatively brief, the zone contains the epicenters of approximately 30 earthquakes that had total felt areas of more than 10,000 km^2. The relatively well-defined seismic lineament that forms the zone and the few earthquake mechanisms within the zone, suggest that the Wichita-Ouachita Zone represents a zone of crustal weakness acted upon a compressive stress oriented east-northeast. Gordon proposes that the seismicity may be a manifestation of "wrench fault tectonics" dominated by left-lateral slip on an east-southeast trending basement fault. The association of geologically ancient structural trends and historic epicenters suggests that the zone may extend northwest to the Rocky Mountains region.

The attached figure shows instrumental seismicity (magnitude 3.0 and greater) in the vicinity of the Meers fault for the period 1925-1980. Octagons are epicenters determined by Joint Hypocenter Determination and are shown with their associated 95-percent-confidence ellipses. Asterisks represent those previously accepted epicenters that lie outside the confidence ellipses of the corresponding revised epicenters. The very thick line represents a geologically young scarp on the Meers fault.

Reports

Dewey, James W., 1985, Instrumental seismicity of central Idaho, in Stein, R. S., and Bucknam, R. C., eds., Proceedings of Workshop XXVIII on the Borah Peak, Idaho, Earthquake: U.S. Geological Survey Open-File Report 85-290, 21 p., in press.

Dewey, James W. (submitted), A review of recent research on the seismotectonics of the Southeastern Seaboard and an evaluation of hypotheses on the source of the 1886 Charleston, S.C., earthquake: Submitted to the Nuclear Regulatory Commission as a NUREG Technical Report, 70 p.

Gordon, D. W., and Dewey, J. W., 1985, The Wichita-Ouachita Seismic Zone - southern Oklahoma seismicity in a regional context: Earthquake Notes, v. 55, no. 1, p. 2.

Gordon, D. W. (submitted), Revised instrumental hypocenters and correlation of earthquake locations and tectonics in the central United States: U.S. Geological Survey Professional Paper, 182 p.
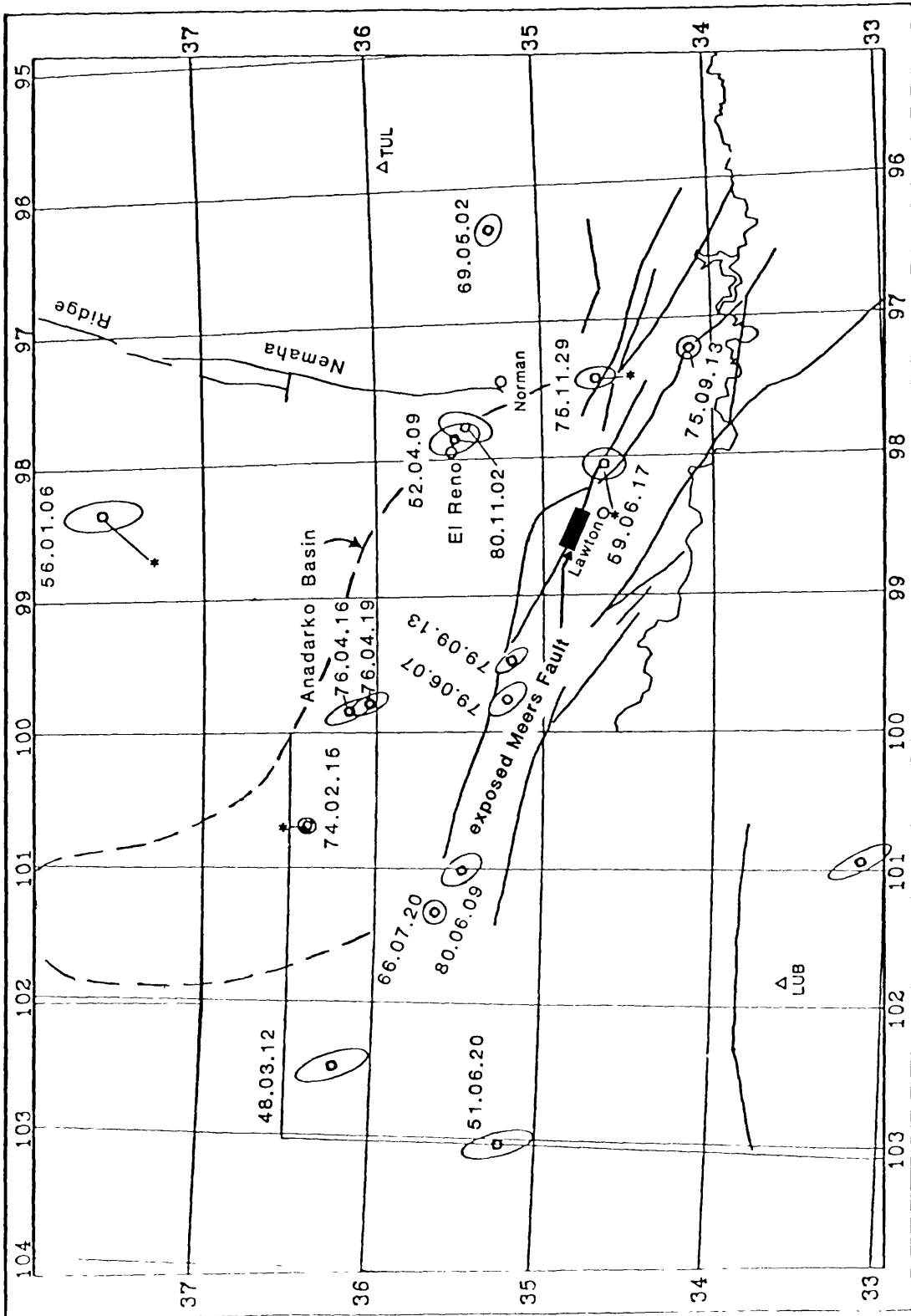
Global Seismology

9920-03684

E. R. Engdahl
Branch of Global Seismology and Geomagnetism
U.S. Geological Survey
Denver Federal Center
Box 25046, Mail Stop 967
Denver, Colorado 80225
(303) 236-1506

Investigations

1. **Depth Phases.** Establish criteria for the proper identification of depth phases from sub-oceanic earthquakes.

2. **Earthquake Location in Island Arcs.** Develop practical methods to accurately locate earthquakes in island arcs.

3. **Subduction Zone Structure.** Develop techniques to invert for subduction zone structure using seismic travel times.

4. **Global Synthesis.** Synthesize recent observational results on the seismicity of the earth and analyze this seismicity in light of current models of global tectonic processes.

Results

1. **Depth Phases.** Focal depths of sub-oceanic subduction zone earthquakes are best determined by the careful identification and analysis of teleseismic depth phases. On short-period vertical-component seismograms, arc crustal structure can cause water-surface reflections (pwP and swP) and sediment-basement reflections with amplitudes comparable to those of water-sediment reflections (pP and sP). However, the occurrence of these short-period depth phases is a higly unpredictable phenomenon, subject to changes in source mechanism and local variations in arc structure.

Digital and analog vertical-component seismograms were examined from nearly 400 teleseismically recorded central-Aleutian earthquakes that occurred during the period 1964 to 1984. A data set consisting of the travel times relative to P of short-period depth phases was assembled for 54 shallow-depth earthquakes and 33 earthquakes deeper than 50 km across the arc. In addition, long-period waveforms for the larger events were examined. Magnitude 4.8 was approximately the lower limit for useful depth phase arrivals.

Short-period reflected phases from shallow-depth earthquakes were analyzed by matching observed travel times relative to P to theoretical values computed for a two-dimensional model of arc crustal structure. Depths resolved in this fashion provide a sharper depth profile of the shallow seismic zone in the central Aleutians than previously available. Outer rise and trench earthquakes occur over a narrow range of subcrustal depths. North of the trench

the plate dips gently beneath the terrace and appears to descend gradually into the mantle. The thickness of the interplate thrust-earthquake zone is no more than 10-15 km. Earthquakes near the volcanic arc and above the plate interface occur at depths beneath the sediment-basement interface. Estimation of the focal depths of earthquakes deeper than 50 km poses a special problem because an accurate specification of slab structure is needed to correct for path effects.

The phases pwP and swP are not ordinarily observed on long-period vertical-component seismograms. However, long-period waves reflected from boundaries with sharp long-period impedance contrasts, such as the sea bottom and the sediment-basement interface, are observed. Moment tensor depths for shallow earthquakes based on the inversion of long-period waveforms using a standard earth model, once transformed into true depths within a model of arc crustal structure for the central Aleutians, agree with depths determined from short-period reflected phases alone to within a few kilometers.

Reported depth phases are routinely used for depth determination by the Preliminary Determination of Epicenters (PDE) and the International Seismological Centre (ISC) services. However, the phases pP and sP are often obscured in the P coda and for sub-oceanic earthquakes, for example, pwP is misidentified and reported as pP. This can result in the overestimation of the focal depths of routinely determined hypocenters reported by these services.

Broadband Graefenberg (GRF) array data from 11 moderate-size shallow-depth earthquakes in the central Aleutians were used to study the effects of focal depth and structure across the arc on observed waveforms. Details of arc crustal structure and the earthquake locations, depths, and source mechanisms are well known from previous related studies. Based on these parameters, depth phase arrival times relative to P and theoretical seismograms were computed. The theoretical results, primarily phase arrival times, suggest that arc structure is responsible for many of the complicated features seen on vertical-component summation seismograms simulated with different instrument responses from the broadband array data. The effect of the water layer is to produce a pwP phase which has strong energy at short and intermediate periods and is often observed as a low-amplitude signal on long-period seismograms. Except for one trench event, all the earthquakes studied occurred along the plate interface zone, had similar thrust focal mechanisms, and differed only in depth. As a result, the effects of depth phases on observed GRF waveforms across the arc were found to be systematically related to the increase in focal depth along the shallow-dipping seismic zone. A broadening and delay of the second and third half-cycles of the long-period P-wave signal with increasing source depth are apparently related to the constructive interference of primary reflections in the crust and their reverberations. Moreover, as the focal depth increases, a greater number of reflections from overlying boundaries are produced. Reverberations deep within the downgoing plate may also occur. For sources along the dipping seismic zone with distances from the trench greater than about 85 km, these effects apparently combine to produce an increase in the short-period complexity of GRF seismograms.

2. <u>Earthquake Location in Island Arcs</u>. An extended data set of central Aleutian earthquakes, that includes events with well determined depths as previously described, has been relocated using the JHD approach. It is shown that by careful selection of observing stations, proper analysis of depth phases and the availability of local network calibration events, this approach can reduce hypocentral uncertainties to less than 15 kilometers over a broad region of the subduction zone. These results and their tectonic significance will be the subject of a paper in preparation.

3. <u>Subduction Zone Structure</u>. First results of a cooperative research project with Dr. D. Gubbins at Cambridge University to jointly invert seismic travel times for hypocenters and structure in the central Aleutian subduction zone are now available. For a coarse two-dimensional grid and spherically symmetric starting model, a plate model 80-100-km thick, 360 km in length, and with 6-8 percent higher average velocities than the surrounding mantle was obtained. Travel times of depth phases from deep earthquakes proved to be the only data available to determine back arc structure and to locate the top of the plate. The work continues using a finer grid structure and iterating on the hypocenters.

4. <u>Global Synthesis</u>. Development of a framework for this synthesis study continues.

<u>Reports</u>

Engdahl, E. R., and Billington, S., 1985, Focal depth determination of central Aleutian earthquakes: Bulletin of the Seismological Society of America, submitted.

Engdahl, E. R., and Kind, R., 1985, Interpretation of broadband seismograms from central Aleutian earthquakes: Ann. Geophysicae, submitted.

Seismic Observatories

9920-01193

Leonard Kerry
Branch of Global Seismology and Geomagnetism
U.S. Geological Survey
Denver Federal Center, MS 967
Denver, Colorado 80225
(303) 236-1506

Investigations

Recorded seismological data at Albuquerque Albuquerque Seismological
Laboratory, New Mexico (ASL) on a continuing basis. Recorded and
provisionally interpreted seismological and geomagnetic data at observatories
operated at Newport, Washington; Cayey, Puerto Rico; and Agana, Guam.
Assisted in the operation of the Puerto Rican Seismic Telemetry Network from
the main base located in Cayey, Puerto Rico. Operated advanced equipment for
gathering research data for universities and other agencies at Cayey, Puerto
Rico and Agna, Guam. At Agana, Guam, a 24-hour standby duty was maintained to
provide input to the Tsunami Warning Service operated at Honolulu Observatory
by NOAA and to support the Early Earthquake Reporting function of the National
Earthquake Information Service.

Results

Provided data on an immediate basis to the National Earthquake Information
Service and the Tsunami Warning Service. Continued to send seismograms
obtained from the WWSSN Systems to NEIS for use in the ongoing USGS
programs. Analog seismic records and digital seismic tape records were
obtained from the SRO system and forwarded to ASL for use in ongoing USGS and
other users' programs. Data from advanced research equipment was forwarded to
universities or other agencies working in conjunction with USGS. Seismic data
from the Puerto Rican net was provided on a continuing basis to the University
of Puerto Rico for their use in studying and research of the seismicity of the
Puerto Rican area.

Responded to requests from the public, interested scientists, universities,
state, and Federal agencies regarding geophysical data and phenomena.

Global Seismograph Network Evaluation and Development

9920-02384

Jon Peterson
Branch of Global Seismology and Geomagnetism
U. S. Geological Survey
Building 10002, Kirtland AFB-East
Albuquerque, New Mexico   87115-5000
(505) 844-4637

Investigations

Work continued on the development and testing of hardware and software for the China Digital Seismograph Network.

Results

The sensor system testing and analysis was completed, and the results were published in an Open-File report. E. Tilgner spent approximately two months in China demonstrating broadband seismometer installation and test procedures and assisting the Chinese in the first two installations.

The station power systems were assembled and tested by the Albuquerque Seismological Laboratory (ASL) engineering group. They have been crated and shipped via surface transport to China with scheduled arrival in mid-May. The units will be transported to the stations and installed by the Chinese.

The station recording systems have been designed and are being assembled by the ASL engineering group. Problems related to write and read errors in the cartridge drive have forced a redesign of software, and this is causing delays.

The data management system is fully assembled and the software is being tested.

Reports

Peterson, J., and E. E. Tilgner, 1985, Description and preliminary testing of the CDSN sensor systems, U. S. Geological Survey Open-File Report 85-288, 60 p.

Global Digital Network Operations

9920-02398

Robert D. Reynolds
Branch of Global Seismology and Geomagnetism
U.S. Geological Survey
Albuquerque Seismological Laboratory
Building 10002, Kirtland AFB-East
Albuquerque, New Mexico 87115-5000
(505) 844-4637

Investigations

The Global Network Operations continued to provide technical and operational support to the SRO/ASRO/DWWSSN observatories which include operating supplies, replacement parts, repair service, redesign of equipment, training and on-site maintenance, recalibration and installation. Maintenance is performed at locations as required, when the problem cannot be resolved by the station personnel. The Bendix O&M contract personnel level remains at one team leader, four field engineers, and one digital technican.

The SRO enhancement program continued at the SRO stations. These enhancements consist of adding the two short-period horizontal components to the digital data, removal of the six second notch from the long-period filters, and installation of clip detectors on each seismometer module.

The following station maintenance activity was accomplished:

ANMO - Albuquerque - SRO
Two maintenance visits

SHIO - Shillong, India - SRO
One maintenance visit

ZOBO - La Paz, Bolivia - ASRO
Two maintenance visits

DWWSSN

BDF - Brasilia, Brazil
One maintenance visit

HON - Honolulu, Hawaii
One maintenance visit

LEM - Lembang, Indonesia
One maintenance visit

SCP - State College, Pennsylvania
One maintenance visit

TOL - Toledo, Spain
One maintenance visit

WWSSN

SHL - Shillong, India
One maintenance visit

ASL Repair Facility

As much routine repair as possible was done during this period to support the field maintenance activity. The station maintenance files have been transferred to the IBM PC/XT computer system and software development was started to put the inventory of electronic components on the computer system.

Special Activity

A site survey was conducted in Israel to help select a location for a SRO station to be installed there in the near future.

The KS36000 seismometer system was removed from the Guam (GUMO) station and shipped to China.

A three-component set of Streckeisen seismometers were installed and connected to the SRO recording system to replace the KS36000.

Results

The digital network continues with a combined total of 29 SRO/ASRO/DWWSSN stations. The main effort of this project is to perform as much on-site maintenance and training as possible in order to provide the highest quality digital data for the worldwide digital database.

Seismicity and Tectonics

9920-01206

William Spence
Branch of Global Seismology and Geomagnetism
U.S. Geological Survey
Denver Federal Center, MS 967
Denver, Colorado 80225
(303) 236-1506

Investigations

Studies carried out under this project focus on detailed investigations of large earthquakes, aftershock series, tectonic problems,and earth structure. Studies in progress have the following objectives:

1. Provide tectonic setting for and analysis of the 1977 Sumba earthquake series (W. Spence).

2. Generalize the role of the slab pull force in determining the primary tectonic features at subduction zones and in contributing to stresses that cause subduction zone earthquakes (W. Spence).

3. Provide tectonic setting for and analysis of the 1974 Peru gap-filling earthquake (W. Spence and C. J. Langer).

4. Determine faulting parameters (strike, dip, slip) for aftershocks of the great (M_S 7.7) Colombia earthquake of December 1979 and infer rupture characteristics of the main shock (C. Mendoza).

5. Determine the maximum depth and degree of velocity anomaly beneath the Rio Grande Rift and Jemez Lineament by use of a 3-D, seismic ray-tracing methodology (W. Spence and R. S. Gross) source-parameter information for moderate-magnitude aftershocks that followed the large (M_S-7.7) Colombia

Results

1. The great (M_O = 4 x 10^{28} dyne-cm), normal-faulting Sumba earthquake of 1977 occurred at the Java Trench, just west of the zone where the Australian continental lithosphere is in collision with the Java arc. Aftershocks of the Sumba earthquake have been relocated by the joint hypocenter method and occur in two zones: an east-west trending zone, mostly east of the main shock, and a triggered northwest- southeast-trending zone located about 180 km northwest of the main shock. Both sets of earthquakes are confined to the 40-km-thick brittle portion of the oceanic lithosphere. Focal mechanism data for the aftershocks in the main shock zone and in the triggered zone combined with study of the detailed tectonic setting support the conclusion that both the Sumba main shock and the triggered group of earthquakes occurred directly as a result of the slab pull.

2. In spite of the recognized strong influence of the slab pull force in moving tectonic plates, the influence of this force in causing tectonic phenomena occurring on the order of days to several years generally has been neglected. In addition to reviewing evidence that the slab pull force is responsible for most steady-state features associated with mature subduction zones, this study considers a time-dependent model that describes the slab pull force and the weaker ridge push force through a cycle of great subduction zone earthquakes. The steady-state and short-term behaviors of a predominant slab pull force are demonstrated to be consistent with most seismic and tectonic data that exist for mature subduction zones and are used to provide a physical basis for several important and previously unexplained observations.

3. The great 1974 Peru thrust earthquake (M_S 7.8, M_W 8.1) occurred in a documented seismic gap, between two earthquakes each with magnitude of about 8, occurring in 1940 and 1942. Additional major earthquakes occurred in this region in 1966 and in 1970; all but the 1970 shock represent thrust faulting. The stress release of the October 3, 1974 main shock and aftershocks occurred in a spatially and temporally irregular pattern. The multiple-rupture main shock produced a tsunami with wave heights of 0.6 ft at Hawaii and which was observed, for example, at Truk Island and at Crescent City. The aftershock series essentially was ended with the occurrence of a M_S 7.1 aftershock on November 9, 1974. The several years of preseismicity data to this earthquake include an unusually clear example of the "Mogi donut" pattern.

4. Three large earthquakes, occurring in 1942, 1958, and 1979, have reruptured the zone of the single great Colombia-Ecuador earthquake (M_S 8.6, M_W 8.8) of January 31, 1906. The last of these (December 12, 1979; M_S 7.7) ruptured the northernmost part of the 1906 rupture. Love and Rayleigh-wave signals recorded by the Global Digital Seismograph Network have been used to retrieve source-parameter information for moderate-magnitude aftershocks that followed the earthquake of 12 December 1979. In the procedure, observed Love/Rayleigh amplitude ratios in a 30-80 second passband are compared against theoretical values calculated for a suite of source models fixed at aftershock depths computed with a Joint Hypocenter Determination method of relocation using depth-phase arrival times. In addition, a reference earthquake with known focal mechanism and depth is used to calibrate the procedure and to minimize the path and size effects.

Aftershocks within the asperity region from which most of the moment release originated during the 1977 main shock denote thrust faulting very similar to that of the mainshock and occur at or near the gently dipping Nazca-South America plate boundary. A few aftershocks are within 45 km of the axis of the Colombia Trench and seaward of the region of maximum energy release and probably represent secondary deformation resulting from stress readjustment following seismogenic failure of the asperity region, rather than a propagation of rupture seaward to the trench axis along the plate interface. At least one of the near-trench aftershocks is a normal-faulting event that occurred within the accretionary wedge of material above the interplate boundary. The other near-trench shocks are probably intraplate events within the subducting slab.

The results are consistent with a propagation of rupture from the mainshock hypocenter to the northeast along the plate boundary for a distance of 230 km. North of this point, aftershock activity probably occurred along a separate, offset segment of the Nazca-South America plate boundary.

5. To a depth of about 160 km, the upper mantle P-wave velocity beneath the Rio Grande rift and Jemez lineament is 4-6 percent lower than beneath the High Plains Province. A 3-D, P-wave velocity inversion shows scant evidence for pronounced low P-wave velocity beneath the 240-km-long section of the Rio Grande rift covered by our array. However, the inversion shows a primary trend of 1-2 percent lower P-wave velocity underlying the northeast-trending Jemez lineament, down to a depth of about 160 km. The Jemez lineament is defined by extensive Pliocene-Pleistocene volcanics and late Quaternary faults. The upper mantle low-velocity segment beneath the Jemez lineament is at most 100 km wide and at least 150-200 km long, extending in our inversion from Mt. Taylor through the Jemez volcanic center and through the Rio Grande rift. A Backus-Gilbert resolution calculation indicates that these results are well-resolved.

Reports

Mendoza, C., 1985, Study of aftershock source properties using digital surface-wave data: The December 1979 Colombia earthquake: Golden, Colo., Colorado School of Mines Ph. D. thesis, 166 p.

Spence, W., 1985, The 1977 Sumba earthquake series: direct evidence for slab pull: Journal of Geophysical Research (in press).

Spence, W., 1985, Slab pull: Nature (submitted).

United States Earthquakes

9920-01222

Carl W. Stover
Branch of Global Seismology and Geomagnetism
U.S. Geological Survey
Denver Federal Center, MS 967
Denver, Colorado 80225
(303) 236-1500

Investigations

1. One hundred seven earthquakes in 16 states were canvassed by a mail questionnaire for felt and damage data. Thirty three of these occurred in California, and 22 in Alaska. The most significant event was the Laramie Mountains, Wyoming, earthquake of October 18, 1984, which was located at 42.364°N., 105.692°W., magnitude 5.3 mb, 5.1 MS, and 5.5 ML. This earthquake and one on November 3, 1984, both in Wyoming, were the only damaging events for this period. Both had a maximum MM intensity of VI.

2. The earthquakes in the United States for the period October 1, 1984 through March 31, 1985, have been located and the hypocenters, magnitudes, and maximum intensities have been published in the Preliminary Determination of Epicenters.

Results

A maximum Modified Mercalli intensity of VI was assigned to the October 18, 1984, Laramie Mountains, Wyoming, earthquake. No major damage resulted from this event even though it was felt over an area of 287.000 km^2 of 7 states (fig. 1). The most severe damage was cracks in exterior brick walls in the Douglas and Medicine Bow, Wyoming area and a few cracked chimneys in Casper, Guernsey, Lusk, and Rock River, Wyoming. Other cities reporting minor damage were Hanna, McFadden, and Shirley Basin, Wyoming. This was the largest magnitude event to be located in eastern Wyoming.

United States Earthquakes, 1982, has received director's approval and will be published in U.S. Geological Survey Bulletin 1655.

Reports

Stover, C. W., 1984, United States earthquakes, 1981: U.S. Geological Survey Special Publication, 136 p.
Stover, C. W., 1984, Intensity distribution and isoseismal map for the Morgan Hill, California, earthquake of April 24, 1984, in the Morgan Hill, California, earthquake: California Department of Conservation, Division of Mines and Geology, Special Publication 68, p. 1-4.
Stover, C. W., 1985, Preliminary isoseismal map and intensity distribution for the Laramie Mountains, Wyoming, earthquake of October 18, 1984: U.S. Geological Survey Open-File Report 85-137, 9 p.
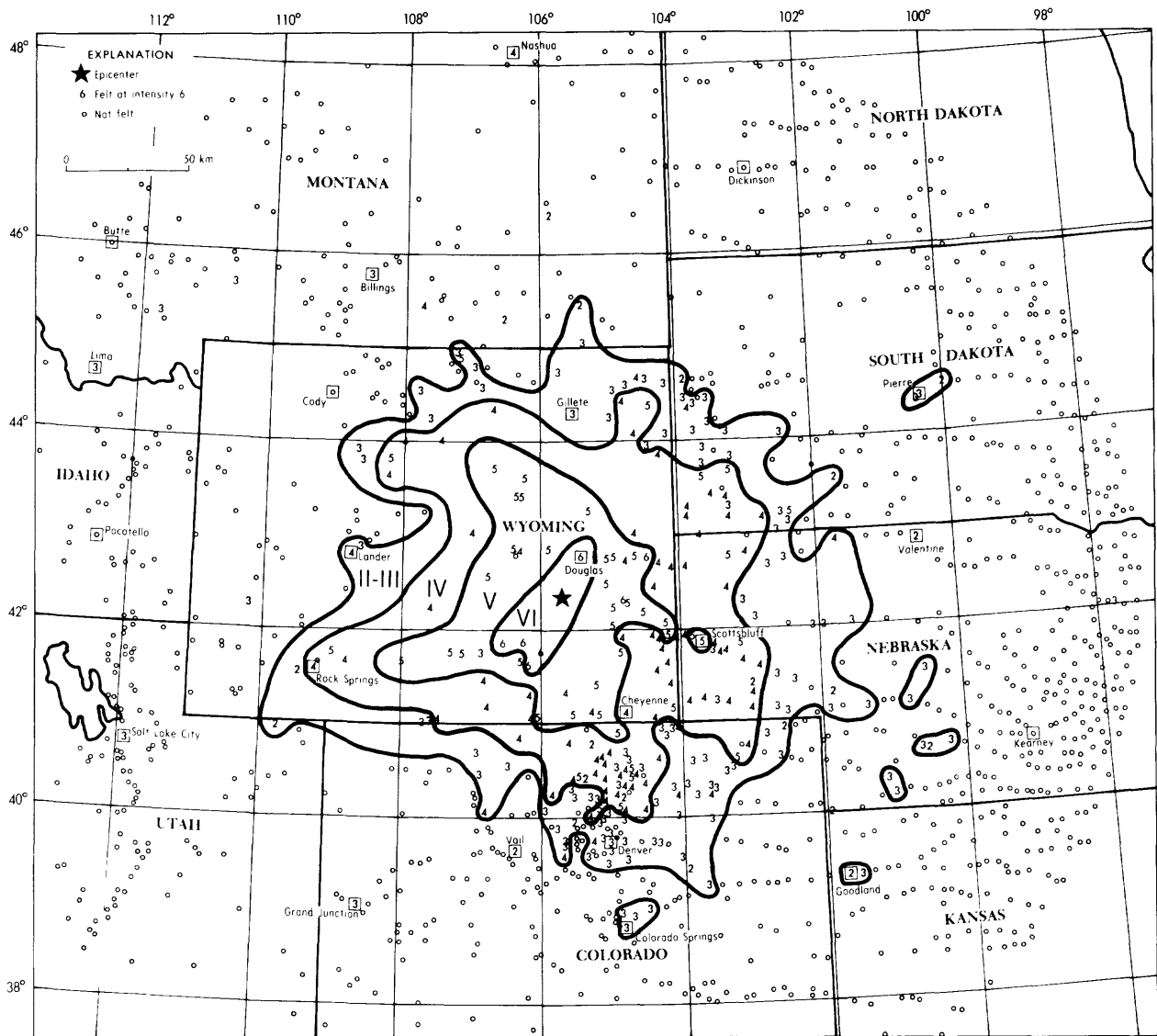
Figure 1.--Isoseismal map for the October 18, 1984 Laramie Mountains, Wyoming, earthquake.

Data Processing

5-9920-02217

John Hoffman
Branch of Global Seismology and Geomagnetism
U. S. Geological Survey
Albuquerque Seismological Laboratory
Building 10002, Kirtland AFB-East
Albuquerque, New Mexico   87115-5000
(505) 844-4637

Investigations

1. Data Management Center for the China Digital Seismograph Network: The data processing equipment required to process the digital tapes from the China Network is in its final stages of testing at the Albuquerque Seismological Laboratory. Most of the software has been written and tested, and the system should be forwarded to China within the next three months.

2. Data Processing for the Global Digital Seismograph Network: All of the digital data received from the Global Network and other contributing stations are reviewed and checked for quality.

3. Network-Day Tape Program: Data from the Global Network stations are assembled into Network-Day Tapes which are distributed to regional data centers and other Government agencies.

Results

1. Data Management Center for the China Digital Seismograph Network: All of the hardware has been purchased, and most of the software has been written to process the data for the China Network. There has been a problem with the 3-M cartridge tape drive systems, but that appears to be resolved. Several software drivers for some of the newer peripherals had to be written, and this has been completed. The complete system should be shipped to China within the next three months.

2. Data Processing for the Global Digital Seismograph Network: During the past six months 642 digital tapes (203 SRO/ASRO, 294 DWWSSN, and 145 RSTN) from the Global Network and other contributing stations were edited, checked for quality, corrected when feasible, and archived at the ASL. The Global Network is presently comprised of 11 SRO stations, 4 ASRO stations, and 15 DWWSSN stations. In addition, there are six contributing stations which include Glen Almond, Canada, plus the five RSTN stations which are supported by Sandia National Laboratories.

3. Network-Day Program: The Network-Day Tape Program is a continuing program which assembles all of the data recorded by the Global Digital Seismograph Network plus the contributing stations for a specific calendar day onto one magnetic tape. This tape includes all the necessary station parameters, calibration data, frequency response, and time correction information for each

station in the network. A sixth edition of the National Earthquake Information
Center Newsletter containing information on the Global Digital Seismograph
stations was distributed in December 1984. These newsletters are published
twice a year and copies are forwarded to all digital data users.

Reports

Newsletter:
Hoffman, J. P., R. Buland, and M. Zirbes, National Earthquake Information
   Center Newletter, December 1984, V. 3, No. 2, 8 pp., available from
   Albuquerque Seismological Laboratory, Albuquerque, New Mexico.

Seismic Review and Data Services

9920-01204

R. P. McCarthy
Branch of Global Seismology and Geomagnetism
U.S. Geological Survey
Denver Federal Center, MS 969
Denver, Colorado 80225
(303) 236-1513

Investigations and Results

Technical review and quality control were carried out on 506 station-months of seismograms from the World-Wide Standardized Seismograph Network (WWSSN). Seventy-five station-months of Seismic Research Observatory (SRO & ASRO) seismograms were provided to the National Earthquake Information Service (NEIS) for their PDE programs on a current basis. An average of thirty-six WWSSN current station-months were supplied monthly for the NEIS fault plane solution program. Under the cooperative WDC-A International Data Exchange (IDE), seismograms from the WWSSN sent for this program outside normal schedules were forwarded to the WDC-A covering three separate events.

Fifty-two annual Station Performance Reports have been completed. The remaining forty-four are in preparation. The overall standards remain consistently high. The timing systems generally operated below 50 milliseconds of error daily. Paper shortages at a few stations due to delivery problems were corrected. The Caico (CAI), Brazil and the Galapagos Islands (GIE) stations, the former replacing Natal (NAT), and the latter returning to operation after a two-year inactive period, have not forwarded any of their seismograms to date. Ninety-six WWSSN stations are operational, plus eight of questionable status.

The special filming project was resumed without any problems. Filming has just about been caught up. The monthly reports covering digital and analog seismograms received from the WWSSN, SRO, and ASRO networks were distributed to USGS, NOAA, and DOD officials and researchers. Information, advice, and consultations regarding WWSSN matters, other seismograph networks, archiving seismic data, World Data Center IDE events, and other special events of interest were carried out with The U.S. Geological Survey, other governmental agencies, universities, and private research groups.

Data Processing, Golden

9950-02088

Robert B. Park
Branch of Engineering Geology and Tectonics
U.S. Geological Survey
Box 25046, MS 966, Denver Federal Center
Denver, CO 80225
(303) 236-1638

Investigations

The purpose of this project is to provide the day-to-day management and
systems maintenance and development for the Golden Data Processing Center.
The center supports Golden-based Office of Earthquakes, Volcanoes, and
Engineering investigators with a variety of computer services. The systems
include a PDP 11/70, several PDP 11/03's and PDP 11/23's, a VAX/750, a VAX/780
and two PDP 11/34's. Total memory is 6.4 mbytes and disk space will be
approximately 3.4 G bytes. Peripherals include five plotters, ten mag-type
units, an analog tape unit, five line printers, 5 CRT terminals with graphics
and a Summagraphic digitizing table. Dial-up is available on all the major
systems and hardwire lines are available for user terminals on the upper
floors of the building. Users may access any of the systems through a Gandalf
terminal switch. Operating systems used are RSX11 (11/34's), Unix (11/70),
RT11 (LSI's) and VMS (VAX's).

The three major systems are shared by the Branch of Global Seismicity and
Geomagnetism and the Branch of Engineering Geology and Tectonics.

Results

Computation performed is primarily related to the Global Seismology and
Hazards programs; however, work is also done for the Induced Seismicity and
Prediction programs as well as for DARPA, ACDA, MMS, U.S. Bureau of
Reclamation and AFTAC, among others.

In Global Seismology and Geomagnetism, the data center is central to nearly
every project. The monitoring and reporting of seismic events by the National
Earthquake Information Service is 100 percent supported by the center. Their
products are, of course, a primary data source for international seismic
research and have implications for hazard assessment and prediction research
as well as nuclear test ban treaties. Digital time series analysis of Global
Digital Seismograph Network data is also 100 percent supported by the data
center. These data are used to augment NEIS activities as well as for
research into routine estimation of earthquake source parameters. The data
center is also intimately related to the automatic detection of events
recorded by telemetered U.S. stations and the cataloging of U.S. seismicity,
both under development.

In Engineering Geology and Tectonics, the data center supports research in assessing seismic risk and the construction of national risk maps. It also provides capability for digitizing analog chart recordings and maps as well as analog tape. Also, most, if not all, of the research computing related to the hazards program are supported by the data center.

The data center also supports equipment for online digital monitoring of Nevada seismicity. Also, it provides capability for processing seismic data recorded on field analog and digital cassette tape in various formats. Under development is a portable microprocessor-based system to be used by the field investigations group to do preliminary analysis and editing of temporary local networks and the GOES Satellite Event Detect System. Recent acquisitions include the VAX/750, laser plotter, three additional tape drives, two HP plotters, DECNET/ETHERNET, and 800 MB of disk storage. A VAX-based accounting system has been developed for an up-to-date reporting capability on branch projects.

National Earthquake Information Center

9920-01194

Waverly J. Person
Branch of Global Seismology and Geomagnetism
U.S. Geological Survey
Denver Federal Center, MS 967
Denver, Colorado 80225
(303) 236-1500

Investigations and Results

The weekly publication, Preliminary Determination of Epicenters (PDE), continues to be published, averaging about 80 earthquakes per issue. The PDE Monthly Listing and Earthquake Data Report (EDR) continue to be prepared on the VAX/1180, with very little down time encountered.

Quick Epicenter Determinations (QED) became available in November to individuals and groups having access to a 300-baud terminal with dial-up capabilities to a commercial telephone number in Golden, Colorado. The time period of data available in the QED is approximately 3 weeks--from about 2 days behind real time to the current PDE in production. The QED program is available on a 24-hour basis, 7 days a week.

We continue to receive telegraphic data from the USSR in a very timely manner on magnitude 6.5 or greater earthquakes and some smaller damaging earthquakes in the USSR and bordering countries. Data from the People's Republic of China via the American Embassy are also being received in a very timely manner and in time for the PDE publication. We continue to receive 4 stations on a weekly basis from the State Seismological Bureau of the People's Republic of China and about 22 by mail, which are in time for the Monthly. We have rapid data exchange (alarm quakes) with Centre Seismologique European-Mediterranean (CSEM), Strasbourg, France and Instituto Nazionale de Geofisica, Rome, Italy and data by telephone from Mundaring Geophysical Observatory, Mundaring, Western Australia.

The Monthly Listing of Earthquakes is up to date. As of March 31, 1985, the Monthly Listing and Earthquake Data Report (EDR) were completed through November 1984. A total of 5,320 events were published for the 6-month period; for the calendar year 1984, 10,528 events were published. During 1984, we received 619,459 readings groups from 1,785 stations throughout the world. This compares with 581,453 groups from 1,736 stations during 1983. Fault plane solutions continue to be determined when possible and published in the monthly listing and EDR for any earthquake having an mb magnitude $\geq$ 5.8. Centroid moment tensor solutions from Harvard University continue to be published in the Monthly Listing and EDR. Moment tensor solutions are being computed by the U.S. Geological Survey and are also published in the above publications. Waveform plots are being published for selected events having mb magnitudes $\geq$ 5.8.

The Earthquake Early Alerting Service continues to provide information on recent earthquakes on a 24-hour basis to the OEVE, scientists, news media, other government agencies, foreign countries, and the general public. Forty-eight releases were made from October 1, 1984 through March 31, 1985. The largest earthquake released during this time was a magnitude 7.8MS on March 3, 1985 near the coast of central Chile. In the United States, the largest earthquakes were a magnitude 5.5 on October 18, 1984 in Wyoming, a 6.0 on March 9, 1985 in Alaska, and a 6.3 on March 13, 1985 off the coast of Oregon.

Reports

Preliminary Determination of Epicenters (PDE)
  26 weekly publications from October 4, 1984 to March 28, 1985--Numbers 37-84 through 10-85. Compilers: W. L. Irby, Willis Jacobs, John Minsch, W. Person, B. Presgrave, W. Schmieder.
Monthly Listing of Earthquakes and Earthquake Data Reports (EDR)
  6 publications from June 1984 through November 1984. Compilers: W. Irby, Willis Jacobs, John Minsch, R. Needham, W. Person, B. Presgrave, W. Schmieder.
Seismological Notes, BSSA, Waverly J. Person
  Vol. 74, No. 5--November-December 1983; Vol. 74, No. 6--January-February 1984; Vol. 75, No. 1--March-April 1984; Vol. 75, No. 2--May-June 1984.
Earthquake Information Bulletin "Earthquakes," Waverly J. Person
  Vol. 16, No. 4--November-December 1983; Vol. 16, No. 5--January-February and March-April 1984; Vol. 16, No. 6--May-June 1984.

National Earthquake Catalog

9920-02648

J. N. Taggart
Branch of Global Seismology and Geomagnetism
U.S. Geological Survey
Denver Federal Center, MS 967
Denver, Colorado 80225
(303) 236-1506

Investigations

1. Assembled, annotated, and evaluated references (mostly in Spanish) on historical seismicity in Mexico.
2. Began an investigation of path-dependent attenuation of L_g waves.

Results

1. Through interlibrary loans, Carol Thomasson has obtained and annotated references, mostly in Spanish, on historical seismicity in Mexico. Several of the references are reprinted chronicles of the Colonial, Early Republic, and Imperial periods, generally written by priests, which contain brief descriptions of seismic damage to churches and public buildings. The purpose of the investigation is to identify possible recurrence among major earthquakes in the historical record and to provide data for the seismicity map of the Geological Society of America's DNAG Project.
2. Singh and Herrman (1983) suggest that values of short-period coda Q and intrinsic Q_β appear to be similar and that code Q may be useful in the estimation of the path-dependent attenuation of L_g waves. Using their map of coda Q for the United States, Taggart developed a geographic grid of γ_0 values, the coefficient of anelastic attenuation of 1.0 Hz L_g waves. Interpolated at intervals along paths as great as 30°, the grid everywhere yields stable averages of γ_0 from six or more samples per path. A frequency dependent Q model of Singh and Herrmann (1983) was combined with averaged grid values of γ_0 to obtain path-dependent estimates of L_g magnitudes for earthquakes throughout the United States. Preliminary results suggest that very little adjustment to the grid will be necessary in the eastern United States. Data collection is in progress for an evaluation of the procedure when applied to earthquakes in the western United States.

References

Herrmann, B., and Kijko, A., 1983, Short-period L_g magnitudes: Instrument, attenuation, and source effects: Bulletin of the Seismological Society of America, v. 73, p. 1835-1850.
Singh, S., and Herrmann, R. B., 1983, Regionalization of crustal Q in the continental United States: Journal of Geophysical Research, v. 88, p. 527-538.

Strong Motion Data Management

9910-02757

A.G. Brady
Branch of Engineering Seismology and Geology
U.S. Geological Survey
345 Middlefield Road, MS 977
Menlo Park, California 94025
(415) 323-8111, ext. 2881

Investigations

Research using analytical test records continues in cooperation with digitizing and processing groups in Europe, within the European Association of Earthquake Engineering.

Results

Routine digitizing (indicated by (D)) and computer processing (indicated by (P)) of strong motion earthquake recordings continues: 8 records (P) explosive test for soil/structure interaction, July-August 1984; 2 records (D) downhole from McGee Creek, Mammoth Lakes, 23 November 1984; 2 records (D) for digitizing and processing test with EAEE; 3 records (P) Monasavu Dam, Fiji, February 1983; 5 records (P) Bougainville Island, Papua New Guinea, 1981 and 1983; 5 records (P) Coalinga aftershock July 9, 1983 074UTC.

Reports

Silverstein, B., and Brady, A.G., 1984. Data processing for the Coalinga aftershock of July 22, 1983 0239 UTC: *U.S. Geological Survey Open-File Report 82-250.*

Silverstein, B.L., 1985. Processed strong-motion records from the Solomon Islands Earthquakes of December 13, 1981 and March 18, 1983: *U.S. Geological Survey Open-File Report 85-261.*

Silverstein, Barry, 1985. Processed strong-motion records from Monasavu Dam, Fiji; Earthquakes of February 13, 14, and 23, 1983: *U.S. Geological Survey Open-File Report 85-* (in press).

NATIONAL STRONG-MOTION NETWORK
DESIGN, DEVELOPMENT, AND OPERATIONS
9910-02763, 02764, 02765

R.P. Maley and E.C. Etheredge

Branch of Engineering Seismology and Geology
U.S. Geological Survey
345 Middlefield Road, MS 977
Menlo Park, California 94025
(415) 323-8111, ext. 2881

Investigations

The Strong-Motion laboratory, in concert with several federal, state, and local agencies and advisory engineering committees, designs, develops, and operates an instrumentation program in 41 states and Puerto Rico. Program goals include: (1) recording of potentially damaging ground motion in regional networks and in closely spaced sensor arrays; and (2) monitoring the structural response of buildings, bridges and dams with sensors placed in critical locations. The present coordinated network consists of more than 1,000 recording units installed at approximately 600 ground sites, 52 buildings, 5 bridges, 54 dams, and 2 pumping plants.

Among the ground motion arrays developed are: (1) digital recording surface arrays 305 to 610 meters long with up to 7 triaxial accelerometers located along these short baselines (Figure 1); (2) liquefaction arrays designed to simultaneously monitor transient changes in pore pressure and ground acceleration utilizing vertically aligned downhole transducers; and (3) a 21-channel downhole system of acceleration and velocity transducers set at depths up to 165 meters near Mammoth Lakes, California.

Recent structural arrays completed:

1. Three-dimensional arrays at earth fill dams combining surface and downhole accelerometers (Figure 2);
2. A 39-channel system used to record ground and building response data on and near a 7-story steel frame building (Figure 3);
3. A 27-channel system installed in the tallest ductile concrete frame building in the San Francisco area (30 stories);
4. Instrumentation installed on a 122-meter bridge span (Figure 4).

Twenty-eight ground stations were established in California, Washington, Hawaii, and Alaska. These new stations constitute additions to existing local networks including those integrated with extensive structural monitoring systems.

Results

A series of earthquakes, beginning with a magnitude 5.8 event on November 23, 1984, were recorded by downhole acceleration/velocity transducers installed near Mammoth Lakes (McGee Creek) only a few days earlier. Peak accelerations recorded at the surface measured .10 g to .12 g for the two largest events,

considerably amplified over that recorded at 35 meters in glacial moraine and at 165 meters in bedrock. These accelerograms represent the first obtained by this group among the many downhole sytems presently being operated.

A 13-story building was instrumented in Berkeley, California relying on extensive analysis of ambient vibration recordings to select appropriate transducer locations within the structure. The recording plan and analyses will be presented in a forthcoming U.S. Geological Survey report by Sotoudeh (Stanford University) and Brady (USGS). This technique has been developed for application to specific structural response studies being conducted in California and in other selected earthquake prone areas.

More than 50 accelerograms were recovered and processed for inclusion into the SMIRS data base.

Reports

Archuleta, R.J. (University of California, Santa Barbara), Gibbs, J., Etheredge, E., Sena, J., Warrick, R., and Borcherdt, R., 1985, Downhole measurements of strong ground motion [abs.]: *Seismological Society of America Annual Meeting*, Austin, Texas.

Maley, R.P., and Etheredge, E.C., 1984, The development of ground and structural response strong-motion instrumentation arrays in the United States: *Eighth World Conference on Earthquake Engineering*, San Francisco, California, 8 p.
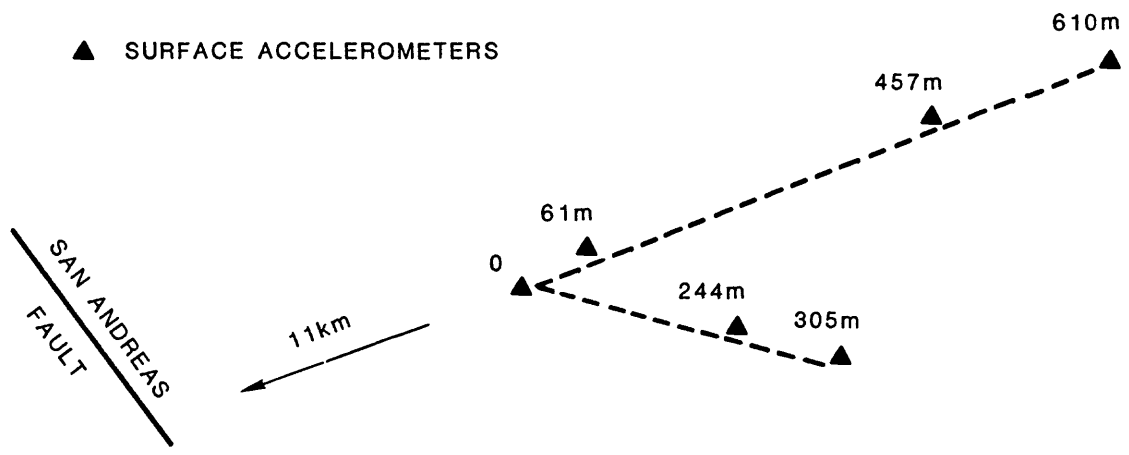
Figure 1.- The Hollister, California Differential Array.
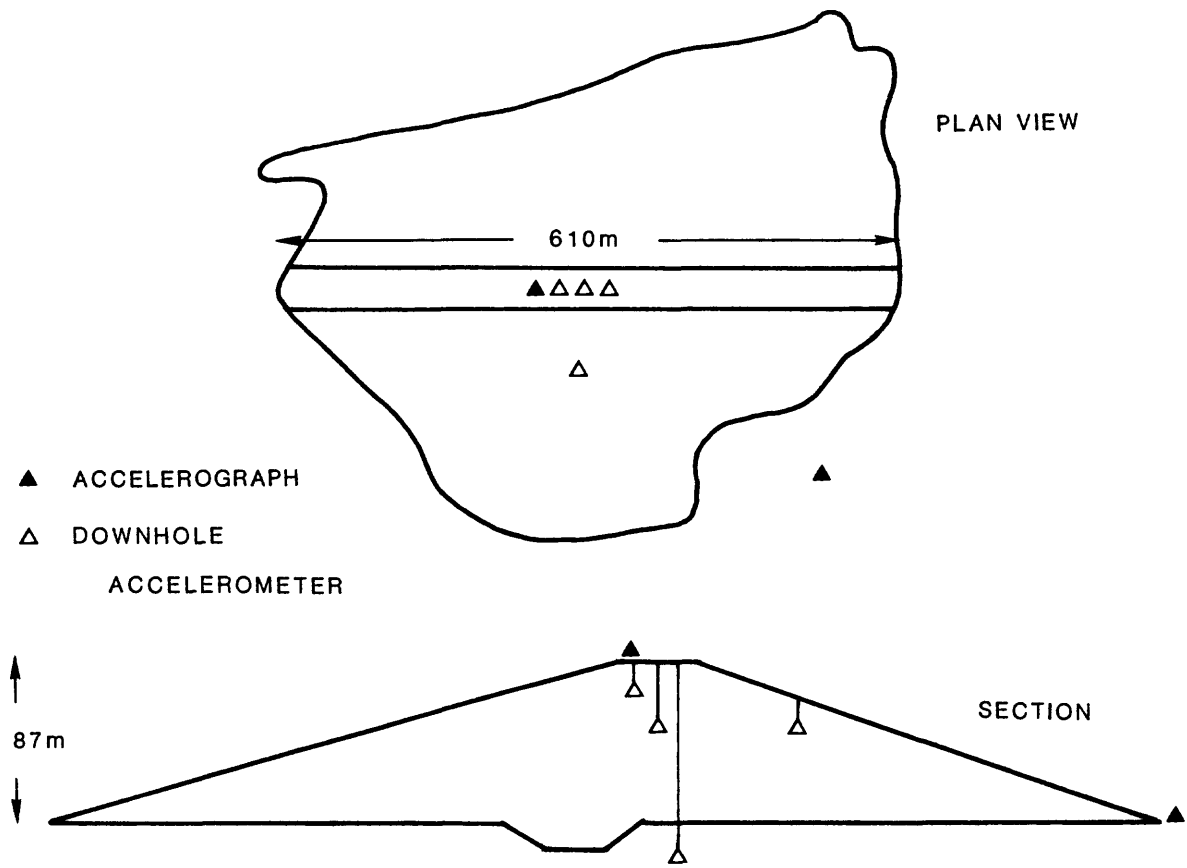
Figure 2.- Instrumentation at Casitas Dam, California.

35m

PLAN VIEW UPPER FLOOR

FOURTH
FLOOR ONLY

8m

PLAN VIEW BASEMENT

41m

CAISSON

141m

SITE PLAN WITH
FREE-FIELD ACCELEROGRAPHS

NEW BLDG

OLD BLDG

● → SINGLE AXIS
ACCELEROMETER

▲ TRIAXIAL
ACCELEROMETER
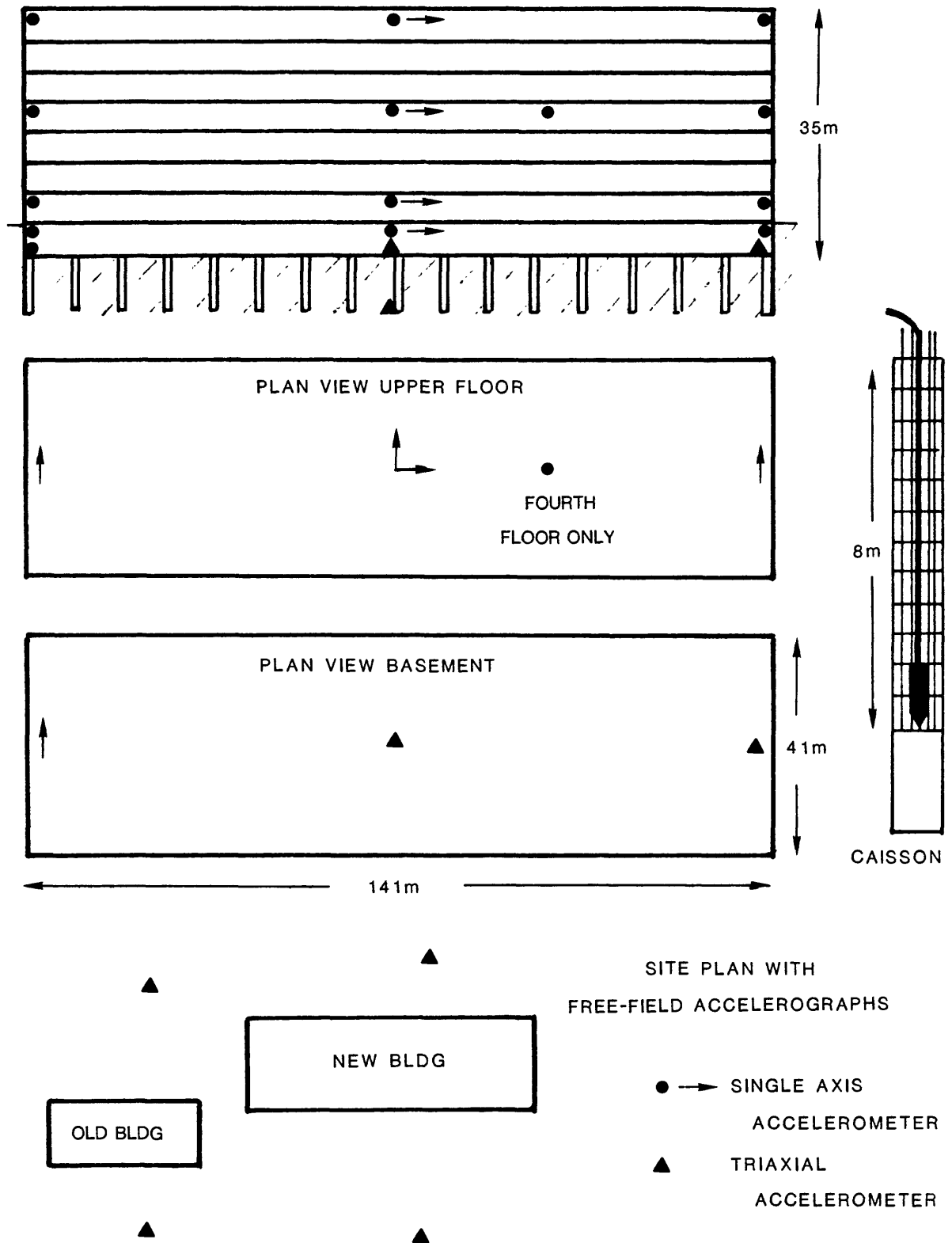
Figure 3.- Strong-motion system, 7 story building near Los Angeles.

SINGLE AXIS ACCELEROMETER

TRIAXIAL ACCELEROMETER

PLAN VIEW

SECTION

122m

5.4 m
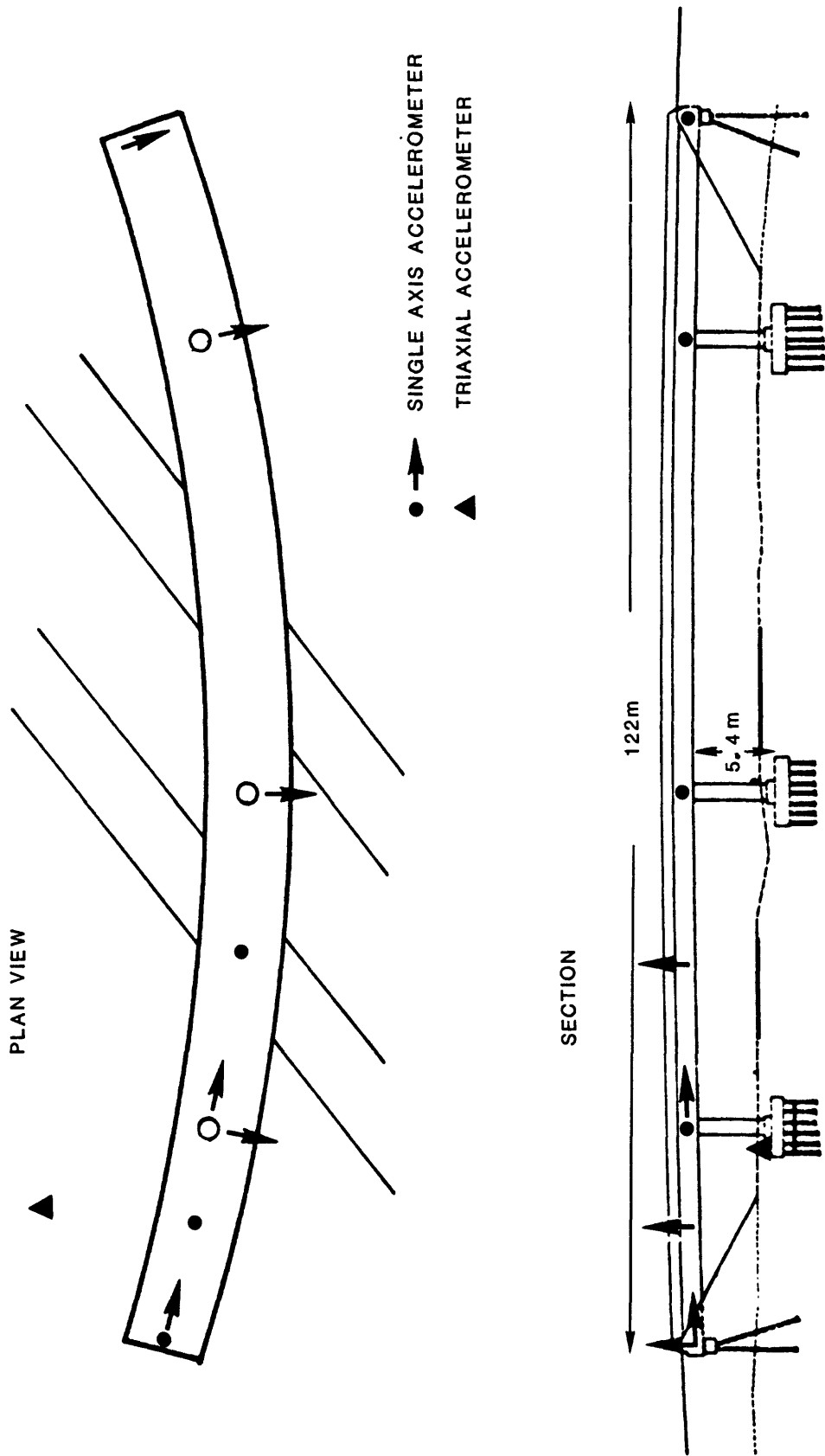
Figure 4.- Instrumentation on the Bellingham, Washington overcrossing.

Physical Constraints on Source of Ground Motion

9910-01915

D. J. Andrews
Branch of Engineering Seismology and Geology
U.S. Geological Survey
345 Middlefield Road, MS 977
Menlo Park, California 94025
(415) 323-8111, ext. 2752

Investigations

Application of the diffusion equation to scarp degradation.

Separation of site effects from spectra of recorded ground motion and an objective method to determine source parameters.

Results

Synthetic modeling of diffusive scarp degradation was completed and a paper was written. The inverse method, based on an objective measure of mean square horizontal extent of a scarp profile, was applied to Lahontan shoreline scarps, and showed apparent diffusion age increasing with scarp height. This requires either a rather small initial scarp slope or, more likely, that diffusive mass flux is a non-linear function of ground slope.

In mid-March I returned my attention to analysis of digital ground motion records from the 1980 Mammoth Lakes earthquake sequence. The objective is to find accurate values of source parameters by an objective methodology, taking into account local site effects. Recent work confirms earlier conclusions that dynamic stress drops are independent of corner frequency (and hence source radius). Ratios of Hanks dynamic stress drop to Brune static stress drop cluster tightly around the value 1, and are independent of corner frequency. This indicates that spectral shape does not vary with source radius. This is striking evidence of similarity of earthquakes of different size.

Reports

Andrews, D. J. and T. C. Hanks, 1985, Scarp degraded by linear diffusion: inverse solution for age, submitted to Journal of Geophysical Research.

Soil-Structure and Structural Response Studies

9910-02760

A.G. Brady and G.N. Bycroft

Branch of Engineering Seismology and Geology
U.S. Geological Survey
345 Middlefield Road, MS 977
Menlo Park, California 94025
(415) 323-8111, ext. 2881

Investigations

1. ## Instrumentation of San Francisco Bay Area Structures.

    The dynamic study of the Great Western building in Berkeley and the resultant permanent instrumentation have been completed and a report has been prepared. Work proceeds on this project in cooperation with the Blume Center for Earthquake Engineering at Stanford.

2. ## Time Dependent Structural Response.

    Current results justify the assumptions made regarding the displacements attained by structures exhibiting elasto-plastic force displacement characteristics and the displacements attained by structures with unlimited elastic capacity.

3. ## Soil Structure Interaction and Differential Ground Motion.

    The data from the experiments conducted with S.R.I. International at Camp Parks, California was analyzed and compared favorably with analytical predictions. A paper was written on the results. These results are important for correcting seismograms for the effects of soil structure interaction. Research continued on the effect of soil structure interaction and differential ground motions on the behavior of structures.

4. ## Analysis of Bridge Records.

    Fifteen channels of acceleration data were obtained from a 3-span freeway bridge during the Morgan Hill earthquake of April 24, 1984. An investigation was carried out to ascertain the behavior of the bridge, and to verify that a sudden spike in the records obtained within the box girder at the abutment end was not associated with any damage.

Reports

Bycroft, G.N., 1985, Tests of soil structure interation theory: *Bulletin, Seismological Society of America,* in press.

Sotoudeh, V., and Brady, A.G., 1985, Dynamic study of the Great Western Building, Berkeley, California: *U.S. Geological Survey Open-File Report 85-* , in press.

Celebi, M., and Brady, A.G., 1985, Earthquake performance of a bridge deck and abutment: *Second International Conference on Soil Dynamics and Earthquake Engineering,* New York, June 28-July 3, 1985.

Strong Ground Motion Prediction in
Realistic Earth Structures

9910-03010

P. Spudich
Branch of Engineering Seismology and Geology
U.S. Geological Survey
345 Middlefield Road, MS 977
Menlo Park, California 94025
(415) 323-8111, ext. 2395
October 1, 1984 to March 31, 1985

Investigations

1. Analysis of the strong motion records from the 1984 Morgan Hill earthquake.

2. Preliminary design of a short-baseline two-dimensional accelerometer array for installation at Parkfield, California, for the observation of earthquake rupture dynamics.

Results

1. The Morgan Hill earthquake of April 24, 1984 (M_L = 6.2) occurred on the Calaveras fault and was well recorded by CDMG and USGS strong motion stations. We have used a fast asymptotic technique developed by Spudich and Frazer (*BSSA*, 1984) to calculate synthetic acceleration and velocity seismograms for stations close to the fault. A realistic laterally homogeneous crustal velocity model is used in the calculations. Theoretical seismograms are compared with the corrected acceleration and velocity data in an attempt to model the slip history on the fault, using the aftershock distribution, the instrumental hypocenter, and the geodetic estimate of the moment for a starting model. The location of the hypocenter at the northwest end of the aftershock zone suggests that rupture was primarily unilateral towards the southeast. The strong motion data indicate considerable heterogeneity in the rupture process, and a laterally varying velocity structure. If rupture propagation is unilateral to the southeast, the large late pulse at the Hall's Valley station is of anomalously large amplitude. It is possible that the low velocity zone in the fault acts as a waveguide for this station and may act similarly for the Coyote Creek and Gilroy 6 stations.

2. The successful observation of rupture propagation using a 213-m-long line of accelerometers (Spudich and Cranswick, *BSSA*, December 1984) has motivated us to investigate the feasibility of using frequency-wave-number (f-k) processing of data from a two-dimensional array of accelerometers to observe rupture propagation. In a hypothetical test, we placed 21 array elements in a 3 km^2 region located 6 km away from a 6 x 10 km fault. We perform f-k analysis on sequential time windows of the array data. For each 0.6-s-long window, the power distribution in f-k space is converted into the frequency-slowness domain. Each point in the slowness plane corresponds to a seismic ray incident upon the array with known angle of incidence and azimuth of approach. By using ray-tracing, each

ray is projected back onto its point of origin on the fault, yielding a snapshot of the power radiated from the rupturing fault for each time window. The expanding rupture can be seen in the sequence of snapshots. We plan to install a dense array of accelerometers in the Parkfield, California, region to record the next major Parkfield earthquake, and we hope to use this technique to observe its rupture propagate.

Reports

Beroza, G., Spudich, P., and Cormier, V., 1984, Modeling rupture of the Morgan Hill earthquake using near field data, *EOS*, **65**, p. 1004.

Spudich, P., and Oppenheimer, D., 1984, Imaging earthquake rupture by using dense accelerometer arrays, *EOS*, **65**, p. 1005.

Aftershock Investigations and Geotechnical Studies

9910-02089

Richard E. Warrick
Eugene D. Sembera

Branch of Engineering Seismology and Geology
345 Middlefield Road, MS 977
Menlo Park, CA 94025
(415) 323-8111, ext. 2757

Investigations

1. The development of techniques for the improvement of field data acquisition, specifically in the application of triggered digital recording systems to aftershock studies.

2. Improvement in the methods used in generating recording, and interpreting shear waves in downhole surveys.

Results

1a. Field testing of the GEOS systems continue with these deployments:

Maine experiments, October 1984 (Boatwright, Cranswick, and Sembera).

Chile earthquake aftershocks, March 1985 (Algermissen, Celebi, and Sembera).

1b. The DR-100 recorders were used in the continuing Anza experiment: January 1985 on (Fletcher, Sembera, and Haar).

1c. The maintenance facility for the GEOS systems was set up by J. Sena, who together with G. Jensen, R. McClearn, C. Dietel, G. Maxwell, and C. Criley are cooperatively proceeding with the building of new systems and the debugging of existing units.

1d. The downhole and surface instrumentation was installed at the McGee Creek site and recording of nearby earthquakes were made on GEOS and CRA-1 recorders (Archuleta, Gibbs, Sena, Etheredge, Salsman, Roth, and Forshee).

2a. Plans for a power driven shear wave generator were completed and construction of a prototype is underway (H.-P. Liu, and Westerlund).

Reports

Borcherdt, R.D., Fletcher, J.B., Jensen, E.G., Maxwell, G.L., VanSchaack, J.R., Warrick, R.E., Cranswick, E., Johnston, M.J.S., and McClearn, R., 1985, A general earthquake observation system (GEOS): submitted *Bulletin, Seismological Society of America.*

Mueller, C.S., Sembera, E., and Wennerberg, L., 1984, Digital recordings of aftershocks of the May 2, 1983 Coalinga, California earthquake: *U.S. Geological Survey Open-File Report 84-697*, 57 p.

Late Pleistocene-Holocene Soil Chronology for
Evaluating Tectonic Framework and Events

14-08-0001-21829

Edward A. Keller
Department of Geological Sciences
University of California
Santa Barbara, California 93106
(805) 961-4207

D. L. Johnson
Department of Geography
University of Illinois
Urbana, Illinois 61801
(217) 333-0589

T. K. Rockwell
Department of Geological Sciences
California State University
San Diego, California 92182
(619) 265-4441

Objective: 1) Develop a chronology for Holocene and late Pleistocene deposits based upon relative development of soils; and 2) apply the chronology to evaluate late Pleistocene and Holocene tectonic framework and events in three study areas: 1) Wheeler Ridge south of Bakersfield, California; 2) the northern front of the San Emigdio Mountains west of Wheeler Ridge, and 3) Frazier Mountain near Gorman, California.

Investigations: The primary task is the development of soil chronosequences for the three study areas. A secondary activity is the application of the soil chronosequence work to develop preliminary rates of uplift associated with folding on the upper plates of concealed reverse faults.

Results and Discussion: Approximately fifty soil profiles in the study areas have been described and sampled. Soil samples are being analyzed at the soils laboratory of the University of New Mexico for particle size and determination of carbonate content.

Soils in the Frazier Mountain area vary from young A-C profiles with minimum development to well developed soils with argillic B horizons; 5YR 5/6, pebbly clay loam, moderate angular blocky structure, and many medium, continuous clay films. These B horizons extend to a depth of several meters and overlie a horizon with calcium carbonate coated pebbles. High geomorphic surfaces on the southeast side of Frazier Mountain have apparent anomalously weakly developed soils compared to the soils on the high surfaces on the northwest side of the mountain.

Soils on the north flank of the San Emigdio Mountains also vary from weak A-C profiles to soils with well developed argillic B horizons with up to Stage IV calcic horizons (Table 1).

Table 1

Generalized soil characteristics for the north front of the San Emigdio Mountains.

Geomorphic Surface	Soil Thickness (cm)	B Horizon					Carbonates	Approximate Age
		Type	Color	Texture	Structure	Clay Films		
Q_1	50-68	A-C Profile, primary fluvial stratification					Weak Stage I	Historic(?)
Q_2	100-191+	A-C Profile, primary fluvial stratification					Stage I	700 RYBP
Q_3	130+	Cambic	10YR 3/3 m	loamy sand - silty clay loam	massive-strong coarse, pris-matic	None	Stage II	<6360 RYPB
Q_4	250+	Argillic	7.5YR 4/6 m	sandy clay loam	coarse, angular blocky	Many, thick, continuous	Stage IV	Late Pleistocene

Soils on Wheeler Ridge (Table 2) are similar to those of the San Emigdio Mountains, varying from A-C profiles to soils with well developed argillic B horizons and carbonate (K) horizons. The stage of carbonate development in K horizons is one of the most distinguishing characteristics of the soils at Wheeler Ridge. The youngest soils are A-C profiles and as the soil development becomes stronger the carbonates increase from Stages I through IV.

Age control for the Holocene soils in the study areas come from ^{14}C dates on charcoal or carbonate rinds from clasts in the calcic horizons. Absolute dates on the late Pleistocene and older soils are crucial to the tectonic interpretation but are more difficult to obtain. We are attempting uranium-thorium (U series) dates on three samples. The presence of abundant carbonate coatings on many of the clasts is encouraging, and we are hopeful that we will be able to successfully date the older geomorphic surfaces.

Interpretation of the tectonic framework based on limited soil chronology and radiocarbon dates in the San Emigdio Mountains and Wheeler Ridge areas suggests several hypotheses. First, Wheeler Ridge is an active anticline growing at a measurable rate to the east. Uplift, tilting, and faulting associated with the growth of Wheeler Ridge is denoted by soils on geomorphic surfaces that are higher and older to the west of the eastern terminus of the anticlinal structure (Figure 1). Absolute dates on two of the younger surfaces being actively folded (Figure 2) suggest that the uplift rate is approximately 0.5 to 2.0 mm/yr.

The Los Lobos folds are anticlinal uplifts located 15 km to the west of the central part of Wheeler Ridge. The folds are active and Figure 3 shows several radial profiles for the San Emigdio Creek alluvial fan. Figure 4 shows the profile of an abandoned Holocene channel ([14]C < 6360 ± 280 ybp) which is on a fan segment that crosses the Los Lobos folds. This profile suggests that during the last 6,000 years the rate of uplift has been at least 0.33 mm/yr. The true uplift rate is likely to be greater as the ^{14}C date is for a buried "A" horizon of a well developed late Pleistocene soil folded over the Los Lobos fold. The Holocene channel is cut in materials that overlie this buried "A" horizon and the true age of the channel must be younger, giving a greater rate of uplift. Charcoal from the younger deposits has been collected and submitted for age determination.

Mountain fronts of the San Emigdio Mountains have migrated north during the Pleistocene, thrusting these mountains over the Piedmont alluvial fans at the southern end of the San Joaquin Valley, as suggested by Davis (1983). Figure 5 shows a cross-section from the San Emigdio Mountains to the San Joaquin Valley. Of particular importance is the late Pleistocene paleosol that is folded north of the White Wolf-Wheeler Ridge fault system which deforms the Pleistocene gravels. We are hopeful that a U-series date on the paleosol will provide better constraint on the rate of uplift of the Los Lobos fold, which we expect is related to the seismic history of the San Emigdio front at this area.

Reference Cited

Davis, T. L., 1983. Late Cenozoic structure and tectonic history of the western "Big Bend" of the San Andreas fault and adjacent San Emigdio Mountains. Unpublished Ph.D. dissertation, University of California, Santa Barbara.

Table 2

Wheeler Ridge: Geomorphic surfaces and soil chronosequence.

Geomorphic Surface	Soil Thickness (cm)	B Horizon					Carbonates	Approximate Age	Approximate Elevation
		Type	Color	Texture	Structure	Clay Films			
Q1	50-80	A-C Profile, primary fluvial stratification					Weak Stage 1	7000 (14_C)	300
Q2	240+	Argillic	10YR 4/4 m	Gravelly sandy loam - sandy clay loam	Moderate coarse subangular blocky	Few very thin to moderately thick	Stage I - II	12000 (14_C)	320
Q3	270+	Argillic	10YR 4/4 m	Clay loam to sandy clay loam	Weak medium sub-angular blocky	Common, moderately thick	Stage II	Late Pleistocene	330
Q4	307+	Argillic	7.5YR 4/6 m	Very gravelly sandy clay loam	Massive breaking to fine subangular blocky	Many to continuous thin to moderately thick	Stage II-III	Late Pleistocene	410
Q5	N/A	B Horizon stripped					Stage IV	Mid-Late Pleistocene	590
Q6	N/A	B Horizon stripped					Stage IV	Mid-Late Pleistocene	635
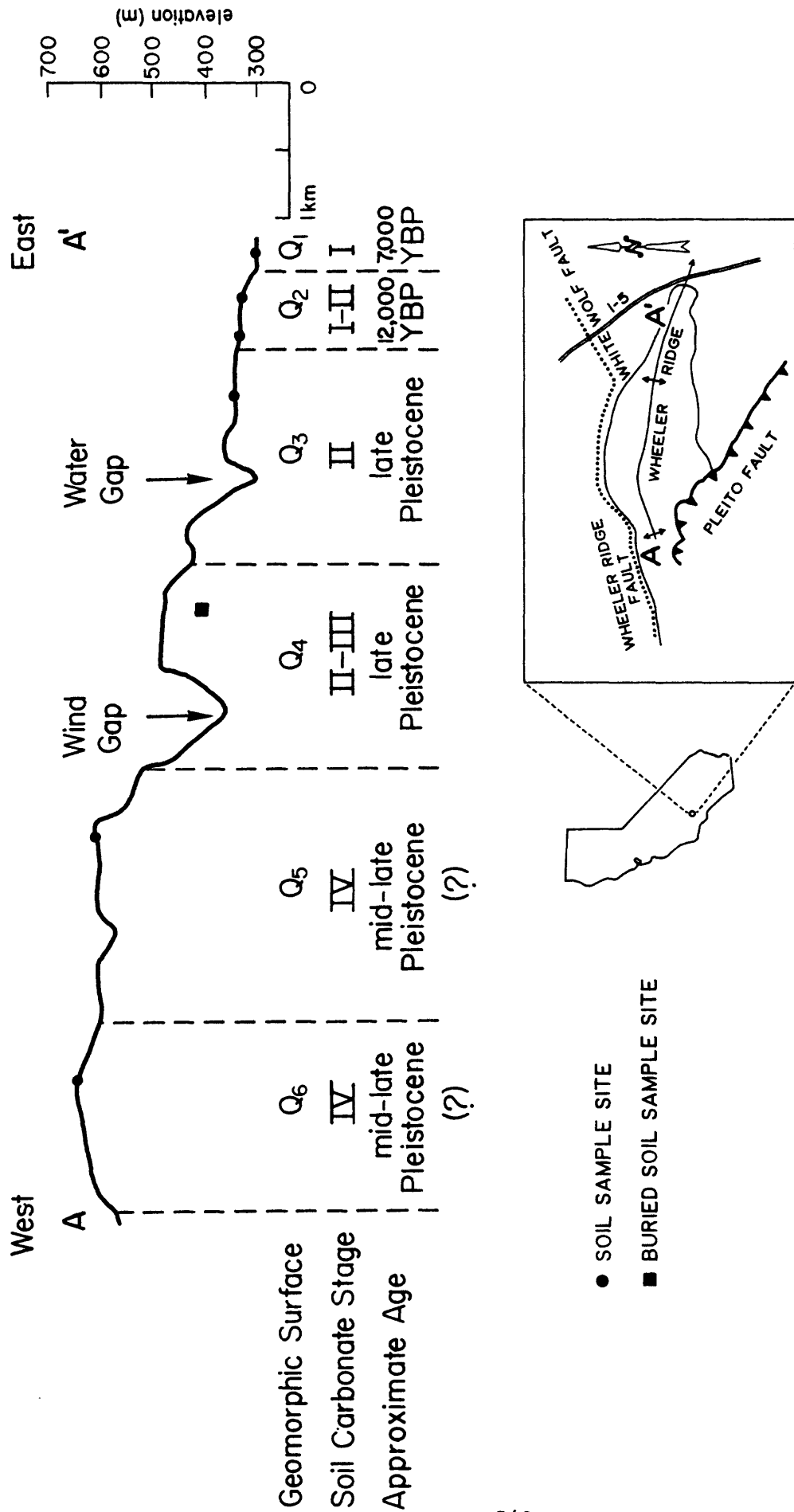
Figure 1. Geomorphic surfaces and soil sample sites along the crest of Wheeler Ridge.
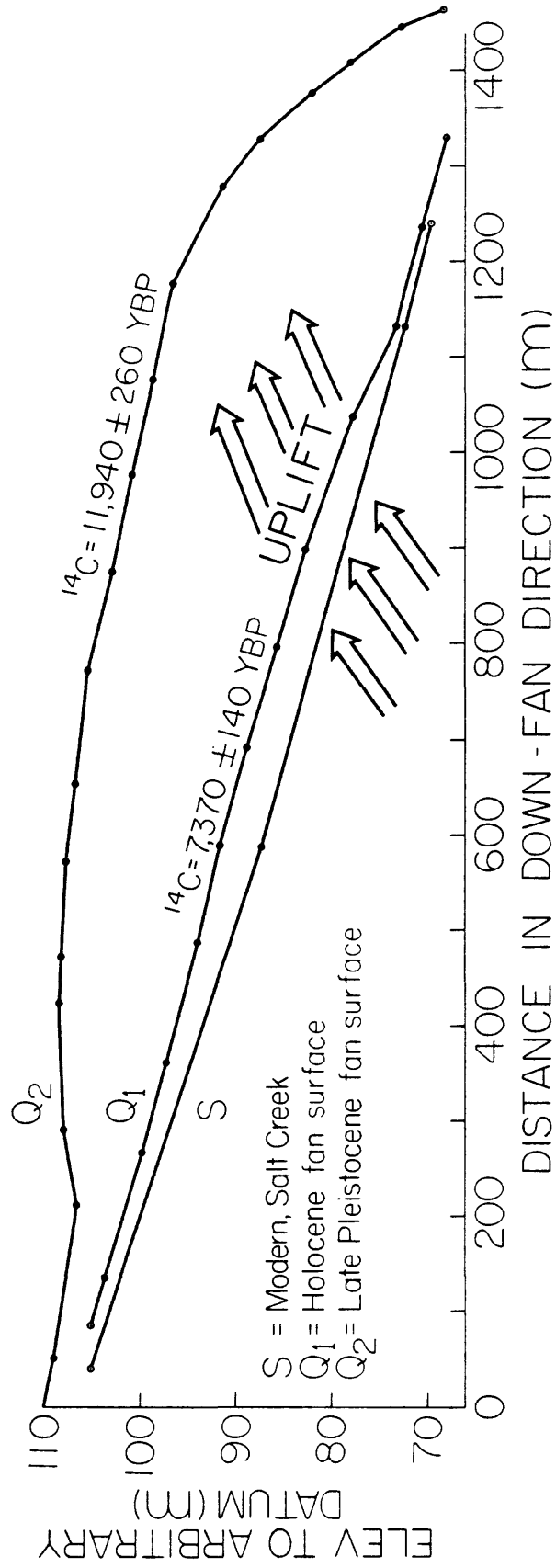
Figure 2. Folded fan segments at the eastern end of Wheeler Ridge.

S = Modern, Salt Creek
Q_1 = Holocene fan surface
Q_2 = Late Pleistocene fan surface

^{14}C = 11,940 ± 260 YBP

^{14}C = 7,370 ± 140 YBP

UPLIFT

Q_2

Q_1

S

ELEV TO ARBITRARY DATUM (m)

DISTANCE IN DOWN-FAN DIRECTION (m)
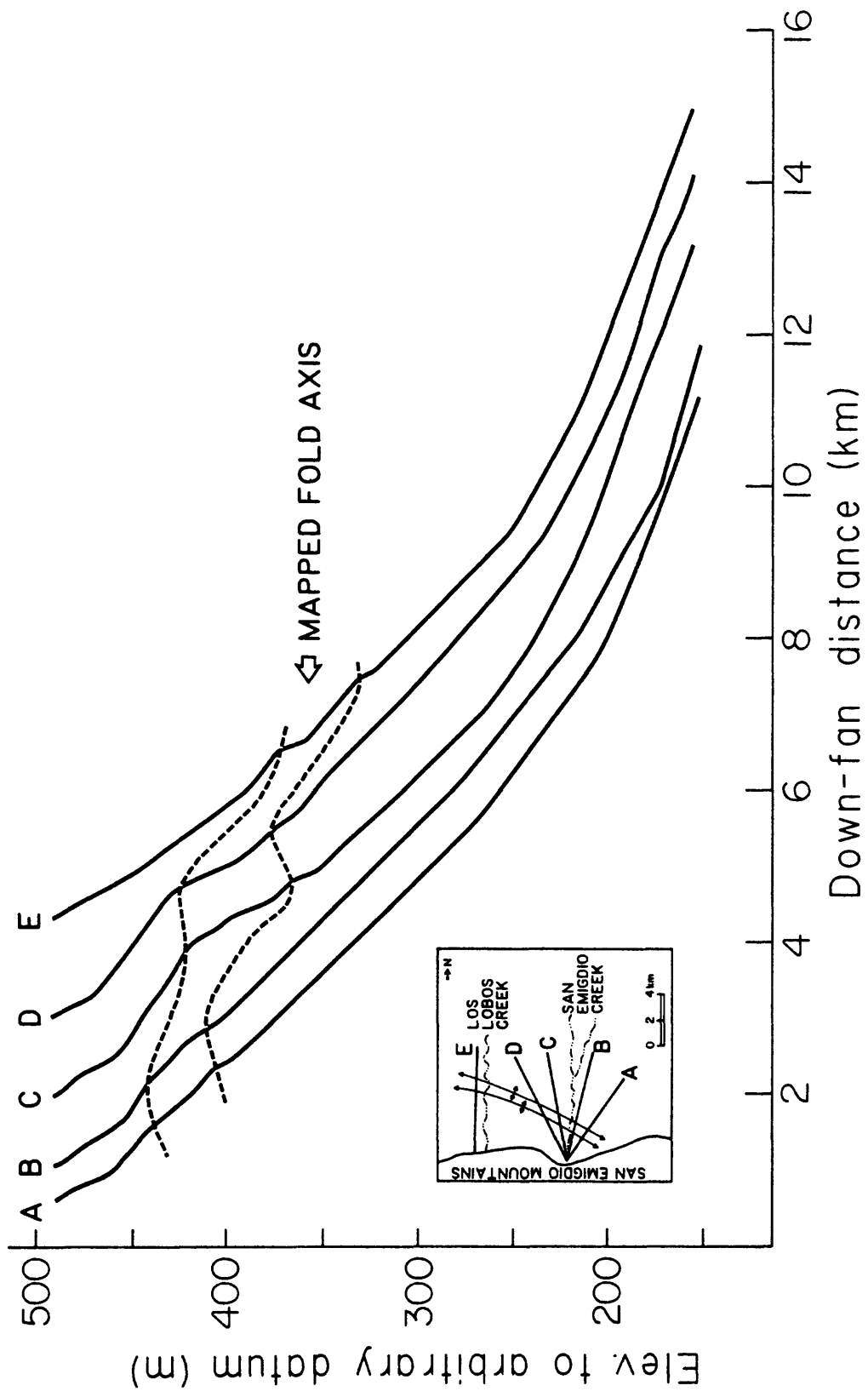
Figure 3. Radial profiles down the San Emigdio alluvial fan showing folded fan segments.
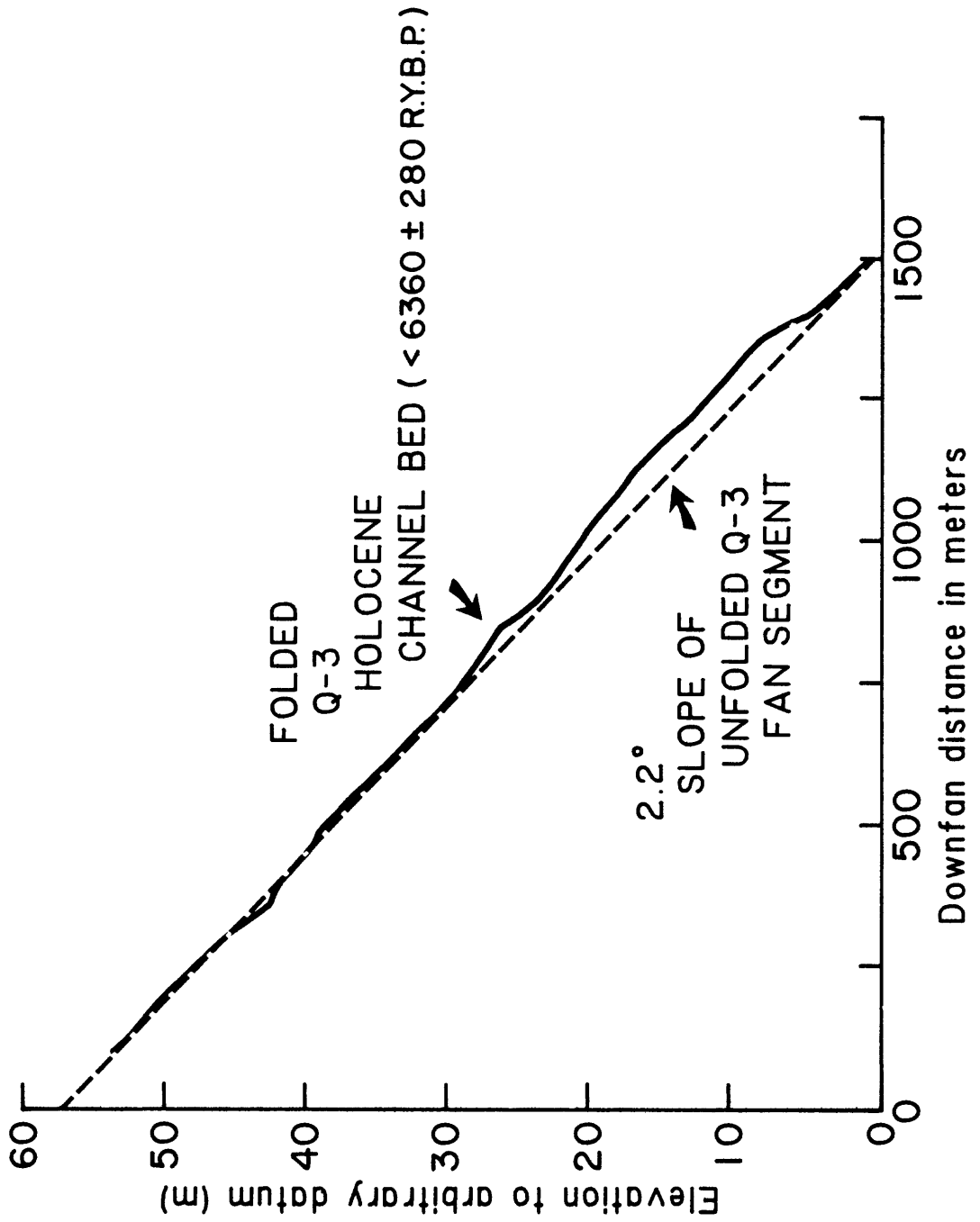
Figure 4. Deformed, abandoned, Holocene channel on the San Emigdio alluvial fan.

TOPOGRAPHIC PROFILE
SAN EMIGDIO CANYON

Holocene gravels (<6360±280 R.Y.B.P.)

Late pleistocene gravels

Bedrock

Paleosol

x4 vertical exaggeration

S

San Emigdio Mts.

Pastoria fault (?)

N

San Joaquin Valley

Los Lobos fold

White Wolf fault

Wheeler Ridge fault

Pleito fault zone

Elevation (km)

Distance (km)
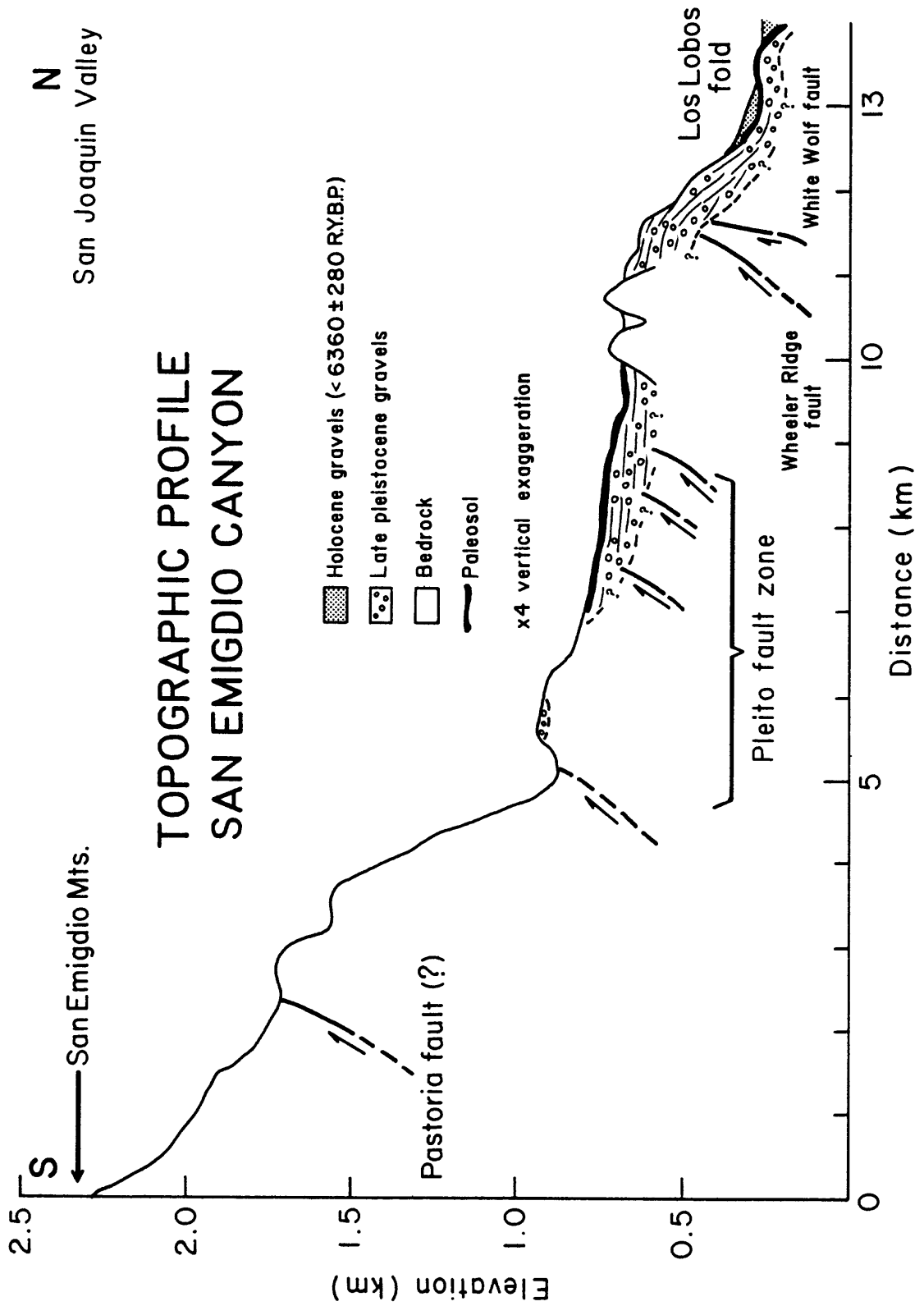
Figure 5. Topographic section from the San Emigdio Mountains to the San Joaquin Valley showing major faults and Los Lobos fold.

STUDY OF SEISMIC ACTIVITY BY
SELECTIVE TRENCHING ALONG THE
ELSINORE FAULT ZONE, SOUTHERN CALIFORNIA

Contract 14-08-0001-21376

T. K. Rockwell
Geology Department
San Diego State University
San Diego, CA 92182

and

D. L. Lamar
Lamar-Merifield Geologists, Inc.
1318 Second Street, Suite 25
Santa Monica, CA 90401
Telephone: (213) 395-4528

Investigations

Study and logging of exposures in trenches across the Glen Ivy North fault, a strand of the Elsinore fault zone between Corona and Lake Elsinore, have continued. Displaced peat layers have been dated by Carbon 14 methods and dendrochronologically corrected.

Results

The fault zone has been logged at 30-cm intervals to reveal the relationships in three dimensions. Figure 1 is an example log showing peat layers (numbered), sediments between the peats (lettered) and fault strands. Analysis of six similar logs and Carbon 14 dating of peat layers has revealed the following events:

Time	Vertical Separation (cm)	Horizontal Separation (cm)
Post-1660 A.D., historical*	30-50	unknown
Between 1300 and 1600 A.D.	2-3	unknown
About 1300 A.D.	±20	90+
Pre-1275 A.D.	3-5	unknown
Pre-1275 A.D.	1-3	unknown

* Glass and pottery shards in liquefied sand related to the earthquake.

There is some evidence of two post-1660 A.D. events. These results suggest a maximum earthquake recurrence interval of 300 years.

Reports

Rockwell, T. K., Lamar, D. L., McElwain, R. S. and Millman, D. E., 1985, Late Holocene faulting on the Glen Ivy North strand of the Elsinore fault, southern California: abstract accepted for presentation at the Cordilleran Section, Geological Society of America.

42285B
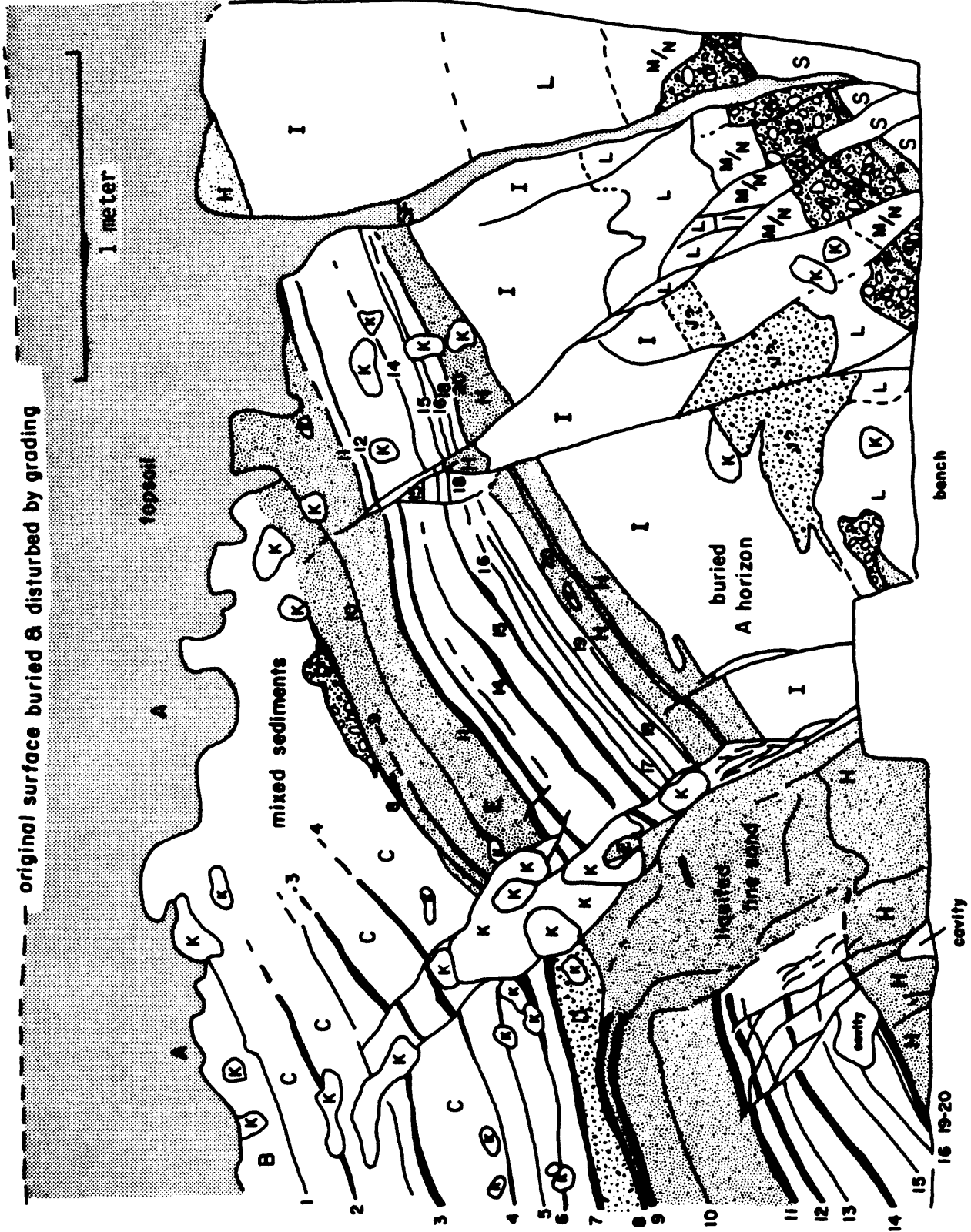
Fig. 1 - Log of displaced strata exposed in trench across Glen Ivy North fault.

INDEX 1

INDEX ALPHABETIZED BY PRINCIPAL INVESTIGATOR

551

Lester, F. W.	U.S. Geological Survey	24
Levi, S.	Oregon State University	96
Li, V. C.	Massachusetts Institute of Technology	380
Lindh, A. G.	U.S. Geological Survey	283
Liu, H. -P	U.S. Geological Survey	383
Logan, J. M.	Texas A&M University	385
Madole, R. F.	U.S. Geological Survey	470
Madden, T. R.	Massachusetts Institute of Technology	287
Maley, R. P.	U.S. Geological Survey	528
Matti, J. C.	U.S. Geological Survey	100
McCalpin, J.	Utah State University	105
McCarthy, R. P.	U.S. Geological Survey	521
McNally, K.	California, University of, Santa Cruz	53
McNally, K.	California, University of, Santa Cruz	168
McNally, K.	California, University of, Santa Cruz	288
Mooney, W. D.	U.S. Geological Survey	388
Morrissey, S-T	Saint Louis, University of	289
Morrissey, S-T.	Saint Louis, University of	296
Morrissey, S-T.	Saint Louis, University of	299
Mortensen, C. E.	U.S. Geological Survey	294
Mueller, R. J.	U.S. Geological Survey	170
Myren, G. D.	U.S. Geological Survey	302
Niazi, M.	Tera Advanced Service Corporation	172
Obermeier, S. F.	U.S. Geological Survey	109
Oppenheimer, D. H.	U.S. Geological Survey	418
Park, R. B.	U.S. Geological Survey	522
Person, W. J.	U.S. Geological Survey	524
Peterson, J.	U.S. Geological Survey	511
Power, M. S.	Woodward-Clyde Consultants	474
Prescott, W. H.	U.S. Geological Survey	177
Ratcliffe, N. M.	U.S. Geological Survey	54
Reimer, G. M.	U.S. Geological Survey	183
Reynolds, R. D.	U.S. Geological Survey	512
Rice, J. R.	Harvard University	393
Robertson, E. C.	U.S. Geological Survey	398
Rockwell, T. K.	San Diego State University	547
Rogers, A. M.	U.S. Geological Survey	493
Ross, D. C.	U.S. Geological Survey	59
Rudnicki, J. W.	Northwestern University	185
Ryall, A. S.	Nevada, University of	27
Ryall, A.S.	Nevada, University of	112
Sass, J. H.	U.S. Geological Survey	400
Sacks, I. S.	Carnegie Institute of Washington	186
Sacks, I. S.	Carnegie Institute of Washington	312
Sato, M.	U.S. Geological Survey	191
Schulz, S. S.	U.S. Geological Survey	306
Segall, P.	U.S. Geological Survey	421

Shapiro, M. H.	California Institute of Technology	323
Shaw, H. R.	U.S. Geological Survey	199
Sieh, K.	California Institute of Technology	116
Sieh, K.	California Institute of Technology	117
Simpson, D. W.	Lamont-Doherty Geological Observatory	424
Simpson, D. W.	Lamont-Doherty Geological Observatory	426
Simpson, R. W.	U.S. Geological Survey	403
Slater, L. E.	Colorado, University of	328
Slater, L. E.	Colorado, University of	329
Smith, R. B.	Utah, University of	61
Spence, W.	U.S. Geological Survey	427
Spence, W.	U.S. Geological Survey	514
Spudich, P.	U.S. Geological Survey	535
Stauder, W.	Saint Louis University	299
Steeples, D. W.	Kansas, University of	429
Stein, R. S.	U.S. Geological Survey	330
Stewart, G. S.	Pacific Geophysics, Inc.	202
Stewart, S. W.	U.S. Geological Survey	30
Stover, C. W.	U.S. Geological Survey	517
Stuart, W. D.	U.S. Geological Survey	404
Sykes, L. R.	Lamont-Doherty Geological Observatory	203
Taber, J.	Lamont-Doherty Geological Observatory	32
Taber, J.	Lamont-Doherty Geological Observatory	206
Taggart, J. N.	U.S. Geological Survey	526
Talwani, P.	South Carolina, University of	433
Tarr, A. C.	U.S. Geological Survey	441
Tarr, A. C.	U.S. Geological Survey	494
Teng, T.	Southern California, University of	35
Teng, T.	Southern California, University of	336
Tinsley, J. C.	U.S. Geological Survey	119
Toksoz, M. N.	Massachusetts Institute of Technology	342
Toksoz, M. N.	Massachusetts Institute of Technology	478
Tullis, T. E.	Brown University	407
Van Schaack, J.	U.S. Geological Survey	39
Van Schaack, J.	U.S. Geological Survey	41
Wallace, R. E.	U.S. Geological Survey	482
Walsh, J. B.	Massachusetts Institute of Technology	411
Warrick, R. E.	U.S. Geological Survey	537
Weaver, C. S.	U.S. Geological Survey	66
Wentworth, C. M.	U.S. Geological Survey	123
Wesson, R. L.	U.S. Geological Survey	211
White, R. A.	U.S. Geological Survey	213
Wyatt, F.	California, University of, San Diego	345
Wyatt, F.	California, University of, San Diego	347
Wyatt, F.	California, University of, San Diego	352
Wu, F. T.	State University of New York, Binghamton	218
Yeats, R. S.	Oregon State University	125
Yerkes, R. F.	U.S. Geological Survey	127
Ziony, J. I.	U.S. Geological Survey	484
Zoback, M. L.	U.S. Geological Survey	486

INDEX 2

INDEX ALPHABETIZED BY INSTITUTION

Lamont-Doherty Geological Observatory	Simpson, D. W.	424
Lamont-Doherty Geological Observatory	Simpson, D. W.	426
Lamont-Doherty Geological Observatory	Sykes, L. R.	203
Lamont-Doherty Geological Observatory	Taber, J.	32
Lamont-Doherty Geological Observatory	Taber, J.	206
Massachusetts Institute of Technology	Aki, K.	130
Massachusetts Institute of Technology	Li, V. C.	380
Massachusetts Institute of Technology	Madden, T. R.	287
Massachusetts Institute of Technology	Toksoz, M. N.	342
Massachusetts Institute of Technology	Toksoz, M. N.	478
Massachusetts Institute of Technology	Walsh, J. B.	411
Nevada, University of	Ryall, A. S.	27
Nevada, University of	Ryall, A. S.	112
New York, State University of, Binghamton	Wu, F. T.	218
Northwestern University	Rudnicki, J. W.	185
Oregon State University	Levi, S.	96
Oregon State University	Yeats, R. S.	125
Pacific Geophysics, Inc.	Stewart, G. S.	202
Queensland, University of	Gladwin, M. T.	243
Saint Louis University	Morrissey, S-T.	289
Saint Louis University	Morrissey, S-T.	296
Saint Louis University	Morrissey, S-T.	299
San Diego State University	Kern, P.	50
San Diego State University	Rockwell, T. K.	547
San Francisco State University	Galehouse, J. S.	238
Sierra Geophysics, Inc.	Ihnen, S. M.	464
South Carolina, University of	Talwani, P.	433
Southern California, University of	Aki, K.	132
Southern California, University of	Haukson, E.	136
Southern California, University of	Henyey, T. L.	249
Southern California, University of	Leary, P. C.	278
Southern California, University of	Teng, T.	35
Southern Califounia, University of	Teng, T.	336
Tera Advanced Services Corporation	Niazi, M.	172
Texas A&M University	Logan, J. M.	385
U.S. Geological Survey	Algermissen, S. T.	446
U.S. Geological Survey	Allen, R. V.	223